Structure and Function of the VAL Family in *Brugia malayi* and *Heligmosomoides polygyrus.*

PART I

Janice Murray

A thesis submitted for the degree of Doctor of Philosophy.

University of Edinburgh

2014

Declaration

I declare that this thesis has been composed by myself, describes my own work and that the work has not been submitted towards any other degree.

Experiments in Chapter 3 were carried out in close collaboration with Dr H McSorley.

Selected experiments throughout this thesis were carried out in close collaboration with Dr J Hewitson. These have been published and are attached at the end of the thesis (see Appendix).

Janice Murray
February, 2015.

Acknowledgments

I think in this part I am allowed to be "too personal", include "verbal vague" and to get a bit chatty! These are all little nuances, of which I was guilty when writing this thesis, and which my very clever, patient and understanding supervisor Rick made me aware. He has remained supportive and positive throughout my PhD and for this and the simple fact that he allowed me the opportunity in the first place, I thank him.

My lab guys….
Kara and Lisa…you have both moved on to pastures new and I am absolutely sure you will both be amazing! I miss you both… I have to say I think we were onto something with our geeky, science film nights. I know of no one else who finishes a film with an Excel spread sheet! I really wish you had both been here to experience this last chapter (pun intended) of my PhD journey. We had the best time…. heart you both!
Yo James! Do you know that I often had to go and have a "wee sit down" after you had chatted science to me! Your knowledge, level of commitment and attention to detail for our research was often super-human. Your singing voice however…..

Henry, you were here...then you left…then you came back…and I was still doing this PhD. That's how long I've known you! You've gone from student to fellow in that time, single to married. Along the way, you always had time to help me out and always kept a straight face and a conciliatory hug, even when you knew my hopes for an experiment were about to be dashed! Thank you for mouse grabbing, footpad measuring, trampolining, poling, whisky drinking, ceilidhs and broken toes!

The Maizelettes, past and present, are an amazing group of talented and gifted individuals! Danielle, I've not known you for very long but I think, after spending a week in Hydra with you ;-), we're on the same wavelength! Thank you for being a calm face through lab moves, poster pitches and ultimately thesis preparation! Chris! Please make me an espresso martini! BW, JM.

Lidia, you were there at the very *Leishmaniacal* start, which seems like a lifetime ago! Thanks for being a great friend and now and pole buddy. Now, after my thesis confinement, we have some catching up to do!!

The 3rd floor of Ashworth has a huge wealth of fabulous people! Judi, you and your group are wonderful colleagues who make science (and Christmas dinners) all the more fun! Dom, you were a calm face when I needed it before AIM meetings (and you make a helluva Caipirinha!). Tara, I've often popped along in a bit of a tizz, you

never told me to go away and always found time to help me out, ☺. Lucy and Lauren, you also experienced the PhD journey at the same time as myself (and Kara and Lisa) and have helped me understand that my crazy brain is actually reacting in a normal way to the stresses!. Many lovely lunches by The Wall….

My thanks also go to Dianne Murray who has spent many hours in the darkness of the confocal facility with me. She has been ever so patient with my "just one more image should do it…". She has shared in my successes and my disappointments and, if I'm honest, I think she has developed a wee soft spot for good ole *H.poly*!

Oddly now… my brother-in-law Andrew…. I believe he placed a seedling of a notion in my mind to undertake this task a few years back. He remains baffled however, as to why I chose to write a thesis rather than submit by publication! I'm guessing that publishing in the field of luminescence dating (Pederson et al., 2014) happens a little faster than in parasite immunology!

* * * * * * * * * * * *

Adrian, Euan and Douglas…. I'm back!

I feel like I have been away from you guys for too long, whilst this thesis has consumed me during its construction. You have been so patient and I love you all. Adrian, I absolutely could not have done this without your constant, unwavering support and belief in me. Now onwards with your birthday preparations ☺! My boys…. so many hugs while I was attached to the computer you have no idea how they lifted my spirits. You've kept me on the right side of sanity although at times it may not have seemed like that. I now vacate the study…Euan, it's all yours!

Mum and dad, you have been wonderfully supportive throughout this whole extravaganza! I hope my lay summary gave you a hint of what it's all about…worms, asthma, immunology, parasites, microscopes, very cool pics, bla de bla de bla. Mum…. I'm done. (and I only had to find my way to the roof once).

Abstract

Evasion of an immune response mounted by a host is fundamental to the survival of a parasite. Immune evasion can be mediated in many ways from the production of molecules by the parasite which mimic cytokines produced by the human immune system to hiding from the immune system by locating within host cells. The production of immune cell mediating molecules in excretory secretory products is another means by which the parasite can tailor its surroundings to facilitate prolonged survival. The hypothesis of immunosuppression by parasite products, in particular members of the Venom Allergen Like (VAL) family, is key to this thesis.

VAL proteins are members of the much larger SCP/TAPS family, which covers proteins from parasitic helminths such as *Heligmosomoides polygyrus* (*H.polygyrus*)to the free-living nematode *Caenorhabditis elegans*. These nematodes may have one or more genes encoding proteins that contain the SCP/TAPS domains often choosing to express these proteins at critical points within the helminths lifecycle. Phylogenetic analysis of a selection of these proteins revealed that their classification could be determined based upon the number of SCP/TAPS domains. Alternatively the presence or absence of the signal sequence combined with conserved cysteine residue data could be used. Further investigations into possible functions of the VAL proteins from *H.polygyrus* were carried out using recombinant protein produced in an insect cell expression system.

To further examine the function of VAL genes a system that allows the heterologous expression of a gene in the well-documented *Leishmania* infection setting was employed. *In vitro* and *in vivo* studies were carried out which examined various infection parameters. Parasite infectivity in bone marrow derived macrophages *in vitro* along with cytokine production was observed. *In vivo* the development of lesions and subsequent parasite recovery from infected mice gave indications of changes in virulence that could be attributed to the presence and expression of the HpVAL genes.

The ability of parasites to ameliorate symptoms of allergic and autoimmune diseases is now well documented with the most extreme use of this knowledge resulting in administration of an active parasitic infection as a treatment regime. We hope to identify individual molecules from a parasite that is known to reduce allergic symptoms in the allergic airway inflammation (AAI) model and produce these in a more structured and regulated fashion. It is plausible that VAL proteins from *H.polygyrus* may possess these regulatory properties, as has been shown for the excretory secretory products (HES) of the parasite; to that end HpVAL-1 and HpVAL-4 were tested in the allergic airway inflammation model and were shown to reduce both cell numbers in the bronchioalveolar lavage fluid and eosinophilia.

Finally, the position of the parasite and products secreted by the parasite was examined. Directly labelled HES and recombinant VAL proteins were used to identify binding sites inside the parasite and within the parasites' locality in the host i.e. the gut. Confocal microscopy revealed binding of HES to the parasites surface and internal structures and of both HES and HpVAL-4 to goblet cells and Paneth cells inside the gut. Paneth cells may affect parasite survival by influencing the gut microbiota and goblet cells have been shown to influence parasite persistence by production of mucus. Thus HES and more specifically HpVAL proteins may, through their interactions with these cells, interfere with mechanisms employed by the host to expel the parasite.

Lay Summary

Parasites by definition are organisms that can survive inside or upon another individual called its host, which can be plant or animal. Many parasites, such as malaria, can infect human hosts. Sometimes these parasites cause harm to their host, as is the case with the malaria parasite but often parasites can live within their host for many years causing them little or no harm at all. Oddly, when the latter is the case, if an immune response did occur it could be detrimental to both host and parasite. Why then do human hosts fight some infections like flu viruses and food poisoning but to all intents and purposes ignore a parasitic guest?

We believe that the parasite itself may have a bearing on whether or not the host attempts eviction by mounting an immune response. We also think that this is achieved through a cocktail of molecules produced by the parasite, which can affect the cells involved when a person raises an immune system.

By keeping parasites in a test tube and collecting everything that they produce we have been able to show that one parasite in particular, *Heligmosomoides polygyrus,* a mouse parasite, produces hundreds of different molecules. We can then identify these molecules based on their DNA or protein patterns. Once identified we can make these molecules artificially in the lab, then test them to see if they had any effect on immune cells. If they affect immune cells then this information can be used to generate new medicines against the parasite or even more remarkably can be used to make treatments for allergies and auto-immune diseases which both result from immune cells behaving in an inappropriate manner.

Abbreviations

Amp	Ampicillin
ASP	*Ancylostoma* secreted protein
APC	antigen presenting cell
Arg-1	Arginase 1
BAL	Bronchoalveolar lavage
BES	*Brugia malayi* excretory secretory products
BM (φ)	Bone marrow (macrophage)
CIP	Calf Intestinal Phosphatase
CPI	Cysteine protease inhibitor
DAPI	4',6-diamidino-2-phenylindole
DC	Dendritic cell
DNA	Deoxyribonucleic acid
DMSO	Dimethyl sulfoxide
EDTA	Ethylenediaminetetraacetic acid
ELISA	Enzyme-linked immunosorbent assay
EPB	Electroporation buffer
ES	Excretory secretory products
FACS	Fluorescence activated cell sorting
FCS	Fetal calf serum
x*g*	G-force
GM-CSF	Granulocyte macrophage colony stimulating factor
KAN	Kanamycin
IL	Interleukin
IFN	Interferon
Ig	Immunoglobulin
i.n.	Intra-nasal
i.p.	Intra-peritoneal
H&E	Hematoxylin and eosin
HES	*Heligmosomoides polygyrus* excretory secretory products
HRP	Horseradish peroxidase

HBSS	Hanks balanced salt solution
LB	Luria broth
LPS	lipopolysaccharide
mAb	Monoclonal antibody
MHC	Major histocompatibility complex
MUC	Mucin
MW	Molecular weight
MWCO	Molecular weight cut off
OVA	Ovalbumin
PAS	Periodic acid-Schiff
PBS	Phosphate buffered saline
PCR	Polymerase chain reaction
PEG	Polyethylene glycol
PFA	Paraformaldehyde
PMA	Phorbol Myristate acetate
qPCR	Quantitative PCR
RNA (ss & ds)	Ribonucleic acid (single stranded &double stranded)
RNAi	Ribonucleic acid interference
rpm	Revolutions per minute
RT-PCR	Reverse transcription PCR
TBE	Tris/ borate/ EDTA
TBS	Tris buffered saline
TBS-T	Tris buffered saline with Tween 20
TGF-β	Transforming growth factor- β
SDM	Semi-defined media
SDS PAGE	Sodium dodecyl sulphate polyacrylamide gel electrophoresis
TLR	Toll like receptor
VAL	Venom allergen like
WT	Wild type

Table of Contents

ABSTRACT 5

LAY SUMMARY 7

ABBREVIATIONS 8

INTRODUCTION 21

HELMINTHS 21
IMMUNE EVASION: CONCEPT AND STRATEGIES. 23
Cystatins: Bm-CPI-2 27
Cytokine mimics: Macrophage-migration inhibition factors (MIFs) 28
Cytokine mimics: TGF-β 29
Prominent ES molecules: Abundant larval transcripts (ALTs) 32
Parasite excretory secretory products 34
HOST TARGETS: CELLS AND TISSUES 35
Macrophages. 36
Dendritic cells. 39
Granulocytes: Neutrophils, eosinophils and basophils. 39
T Cells 43
Innate lymphoid cells 46
B cells and antibody responses 49
PARASITES AND ANIMAL MODELS 50
Heligmosomoides polygyrus 50
EPITHELIAL CELLS 53
Lung epithelium: 53
Gut epithelium: 55
THE HOST MICROBIOTA 56
AIM AND HYPOTHESES **58**

MATERIAL AND METHODS 60

PARASITE METHODS 60
Preparation of *H.polygyrus* excretory secretory products (HES) 60
Preparation of *H.polygyrus* extract (HEx) 60
Parasite Egg Counts 60
Brugia malayi 65
Nippostrongyus brasiliensis 67
MOLECULAR BIOLOGY AND PROTEIN TECHNIQUES 69
PCR 69
A-Tailing 69
Dephosphorylation of vectors. 70
Restriction Digests 70
Agarose Gel Electrophoresis 70
Gel Purification 71
Ligation 71
Bacterial Transformation 71
PCR Colony Screen 71

Sequencing 72
PROTEIN METHODS 73
SDS-Protein Gel Electrophoresis (SDS-PAGE) 73
Western Blotting Detection of Protein 74
Antibody detection of proteins 74
RNA Extraction 75
DNase Treatment 75
Reverse transcription 75
Large Scale RNA using T7 RiboMAX™ System 76
RNAi protocol. 76
Modified RNAi protocol using siRNA. 79
Transformation 80
Growth and Induction 80
Assessment of the solubility of recombinant protein. 81
Purification of Recombinant Proteins 81
LPS depletion using Triton X114 81
MICROSCOPY TECHNIQUES 83
Freezing Tissue and Sectioning 83
Immunofluorescent Staining 83
Whole Mount tissue preparation. 84
Staining Whole Mount Tissue 85
INSECT CELL CULTURE 86
Transfection of Insect Cell Lines 87
Freezing Cell Lines 88
LEISHMANIA METHODS 89
Recovering Frozen Parasites. 89
Cryopreservation of parasites 89
Culture of *Leishmania mexicana* promastigotes. 89
Transfection of *L.mexicana* promastigotes. 90
Cytomix Method for parasite transfection 91
IMMUNOLOGICAL METHODS 92
Cytokine ELISA (Enzyme Linked Immunosorbent Assay) 92
Serum Antibody ELISA 94
Cell Isolation for Fluorescence Activated Cell Sorting (FACS), Intracellular Cytokine Staining (ICCS) or restimulation. 95
Restimulation of Cells 96
Cell surface staining for flow cytometry 96
Cytometric Bead Array Assay (CBA Assay) 98
Alum Precipitation 99
BUFFERS AND MEDIA 102
Mice 104
Statistics 104
Computer Software 105

CHAPTER 1 109

VALS: THE GENE, GENE FAMILY AND THE PROTEIN. 109
INTRODUCTION 109
The SCP/TAPS family. 109

RESULTS 115
1.2 - 1.4 Phylogenetic tree of the VAL protein family in *H.polygyrus*. 115
1.5 Phylogeny of SCP/TAPS family members across species. 123
1.6 – 1.10 HpVAL-1 & 4 have structural similarity to proteins with known SCP domains. 126
1.8 HpVAL-4 showing SCP domain and secondary structure. 130
1.9 HpVAL-4 SCP domain aligns to the C terminal domain of HpVAL-1. 130
1.10 HpVAL-1 and HpVAL-4 3D structures align with Ves v5, a major allergen from Yellow-jacket venom. 133
1.11 Insect cell expression. 135
1.12 Codon Optimization for enhanced protein expression. 137
1.13 HpVAL-1 & 4 both express in Hi5 and SF9 insect cells 138
1.14 Purification of recombinant proteins Hp-VAL-1, HpVAL-2, BmVAL and Ce-VAL. 140
1.15 Recombinant HpVAL-4 is bound by conformation dependent antibody but does not recognise an antibody that binds HpVAL-1. 142
1.16 Biotinylation of HpVAL proteins. 144
1.17 Biotinylated recombinant HpVAL binds naïve B cells. 146
1.18 Do all VAL proteins bind naive B cells? 148
1.20 HpVAL-4 and β-tubulin sequences for insertion into L4440 RNAi vector. 150
1.21 RNAi of HpVAL-4. 153
1.22 RNAi on exsheathed *H.polygyrus* larvae. 155
1.23 RNAi optimization reveals no knockdown of HpVAL-4. 155
1.24 A modified RNAi protocol using siRNA. 158
1.25 Exsheathed larvae cannot mount an infection in mice. 160
1.26 Genes required for efficient RNAi processing. 162
DISCUSSION 164

CHAPTER 2 173

GENE FUNCTION ANALYSIS USING A NOVEL TRANSGENIC APPROACH. 173
INTRODUCTION 173
RESULTS 177
2.3 Vectors used in the cloning of Bm-VAL, Ce-VAL, and Hp-VAL1 into the *Leishmania* expression system. 177
2.4 In vitro infection of bone marrow derived macrophages. *(BMDM)* 180
2.5 Expression of arginase, iNOS, IL13 & Il10 in infected BMDM by quantitative RT-PCR. 182
2.7 Experimental protocol for *in vivo* assessment of Bm-VAL-1 gene function. 185
2.8 Time course of cutaneous lesion development. 186
2.9 Mice infected with Bm-VAL transgenic parasites have a higher parasite burden than those infected with wild type *L.mexicana*. 188
2.10 Immune responses in popliteal lymph node. 190
2.11 Experimental protocol for *In vivo* assessment of Bm-VAL-1 gene function. 192
2.12 Time course of Lesion Development. 192
2.13 Parasites recovered from foot and spleen of infected mice. 195
2.14 Immune responses in popliteal lymph node. 197
2.15 Experimental protocol for *In vivo* assessment of Bm-VAL-1 gene function. 199

2.16 Growth curves of *Leishmania* promastigotes transfected with pSSU, Bm-VAL or Ce-VAL. 201
2.17 Time course of Lesion Development. 203
2.18 Parasites recovered from foot and spleen of infected mice. 205
2.19 Immune responses in popliteal lymph node. 206
2.20 Experimental protocol for *In vivo* assessment of Bm-VAL-1 gene function. 208
2.21 Time course of Lesion Development. 208
2.22 Parasites recovered from foot and spleen of infected mice. 211
2.23 Immune responses in popliteal lymph node. 211
2.24 Collated lesion development time course data from *Leishmania in vivo* experiments. 214
2.25 Collated parasite recovery data from *Leishmania in vivo* experiments. 216
2.26 Summary of experimental readouts from 4 *in vivo* infection experiments. 218
DISCUSSION 220

CHAPTER 3 223

VAL, A COMPONENT OF HES, AND ITS EFFECT IN THE ALLERGIC AIRWAY INFLAMMATION MODEL 223
INTRODUCTION 223
RESULTS 228
3.3 Can recombinant HpVALs induce a Th2 response? 228
3.4 Cytokines produced in response to recombinant VALs are significantly lower than seen in response to HES. 230
3.5- 3.6 Profile of cells recruited in response to HES and recombinant VALs. 233
3.7- 3.8 Levels of RELM-α and YM-1 in peritoneal lavage fluid 236
3.9- 3.10 Experiment 1: Hp-VAL, a component of HES, reduces cell numbers and eosinophil numbers in BAL fluid in the A.A.I. model. 239
3.11 Analysis of BAL fluid shows a reduction in proportions and absolute numbers of T helper cells after administration of HES and Hp-VAL4. 244
3.12- 3.13(i) & (ii) An overall reduction in cytokines produced is observed in mice treated with HES and HpVAL-4. 246
3.14 Levels of OVA specific IgE are reduced with HES treatment but not by HpVAL-4. 250
3.15 Levels of RELM-α in BAL and lung homogenate are reduced by HES treatment, whereas YM-1 levels appear to increase. 253
3.16 Differences between treatment groups illustrated by immunohistochemistry. 255
3.17 Experiment 2: Do other VAL molecules suppress AAI? 257
3.18 Enumeration and characterization of BAL cells. 259
3.19 Enumeration and characterization of lung homogenate cells. 261
3.20 (i-iii) Intracellular cytokine profile of BAL and lung homogenate cells by CBA assay. 264
3.21 Levels of RELM-α in BAL and lung homogenate are reduced by VAL treatment. Conversely, YM-1 levels increase upon treatment with CeVAL. 268
3.22 Experiment 3: Is the reduction of airway eosinophilia dependent on VAL structure? 270
3.23 Enumeration and characterization of BAL cells. 272
3.24 Experiment 4: Can the initial suppression of AAI by HpVAL be repeated? 274
3.25 Enumeration and characterization of BAL cells. 276

3.26 Pooled data from 4 investigations showing that Hp-VAL4 reduces numbers of eosinophils as seen with HES. 278
DISCUSSION 280

CHAPTER 4 285

INTERACTIONS CONCERNING HES, VAL, *H.POLYGYRUS* AND THE GUT. 285
INTRODUCTION 285
RESULTS 291
SECTION 1: PROBING THE ADULT SURFACE OF *H.POLYGYRUS*. 291
4.3 Monoclonal antibody binds to carbohydrates on the surface of the parasite. 291
4.4 Polyclonal α-HES and α- Glycan A antibodies recognise the surface and some internal structures of the parasite. 293
4.5 Characterisation of antibody binding reveals that monoclonal and polyclonal antibodies, which recognise HpVAL-1 & -4, bind to different structures of the parasite. 297
4.6 Biotinylated lectins do not bind cuticle carbohydrates. 300
4.7 - 4.10 Are VAL proteins associated with the cuticle and can they be recovered by chemical or detergent treatment? 303
4.11 Acetone precipitated parasite cuticle reveals a 62kDa protein which is recognised by α-HES and α-Glycan A antibodies. 309
SECTION 2: DO *H.POLYGYRUS* PRODUCTS BIND TO HOST CELLS? 311
4.12 Alexa647 labeled HES binds to cells recruited to granulomas present in *H.polygyrus* infection. 311
4.13 (i) & (ii). Alexa647 labelled HES binds to the surface of the parasite throughout an infection time-course. 313
4.14 - 4.16 Is the binding of HES to *H.polygyrus* and Paneth cells CD24 dependent? 317
4.15-(i) & (ii) Binding of HES to *H.polygyrus* and Paneth cells is not CD24 dependent (DAY 7). 317
4.16 (i)-(ii) Binding of HES to *H.polygyrus* and Paneth cells is not CD24 dependent (DAY 28). 322
4.17 HES binding to Paneth cells is heat stabile. 326
4.18-4.19 Cuticle binding of HES in *H.polygyrus* is not antibody mediated. 328
4.20 Preparation of intestinal epithelium for whole mount staining. 332
4.21 Immunostaining of intestinal villi and crypts. 334
4.22 HES binds to cells on the surface of the villus. 338
4.23 HES and HpVAL-4 bind to villus goblet cells. 340
4.24 HpVAL-4, not HpVAL-1, binds intestinal goblet cells. 342
4.25 - 4.26 HpVAL-4 and MUC2 binding within the goblet cell. 344
4.27 Intestinal goblet cells from CD24-/- mice bind HES and HpVAL-4 but not HpVAL-1; Paneth cells bind all three. 346
4.28 Summary of villi and crypt staining. 350
DISCUSSION 351

FINAL DISCUSSION AND FUTURE DIRECTIONS 355

Published Papers 394

List of Figures

Introduction

Fig 1. Global distribution of helminth infection (World Health Organisation). 22
Fig 2. *Brugia malayi* life cycle. 33
Fig 3. Cells of the innate and adaptive immune system. 35
Fig 4. Polarisation of macrophages during infection. 38
Fig 6 Male and female *Heligmosomoides polygyrus* (*H.polygyrus*). 51
Fig 7. Scanning electron micrograph showing club cells rat bronchiole. 53
Fig 8. A. *H.polygyrus* life cycle 63
B. Preparation of *H.polygyrus* excretory/secretory products (HES). 63
Fig 9. Maintenance of the *B.malayi* laboratory life cycle. 66
Fig 10. Maintenance of the *N.brasiliensis* laboratory life cycle. 68
Fig.11 SeeBlue® Plus pre-stained markers. 73
Fig. 12 RNAi protocol. 77
Fig. 13 Modified RNAi protocol using siRNA. 79

Chapter 1

Fig 1.1 Structural configuration of SCP/TAPS proteins. 113
Fig 1.2 Phylogenetic tree of the complete VAL protein family in *H.polygyrus*. 117
Fig 1.4 (A) Phylogenetic tree showing SCP/TAP domains of the VAL protein family in *H.polygyrus*. 119
Fig 1.4 (B) Phylogenetic tree showing SCP/TAP domains of the VAL protein family in *H.polygyrus* and *S.mansoni*. 121
Fig 1.5 Phylogeny of SCP/TAPS family members across species. 124
Fig 1.6 HpVAL1 has structural similarity to proteins with known SCP domains. 128
Fig 1.7 HpVAL-1 Showing primary and tertiary structure 129
Fig 1.8 HpVAL-4 Showing SCP domain and tertiary structure. 131
Fig 1.9 HpVAL-4 SCP domain aligns with the C terminal domain of HpVAL-1. 132
Fig 1.10 HpVAL-1 and HpVA-4 3D structures align with Ves v5, a major allergen from Yellow-jacket venom. 134
Fig 1.11 Insect cell expression vector map. 136
Fig 1.12 HpVAL-1 and 4 both express in Hi5 and SF9 insect cells. 139
Fig 1.13 Purification of recombinant proteins HpVAL-1, HpVAL-4, Bm-VAL and Ce-VAL. 141
Fig 1.14 Recombinant HpVAL-4 is bound by conformation dependent antibody but does not recognise an antibody that binds HpVAL-1. 143
Fig 1.15 Biotinylation of HpVAL proteins. 145
Fig 1.16 Biotinylated recombinant HpVAL binds a splenocyte subset. 147
Fig 1.17 Do all VAL proteins bind naive B cells? 149
Fig 1.18 Genomic maps of HpVAL-4 and HpTubulin: Primer design for RNAi constructs. 151
Fig 1.19 HpVAL-4 and β-tubulin sequences for insertion into L4440 RNAi vector. 152
Fig 1.20 RNAi of HpVAL-4. 154
Fig 1.21 RNAi on exsheathed *H.polygyrus* larvae. 156
Fig 1.22 RNAi optimization reveals no knockdown of HpVAL-4. 157

Fig 1.23 A modified RNAi protocol using siRNA. 159
Fig 1.24 Exsheathed larvae cannot mount an infection in mice. 161
Fig 1.25 CRISP Family hierarchy 165
Fig. 1.26 Post-translational modifications added to recombinant proteins in 3 protein expression systems 168
Fig. 1.27 2D electrophoresis of excretory/secretory products from *H.polygyrus*. 170

Chapter 2

Fig 2.1 Forward and reverse genetics 174
Fig 2.2 Construct design for cloning into pSSU vector. 176
Fig 2.3 Vectors used in the cloning of Bm-VAL, Ce-VAL and Hp-VAL1 into the *Leishmania* expression system. 179
Fig 2.4 *In vitro* infection of bone marrow derived macrophages. (BMDM) 181
Fig 2.5 Expression of arginase, iNOS, IL13 & Il10 in infected BMDM by quantitative RT-PCR. 183
Fig 2.6 Macrophage responses to *Leishmania* infection 184
Fig 2.7 Experimental protocol for *In vivo* assessment of Bm-VAL-1 gene function. 185
Fig 2.8 Time course of cutaneous lesion development. 187
Fig 2.9 Mice infected with Bm-VAL transgenic parasites have a higher parasite burden than those infected with wild type *L.mexicana*. 189
Fig 2.10 Immune responses in popliteal lymph node. 191
Fig 2.11 Experimental protocol for *In vivo* assessment of Bm-VAL-1 gene function. 193
Fig 2.12 Time course of Lesion Development. 194
Fig 2.13 Parasites recovered from foot and spleen of infected mice. 196
Fig 2.14 Immune responses in popliteal lymph node. 198
Fig 2.15 Experimental protocol for *In vivo* assessment of Bm-VAL-1 gene function. 200
Fig 2.16 Growth curves of *Leishmania* promastigotes transfected with pSSU, Bm-VAL or Ce-VAL. 202
Fig 2.17 Time course of Lesion Development. 204
Fig 2.18 Parasites recovered from foot and spleen of infected mice. 205
Fig 2.19 Immune responses in popliteal lymph node. 207
Fig 2.20 Experimental protocol for *In vivo* assessment of Bm-VAL-1 gene function. 209
Fig 2.21 Time course of Lesion Development. 210
Fig 2.22 Parasites recovered from foot and spleen of infected mice. 212
Fig 2.23 Immune responses in popliteal lymph node. 213
Fig 2.24 Collated lesion development time course data from *Leishmania in vivo* experiments. 215
Fig 2.25 Collated parasite recovery data from *Leishmania in vivo* experiments. 217
Fig 2.26 Summary of experimental readouts from 4 *in vivo* infection experiments. 219

Chapter 3

Fig 3.1 Immunoregulatory setting induced by the presence of helminths and bacteria. 224

Fig 3.2 Lung tissue and cells that may come into contact with *H.polygyrus* ES in the A.A.I. model. 226
Fig 3.3 Can recombinant HpVALs induce a TH2 response? 229
Fig 3.4 Cytokines produced in response to recombinant VALs are significantly lower than seen in response to HES. 231
Fig 3.5 Profile of cells recruited in response to HES and recombinant VALs. 234
Fig 3.6 Summary of cell types recruited to peritoneal cavity. 235
Fig 3.7 Levels of RELM-α and YM-1 in peritoneal lavage fluid 237
Fig 3.8 Summary of the effects seen upon injection of the peritoneal cavity with HES or VAL proteins. 238
Fig 3.9 Allergic Airway Inflammation model 241
Fig 3.10 Experiment 1: Hp-VAL, a component of HES, reduces cell numbers and eosinophil numbers in BAL fluid in the A.A.I. model. 242
3.11 Analysis of BAL fluid shows a reduction in proportions and absolute numbers of T helper cells after administration of HES and Hp-VAL4. 245
Fig. 3.12 BD Cytometric Bead Array 246
Fig 3.13 (i) An overall reduction in cytokines produced is observed in mice treated with HES and HpVAL-4. 248
Fig 3.13 (ii) An overall reduction in cytokines produced is observed in mice treated with HES and HpVAL-4 (cont'd). 249
Fig 3.14 Levels of OVA specific IgE are reduced with HES treatment but not Hp-VAL4. 252
Fig 3.15 Levels of RELM-α in BAL and lung homogenate are reduced by HES treatment, whereas YM-1 levels appear to increase. 254
Fig 3.16 Differences between treatment groups illustrated by immunohistochemistry. 256
Fig 3.17 Experiment 2: Do other VAL molecules suppress AAI 258
Fig 3.18 Enumeration and characterisation of BAL cells. 260
Fig 3.19 Enumeration and characterisation of lung homogenate cells. 262
Fig 3.20(i) Intracellular cytokine profile of BAL and lung homogenate cells by CBA assay. 265
Fig 3.20 (ii) Intracellular cytokine profile of BAL cells by CBA assay (contd.) 266
Fig 3.20 (iii) Intracellular cytokine profile of BAL cells by CBA assay (contd.) 267
Fig 3.21 Levels of RELM-α in BAL and lung homogenate are reduced by VAL treatment. Conversely, YM-1 levels increase upon treatment with CeVAL. 269
Fig 3.22 Experiment 3: Is the reduction of airway eosinophilia dependent on VAL structure? 271
Fig 3.23 Enumeration and characterisation of BAL cells. 273
Fig 3.24 Experiment 4: Can the initial suppression of AAI by HpVAL be repeated? 275
Fig 3.25 Enumeration and characterisation of BAL cells. 277
Fig 3.26 Pooled data from 4 investigations showing that Hp-VAL4 reduces numbers of eosinophils as seen with HES. 279

Chapter 4
Fig 4.1 The hookworm lifecycle. 286
Fig 4.2 The intestinal epithelial layers. 288

Fig 4.3 Monoclonal antibody binds to carbohydrates on the surface of the parasite. 292
Fig 4.4 Polyclonal α-HES and α- Glycan A antibodies recognise the surface and some internal structures of the parasite. 295
Fig 4.5 Characterisation of antibody binding reveals that monoclonal and polyclonal antibodies, which recognise HpVAL-1 & -4, bind to different structures of the parasite. 299
Fig 4.6 Biotinylated lectins do not bind cuticle carbohydrates. 302
Fig 4.8 Sequential treatments to remove parasite cuticle components: Tween-20 306
Fig 4.9 Sequential treatments to remove parasite cuticle components: Cetyltrimethylammonium cationic detergent (CTAB) 307
Fig 4.10 Tween & CTAB treatment of eggs 308
Fig 4.11 Acetone precipitated parasite cuticle reveals a 62kDa protein which is recognised by α-HES and α-Glycan A antibodies. 310
Fig 4.12 Alexa647 labelled HES binds to the surface of the parasite and to cells recruited to the resulting granuloma. 312
Fig 4.13(i) Alexa647 labeled HES binds to the surface of the parasite throughout an infection time-course. 315
Fig 4.13(ii) Alexa647 labeled HES binds to the surface of the parasite throughout an infection time-course. 316
Fig 4.14 Is the binding of HES to *H.polygyrus* and Paneth cells CD24 dependent? 318
Fig 4.15-i 319
Fig 4.15-ii 320
Fig 4.16-(i) 323
Fig 4.16-(ii) 324
Fig 4.17 Paneth cell binding of HES is heat stabile. 327
Fig 4.18 Cuticle binding of HES in *H.polygyrus* is not antibody mediated. 329
Fig 4.19 Cuticle binding of HES in *H.polygyrus* is not antibody mediated. 330
Fig 4.20 Preparation of intestinal epithelium for whole mount staining. 333
Fig 4.21 Immunostaining of intestinal villi and crypts. 337
Fig 4.22 HES binds to cells on the surface of the villus. 339
Fig 4.23 HES and HpVAL-4 bind to villus goblet cells. 341
Fig 4.24 HpVAL-4, not HpVAL-1, binds intestinal goblet cells. 343
Fig 4.25 Goblet cell structure 344
Fig 4.26 HpVAL-4 and MUC2 binding within the goblet cell. 345
Fig 4.27 Intestinal goblet cells from CD24-/- mice bind HES and HpVAL-4 but not HpVAL-1; Paneth cells bind all three. 348
Fig 4.28 Summary of villi and crypt staining. 350

Final Discussion
Fig D1. Interactions between *H.polygyrus*, intestinal cells, mucus and the microbiota. 360

List of Tables

Introduction
Table 1: Immunomodulatory molecules 26

Materials and Methods
Table 1: PCR Programmes. 69
Table 3: Immunohistochemistry Antibodies and Reagents 85
Table 4: Insect Cell Lines 86
Table 5. Insect Cell Line Freezing Media 88
Table 6: Cytokine ELISA Antibodies 93
Table 7: Flow cytometry Antibodies 97
Table 8: Primers 100
Table 9: Vector Table 106

Chapter 1
Table 1.2 Identity shared between VAL proteins and HpVAL-1 126
Table 1.3 Amino acid identities shared between VAL proteins and Ves v5. 133
Table 1.4 Codon usages for serine. 137
Table 1.5 Genes required for efficient RNAi processing. 163

Chapter 2
Table 2.1 178

Chapter 3
Table 3.1 Antibody responses throughout A.A.I model in response to either H.polygyrus infection or treatment with HES. 250
Table 3.2 Summary of CBA cytokine data 264

Chapter 4
Table 4.1 297
Table 4.2 300
Table 4.3 Murine intestinal cell types. 334
Table 4.4 Antibodies and fluorescent conjugates for confocal microscopy on VCP tissue. 336

Introduction

Helminths

The phrase "helminth parasite" covers a vast and complex group of organisms, which fall into two major phyla: the **Platyhelminths**, which are further segregated into cestodes and trematodes and the **Nematodes** (http://parasite.org.au/para-site/contents/helminth-intoduction.html). These organisms are estimated to infect over a billion people worldwide with the majority of those infected living in sub-Saharan Africa, Asia, and the Americas (Fig 1.) (Lustigman et al., 2012). Diseases such as ascariasis (caused by soil-tramsmitted helminths such as *Ascaris lumbricoides*), onchocerciasis (caused by *Onchocerca volvulus*), schistosomiasis (caused by *Schistosoma mansoni* and *Schistosoma haematobium*) and lymphatic filariasis (caused by *Wuchereria bancrofti, Brugia malayi* and *Brugia timori*) cause wide ranging disabilities such as diarrhoea and dysentery (Organization, 2014d), blindness (Organization, 2014b), anaemia and malnutrition (Organization, 2014c) and lymphoedema (tissue swelling) or elephantiasis (Organization, 2014a) respectively. Each disease has major socio-economic implications with individuals rendered unable to thrive due to malnutrition, unable to work due to physical symptoms of disease and the young often displaying reduced cognitive development with subsequently reduced educational results. Apart from the initial disease related symptoms, individuals often suffer accentuated effects from co-infections such as malaria (Mulu et al., 2013), however co-infection studies focusing on helminths and HIV indicated no increase in viral load or disease progression (Brown et al., 2004).

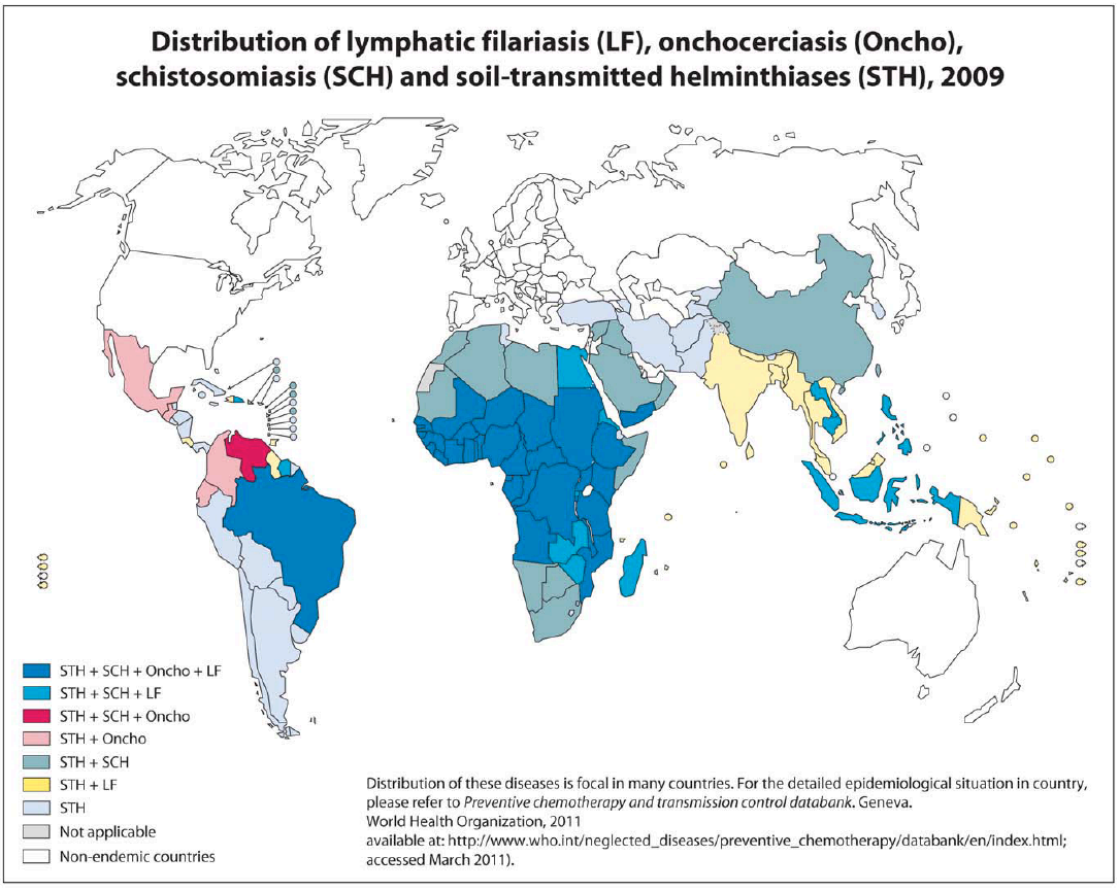

Fig 1. Global distribution of helminth infection (World Health Organisation).

Members of both the platyhelminths and the nematodes share the ability to reside within the host for extended periods of time, in some cases for as long as a decade. The size of the organism involved precludes them from hiding from immune attack within host cells, as a *Leishmania* parasite would by residing in a host macrophage. Thus these complex, multi-cellular organisms must find alternative methods to avoid expulsion by the host.

Immune evasion: Concept and strategies.

The ability of parasites to inhabit a host for lengthy periods of time presents many interesting questions. Does the host mount an immune response, which ultimately fails? Does the parasite cause the failure of such a response? Or, does the host ignore the presence of the parasite, instead choosing a path of cohabitation, which may or may not eventually lead to immunopathology, as observed in filarial infections that affect the lymphatics (Babu & Nutman, 2012). If cohabitation is the immunological outcome, was this route driven by the parasite itself?

Different mechanisms are employed by the parasite depending on the nature of its lifecycle. Evasion of an immune response may result in a parasite hiding in areas of the host, which are poorly protected by immune cells such as the eye or the brain in a *Toxoplasma gondii* infection (Bhopale, 2003). The invasion of a specialised immune cell such as a macrophage may seem reckless, however this is precisely the mechanism used by *Leishmania*, *Toxoplasma* and *Tyrpanosoma cruzi* to avoid expulsion by the host (Bloom, 1979). One of the most exquisite methods of immune evasion, antigenic variation, is demonstrated by African trypanosomes (Pays, Vanhamme, & Perez-Morga, 2004), (Stockdale, Swiderski, Barry, & McCulloch, 2008). *Trypanosoma brucei* displays around 10^7 variant surface glycoproteins (VSG) on its surface. As a host generates antibodies directed against the VSG molecules, the parasite has already generated a new population with a different suite of VSG molecules on their surface, thus allowing them to avoid anti-VSG killing. This is achieved with the help of a set of genes, which code for antigenically distinct surface antigens. The parasite must have the ability to express these one at a time and be able

to change expression profiles between the variant. Depending on the parasite, two methods for achieving this are employed. *Giardia lamblia* (Prucca & Lujan, 2009) and *Plasmodium falciparum* (Scherf, Lopez-Rubio, & Riviere, 2008) use transcriptional mechanisms to either express or silence the gene required for the expression of a particular VSG, whereas *Neisseria* species utilise a method of recombination to ensure antigenic immune avoidance (Mehr & Seifert, 1998). Another method that many parasites employ to evade immune detection involves a period of dormancy during their life cycle, which enables them to remain undetected by the host immune system. *Plasmodium* sporozoites have been described as having a quiescent stage, the hypnozoite, which can reside within the liver for many months without detection (Gomes-Santos et al., 2011), (Markus, 2011), (Dembele et al., 2014).

The methods detailed above can help the parasite avoid detection, however these are all **passive** tactics which alone would be unable to achieve the long-lived evasion attained by some parasites. In a recent review by McNeilly and Nisbet (McNeilly & Nisbet, 2014), immunomodulatory mechanisms employed by parasites are discussed with implications for future vaccine developments being outlined. This review detailed mechanisms and molecules employed and produced by parasites and described how these interfere with host immunity e.g. *Fasciola hepatica (F.hepatica),* a ruminant trematode, drives host immune responses towards Th2. This is beneficial for the parasite as its survival is dependent on a failing host protective Th1 response. Molecules found in the excretory/secretory products from *F.hepatica* such as apyrases, galectins and MIFs are discussed. These can be **actively** produced and complement the passive strategies employed by parasites and allow further immune evasion (Table 1). Similar excretory/secretory products produced by *Heligmosomoides polygyrus* and *Brugia* malayi and their ability to influence immune responses will be examined in Chapters 2, 3 and 4, where interactions between host cells such as macrophages, eosinophils and goblet cells will be examined. These molecules, which from part of parasite's excretory/secretory repertoire, may block or modulate host immune responses or have direct effects upon host immune cell

functions (Lightowlers & Rickard, 1988). A selection of molecular candidates is discussed below.

Molecule family	Function	Molecule and parasite	Reference
Protease inhibitors	Interference with Ag processing	Bm-CPI-2, *Brugia malayi*	Manoury et al, 2001
		Onchocystatin, *Onchocerca volvulus* *Acanthocheilonema viteae* cystatin *Acanthocheilonema viteae* cystatin	Schonemeyer et al, 2001 Schnoeller et al, 2008 Figueiredo et al, 2009
		Nippocystatin, *Nippostrongylus brasiliensis*	Dainichi et al, 2001
	Immunomodulation	Bm-SPN-2, *Brugia malayi*	Zang et al, 1999
		TvSERP, *Trichostrongylus vitrinus*	MacLennan et al, 2005
Cytokine mimics	Immune response interference by parasite derived homologues of host cytokines	Bm-tgh-1, *Brugia malayi*	Gomez-Escobar et al, 1998
		Bp-trk-1, *Brugia pahangi*	Gomez-Escobar et al, 1997
		Bm-MIF-1, *Brugia malayi*	Pastrana et al, 1998
		Bm-MIF-2, *Brugia malayi*	Zang et al, 2002
		Ts-MIF, Trichinella spiralis	Pennock et al, 1998
Prominent ES proteins	Various immunomodulatory properties	Bm-VAL-1, *Brugia malayi*	Murray et al, 2001
		Ac-ASP-2, *Ancylostoma caninum*	Hawdon et al, 1999
		Na-ASP-2, *Necator americanus*	Goud et al, 2005
		Bm-ALT, *Brugia malayi* Ov-alt-1, *Onchocerca volvulus* Av18, *Acanthocheilonema viteae*	Gomez-Escobar et al, 2005 Joseph et al, 1998 Pogonka et al, 1999
		Tci-APY-1, *Teladorsagia circumcincta*	Nisbet et al, 2011

Table 1: Immunomodulatory molecules

Cystatins: Bm-CPI-2

Cysteine protease inhibitors (cystatins) have been described in a number of parasites such as *O.volvulus* (Schonemeyer et al., 2001), *Nippostrongylus brasiliensis* (Dainichi et al., 2001) and *B.malayi* (Manoury et al., 2001). Given their homology to mammalian cystatins, which have been shown to be involved in regulation of the MHC class II pathway (Watts, 2001), it was not surprising to discover that the *B.malayi* cystatin, Bm-CPI-2, also blocked the presentation of antigenic peptides in this manner (Manoury et al., 2001). Cystatins are notable by the fact they can contain two inhibitory sites: 1) for the inhibition of cysteine proteases such as papain, and a second site, 2) for the inhibition of asparaginyl endopeptidase (AEP). Not all cystatins contain this second inhibitory site and if they do it may not necessarily be functional. As mentioned above the *B.malayi* cystatin, Bm-CPI-2, was capable of inhibiting cysteine protease. Furthermore it also contains a functional AEP site as demonstrated by its ability to inhibit the processing of the tetanus toxin C fragment (Manoury et al., 2001). Site-directed mutagenesis of the AEP sequence ablated this activity but had a minimal effect on papain processing (Murray, Manoury, Balic, Watts, & Maizels, 2005).

Interestingly the free-living nematode *Caenorhabditis elegans* (*C.elegans*) also has sequence similarities indicating putative inhibitory sites, however when tested it was only able to process the Cathepsin S substrate and had no effect on the AEP substrate. Sequence similarities have been described between other filarial cystatins including *O.volvulus* (Lustigman, Brotman, Huima, Prince, & McKerrow, 1992), *Acanthocheilonema viteae* (Hartmann, Kyewski, Sonnenburg, & Lucius, 1997) and *Litomosoides sigmodontis* (Pfaff et al., 2002), identifying putative AEP sites and addressing the possible immunomodulatory roles these molecules could play.

More recently, Whelan et al described a genetically modified bacterium (*Escherichia coli* Nissle 1917), altered to secrete a cystatin from *Acanthocheilonema viteae*, which decreased intestinal inflammation in a murine model of colitis and in post-weaning pigs (Whelan et al., 2014).

Cytokine mimics: Macrophage-migration inhibition factors (MIFs)

Released as a soluble factor from activated lymphocytes, macrophage-migration inhibitory factor was one of the first immune system cytokines to be defined. Its ability to inhibit the migration of macrophages was first described and this has become the accepted way to refer to the molecule (Bloom & Bennett, 1966). Interestingly, in the intervening years, many more functions have been attributed to MIF and additionally, expression patterns for MIF have been described in most parts of the body (eyes, ears, brain, spleen, kidneys and skin), but particularly by epithelial cells (Maaser, Eckmann, Paesold, Kim, & Kagnoff, 2002) and tissues that come into direct contact with the host's natural environment (Fig 2) (Calandra & Roger, 2003). Being expressed by so many tissues it therefore follows that a large range of different cell types also express MIF such as B cells, macrophages, monocytes, blood dendritic cells, neutrophils, eosinophils, mast cells and basophils (Lue, Kleemann, Calandra, Roger, & Bernhagen, 2002), (Bernhagen, Calandra, & Bucala, 1998). Analysis of the biochemical qualities possessed by MIF reveals the absence of a signal peptide (Swope, Sun, Blake, & Lolis, 1998), and shows the presence of two sites of enzymatic activity, specifically a tautomerase site (Rosengren et al., 1996), (Lubetsky, Swope, Dealwis, Blake, & Lolis, 1999) and an oxidoreductase site (Kleemann et al., 1998).

Largely designated as a pro inflammatory cytokine, MIF was found to stimulate the release of IL-6, IL-8 and TNF-α *in vitro* accompanied by the secretion of endogenous MIF from human monocytes or mouse macrophages. Moreover MIF was found to synergize with lipopolysaccharide (LPS), consequently accentuating toxic shock (Bernhagen et al., 1993). Interestingly, MIF-/- mice survived after they had been administered with, what would normally be considered a lethal dose of LPS (Bozza et al., 1999). A further demonstration of the requirement of MIF to maintain an inflammatory situation was described by de Jong et al, whereby MIF -/- mice failed to develop experimental colitis (de Jong et al., 2001). MIF -/- mice also do not develop allergic asthma after sensitization and challenge with ovalbumin (Magalhaes et al., 2007). The absence of MIF renders mice more susceptible to protozoan

infections such as *Leishmania major* (Satoskar, Bozza, Rodriguez Sosa, Lin, & David, 2001) and *Toxoplasma gondii* (Terrazas et al., 2010) and also reduces eosinophilia in *Schistosoma mansoni* infection whilst having no direct effect on the Th2 response mounted against the infection (Magalhaes et al., 2009).

Cytokine mimics: TGF-β

The TGF-β superfamily encompasses a large group of cytokines, which have a range of functional properties beyond those involved in immune regulation, with roles described amongst others for the nervous system (Bottner, Krieglstein, & Unsicker, 2000), the respiratory system (Kunzmann, Collins, Kuypers, & Kramer, 2013) and the digestive system (Ruemmele & Garnier-Lengline, 2013). The effects that TGF-β can exert on the immune system can be both stimulatory and inhibitory, with many cell types being influenced by this powerful cytokine (Yoshimura & Muto, 2011). The most profound effect is to be observed on T cells where proliferation, differentation and survival are all influenced (Gorelik & Flavell, 2002). B cell proliferation is also influenced by TGF-β along with the induction of apoptosis of immature and resting B cells(Stavnezer, 1995).

TGF-β also influences many other cells of the immune system such as dendritic cells (DCs), macrophages, mast cells and granulocytes. Dendritic cell maturation has been shown to be regulated by TGF-β in both human and murine studies where DCs generated in the presence of TGF-β exhibit an immature phenotype(Ronger-Savle et al., 2005), (Yamaguchi, 1998). Antigen presentation *in vitro* by mature DCs is also regulated by TGF-β as shown by Geissmann et al (Geissmann et al., 1999) where DCs cultured with lipopolysaccharide (LPS) and TGF-β failed to express MHC class II and related costimulaory molecules. Interestingly TGF-β is expressed by immature bone marrow-derived DCs although the reason for this remains unclear (Morelli et al., 2001). TGF-β also exerts pro and anti-inflammatory qualities over monocytes and macrophages respectively. By acting as a chemoattractant TGF-β can recruit monocytes to a site of injury. This recruitment and migration can also occur upon

TGF-β induced production of matrix metalloproteinases (Wahl et al., 1987), (Wahl, Allen, Weeks, Wong, & Klotman, 1993).

Macrophage phagocytosis, activation and presentation are all affected by TGF-β. Phagocytosis is downregulated by a lowering of expression of the two IgG receptors FcγRI and FcγRIII (Tridandapani et al., 2003) whilst macrophage activation is regulated by TGF-β inhibition of inflammatory mediators such as TNF-α and MMP-12 (Werner et al., 2000). Antigen presentation by macrophages is also affected by TGF-β in two ways. Primarily, TGF-β inhibits the expression of MHC class II molecules on the macrophage along with the inhibition of expression of CD40 and IL12p40 (Nandan & Reiner, 1997),(Takeuchi, Alard, & Streilein, 1998),(Du & Sriram, 1998). Like dendritic cells, macrophages can also produce TGF-β. This can occur, for example, following uptake of mycobacteria. A macrophage will produce TGF-β which results in the suppression of macrophage antibacterial activity thus aiding the survival of the bacteria (Dahl, Shiratsuchi, Hamilton, Ellner, & Toossi, 1996).

Mast cells release effector molecules such as histamines and proteases as well as TNF-α in response to allergens or to protect a host from parasitic diseases. This release occurs after their recruitment which is driven by TGF-β (Gruber, Marchese, & Kew, 1994). Activation of mast cells occurs when IgE binds to the FcεR receptor, expression of which can be reduced by TGF-β (Gomez et al., 2005). TGF-β is also capable of recruiting granulocytes to a site of infection, whilst at the same time exhibiting downregulatory properties on endothelial IL-8, which is also capable of granulocyte attraction (Reibman et al., 1991). Whether or not TGF-β can influence the regulation of granulocyte acitvation and granulocitic effects reamins unclear (Balazovich, Fernandez, Hinkovska-Galcheva, Suchard, & Boxer, 1996).

TGF-β and parasites.

Many parasites including *B.malayi* and *Brugia pahangi* (Gomez-Escobar et al., 1997), (Gomez-Escobar et al., 1998), *Heligmosomoides polygyrus* (McSorley et al., 2012), *S.mansoni* (Davies, Shoemaker, & Pearce, 1998)and *O.volvulus* (Korten et al., 2009) all express either a TGF-β mimic or a receptor (Gomez-Escobar et al., 1997).

The case for parasites producing TGF-β-like molecules in their excretory-secretory (ES) products is elegantly posed by Graniger et al (Grainger et al., 2010), who demonstrated that the ES products from *H.polygyrus* contained TGF-β activity which acted directly on T cells generating a population of $Foxp3^+$ T regulatory cells, which may hamper the host immune response.

Prominent ES molecules: Abundant larval transcripts (ALTs)

Elements secreted by parasites are often examined for their ability to help the parasite evade the host immune responses. One factor, which is also important when examining ES proteins, is the life cycle stage of the parasite that expressed the gene to produce the particular protein. Often proteins produced when a parasite is infective are studied as they may be required to interact with the host immune reply to its presence. One such molecule is the **A**bundant **L**arval **T**ranscript (ALT). Described by Gregory et al, (Gregory, Blaxter, & Maizels, 1997), (Gregory, Atmadja, Allen, & Maizels, 2000) and Gomez-Escobar et al, (Gomez-Escobar et al., 2005) this molecule is highly expressed by the infective larval stage of the parasite *B.malayi* (Fig 3) and was shown to amplify Th2 responses following *in vitro* infection of macrophages with transgenic, Bm-ALT expressing *Leishmania* parasites. Similar molecules have been described from *O.volvulus* (Joseph et al., 1998), *L.sigmodontis* (Allen et al., 2000), *Dirofilaria immitis* (Frank et al., 1999) and *A.viteae* (Pogonka et al., 1999), all expressing the ALT-like proteins in their infective L3 stage.

Antibodies from *O.volvulus* infected patients recognised the Ov-alt-1 recombinant protein by enzyme linked immunosorbent assay (ELISA), with 88% of putatively immune and 95% of infected individuals responding (Joseph et al., 1998). When jirds were vaccinated with recombinant Bm-alt-1, reductions in parasite burden were reported at 76% (Gregory et al., 2000).

Other highly produced molecules, which are present in the ES products of parasites, include apyrases (Nisbet et al., 2011), serpins (Zang et al., 1999), calreticulin (Ramirez et al., 2012), IPSE/alpha1 (Schramm et al., 2007) and galectins (Kim et al., 2010). These are all potential immunomodulators, which either alone or in combination with other factors assist the parasites in its endeavours to remain within the host.

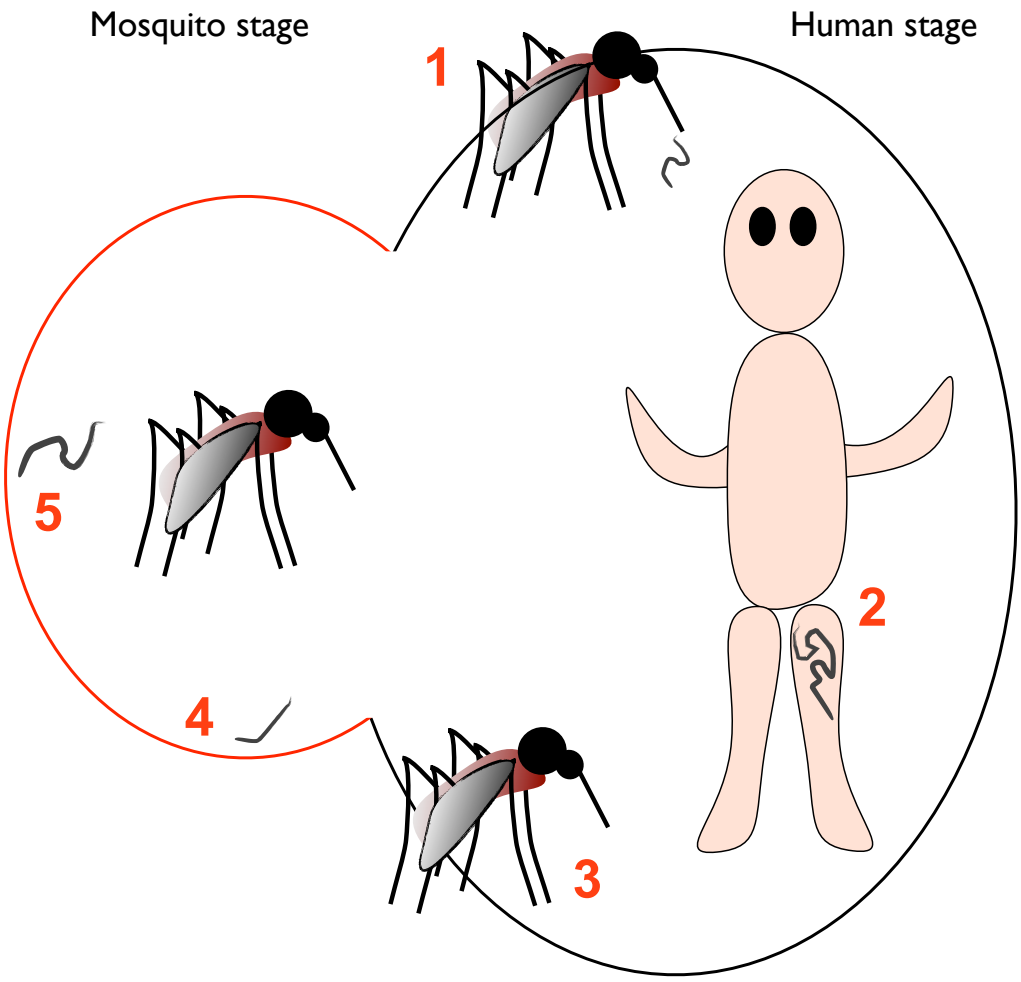

Fig 2. *Brugia malayi* life cycle

1. Infected adult mosquitos feed on individual thus allowing infective L3 larvae to enter a new host.
2. Adult male and female parasites migrate to the lymphatic system.
3. Sheathed microfilariae are produced by adult in blood stream where they can be transmitted to mosquitoes during a blood meal.
4. Microfilariae then exsheath, penetrate the mosquito midgut and migrate to thoracic muscles as L1 larvae.
5. Larvae moult from L1 stage to infective L3 stage and migrate to mosquito head and proboscis where they can be transmitted during the next blood meal.

Parasite excretory secretory products

Many parasites secrete a cocktail of molecules throughout their lifecycle, which have become the focus of immunologists interested in host-parasite interactions. The excretory secretory (ES) products of parasites will be in contact with many of the host tissues and cells and as such may affect the host responses and subsequent immunological reactions. As such they are increasingly looked to for potential immune mediators, vaccine candidates and therapeutic drugs (El Ridi & Tallima, 2013), (Bahlool, Skovgaard, Kania, & Buchmann, 2013), (El Ridi & Tallima, 2009).

To further elucidate the potential of ES products that may influence damaging host immune responses, often the infective larval stage of a parasite is the target, as it is this stage that will encounter the full force of the host immune reaction. Thus, many studies of ES products now separate the life cycle stages and examine each independently (Hewitson et al., 2011b), (Cui et al., 2013b), (Butter et al., 2013). Proteome and secretome information coupled with genomic and transcriptomic data is proving to be a very powerful resource (Aebischer, 2014), (Thompson & Monis, 2012).

****

All of the discussed immune evasion molecules are present in the excretory/secretory products from *H.polygyrus* thus it is possible that this parasite may utilise one or more of these products in order to manipulate the host immune response to ensure its survival. Experiments discussed throughout this thesis aim to examine this possibility.

Host targets: Cells and tissues

As the parasite enters the host it is accompanied by an entourage of molecules and modulators, some of which have been discussed above. Each parasite and each modulatory molecule will have interactions with specific cells and tissues of the host immune system. I will now discuss some of these cells and tissues, which are directly involved in the interactions described later in this thesis. Fig 3 illustrates cells that are involved in the innate and adaptive immune responses.

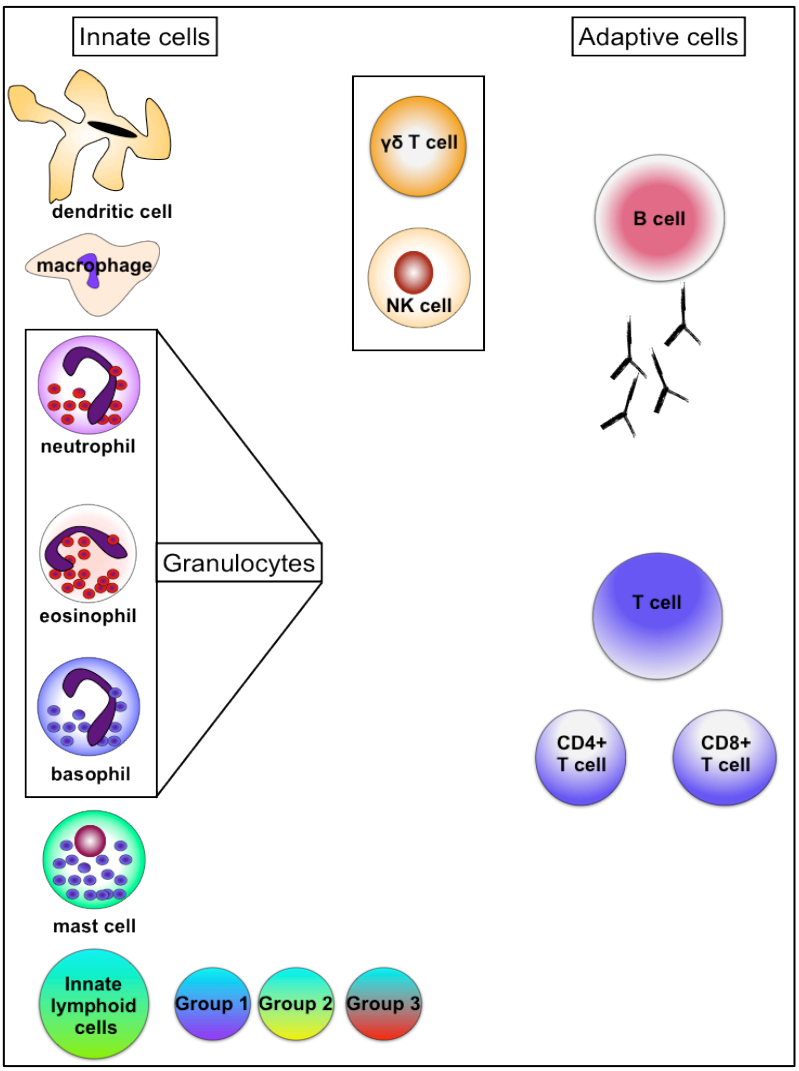

Fig 3. Cells of the innate and adaptive immune system.
Illustrations of cells involved in the innate and adaptive immune repsonses will be used throughout this chapter.

Macrophages.

Derived from bone marrow precursors, macrophages are one of the first lines of defence against invading pathogens. Their method of dispensing with microbes depends first upon detection and subsequent phagocytosis. Recognition of pathogens is facilitated via a range of pathogen recognition receptors (PRRs) (Dale, Boxer, & Liles, 2008), (Erwig & Henson, 2007). Depending upon the stimulus received by the macrophage its fate lies in one of two directions: classically activated or alternatively activated (also termed M1 and M2 macrophages respectively) (Mege, Mehraj, & Capo, 2011), (Benoit, Desnues, & Mege, 2008). This polarisation of macrophages is illustrated in Fig 4. As a cell type involved in the immune response during infection with *Leishmania*, macrophages will be closely examined throughout Chapter 2.

Classically activated macrophages (CAM): Stimulation with interferon-γ (IFNγ) from Th1 and NK cells and tumour necrosis factor (TNF) from antigen presenting cells gives rise to classically activated macrophages. Indeed mice lacking IFNγ expression are more susceptible to various bacterial infections (Filipe-Santos et al., 2006). Classically activated macrophages have augmented microbial properties and secrete high levels of pro-inflammatory cytokines such as IL-1, IL-6 and IL-23, which if left unchecked can lead to host tissue damage leading to the immunopathology as observed in rheumatoid arthritis (Langrish et al., 2005), (Veldhoen, Hocking, Atkins, Locksley, & Stockinger, 2006), (Szekanecz & Koch, 2007) and inflammatory bowel disease (Zhang & Mosser, 2008). Indicators of classically activated macrophages include IL-12, iNOS, CCL15, CCL20, CXCL9, CXCL10 and CXCL11 (Mosser & Edwards, 2008).

Alternatively activated macrophages (AAM): Production of IL-4 and IL-13 by $CD4^+$ T cells results in a population of macrophages termed **A**lternatively **A**ctivated **M**acrophages (AAM), which are a characteristic cell type described in helminth infection settings (Stein, Keshav, Harris, & Gordon, 1992), (Jenkins & Allen, 2010). Other sources of IL-4 include basophils and mast cells with other granulocytes potentially contributing (Brandt, Woerly, Younes, Loiseau, & Capron, 2000). Additionally IL-21/ IL-21R and IL-33/ST2 are involved in activation of AAMs

(Frohlich et al., 2007). As well as a key role in immunity tohelminths, alternatively activated macrophages have been implicated in wound healing due to the high levels of arginase secreted which converts arginine to ornithine. Ornithine is a precursor of polyamines and collagen, both components required for production of the extracellular matrix (Kreider, Anthony, Urban, & Gause, 2007). Proteins expressed by alternatively activated macrophages include the mannose receptor, Arginase1, RELMα and YM-1 (Stein et al., 1992). The role of alternatively activated macrophages in a helminth infection setting has been extensively researched. During infection with *Nippostrongylus brasiliensis*, AAMs proved essential for worm expulsion (Zhao et al., 2008) a situation also seen in *Heligmosomoides polygyrus* infection settings (Anthony et al., 2006).

Key proteins expressed by AAMs are Arginase, RELMα and YM-1.
Arginase: converts arginine to ornithine thus aiding tissue repair. Anti-inflammatory and host protective properties were described following reduced intestinal inflammation that normally occurs due to egg production from *Schistosoma mansoni* (Pesce et al., 2009a).
RELMα: also expressed by eosinophils and epithelial cells, RELMα was originally described in allergen-induced pulmonary inflammation where it was designated FIZZ1 (Holcomb et al., 2000) (found in inflammatory zone). During helminth infection RELMα had a negative regulatory effect on Th2 immune repsonses suppressing resistance to nematode infections (Pesce et al., 2009b).
YM-1: chitin binding protein with no chitinase activity. Shown to have potent chemotactic properties for eosinophils (Owhashi, Arita, & Hayai, 2000), Ym1 may be involved in the enhancement of host effector responses by mediating eosinophil recruitment.

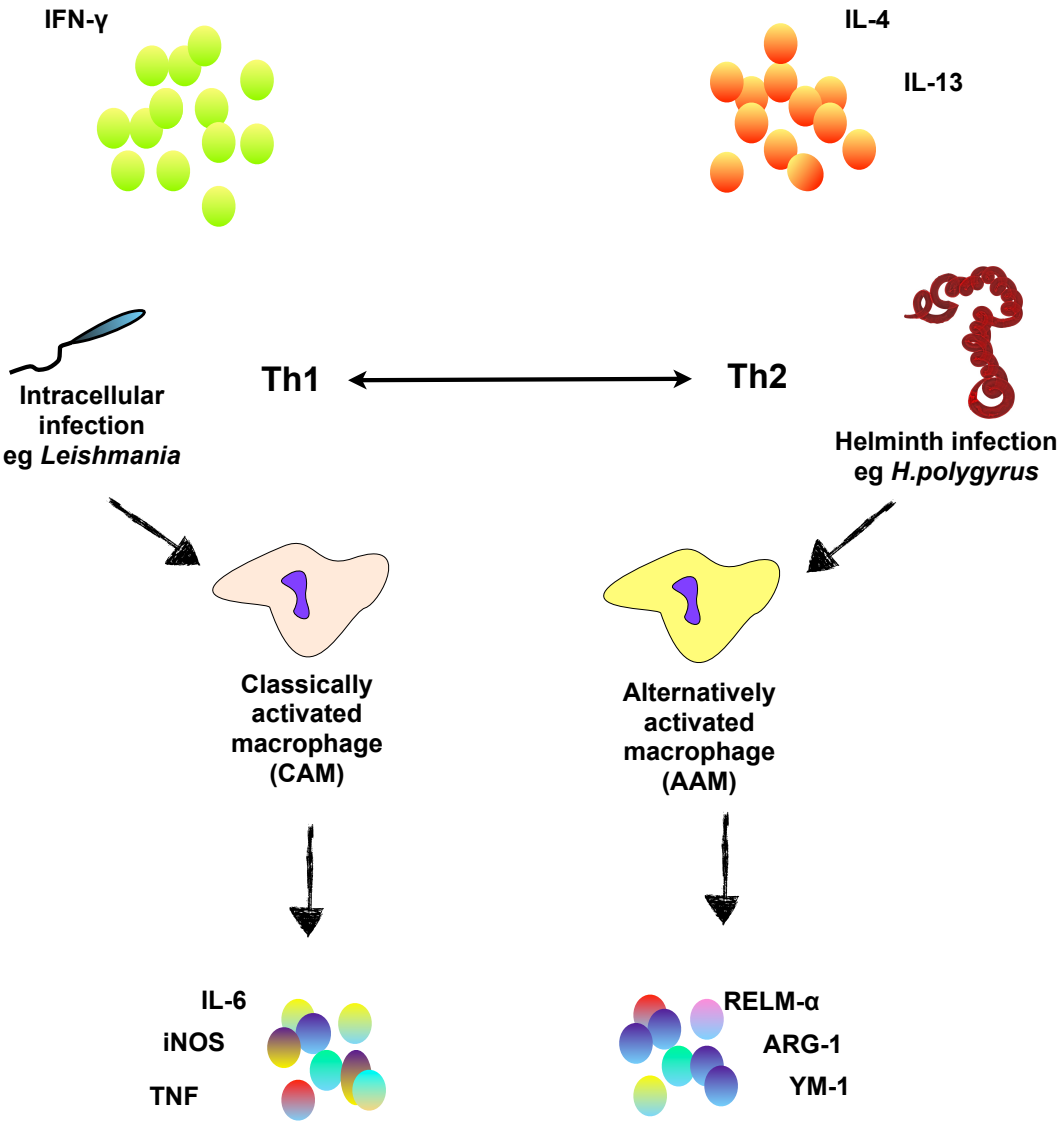

Fig 4. Polarisation of macrophages during infection.
Macrophages become polarised to either a **classically** activated or an **alternatively** activated phenotype depending upon the stimulus they receive. Classical activation occurs during infection with bacteria or intracellular parasites and results in the production of IL-6, iNOS and TNF. Alternative activation occurs during infection with helminth parasites and induces the production of RELM-α, ARG-1 and YM-1.

Dendritic cells.

Dendritic cells could be referred to as the sentinels of the immune system due to their locale and function. Situated throughout the body, they are located close to epithelial cells where they are able to capture, process and present antigens to T cells. Various receptor groups facilitate antigen detection (toll-like receptor, C-type lectin receptor, NOD-like receptor, RIG-like receptor). Dendritic cell activation generally consists of the up regulation of a suite of costimulatory molecules (CD40, CD80 and CD86) and cytokines (IL-12, IL-6, Il-23 and TNF) (Kapsenberg, 2003). Known as "classical activation" of dendritic cells, this generally fails to occur during helminth infections (MacDonald & Maizels, 2008), (White & Artavanis-Tsakonas, 2012). Dendritic cells exposed to the excretory/secretory products from *S.mansoni* (SEA) (Perona-Wright, Jenkins, & MacDonald, 2006) or *A.viteae* (Whelan et al., 2000) do not respond as described above, yet induction of the Th2 response still occurs. However, Balic et al showed that stimulation of DCs with *N.brasiliensis* (NES) up-regulated CD86 and OX40Ligand, and stimulated DCs to produce IL-6 and IL12p40, all indicators of DC maturation (Balic, Harcus, Holland, & Maizels, 2004). Moreover, these activation signals could not be detected from DCs pulsed with heat-inactivated NES suggesting that a soluble protein present in NES be responsible for DC activation. Whereas protein moieties are often implicated in DC responses, it has been shown that carbohydrates present in parasite excretory/secretory products of *H.polygyrus* and *N.brasiliensis* are able to induce a Th2 response in BMDCs (Massacand et al., 2009), (White & Artavanis-Tsakonas, 2012). Once activated DCs then present Ag peptides to $CD4^+$ T helper cells. Given their distribution throughout different tissues, it must be considered that DCs in varying locations will display different suites of activation markers and subsequent Th2 inducing signals. This enables DCs to respond in the most appropriate manner to the stimuli they encounter.

Granulocytes: Neutrophils, eosinophils and basophils.

Generated from hematopoetic stem cells, granulocytes are differentiated from other leukocytes by the presence of a segmented nucleus and numerous secretory granules in the surrounding cytoplasm. Release of the contents of these granules is considered to play a role in innate and adaptive immunity (Sorci & Faivre, 2009), however if

these cells remain unregulated then tissue damage and immunopathology may occur as seen in cases of asthma (Shamri, Xenakis, & Spencer, 2011).

Neutrophils: Comprising over 50% of human white blood cells, neutrophils are crucial, primary responders during inflammation where they can eliminate foreign microorganisms by phagocytosis (Mantovani, Cassatella, Costantini, & Jaillon, 2011). During *Leishmania* infection neutrophils are the first cell to be recruited to the initial site of infection (Tkalcevic et al., 2000) and this influx of neutrophils occurs if parasites have been delivered into the host by the bite of a sand fly or the use of a laboratory needle. Recruitment to the site of infection may occur in response to tissue damage and the need for tissue repair but is also driven in response to the actual sand fly bite, the saliva injected with the parasites and the infectious status of the parasites (Peters et al., 2008), (Ribeiro-Gomes, Peters, Debrabant, & Sacks, 2012).
The innate immune response observed during *Strongyloides stercoralis* is also characterized by the early recruitment of neutrophils. Accompanied by macrophages and eosinophils parasites are met by the release of granular components from these cells. Indeed, removal of neutrophils and eosinophils from naïve mice using a αGr-1 antibody resulted in an increase in parasite survival (O'Connell et al., 2011).
During an infection with *H.polygyrus*, once more, neutrophils and eosinophils are recruited into the mucosa and submucosa of the mouse intestinal epithelium (Liu, Cypess, & van Zandt, 1974) with neutrophils accumulating around the parasite before the appearance of DCs, AAMs, T cells and eosinophils (Morimoto et al., 2004). These responses however are more likely to play a complimentary role to type-2 responses, such as mucus production, than stand alone as potent immune challenges.

Eosinophils: Originating from $CD34^+$ cells in the bone marrow and maturing under the control of IL-5, IL-3 and GM-CSF, eosinophils are characterized by a segmented nucleus, which is surrounded by granules containing Charcot-Leyden Crystal protein (CLC, galectin 10), major basic protein (MBP), eosinophil cationic protein (ECP), eosinophil peroxidase (EPO) and eosinophil neurotoxin (EDN)(Dvorak & Weller, 2000). Eosinophils can be detected predominantly in the gastrointestinal tract,

thymus and mammary glands however they can accumulate causing eosinophilia during certain infections and allergic conditions. During helminth infection eosinophils were shown to bind to various life-cycle stages of *H.polygyrus*, indeed binding of the eosinophils to the parasite was antibody mediated and was mainly directed at the infective larval stage (Penttila, Ey, & Jenkin, 1983). Eosinophil binding to the filarial parasite *Brugia malayi* was also observed by Hamann et al, (Hamann et al., 1990). Eosinophils have likewise been shown to adhere to *S.mansoni*, *Trichinella spiralis* and *N.brasiliensis* with resultant degranulation and expulsion of the granule contents however little damage appears to be inflicted upon the parasites irrespective of the life cycle stage involved (McLaren, Mackenzie, & Ramalho-Pinto, 1977), (Shin, Lee, & Min, 2009). Responding to this attack, it has been demonstrated that excretory/secretory products from *H.polygyrus* can reduce levels of IFNγ and IL-12 and concurrently reduce levels of eosinophilia (Rzepecka, Donskow-Schmelter, & Doligalska, 2007), (Hogan et al., 2008). The effect of helminth infection on eosinophil recruitment during a laboratory model of asthma was examined by Wilson(Wilson et al., 2005) et al, where they showed that eosinophil numbers were reduced in the presence of an infection with *H.polygyrus*. Subsequent investigations by McSorley et al noted that this reduction in eosinophil numbers did not require the presence of the parasite but could be achieved using the excretory/secretory products from the parasite alone (McSorley et al., 2012). In Chapter 3 the allergic airway inflammation model will be examined using a single, highly expressed molecule that is secreted by *H.polygyrus*.

Basophils: Forming less than 1% of the total leukocyte population, basophils are comparatively rare and as such have been overlooked to a certain degree. Circulating in the blood they respond to IL-3 and thymic stromal lymphopoietin (TSLP) in order to activate, expand and survive (Lantz et al., 1998), (Siracusa et al., 2011). Granules located within the basophil contain leukotriene C4, histamine and the cytokines IL-4 and IL-13, which are released upon ligation via the IgE binding FcεRI (Sullivan & Locksley, 2009). It has been proposed that basophil activation may occur in response to some parasite products. Human basophils became activated, *in vitro,* upon

stimulation with purified protoscolices or metacestodes from the platyhelminth *Echinococcus multilocularis*, resulting in the release of IL-4, IL-13 and degranulation of the mast cell (Aumuller et al., 2004). Similarly, basophils which were isolated from naïve human donors, were incubated with *Schistosoma mansoni* egg antigen (SEA) in the presence of IL-3. This resulted in the release of IL-4 and was accompanied by degranulation of the mast cell causing the discharge of their granular contents (Falcone et al., 1996). These studies were however all carried out *in vitro* and when patient records were examined from individuals infected with a range of parasitic diseases, both helminthic and protozoan, minimal evidence (0.6%) of basophilia was recorded (Mitre & Nutman, 2003). It may be that helminth products, such as the glycoproteins described form *Scistosoma mansoni* (Haisch et al., 2001), can induce the activation of basophils but are not able to encourage proliferation.

Mast cells. The long-lived mast cell (weeks-months) shares many properties with their bone marrow derived cousins the basophils. Both have a multi-lobed nucleus, which is surrounded by cytoplasmic granules; express the high-affinity IgE receptor Fc**e**R1 and both are capable of histamine release. Mast cells however exit the bone marrow as progenitors and complete their maturation in the tissues. Granules in the mast cell, containing proteases, histamines, proteoglycans and cytokines can be released in one of two manners. Anaphylactic degranulation involves all granular contents being released simultaneously whereas piecemeal degranulation describes a more gradual and slow release of granules (Crivellato, Nico, Mallardi, Beltrami, & Ribatti, 2003).

During an *H.polygyrus* helminth infection mast cells infiltrate the mucosa and submucosa (Liu et al., 1974) along with neutrophils and eosinophils. The role of mast cells during the expulsion of parasites varies depending on the infection. During infection with *T.spiralis* or *Strongyloides venezuelensis* mast cell hyperplasia is observed and expulsion of the parasites is mast cell dependent (Knight, Wright, Lawrence, Paterson, & Miller, 2000), (Lantz et al., 1998). However, no significant role has been attributed to mast cells during *N.brasiliensis* or *H.polygyrus* infections (Crowle & Reed, 1981), (Anthony, Rutitzky, Urban, Stadecker, & Gause, 2007).

T Cells

T cell biology is a vast and complicated arm of immunology. Here, I will briefly outline T cell polarisation mechanisms, the effects of parasitic infections and the implications of parasitic immunomodulatory factors.

Naïve T lymphocytes will, depending upon the stimulus they receive, differentiate and form a population of cells which are either **pro** or **anti**- inflammatory. **CD4** expressing T cells, also know as T helper cells, are prolific cytokine producers and are further split into **Th1** or **Th2** subsets depending on the suite of cytokines that they produce. **Th1** T cells are generated in response to bacteria or viruses and primarily secrete **IFNγ, IL-2** and **lymphotoxin**. If these cells and their products are left unchecked this may lead to tissue damage, thus a balance must be struck by **Th2** cells secreting **IL-4, IL-5** and **IL-13.** Together along with IgE and IL-10 these create an anti-inflammatory balance to the Th1 situation (Berger, 2000).

Th1 cells: Produced in response to bacteria, viruses or protozoa, these cells secrete IFNγ, which can influence innate cells such as macrophages (generating classically activated macrophages) and can also activate $CD8^+$ cytotoxic T cells that can kill virus-infected cells. Toll-like receptors 4, 5 and 12 further drive the Th1 response when stimulated by LPS, flagellin and profilin respectively (Akira, Uematsu, & Takeuchi, 2006), (Koblansky et al., 2013). The transcription factor NF-κB is subsequently activated and this further stimulates the production of more pro-inflammatory cytokines (IL-1, IL-6, TNF-α and IL-12p40) (Walsh & Mills, 2013).

Th2 cells: Generated in response to helminth infection these cells produce IL-4, IL-5 and IL-13 (Allen & Maizels, 2011). Under the influence of IL-4 and IL-13, macrophages move toward the alternative activation pathway, which in turn stimulates tissue repair, and class switching in B cells generates IgG1 and IgE. IL-13 may be particularly important in intestinal helminth infection due to its ability to initiate mucin production from goblet cells (Allen & Maizels, 2011). Induction of Th2 responses by helminths and parasites is less defined than that for a Th1 response. As invaders become more complex, so too does the initiation of a defence by the host. Secreted products from the parasite may initiate induction of the Th2 response, such as Omega1 (a glycosylated ribonuclease secreted by *S.mansoni* eggs),

which was shown by Everts to generate a Th2 response via dendritic cell activation (Everts et al., 2012). However recent studies by McSorley suggest that excretory secretory products from the intestinal helminth *H.polygyrus* strongly suppress Th2 inflammatory responses in an airway allergy model (McSorley, Blair, Smith, McKenzie, & Maizels, 2014).

Th17 cells: As the name would suggest TH17 cells are responsible for the production of IL-17 along with IL-22, GM-CSF and TNF-α and have a key role in the pathogenesis of organ-specific autoimmune disease (Mills, 2008). Derived in response to TGF-β, IL-6 and IL-21, Th17 cells activate macrophages and neutrophils resulting in inflammation and tissue damage (Jovanovic et al., 1998), (Mills, 2008). Apart from their inflammatory role in autoimmunity Th17 cells are also key mediators in immunity to pathogens as they recruit and activate neutrophils to the site of infection (Kumar, Chen, & Kolls, 2013).

T_{reg} cells: Regulation of immune responses to self antigens is the responsibility of the T_{reg} cell accompanied by its ability to dampen T effector responses thus avoiding immunopathology (Belkaid & Rouse, 2005). Following maturation and induction in the thymus, natural T_{reg} cells are located in the periphery and constitutively express CD25, CTLA-4 and the glucocorticoid-inducible tumor necrosis factor. Adaptive T_{reg} cells are induced in the periphery and depending on disease status and setting can express variable levels of CD25 (Bluestone & Abbas, 2003).

Regulatory T cells may have evolved from cells that were required for wound repair in response to damage caused in the first instance by the parasite. This has unexpected benefits for the parasite, as the response results in a state of immune tolerance and reduced possibilities of host tissue damage, rather than an inflammatory response which may result in subsequent expulsion or killing of the parasite.

During infection with *H.polygyrus* the population of T_{regs} in the mesenteric lymph node expands and becomes activated during the early phase of infection. This was noted in C57BL/6 mice, which are susceptible to infection with this parasite (Finney, Taylor, Wilson, & Maizels, 2007). Metwali et al described a population of CD8+ regulatory cells in the lamina propria of *H.polygyrus* infected mice. These cells

inhibited T-cell proliferation and in so doing prohibited the development of experimentally induced colitis (Metwali et al., 2006).
Tregs may also have a role in the suppression of inflammatory immune responses such as those induced by schistosome eggs. Originally thought to be IL-10 dependent recent studies indicate suppression may be IL-10 independent however the mechanisms by which this is mediated is still unclear (Hesse et al., 2004), (Baumgart, Tompkins, Leng, & Hesse, 2006). Interestingly T_{regs} are also thought to regulate Th2 immune responses in schistosomiasis indicating that they may play a pivotal role in balancing the immune response as disease progresses into the chronic, long lasting phase (Taylor, Mohrs, & Pearce, 2006).

CD8+ T cells: Generation of $CD8^+$ T cells occurs after antigenic peptides are presented by antigen presenting cells following processing by the endogenous MHC class I pathway. Generally regarded as facilitators of adaptive immunity to cytosolic pathogens such as viruses, bacteria and protozoa they can also respond to non-cytosolic antigens processed via exogenous MHC class I pathways (Harty, Tvinnereim, & White, 2000). Once activated, $CD8^+$ T cells generate IFN-γ, TNF and chemokines that facilitate the recruitment of macrophages and neutrophils (Harty & Bevan, 1999).
As mentioned above, CD8+ T cells play an important role in protection against intracellular pathogens such as *T.gondii* (Brown & McLeod, 1990).
Interestingly, the development of a population of CD8+ T cells during *T.gondii* infection was inhibited when mice were already infected with *H.polygyrus* (Khan et al., 2008). *H.polygyrus* is a potent stimulator of a Th2 response; consequently as CD8+ T cells require a Th1 immune environment with particular emphasis on the presence of IFN-γ, development of this subset of T cells failed to occur (Khan et al., 2008).

Innate lymphoid cells

One of the most recent findings in the field of cellular immunology is the discovery of a population of cells now known as innate lymphoid cells (ILCs). Cytokine secretion was generally thought to be under control of the adaptive Th1 and Th2 cells, each secreting a discrete set of cytokines. In addition to cytokines produced by the adaptive response a second source of cytokines was discovered; the ILCs. Distinct from adaptive cells, ILCs produce many cytokines in common with their adaptive cousins however they do not share many surface makers. Also lacking a T cell receptor, ILCs do not respond in an antigen specific manner. ILCs have now been classified into three groups dependant on surface maker expression and their secreted cytokine repertoire.

Group 1 ILCs include NK cells and are characterised by their production of type 1 cytokines such as INF-γ and tumour necrosis factor (TNF). NK cells not only are capable of producing INF-γ but also display cytotoxic activity towards tumour cells (Kiessling, Klein, Pross, & Wigzell, 1975). Equally they are also involved in the clearance of cells that have become infected with virus by directly inducing cell death (Vivier et al., 2011). Expression of perforin and granzymes enables induction of granule-mediated cytotoxicity (Walker, Barlow, & McKenzie, 2013).

Group 2 ILCs produce type 2 cytokines such as IL-4, 5 and 13. Fallon et al described a population of non-B, non-T cells that were capable of producing type 2 cytokines during infection with *N.brasiliensis* (Fallon et al., 2006). Termed natural helper cells, nuocytes and innate helper 2 cells, ILC2s are found in mesenteric lymph nodes, spleen, liver and the intestines, and have also been detected in the airways (Walker et al., 2013), (Barlow et al., 2012; Bartemes et al., 2012). ILC2s produced their array of cytokines following stimulation with IL-7, IL-25, IL-33 and thymic stromal lymphopoietin (TSLP) (Fort et al., 2001), (Hurst et al., 2002), (Spits et al., 2013). During infection with helminths or in an allergic situation ILC2s respond to TSLP, IL-25 and IL-33, which are released as a consequence of tissue damage or allergen exposure, by producing IL-5, -9 and -13 (Licona-Limon, Kim, Palm, & Flavell, 2013). ILC2s respond to helminth infection and aid protection with IL-13

release, which is instrumental in up-regulation of goblet cell mucus secretion and smooth muscle cell contraction (Fallon et al., 2002), (Finkelman et al., 2004), (Walker et al., 2013). During an allergic response it was understood that T_h2 cells were solely responsible for the production inflammatory type 2 cytokines, however Barlow et al demonstrated that ILC2s were responsible for the majority of IL-13 expression in the lung (Barlow et al., 2012), (Klein Wolterink et al., 2012). Indeed in IL-13-/- mice that are normally not susceptible to allergic lung inflammation, airway hyper-reactivity was restored following the transfer of IL-13 expressing ILC2 cells (Barlow et al., 2012).

Group 3 ILCs are sub-divided into ILC3s and LTi cells. ILC3s express NKp46, which is the NK cell activating receptor. However, unlike NK cells they do not produce IFN-γ or TNF instead they produce the cytokine IL-22 (Satoh-Takayama et al., 2008) and are predominantly located in mucosal tissues of intestinal tract. Unlike ILC3 cells, LTi cells do not express NKp46 but do secrete IL-22 in addition to IL-17. These cells were first described in foetal and neonatal lymph nodes and early studies suggest a role in innate repsonses due to their capacity to produce IL-17A and IL-22 as mentioned above (Takatori et al., 2009). Figure 5 shows ILC groups with their associated surface markers and cytokine profiles.

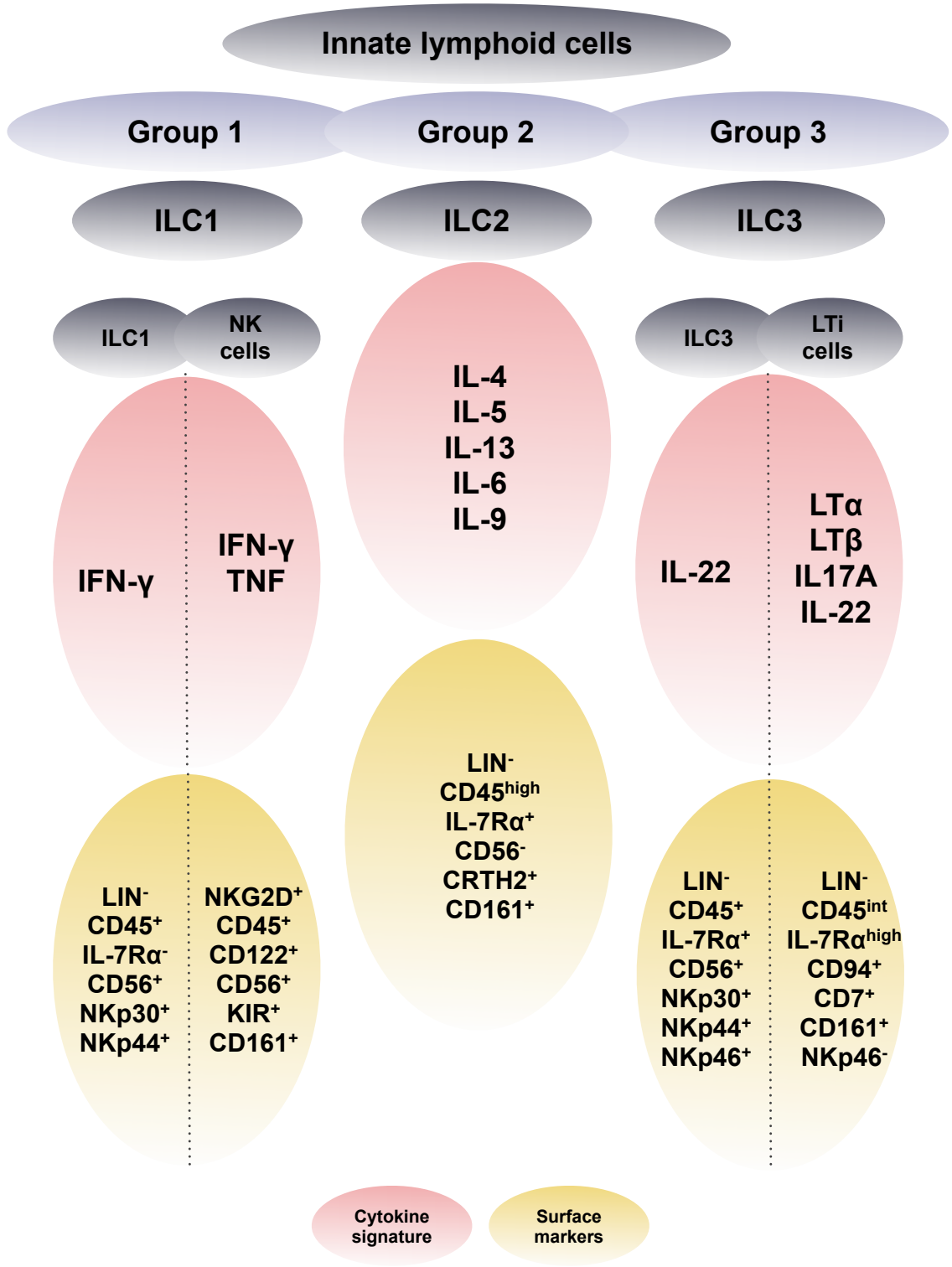

Fig 5. Innate lymphoid cells.

B cells and antibody responses

Produced in the bone marrow, B cells mature in the spleen and secondary lymphoid tissues with antibody production being their main role in humoral immunity. Pathogen antigens bind to the B cell via the B cell receptor (BCR) resulting B cell activation. Following activation, B cells then proliferate and subsequently differentiate into plasma or memory B cells.

Given that immunity to helminths is primarily driven by a strong Th2 response, it is very interesting to note that there is substantial evidence for antibody-mediated protection and expulsion of the gastrointestinal parasite *H.polygyrus* (McCoy et al., 2008), (Horsnell & Brombacher, 2008). Upon infection with *H.polygyrus*, stimulation of B cells results in hypergammaglobulinaemia, which is restricted to IgG1 and IgE (Chapman, Knopf, Hicks, & Mitchell, 1979). Indeed, levels of IgG1 can reach 20-40mg/ml following secondary infection, which is in stark contrast to the < 1mg/ml observed in an uninfected individual (Williams & Behnke, 1983). This immune serum also demonstrated protective effects following passive transfer into naïve recipients (Williams & Behnke, 1983). Moreover, serum from immune mice restored protection during a challenge *H.polygyrus* infection in μMT mice, with resultant worm expulsion, however, the role of B cells in infection with a second gastrointestinal parasite, *Nippostrongylus brasiliensis,* demonstrated no such role for the B cell in parasite removal (Liu et al., 2010).

During infection antibodies and cytokines alike, both produced by the B cell, are required to successfully expel *H.polygyrus* parasites. These B cell generated moieties work in tandem with, and promote, Th2 memory cells (Wojciechowski et al., 2009). Additionally, B cells may be involved with parasite expulsion, as during secondary infection with *Litosomoides sigmodontis*, *S.mansoni* and *H.polygyrus,* parasite numbers increased when B cells were absent (Martin et al., 2001), (Bickle, 2009), (Wojciechowski et al., 2009).

****

Thus, if a soluble molecule is responsible for manipulation of the host immune response its effect on host immune cells and tissues would be paramount. Some of these cells, in particular gut cells and tissues, are discussed in later chapters.

Parasites and Animal models

Examining the potential of parasite products to manipulate and modulate immunity would be almost impossible were it not for the existence of a suitable parasite to study accompanied by a suitable model in which to test it.

Heligmosomoides polygyrus

The mouse parasite *H.polygyrus* is one such organism and is commonly used as a model for chronic gastrointestinal nematode infection in the laboratory. Although this parasite has been utilised in a laboratory setting for a number of decades, recently debate arose with regards to the nomenclature of the parasite currently being used. In 1845, the naming of a parasite as *Strongylus polygyrus* isolated from wood mice, and shortly afterwards (1878) isolated from voles, may be the earliest records of the parasite in question (Dujardin, 1845), (Hall, 1878). Later, a strain referred to as *Nematospiroides dubius* Baylis was used experimentally in the laboratory by a group in Arizona studying host-parasite relations (Spurlock, 1943). Bryant et al described the life cycle of the *Nematospiroides dubius* Baylis in 1973 (Bryant, 1973). Between 1950 and 1967 nomenclature became confusing with both *Nematospiroides dubius* Baylis and *Heligmosomoides polygyrus*, the latter coined by Cram in 1927, (Cram, 1927). In 1992 Bhenke et al discuss the nomenclature of the parasite, and propose that *Nematospiroides dubius* be abandoned in favour of *Heligmosomoides polygyrus bakeri* when referring to laboratory maintained parasites (Behnke, Keymer, & Lewis, 1991). However nomenclature concerns continue with reviews from Bhekne and Maizels continuing to debate the issue (Behnke & Harris, 2010), (Maizels, Hewitson, & Gause, 2011). For clarity, the parasite will be referred to as *Heligmosomoides polygyrus* (*H.polygyrus*) throughout this thesis. *H.polygyrus* is a naturally occurring dioecious parasite that is found in wild mouse populations. Male and female adult parasites, measuring approximately 12mm and 6mm respectively, can be distinguished primarily by the size but also by the presence of the copulatory bursa found at the posterior end of the male (Fig 6 A & B).

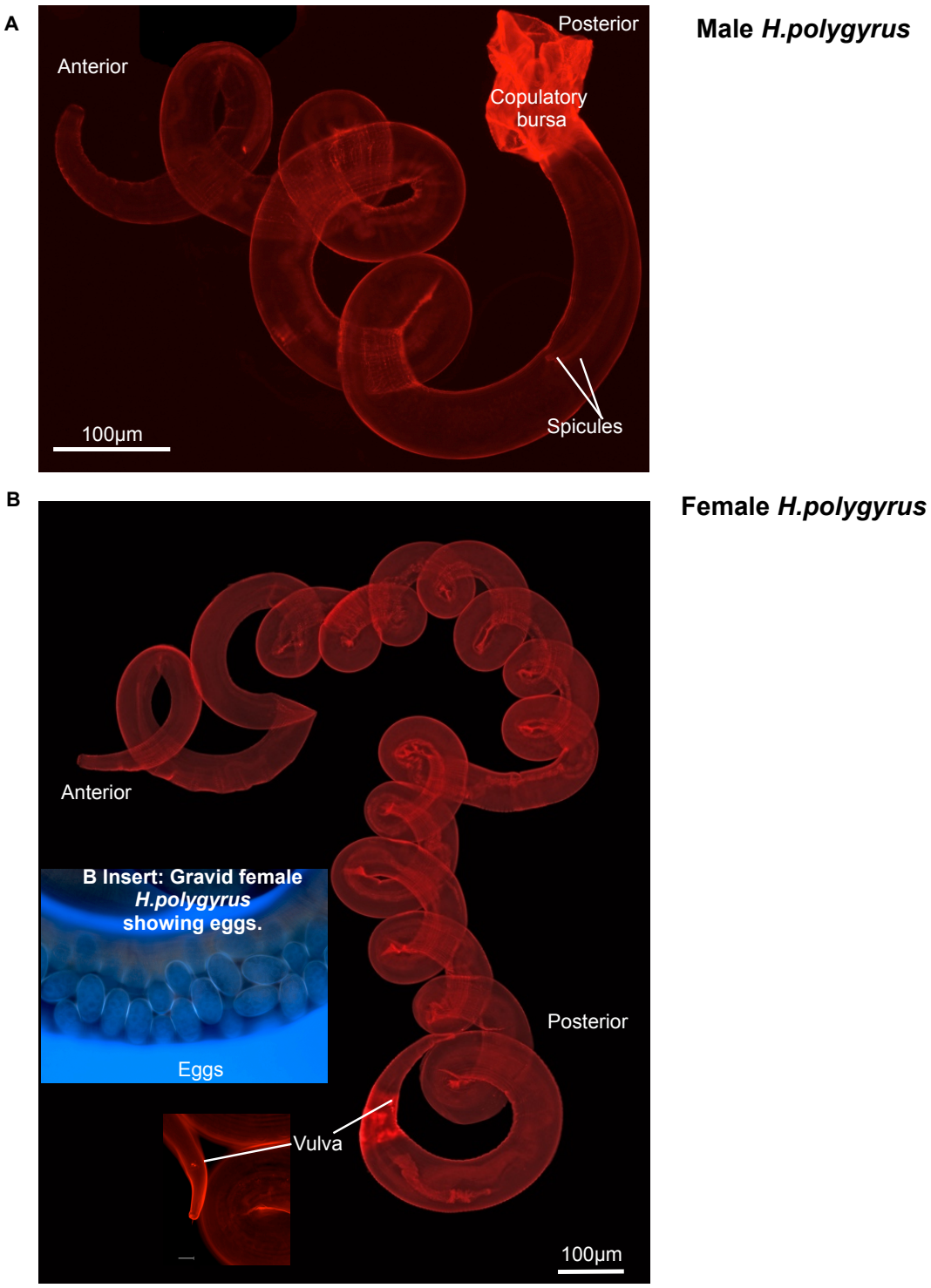

Fig 6 Male and female *Heligmosomoides polygyrus* (*H.polygyrus*).

Fig 6 Male and female *Heligmosomoides polygyrus* (*H.polygyrus*).

A. Male *H.polygyrus* showing the copulatory bursa and spicules, both of which are required for reproduction. **B**. Female *H.polygyrus* **B-insert.** Eggs within gravid female parasite. Parasites were stained in round-bottomed 96-well plates on ice. 1° antibody: rat α-HES, 1:100. 2° antibody: α-rat TRITC, 1:100.
Parasites were visualised using an Olympus fluorescent microscope.

Epithelial cells

The parasites, life cycles and parasite products described above will feature prominently throughout this thesis as I discuss interactions between them and the host cells with which they come into contact. One of the primary sites for host-parasite interactions, whether they occur in the lung or the gastrointestinal tract, is the epithelium.

Lung epithelium:

The **Clara/ club cell** (Fig 7), first identified in 1881 by Kolliker and subsequently named after Max Clara, is a multi-functional cell residing in the terminal bronchioles. More recently in 2013, editorial boards from a number of journals decided to rename them Club cells due to the circumstances which shadowed their discovery (Irwin et al., 2013). Unlike other lung cells, club cells have no cilia but do contain granules within the cytoplasm. Involved in lung protection they control inflammation, aid clearance of environmental agents and help maintain ciliated cell numbers by proliferation (Reynolds & Malkinson, 2010). Club cell secretion can be stimulated *in vivo* by intratracheal instillation of bleomycin, which results in part of the cell protruding into the lumen of the bronchiole (Peao, Aguas, de Sa, & Grande, 1993). One component of the secretory granules is club cell secretory protein (CCSP), which has anti-inflammatory and immunomodulatory roles in the lung (Wang, Rosenberger, Bao, Stark, & Harrod, 2003), (Harrod, Mounday, Stripp, & Whitsett, 1998). Club cells are also the progenitor cells for the goblet cell in the respiratory epithelium. Inflammation in the lung due to the presence of pulmonary allergens and IL-13 causes goblet cell hyperplasia and the associated production of excess mucus. Accompanying this, goblet cell differentiation of club cells occurs upon the increased expression of SAM-pointed domain–containing Ets-like factor (SPDEF). SPDEF expression in the club cell, has been shown to regulate a transcriptional network, preventing club cell differentiation and inducing goblet cell differentiation and mucus production (Chen et al., 2009), (Park et al., 2007).

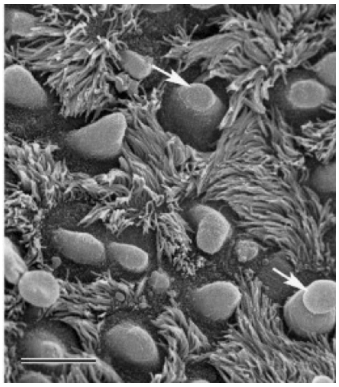

Fig 7. Scanning electron micrograph showing club cells rat bronchiole.
Scanning electron micrograph showing club cells located in a rat bronchiole. Arrows indicate actively secreting cells. Taken from Reynolds et al (Reynolds & Malkinson, 2010).

Goblet cells are generally found in low numbers in the airway epithelium until the presence of an inhaled airway insult, such as allergens, particulates or pathogens are detected. The primary role of the goblet cell, be it airway or gastro-intestinal, is to produce mucin to cover the surface of the epithelium which acts as a protective barrier. Mucins help protect the underlying cells from inhaled particulates. Upon exocytosis from the goblet cell mucins, which can expand in volume up to 600-fold, mix with proteins, lipids and glycoconjugate components to form mucus (Rogers, 2003). The main mucins produced in the airway are MUC5AC and MUC5B, which are packed into the secretory granules of the goblet cells ready for expulsion or produced by the submucosal glands respectively (Hovenberg, Davies, & Carlstedt, 1996), (Thornton et al., 1996), (Rogers, 1994). Inflammatory cell recruitment is thought to play a role in the increased production of mucin from goblet cells (Haile et al., 1999), (Jackson, 2001).

During infection with the intestinal parasite *N.brasiliensis*, which also has an airway/ lung infection stage (Fig 10), goblet cell hyperplasia has been described in both the airway and the intestine (Tomita, Kobayashi, Itoh, Onitsuka, & Nawa, 2000). Tsubokawa et al noted that qualitative and quantitative changes occurred in rat mucins as a result of contact with parasite antigens (Tsubokawa et al., 2012). Interestingly, it has been shown that infection with *N.brasiliensis* reduces eosinophilia, eotaxin levels and levels of IgG1 and IgE in an airway allergy model, however no change in goblet cell metaplasia or mucus production was observed (Wohlleben et al., 2004). However, administration of the excretory/secretory products from *N.brasiliensis* alone in an airway allergy model not only reduced eosinophilia, allergen specific IgG1 and IgE but also ablated goblet cell metaplasia and mucus production (Trujillo-Vargas et al., 2007). Similar observations have been described during infection with *H.polygyrus* and likewise with administration of *H.polygyrus* excretory/secretory products (Wilson et al., 2005), (McSorley et al., 2012).

Ciliated cells are located primarily in the tracheal and bronchial regions. Functioning as part of the mucociliary escalator, these columnar shaped cells have cilia, which

work to move mucous produced by goblet cells and environment particulates out of the lungs (Alberts B, 2002).

Alveolar macrophages (AMs) arise from precursors in the bone marrow and can respond quickly when the airways encounter inhaled particulates. Forming 95% of the bronchoalveolar lavage, AMs arise in the presence of IFN-γ and lipopolysaccharide (LPS) and are important for the production of cytokines, which produce pro and anti-inflammatory responses in the lung (Flaherty, Monick, & Hinde, 2006). During infection with *N.brasiliensis,* AMs recruited to the lungs exhibited and alternatively activated profile with increased expression of the markers YM-1, FIZZ1 and Arginase1 (Reece, Siracusa, & Scott, 2006) raising the possibility of their involvement in tissue repair and remodelling that is required during helminth infection.

Gut epithelium:

Generally, helminths set up a chronic infection in a host leading not to death, but to conditions that have an impact on the overall health of an individual such as malnutrition, growth retardation and vitamin deficiencies (Pawlowski Z. Schad G and Stott G, 1991). An infection with the hookworm *Ancylostoma duodenale* or *Necator americanus* will, for example, lead to iron-deficiency anaemia. Research into these infections is commonly undertaken by studying responses observed in animal models. *H.polygyrus* infection was shown to ameliorate symptoms in a model of the inflammatory bowel condition colitis, however when examined during coinfection with *Plasmodium chabaudi,* a previously efficacious vaccine failed to induce protection (Elliott et al., 2004), (Su, Segura, & Stevenson, 2006). *H.polygyrus* resides in the gut of the mouse and passes through the gut epithelium. Interactions between parasite, parasite secretions, gut tissue and specialised gut cells (goblet cells and Paneth cells), are introduced and explored fully in Chapter 4.

The host microbiota

Closely associated with the gut epithelium, the aforementioned goblet cells and mucus, and the Paneth cells, the gut microbiota is crucial to the development of a balanced immune system and immune responses that go beyond the immediate intestinal setting. The microbiota of an individual is laid down immediately during birth (Neu & Rushing, 2011), although some suggest colonisation may occur in utero via ingestion of amniotic fluid by the foetus (Goldenberg, Culhane, Iams, & Romero, 2008). Studies have shown that infants born by vaginal delivery come into contact with a range of beneficial, maternal bacteria, whereas infants delivered by Caesarean section (CS) are exposed to non-maternal, environmental bacteria (Biasucci, Benenati, Morelli, Bessi, & Boehm, 2008), (Biasucci et al., 2008), (Gronlund, Lehtonen, Eerola, & Kero, 1999). Another study, which examined the composition of the gut microflora from babies delivered by both methods, found that babies born vaginally had a predominance of *Lactobacillus* bacteria, in stark contrast to infants born by CS, whose microbiota consisted mainly of potentially pathogenic *Staphylococcus* and *Acinetobacter* (Dominguez-Bello et al., 2010). With this in mind, there have been a number of studies investigating the increase in prevalence of atopic disease, such as asthma, with an increase in CS delivery (Werner, Ramlau-Hansen, Jeppesen, Thulstrup, & Olsen, 2007), (Kero et al., 2002), (Decker et al., 2010).

In addition to how an infant is delivered, whether or not a child is breast-fed also influences the "set-up" of the gut microbiota. Breast milk has been shown to contain prebiotic oligosaccharides, which pass through to the colon where they are fermented by resident bacteria. This fermentation results in a pH-suitable environment for the proliferation of bifidobacteria and lactobacilli (probiotics) (Forchielli & Walker, 2005). These in turn stimulate the production of a defensive layer of IgA, which coats mucosal surfaces (Hooper et al., 2001). In experimental systems where mice have no colonizing gut microbes, as is the case in germ free mice, IgA-secreting-plasmocytes were absent. Accompanied with smaller Peyer's patches and fewer intraepithelial lymphocytes (Moreau & Corthier, 1988), (Lefrancois & Goodman, 1989) these changes in gut associated lymphoid tissues illustrate the requirement for a diverse microbiota in the intestine.

When the microbiota is absent, as is the case in germ-free mice, specialised cells of the intestinal epithelium (IECs) fail to act appropriately, with changes in cytokines, TLR expression and alterations to the production of anti-microbial peptides among some of the defects that can occur. An illustration of this happens when there is a lack of the gram-negative bacteria *Bacteroides thetaiotaomicron*, which induces expression of the anti-microbial peptide REG3γ by the Paneth cells. REG3γ activity is directed against Gram-positive bacteria, and in so doing helps to maintain a suitable environment for gram-negative colonisation (Cash, Whitham, Behrendt, & Hooper, 2006).

Thus, the composition of the gut microbiota from the outset, determines the development of the early gut mucosal immune system. Stimulation by these bacteria of gut associated lymphoid tissues (GALT) instructs the production of antibodies to pathogenic bacteria and allows non-pathogenic species to remain unchallenged. This was initially called the "old friends" hypothesis (see Chapter 3) and has more recently set the foundations for the hygiene hypothesis (Rook, 2010).

Throughout infection with an intestinal helminth, both the parasite and the microbiota have the ability to interact directly with the IECs. How they do so impacts on the survival prospects of both. Indeed, it has been recently demonstrated that such a relationship exists between the helminth *H.polygyrus* and the intestinal *Lactobacillus* population, with a positive correlation between infection and *Lactobacillus* abundance being demonstrated (Reynolds et al., 2014). Conversely, mice infected with *H.polygyrus* were more likely to develop *Citrobacter rodentium* induced colitis with none of the aforementioned protective characteristics evident (Chen, Louie, McCormick, Walker, & Shi, 2005).

Thus, as helminths, their products and the gut microbiota all inhabit the same area of the intestine, it is not unreasonable to assume interactions occur between them to ensure the optimum environment exists for each to flourish.

Aim and Hypotheses

This thesis aims to describe and comprehend interactions that occur between a parasite and its host, which allow both to survive. To understand this relationship a number of approaches were employed taking the study from a molecular level, in which putative immunomodulatory proteins and protein families were described, through to the utilisation of model experiments which attempted to appreciate, at a functional level, how these interactions may be occurring.

Chapter 1 aims to describe the VAL gene family and the reasoning for choosing VAL proteins as putative immunomodulatory molecules is set out. The hypothesis of this chapter is based on the ability of parasites to remain in their host unchallenged for long periods of time and the suggestion that a parasite produced moiety is responsible for this by interfering with or modulation of the host immune response. VAL proteins are well known candidates for immunomodulation in other parasite systems, sometimes due to the timing of their release or perhaps due to the quantities in which a parasite produces them. Thus VAL proteins from the murine gastro-intestinal parasite *Heligmosomoides polygyrus* and the human filarial parasite *Brugia malayi* will be examined for immunomodulatory potential.

Chapter 2 describes the first of three approaches used to study gene expression and protein function. *Leishmania* parasites have a well-documented and understood mode of infection with thoroughly described immune responses, both in the human host and during *in vitro* infection of macrophages. The aim was to create transgenic parasites and examine immune responses to these parasites in comparison to wild type parasites. It may be hypothesised that any changes in virulence were the direct result of the inserted gene and subsequent production of the related protein.

Chapter 3 explores an allergic airway inflammation model, which has been used previously to demonstrate amelioration of allergic responses upon administration of excretory/secretory products from *H.polygyrus* (HES) (McSorley et al., 2012). As VAL proteins are the most highly represented protein family in HES it was

hypothesised that they may be the responsible moiety for the suppression observed. This chapter details a set of experiments undertaken to study the effects of VAL proteins in a murine model of asthma.

Chapter 4 examines recombinant VAL proteins and the excretory/secretory products from (HES), and attempts to establish where and with which cells it may interact. As *Heligmosomoides polygyrus* inhabits the intestine of the mouse it was postulated that interactions might occur between HES, VAL proteins and cells of the murine intestinal epithelium. Thus, a combination of immunohistochemistry and confocal microscopy were employed to visualise possible protein-cell binding events.

Material and Methods

Parasite Methods

Preparation of *H.polygyrus* excretory secretory products (HES)

The lifecycle of *H.polygyrus* was maintained as described previously in F1 mice (Camberis, Le Gros, & Urban, 2003). 400 *H.polygyrus* L3 stage larvae were administered to CBAxC57BL/6F1 mice by oral gavage. 14 days later adult parasites were recovered from the gut of infected mice, washed extensively and then cultured in serum free RPMI 1640 medium (Gibco) supplemented with 1% glucose, 100U/ml penicillin, 100µg/ml streptomycin, 2mM l-glutamine and 100µg/ml gentamicin (Gibco). Supernatant from the first 24 hours of culture was collected separately, with subsequent collections harvested every 2-3 days, centrifuged at 400 *g* for 10 minutes to remove eggs and then concentrated using an Amicon diafiltration device with a 3000 molecular weight cut off membrane. The supernatant was concentrated 200-fold (1 litre concentrated to 5ml) before washing the membrane with a further 50ml PBS, which was reduced to 5ml. The concentrated supernatant was sterile filtered through a 0.2µm filter (Millipore) and was then frozen at -80°C. Protein concentrations varied from batch to batch but was generally 1mg/ml.

Preparation of *H.polygyrus* extract (HEx)

Adult *H.polygyrus* parasites were harvested from the gut tissue of mice by gently scraping the gut tissue after slicing open longitudinally. Parasites were homogenised in cold PBS on ice using a hand held homogeniser or by using a TissueLyser (Qiagen). Homogenised tissue was then centrifuged at 13,000g for 30 minutes and the supernatant stored frozen at -80°C.

Protein concentrations of both HES and Hex were determined by Bradford assay.

Parasite Egg Counts

2-3 faecal pellets were collected and weighed before suspending in 2ml of distilled water. 2ml of saturated NaCl solution was added and eggs were then counted using a

McMaster egg counting chamber. Egg counts shown are per gram of faecal matter and were calculated as follows:

$$\text{Eggs/gram of faeces} = \frac{\text{egg count} \times 26.67^{*}}{\text{faeces mass (g)}}$$

* = calculated as: volume of liquid faeces was dissolved in (4ml) chamber volume (0.15ml)

To maintain the lifecycle of *H.polygyrus* in laboratory setting, 400 L3 larvae were introduced to F1 CBA mice by oral gavage (Fig 8A-1). Larvae migrate down to the small intestine where they penetrate the duodenal mucosa (Fig 8A-2). Whilst resident in the muscularis they undergo two moults over a period of 7 days (Fig 8A-3), subsequently emerging into the lumen of the gut as adult parasites (Fig 8A-4). Whilst in the lumen, adult parasites anchor themselves by wrapping around intestinal villi (Telford, Wheeler, Appleby, Bowen, & Pritchard, 1998). Male and female parasites mate and the female commences the production of eggs, which are then expelled from the mouse in the faeces (Fig 8A-5). To maintain a stock of infective larvae, faeces from infected mice were mixed with charcoal and kept in a humid container for up to 14 days. Larvae should hatch after 5 days and can be harvested and stored at 4°C (Fig 8A-4.1).

The excretory/ secretory products produced by *H.polygyrus* (HES) are key to a number of subjects discussed later in this thesis (Hewitson et al., 2011b), (Hewitson, Grainger, & Maizels, 2009), (McSorley, Hewitson, & Maizels, 2013), (Maizels et al., 2012). To produce HES, adult parasites were collected from the small intestine of Day 14 infected mice (Fig 8B-1). Using a Baermann apparatus lined with muslin, adult worms were separated from the contents of the intestine. Worms migrate through the muslin, which was immersed in HBSS, and settle in a collection tube, over a period of two hours at 37°C (Fig 8B-2). Worms were washed thoroughly with HBSS and finally HBSS containing penicillin/ streptomycin. Worms were then steeped in 10% gentamycin before final washes in HBSS. Finally the worms were place in 25cm^2 tissue culture flasks in RPMI containing glucose, penicillin/ streptomycin and l-glutamine. Worms were cultured for 3 weeks, with media being harvested and replaced every 2-3 days (Fig 8B-3). During the final step in the process HES was filtered and concentrated using an Amicon diafiltration device fitted with a 3000 molecular weight cut-off filter (Fig 8B-4). The HES was then sterile-filtered and stored at -80°C.

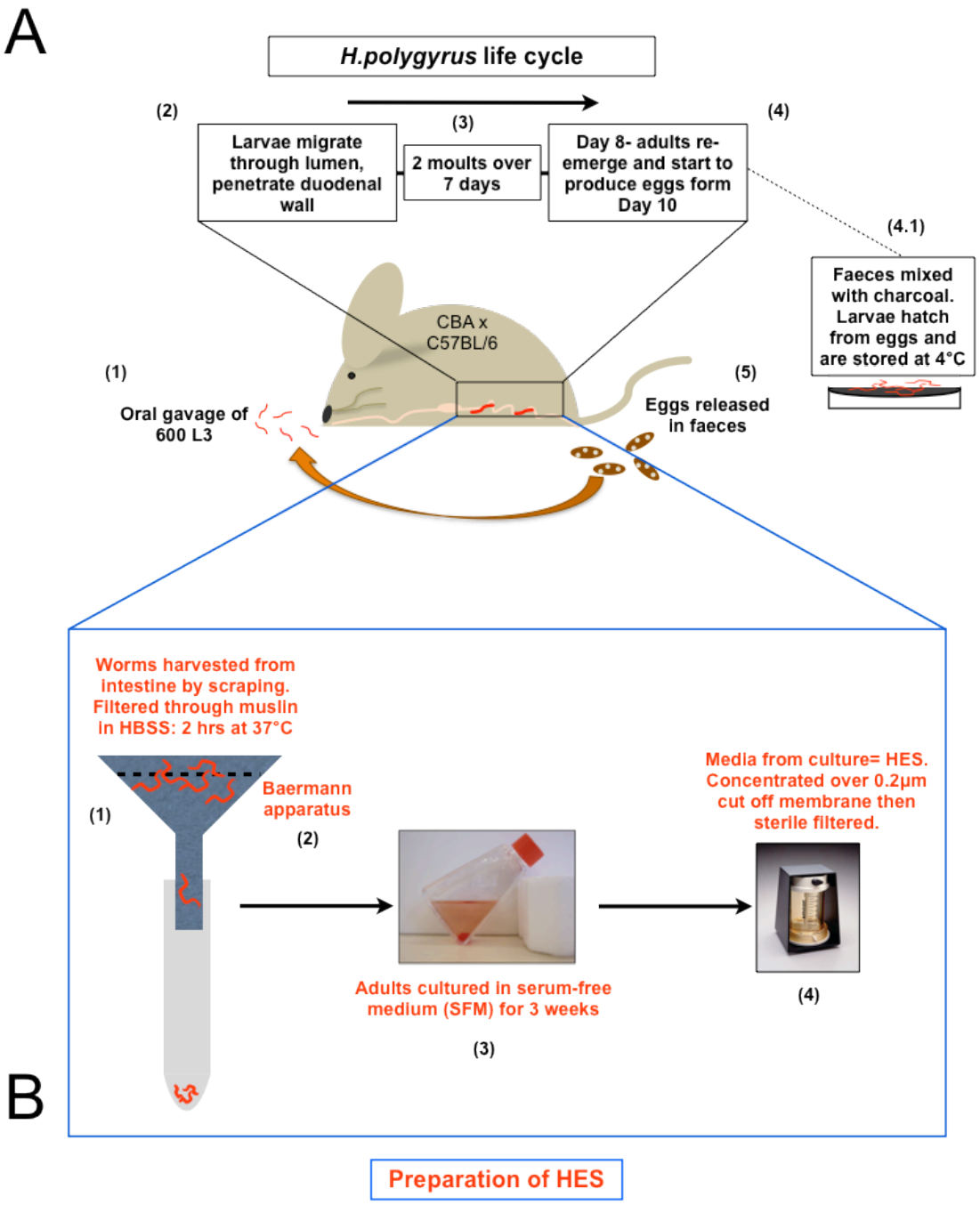

Fig 8. A. *H.polygyrus* life cycle

B. Preparation of *H.polygyrus* excretory/secretory products (HES).

Fig 8. A. *H.polygyrus* life cycle

1. Mice were gavaged with 600 L3 *H.polygyrus* larvae.
2. Larvae migrate through the lumen of the gut, penetrating the duodenal wall.
3. Over the next 7 days larvae undergo 2 further moults.
4. Around Day 8 adult parasites emerge into the gut lumen where they mate and the female parasites begin to produce eggs.
    4.1 For propagation of the life cycle in the lab, eggs were collected from the faeces and were mixed with charcoal. This was plated out onto moist filter paper in petri dishes. Larvae were later collected and stored at 4°C.
5. Eggs are released into the environment in the faeces from the mouse.

Fig 8. B Preparation of *H.polygyrus* excretory/secretory products (HES).

1. & 2. Adult parasites were harvested from the intestine of the mouse into muslin bags suspended on a Baermann apparatus (2.) Parasites were then incubated in HBSS at 37°C for two hours. During this time, parasites migrate through the muslin bag and were collected in a test tube below.
3. Adult parasites can be cultured in the lab for up to 3 weeks in serum free media. Parasite excretory/ secretory products (ES) were collected at regular intervals.
4. The ES is then filtered and concentrated through an Amicon diafiltration device.

Brugia malayi

The life cycle of the filarial parasite *Brugia malayi* (*B.malayi*) was described and shown earlier (Fig 2) with regard to the timing of expression of Bm-alt-1. The parasite can be maintained in a laboratory setting. Figure 8 shows the life cycle of *B.malayi* in a laboratory setting, where the gerbil (*Meriones unguiculatus*) acts as a host. Infective L3 larvae were injected intra-peritoneally (IP) in RPMI media containing penicillin and streptomycin, where they will develop into adult parasites and produce microfilariae (Mf) (Fig 9-1). Microfilariae, which were harvested from the peritoneal cavity of the jird by lavage with RPMI containing heparin, were then used to inoculate fresh mammalian blood at a concentration of 10-15,000/ml (Fig 9-2). Blood feeders (containers with a sausage skin membrane for the mosquito to feed at) were dosed with Mf infected blood and placed on to of mosquito cages. The mosquitoes, which have been fasted for 24 hours, ingest a blood meal thus take up Mf. Over a period of 10-14 days the Mf will develop into L3 larvae during which it will migrate through the mosquito midgut, the thoracic muscles and thence towards the mosquito head and proboscis (Fig 9-3).

For experimental purposes such as the collection of excretory/ secretory products by *in vitro* culture, the infective L3 stage can be collected by crushing the infected mosquitos and allowing larvae to be collected using a Baermann apparatus. As a model of filarial infection adult parasites can be implanted into the peritoneal cavity of mice (MacDonald AS, 1998). This model was used by MacDonald to show that IL-4 was required to promote proliferative suppression by filarial parasites.

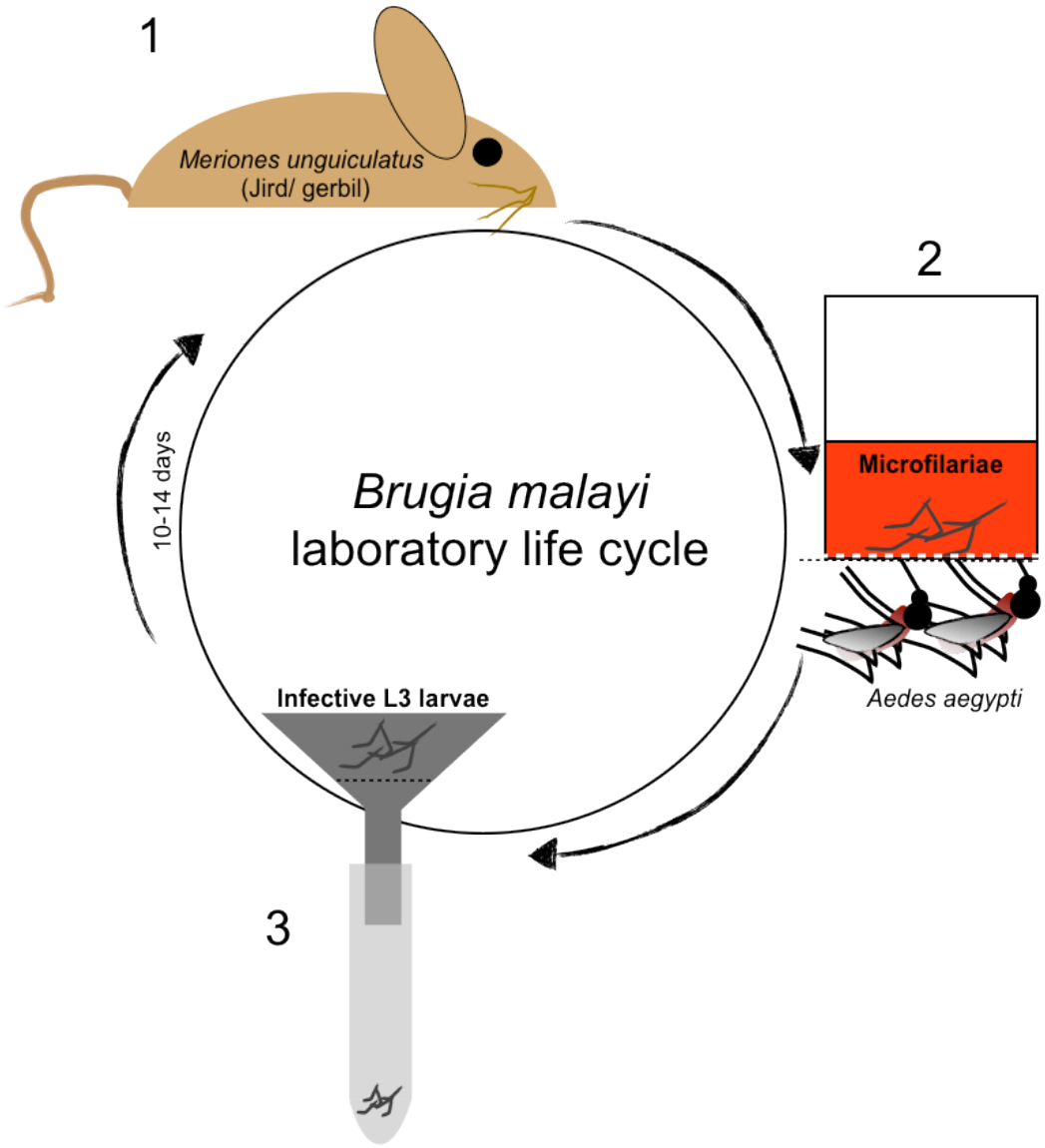

Fig 9. Maintenance of the *B.malayi* laboratory life cycle.
1. *B.malayi* L3 larvae were injected into the peritoneum of laboratory gerbils in RPMI media containing antibiotics.
2. Mammalian blood is seeded with microfilariae which had been collected from the peritoneal cavity of gerbils. *Aedes aegypti* mosquitoes had been fasted for 24 hours were then fed using blood feeders as shown.
3. Two weeks after being blood fed the mosquitoes were crushed using a plastic pipette to harvest the infective L3 stage of the parasite.

Nippostrongyus brasiliensis

Nippostrongylus brasiliensis (*N.brasiliensis*) is used in the laboratory as a model of acute infection, with duration of infection lasting 9-14 days and no intermediate host (Camberis et al., 2003). Infective third-stage larvae were injected sub-cutaneously into the host (rat) where they proceed to migrate, via the lymphatic system, to the lungs where they can be detected 15 hours after infection (Ogilvie & Jones, 1971) (Fig 10-1). After moulting the L4 larvae migrate via the trachea and the oesophagus to the small intestine (Fig 10-2 & 9-3) and the duodenum. Here the larvae moult to become L5 or adult parasites and commence egg production after around 7 days, which are passed into the environment in the faeces (Fig 10-4). The food source of *N.brasiliensis* does not appear to be the host ingesta but host intestinal tissue (Bansemir & Sukhdeo, 1994), (Bansemir & Sukhdeo, 2001).

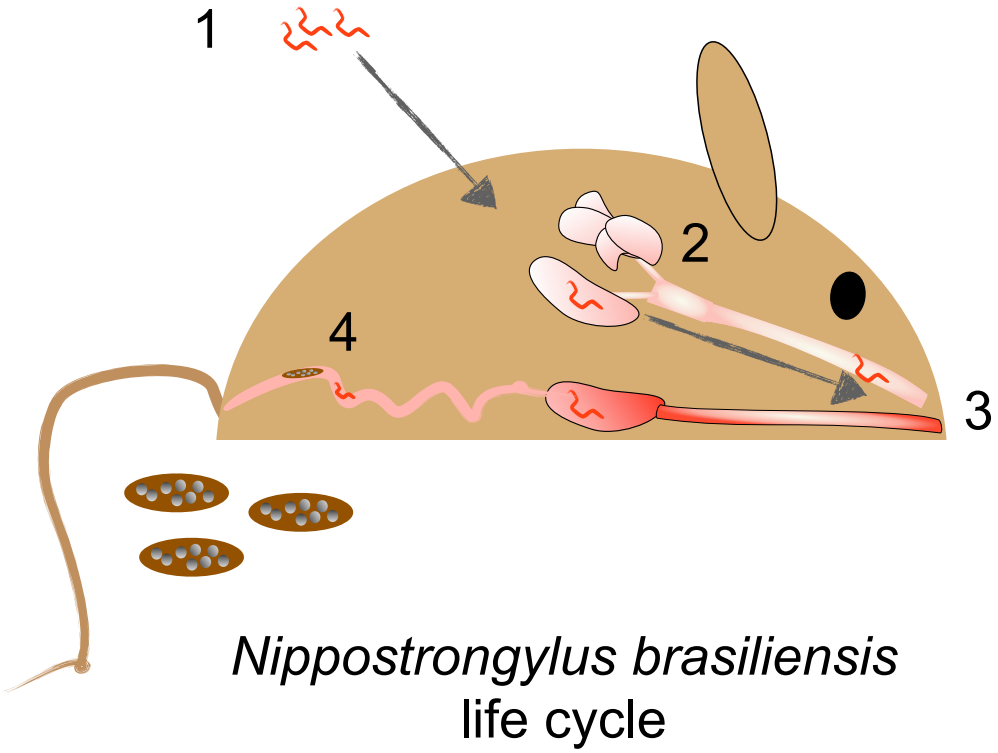

Fig 10. Maintenance of the *N.brasiliensis* laboratory life cycle.

1. Infective third stage larvae were injected subcutaneously into rats.
2. From the site of injection the larvae migrate via the lymphatic system to the lungs where they under go a moult to become l4 larvae.
3. L4 larvae migrate via the trachea and oesophagus to the small intestine and duodenum where they undergo a further moult (L5) and finally become adult parasites.
4. Eggs produced by adult parasites are passed into the environment in the faeces of the rat.

Molecular Biology and Protein Techniques

PCR

PCR reactions were performed using primers synthesised by MWG. These were diluted initially to a concentration of 1µg/ml for stocks, and subsequently diluted to100ng/ml for PCR or 10ng/ml for sequencing. Taq polymerase from Promega was used and reactions were carried out in a MJ Research DNA Engine. Each reaction was designed taking into account the melting and annealing temperatures for each primer.

Table 1: PCR Programmes.

Name	1°denature	Dentauring	Annealing	Extension	Cycles
PCR-60	4mins 95°C	1 min 95°C	1 min 60°C	1 min 72°C	34
PCR-55	4mins 95°C	1 min 95°C	1 min 50°C	1 min 72°C	34
Sequencing	-	30 sec 95°C	20 sec 50°C	4 mins 60°C	25
A-Tailing	-	-	20mins 70°C	-	-

A-Tailing

When performing a PCR reaction, use of a proofreading enzyme such as Pfu results in a blunt ended product. In order to ligate this product into pGEM-T it must have an overhanging nucleotide. 12µl of PCR product is mixed in a tube with 2µl Taq buffer, 2µl dATP (2nm), 2µl H_2O, 2µl Taq and 1.2µl $MgCl_2$. This was incubated at 70°C for 20 minutes.

Dephosphorylation of vectors.

In order to prevent the recircularisation of a vector during the ligation process, digested vectors can be treated with **c**alf **i**ntestinal alkaline **p**hosphatase (CIP). Alkaline phosphatases remove 5' phosphate groups from DNA thus preventing self-ligation. A control ligation tube where no insert is included was set up to evaluate the efficiency of the CIP treatment. Briefly, 5µl of 10X CIP buffer was added to the purified, digested vector. 2.5µl (25 units) of enzyme was added and incubated at 37°C for 30 minutes. A further 2.5µl (25 units) of enzyme was added with a second 30-minute incubation. Buffer and enzyme were removed from the reaction using an Amicon Microcon column as follows: CIP reaction was added to column and the volume made up to 500µl. The column was then centrifuged at 400*g* for 10 minutes. Buffer was removed from the reservoir and the volume in the column was topped up to approximately 500µl again. This procedure was repeated twice (three spins in all).

Restriction Digests

Restriction enzymes were purchased from Promega, New England BioLabs and Fermentas. Each enzyme was used with its corresponding buffer and the appropriate temperature for optimal enzymatic activity was used. Where double digests were carried out buffer charts were consulted to choose a compatible buffer for both enzymes.

Agarose Gel Electrophoresis

DNA from PCR reactions, ligations or colony screens was analysed for purity and size determination using agarose gels stained with ethidium bromide. Gels were usually 1% unless the anticipated product required a higher or lower percentage for good resolution. Ethidium bromide was added to 0.5X TBE buffer at a concentration of 0.5 mg/ml. DNA was electrophoresised at 100V until separation of products was achieved. Products were visualised using an Alpha Innotech gel imaging system.

Gel Purification

The purification of DNA following restriction digest whilst removing enzymes and buffer salts from the previous reaction, is also required to ensure that a product of a single size is taken forward in the cloning procedure. Qiagen gel extraction columns were used according to manufacturers instructions to purify DNA products that had been excised from an agarose gel.

Ligation

Ligations were carried out using Promega T4 DNA ligase generally with 2X rapid ligation buffer supplied in the pGEM-T easy kit®. Where 2X rapid buffer was used ligation reactions were carried out at room temperature for one hour, all other ligations where 10X ligation buffer was used or where the maximum number of transformants are required e.g. colony screening, were carried out at 4°C overnight.

Bacterial Transformation

Following ligation, reaction mixes were transformed into competent bacteria to allow for the selection of positive clones. 50µl competent JM109 cells (Promega) were defrosted on ice before adding 2-3µl of ligation reaction. This was incubated on ice for 30 minutes and was then heat shocked at 42°C for 40 seconds. The cell/ligation mix was then returned to ice for two minutes before the addition of 500µl of SOC media (Sigma) and incubated at 37°C for one hour. After the hour incubation, the transformation was spun briefly to pellet the cells, which were then plated out onto LB agar plates containing the appropriate antibiotic (50µg/ml).

PCR Colony Screen

Following the transformation of a ligation reaction it is necessary to isolate a positive integrant. Individual colonies were picked from the plated out ligation mix and were transferred into 50µl of LB media. 19µl of a master mix containing the appropriate primers, dNTP's, $MgCl_2$, Taq enzyme and water was added to thin wall PCR tubes. Then 1µl of the LB/colony mix was added to the master mix.

PCR colony screen programme:	94°C, 10 minutes – 1 cycle
	94°C, 15 seconds denaturing
	55°C, 20 seconds annealing
	72°C, 90 seconds extension
	33 cycles
	72°C, 10 minutes

In the event of a colony being positive, the remainder of the colony/ LB mix was then used to inoculate 10ml of LB media, containing the appropriate antibiotic, for overnight culture.

Sequencing

PCR and ligation product sequences were verified using Big Dye® terminator reagent (Life Technologies). 3µl BigDye buffer, 2µl BigDye enzyme and 1µl primer were added to a tube containing the template to be sequenced. The volume of product and H_2O were determined empirically for each reaction.

Protein Methods

SDS-Protein Gel Electrophoresis (SDS-PAGE)

Generally samples were diluted in NuPage® LDS loading buffer (4X) and boiled for 5 minutes before electrophoresis. Protein samples were analysed using the Invitrogen NuPAGE® Novex gel system. To achieve the best separation for the proteins of interest 4-12%, gradient Bis/TRIS gels were used with NuPAGE® MES running buffer. Gels were run at 200V for 40 minutes; this allowed separation of proteins in the range of 3-188 kDa. Protein molecular weight markers used were Invitrogen SeeBlue® Plus2 pre-stained markers (Fig. 11). Separated proteins were visualised using a Coomassie blue solution for 1 hour followed by destaining in methanol/acetic acid.

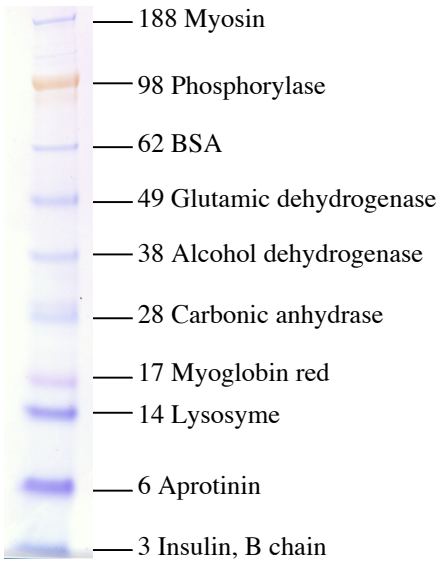

Invitrogen SeeBlue® Plus2 pre-stained markers run on a 4-12% SDS pre cast gel using Invitrogen NuPAGE® MES running buffer.

Fig.11 SeeBlue® Plus pre-stained markers.
Protein sizes shown in kDa.

Western Blotting Detection of Protein

Separated proteins were transferred from the SDS-PAGE gel onto Bio-Rad Trans-Blot® nitrocellulose membrane using a Bio-Rad semi-dry blotting system and NuPage® transfer buffer. Electrophoresis was carried out at 1mA/cm^2 for 1 hour for a 10cm x 10 cm gel. After blotting, the nitrocellulose was transferred to a solution of Ponceau S (Sigma, 0.1 % (w/v) in 5% acetic acid (v/v)) to check for successful transfer. Blots were then blocked in a solution of PBS/ 5% milk powder (Marvel) at 4°C overnight.

Antibody detection of proteins

After overnight incubation in block buffer (PBS/ 5% milk powder (Marvel), blots were washed for 5 minutes in PBS, before incubating for 1.5 hours at room temperature in a solution of the primary antibody at an appropriate concentration. Antibodies were diluted in PBS containing 5% w/v Marvel, 0.1% v/v Triton X-100, 0.05% v/v Tween 20. Blots were then given 3 x 5 minute washes in PBS/ Triton X-100/ Tween20. Secondary antibodies (e.g. mouse α-IgG-HRP (DAKO)) were diluted 1:2000 using PBS containing 5% w/v Marvel, 0.1% Triton v/v X-100, 0.05% v/v Tween 20, and were incubated at room temperature for 1 hour. A further 3 x 5 minute washes followed by 1 x 5 minute wash in distilled water were performed before detection using the Amersham ECL Plus™ detection system according to manufacturers instructions. This is a chemiluminescent detection system, which is visualised using a Molecular Devices Gel Doc.

RNA Extraction

Samples requiring RNA extraction were stored at –80°C in TRIzol® reagent (Life Technologies). Once defrosted, samples were pelleted by centrifuging at 400g for 10 minutes, before resuspending in 1ml of TRIzol®. 0.2ml of chloroform was added to each tube and mixed vigorously. This was incubated at room temperature for 2-3 minutes and followed by a 4°C, 15 minute spin at 13000g. The aqueous phase (upper layer) was removed and transferred to clean RNase free tubes. 0.5ml of isopropanol was added to each tube and mixed before incubating at room temp (15-30°C) for 10 minutes. Samples were spun again at 4°C, 13000g for 10 minutes. The isopropanol was removed from the tubes and the resultant pellet was carefully washed using 1ml of 75% ethanol. 75% ethanol was prepared using DEPC treated water. Ethanol was removed and the pellet was allowed to dry before resuspending with 20µl of DEPC water. RNA samples were routinely stored at –80°C.

DNase Treatment

Before further processing by reverse transcription and PCR, samples were treated with DNase to remove any contaminating genomic DNA. DNA-free™ (Ambion) was used for this purpose. 2µl of 10X buffer was added to each RNA sample. This was followed by 2µl of DNase1 enzyme. Samples were then incubated at 37°C for 30 minutes before the addition of 5µl of DNase inactivation reagent. Samples were then spun at 16.2x*g* for 2 minutes. The supernatant was removed to clean RNA free tubes.

Reverse transcription

cDNA is generated from DNase treated RNA using reverse transcriptase. 2µl of 10X RT buffer, 2µl dNTP (10mM), 1µl oligo dT (500µg/ml), 0.5µl RNasin (40U/µl) and 1µl of reverse transcriptase (50U/µl) was used per reaction. 1µg or 0.5µg RNA was used in each reaction. The total reaction volume was made up to 20µl.
RT-PCR programme: 20°C for 10 minutes, 37°C for 60 minutes, 99°C for 5 minutes.

Large Scale RNA using T7 RiboMAX™ System

In order to produce large quantities of pure RNA for the purpose of RNAi investigations, the T7 RiboMAX Express Large Scale RNA Production System by Promega was used according to manufacturers instructions. Briefly, DNA templates were linearised with the appropriate restriction enzyme, checked for complete digestion by agarose gel electrophoresis and gel purified. The DNA was then further purified using a phenol/ chloroform extraction protocol. 100µl of phenol/chloroform (Sigma) was added to the gel extracted DNA. This was mixed before centrifuging at 16000g for 15 seconds. The upper aqueous phase was transferred to a clean tube and 100µl of chloroform was added. The sample was again mixed prior to centrifuging and transferred to another tube. DNA was precipitated using sodium acetate and cold ethanol before the concentration of the precipitated DNA was measured using a Nanodrop spectrophotometer.

Transcription reactions were set up by mixing RiboMAX T7 Express buffer, template DNA, water and T7 Express enzyme mix (a mixture of T7 RNA polymerase, recombinant RNasin ribonuclease inhibitor and recombinant inorganic pyrophosphatase). This reaction was incubated at 37°C for 30 minutes before RNase free DNase was added to ensure that no DNA template remained. The sample was again further purified by phenol/ chloroform extraction followed by ethanol precipitation. RNA concentration was measured using a Nanodrop spectrophotometer.

RNAi protocol.

Various protocols abound for the knockdown of genes by RNAi; Samarasinghe et al used the following protocol to successfully knockdown a VAL protein in *H.contortus* (Samarasinghe, Knox, & Britton, 2010).

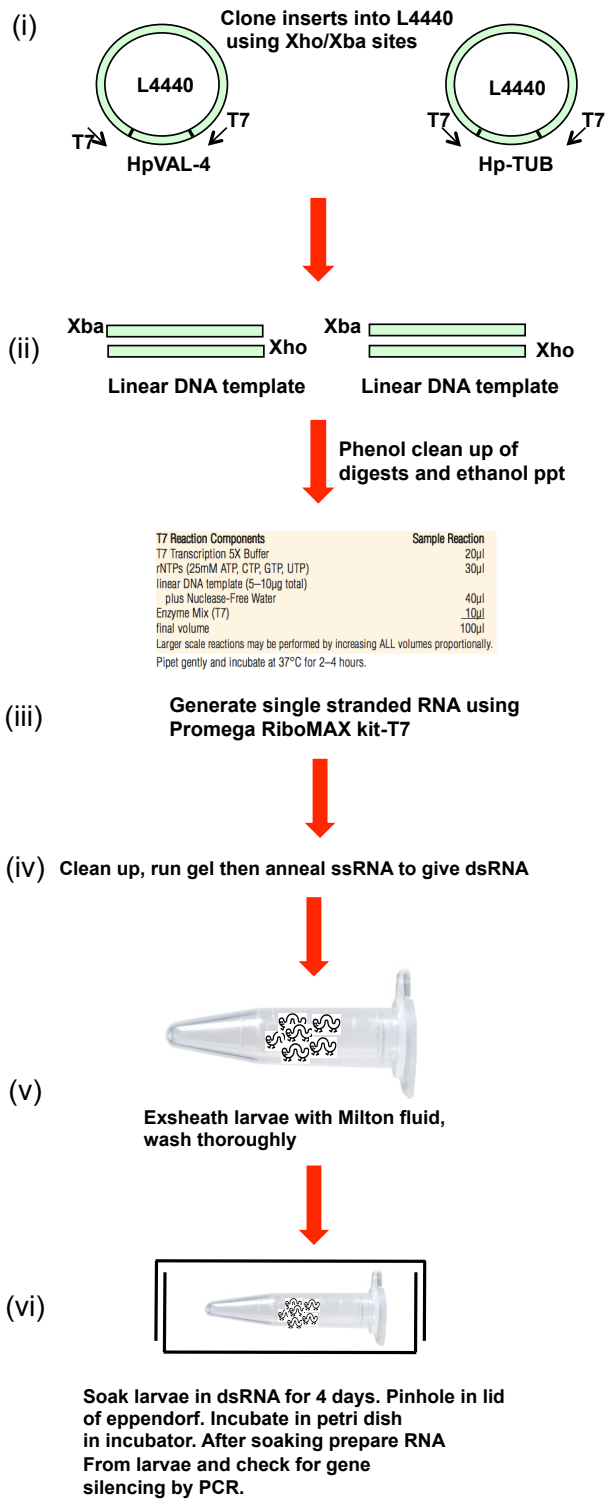

Fig. 12 RNAi protocol.

RNAi protocol

(i) Primers 1&2 (Fig 12) were used to amplify a product from cDNA (tubulin reaction) or from plasmid DNA (HpVAL-4 reaction). PCR products were ligated into the pGEM vector for colony screening and sequencing. Positive clones and the L4440 vector were digested with Xho1 and Xba1, electrophoresed and gel purified. (ii) 10µg (2x 5µg) of DNA from positive clones was linearised using either Xho1 or Xba1 and digesting overnight. Complete digestion was confirmed by gel electroproresis. Digests were then treated with phenol chloroform. (iii) ssRNA was generated using a Promega RiboMAX T7kit as per manufacturers instructions. (iv) Complementary strands of ssRNA were mixed together with injection buffer and DEPC water, incubated at 37°C for 30 minutes and allowed to anneal to form dsRNA, before cooling to room temperature. (v) 1000 larvae in 1ml were exsheathed by adding 25µl of Milton fluid. Exsheathment was complete within 30 minutes. Larvae were then washed thoroughly. (vi) dsRNA was added to Lipofectamine 2000/ Cellfectin and incubated for 10 minutes before adding to washed larvae and transferring to a 1.5ml eppendorf tube containing a small pinhole in the lid to allow gas transfer. Larvae were soaked for 4 days.

Modified RNAi protocol using siRNA.

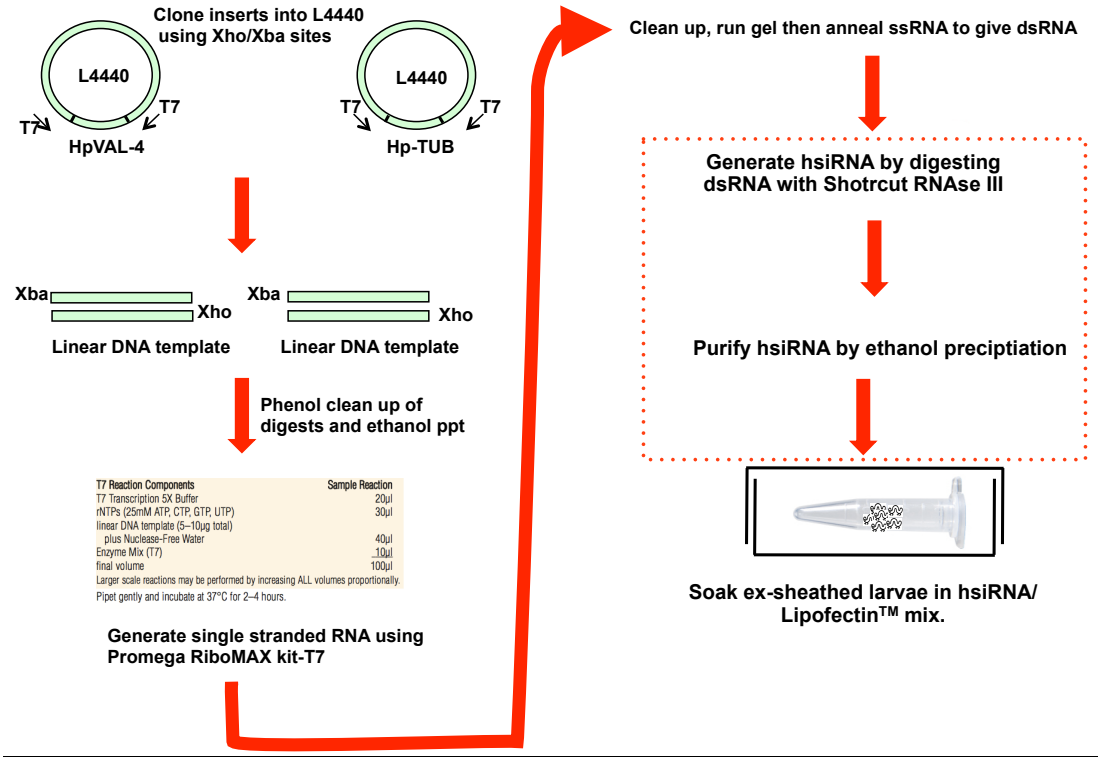

Fig. 13 Modified RNAi protocol using siRNA.

Modification of the RNAi protocol described in Fig. 12 used RNase III to digest the dsRNA into small pieces of heterogeneous short-interfering RNA (hsiRNA) allowing potentially easier uptake by the parasite (see red dashed box).

Recombinant Protein Expression

Transformation

Transformation of bacteria was carried out as previously described with the following exceptions. BL21(DE3) competent bacteria were used (Novagen). These cells carry a copy of the T7 polymerase gene and can therefore be used when expressing proteins that are encoded in plasmids with the T7 RNA polymerase promoter, in this case pET29 (Novagen). As it was plasmid DNA that was being transformed it was necessary to dilute the plasmid DNA 1:50 and then add 1µl (min concentration required 1µg/ml) of this to 50µl of competent cells. Transformed bacteria were then plated out on LB agar plates containing the appropriate antibiotic.

Growth and Induction

In the first instance, a single colony was picked from the overnight LB plate and inoculated into100ml of LB broth containing the correct antibiotic. This was grown at 37°C in an orbital shaking incubator at 300r.p.m. until an optical density (OD_{600}) of 0.6 was achieved. At this point 1ml of culture was removed, and spun down at 16000*g* for 1 minute to pellet the cells. The pellet (uninduced control), which was resuspended in 50µl of SDS PAGE loading buffer, was stored at –20°C until required.

The pET29 plasmid carries a T7lac promoter and thus requires IPTG with a final concentration of 1mM for induction of protein expression. 1ml aliquots of culture were removed at 1-hour intervals to monitor expression levels over time. After 3 hours, the culture was centrifuged at 6000*g,* using a Sorvall SLA3000 rotor for 20 minutes at 4°C. The pelleted bacteria were then resuspended in 10ml of 1X binding buffer. This was sonicated on ice for 1 minute using 10-second bursts with 10 second rests to reduce the build up of heat. The sonicated bacteria were then centrifuged at 16000*g*, using a Sorvall SS-43 rotor, for 20 minutes at 4°C. The supernatant was retained for SDS PAGE analysis.

Assessment of the solubility of recombinant protein.

Cultures were pelleted at 6000*g*. and were resuspended in 1X binding buffer. After the first sonication, (as described above) the supernatant was kept and represented the "soluble fraction". The remaining pellet was then resuspended in 10ml of 1X binding buffer containing 8M urea. This was then sonnicated as before and centrifuged. This supernatant was retained and represented the "insoluble fraction". All fractions were analysed by SDS PAGE. Recombinant protein solubility varies between molecules with some being highly soluble thus showing little or no protein in the insoluble fraction.

Purification of Recombinant Proteins

After the solubility of a particular protein has been determined the cell sonication supernatant is filtered, first through a 0.45µm filter then a 0.2µm filter. This is then diluted at least two fold with binding buffer (20mM sodium phosphate, 0.5M NaCl, 10mM imidazole). HIS tagged recombinant proteins were purified using an ÄKTAprime™ chromatography system from GE Healthcare. Filtered bacterial supernatant was applied to a nickel chelate column (GE Healthcare # 17-0408-01), which was used to bind the 6xHIS tag. Columns were charged with $NiSO_4$ buffer before application of the filtered bacterial supernatant. Recombinant protein was eluted using an imidazole gradient programme (20mM sodium phosphate, 0.5M NaCl, 500mM imidazole). 1ml fractions were collected using an automated fraction collector.

LPS depletion using Triton X114

When recombinant proteins are to be used for *in vivo* experiments, it is important to ensure that levels of LPS are measured and found to be negligible. LPS levels were determined using a quantitative chromogenic Limulus Amebocyte lysate (LAL) assay (Lonza) according to manufacturer instructions.

Triton X114 was added at a 1:100 dilution to the recombinant protein and was incubated at 4°C on a rotating wheel for a minimum of 30 minutes. During this incubation the Triton X114 binds to any LPS in the sample. The sample was then heated to 37°C 10 minutes to allow the formation of micelles which are removed by centrifugation at 16000*g*. The top aqueous layer was removed to a clean tube. Addition of Triton X114 was repeated a further two-three times leaving a small amount in the tube after the final wash to ensure no carry over of Triton into the sample.

Microscopy Techniques

Freezing Tissue and Sectioning

Tissue to be examined by immunofluorescent staining was dissected from the mouse and placed into an embedding mould on dry ice. Cryo-m-Bed (Bright Instruments) mounting fluid was poured over the section and allowed to solidify completely before storage of the sample at -80°C. Sections between 5-10μm were cut using a Leica cryostat and were mounted onto Polysine slides (Thermo Scientific).
Samples to be mounted in paraffin were outsourced to the histology department (SuRF) at QMRI, Edinburgh where H&E and PAS staining were also performed if required.

Immunofluorescent Staining

Paraffin sections were dewaxed in Histoclear (Brunel Microscopes) for 5 minutes in a fume hood. Sections were then rehydrated through a series of ethanol baths- 100%, 95% and 70% before washing in running tap water for 5 minutes.
Where a sample had been fixed using formalin and then mounted in paraffin, it was necessary to perform an antigen retrieval step. Citrate buffer antigen retrieval works in two ways by, 1) heating the sample to encourage protein epitope refolding and 2) citrate buffer treatment to ensure conformation stability of the refolded protein. Thus samples were incubated for 20 minutes in citrate buffer at 95°C before cooling at room temperature for a further 20 minutes. Sections were washed in TBS-T for 2X 5 minutes. Sections were blocked for 1 hour in block solution. (TBS-T, 10% FCS, 1% BSA, 250μg/ml rat IgG). Before proceeding to the next steps the samples were encircled with a wax histology pen. This ensured the antibodies remain on the sample during incubations and minimised the risk of drying out. Incubations with 0.0001% biotin and avidin were performed to block any endogenous tissue biotin avtivity. This is necessary when using streptavidin conjugated antibodies. Primary antibodies, diluted in PBS/ 2% FCS / 0.2% BSA, were incubated overnight at 4°C at

various concentrations (see Table 3) followed by 3 washes in PBS-T. Secondary antibodies were prepared in PBS/ 2% FCS / 0.2% BSA and were incubated on the sample for 30 minutes at room temperature. 3 final washes in PBS-T, PBS and finally H_20 before mounting in Vectashield containing DAPI.

Whole Mount tissue preparation.

In order to examine the complete structure of the villi in the gut, a whole mount procdure was used. It is vitally important that gut tissue is removed from the mouse and processed immediately. Hence, small intestine tissue was removed from the mouse and was flushed with cold Hank Balanced Salt Solution (HBSS). This helps to remove faeces and mucus from the lumen. The gut tissue was then inverted on pre-soaked, wooden brochette sticks (approx 20cm long x 4mm). Inverted gut tissue was washed gently, in a 15ml tube containg cold HBSS on ice for 5 minutes. A sharp, curved blade was then used to slice down one side of the gut and gently remove the tissue into another 15ml tube containing cold 30mM EDTA. Tissue was incubated in the EDTA for 10 minutes on ice. Tissue was removed after 10 minutes and was transferred to a tube containing cold HBSS to remove the EDTA. A further HBSS wash was performed before removing the tissue and placing onto a glass plate under a dissecting microscope. With the tissue facing luminal side up, two bent 20G needles were used to gently scrape the surface of the gut removing the villi and crypts. The scraped epithelium was transefrred to 4% formalin using a yellow tip with the end removed. Large pieces of tissue were broken up by gentle shaking then the tissue was fixed overnight at 4°C. (See Chapter 4, Fig 4.20).

Staining Whole Mount Tissue

Fixed tissue was gently washed 3X 5 minutes in PBS-T. Tissue was then permeabilised using PBS-Triton X-100 (0.5%) for 30 minutes on ice. TBS containing 5% Marvel, 0.1% Triton X-100 (blocking buffer) was used to block the tissue for 1 hour on ice. After blocking, if tissues were to be stained with biotinylated antibodies then endogenous biotin activity had to be blocked by two incubations, one with 0.001% avidin and a subsequent incubation with 0.001% biotin. Primary antibodies (see Table 3 for dilutions) in blocking buffer were incubated on samples overnight at 4°C. After incubation with the primary antibody samples were washed 4 times- 5 min, 10 min, 15 min and finally 20 min in PBS-T. Secondary antibodies were diluted in PBS-T (See Table 3) for 1 hour at room temperature. 3 washes in PBS-T, 5, 10 and 15 minutes respectively followed by 1X 5 minute wash in PBS alone. Samples were then mounted onto polysine slides in Vectashield mountant containing DAPI.

Table 3: Immunohistochemistry Antibodies and Reagents

Antibody	Dilution	Supplier/ Cat No	Method
Rabbit α lysosyme	1:500	Dako, A0099	WM
Mouse α β-catenin	1:400	BD Bioscience, 610154	WM
Rat α CD24	1:200	Santa Cruz, sc-19651	WM
α-mouse F4/80	1:100	Invitrogen, MF48000	Cryo sections
Rabbit αMuc2	1:400	Santa Cruz, sc15334	WM
Streptavidin 488	1:100	Vector, SA488	WM
Extravidin TRITC	1:200	Sigma, E3011	Cryo sections
α-rabbit 647	1:100	Life Technologies, Z25308	WM
α-rabbit 488	1:100	Invitrogen, A11034	WM
α-mouse 488	1:100	Biolegend, A11001	WM
Streptavidin FITC	1:100	Biolegend, 405201	Cryo sections
Streptavidin PE	1:100	Vector, SA5201	Cryo sections

WM- whole mount Light yellow shading: Primary antibodies

Dark yellow shading: Secondary antibodies

Insect Cell Culture

Recombinant proteins were expressed using an insect cell expression system that allows expressed proteins to be secreted and the generation of stable cell lines.

Table 4: Insect Cell Lines

Cell Line	Origin	Media	Comments
Hi5	*Trichopulsia ni*	Express Five (Life Technologies)	Grows in both adherent and suspension culture. Doubling time: 18-24 hours
Sf9	*Spodoptera frugiperda*	ExCell 402 (Sigma)	This is a subclone of Sf21. Grows in both adherent and suspension culture. Doubling time: 24-30 hours
Sf21	*Spodoptera frugiperda*	ExCell 402 (Sigma)	Grows in both adherent and suspension culture. Doubling time: 24-30 hours. May express more recombinant protein than Sf9.

Cell lines were recovered from liquid nitrogen storage by defrosting vials quickly in a 37°C water bath into the appropriate pre-warmed media. Cells were transferred to tissue culture flasks and allowed to adhere for 30 minutes, before changing the media to remove any DMSO present from the freezing process. Cell lines were grown in flasks until they were almost confluent, at which point sub culturing by sloughing the cells from the flask using a disposable cell scraper, was undertaken. Adaptation of adherent cells to spinner flasks was carried out according to manufacturer's instructions. Briefly, cells were seeded into a spinner flask at a density of between

$2x10^5$ and $4x10^5$ for Hi5 cells and $0.5x10^6$ for Sf9 and 21 cells. Heparin at 10U/ml was added to cultures in the first instance to reduce the formation of clumps. The concentration of heparin (Sigma) in culture was reduced step-wise over a number of passages. This was determined empirically for each culture. Cells were agitated in stirrer flasks containing a hanging stir-bar, at a rotation speed of 80-90rpm, and were passaged when a cell density of between 2 $x10^6$/ml to $4x10^6$ /ml was achieved.

Transfection of Insect Cell Lines

An optimum cell density of 50-60% confluence was achieved by plating out 100µl, 250 µl, 500 µl, 750 µl and 1ml of cells in a total of 3ml media into wells on a 6-well plate to see which gave the appropriate well coverage. Cells were then allowed to adhere to the well whilst the transfection mix was prepared. Between 1-5 µg of plasmid DNA was mixed with 30 µl Cellfectin®/media mix. This was added to the adhered cells, before incubating at room temperature for 4 hours in a humidified box. A further 3ml media was added to each well and cells were incubated at 28°C. Cell extracts and concentrated cell media were tested on days 2,3 and 4 post transfection for the expression of recombinant protein. Stable lines of cells expressing recombinant protein were established under drug selection with Blasticidin S HCL (Invitrogen), at an initial concentration of between 50-80 µg/ml and were then maintained with the drug at 10 µg/ml. Cell media containing secreted recombinant protein was centrifuged and filtered before concentration in an Amicon diafiltration device. Recombinant protein was then purified from the concentrated insect cell supernatant using an ÄKTApurifier chromatography system (see section on "Purification of Recombinant Proteins" on page 80). The ÄKTApurifier system (purification runs, elution and sample analysis) is controlled using Unicorn software by GE healthcare.

Freezing Cell Lines

Cells achieving 90% viability, which are in mid-log phase growth, were frozen down for stocks. See Table 5 for freezing media for each cell line.

Table 5. Insect Cell Line Freezing Media

Cell Line	Freezing Media	Cell Density
Hi5	45% conditioned media 45% Express5 media 10% DMSO	> $1x10^7$
Sf9	80% conditioned media 10% FCS 10% DMSO	> $1x10^7$
Sf21	80% conditioned media 10% FCS 10% DMSO	> $1x10^7$

Leishmania methods

Recovering Frozen Parasites.

Parasites stored in liquid nitrogen were defrosted by removing the cryo-vial and immediately immersing into a 37°C water bath. After defrosting the parasites 10ml of preheated 1x SDM (semi-defined media) was added in order to dilute the DMSO . This was then centrifuged at 1000g for 10 minutes to pellet the parasites. The media, containing 10% DMSO, was then removed and replaced with a further 10ml of preheated 1x SDM with no DMSO present. DMSO is added to the freezing media to prevent the formation of ice crystals, which would damage the parasites and reduce viability. Parasites were transferred into a $25cm^2$, vented tissue culture flask for culture.

Cryopreservation of parasites

Where positive lines of transfected *Leishmania mexicana* had been identified, these were kept for long-term storage in liquid nitrogen. The parasites, grown in the presence of puromycin, were frozen down after centrifugation for 8 minutes to pellet and subsequent resuspension in freezing solution (FCS containing 10% DMSO). Parasites in cryotubes were then placed in a thick layer of blue towel to slow down the freezing process and reduce the possibility of crystal formation and frozen, first at –80°C overnight and then transferred to liquid nitrogen for long term storage.

Culture of *Leishmania mexicana* promastigotes.

L.mexicana promastigotes were cultured in semi-defined media (SDM) containing 10% FCS. To passage parasites, 10µl of a confluent culture was inoculated into 10 ml of complete media in a $25cm^2$ flask. These were then cultured at 26°C. Parasites were passaged routinely once a week. Puromycin was added at a 1:1000 dilution to

lines of parasites that were under selection. All used media and plastics were disposed of in a vessel containing a Presept™ tablet dissolved in water.

Transfection of *L.mexicana* promastigotes.

Parasites were split 1:10 (1ml parasites + 9ml SDM) two days prior to transfection to ensure that they were in a logarithmic growth stage. 10μg of the desired DNA was linearised with restriction enzyme Pme1 (New England Biolabs) before transfection. DNA was digested overnight at 37°C. Linearised DNA was then gel purified using a Qiagen gel purification kit.
On the day of transfection, parasites were pelleted at 1000*g* for 10 minutes. Media was decanted and the parasites were then resuspended in 10ml of electroporation buffer. In order to count the parasites, 10μl of parasites was added to 190μl of 4% formaldehyde. 10μl of fixed parasites was then added to a haemocytometer and counted. Parasites in electroporation buffer (EPB) were spun again at 1.4x*g* and were resuspended at a concentration of 1x 10^7 parasites/ ml. Parasites were placed on ice for 10 minutes before adding to 0.2cm pre-chilled electro-cuvettes. Linearised DNA was added to the cuvettes followed by 400μl of parasites. These were mixed and incubated on ice for a further 10 minutes. Electroporation settings are as follows:

Electroporation settings: Volts: 0.45kV, capacitance 500μFd.
Time constant: 3.5-4.0

Parasite/ DNA mix was added to 10ml of complete SDM. This was incubated overnight at 26°C. The following day this was made up to a volume of 24ml with SDM and was plated out onto a 24 well plate (1ml/well). Puromycin was added at a concentration of 40μM to allow selection of positive integrants to begin.

Cytomix Method for parasite transfection

Log phase parasites were counted and adjusted to $1x10^8$ prior to pelleting at 1.4x*g* for 10 minutes. The pellet was resuspended in half of the original volume of ice cold Cytomix and then spun again at 1000*g* for 10 minutes. The final pellet was resuspended again in ice cold Cytomix this time at a concentration of $2x10^8$ cells/ml. 10- 50 µg of plasmid DNA was added to a pre-chilled 4mm electroporation cuvette followed by 500µl of cells in Cytomix.

Settings for electroporation were: 25µF, 1500V (3.75kV/cm)

Electroporated parasites were allowed to recover for 10 minutes on ice before being transferred to a tissue culture flask containing 10ml media. This was then split again into two flasks and made up to a final volume of 24ml per flask. Each 24ml was then split into 24well plates.

Immunological Methods

Cytokine ELISA (Enzyme Linked Immunosorbent Assay)

Soluble cytokines that were released into cell media in response to either parasite infection or stimulation of macrophages with a recombinant protein were measured using a standard ELISA protocol. Supernatants were stored until analysis at -20°C in the short term or -80°C for the longer term.

Capture antibodies were prepared in 0.06M bicarbonate buffer (pH9.6) (See Table 6 for antibody dilutions). Standard NUNC Maixsorp ELISA plates (# 439454) were coated with 50µl per well of the capture antibody and were incubated overnight at 4°C. The following day plates were blocked with TBS/ 10% FCS/ 0.05% Tween20. 200µl of blocking solution was used per well. Plates were blocked at 37°C for two hours. Standard curves were prepared in media for each assay with the top concentration being determined individually for each cytokine. After blocking, plates were washed 3 times in TBS/ Tween20 before the addition of standards and samples. 50µl of each was added to the wells with samples being loaded in duplicate. Standards and samples were incubated at 4°C overnight.

After sample incubation, plates were again washed 3 times with TBS/ Tween20. Detection antibody was prepared in TBS/ 10% FCS/ 0.05% Tween20. 50µl of detection antibody was added per well, and plates incubated at 37°C for 1 hour. Plates were washed 3 times and then Extravidin AP conjugate was added at a dilution of 1:10,000 (100µl/ well). Conjugate was incubated at 37°C for one hour before 4 washes with TBS/ Tween20 followed by 1 distilled water wash. 100µl per well of pNPP substrate was added and allowed to develop in the dark. Plates were read at 405nm.

Table 6: Cytokine ELISA Antibodies

Capture Ab (concentration)	Clone number and supplier	Top standard concentration	Detection Ab (concentration)	Clone number and supplier
IL-10 4µg/ml	JES5-2A5 Pharmingen	10ng/ml	2µg/ml	SXC-1 Pharmingen
IL-6 2µg/ml	MP5-20F3 Pharmingen	100ng/ml	0.5µg/ml	MP5-32C11 Pharmingen
IL12p40 2µg/ml	C15.6 Pharmingen	200ng/ml	0.5µg/ml	C17.8 Pharmingen
IL12p70 2µg/ml	9A5 Pharmingen	10ng/ml	0.5µg/ml	C17.8 Pharmingen

Serum Antibody ELISA

To measure antibodies present in serum, whole blood was clotted at 4°C overnight and was then spun at 16000*g* for 20 minutes to remove red blood cells. ELISA plates coated overnight with either goat anti-mouse IgG/A/M at 1µg/ml (Southern Biotech) or anti IgE at 1.5 µg/ml (Clone R35-72, BD Pharmingen) diluted in carbonate buffer were blocked for 2 hours at 37°C with 2% BSA in carbonate buffer. Serial dilutions (3-fold down 8 wells) of the serum were prepared in blocking buffer, added to the ELISA plates and incubated overnight at 4°C. The following day antibody binding was detected with the following HRP-conjugated antibodies: Goat anti-mouse IgG1, IgG2a or IgE (all Southern Biotech) and subsequent ABTS peroxidase substrate (KPL) colour changes being read at 405nm. Where IgE was being measured, the serum had to be depleted of total IgG by overnight incubation with Protein G agarose Fast Flow beads (Millipore).

Cell Isolation for Fluorescence Activated Cell Sorting (FACS), Intracellular Cytokine Staining (ICCS) or restimulation.

Spleen and lymph node preparation: In order to prepare a single cell suspension for staining, relevant organs were removed from the mouse, passed through a 70μm cell strainer (BD) and diluted into 2ml complete RPMI media (cRPMI). Red blood cells, present in the sample, were lysed by adding 4ml red blood cell lysing solution (Sigma) and incubating for 4 minutes. A further 9ml of cRPMI was added and cells were spun for 5 minutes. Cells were resuspended in 3ml of cRPMI, counted and adjusted to $1x10^7$.

Bronchiolar Lavage preparation: Lungs were flushed 3 times with 0.5ml PBS/ 0.5% BSA. Supernatant from the first 0.5ml retained after centrifugation for analysis by ELISA. Cells from this centrifugation were then added to the 2^{nd} and 3^{rd} 0.5ml washes for FACS staining. Cells were spun for 5 minutes to pellet the cells. Red blood cells present were lysed by the addition of 0.5ml RBC lysis (Sigma) solution as for spleen and lymph node preparation, and incubated for 4 minutes. 1ml PBS/ 0.5%BSA was added to stop the lysis reaction and the cells were centrifuged again. Cells were resuspended and counted for staining.

Lung Homogenate: Single lobes of lung were digested in 2U/ml liberase TL (Roche), 80 U/ml DNase. Single cell suspensions were achieved by maceration through a 70μm cell strainer (BD) and RBC lysed as described previously.

Peritoneal Lavage: Cells present in the peritoneum were collected for analysis by flushing the peritoneum with 2x 5ml RPMI media using a 23G needle. Red blood cells present were lysed as described previously.

Restimulation of Cells

Cells were restimulated with either 1) recombinant protein (1µg/ml) or 2) HES (2µg/ml) for 4 days at 37°C. Cell supernatants were harvested and analysed for cytokine presence by ELISA.

Cell surface staining for flow cytometry

Cells were stained in 96-well round-bottomed plates. Cells were pelleted by centrifugation for 3 minutes and were washed 2x in PBS. Prior to antibody staining cells were incubated with a 1:1000 dilution in PBS of Live/Dead Aqua stain (Invitrogen) for 15 minutes at 4°C followed by two washes. Fc receptors were blocked by adding 50µl per well of a 1:50 dilution of naïve rat IgG (Sigma) prepared in FACS buffer and incubated for 10 minutes at 4°C. Cells were washed 3 times in FACS buffer before incubation for 20 minutes at 4°C with surface antibody stains which had been prepared at 1:100 in FACS buffer. Where biotinylated 1° antibodies were being used 1:100 dilutions of the appropriate streptavidin 2° was added for 20 minutes at 4°C. Finally cells were washed 3X in FACS buffer before resuspending in 300µl for FACS analysis on a BD FACS Canto.
Intracellular cytokines were measured following stimulation of cells at 37°C for 4 hours with Phorbol Myristate acetate (PMA, Sigma, 500ng/ml), Ionomycin (Sigma, 1µg/ml) and Brefeldin A (Sigma, 10µg/ml). Cells were then surface stained for CD4 followed by a permeabilisation step for 30 minutes at 4°C using BD Biosciences Cytofix/Cytoperm solution. Cells were washed twice with Perm/Wash buffer (BD) and subsequently stained for the presence of intracellular cytokines. After staining cells were washed twice and resuspended in 200µl FACS buffer.
Samples were acquired using a Becton-Dickinson FACSCanto flow cytometer and data was analysed using FlowJo software (Tree Star).

See Table 7 for flow cytometry antibodies used.

Table 7: Flow cytometry Antibodies

Marker	Fluorophore	Clone number	Supplier	Cat/ no.
CD4	PE	RM4-5	Biolegend	1005112
CD8	PE	53-6.7	Biolegend	100707
IL-10	PE	-	Biolegend	554467
Siglec F	PE	E50-2440	Biolegend	552126
CD4	FITC	GK1.5	Biolegend	100406
CD8	FITC	53-6.7	Biolegend	100706
Gr-1	FITC	RB6-8l5	Biolegend	108406
IFNγ	FITC	XMG1.2	Biolegend	505806
CD11c	FITC	N418	Biolegend	117306
F4/80	FITC	BM8	Caltag	123108
CD69	FITC	-	Caltag	HM4001S
STREPTAVIDIN APC	**-**	**-**	**Biolegend**	**405207**
IL-10	APC (Allophycocyanin)	JES5-16E3	Biolegend	505010
Gr-1	APC	RB6-8l5	Biolegend	108412
MHC II	PerCP	MB/114.152	Biolegend	107623
F4/80	PerCP	BM8	Biolegend	123128

Cytometric Bead Array Assay (CBA Assay)

Cytokine levels in bronchoalveolar lavage (BAL) and lung homogenate were measured using a Cytometric Bead Array Assay from BD. This kit allows the measurement of a number of cytokines, present at low concentrations, in low volume samples. Beads with distinct fluorescent properties are coated with antibodies. Samples to be analysed are then added to a cocktail of beads, followed by detection antibodies, which together then form complexes. The complexes are measured by flow cytometry. The concentration of each cytokine is measured by fluorescence intensity in the phycoerythrin (PE) channel.

BAL and lung homogenate samples were defrosted and spun at 16000*g* for 5 minutes at 4°C to remove any particulate matter. 50µl of each supernatant was transferred to a 96-well round-bottomed plate and was kept cold on ice. Cytokine standard curves were prepared in filtered FACS buffer.
Cytokine bead cocktails were prepared by vortexing the bead stocks before using 0.2 µl of beads per well, diluted in 50 µl FACS buffer (1:250). Bead cocktails were then added to the wells containing samples and standards. The sample/ bead mixes were then mixed gently on a plate shaker (300 rpm for 1 minute) before wrapping in foil and incubating at 4°C for 1 hour.
Detection antibodies were prepared in the same manner as for the beads with 50µl being added to each well before a brief mixing step and a further 1 hour incubation at 4°C. Samples were washed once with filtered FACS buffer before bing resuspended in FACS buffer. Samples were acquired on a BD FACS Array machine.

Alum Precipitation

Recombinant protein, HES or OVA was mixed with an equal volume of 9% potassium alum (Sigma A7167) (Wilson et al., 2005) (3ml+3ml). A drop of phenol red pH indicator was added. 1M NaOH was added drop-wise until the colour of the solution turned from yellow to bright pink. This was incubated at room temperature for 30 minutes with mixing before washing 3 times with PBS. Washing was carried out by centrifuging the solution (2000g) for 10 minutes and then discarding the supernatant. The pellet was then resuspended in PBS. When the pellet retains a white colour it is then resuspended up to the original volume, taking into account the volume of the pellet.

Table 8: Primers

Name	Sequence	Comments
Bm-VAL_insect F	CGCGGATCCGTGTCCAGGAGGTCGACTA	Insect select cloning: BamH1
Bm-VAL_insect R	CCGACCGGTTTTTCTACACAATCCAGA	Insect select cloning: Age1
BmVAL-ins-R-stop	CCGACCGGTTCATTTTCTACACAATCCAGA	Age1 restriction site
Ce-VAL_insect F	CGCGGATCCGCAGTTCACCAGTACTGGC	Insect select cloning: BamH1
CeVAL_insect R	CCGACCGGTAGCGCAAAGTCCAGAAGA	Insect select cloning: Age1
CeVAL-ins-R-stop	CCGACCGGTTTAAGCGCAAAGTCCAGAAGA	Age1 restriction site
Actin-F	TGA GCA CGG TAT CGT CAC CAA C	RT-PCR
Actin-R	TTG AAG GTC TCG AAC ATG ATC TG	RT-PCR
YM-1-F	TCACAGGTCTGGCAATTCTTCTG	RT-PCR
YM-1-R	TTTGTCCTTAGGAGGGCTTCCTC	RT-PCR
Hp-VAL-1_leish -F	CCGCTCGAGATGTGGCTTCCGCTCATTTTG	pSSU cloning primer: Xho1
Hp-VAL-1_leish -R	CGCGGATCCTTAAGGGAGGCAAAGTCCTTG	pSSU cloning primer: BamH1
Hp-VAL-2_leish -F	CCGCTCGAGATGAAGCGTATAATCATTCTG	pSSU cloning primer: Xho1
Hp-VAL-2_leish -R	TGCTCTAGATCAAGACAGAGAACGAAGAGG	pSSU cloning primer: Xba1
Hp-VAL-2-5'ins-check	TTGGTACATATTAAATGA	Sequence verification
Hp-VAL-2-3'ins-check	GACGCTGTGATTTCGGCCTCGCAA	Sequence verification
Hp-VAL-4_ins-F	CGCGGATCCAGAGTTCGGATGCGATGGCACT	Insect select cloning: BamH1
Hp-VAL-4_ins-F	CCGACCGGTGCGCAGAGGTTGGAGCGTA	Insect select cloning: Age1
Arginase F	CAGAAGAATGGAAGAGTCAG	RT-PCR
Arginase R	CAGATATGCAGGGAGTCACC	RT-PCR
pSSU-R	GCTGCATCAGGTCGGAGA	Sequence verification

Hp-SOD-F	AGGTCGACGCGTCGCAGAGAATGA	RNAi primers
Hp-SOD-R	GTCTTCAGAGATCGTCCTTCTTC	RNAi primers
HpVAL1 codopt-F	CGGGGATCCAACCACTTGCCCCGGCAACTCC	Codon opt cloning: BamH1
HpVAL1 codopt-R	CGCACCGGTGGTTTCCAGGGGCAGAGTGCA	Codon opt cloning: Age1
HpVAL4 codopt-F	CGCGGATCCAGAGTTCGGTTGCGACGGCACC	Codon opt cloning: BamH1
HpVAL4 codopt-R	CGCACCGGTGCGAGCGGAGGTGGGAGCGTA	Codon opt cloning: Age1
OpIE2-Forward	CGCAACGATCTGGTAAACAC	Supplied with pMIBV5HIS vector
OpIE2-Reverse	GACAATACAAACTAAGATTTAGTCAG	Supplied with pMIBV5HIS vector
HpVAL-4 RNAi 1	TCTAGAACTTCTAAGCGTAGACCTCCCTGA	RNAi primers
HpVAL-4 RNAi 2	CTCGAGACATCTGCGGGTGCGATGGCAGTT	RNAi primers
HpVAL-4 RNAi 3	GAAATGGAGCTGTGATCTGGAAGA	RNAi primers
HpVAL-4 RNAi 4	CTAGCGCGCAGAGGTTGGAGCGTA	RNAi primers
HpTUB RNAi 1	TCTAGACGCTACCCTTTCTGTCCATCAACT	RNAi primers
HpTUB RNAi 2	CTCGAGGTGCAAAGCCAGGCATAAAGAAGT	RNAi primers
HpTUB RNAi 3	ATGGCTTCATTCTCCGTTGTTCCA	RNAi primers
HpTUB RNAi 4	CTGTGTAAGCTCGGCAACGGTTAA	RNAi primers

Red text denotes restriction site.

Buffers and Media

Complete RPMI	RPMI 1640 (Gibco) 10% foetal calf serum (FCS;Hyclone) 2 mM L-glutamine (Gibco), 100 U/ml Penicillin 100 µg/ml Streptomycin (Gibco).	
Protein gel buffers	NuPage MES buffer (Life Technologies)	
	NuPage LDS Loading buffer (Life Technologies)	
	Coomassie Blue	2% Coomassie blue
		25% methanol
		7.5% acetic acid
		Filter through Whatman No.1
	Destain	25% methanol
		7.5% acetic acid
AKTA buffers	Charge buffer (8x):	400mM $NiSO_4$
	Binding buffer (1x):	20mM sodium phosphate
		0.5M NaCl
		10mM imidazole
	Elution buffer (1x):	20mM sodium phosphate
		0.5M NaCl
		500mM imidazole
	Strip buffer (8x):	400mM EDTA
		2M NaCl
		80mM Tris HCL pH7.9
ELISA buffers	Carbonate buffer	45.3ml 1M $NaHCO_3$
		18.2ml 1M $NaCO_3$
		up to 1L
		Adjust pH to 9.6 if necessary
	Wash buffer	1L PBS
		0.5ml Tween20 & 10ml FCS

***Leishmania* buffers**

Electroporation buffer (EPB)	21 mM HEPES pH7.5
	137mM NaCl
	5mM KCl
	0.7mM Na_2PO_4
	6mM Glucose
	Filter sterilise and store at 4°C

Semi-defined medium (2x)

Minimum essential medium (S-MEM) (containing Earle's salt, L-glutamine, without Na2CO3)	140g
M199 medium (containing Hank's solution, L-glutamine, without Na2CO3)	40g
MEM essential amino acids	160ml
MEM non-essential amino acids	120ml
Glucose	20g
HEPES buffer	160g
MOPS buffer	100g
Sodium pyruvate	2g
L-alanine	4g
L-glutamine	6g
L-arginine	2g
L-methionine	1.4g
L-phenylalanine	1.6g
L-proline	1.2g
L-serine	1.2g
L-taurine	3.2g
L-threonine	7g
L-tyrosine	2g
Adenosine	0.2g
Guanosine	0.2g
Glucosamine-HCl	1.0g
Folic acid	0.08g
p-aminobenzoic acid	0.04g
Biotin	0.004g

The above components were sufficient for 10L of media. Components were dissolved in ddH_2O and adjusted to pH 7.0 before 40g of NaHCO3 was added and the pH was readjusted to 7.3. The solution was then filtered through a 0.2μm filter before storing at -20°C until required.

Saturated salt buffer (egg counts): 400g NaCl dissolved in 1L ddH_2O

Citrate buffer (antigen retrieval): 0.96g citric acid, 0.25ml Tween-20 in 500ml ddH_2O.

RNAi Buffers

Injection buffer: 20mM KPO_4
3mM potassium citrate
2% polyethylene glycol (PEG)
pH 7.5

Potassium buffer: K_2HPO_4 17.4g in 100ml
KH_2PO_4 13.6g in 100ml
The above buffers were used to create potassium phosphate buffer.
e.g. To achieve pH 7.4 add 80.2ml K_2HPO_4 to 19.8ml KH_2PO_4. Dilute this up to 1L.

Mice

BALB/c, C57BL/6, CBA, μMT (C57BL/6) and MyD88-/- mice were bred in-house, housed in individually vented cages according to UK Home Office regulations.

Statistics

Data was analysed for statistical information using Prism5 (Graphpad Software). When two groups were being compared Students t test was used and for 3 or more groups a one-way ANOVA with a Tukey's multiple comparison test used. Unless otherwise shown differences were not significant.
*= $p < 0.05$, **= $p < 0.01$ and *** $p = < 0.001$.

Computer Software

Flowjo © Tree Star was used for flow cytometry analysis.

MacVector was used for sequence analysis.

Volocity 3D Image Analysis software (PerkinElmer) was used to generate and analyse confocal images.

Openlab software (PerkinElmer) was used to generate fluorescent and light microscope images.

MacPyMOL and 3DJigsaw were used to generate 3D protein structures.

COBALT (NCBI) was used to generate sequence alignments and phylogenetic trees. All radial trees were generated using Fast Minimum Evolution (*Desper R and Gascuel O, Mol Biol Evol 21:587-98, 2004 PMID: 14694080*) with a maximum sequence difference of 0.85 and distance based on the Grishin model (*Grishin NV, J Mol Evol, 41:675-79, 1995 PMID: 18345592*).

Table 9: Vector Table

Name	Application	Manufacturer
pSSU	*Leishmania* vector	Dr A Aebischer lab
pMIBV5His	Insect select expression vector	Invitrogen
pGEM-T	Cloning vector	Promega
L4440	RNAi	Dr C Britton lab

Table 10: Restriction Digest Enzymes

Name	Supplier	Sequence showing restriction sites
Age1	Fermentas	A-CCGGT
BamH1	Fermentas	G-GATCC
BamH1	New England Biolabs	G-GATCC
Dpn1	New England Biolabs	GA-TC
EcoRV	New England Biolabs	GAT-ATC
Nde1	New England Biolabs	CA-TATG
Pme1	New England Biolabs	GTTT-AAAC
Xho1	New England Biolabs	C-TCGAG
Xba	Promega	T-CTAGA
Xho1	Promega	C-TCGAG

Table 11: Molecular biology enzymes

Name	Supplier	Cat number
Bovine serum albumin (BSA)	Promega	R396D
Calf intestinal phosphatase	New England Biolabs	M0290s
Taq	Promega	M3001
Ligase	Promega	M180A

Chapter 1

VALs: the gene, gene family and the protein.

Introduction

The SCP/TAPS family.

The **SCP** (sperm-coating protein)/ **TAPS** (Tpx-1/Ag5/PR-1/Sc7), Pfam: PF00188 has evolved over time as more and more research has been carried out into these fascinating proteins. The number of proteins bearing this motif has increased dramatically with new members described from many different species. All share the same conserved cysteine residues, which form the **SCP/TAPS** domain. One early reference to this region of the protein as a SCP domain was noted by (Kovalick & Griffin, 2005) where they examined 26 SCP/TAPS proteins from *Drosophila melanogaster*. This first reference to the SCP/TAPS family came after a 2003 release of the InterPro database (Mulder et al., 2003). The InterPro search facility now lists over 5600 proteins that are predicted to be part of the SCP/TAPS family, http://www.ebi.ac.uk/interpro/entry/IPR001283, CAP domain: http://www.ebi.ac.uk/interpro/entry/IPR014044. Even since this early mention of the SCP/TAPS domain, proteins bearing these characteristics have indeed been linked together based on both nucleotide and protein sequence; however the usage of a consistent name has eluded them. VAL molecules (**V**enom allergen/ **A**ncylostoma secreted protein-**l**ike) (Murray et al., 2001), ASP-like (***A****ncylostoma* **s**ecreted **p**rotein) (Saverwyns et al., 2008), ASP (MacDonald et al., 2005), VAH (**v**enom **a**llergen **h**omolog) (Tetteh, Loukas, Tripp, & Maizels, 1999) are all examples of terms coined to describe these proteins.

Interest in these molecules stems from the fact that they are expressed by the parasite at critical stages during the life cycle. For most helminths more than one of these molecules is found with some having as many as 25+ variants. Could it be that for a

parasite with a lifecycle that encompasses different tissues, locations or even hosts, as is the case for *Schistosoma mansoni,* that these proteins have been adapted for use at each different stage?

An early example of a filarial SCP/TAPS protein was discovered as the result of a World Health Organisation (WHO) initiative, which would see high quality cDNA libraries generated from the filarial parasite *Brugia malayi* (*B.malayi*). New genes could be identified from these libraries using an expressed sequence tag (EST) approach (Williams et al., 2000), which involves a single pass sequencing read. Of particular interest were genes from the L3 infective larvae stage, notably a homologue of an SCP/TAPS protein from the dog hookworm *Ancylostoma caninum*, Ac-ASP-1 (*Ancylostoma* secreted protein) (Hawdon, Jones, Hoffman, & Hotez, 1996). The *B.malayi* homologue was isolated using gene specific nondegenerate primers on a cDNA library. The resulting gene and protein was termed Bm-VAL-1, for **V**enom allergen/ **A**ncylostoma secreted protein-**l**ike and protein (Maizels, Gomez-Escobar, Gregory, Murray, & Zang, 2001).

The murine nematode *Helimosomoides polygyrus* (*H.polygyrus*) expresses a large SCP/TAPS family, members of which are shown in Table 1.1. These proteins follow the required amino acid sequence required to attain the SCP/TAPS nomenclature, all containing either one or two SCP domains characterized by the 6 conserved cysteine residues (Fig 1.1A). Where two domains are present these are hinged together by a threonine rich region.

Both single and double domain proteins have representatives across many different species. Examples of these are shown in Fig 1.1B listing amongst others proteins from *Necator americanus*, *Onchocerca volvulus* and *Haemonchus contortus* with putative functions ranging from transition to parasitism as described for Ac-ASP-2 (Hawdon et al., 1996) to the interaction of *H. glycines* with its host plant due to the protein being expressed in the subventral oesophageal gland cells (Gao et al., 2001a). In this chapter, I have examined the VAL family members present in *H.polygyrus.* I have examined sequence characteristics at both the DNA and protein level and

subsequently expressed them in a manner, which we hope will retain tertiary structure and thus maintain possible function. In a further attempt to search for a function to attribute to these proteins gene knockdown was attempted using RNAi, which culminated in a survey of *H.polygyrus* genes required for the success of the RNAi technique.

In depth phylogenetic analysis has been carried out for *Schistosoma mansoni* (*S.mansoni*) (Chalmers et al., 2008), (Chalmers & Hoffmann, 2012), *Drosophila melanogaster,* (Kovalick & Griffin, 2005) and parasitic trematodes, namley *Clonorchis sinensis*, *Opisthorchis viverrini*, *Fasciola hepatica* and *F. gigantica*, *Schistosoma mansoni*, *S. japonicum* and *S. haematobium* (Cantacessi et al., 2012). One study in particular carried out by Yoshino et al. (Yoshino et al., 2014) describes a venom allergen like protein from *S.mansoni,* SmVAL9, and suggests a role during tissue reorganisation and extracellular matrix remodelling.

	Name	Domains	Size (amino acids)	Location L4ES	Location HES	Location ERM	ACCESSION NUMBER
*(7)	HpVAL-1	Double	472				AEP82912.1 GI:348659350
*(3)	HpVAL-2	Double	470				AEP82917.1 GI:348659360
*(2)	HpVAL-3	Double	469				AEP82918.1 GI:348659362
	HpVAL-4	Single	213				AEP82919.1 GI:348659364
	HpVAL-5	Double	481				AEP82920.1 GI:348659366
	HpVAL-6	Double	417				AEP82921.1 GI:348659368
*(5)	HpVAL-7	Single	235				AEP82922.1 GI:348659370
*(3)	HpVAL-8	Double	419				AEP82925.1 GI:348659376
	HpVAL-9	Double	443				AEP82926.1 GI:348659378
	HpVAL-10	Single	257				AEP82927.1 GI:348659380
	HpVAL-11	Single	267	SEQUENCE INFORMATION NOT COMPLETE			
	HpVAL-12	Double	453				AEP82928.1 GI:348659382
	HpVAL-13	Single	232				AEP82929.1 GI:348659384
	HpVAL-14	Double	440				AEP82930.1 GI:348659386
	HpVAL-15	Single	223				AEP82931.1 GI:348659388
	HpVAL-16	Double	464				AEP82932.1 GI:348659390
	HpVAL-17	Double	462				AEP82933.1 GI:348659392
	HpVAL-18	Double	462				AEP82934.1 GI:348659394
*(2)	HpVAL-19	Double	467				AEP82935.1 GI:348659396
	HpVAL-20	Double	473				AEP82936.1 GI:348659398
	HpVAL-21-25	Double	SEQUENCE INFORMATION NOT COMPLETE				

High level gene expression

Medium level gene expression

Low level gene expression

VAL proteins with isoforms. *

Table 1.1 VAL proteins from *H.polygyrus.*

VAL proteins identified from *H.polygyrus* are shown with accession numbers, protein size and domain number. Gene expression levels are also indicated by blue, pink or red shading (Hewitson et al, 2013).
L4 ES: excretory/ secretory products from 4th stage larvae. HES: adult excretory/ secretory products. ERM: egg released material. The number of isoforms for a given protein is also shown in brackets with an asterisk *.

A

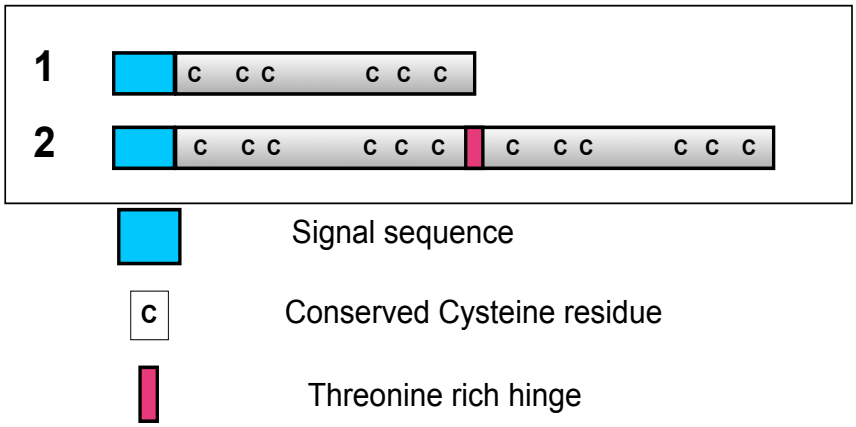

B

Species	Protein	Accession number	Predicted function
SINGLE DOMAIN PROTEINS			
Ancylostoma caninum	ASP-2	AAC35986	Transition to parasitism
Necator americanus	Na-ASP-2	AAP41952	Unknown
Haemonchus contortus	Haemonchus 24kDa	U64793	Unknown
Onchocerca volvulus	OvASP-2	AAB69625	Unknown
Brugia malayi	Bm-VAL-1	AAK12274	Invasion of host
Meloidogyne incognita	*Meloidogyne* secreted protein	AF0132289	Unknown
Heterodera glycines	Hd-VAL-1	AF374388	Relationship with host
DOUBLE DOMAIN PROTEINS			
Ancylostoma caninum	ASP-1	AAD13339	Released during infection
Ancylostoma ceylanicum	AcASP-2	AAN11402	Unknown
Necator americanus	NaASP-1	AAD13340	Unknown
Haemonchus contortus	Haemonchus 40kDa	AAC03562	Unknown

Fig 1.1 Structural configuration of SCP/TAPS proteins.

Fig 1.1 Structural configuration of SCP/TAPS proteins.

A. VAL proteins belong to the larger SCP/TAPS: **SCP**: **s**perm **c**oating **p**rotein, **TAPS**- **T**px-1, **A**g5, **P**r-1, **S**c7, family which is characterised by the presence of a conserved group of 6 cysteine residues. These conserved residues make up the **SCP** domain.
VAL proteins fall into one of two categories: **single** or **double** domain. Where a protein has two SCP domains present these are hinged together by a threonine rich hinge like region.

B. SCP/TAPS proteins have been identified in many parasitic nematodes. A selection of single and double domain proteins with their accession numbers and possible functions is shown.

Results

1.2 - 1.4 Phylogenetic tree of the VAL protein family in *H.polygyrus*.

Most VAL proteins identified from *H.polygyrus* fall into two discrete groups based on the number of SCP domains present, however HpVAL3, 6 & 8 (shown with purple arrows) are double domain proteins within lineages of single domain homologues. This can be seen in Fig 1.2 where a radial phylogenetic tree, based on that as described by (Desper & Gascuel, 2004), was generated using COBALT (Constraint-based multiple alignment tool, NCBI). Results here underline the broad evolutionary diversity found in the HpVAL family. This diversity continues with regards to stage specificity (Hewitson et al., 2013) as VAL proteins can be detected in adults (HpVAL-1), day 3/day 5 larvae (HpVAL-28) but HpVAL-4 can be detected in stages from day 3 larvae through to adults.

The double domain members of the HpVAL family were further examined in Fig 1.3 where radial trees were generated. Generally, isoforms of each VAL protein, grouped together as would be expected and has been described for VAL proteins from *A.caninum* (Qiang et al., 2000) and *Cooperia punctata* (Yatsuda, Eysker, Vieira-Bressan, & De Vries, 2002). Fig 1.4 (A) shows a phylogenetic tree generated to examine the similarities of N and C-terminal SCP domains and how they relate to the single domain VAL proteins within the *H.polygyrus* family. The resulting tree shows N and C terminal domains grouping together as would be expected, however two of the single domain VALs (VAL-4 & 15) group with the N-terminal domains and another two (VAL 7 & 10) group with the C-terminal domains. Notably, if two VAL N-terminal SCP domains are closely associated it does not follow that the C-terminal SCP domains will be, e.g. the C-terminal domains of HpVAL-18 is most similar to HpVAL-19, the same is true for their N-terminal domains. However, the C-terminal domain of HpVAL-12 is most similar to HpVAL-9&5 but the N-terminal domain groups with HpVAL-3.1.

Fig 1.4 (B) illustrates VAL protein families from both *H.polygyrus* and *Schistosoma mansoni.* Both of these parasite species have large VAL families, however *S.mansoni* has predominantly single domain VAL proteins. The phylogenetic tree shows that although VAL proteins from *S.mansoni* are quite different from *H.polygyrus* VALs, they are more similar to the C-terminal domains of VALs found in *H.polygyrus*.

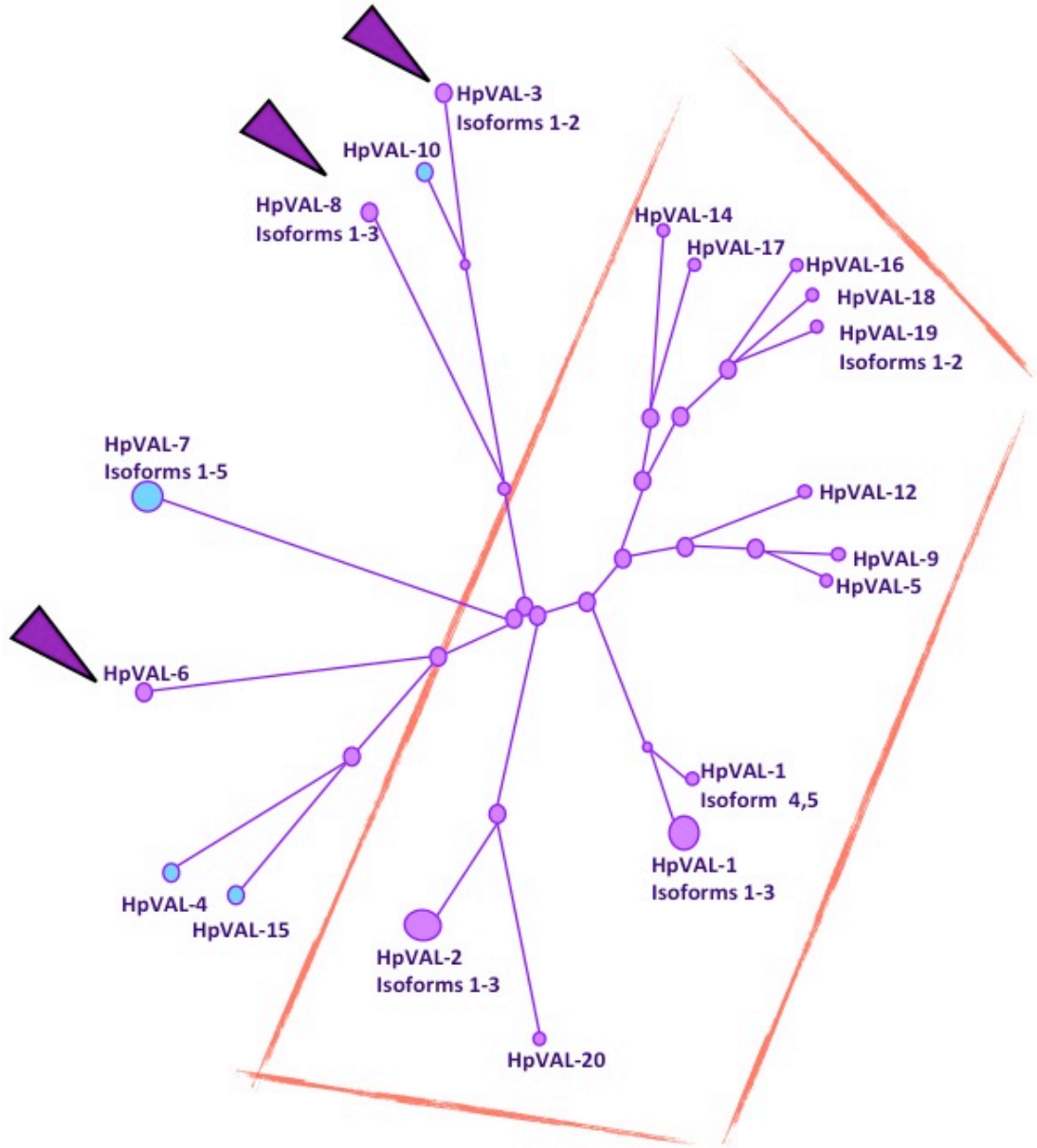

Fig 1.2 Phylogenetic tree of the complete VAL protein family in *H.polygyrus*.

Protein sequences for VAL members in *H.polygyrus* were submitted to COBALT. A radial tree was generated using Fast Minimum Evolution (*Desper R and Gascuel O, Mol Biol Evol 21:587-98, 2004 PMID: 14694080*) with a maximum sequence difference of 0.85 and distance based on the Grishin model (*Grishin NV, J Mol Evol, 41:675-79, 1995 PMID: 18345592*).

Single domain VAL proteins are labeled pale blue. Large circles indicate more than one sequence variant. Double domain proteins (boxed in red) are labeled purple and appear to have diverged at some point from single domain VALs. Purple arrows show double domain VAL proteins within lineages of single domain homologues.

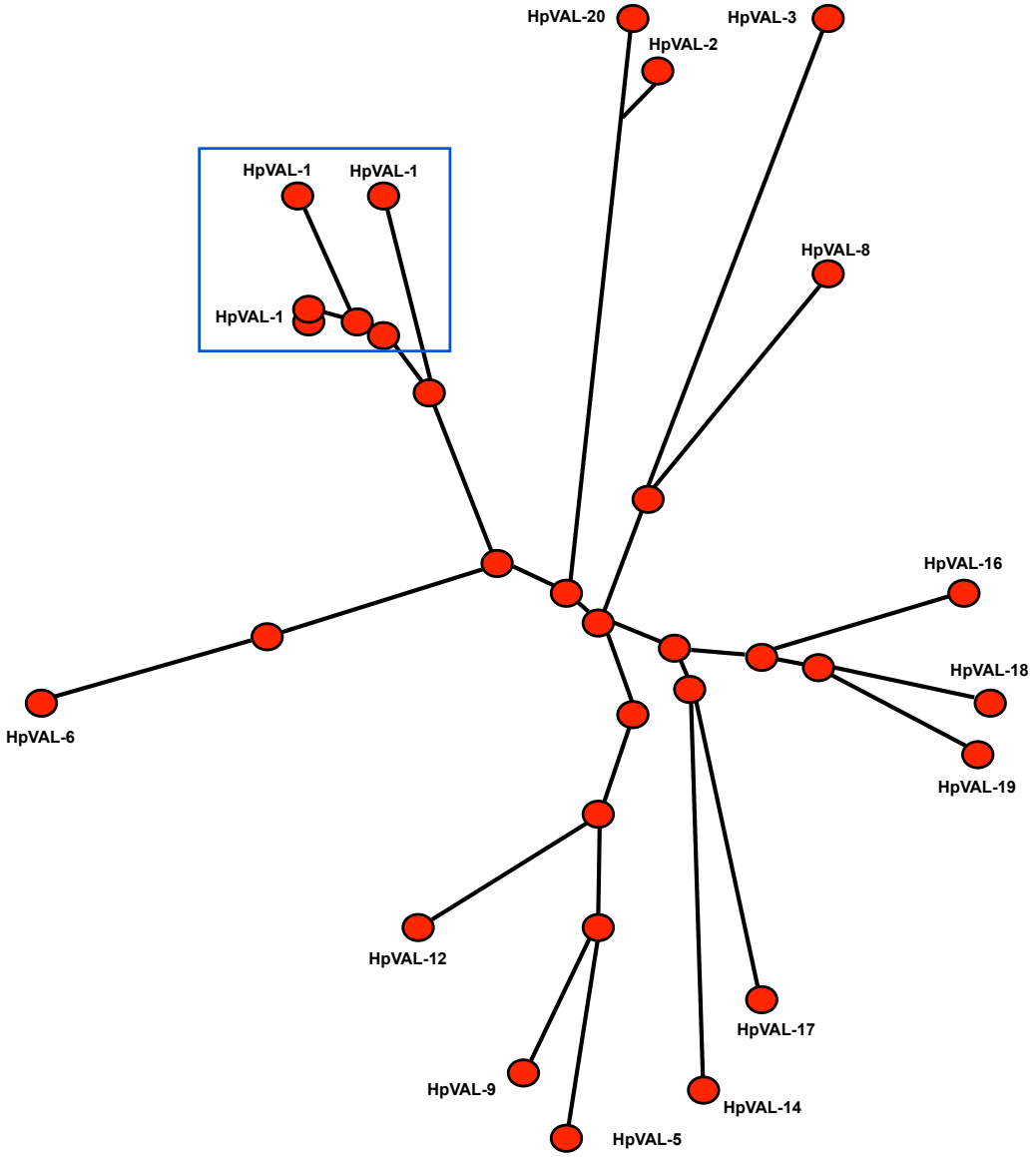

Fig 1.3 Phylogenetic tree showing double domain members of the VAL protein family in *H.polygyrus*.

Protein sequences for double domain VAL members in *H.polygyrus* were submitted to COBALT. Radial tree was generated using Fast Minimum Evolution (*Desper R and Gascuel O, Mol Biol Evol 21:587-98, 2004 PMID: 14694080*) with a maximum sequence difference of 0.85 and distance based on the Grishin model (*Grishin NV, J Mol Evol, 41:675-79, 1995 PMID: 18345592*). Double domain VAL proteins- HpVAL-1, 2, 3, 5, 6, 8, 9,12,14,16,17,18,19, 20. 3,6 & 8 fall with single domain VALs in full phylogenetic tree, Fig. 1.2.

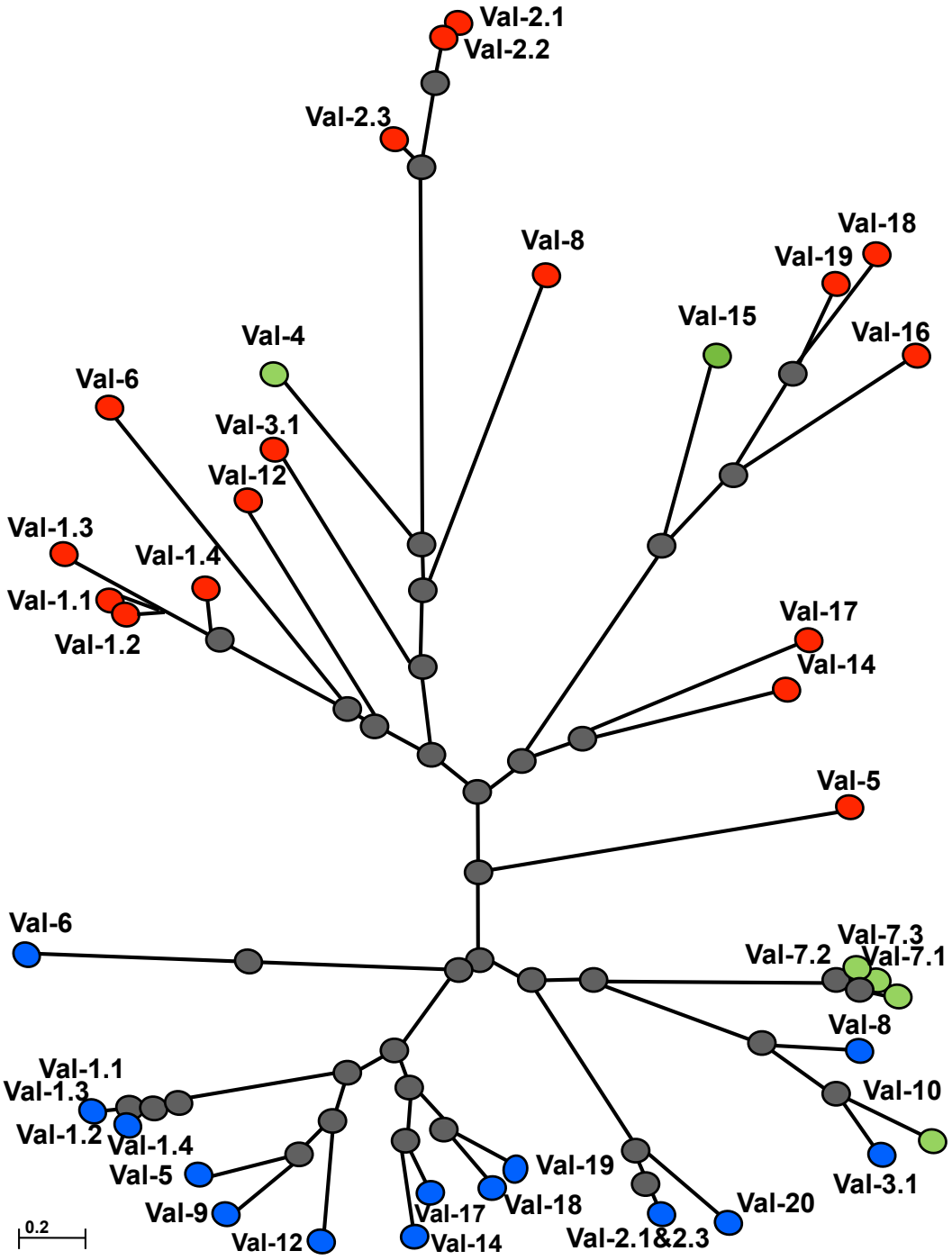

Fig 1.4 (A) Phylogenetic tree showing SCP/TAP domains of the VAL protein family in *H.polygyrus*.

Fig 1.4 (A) Phylogenetic tree showing SCP/TAP domains of the VAL protein family in *H.polygyrus*.

Protein sequences for N (RED) and C-terminal (BLUE) SCP domains in *H.polygyrus* were submitted to COBALT. A radial tree was generated using Fast Minimum Evolution (*Desper R and Gascuel O, Mol Biol Evol 21:587-98, 2004 PMID: 14694080*) with a maximum sequence difference of 0.85 and distance based on the Grishin model (*Grishin NV, J Mol Evol, 41:675-79, 1995 PMID: 18345592*). Generally N and C-terminal domains group together with HpVAL-4 and 15 grouping with N-terminal domains and HpVAL-7 and 10 grouping with C-terminal domains.

N-terminal SCP domain- blue nodes
C-terminal domain- red nodes
Single domain- green nodes

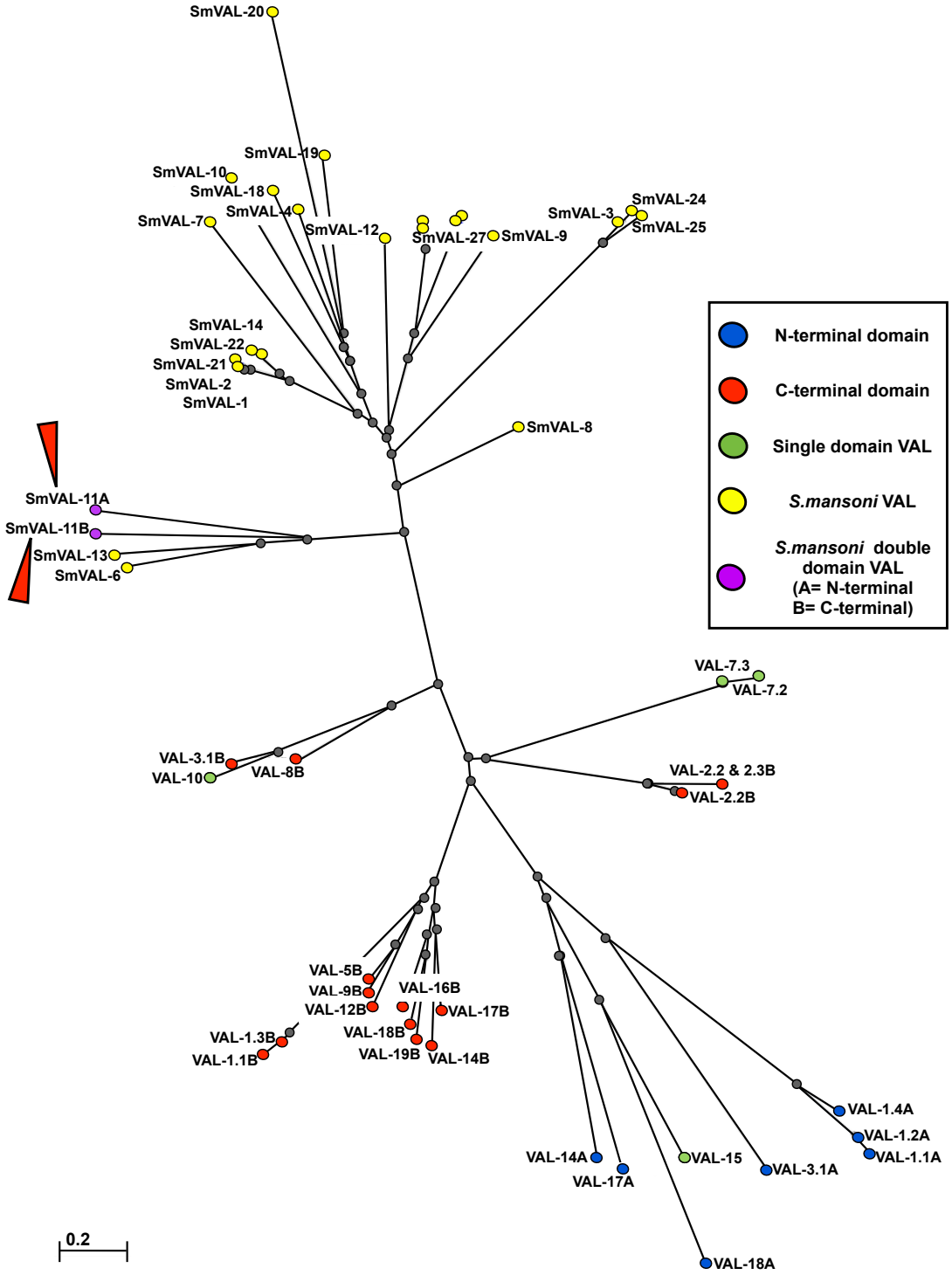

Fig 1.4 (B) Phylogenetic tree showing SCP/TAP domains of the VAL protein family in *H.polygyrus* and *S.mansoni*.

Fig 1.4 (B) Phylogenetic tree showing SCP/TAP domains of the VAL protein family in *H.polygyrus* and *S.mansoni*.

Protein sequences for N (RED) and C-terminal (BLUE) SCP domains in *H.polygyrus* were submitted to COBALT. *S.mansoni* sequences are denoted by yellow symbols and the S.mansoni double domain VAL is shown in pink and highlighted with red arrows.

A radial tree was generated using Fast Minimum Evolution (*Desper R and Gascuel O, Mol Biol Evol 21:587-98, 2004 PMID: 14694080*) with a maximum sequence difference of 0.85 and distance based on the Grishin model (*Grishin NV, J Mol Evol, 41:675-79, 1995 PMID: 18345592*). Generally *S.mansoni* VAL proteins appear to have evolved quite separately from *H.polygyrus* VAL proteins, however they are more similar to the C-terminal domains of *H.polygyrus* VAL proteins

H.polygyrus N-terminal SCP domain- blue nodes
H.polygyrus C-terminal domain- red nodes
Single domain- green nodes
S.mansoni VAL proteins- yellow nodes
S.mansoni double domain VAL- pink nodes

1.5 Phylogeny of SCP/TAPS family members across species.

There is great sequence diversity in the SCP/TAPS family at both the nucleotide and protein level. When *H.polygyrus* VAL protein sequences are aligned the resultant phylogenetic tree separates the proteins based on the number of SCP domains present (Fig 1.2). When VAL protein sequences from other nematodes, both parasitic and free-living, are included the double domain VAL proteins from *H.polygyrus* form a group distant from most other VAL representatives of both the single and double domain variety.

The VAL protein family from *S.mansoni* was found to also split in two distinct groups (Chalmers et al., 2008). This grouping was based not on SCP domain number but on the presence or absence of a signal sequence and a set of conserved cysteine residues for members of Group 1 and 2 respectively. By far the majority of VALs contained a signal sequence and the conserved cysteines thus were found in Group 1. But a small number, SmVAL6, 13, 16, 17 and 11 contained no signal sequence and were found in Group 2. These proteins also contained two sequence insertions not found in Group 1. Interestingly, when any of the Group two SmVAL sequences were included in an assembly of HpVAL proteins, a proper alignment was not achieved. However when members of Group one were included assembly of amino acids could be achieved, with SmVAL2, 4 and 6 clustering with HpVAL-3, 4 and 10 (pink grouping) (Fig 1.5).

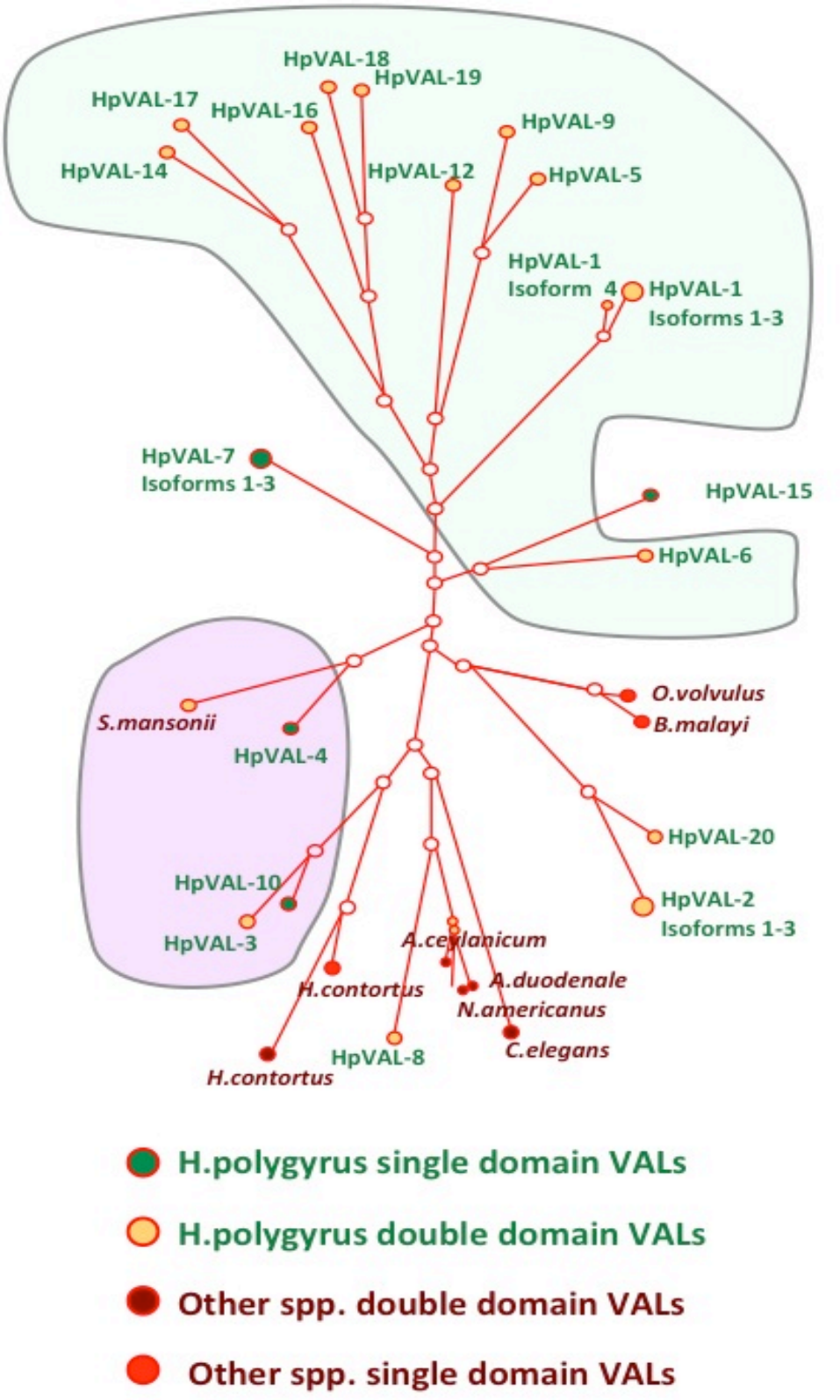

Fig 1.5 Phylogeny of SCP/TAPS family members across species.

Fig 1.5 Phylogeny of SCP/TAPS family members across species.

Protein sequences for SCP/TAPS members in *H.polygyrus* and other nematodes were submitted to BLAST. Radial tree was generated using Fast Minimum Evolution (*Desper R and Gascuel O, Mol Biol Evol 21:587-98, 2004 PMID: 14694080*) with a maximum sequence difference of 0.85 and distance based on the Grishin model (*Grishin NV, J Mol Evol, 41:675-79, 1995 PMID: 18345592*).

S.mansoni: gi/353232981, *H.contortus*: gi/2329928, *A.ceylanicum:* gi/23268455, *A.duodenale:* gi/3719257*, H.contortus:* gi/ 2905792*, O.volvulus:* gi/ 5868902*, B.malayi:* gi/ 3095442*, C.elegans:* gi/ 74963711*, N.americanus:* gi/ 3396070.

1.6 – 1.10 HpVAL-1 & 4 have structural similarity to proteins with known SCP domains.

Cysteine-rich secretory proteins, **a**ntigen 5 and **p**athogenesis related proteins, the latter group of which VAL proteins fall into, make up the **CAP** superfamily. Studies on the tertiary structure of these proteins show striking conservation based on the core elements namely the SCP domain (Gibbs, Roelants, & O'Bryan, 2008). Protein structural studies on Ves v 5, a major allergen from yellow-jacket venom (Henriksen et al., 2001), *Ostertagia ostertagi* ASP-1 (Borloo et al., 2013), *Necator americanus* Na-ASP-2 (Asojo et al., 2005), (Mason et al., 2014), the plant pathogenesis-related protein P14a (Fernandez et al., 1997), *Ancylostoma ceylanicum* excretory-secretory protein 2 (AceES-2) (Kucera, Harrison, Cappello, & Modis, 2011), platyhelminth VAL studies (Chalmers & Hoffmann, 2012) and the human glioma pathogenesis related protein (HuGliPR) (Szyperski, Fernández, Mumenthaler, & Wüthrich, 1998) have uncovered tertiary structural homologies between these otherwise diverse molecules. Amino acid identities of these VAL proteins are listed in Table 1.2.

	% identity to HpVAL-1
HpVAL-4	23
AceES-2	54
Oo-ASP-1	27
HuGliPR	27
Na-ASP-2	30
Plant pathogenesis protein P14a	44

Table 1.2 Identity shared between VAL proteins and HpVAL-1

MacPymol generated a 3D protein structure of HpVAL-1 (Fig 1.6) from a PDB file made using 3D-Jigsaw, with the N- and C-terminal SCP domains denoted by pink and green respectively. These SCP domains lie as distinct regions of the protein linked by the hinge region denoted in blue. The start and end of the protein are indicated with arrows. The secondary structure of HpVAL-1 was also generated using MacPymol showing the positioning of loop, α-helices and β-sheets (Fig 1.7) coloured in magenta, cyan and red respectively. The N and C-terminal SCP domains differ with the N-terminal domain containing 3 β-sheets and the C-terminal domain containing two.

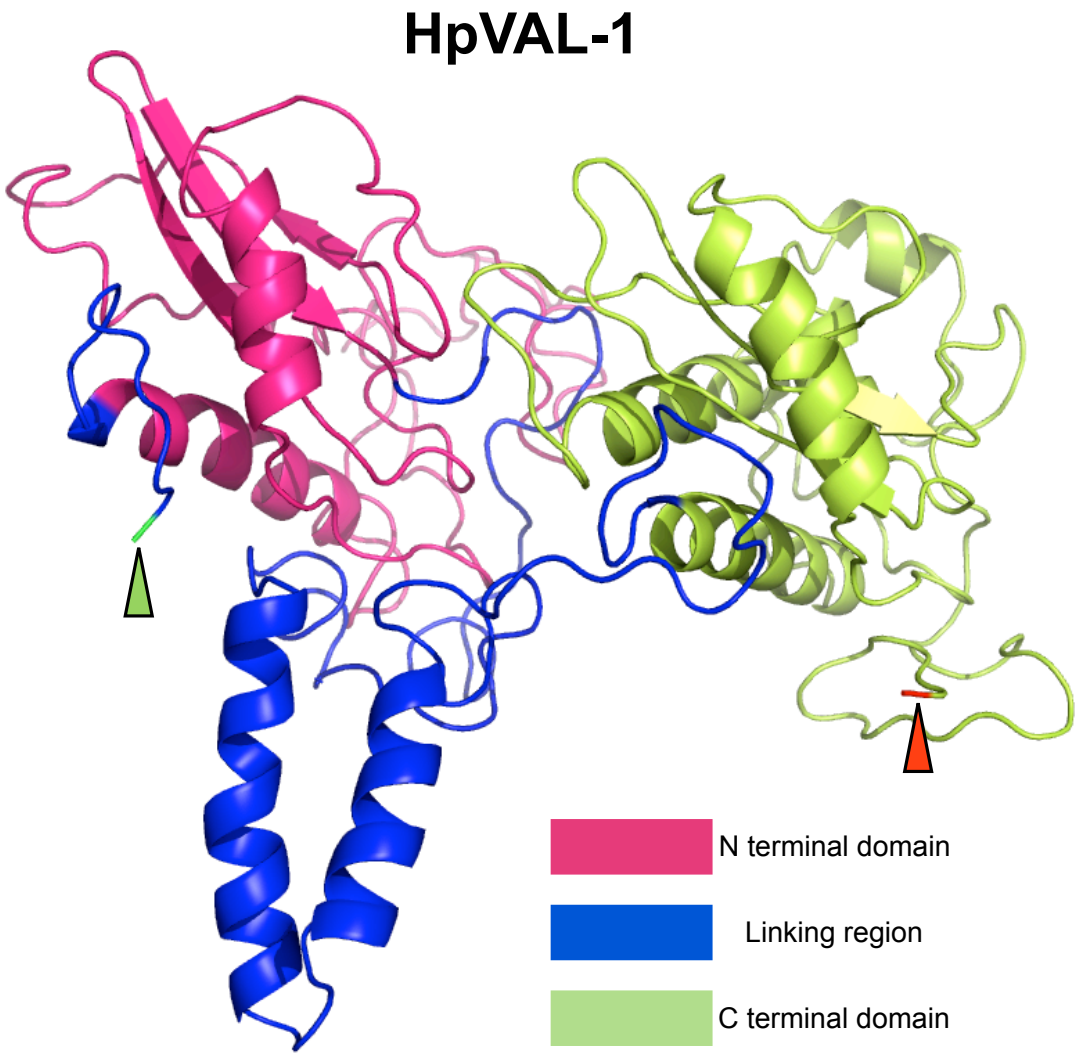

Fig 1.6 HpVAL1 has structural similarity to proteins with known SCP domains.

Amino acid sequence of each VAL protein was copied in the 3Djigsaw (http://bmm.cancerresearchuk.org/~3djigsaw/http://bmm.cancerresearchuk.org/~3djigsaw/) program which generates a PDB file based on sequence similarities within the PDB database. MacPyMOL (PyMOL, DeLano Scientific) was then used to generate a cartoon image showing the 3D structure of the protein based on known structures from the database.

Here the 3-D structure of HpVAL-1 is shown with both the N and C-terminal SCP domains highlighted in pink and green respectively. The N terminal start is shown using a green arrow and end of the protein is shown using a red arrow. β-sheets are shown as flat arrow structures and α-helices as coiled structures.

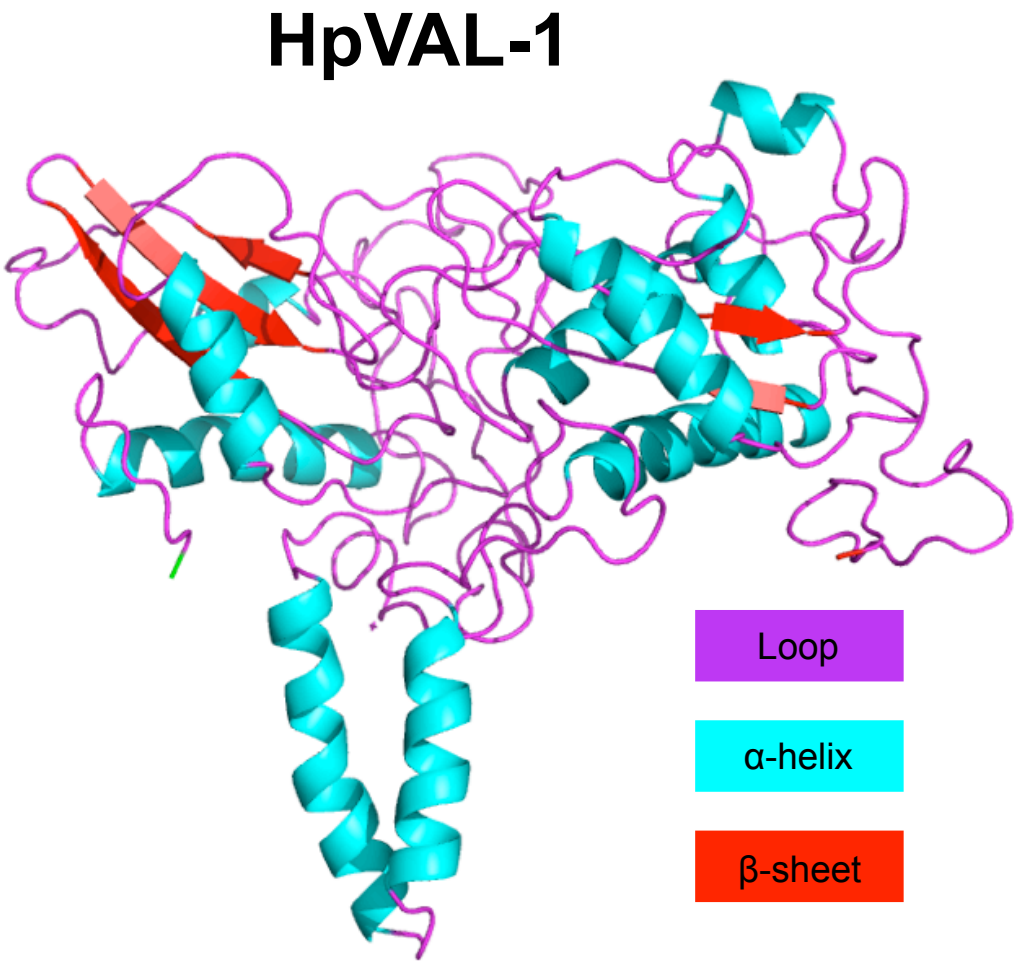


```
  1  mwlplillsa vanregtatt cpgnsgvtda artaaldain earrtavngl mqngatagtn
 61  lphgsnmyml ewdcnleala gvmvpndcsa ptaglpnngl saavvtpapt tadavmtqgv
121  aswpvllqta anafappaag tpvkyegpta gaalpadvlp lgnmirgstt kvgctvkict
181  aqavlvclyd qpdlkqgdtv ydagtgvcqn stadklctly ppptcdiytg lcvktdvttt
241  ttpsatttas tlavfpggag gtggtggsrg tggtggtgga ntrcpqnpqm tddlrylfrd
301  mhnyrrseta lgrtikntgn ylpsssnmqy mryscplevt aihiastcpg sliqsgrlig
361  qvpigaytft tatqdivksl wrvvrqvngp gmqvtfkaqh vgtpiasftq mawaasrrlg
421  cavarcptay iavcnyepig nivgqqiytp gtpctactyg stctatqglc tlp
```

Fig 1.7 HpVAL-1 Showing primary and tertiary structure

The secondary structure of HpVAL-1 was generated using MacPymol. Loop, α-helix and β-sheet structures are denoted in magenta, cyan and red respectively.

1.8 HpVAL-4 showing SCP domain and secondary structure.

3D and secondary structures for HpVAL-4 (Fig 1.8 A and B) were also generated using MacPymol to show the association of the SCP domain with the loop, α-helices and β-sheet structures. Interestingly the SCP domain of HpVAL-4 contained only two β-sheet structures as was seen in the C-terminal SCP domain of HpVAL-1.

1.9 HpVAL-4 SCP domain aligns to the C terminal domain of HpVAL-1.

In Fig 1.9, these 3D structures, HpVAL-1 and HpVAL4, were aligned using MacPymol. Here HpVAL-4 associated more closely with the C-terminal domain from HpVAL-1. This is contrary to the phylogenetic prediction shown in Fig 1.4, which shows the HpVAL-4 SCP domain associating more closely with N-terminal SCP domains. This inability to form a theoretical 3D structure with the N-terminal SCP domain may be due to the presence of two domains and the linker region.

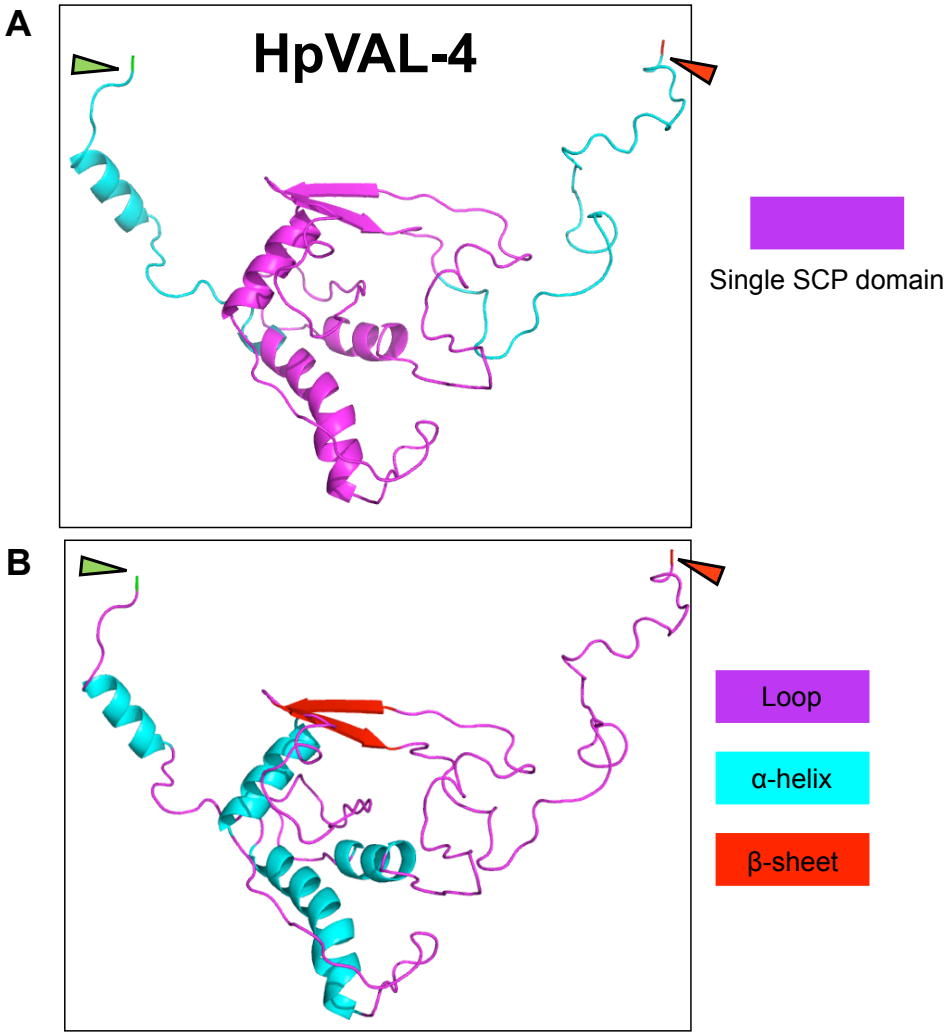


```
1   mstlptvsfl vvlvalgkae fgcdgtleqn dttrevflrf hndvrkfial giypnkvgvl
61  gpaknmyqlk wscdleeeah esiyscsynp lllhpqsysk llsvdlpdtd vvgatlemwt
121 efmriygvnt ktnsynpsfs qfanmayskn tkvgcsykkc ggdtlvtcvy elgvklpshp
181 qmwengptcv cvaytdsicn dnnlceyapt sar
```

Fig 1.8 HpVAL-4 Showing SCP domain and tertiary structure.

A. 3-d structure of the single SCP domain HpVAL-4 protein was generated in as described in Fig 1.6.SCP domain denoted by pink structure. The N and C terminal start and finish of the protein are indicated with arrows.

B. Tertiary structure was generated from primary structure amino acid sequence, which was submitted to MacPymol. Loop, α-helix and β-sheet structures are denoted in magenta, cyan and red respectively.

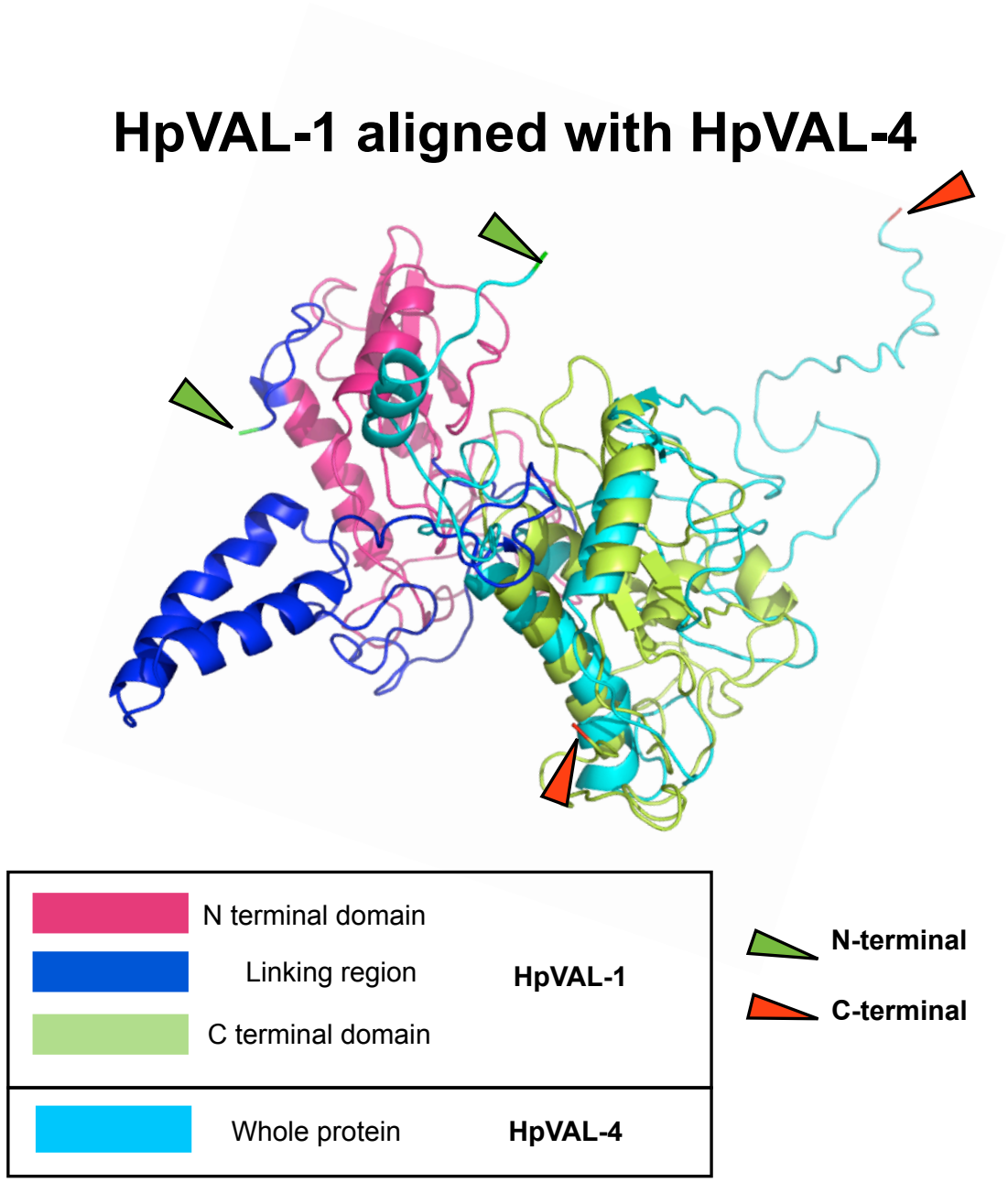

Fig 1.9 HpVAL-4 SCP domain aligns with the C terminal domain of HpVAL-1.

3D structures of HpVAL-1 and HpVAL-4 were aligned using MacPymol. HpVAL-1 is denoted by 3 colours:

N-terminal SCP domain= magenta.
C-terminal SCP domain= green.
Linker region = blue.
HpVAL-4= cyan.

HpVAL-4 aligns to the C-terminal domain of HpVAL-1.

1.10 HpVAL-1 and HpVAL-4 3D structures align with Ves v5, a major allergen from Yellow-jacket venom.

When investigating putative functional properties of a protein, insights can often be gained by examining the 3D structure. As VAL proteins are denoted by the presence of an SCP domain both HpVAL-1 and HpVAL-4 were compared to Ves v5, one of the three main allergens found in yellow-jacket wasp venom (Henriksen et al., 2001) and a protein which is a member of the pathogenesis related proteins group based upon amino acid identity; as such it contains a single SCP domain. VesV5 is also one of the top hits when *H.polygyrus* VALs are submitted to the sequence database.
The 3D protein structure of Ves v5 (1QNX) (Fig 1.10A) was matched against 3D structures from HpVAL-1 (Fig 1.6) and HpVAL-4 (Fig 1.8A). The percentage sequence identities for amino acids between HpVAL-1, HpVAL-4 and Ves v5 are listed in Table 1.3. Interestingly VesV5 also aligns with the C-terminal of HpVAL-1 as was seen for HpVAL-4. Thus the SCP domain of HpVAL-4 groups phylogenetically with N-terminal SCP domains but does not align to these domains based upon 3d structure instead aligning with the C-terminal domain. In addition, a known SCP domain containing venom allergen, Ves v5, also aligns with the C-terminal domain of HpVAL-1.

	% identity to Ves v5
HpVAL-1	24
HpVAL-4	36

Table 1.3 Amino acid identities shared between VAL proteins and Ves v5.

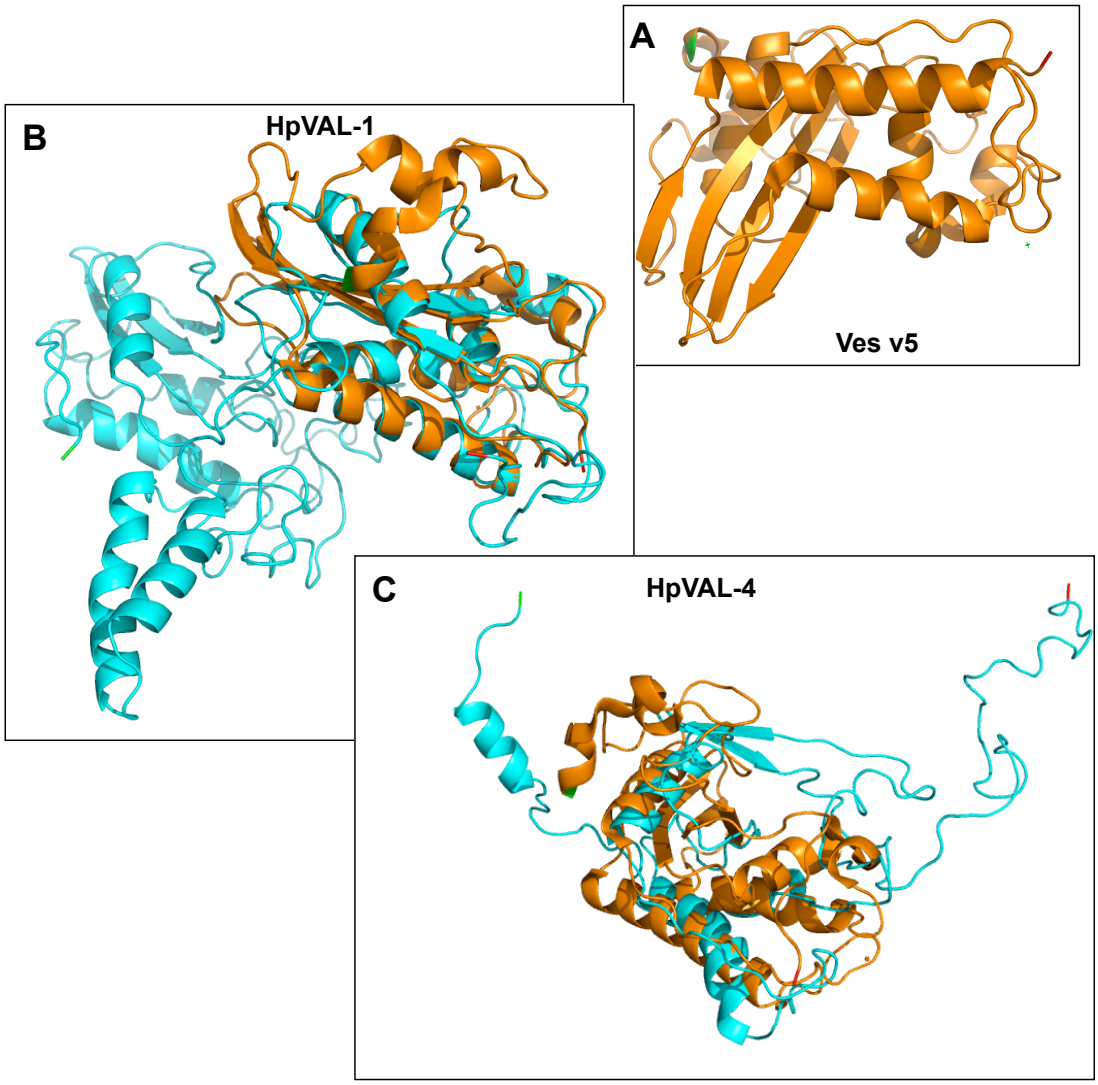

Fig 1.10 HpVAL-1 and HpVA-4 3D structures align with Ves v5, a major allergen from Yellow-jacket venom.

3D structures were generated by submitting a protein database file (pdb) to MacPymol:

A Ves v5: yellow-jacket allergen (single SCP domain)
B HpVAL-1 (double SCP domain) is shown in blue and aligned to Ves v5 which is shown in orange.
C HpVAL-4 (single SCP domain) is shown in blue and aligned to Ves v5 which is shown in orange.

1.11 Insect cell expression.

A number of caveats lie around the use of a recombinant protein when studying the properties that its native form may exert either *in vitro* or *in vivo*; is it folded correctly, are there any contaminants from the expression system, is it degraded or is it indeed at all soluble? Much of the preliminary work done on VAL proteins from either *B.malayi* or *H.polygyrus* has been carried out with recombinant protein produced in a bacterial system. Bacterial expression has many benefits over other systems, being relatively easy to produce good quantities of recombinant protein. Even if this protein is not folded correctly it can be used to produce antibodies with which further characterization can be achieved. However, if there were any requirement to examine protein interactions with specialized cells then conformation of the protein structure would be critical as would be the requirement for it to be free of LPS contamination.

To this end, two HpVAL proteins, the single domain HpVAL-4 and the double domain HpVAL-1, were cloned into an insect cell expression system. The InsectSelect™ system from Invitrogen allows expression of the protein to be driven by the *OpiE2* promoter and secretion of the recombinant protein via a Honeybee melittin secretion (HBM) signal sequence (Tessier, Thomas, Khouri, Laliberte, & Vernet, 1991) (Fig 1.11). The *OpiE2* and *OpiE1* promoters originate from the baculovirus *Orgyia pseudotsugata* allowing protein expression in *Spodoptera frugiperda* (SF9), SF21 and *Trichoplusia ni* (Hi5) insect cell lines. An ampicillin resistance gene is present for the selection of positive clones in *E.coli* during cloning whilst generation of stable cell lines occurs via blasticidin selection. This system also allows transfection of various cell lines so that expression levels for each can be observed empirically. Once expression has been achieved, the recombinant protein can be purified by means of a 6xHIS tag directly from the insect cell media.

Inserts were generated using PCR primers that contained BamH1 and Age1 restriction sites to allow ligation into the vector whilst maintaining reading frame with the HBM signal sequence at the 5' end and the 6xHIS tag at the 3' end.

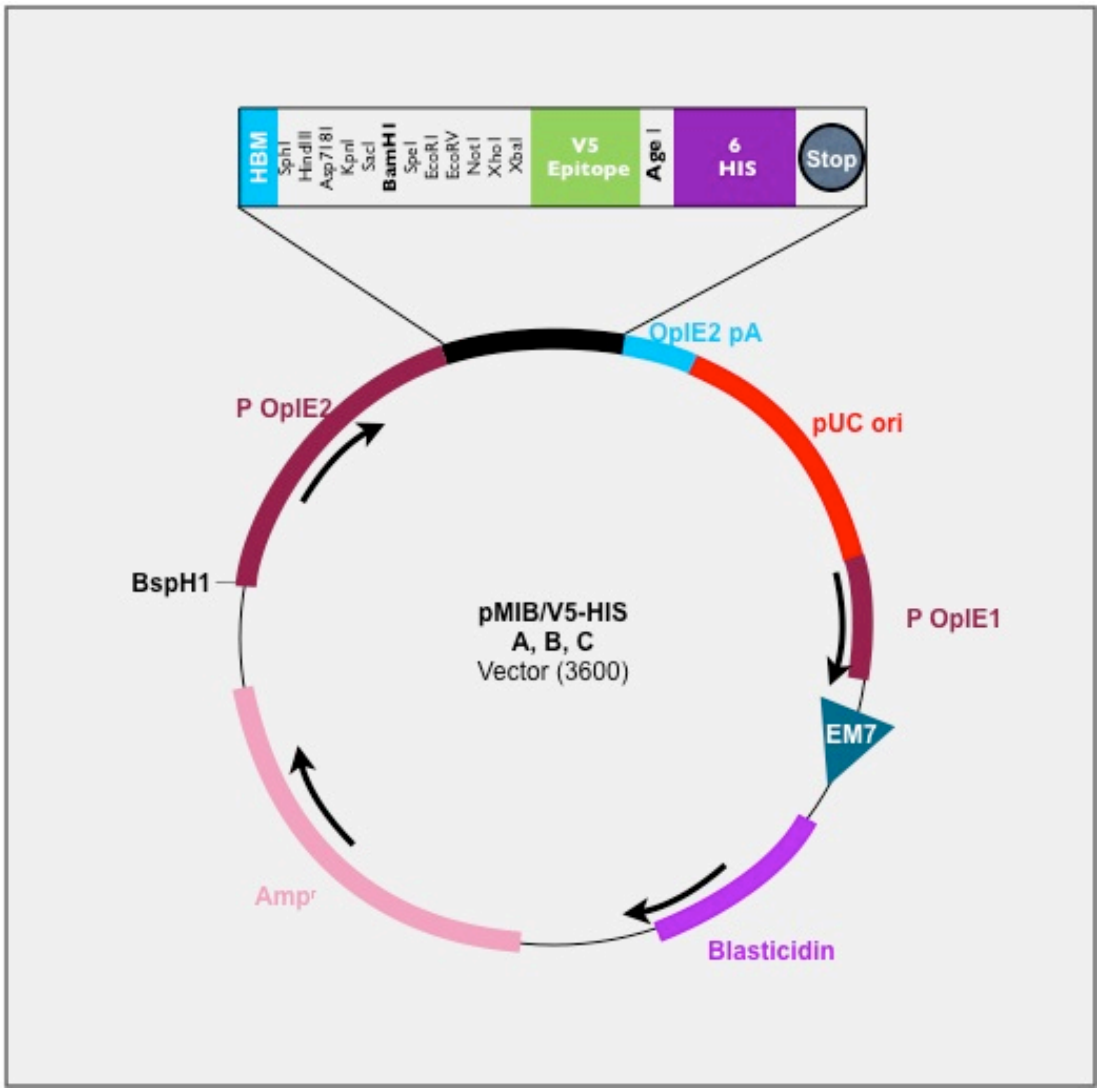

Fig 1.11 Insect cell expression vector map.

HpVAL-1 & 4 cloned into the insect cell expression vector pMIBV5-HIS. **BamH1** and **Age1** restriction sites used, thus retaining the honey bee melittin signal sequence ensuring secretion of the protein and the 6-HIS tag allowing for protein purification.
Presence of the blasticidin resistance gene allowed for the selection of stable cell lines whilst selection of *E.coli* clones was mediated by ampicillin resistance.

1.12 Codon Optimization for enhanced protein expression.

Most amino acids can be coded for by more than one codon and most organisms show a preference for one of the codons able to make a specific amino acid. For example, bacteria may code for a particular amino acid with a different combination of nucleotides to that preferred by helminths or mammals. Table 1.4 shows the nucleotide combinations that can be used to generate the amino acid serine, and the frequency with which different organisms use each arrangement. Due to this having a potentially profound effect on the expression of a protein it is wise to ensure that a sequence being inserted into a vector for the specific purpose of protein production in insect cells should present a set of optimized codons for that particular system.

	Frequency/ 1000					
Serine	TCT	TCC	TCA	TCG	AGT	AGC
E.coli	10.4	9.1	8.9	8.5	9.9	15.2
C.elegans	16.8	10.7	20.4	12.1	12.1	8.3
Insect	10.8	14.1	9.2	7.2	6.7	10.1
Yeast	23.6	14.2	18.8	8.6	14.2	9.7

Table 1.4 Codon usages for serine.
The amino acid serine can be coded for by six different nucleotide combinations. Different organisms will preferentially utilise certain arrangements. When expressing a recombinant protein in a particular system this must be taken into account. Frequency/1000 value represents the No. of codons present per 1000 bases in the input sequence(s) used to generate the codon usage table.

Sequences for HpVAL-1 and HpVAL-4 were submitted to the Graphical Codon Usage Analyser where each triplet position was compared to the usage table of the chosen organism. The codon-optimized sequence was then submitted to GeneArt to synthesise DNA inserts complete with BamH1 and Age1 restriction sites for cloning, which were then supplied in a pMA-T vector. PCR products were ligated into the cloning vector pGEM-T and sequenced. Successful restriction of the insert and ligation into the pMIBV5-HIS vector was also confirmed by sequencing.

1.13 HpVAL-1 & 4 both express in Hi5 and SF9 insect cells

Constructs containing HpVAL-1 and HpVAL-4 in the pMIBV5-HIS vector were transfected into Hi5, SF9 or SF21 cells by lipid mediated transfection. Cell number and concentration of DNA to be transfected were determined empirically. Three days following transfection cells were selected for positive integration of the construct by the addition of Blasticidin S at either 50µg or 80 µg/ml. Two concentrations of Blasticidin S were tested to obtain optimal selection of positive clones. Blasticidin S, isolated from *Streptomyces griseochromogenes,* inhibits protein synthesis in both prokaryotic and eukaryotic cells (Takeuchi, Hirayama, Ueda, Sakai, & Yonehara, 1958; Yamaguchi, Yamamoto, & Tanaka, 1965). Where cells have been successfully transfected by the pMIB/V5 construct the Blasticidin resistence gene (BSD) will allow production of Blasticidin S Deaminase, which converts blasticidin S (BS) to a non-toxic deamino-hydroxy derivative. Supernatants from cell culture were harvested and concentrated using Vivaspin ™ sample concentrators before analysis by SDS PAGE and western blotting using α-HpVAL-1 and α-HpVAL-4 polyclonal antibodies for detection of recombinant protein.

Both HpVAL-1 and HpVAL-4 were produced and secreted into the cell media by Hi5 (Fig 1.12 A) and SF9 (Fig 1.12 B) cells. Once it was determined that recombinant protein was being secreted the concentration of Blasticidn S was reduced to 10µg/ml in order to maintain the plasmid within the cells. SF9 cells were tested following expression analysis in Hi5 cells thus cell extracts were not analysed as secreted expression had already been established in Hi5 cell.

It is important to have putative control proteins that have been produced in the same expression system, thus VAL proteins from *Brugia malayi* (BmVAL-1) and *Caenorhabditis elegans* (Clone F49E11.6) were chosen as examples of single domain VAL proteins from a parasitic and a non-parasitic, free-living nematode respectively (Murray, 2007)(Data not shown).

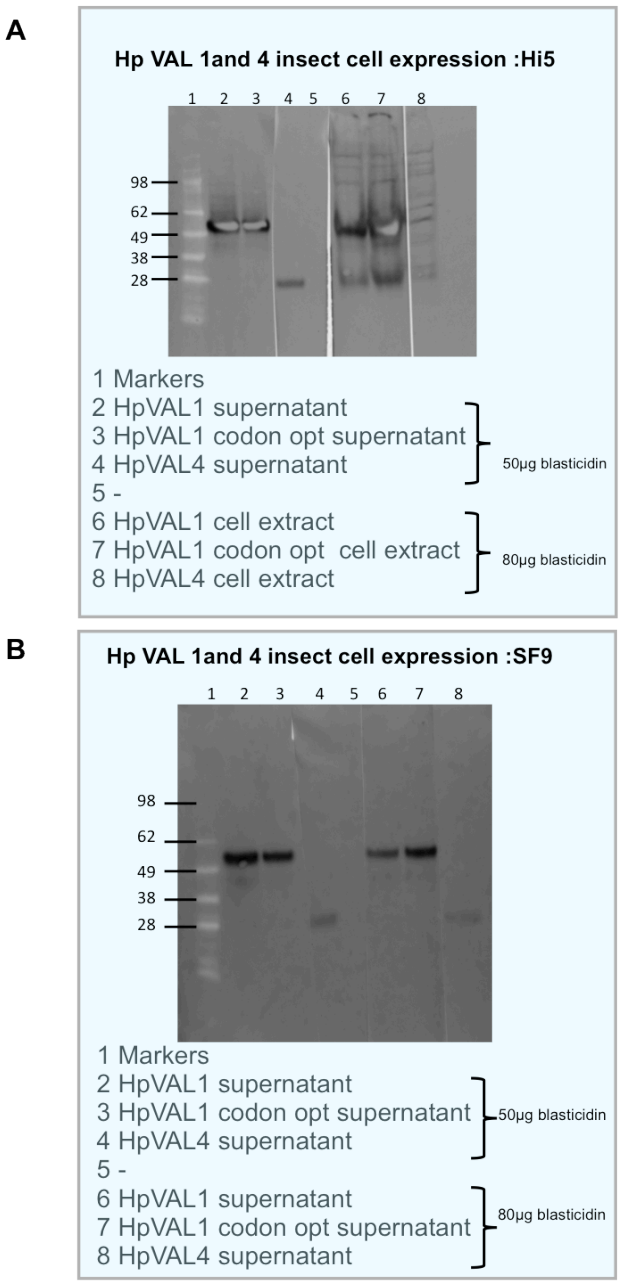

Fig 1.12 HpVAL-1 and 4 both express in Hi5 and SF9 insect cells. HpVAL1and 4 constructs were transformed into **(A)** Hi5 and **(B**) SF9 cells using a lipid based transfection system. Briefly, DNA is incubated with cell culture media and Cellfectin for 30 minutes. Insect cells are plated out at 50-60% confluence and allowed to adhere to the plate prior to incubation with the DNA/Cellfectin mix for 4.5 hours at 27°C. Cells were then washed and fresh media added. Two days post transfection media containing blasticidin was added to commence selection. Two concentration of Blasticidin S were tested to ensure optimal selection of positive clones. For both HpVAL1 and 4, protein can be detected in the media supernatant from both cell lines by western blotting using a polyclonal antibody (1:100 dil^{n}) against each recombinant.

1.14 Purification of recombinant proteins Hp-VAL-1, HpVAL-2, BmVAL and Ce-VAL.

Purification of recombinant protein produced by insect cells transfected with pMIBV5-HIS constructs was facilitated by, in this instance, the presence of a polyhistidine (6xHIS) tag. Cell culture supernatant containing soluble recombinant protein was harvested from cells twice weekly whilst the cells were growing at an optimal level. The supernatant, which was centrifuged at 2000g and filtered through a 0.45μM filter in order to remove cell debris, was then frozen until sufficient had been collected for a purification run.

Prior to purification it was necessary to:

1) Reduce the volume of material to be passed over the chelating column to ensure sample processing was carried out in a reasonable time in order to reduce the possibility of protein degradation.
2) Dialyse the sample into binding buffer.

Serum free media is known to strip nickel ions from chelating columns thus prohibiting binding of the 6xHIS tag. The sample volume was therefore reduced using an Amicon diafiltration device followed by subsequent dialysis into 1X binding buffer and a further filtration step. Samples were loaded onto HiTrap chelating HP columns (GE Healthcare) and affinity purified on either an ÄKTAprime (GE Healthcare) (Fig 1.13 A, C and D) or latterly a ÄKTApurifier (GE Healthcare) (Fig 1.13 C) chromatography system using an imidazole gradient to separate HIS tagged proteins and allow fractionation in a Frac950 fraction collector (GE Healthcare). Each fraction within the vicinity of the peak on the trace was then analysed by SDS PAGE (Novex® NuPAGE ® 4-12% gradient bis-tris gel, Life Technologies) and stained using Coomassie blue reagent. Three of the four recombinant proteins expressed achieved better levels of expression in Hi5 cells with only Bm-VAL expressing more efficiently in Sf9 cells. Fractions containing recombinant protein were then pooled and dialysed into PBS, before assessing protein concentration by Bradford assay and testing for LPS contamination using a quantitative chromogenic Limulus Amebocyte lysate (LAL) assay (Lonza) according to manufacturer instructions.

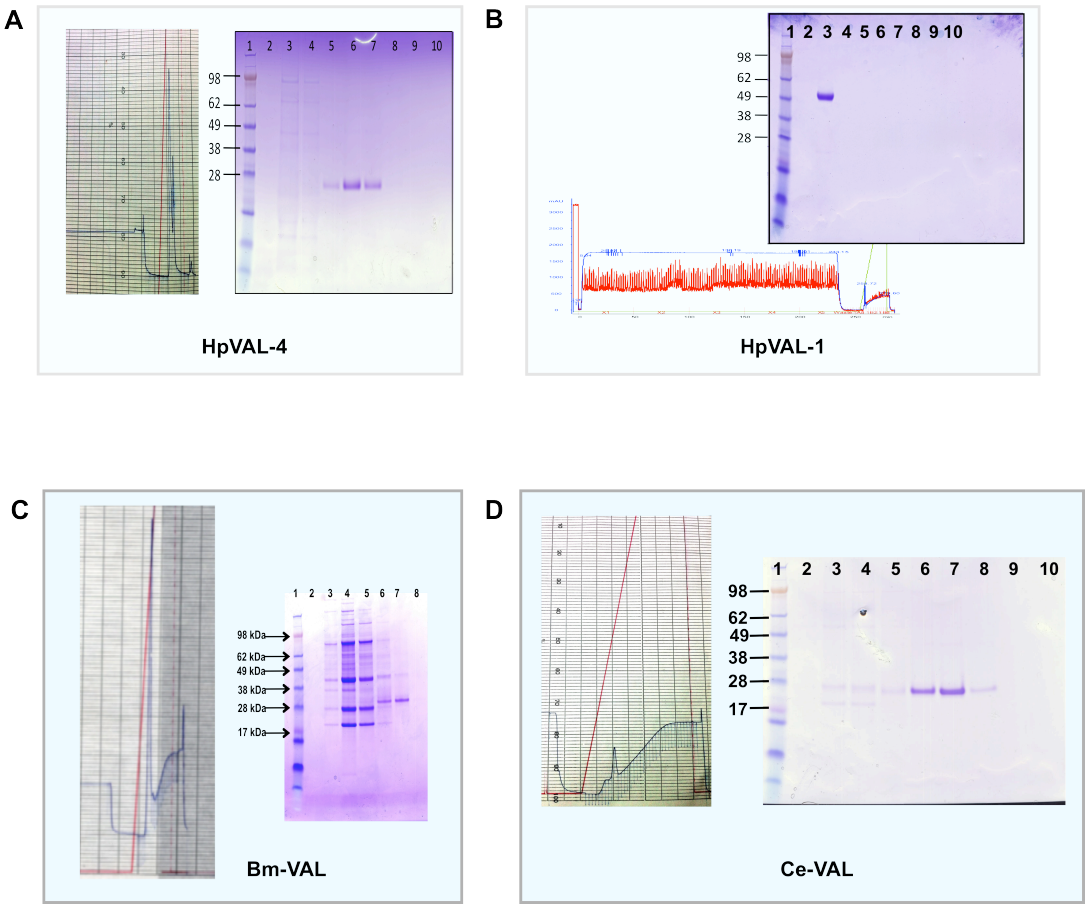

Fig 1.13 Purification of recombinant proteins HpVAL-1, HpVAL-4, Bm-VAL and Ce-VAL.

Insect cell supernatant was harvested from culture and was centrifuged to remove and cell debris. Before 6xHIS tag purification the supernatant was reduced in volume using an Amicon diafiltration device. The supernatant was then dialysed into ÄKTA binding buffer and filtered.

Recombinant proteins were purified over nickel chelating columns using either an ÄKTA Prime HPLC (**A**, **C** and **D**) or an ÄKTA Purifier HPLC (**B**).

Fractions from a purification run were analysed using a Pierce Protein coomassie kit to determine any fractions containing protein. These were then run on a SDS PAGE gel and stained with Coomassie blue to check for size and purity of each fraction (lanes numbers shown on gels A-D).

1.15 Recombinant HpVAL-4 is bound by conformation dependent antibody but does not recognise an antibody that binds HpVAL-1.

In order to test the characteristics of the insect cell derived HpVAL-4 protein, its ability to cross-react with monoclonal antibodies previously shown to bind various VAL proteins (Hewitson et al., 2011a) was assessed by ELISA. Recombinant HpVAL-4 protein was coated overnight onto Nunc Maxisorb® ELISA plates at a concentration of 1μg/ml in carbonate buffer. Plates were blocked with PBS/BSA 5% /Tween 20 0.05% before the addition of either a polyclonal rat antibody raised against HpVAL-4 (prepared by Yvonne Harcus) or one of two monoclonal antibodies, mAb 2.11 or mAb 4-M15, generated from splenocytes isolated from *H.polygyrus* infected mice, within our lab (Hewitson et al., 2011a) which have been shown to bind to HpVAL-4 and HpVAL-1 respectively. After overnight incubation at 4°C antibody binding was detected using an α-rat HRP conjugate for the polyclonal or an α-mouse HRP conjugate for the monoclonals. ABTS substrate was used and read at 405nm on a Molecular Devices VMax microplate reader.

As expected HpVAL-4 recombinant protein bound only the polyclonal antibody and mAb 2.11 which had been previously shown to bind HpVAL-4. Antibody mAb 4-M15, which had been shown to bind HpVAL-1, showed no reactivity to the recombinant (Fig 1.14). This data along with size information from SDS PAGE gel analysis confirms that the recombinant protein secreted from the insect cells was soluble and correctly folded and there was no cross-reactivity between HpVAL-4 and HpVAL-1.

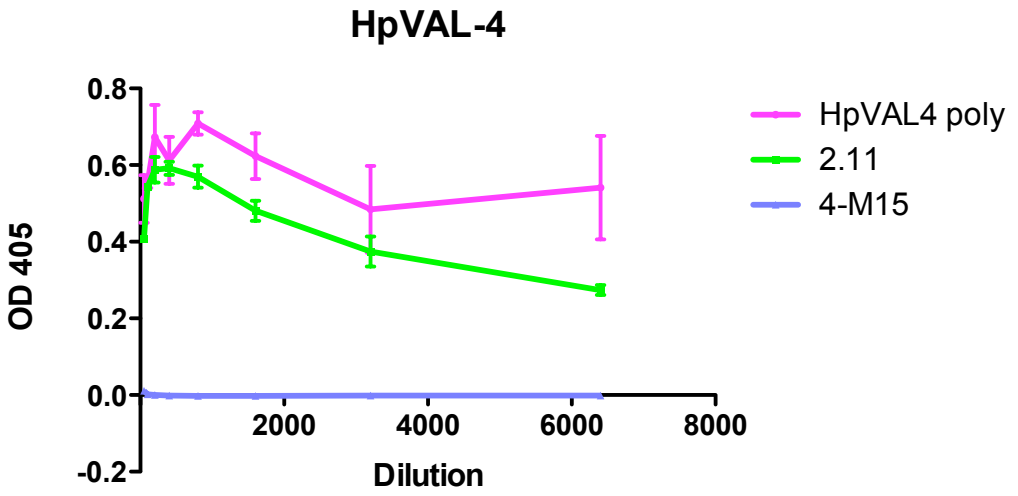

Fig 1.14 Recombinant HpVAL-4 is bound by conformation dependent antibody but does not recognise an antibody that binds HpVAL-1.

ELISA plates were coated overnight at 4°C with 50µl of recombinant HpVAL-4 at 1µg/ml in carbonate buffer. Following blocking with PBS/ BSA 5%/ Tween20 0.05%, a polyclonal α-HpVAL-4 antibody and two monoclonal antibodies, which had been generated from a primary infection with *H.polygyrus* and been shown to react with HpVAL-1 and 4, were diluted down the plate using doubling dilutions in PBS/tween. Samples were incubated overnight at 4°C. The polyclonal antibody was detected the following day using an α-rat HRP conjugate (1:2000) and the two monoclonal antibodies were detected using an α-mouse HRP conjugate (1:2000). Following a one hour incubation at 37°C ABTS peroxidase was used for detection and sample were read at 405nm.

mAb 2.11 has been shown to bind to HpVAL-4. (Hewitson et al, 2011)
mAb 4-M15 has been shown to bind to HpVAL-1. (Hewitson et al, 2011)

1.16 Biotinylation of HpVAL proteins.

Chemical labelling of recombinant protein is a powerful way in which to study the interactions of a protein in an *in vitro* situation. Chemical labels, such as biotin or fluorescent dyes such as Alexa-647, are covalently bonded via chemical groups that react with specific amino acids thus ensuring close proximity of the label to the protein. However this distance can be manipulated by the use of spacer arms between the protein and the label. The EZ-Link NHS-LC-Biotin kit utilizes lysine residues present in the protein, which bind to the N-hydroxysuccinimide element of the reagent (Fig 1.15 A).

Kit instructions imply a minimum protein concentration for labelling to be successful, however achieving these concentrations for recombinant insect cell derived protein proved to be very difficult. In order to examine if lower concentrations of protein could be labelled using the EZ-Link NHS-LC-Biotin kit, varying concentrations of BSA with biotin at the recommended molar excess or higher were labelled and subsequently analysed by western blot. Fig 1.15B shows a western blot in which BSA was biotin labelled at a range on concentrations. Thus HpVAL-1 and HpVAL-4 at 53μg/ml and 63 μg/ml respectively were successfully labeled as shown in Fig 1.15C.

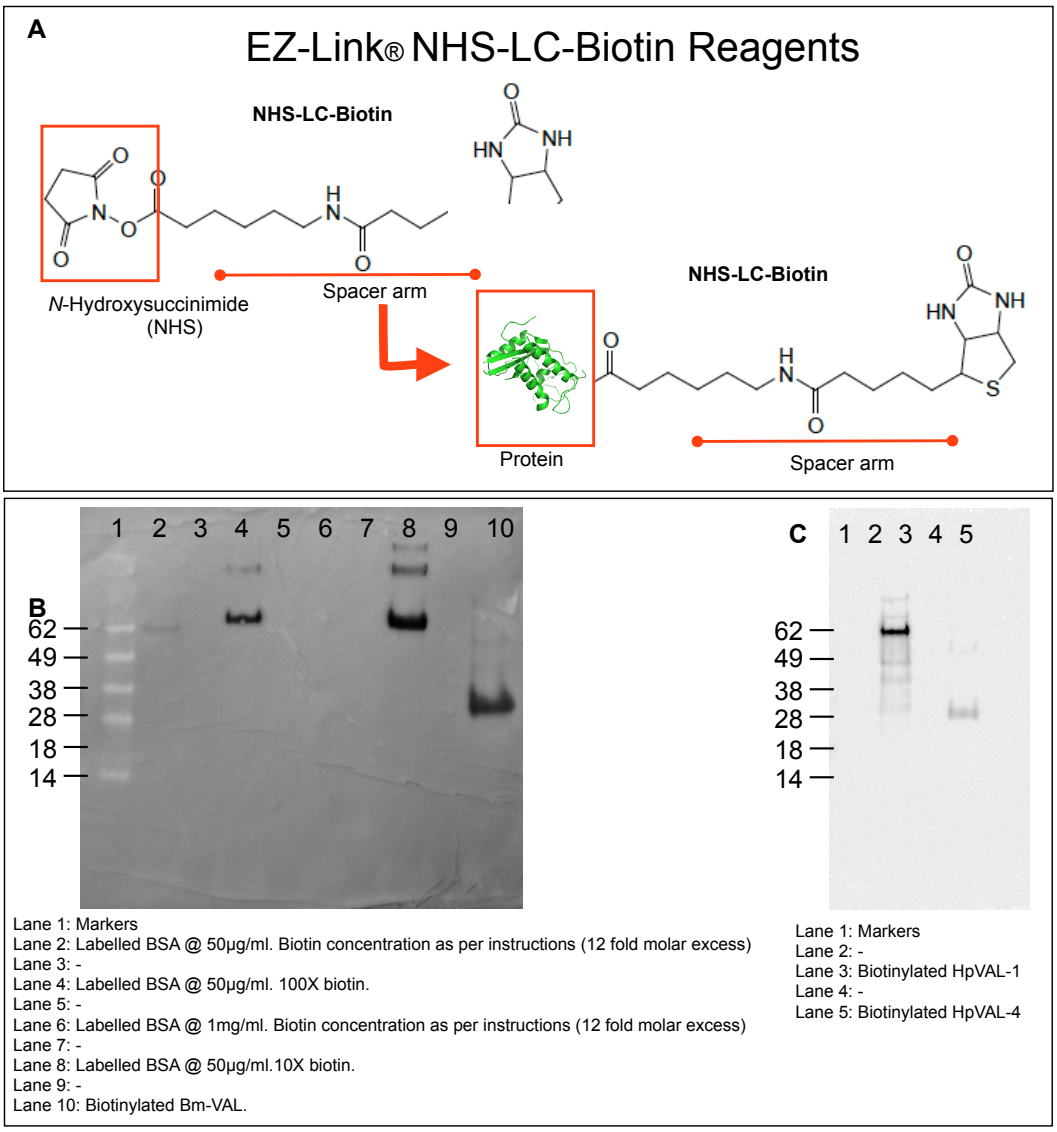

Fig 1.15 Biotinylation of HpVAL proteins.
A. Conjugation of biotin to VAL proteins was achieved using an EZ-Link® NHS-LC-Biotin labelling kit. Primary amines, present in the side chains of lysine (K) residues of the protein to be labelled, bind the N-Hydroxysuccinimide (NHS) element of NHS-Biotin. Upon binding the NHS element becomes non-reactive and is removed during the desalting stage of the protocol.
B. Optimisation of labelling protocol.
BSA was labelled using the NHS-LC-Biotin kit at various concentrations- 50µg/ml and 1mg/ml with various amounts of NHS-Biotin reagent. Labelled BSA was then electrophoresed, blotted and detected using a streptavidin-HRP conjugate.
C. HpVAL-1 and 4 biotinylation.
HpVAL-1 (53µg/ml) and HpVAL-4 (63µg/ml) were biotinylated, electrophoresed and blotted as for BSA.

1.17 Biotinylated recombinant HpVAL binds naïve B cells.

H.polygrus ES had been previously labelled using the EZ-Link NHS-LC-Biotin kit technique described in Fig 1.15. It was observed that biotinylated HES bound to naïve B cells in a CD24-dependent manner (Fig 1.16A). From a population of $CD19^{+}B220^{+}$ cells biotinylated HES bound to CD24 in wild type mice, binding which was completely absent in CD24-/- mice. Similar observations of interactions between a parasite excretory/secretory product and B cells were made with ES-62, an immunomodulatory protein from *Acanthocheilonema viteae,* where ES-62 binding to B cells was blocked by phosphocholine. Subsequent internalization of ES-62 by the B cell was not dependent on TLR-4 as is the case for internalization by macrophages (Harnett, Goodridge, Allen, & Harnett, 2012).

In order to examine if VAL proteins, which are highly represented in HES, are responsible for CD24 binding, biotinylated HES or biotinylated HpVAL-1 were added to naïve splenocytes from a C57BL/6 mouse. Reducing concentrations of biotinylated HES, from 10µg/ml to 1µg/ml were tested alongside bioHpVAL-1 at 1µg/ml. As controls, both biotinylated HES and biotinylated HpVAL-1 were boiled in order to denature the protein structure.

Reductions in the concentration of biotinylated HES showed a marked reduction in the percentage of biotin binding cells, from 47% to 2.6%. Also boiling biotinylated HES reduced binding to 1.33%, the equivalent of no HES being added at all (Fig 1.16B).
Binding of cells was observed with biotinylated HpVAL-1 that was also diminished upon boiling of the protein although not to the same extent (Fig 1.16C). This decrease in binding of cells to biotinylated HES or HpVAL-1 after boiling is further demonstrated in Fig 1.16D where boiled samples (in blue) show a noticeable shift to the left.

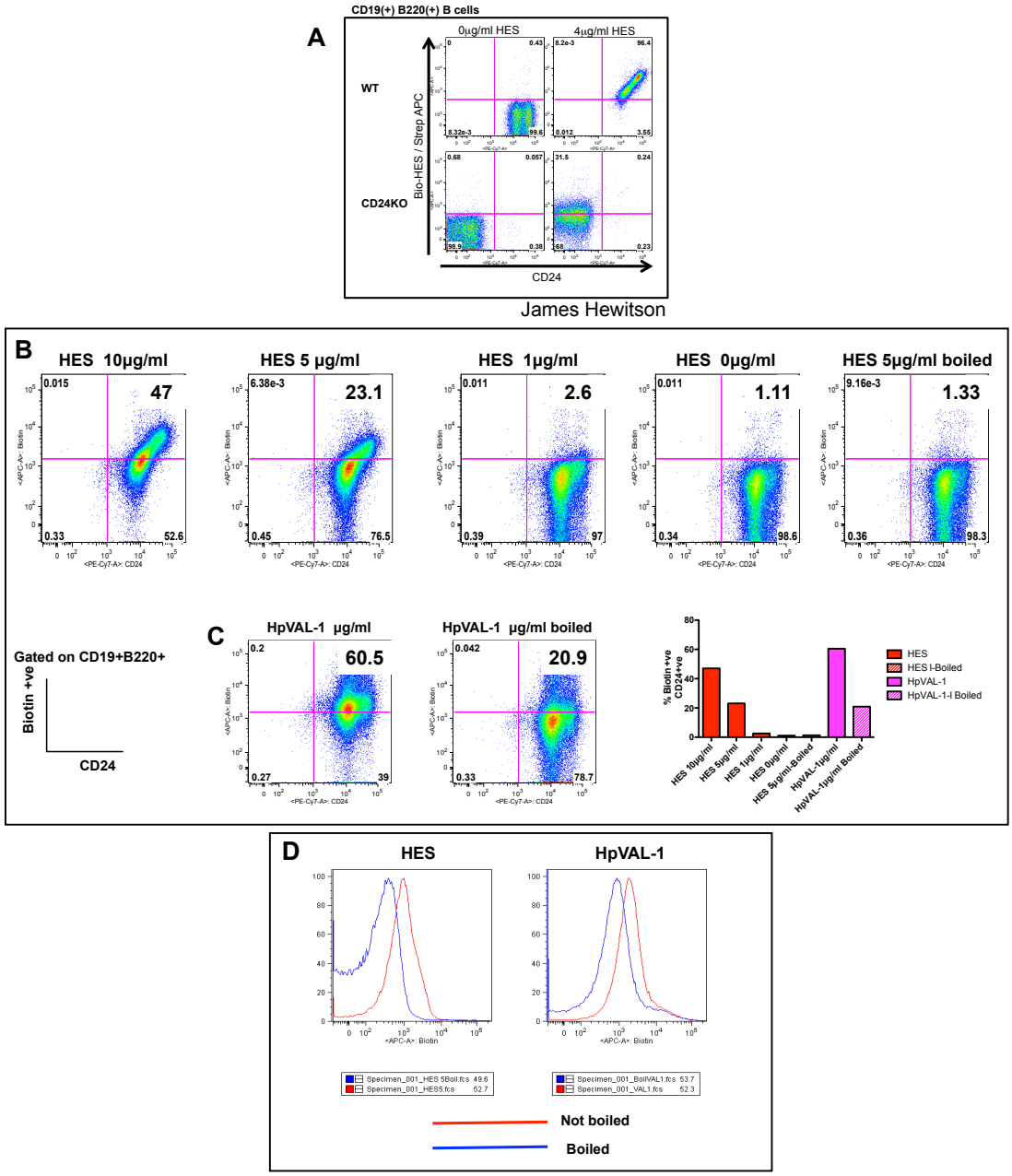

Fig 1.16 Biotinylated recombinant HpVAL binds a splenocyte subset.

A. 5x 10^5 splenocytes, prepared from female C57BL/6 mice, were incubated with (**A**) biotinylated HES (boiled or not boiled) or (**B**) biotinylated HpVAL-1 (boiled or not boiled). At the same time the following staining panel was included: CD19-FITC, CD4-APC Cy7, B220-PerCP, CD24-PeCy7 and CD8-PE.

B. Reduction in binding of biotinylated HES and HpVAL-1 to naïve splenocytes.

1.18 Do all VAL proteins bind naive B cells?

HpVAL-1 was shown to bind to naïve B cells, an effect that was reduced but not completely lost upon boiling the protein. As discussed earlier (see Table 1.1) HpVAL-1 is a single member of a large family of VAL proteins found in the excretory secretory products of *H.polygyrus*. Is this B cell binding property a hallmark of only double domain VAL proteins?

To examine further these binding characteristics two more biotinylated VAL proteins were assessed, HpVAL-4 and BmVAL. Naïve splenocytes from a C57BL/6 mouse were incubated with biotinylated recombinant proteins, either boiled or not boiled. Cells were stained for FACS analysis with CD19-FITC, CD4-APC Cy7, B220-PerCP, CD24-PeCy7 and CD8-PE, CD4-APC.

Both *H.polygyrus* VAL proteins 1 and 4 bound to $CD19^+$ cells, HpVAL-1 more so than HpVAL-4 (Fig 1.17A), an observation that was reduced upon boiling for the double domain HpVAL-1 but not for the single domain VAL protein, HpVAL-4. This may indicate that denaturing the double domain protein disrupts a binding site that relies on the position of the two domains in respect to each other. However, the binding of both HpVAL-1 and HpVAL-4 to $CD24^+$ was reduced upon boiling of the protein in both cases (Fig 1.17B). Interestingly, BmVAL bound to neither $CD19^+$ nor $CD24^+$ as well as its *H.polygyrus* counterparts did.

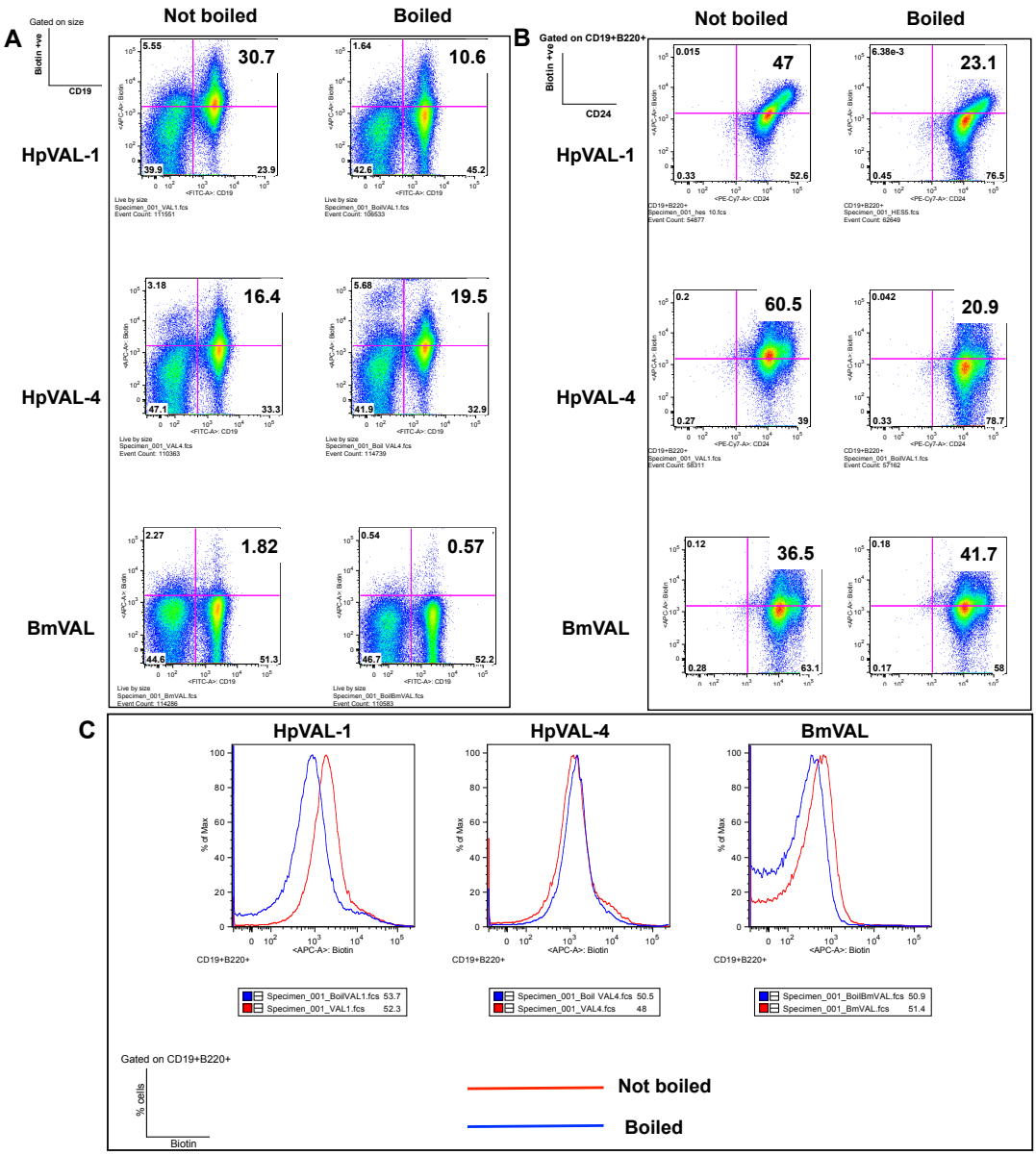

Fig 1.17 Do all VAL proteins bind naive B cells?

5x 10^5 splenocytes, prepared from female C57BL/6 mice, were incubated with biotinylated HpVAL-1 or HpVAL-4 (boiled or not boiled) or Bm-VAL (boiled or not boiled). At the same time the following staining panel was included: CD19-FITC, CD4-APC Cy7, B220-PerCP, CD24-PeCy7 and CD8-PE, CD4-APC.

(**A**) Biotin+CD19+
(**B**) Biotin+CD24+
(**C**) Percentage of biotin+ cells from a population of CD19+B220+ B cells

1.19 Genomic maps of HpVAL-4 and HpTubulin: Primer design for RNAi constructs.

RNAi is a powerful tool allowing researchers to investigate gene function in systems where the ability to use traditional genetics manipulations may elude them. The introduction of complementary double stranded RNA ablates mRNA through means available to most eukaryotes. Whilst RNAi has proved to be an invaluable tool when used to study the free-living nematode *Caenorhabditis elegans* success when studying parasitic nematodes has been proved to be more elusive.

However with recent success in the filarial parasite *Brugia malayi* (Winter, McCormack, Myllyharju, & Page, 2013) and more notably *Haemonchus contortus,* where a VAL homologue was successfully knocked down (Samarasinghe, Knox, & Britton, 2011), primers were designed to examine the potential for knockdown of HpVAL-4, 260b.p. (Fig 1.18A) and HpTubulin, 328 b.p. (Fig 1.18B). HpVAL-4 was chosen above HpVAL-1 due to the fact it contains a single SCP domain as does the successfully knocked down *H.contortus* 40 kDa gene (Accesion number A30245) tested by Samarasinghe et al. For each gene two sets of primers were designed, the first set was designed for the primary amplification of cDNA and contained Xho1 and Xba1 sites for insertion into the L4440 RNAi vector. The vector contains two T7 promoters to allow *in vitro* transcription to occur on both strands (Fig 1.18C) (Fire et al., 1998). The second set was designed to sit out with the first and was used to confirm knockdown. These primers were also designed such that by spanning an intron they would generate a larger product if there were any genomic contamination.

1.20 HpVAL-4 and β-tubulin sequences for insertion into L4440 RNAi vector.

Sequence information for HpVAL-1 is highlighted in pink (Fig 1.19A) and in blue for Hp-Tubulin (Fig 1.19B).

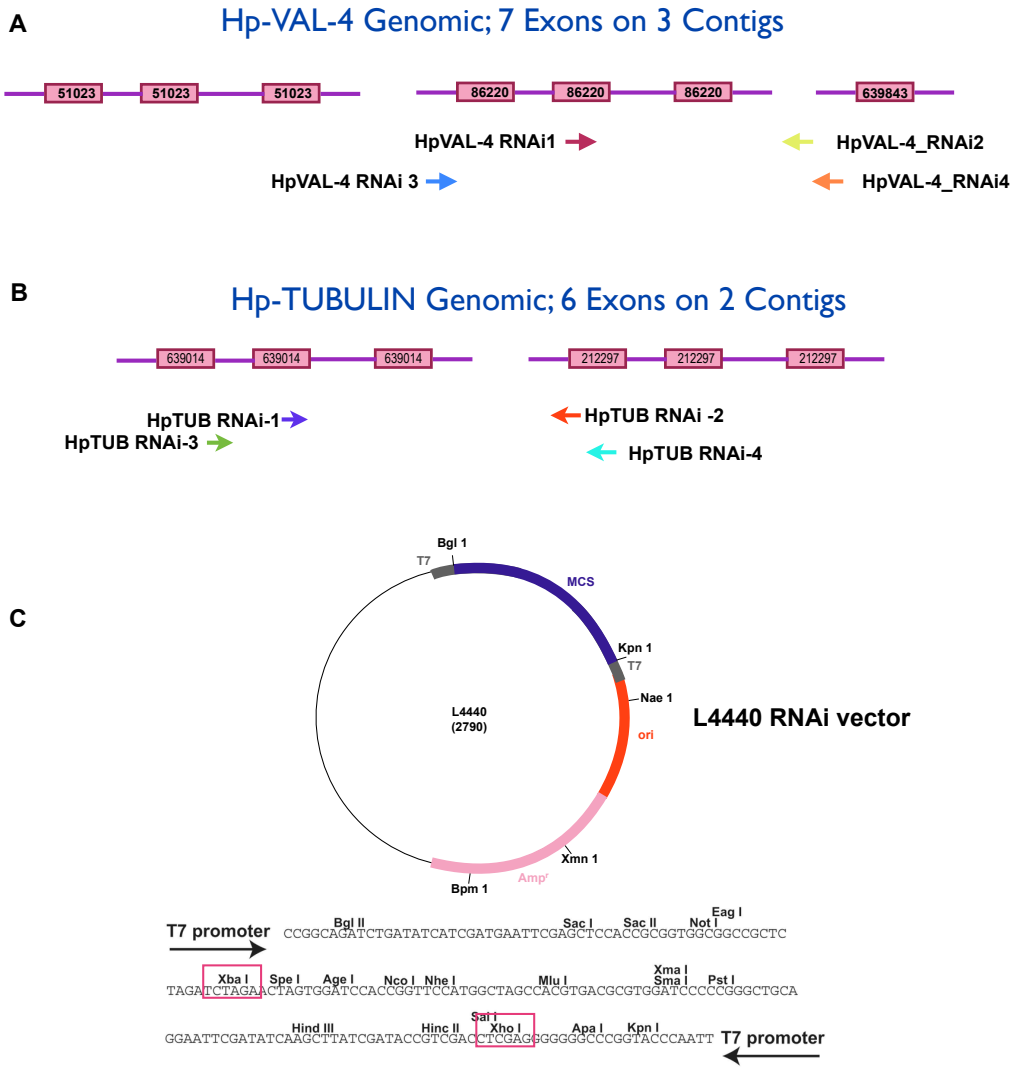

Fig 1.18 Genomic maps of HpVAL-4 and HpTubulin: Primer design for RNAi constructs.

Two sets of primers were designed to facilitate RNAi experiments. Primers 1&2 for both HpVAL-4 (**A**) and HpTubulin (**B**) were designed to amplify a product of the correct size from cDNA.
HpVAL-4, a single domain VAL protein, contains 7 exons sequenced over two contigs.
HpTUBULIN contains 6 exons sequenced over two contigs.

C L4440 vector double T7 promoter vector L4440 (originally designed by A. Fire and kindly gifted by C.Britton, University of Glasgow). Two T7 promoters allow *in vitro* transcription on both strands. Inserts were cloned into vector using Xho and Xba which were then subsequently used to linearise the construct.

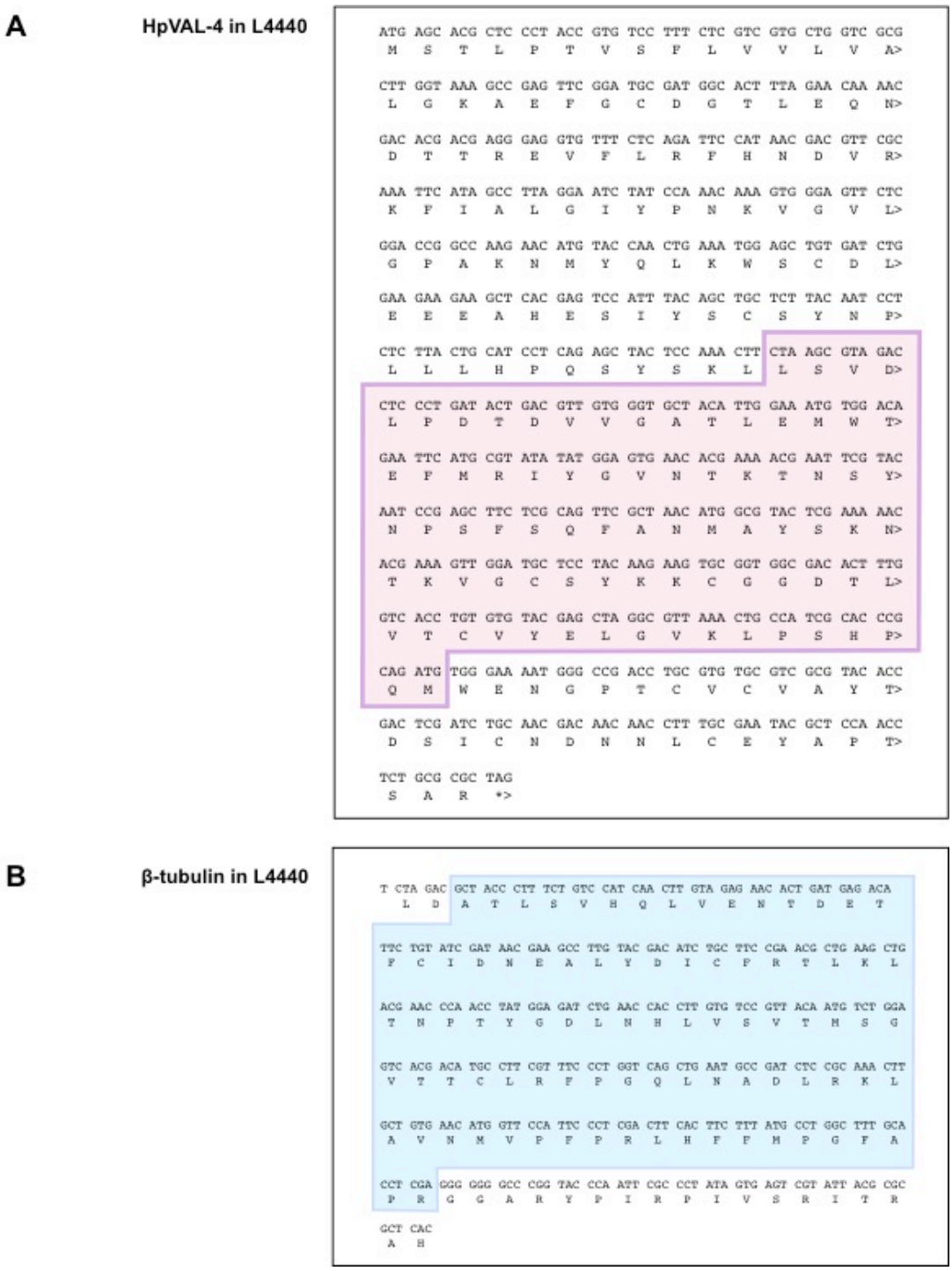

Fig 1.19 HpVAL-4 and β-tubulin sequences for insertion into L4440 RNAi vector.

A Pink block shows sequence that was amplified from plasmid DNA for insertion into L4440 rNAi plasmid.
B Blue block shows sequence that was amplified from cDNA for insertion into L4440 rNAi plasmid.

1.21 RNAi of HpVAL-4.

Primer set 1, Fig 1.18 A&B, was used to amplify inserts which were then ligated into the L4440 using the appropriate restriction enzymes, in this case Xho1 and Xba1. Once cloned into the RNAi vector single digests of plasmid were set up with either Xho1 or Xba1 in order to linearize the DNA. Complete digestion for both L4440 containing HpVAL-1 and L4440 containing HpTubulin was confirmed by agarose gel electrophoresis (Fig 1.20 A). Using the Promega RiboMAX kit-T7 according to the manufacturer's instructions, linearised DNA was then used to generate ssRNA which was subsequently purified by phenol chloroform extraction and incubated with complementary ssRNA to form dsRNA.

Meanwhile, exsheathement of *H.polygyrus* larvae was achieved by incubating in a 2.5% solution of Milton fluid (Fig 1.20 B). Larvae were washed extensively prior to setting up the RNAi reaction. Larvae were soaked, as opposed to electroporated which can have adverse effects on the health of the larvae (Geldhof et al., 2006), in dsRNA /lipofectamine or dsRNA/ cellfectin for 4 days at 37C°, following which they were washed to remove all of the RNAi reaction mix and larval RNA was extracted using TRIzol reagent for analysis by RT-PCR.

A

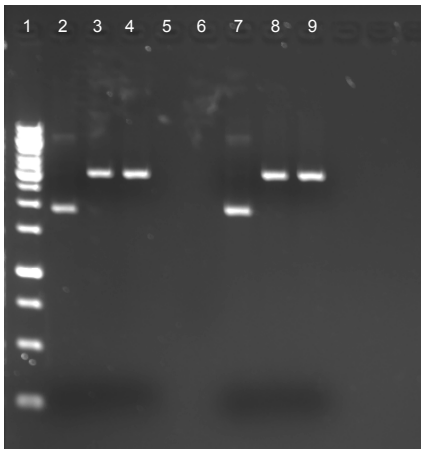

Lane 1: Markers
Lane 2: Undigested Tub/L4440
Lane 3: Tub/L4440- Xho1
Lane 4: Tub/L4440- Xba1
Lane 5: -
Lane 6: -
Lane 7: Undigested HpVAL-4/L4440
Lane 8: HpVAL-4/L4440- Xho1
Lane 9: HpVAL-4/L4440- Xba1

B

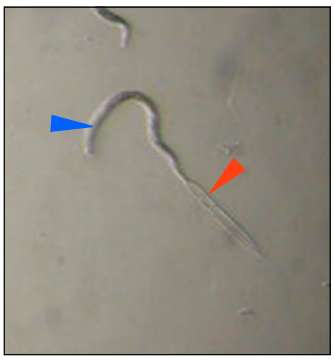

Fig 1.20 RNAi of HpVAL-4.

A 10µg (2x 5µg) of DNA from positive clones containing HpVAL-4 or Hp-Tubulin and the L4440 vector were digested with Xho1 and Xba1, electrophoresed and gel purified.

B 1000 larvae in 1ml were exsheathed by adding 25µl of Milton fluid. Exsheathment was complete within 30 minutes.

1.22 RNAi on exsheathed *H.polygyrus* larvae.

H.polygyrus larvae were exsheathed as previously described and soaked in either HpVAL-4 dsRNA or HpTubulin dsRNA for 4 days at 37°C. RNA was extracted from soaked parasites and cDNA was subsequently generated by reverse transcription. The second set of primers for HpVAL-4 and HpTubulin, as explained in Fig 1.18 A and B**,** were used for PCR reactions. All results were compared to products generated using primers for the constitutively expressed superoxide dismutase (SOD) (Liddell & Knox, 1998).

After 35 cycles initial results show that tubulin levels from larvae soaked in double-stranded Tubulin RNA remain unaffected (Lanes 5 and 6 Fig 1.21A). However there was a notable reduction in HpVAL-4 levels from larvae soaked in double-stranded HpVAL-4 RNA (Lanes 7 and 8 Fig 1.21A). Unfortunately, levels of product from control reactions set up with SOD primers indicate that starting amounts of cDNA may not have been equal for all samples leading to possible discrepancies when gene specific primers were used. It is of vital importance that levels of expression for all samples are equal when generated with housekeeping or constitutively expressed primers are used.

1.23 RNAi optimization reveals no knockdown of HpVAL-4.

Further optimization steps, to achieve comparable levels of transcripts in control reactions where SOD primers were used, were undertaken. These included 1) tightly controlling the concentration of cDNA that was used per reaction by increasing the number of larvae and using various method to quantify DNA, and 2) sampling PCR reactions at lower cycle numbers- 20, 25, 30 and 35 cycles to observe when a reaction reaches a plateau. These alterations to the protocol helped achieve consistent levels of PCR product in control reactions thus allowing appropriate comparisons to be made (Fig 1.22). This however revealed no apparent knockdown of gene expression in samples treated with HpVAL-4.

A

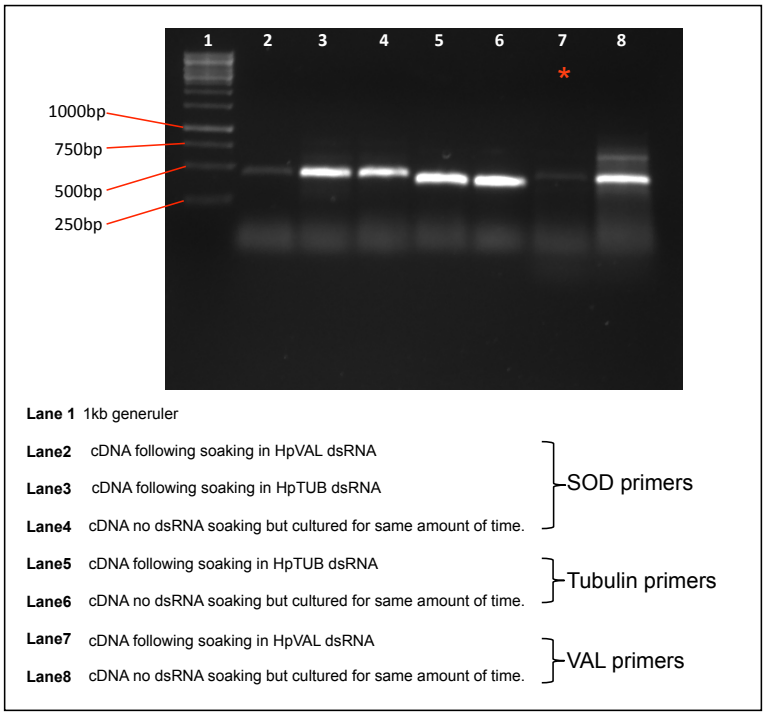

B

Densitometry
Lane 2: 1403350
Lane 3: 7647900
Lane 4: 6448000
Lane 5: 8973250
Lane 6: 10395450
Lane 7: 1145950
Lane 8: 7665450

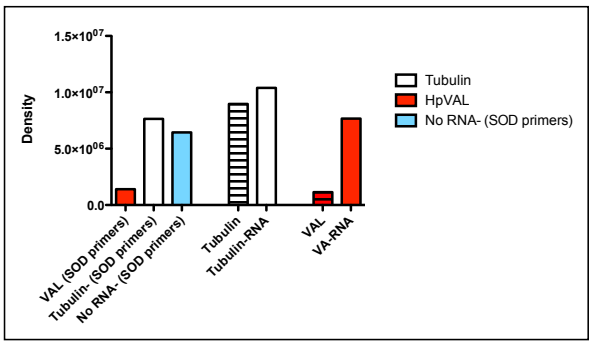

Fig 1.21 RNAi on exsheathed *H.polygyrus* larvae.

A. RNA was extracted from larvae which had been soaked in dsRNA for 4 days at 37°C using the standard TRIzol protocol. RNA was reverse transcribed and gene specific PCR reactions carried out.
Lanes 2-4 show products generated using SOD (superoxide dismutase) primers.
Lanes 5 & 6 show products generated using tubulin primers.
Lanes 7 & 8 show products generated using HpVAL primers.

B. Results were measured by densitometry using a Molecular Devices Gel Doc imager and software.

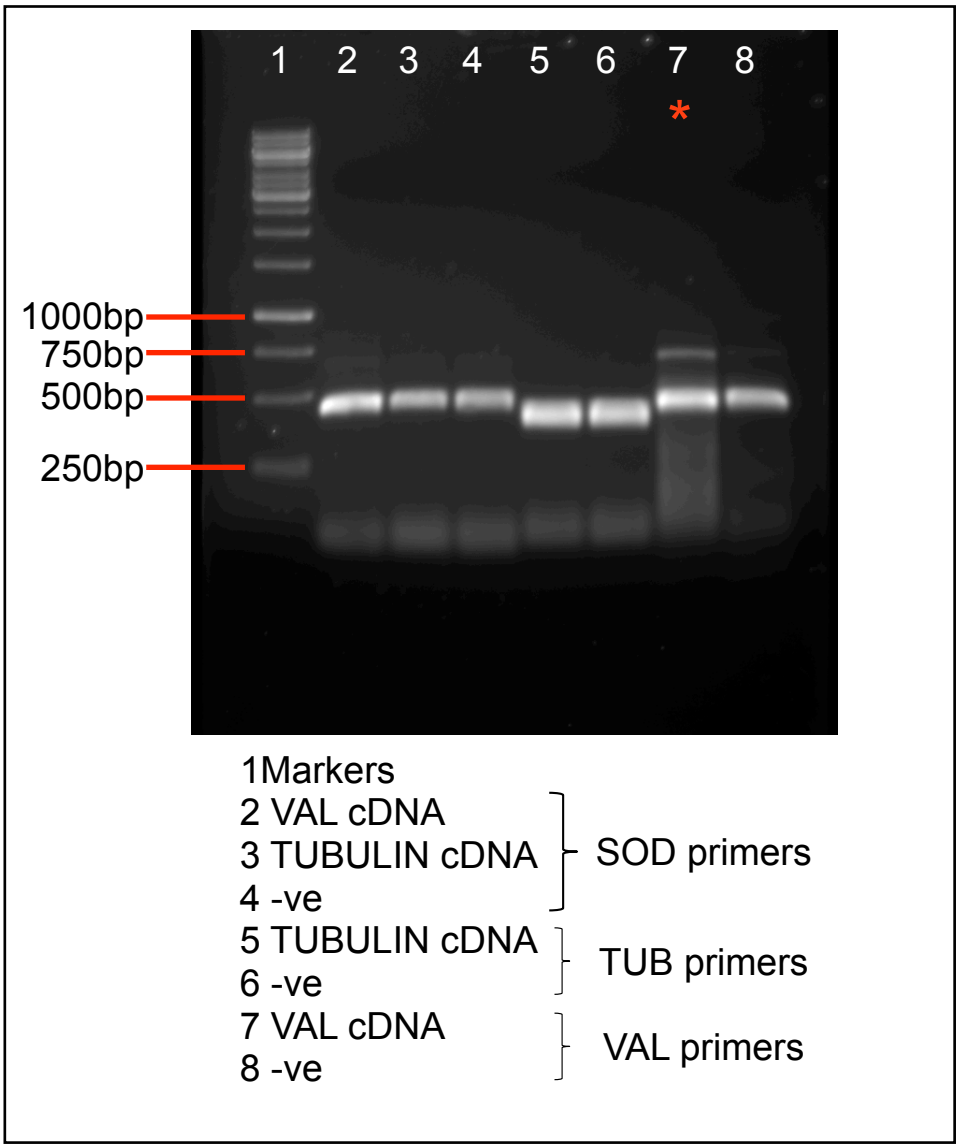

Fig 1.22 RNAi optimization reveals no knockdown of HpVAL-4.

RNA was extracted from larvae which had been soaked in dsRNA for 4 days at 37°C using the standard TRIzol protocol. RNA was reverse transcribed and gene specific PCR reactions carried out.

Lanes 2-4 show products generated using SOD (superoxide dismutase) primers.
Lanes 5 & 6 show products generated using tubulin primers.
Lanes 7 & 8 show products generated using HpVAL primers.

1.24 A modified RNAi protocol using siRNA.

With levels of transcript in control reactions now equivalent over various samples other elements of the experimental protocol were assessed.

One of the main issues described by researchers studying gene knockdown by RNAi is delivery of the dsRNA and the ability of the parasite to enable its uptake (Viney & Thompson, 2008), (Knox, Geldhof, Visser, & Britton, 2007), (Dalzell et al., 2012). With this in mind a modified RNAi protocol, which utilizes heterogeneous short-interfering RNAs (hsiRNAs) was employed with the hope of easier uptake of the RNA by the larvae. This method was used to successfully knockdown the Collagen prolyl 4-hydroxylase genes in the human filarial parasite *Brugia malayi*, although delivery of hsiRNA was by soaking for *B.malayi*, it was achieved by feeding for the control reactions in *C.elegans* (Winter et al., 2013).

The modified RNAi protocol remains the same as previously described up until the point of achieving dsRNA. At this juncture 5µg dsRNA is digested with Shortcut RNase III to generate heterogeneous short-interfering RNAs, which are then used to prepare the hsiRNA/ lipofectin^{TM} reaction mix. Soaking of larvae in 1-2 µM hsiRNA and subsequent RNA extraction and RT-PCR analysis remains the same as described earlier. Results using this modified RNAi protocol seemed to be promising with PCR levels consistent for each control sample, levels of transcript appeared to be reduced in larvae that had been soaked in HpVAL-4 hsiRNA (Fig 1.23).

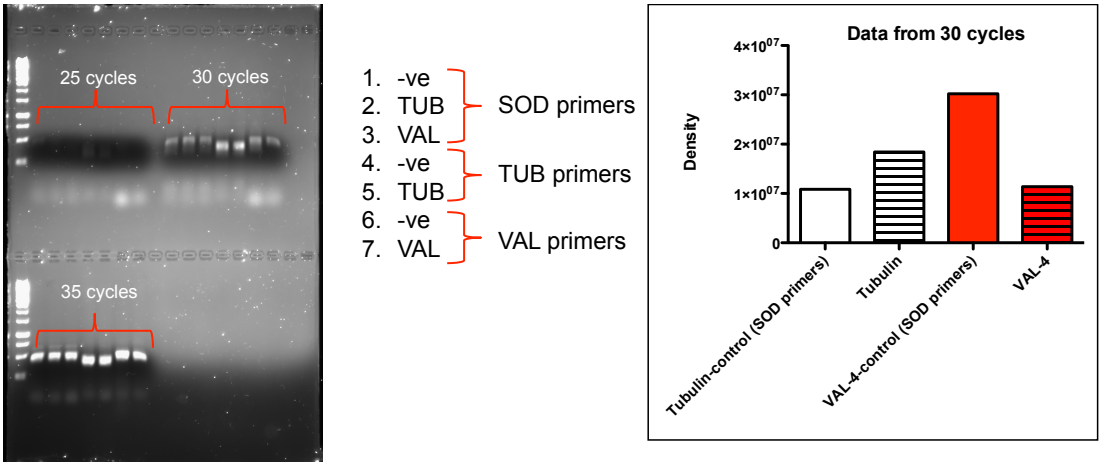

Fig 1.23 A modified RNAi protocol using siRNA.

After soaking in hsiRNA larvae were collected into TRIzol reagent for subsequent RNA extraction, reverse transcription and PCR. Samples were removed from the PCR reactions at 25, 30 and 35 cycles and analysed by gel electrophoresis. Relative densitometry values were determined using a Molecular Devices Gel Doc imager.

1.25 Exsheathed larvae cannot mount an infection in mice.

Uptake of dsRNA remains one of the biggest hindrances for successful RNAi. In the case of *C.elegans*, dsRNA can be actively fed to the nematodes with the physiology of the worm posing no issues to later dissemination of the RNA throughout its body (Timmons, Court, & Fire, 2001; Timmons & Fire, 1998). Interestingly, the method described by Timmons et al in 2001, utilized bacteria that were deficient in RNaseIII, the enzyme being used to generate hsiRNA in the modified RNAi method described earlier (Fig 1.24 A).
With issues still remaining as to which is the best method to deliver dsRNA or hsiRNA to more physiologically complex nematodes e.g. animal parasitic nematodes such as *H.polygyrus* or *H.contortus,* ease of access to the parasite should be enabled by removing the parasite's sheath. This was achieved with ease by soaking *H.polygyrus* larvae in a 2.5% solution of Milton fluid. The effect of removing the larval sheath however is uncertain. Larvae have this sheath present when gavaged into the mouse for the purpose of the *H.polygyrus* lifecycle and go on to mount successful infections.

Therefore, C57BL/6 mice were infected with 200 sheathed or exsheathed larvae as for a routine lifecycle infection (Fig 1.24A). 14 days later, faeces were collected and egg counts enumerated. After 28 days, mice were culled with worm burden and granuloma formation being counted.

Results showed that larvae were completely unable to mount an infection after being exsheathed, with no eggs present in the faeces after 14 days and no worms or granulomas present at day 28 after larval gavage (Fig 1.24B).

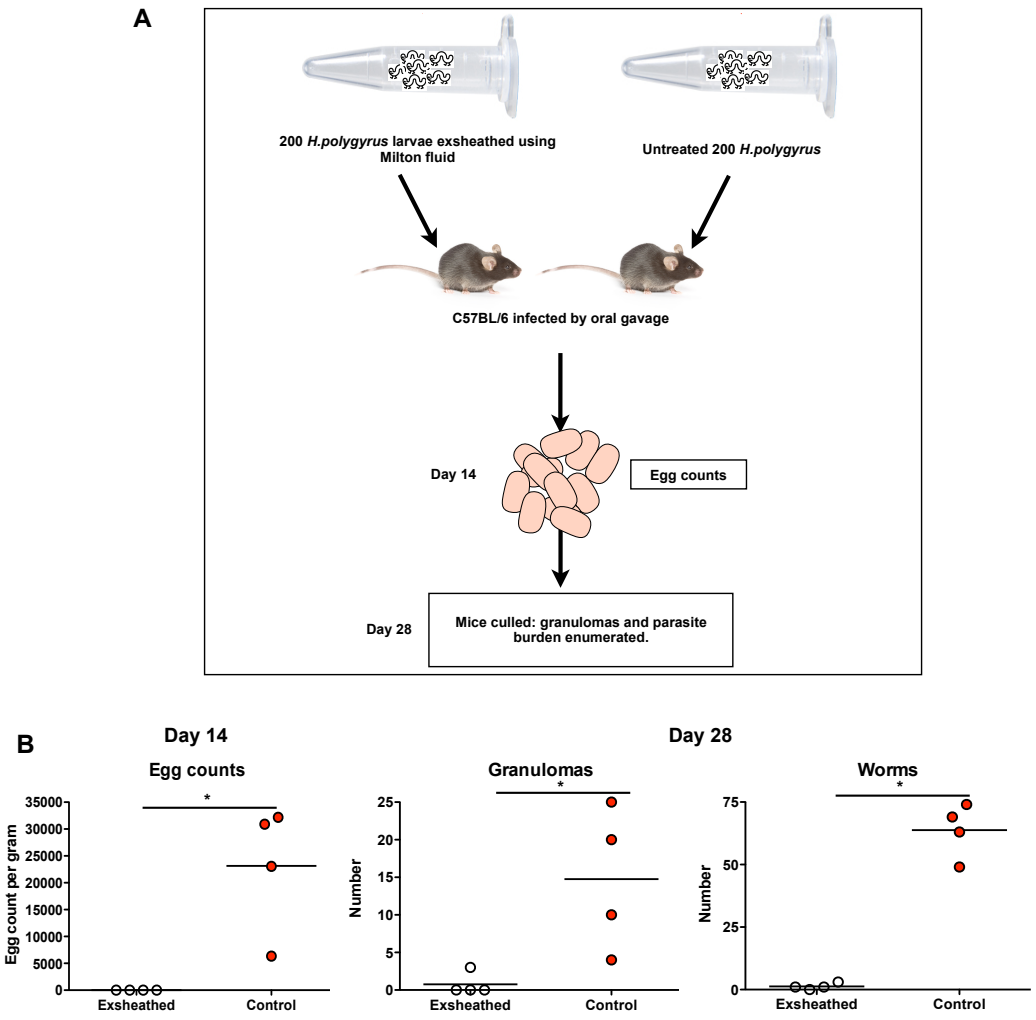

Fig 1.24 Exsheathed larvae cannot mount an infection in mice.

A. 200 *H.polygyrus* larvae were exsheathed by incubation for 30 minutes in dilute Milton fluid (2% sodium hypochlorite/ 16.5% sodium chloride). Following exsheathing C57BL/6 mice were infected by oral gavage with either exsheathed or untreated larvae (200 larvae). Egg counts were performed on Day14. Granuloma formation and parasite burden were enumerated on Day 28.

B. Day 14: egg counts were carried out from mice infected with larvae that were untreated or that had been exsheathed. Briefly, mouse faeces was collected and weighed before transferring to a vial containing 2ml H20 to dissolve. This was then diluted with 2ml saturated NaCl solution before counting the eggs in a McMaster counting chamber. Day 28: mice were culled and both worm and granuloma numbers were enumerated.

1.26 Genes required for efficient RNAi processing.

Due to continually unpredictable results, attention was turned to whether or not *H.polygyrus* has all of the required core proteins for each step in the RNAi pathway. A study by Ledner et al examined three methods of dsRNA delivery to *H.polygyrus,* 1) feeding, 2) electroporation and finally 3) soaking, with varying results. Analysis of databases available at the time showed that genes involved in dsRNA uptake were actually missing in *Brugia malayi* and *Haemonchus contortus* the implication being that successful RNAi in these parasites would not be possible (Lendner, Doligalska, Lucius, & Hartmann, 2008). As *H.polygyrus* databases became available these were then examined for homologous genes to those mined by Ledner for the four main stages of the RNAi process, namely 1) Uptake, 2) Processing, 3) mRNA regulation and 4) Amplification.

Results of this database search are shown in Table 1.5 and clearly show that the genes required for uptake are missing in *H.polygyrus,* with rsd-3 being the exception as is the case for *B.malayi*, *H.contortus* and *S.mansoni*. There are homologous genes for processing, mRNA regulation and for amplification, however with genes for uptake severely underrepresented in these parasites it would be unlikely for an RNAi protocol to be successful.

C.elegans		H.polygyrus		H.contortus		B.malayi		S.mansonii		C.elegans genebank location
Gene	Function	BLAST hit	Homologues	Contig	Score	WGS	Homologues	GAV3	Homologues	
Uptake										
sid-1	Uptake and spread of dsRNA	/	/	102975	3e -07	/	/	6e -13	29192.m000634	http://www.ncbi.nlm.nih.gov/nuccore/AF478687.1
sid-2	Uptake of dsRNA from intestine	/	/	/	/	/	/	/	/	http://www.ncbi.nlm.nih.gov/nuccore/NM_067422
rsd-2	Silencing defect in germline cells	/	/	/	/	/	/	/	/	http://www.ncbi.nlm.nih.gov/nuccore/NM_001047488
rsd-3	Silencing defect in germline cells	isotig 09233	1e -32	116129	1e -08	3e -16	B.malayi ctg_55066	1.1e -24	29116.m002007	http://www.ncbi.nlm.nih.gov/nuccore/NM_077572
rsd-4	Silencing defect in somatic and germline cells	/	/	/	/	/	/	/	/	
rsd-6	Silencing defect in germline cells	/	/	/	/	/	/	/	/	http://www.ncbi.nlm.nih.gov/nuccore/NM_059868
Processing										
dcr-1	Ribonuclease	isotig 16281	7e -97	27546	3e -159	2e -28	B.malayi ctg_57271	5.8e -131	29443.m000270	http://www.ncbi.nlm.nih.gov/nuccore/NM_066360
drh-1	Helicase; req for somatic and germline RNAi	isotig 09412	1e -53	30378	4.1e -54	2e -12	B.malayi ctg_62040	5.1e -11	29372.m000515	http://www.ncbi.nlm.nih.gov/nuccore/NM_068817
rde-1	Accumulation of dsRNA	isotig 00472	5e -71	12769	7e -12	1e -09	B.malayi ctg_63588	7.7e -21	30940.m000077	http://www.ncbi.nlm.nih.gov/nuccore/NM_171525
rde-4	dsRNA recognition and binding protein	isotig 10091	7e -26	/	/	/	/	/	/	http://www.ncbi.nlm.nih.gov/nuccore/NM_066864
mRNA regulation										
tsn-1	nuclease	isotig 02021	e-133	35378	9e -93	1e -34	B.malayi ctg_56603	1.1e -142	29355.m000114	http://www.ncbi.nlm.nih.gov/nuccore/NM_062438
vig-1	RNA binding protein	isotig 10488	3e -72	30623	6e -37	6e -09	B.malayi ctg_62501	1.9e -19	29056.m001365	http://www.ncbi.nlm.nih.gov/nuccore/NM_1709?4
rde-2	Function downstream of rde-1	/	/	/	/	/	/	/	/	http://www.ncbi.nlm.nih.gov/nuccore/NM_001026227
mut-7	RnaseD reqd for RdRP	isotig 05958	4e -25	1999	7.6e -15	/	B.malayi ctg_64140	/	/	http://www.ncbi.nlm.nih.gov/nuccore/NM_066704.6
Amplification										
rrf-1	for somatic RNAi	isotig 10238	e -175	/	/	/	/	/	/	http://www.ncbi.nlm.nih.gov/nuccore/NM_059730.2
ego-1	RdRP	isotig 05904	0	16506	5.2e -68	4e -45	B.malayi ctg_55687	/	/	http://www.ncbi.nlm.nih.gov/nuccore/NM_059731
rde-3/ mut-2	Nucleotidyltransferase: function in RNAi unknown	isotig 11139	1e -53	13595	5.2e -19	4e -07	B.malayi ctg_53347	1.2e -19	29049.m001839	http://www.ncbi.nlm.nih.gov/nuccore/NM_192980
eri-1	Exonuclease: degrades siRNA	isotig 12339	5e -97	17169	3.3e -44	2e -14	B.malayi ctg_52817	1.3e -30	29104.m002062	http://www.ncbi.nlm.nih.gov/nuccore/NM_171244
References										
	http://www.plosntds.org/article/info%3Adoi%2F10.1371%2Fjournal.pntd.0001176									
	http://www.sciencedirect.com/science/article/pii/S0166685108001382									

N.B. *H.polygyrus* BLAST searched with H.contortus orthologue

Table 1.5 Genes required for efficient RNAi processing.

Discussion

In this chapter, I have tried to describe the protein family upon which this thesis is based (Fig 1.25). At first glance, this task is made more complicated by the fact the HpVAL proteins belong to an inconsistently named family of molecules that are found in various different eukaryotic organisms, including parasites. Yet even though there are so many members of this family attributing a function to these proteins often remains elusive. Some putative functions have however been suggested such as aiding the parasite with its transition from a free-living stage to one of parasitism as is the case for ASP-1 (Hawdon et al., 1999). In vertebrates, they are expressed in the epididymal lumen and are thought to be involved in sperm-oocyte binding (Jalkanen, Huhtaniemi, & Poutanen, 2005). SCP/TAPS proteins are also highly represented in both snake and vespid venoms (Yamazaki & Morita, 2004) {Henriksen,
2001 #755} where they are suggested to be involved in trypsin inhibition and the contraction of smooth muscle. Much of the tertiary structure of these proteins has been based upon the crystal structure of Ves V 5, which was deduced as having an α-β-α core by Henriksen et al (Henriksen et al., 2001). It is hoped that with the increase in research and information on these proteins that there will also come an understanding of the need to standardize nomenclature for them, an issue addressed by Cantacessi et al, (Cantacessi et al., 2009).

Based upon their SCP domain content the VAL family in *H.polygyrus* neatly splits into two main groups with members having two domains forming the larger of the two. Of the double domain proteins only HpVAL-3, 6 and 8 fall outwith the group. When phylogenetic trees are generated for the single and double domain VALs separately HpVAL-3 and 8 group together (Fig 1.4).

It is highly possible that single and double domain VAL proteins have evolved for very different roles hence their divergence on the phylogenetic tree. Interestingly, when compared to a mix of single and double domain VAL proteins from other species the majority of *H.polygyrus* double domain VALs still appear to separate from most other proteins be they single or double domain indicating that there has

been extensive radiation and diversification since the parasite has adapted to the mouse host.

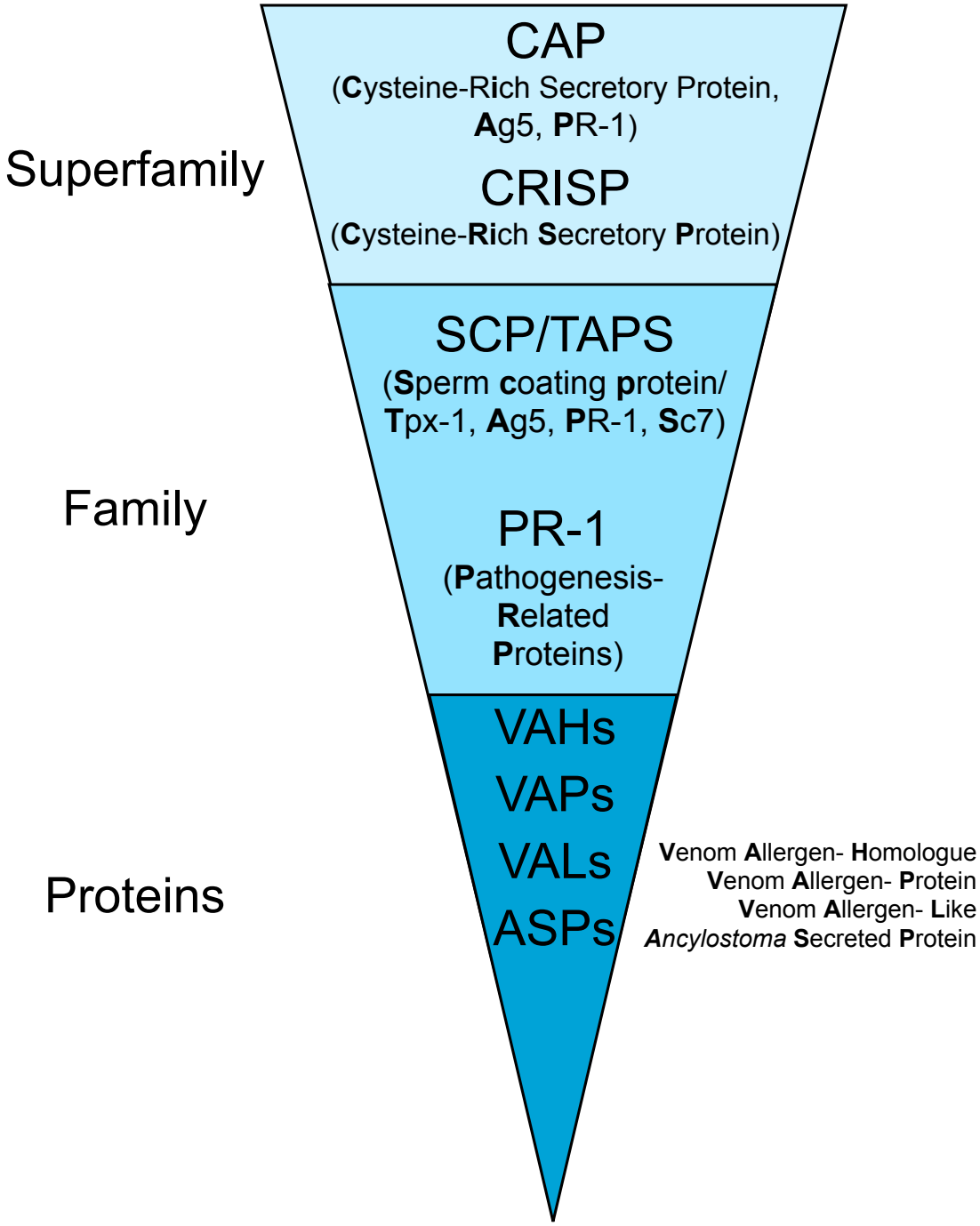

Fig 1.25 CRISP Family hierarchy

Classification of this family of proteins, somewhat like their nomenclature, is developing into a rather complicated scenario. A number of groups have suggested classification based on different criteria. Consideration of primary and predicted secondary structure (Osman et al., 2012), a phylogenetic approach based on amino acid sequence data and utilizing a mathematical/ statistical model (Cantacessi et al., 2009), grouping based on the presence or absence of a signal peptide and conserved cysteine residues (Chalmers et al., 2008) or as I have shown here grouping based on SCP domain content. Undoubtedly, classification for this family of proteins will be a complicated and extensive process. Factors such as SCP domains, site of expression within the organism and the organism itself, the 3D structure in particular any regions of disorder within the molecule that may affect how it folds and finally the presence of any other domains to name but a few.

To express or not to express….? And exactly how to do so…that is the question.

This is not a trivial question. Searching through the literature SCP/TAPS proteins have been studied in no fewer than 3 different systems; bacterial (Murray et al., 2001), (Hawdon et al., 1996), yeast (Goud et al., 2004) and baculovirus (Geldhof, Meyvis, Vercruysse, & Claerebout, 2008) and finally use of native protein purified from parasite excretory/secretory products. Each system has its pros and cons; usually the most pertinent issue is how much recombinant protein can actually be produced. For large-scale production of recombinant protein, bacterial and yeast expression are usually much better than their counterparts. However as I have alluded to in this chapter, structure of the recombinant should not be compromised if cellular assays are to be studied. Proteins produced in these systems can however be used to generate polyclonal antibodies as this process does not require correct structural conformation. In my hands, the VAL protein from *Brugia malayi* (Bm-VAL-1) was very insoluble when expressed in the pET system (Novagen) with just a fraction remaining outwith the inclusion bodies (Murray et al., 2001). Nevertheless, antibodies raised against Bm-VAL-1 recognized proteins in extracts made from microfilariae and larvae and furthermore antibodies present in sera from a set of human filariasis patients recognized the recombinant protein generated.

Murine antibodies to recombinant *Bm*-VAL-1 react with a 28 kDa protein in L3 extracts and recombinant *Bm*-VAL-1 is recognised by murine T cells primed with soluble L3 proteins. Of 82 ESTs corresponding to *Bm-val*-1, 72 are recorded from the infective larval (L3) stage.

Meyvis et al described further evidence that the manner in which a recombinant protein is produced can affect research outcomes. The ASP homologue from *Ostertagia ostertagi* (Oo-ASP-2) had originally been isolated from the excretory/secretory material of the parasite. This had induced protection against challenge in vaccinated calves at a reproducible level of 74% reduction in fecal egg counts (Meyvis et al., 2007), an observation that could not be reproduced using recombinant protein generated in a baculovirus system (Geldhof et al., 2008).

Here I have described the production of recombinant protein in an insect cell system, a choice based upon the level of post-translational modifications bestowed upon the protein by these cells. As shown in Fig. 1.26, proteins produced in a yeast system are decorated with a very high number of sugars; many more than are found in a mammalian system. Thus, the ability of insect cells to fold a protein correctly with a degree of N-glycosylation was chosen above yeast's ability to produce much greater quantities.

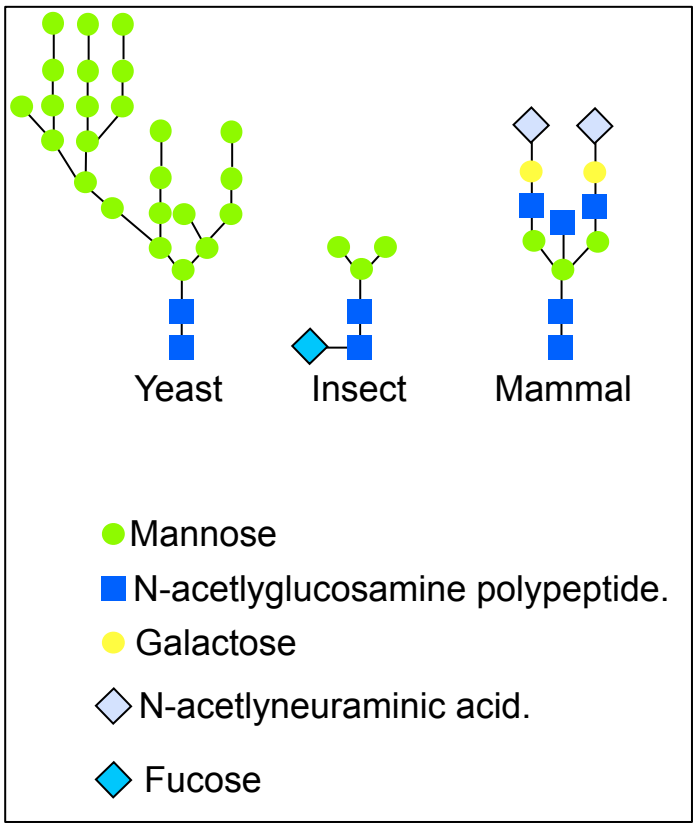

Fig. 1.26 Post-translational modifications added to recombinant proteins in 3 protein expression systems

HES vs. VAL

As the VAL proteins are so well represented in *H.polygyrus* ES it is tempting to try and attribute various HES properties to molecules that have been identified within the HES mixture. Here an observation made in our laboratory whereby HES bound to naïve B cells (James Hewitson, unpublished) was investigated to see if one of the VAL proteins was responsible for this. Biotinylated HES and various biotinylated VAL proteins were incubated with C57BL/6 splenocytes. The original observation was reproduced with HES and a similar but not identical observation was achieved with both HpVAL-1 and HpVAL-4. The binding seen with HES was dependent on conformation of the protein as seen by the loss of binding when the protein had been boiled. For both VAL proteins however, boiling resulted in a reduction of binding and not a total loss. Therefore it is possible that VAL proteins examined here, which are found in HES, are only partly responsible for the CD24 dependent binding seen in B cells. Investigation is also ongoing to examine preliminary data, which shows that recombinant insect cell expressed VAL proteins bind to CD79a, which subsequently forms a complex with CD79b to become part of the B cell receptor complex (Chu & Arber, 2001). This may reveal more information regarding the ability of HES and VAL proteins to bind naïve B cells.

RNA interference (RNAi) has proved to be a very powerful resource for studying gene function in the free-living nematode *C.elegans* (Kamath et al., 2003), (Simpson, Davis, & Boag, 2012). However many attempts to knockdown genes in parasitic nematodes have met with inefficient or inconsistent results. Reports from groups examining this technique in *Ostertagia ostertagi* (Visser et al., 2006) and *Haemonchus contortus* (Geldhof et al., 2006) have met with sporadic success. Of note, even within species differences can make an impact upon the efficacy of the RNAi protocol can be observed between *C.elegans* and *C.briggsae* have differing abilities to uptake dsRNA (Winston, Sutherlin, Wright, Feinberg, & Hunter, 2007).

Thus, the VAL family in *H.polygyrus* has proven to be one with great intra-species variability, a feature shared with ASP-like proteins in other parasitic nematodes. As can be seen from the 2D silver stained gel below (Fig 1.27 (Hewitson et al., 2011b)), VAL proteins comprise a significant proportion of the proteins found in HES however their diversity both at the nucleotide and amino acid levels mean that they form a group of proteins with potential for a functional role in many different environments throughout the parasite. As a main player in the excretory/secretory products of the parasite there is also a very strong chance that they somehow help modulate host immune responses thus allowing their guaranteed persistence.

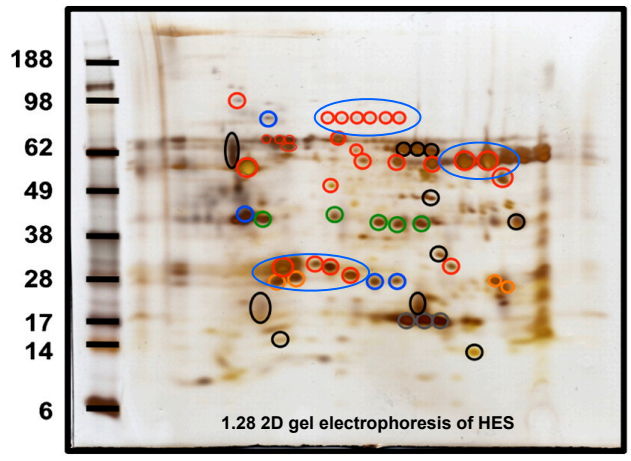

Fig. 1.27 2D electrophoresis of excretory/secretory products from *H.polygyrus*.

The following chapters will investigate potential immunomodulatory effects of these proteins in two different model systems and will attempt to understand how these proteins interact with their immediate surroundings in and around the worm.

Chapter 2

Gene function analysis using a novel transgenic approach.

Introduction

To study the function of a particular gene methods have changed quite dramatically over the past few years. Previously a forward genetic approach would have been employed where the search was for a gene responsible for a known phenotype (Fig. 2.1). With recent advances in whole genome sequencing it is now more often the case that the gene is actually the starting point of the research with the resultant phenotype being the question. As a consequence of this, recent methods for studying gene function have often focussed in on reverse genetic techniques where the known gene sequence can be manipulated by various methods and the phenotype of the altered gene will give clues as to its function. These methods include gene deletion and point mutations, achieved by either chemical mutagenesis or by transposon mediated mutagenesis (Triglia, Duraisingh, Good, & Cowman, 2005), (Murray et al., 2005); homologous recombination is often used and allows very precise and targeted manipulation (McCulloch & Barry, 1999), (Ding et al., 1999).

More recently enriched information from genome studies on schistomosmes has allowed transgenic approaches to be employed using integration competent vectors such as retroviral systems (Brindley et al, 2012), while murine leukemia virus has been successfully used to generate transgenic *S.mansoni* (Rinaldi et al, 2014). Parasitic helminths do not easily lend themselves to some of these methods of study. In general the most widely applied technique would be that of transient RNAi, however even this is very species dependant, working in some systems but remaining elusive in others (Lendner et al., 2008), (Knox et al., 2007). With all of these limitations, researchers have to adapt well-known and used systems to their particular organism with varying degrees of success.

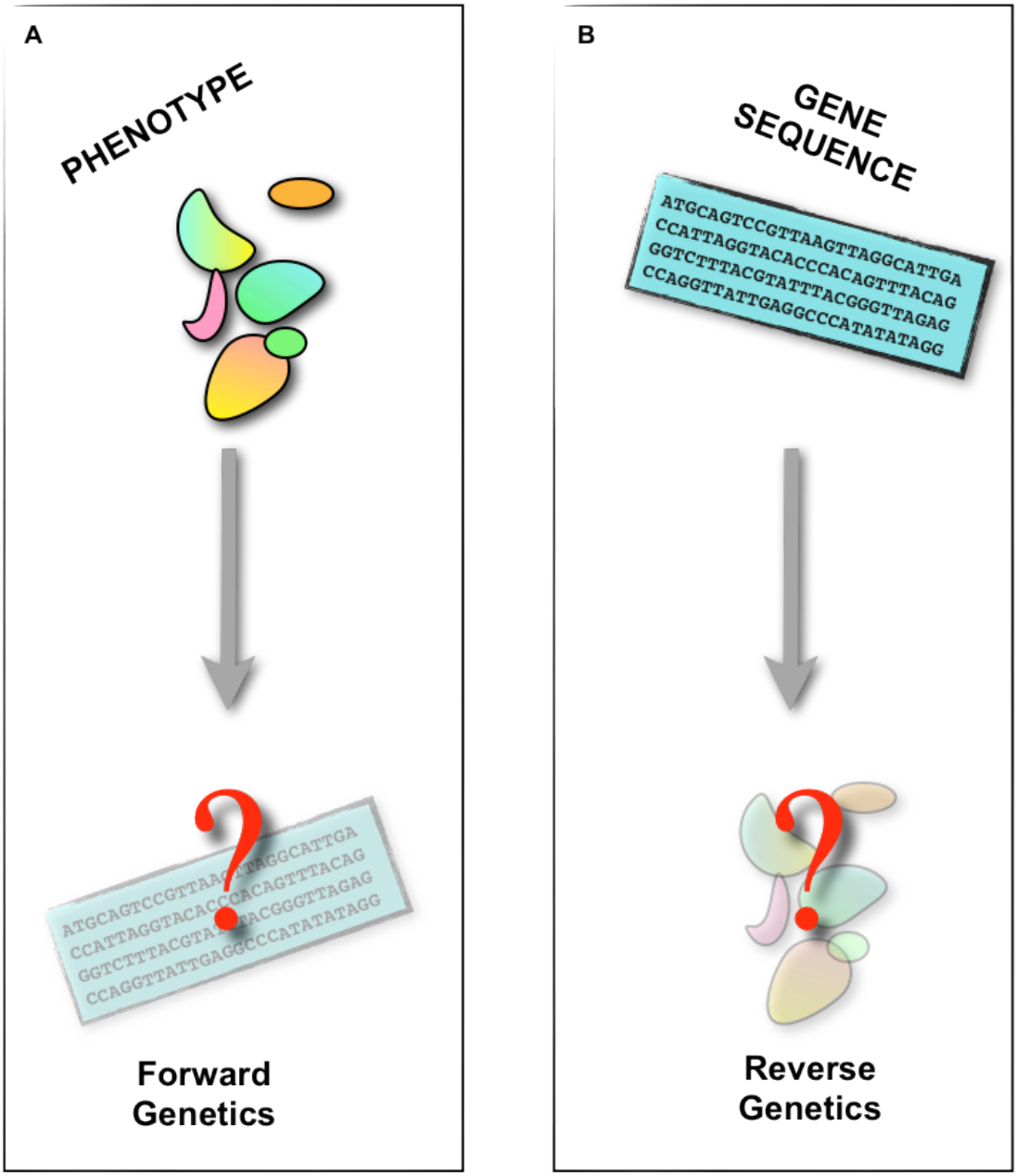

Fig 2.1 Forward and reverse genetics

A. Traditionally research into gene function was performed from the basis of a known phenotype, with experiments carried out to understand the gene sequence responsible for that phenotype. **B**. With much more gene sequence information available now due to the advances in whole genome sequencing technology, more often now researchers start with a gene sequence and modify this to examine the outcome and define genetic phenotypes.

The system studied in this chapter has been used previously in our laboratory to determine the immunological function of a gene from the filarial parasite *Brugia malayi* (Gomez-Escobar et al., 2005). It allows the function of a single helminth gene to be investigated by inserting it into another parasite, in this case *Leishmania mexicana* (*L.mexicana*). The transfected *L.mexicana* can then be tested *in vitro* with regards to their ability to infect macrophages, a cell type known to be involved in filarial infections (Goodridge et al., 2001), (Loke et al., 2002) or *in vivo* where details of their infectivity in various mouse species has been documented (Rosas et al., 2005). *L.mexicana* was chosen over its more virulent cousin *L.major* due to the fact that it can establish an infection *in vitro* in macrophages whether they are *ex vivo* or bone marrow derived. Studies can then be expanded with the same line of transgenic parasites with *in vivo* effects being observed by setting up infections in mice. Miβlitz et al. first described the construction of a DNA cassette, which allowed integration of a gene into a genomic small sub-unit rRNA locus of *Leishmania mexicana* by homologous recombination (Misslitz, Mottram, Overath, & Aebischer, 2000). This system was also used by Bennett to study the role of dendritic cells in a *Leishmania* infection setting (Bennett, Misslitz, Colledge, Aebischer, & Blackburn, 2001). Here they generated *Leishmania* parasites, which expressed the EGFP protein through integration of the pSSU cassette containing the EGFP reported gene. They went on to infect bone marrow derived dendritic cells with EGFP-expressing promastigotes and analysed these using FACS.

Here VAL genes from *B.malayi*, *C.elegans* and latterly *H.polygyrus* were all cloned into the pSSU vector (Fig. 2.2). This allowed a set of *in vitro* and *in vivo* experiments to be carried out to address the hypothesis that the VAL genes, regardless of which organism they are expressed in, play a role in immune system manipulation.

In vitro experiments where bone marrow derived macrophages were infected allowed questions of infectivity, cytokine production and macrophage activations status to be addressed while *in vivo* experiments in mice allow similar questions to be asked but in a much more challenging environment.

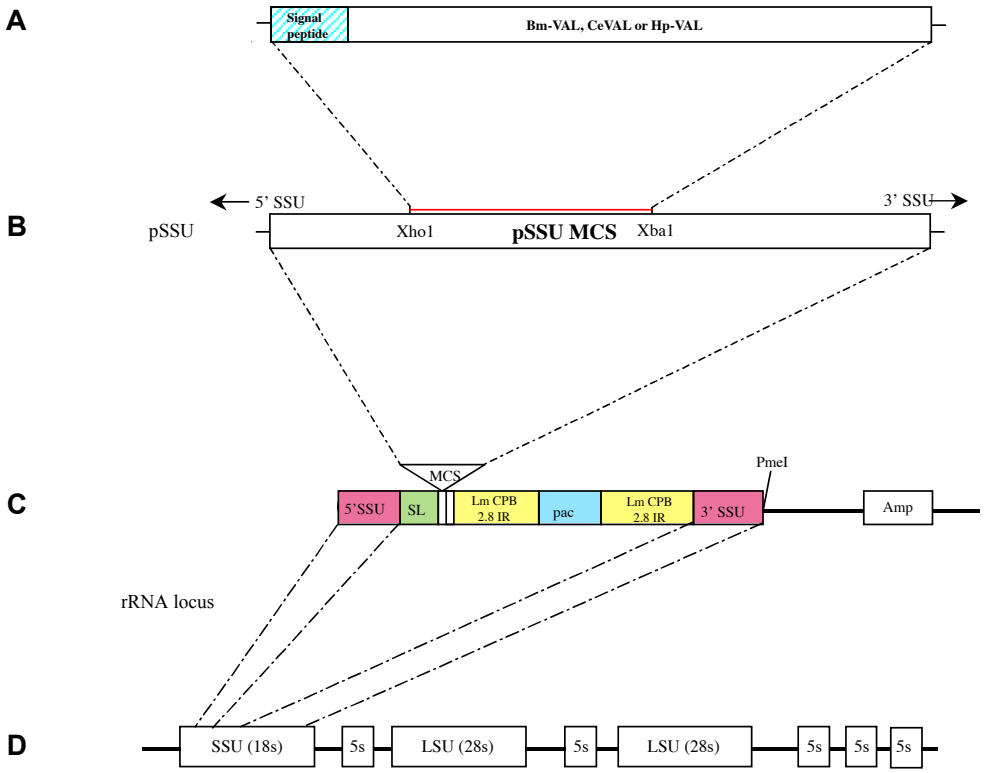

Fig 2.2 Construct design for cloning into pSSU vector.

A VAL gene showing signal sequence which was cloned into pSSU in its entirety.
B Introduction of the VAL gene into the multiple cloning site of pSSU. Xho and Xba were used for all 3 VAL genes.
C 5' SSU and 3'SSU (pink) are sequences required for homologous recombination into an 18s rRNA gene. SL (green) contains a splice acceptor site. LmCPB (yellow) is the *L.mexicana* cysteine proteinase B 2.8 gene which allows high gene expression in the amastigote stage of the parasite life cycle. pac(blue) is required for puromycin selection. The restriction site Pme1 is required for plasmid linearisation.
D Site of integration into an rRNA locus.

Results

2.3 Vectors used in the cloning of Bm-VAL, Ce-VAL, and Hp-VAL1 into the *Leishmania* expression system.

In order to examine the functional effects of the VAL genes it was first of all necessary to clone these genes into a vector that allowed them to be expressed in *L.mexicana*. In the first instance genes were amplified by PCR and were then ligated into the cloning vector pGEM-T (Promega) (Fig. 2.3A). PCR amplification primers (Materials and Methods : Table 8) had included restriction enzyme sites enabling the excision of the gene from pGEM-T and subsequent ligation into the multiple cloning site of pSSU-int (Fig. 2.3B). (Misslitz et al., 2000) This plasmid had originally been designed to enable its introduction by homologous recombination into a genomic small sub-unit rRNA locus. Continued expression of the inserted gene at high levels was ensured by insertion of intergenic regions from a cysteine proteinase B gene cluster known to regulate levels of expression.

Constructs were linearised with Pme1 (Table 2.1) prior to electroporating logarithmic phase promastigotes. 24 hours post electroporation transfection positive parasites were selected by adding puromycin to the culture media with positive lines emerging two to three weeks later. Bm-VAL-1, Ce-VAL, pSSU (control) and Hp-VAL-1 were all cloned and transfected in this manner.

	Gene Length	No. amino acids & Protein size	pI	Signal sequence
BmVAL-1 (single domain)	**663b.p.**	**221 24.76 kDa**	**10.05**	✓
CeVAL (single domain)	**624b.p.**	**208 22 kDa**	**8.94**	✓
HpVAL-1 (double domain)	**1422b.p.**	**474 48.85kDa**	**8.01**	✓

Table 2.1

VAL genes cloned into pSSU vector.
Bm-VAL (*Brugia malayi*), CeVAL (*Caenorhabditis elegans,* F49E11.6), HpVAL-1 (*Heligmosomoides polygyrus*)

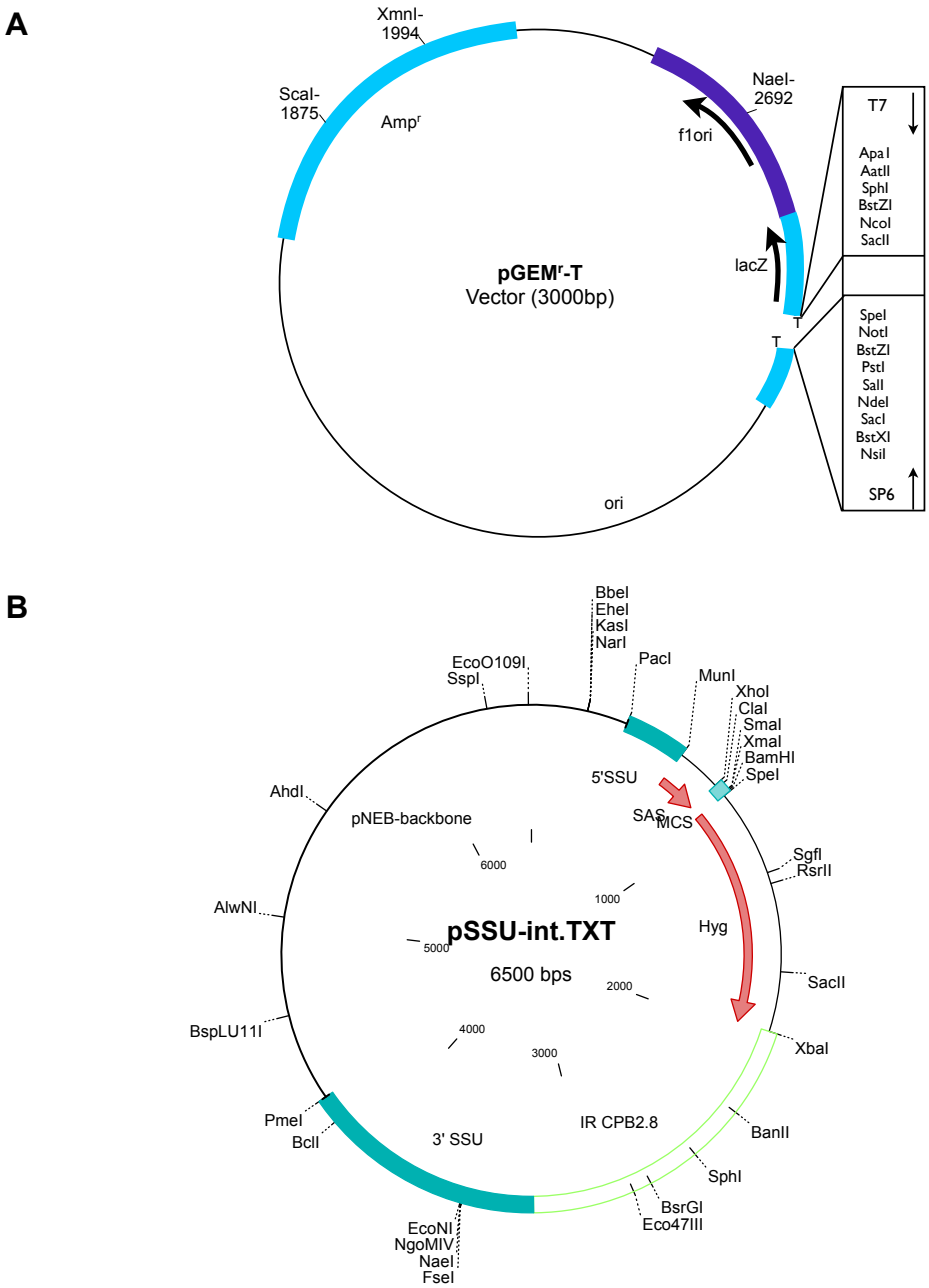

Fig 2.3 Vectors used in the cloning of Bm-VAL, Ce-VAL and Hp-VAL1 into the *Leishmania* expression system.

pGEM-T cloning vector (Promega) was used to sub-clone genes prior to final cloning. Diagram adapted from Promega data sheet (A).
pSSU-int vector showing multiple cloning site (MCS), Pme1 restriction site which was used to linearise constructs prior to electroporation and the position of both the 3' and 5' SSU sequences which allow integration into the 18s rRNA locus (B).

2.4 In vitro infection of bone marrow derived macrophages. *(BMDM)*

Macrophages are readily infected by *Leishmania mexicana* and as such are an appropriate readout to assess the infectivity of wild type and transgenic parasites *in vitro* {Weinheber, 1998 #164}. These cells are also at the forefront of the immune response to filarial infection (MacDonald, Maizels, Lawrence, Dransfield, & Allen, 1998) and as such are particularly relevant to this study.

Bone marrow derived macrophages were cultured on glass cover slips in 24-well plates and were infected with wild type, Bm-VAL or Ce-VAL transgenic parasites (3 cover slips each). At 24 hours (Fig 2.4 A) and 5 days (Fig 2.4B) after infection the coverslips were removed from the wells and were stained using DIFF QUICK. The numbers of parasites per macrophage were then counted with 200 macrophages per coverslip enumerated.

Little difference was noted 24 hours after infection between the parasite lines. However 5 days post infection the number of macrophages containing no parasites was higher in macrophages infected with wild type parasites than with Bm-VAL or Ce-VAL parasites, suggesting that the wild type parasites were less able to infect although this was a subtle observation and did not reach statistical significance. Macrophages containing one or more parasite showed no differences between *Leishmania* lines.

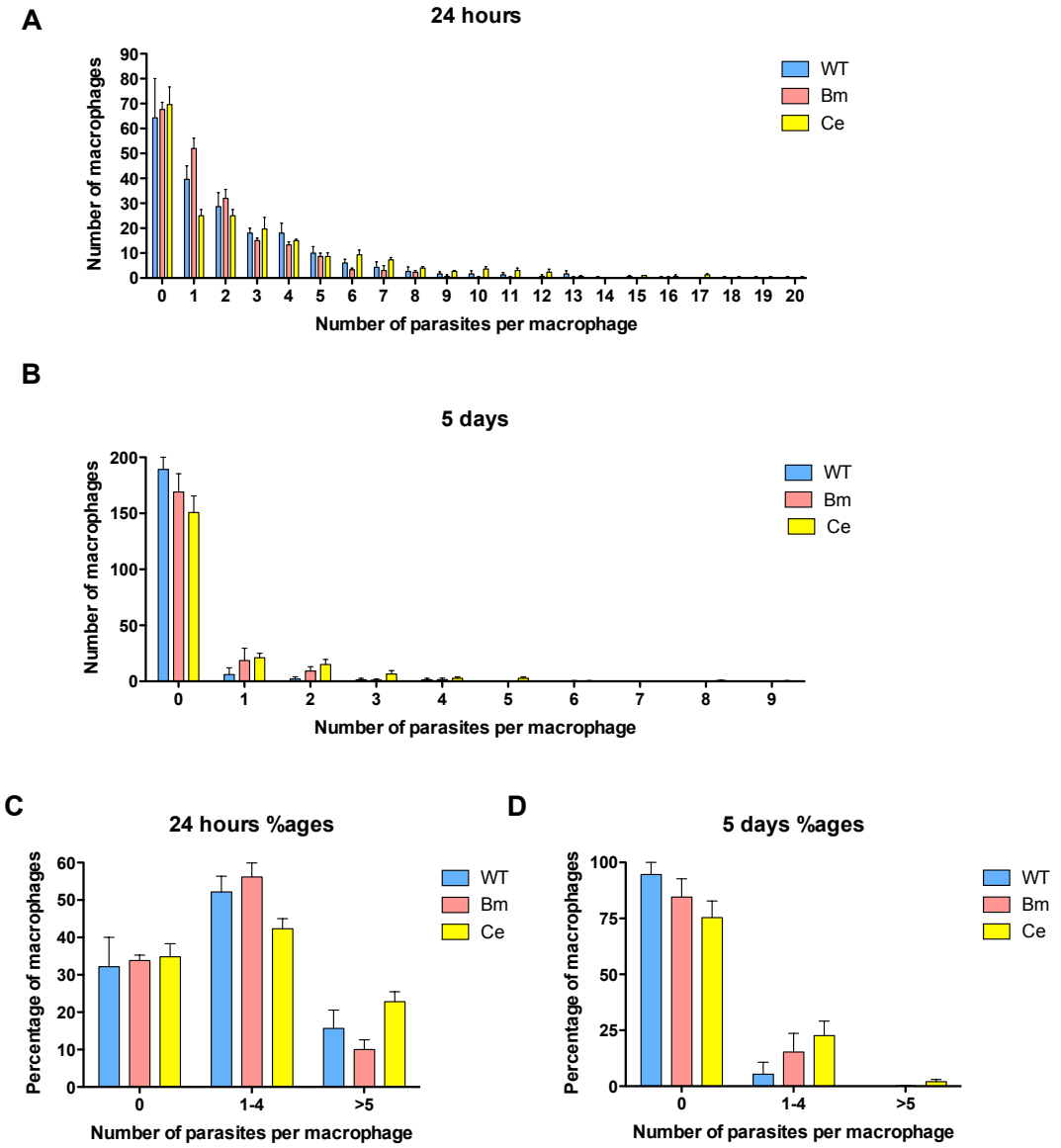

Fig 2.4 *In vitro* infection of bone marrow derived macrophages. (BMDM)

1x10^5 bone marrow derived macrophages from C57/B6 mice were cultured in a 24-well plate prior to infection with W.T., Bm-VAL or CeVAL transgenic *L.mexicana* for a period of 24 hrs (A & C) or 5 days (B & D).

Parasites present in macrophages were detected by DIFF QUICK staining. 200 macrophages were counted for each time point.

2.5 Expression of arginase, iNOS, IL13 & Il10 in infected BMDM by quantitative RT-PCR.

Various parameters were measured in order to assess the internal environment of the macrophage and to see if manipulation of the parasite had affected this in any way. **Arginase** has been shown to be closely involved with the development and maintenance of *Leishmania* infection (Iniesta et al., 2005), (Gaur et al., 2007) with the induction of arginase 1 favouring parasite replication. Host Th2 cytokines **IL-4** and **IL-13** also play a part in the regulation of this induction. When induction of arginase is inhibited parasite numbers are reduced. This mechanism is a result of arginase being produced by the parasite and not by the host as described by (Roberts et al., 2004), where deletion of the gene involved in parasite arginase activity in *L.mexicana* resulted in reduced parasite survival given that parasite produced arginase enhances parasite survival by causing the reduction of the iNOS substrate arginine.

Il-10 that is produced by macrophages in response to IgG1 bound to the surface of *Leishmania* parasites causes a decrease in IL-12 production and **iNOS** expression and a subsequent reduction in the production of parasite killing nitric oxide (Kane & Mosser, 2001), (Buxbaum, 2013) thus favouring parasite survival within the host cell. Fig 2.6 summarizes the interaction of host cytokines and their effect on the activation status of an infected macrophage. Adapted from (Liu & Uzonna, 2012).

In this experiment, total RNA from macrophages that had been infected with parasites for 24 hours was extracted. cDNA was generated by reverse transcription and quantitative real time PCR was carried out for arginase, iNOS, IL-10 and IL-13 (Fig. 2.5 A-D) with levels of gene expression being expressed as a ratio of β-actin. No significant differences were seen in any of the genes tested, but notably both Il-13 and arginase showed increased trends in VAL-transfected settings.

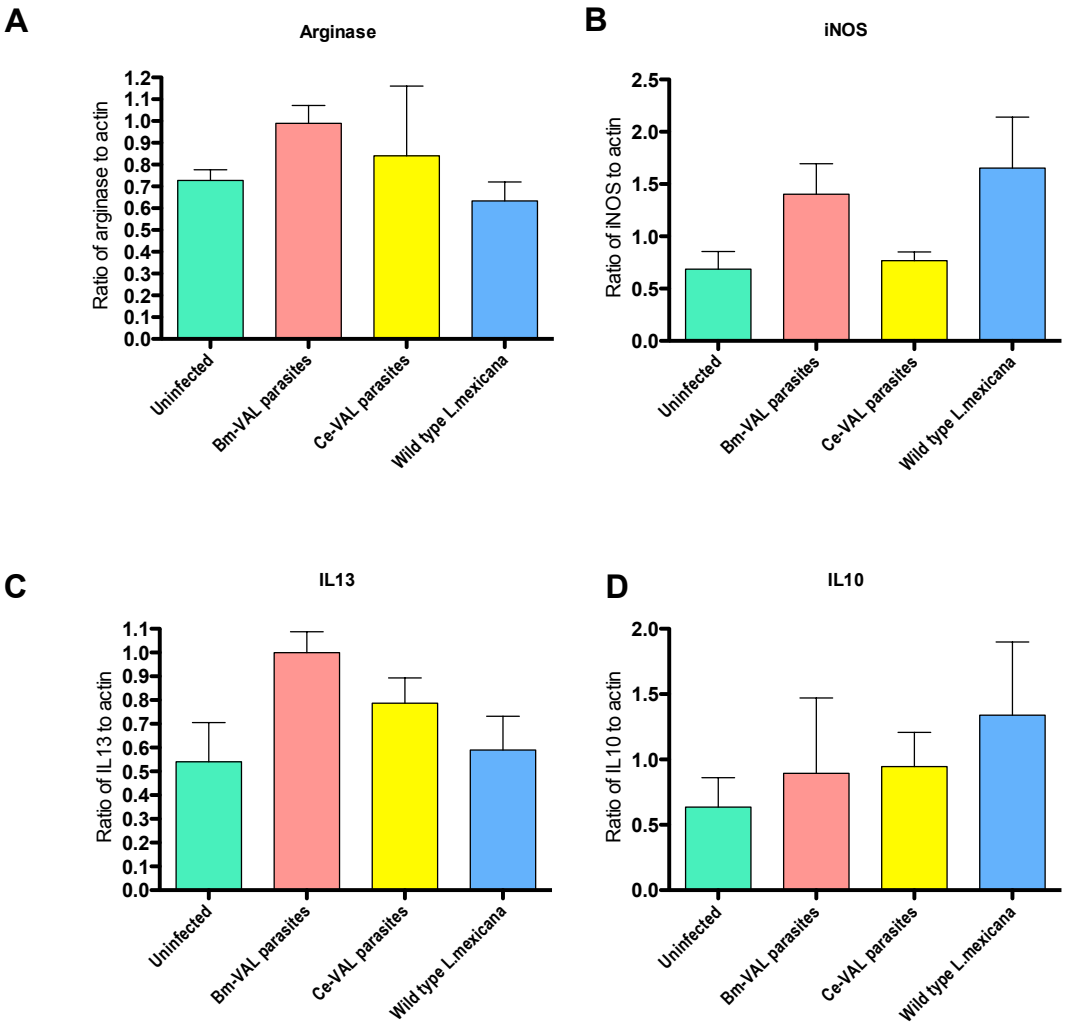

Fig 2.5 Expression of arginase, iNOS, IL13 & Il10 in infected BMDM by quantitative RT-PCR.

Total RNA from uninfected macrophages and macrophages infected with parasites for 24 hours was extracted in order to generate single stranded cDNA. Real time PCR (30 cycles) using the Lightcycler was used to determine expression levels of the following genes of interest:

A. Arginase
B. iNOS
C. IL-13
D. IL-10

These were expressed as a ratio of β-actin.
Differences not significant by T-test analysis. Error bars show SEM.

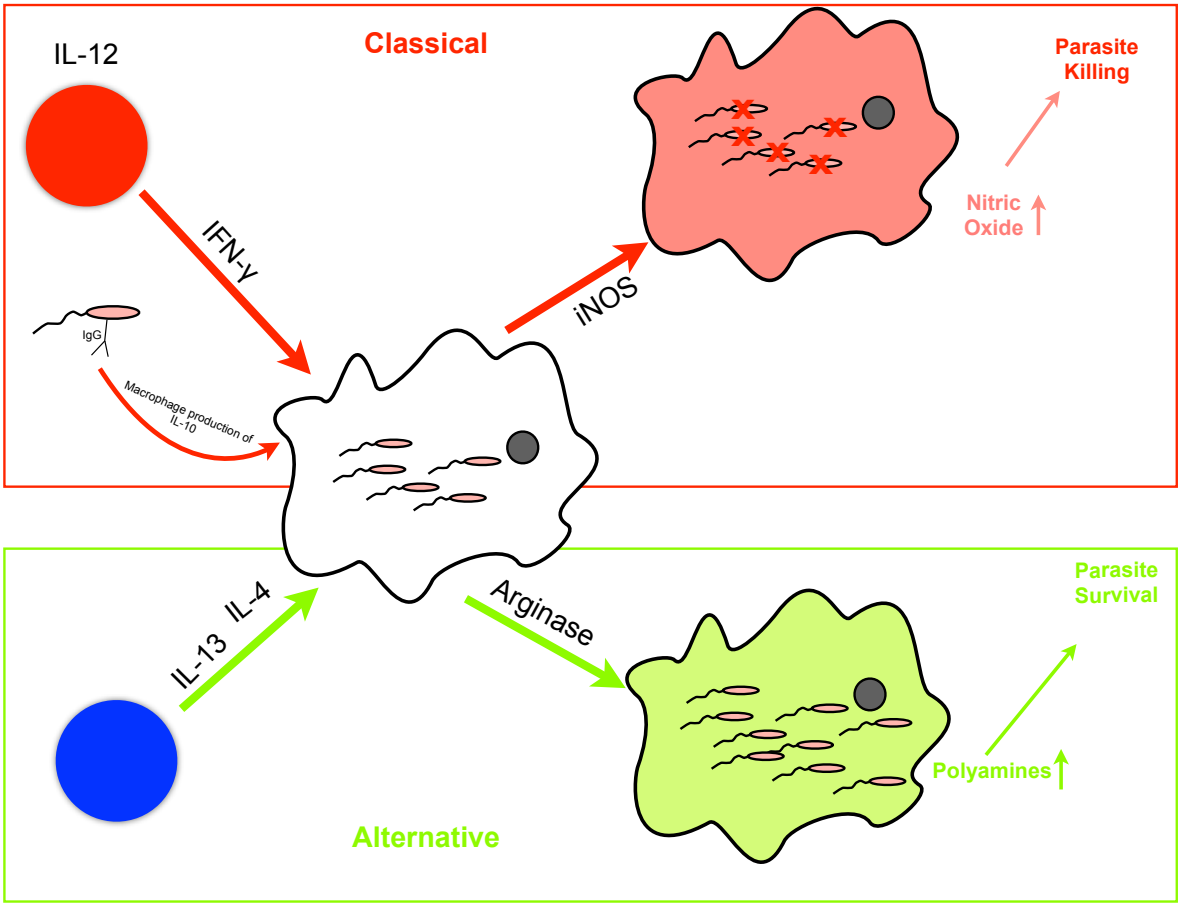

Fig 2.6 Macrophage responses to *Leishmania* infection

2.7 Experimental protocol for *in vivo* assessment of Bm-VAL-1 gene function.

Although assessments of gene function related to the transgenic parasites in an *in vitro* setting can reveal interesting information about the parasites and their influence on specific cell types e.g. macrophages, a far more challenging environment for the parasite is that of an *in vivo* infection setting.

To this end parasites were injected into the footpad of C57/B6 female mice. At week 3-post infection, weekly footpad measurements were taken from the infected foot and the uninfected contra-lateral foot as a control. Measurements were taken using a digital micrometer in a blinded fashion. This experiment ran for 8 weeks after which the final lesion measurement was taken and the infected foot removed from the mouse for parasite recovery data. Popliteal lymph nodes were harvested for analysis of intracellular cytokine production.

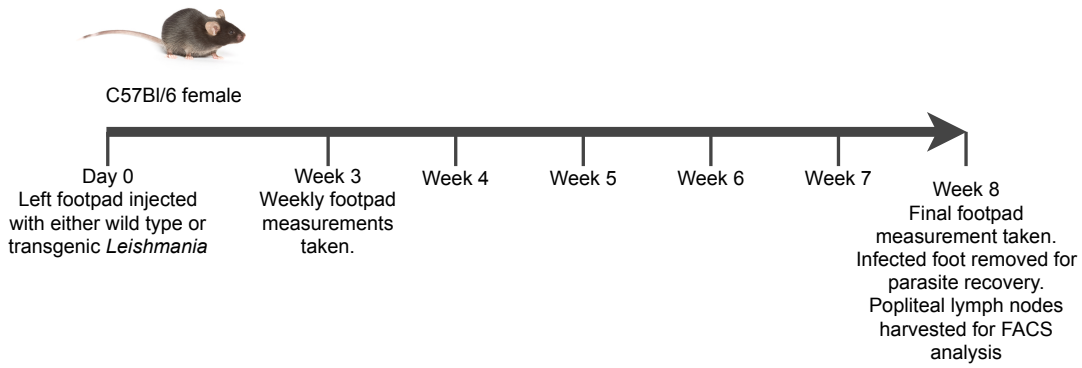

Fig 2.7 Experimental protocol for *In vivo* assessment of Bm-VAL-1 gene function.

Mice were injected subcutaneously in the footpad of the rear left foot with $3x10^6$ wild-type or transgenic parasites. Groups of 8 mice were tested. 3 weeks post injection footpad measurements were taken from both the infected foot and the contralateral uninfected foot.
At week 8 final footpad measurements were taken, the infected foot removed for parasite recovery analysis and popliteal lymph nodes harvested for intracellular cytokine analysis.

2.8 Time course of cutaneous lesion development.

Monitoring of infection progress can be performed throughout the whole experiment in a non-invasive manner by measuring the local swelling that occurs in the injected footpad. This is then compared with a measurement taken from the uninfected contra-lateral footpad and the difference in measurement is plotted. Over time this gives an indication of the progress of the infection and allows comparisons to be drawn between experimental groups but should not however be the sole determinant of infection severity as lesion size does not always correlate with the number of viable parasites. Thus, the previous method (Fig 2.7) whereby viable parasite numbers are recovered at the end of an experiment should be used in conjunction with lesion development measurements.

Here each group consists of 8 female mice per treatment housed in cages of 4 mice per cage. Measurements of swelling was taken weekly from 3 weeks post injection and was plotted as shown for individual mice in Fig 2.8 A & B. In Fig 2.8 C measurements for individual mice were grouped to show more clearly the difference between wild type and transgenic infected mice.

Lesions were much larger in mice infected with Bm-VAL parasites than in mice infected with wild type. This data along with that from the parasite recovery from the footpad would therefore tend to indicate a more severe infection was being mounted by transgenic parasites than that of the wild type.

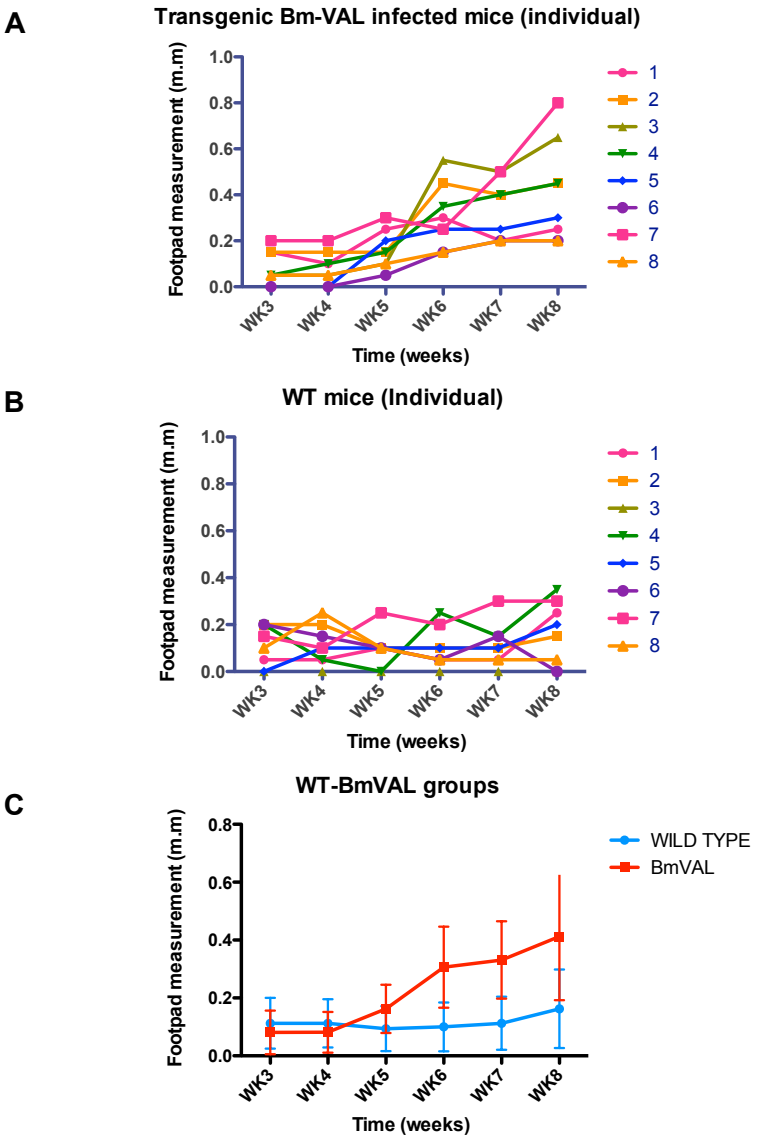

Fig 2.8 Time course of cutaneous lesion development.

A & B Time-course of footpad swelling (lesion development) in individual mice from groups of mice infected with either wild type *L.mexicana* or Bm-VAL transgenic *L.mexicana*. **C** Time-course showing grouped mice measurements.

For **A,B & C** Groups of 8 mice were mice were injected subcutaneously in the footpad of the rear left foot with $3x10^6$ wild-type or transgenic parasites. 3 weeks post injection footpad measurements were taken using a digital micrometer from both the infected foot and the contralateral uninfected foot. At week 8 final footpad measurements were taken, the infected foot removed for parasite recovery analysis and popliteal lymph nodes harvested for intracellular cytokine analysis. Panel C shows the mean measurements for the 8 mice. Error bars show standard deviation.

2.9 Mice infected with Bm-VAL transgenic parasites have a higher parasite burden than those infected with wild type *L.mexicana*.

One of the experimental readouts of *Leishmania* infection *in vivo* is that of parasite burden at the site of infection. The infected footpad was collected at the conclusion of the experiment and samples serially diluted as shown in Fig 2.9A. Following 7 days of incubation at 26°C the number of viable parasites from the footpad was deduced from the highest dilution at which promastigotes could be grown. Significantly more Bm-VAL transfected parasites were present at high dilutions than wild type parasites after 7 days culture (Fig 2.9B, Student t test, * 0.03). These parasites were then tested by RT-PCR for continued expression of the Bm-VAL gene which is shown in Fig 2.9C.

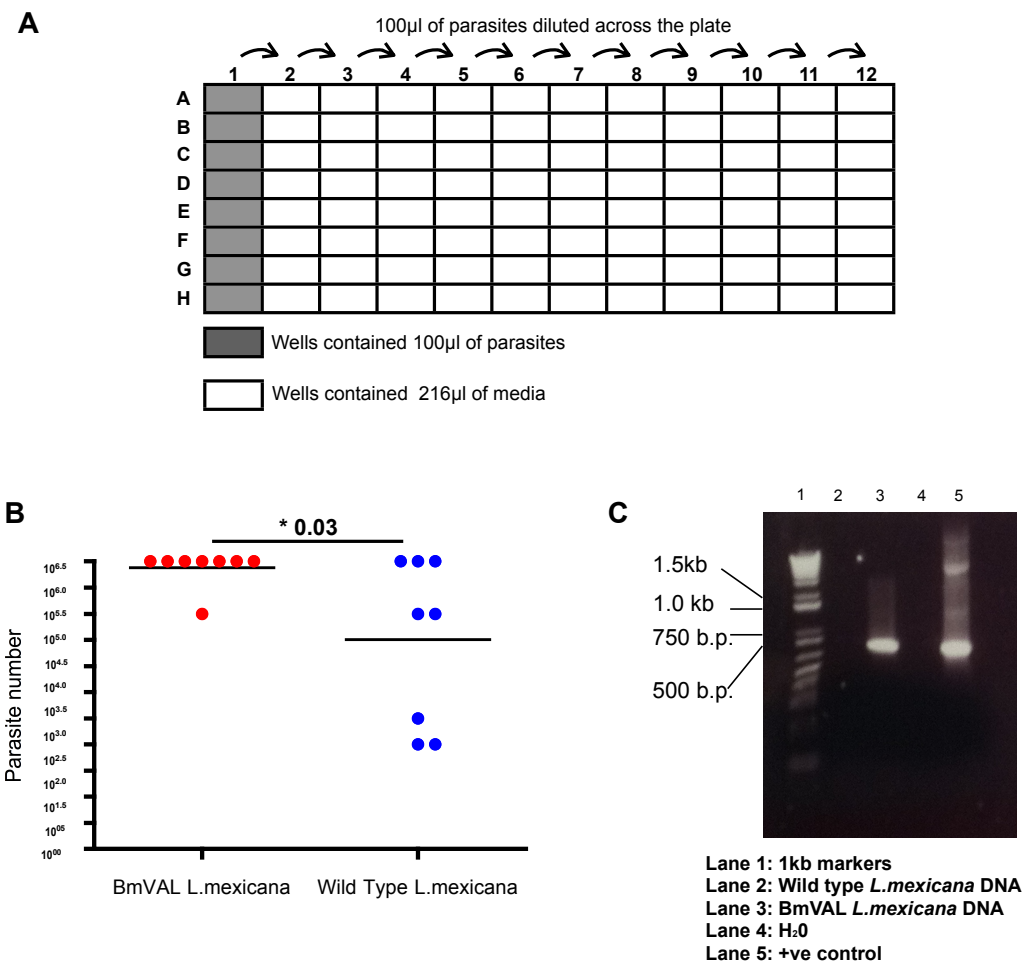

Fig 2.9 Mice infected with Bm-VAL transgenic parasites have a higher parasite burden than those infected with wild type *L.mexicana*.

A Scheme for serial dilution of parasites.

B Parasite recovery from infected footpad after 8 week infection. Parasite numbers were determined by serial dilution as described (**A**). Results statistically significant by Students t test.

C Continued expression of BmVAL by parasites recovered from the footpad was shown in lane 3. RNA was extracted from parasites that had been cultured for 2 weeks after recovery from the infected foot. RT-PCR results with gene specific primer are shown.

2.10 Immune responses in popliteal lymph node.

Immune cytokines produced during an infection are an important measure of the immune response with regards to its nature and provenance. In the case of *Leishmania* infections the type of immune response is critical in determining the outcome as to whether or not the parasite will survive and if lesions will heal or become ulcerative (Liese, Schleicher, & Bogdan, 2008), (Hurdayal & Brombacher, 2014).

To complete the experimental readout for the *in vivo* evaluation of Bm-VAL in the *Leishmania* system, popliteal lymph nodes were harvested from the mice and were examined for their production of intracellular IL-4, IL-10 and IFN-γ. Total cell numbers were enumerated before an initial stimulation with PMA, Ionomycin and Brefeldin A. Cells were then permeabilised using BD Cytofix/ Cytoperm solution prior to surface staining for the lineage marker CD4. Subsequent staining for the individual cytokines mentioned above was then performed.

The analysis showed an elevated number of total cells present in the lymph node of mice infected with Bm-VAL parasites although CD4+ cell numbers were higher in the mice infected with wild type parasites. None of the cytokines measured differed with any significance between the two groups of mice infected.

With tantalising data from lesion development measurements and parasite recovery from the footpad both hinting that Bm-VAL transfected parasites initiate a different response from the host immune system it was decided to carry out a repeat experiment, this time continuing the infection for longer and including parasite recovery information from the spleen.

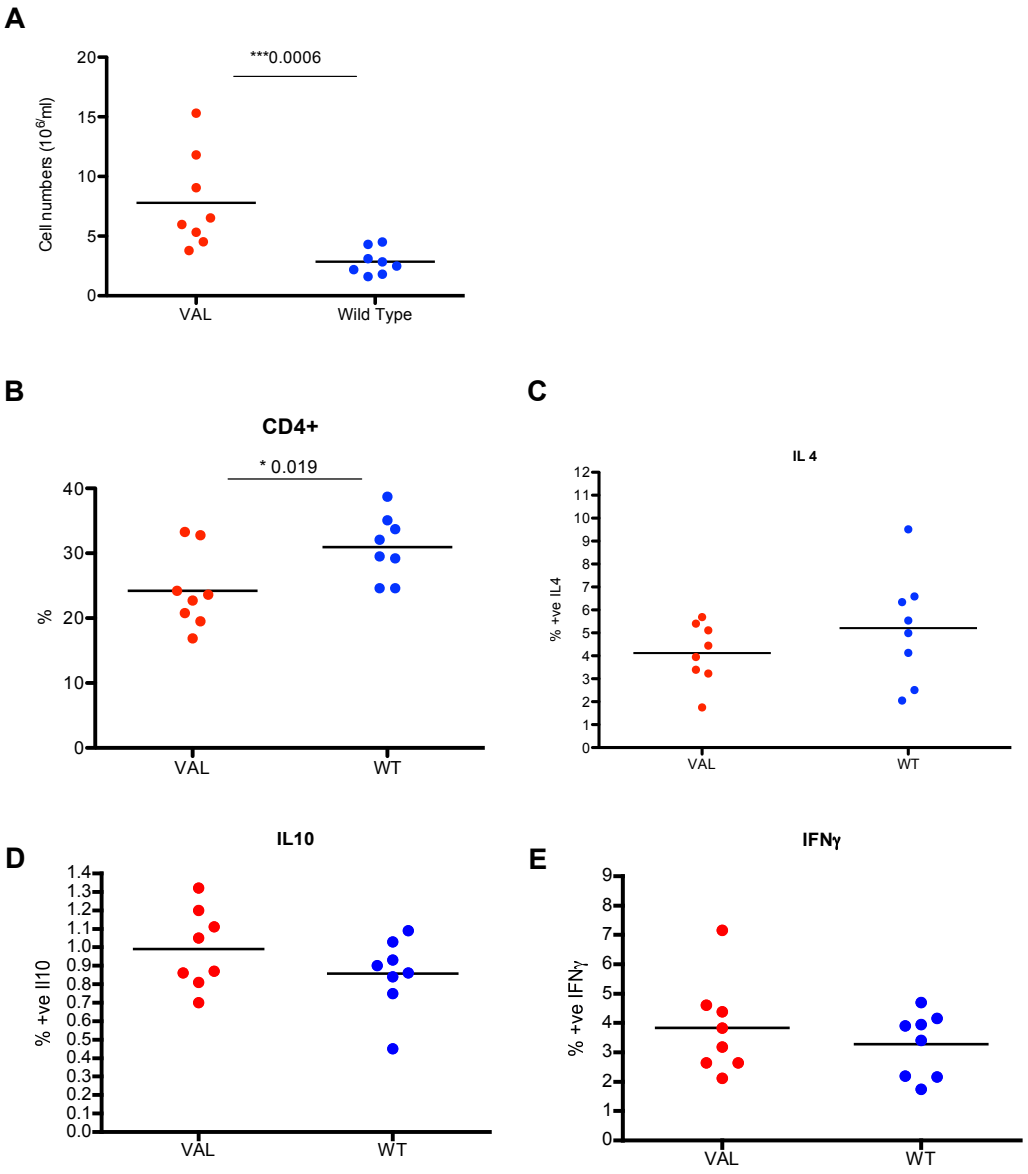

Fig 2.10 Immune responses in popliteal lymph node.

Cells harvested from the draining popliteal lymph node and were stained for the production of intracellular cytokines. Briefly, cells were counted (**A**) and then stimulated with PMA/ Ionomycin and Brefeldin A for 4 hours prior to CD4 cell surface staining (**B**) followed by a permeabilistaion step with BD Bioscieces cytofix/ Cytoperm and subsequent staining for intracellular cytokines, in this case IL10 (**C**) and IFNγ(**D**).

2.11 Experimental protocol for *In vivo* assessment of Bm-VAL-1 gene function.

The first *in vivo* experiment showed that the Bm-VAL gene might be having some effect on either parasite progress or the interactions between the parasite and the host immune system. The protocol in that instance had continued for 8 weeks. Examining lesion development data it appeared that for some mice the response had not plateaued in which case it would be interesting to repeat this but continue the experiment for another 4 weeks. Parasites recovered from that experiment, which had been verified for the continued expression of BmVAL protein, were cultured to ensure stationary growth phase and used to inject female C57/B6 mice sub-cutaneously in the hind footpad with either wild type *L.mexicana* or Bm-VAL transgenic parasites. Weekly measurements of the two hind feet were taken to monitor lesion development and at 12 weeks the experiment was terminated. The infected rear foot and spleen were harvested to check for parasite recovery along with the lymph nodes, which were harvested for cytokine analysis.

2.12 Time course of Lesion Development.

Lesion development is a key indicator of infection progress and intensity. Results from the second *in vivo* experiment showed a distinct trend whereby the sub-cutaneous lesion development in animals infected with wild type parasites was more pronounced than in mice infected with Bm-VAL transgenic parasites. This was in direct contradiction to the first experiment where Bm-Val transgenic parasites induced more swelling than the wild type. Footpad measurements for mice present in the wild type infected group showed slightly more variability than was noted in the transgenic group.

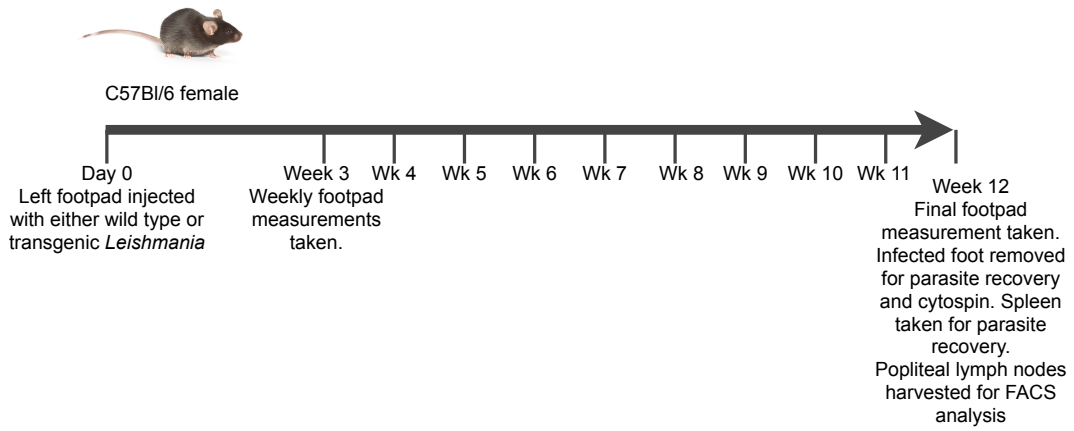

Fig 2.11 Experimental protocol for *In vivo* assessment of Bm-VAL-1 gene function.

Mice were injected subcutaneously in the footpad of the rear left foot with $3x10^6$ wild-type or transgenic parasites which had been recovered from the infected footpads of mice from the previous experiment. Groups of 8 mice were tested. 3 weeks post injection footpad measurements were taken in a blind manner from both rear feet.
At week 12 final footpad measurements were taken, the infected foot removed for parasite recovery analysis and popliteal lymph nodes harvested for intracellular cytokine analysis. This time the spleen was also harvested to check for the presence of parasites.

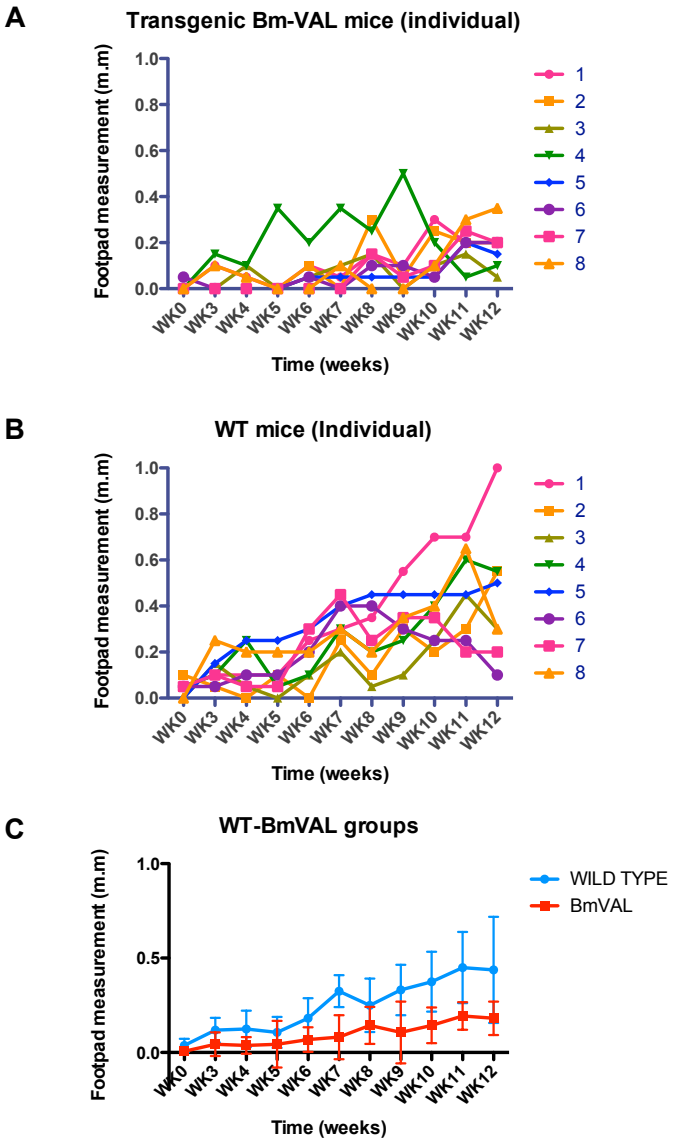

Fig 2.12 Time course of Lesion Development.

A & B Time-course of footpad swelling (lesion development) in individual mice from groups of mice infected with either wild type *L.mexicana* or Bm-VAL transgenic *L.mexicana*. **C** Time-course showing grouped mice measurements.

For **A,B & C** Groups of 8 mice were mice were injected subcutaneously in the footpad of the rear left foot with $3x10^6$ wild-type or transgenic parasites. 3 weeks post injection footpad measurements were taken using a digital micrometer from both the infected foot and the contralateral uninfected foot. At week 12 final footpad measurements were taken, the infected foot removed for parasite recovery analysis and popliteal lymph nodes harvested for intracellular cytokine analysis.
Panel C shows the mean measurements for the 8 mice. Error bars show standard deviation.

2.13 Parasites recovered from foot and spleen of infected mice.

Another key indicator of the intensity of parasite infection is a measurement of parasite burden in the footpad and also in the spleen (Aguilar Torrentera et al., 2002), (Buffet, Sulahian, Garin, Nassar, & Derouin, 1995). These tissues were harvested at the end of the experiment and cell suspensions were prepared. Serial dilutions of each tissue were set up and were cultured for seven days. Cultures were then examined to see at which dilution live parasites were present with the final titre determined as the last well containing at least one live parasite.

Result from both the foot (A) and the spleen (C) showed significantly more parasites present at a higher titration in the wild type infected mice than in the mice infected with transgenic parasites. This data corresponded with that from the lesion measurements but again was found to be contradictory to results found in the first *in vivo* procedure.

RT-PCR, with gene specific primers, on RNA extracted from parasites that had been cultured for 2 weeks after recovery from the infected foot showed continued expression of Bm-VAL in transgenic parasites (B).

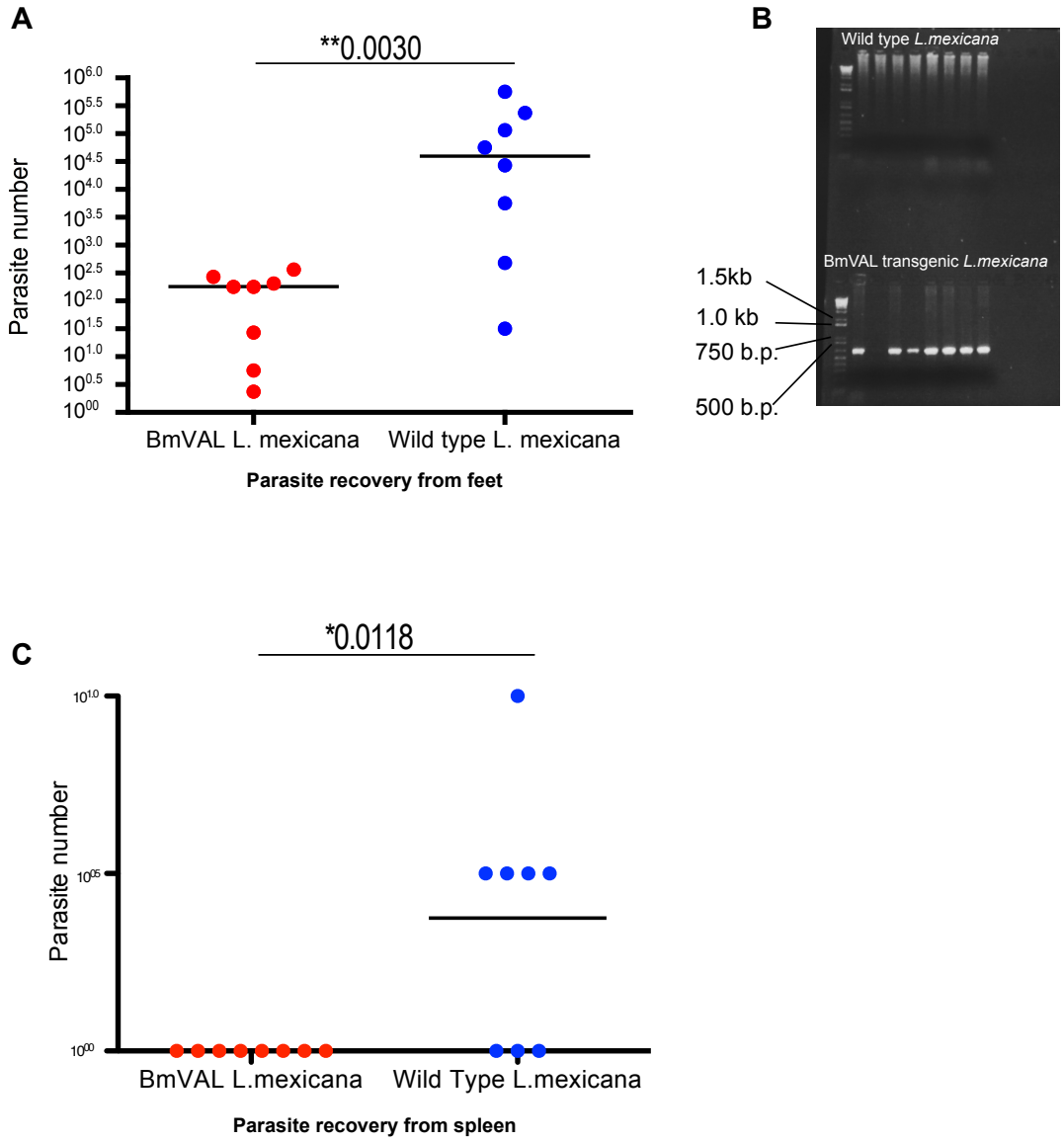

Fig 2.13 Parasites recovered from foot and spleen of infected mice.

The foot (**A**) and spleen (**C**) were recovered from infected mice and were manually disrupted using a syringe plunger. Extracts were centrifuged and then resuspended in 1ml of SDM media prior to serial dilution across a 96-well plate.
B. Expression of BmVAL by parasites recovered from the footpad is shown. RNA was extracted from parasites that had been cultured for 2 weeks after recovery from the infected foot. RT-PCR results with gene specific primers is shown

2.14 Immune responses in popliteal lymph node.

So far, results from the 2nd *in vivo* experiment had been in direct contradiction to those achieved in the first experiment. Lesion development and parasite recoveries had been more pronounced and higher for animals infected with transgenic parasites in the first experiment. However, in the second experiment the wild type infections appeared to be more virulent.

Immune responses in the draining lymph nodes measured from this second experiment were to provide no further insight as to the performance of the two lines of parasite tested. Cell numbers counted from lymph nodes showed no difference (Fig. 2.13A) nor did measurements of CD4+ cells or the production of intracellular IL-10 and IFN-γ (Fig. 2.13C-E). IL-10 and IFN-γ were measured by ELISA with wild type parasites potentially initiating the production of more IL-10.

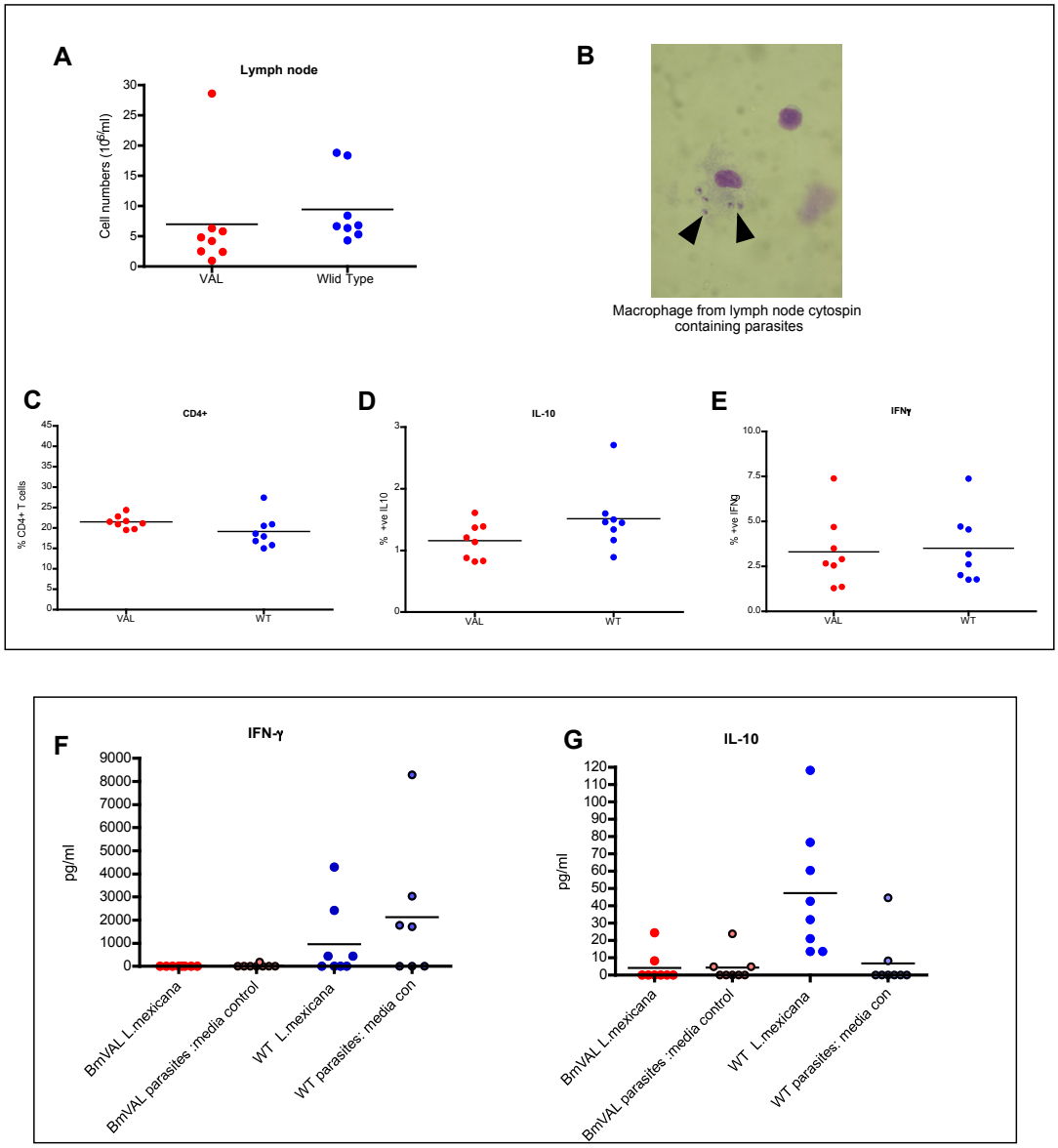

Fig 2.14 Immune responses in popliteal lymph node.

Cells were harvested from the draining popliteal lymph node and were then stained for the production of intracellular cytokines. Briefly, cells were counted (**A**) and then stimulated with PMA/ Ionomycin and Brefeldin A for 4 hours prior to CD4 cell surface staining (**C**) followed by a permeabilistaion step with BD Bioscieces cytofix/ Cytoperm and subsequent staining for intracellular cytokines, in this case IL10 (**D**) and IFNγ(**E**).Panel (**B**) Cytospin showing the presence of *Leishmania* parasites in a macrophage recovered from the lymph node
IFNγ and IL10 levels were also measured by ELISA (**F**) and (**G**).

2.15 Experimental protocol for *In vivo* assessment of Bm-VAL-1 gene function.

It is well documented that *Leishmania* parasites in culture *in vitro* loose their pathogenicity and should be passaged through mice in order to avoid this (Kropf, 1998). An alternative to murine passage is to re-transfect a low passage number wild type parasite with the construct of interest. To ensure that parasites used in my *in vivo* investigations were fully virulent new stable lines of transgenic parasites were generated and the first *in vivo* protocol (Fig. 2.7) was repeated. This involved the subcutaneous injection of parasites in the hind footpad of C57/B6 female mice. Three weeks after injection weekly footpad measurements were taken from both rear feet to measure lesion size and development. At week 8-post infection the experiment was stopped and feet and spleen removed from animals to check for the presence and virulence of parasites. Intracellular cytokines were also measure from the popliteal lymph nodes.

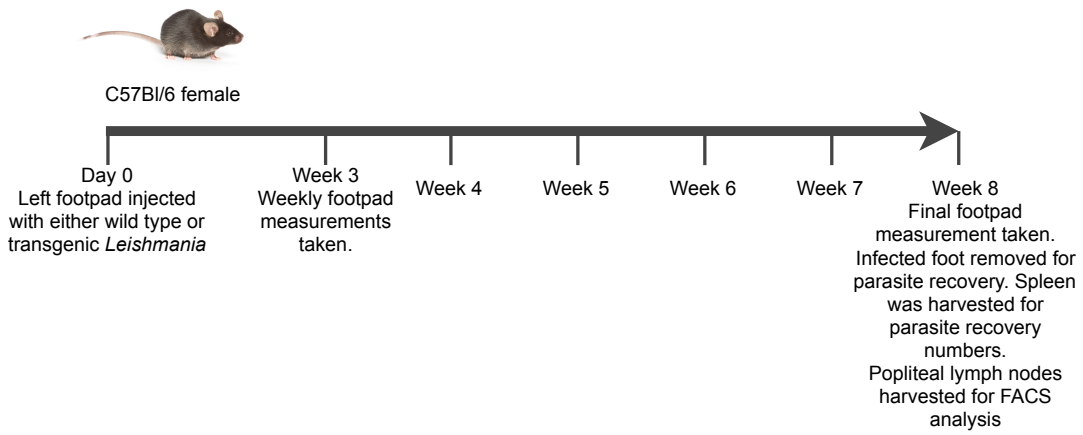

Fig 2.15 Experimental protocol for *In vivo* assessment of Bm-VAL-1 gene function.

New transgenic lines were prepared and mice were subsequently injected subcutaneously in the footpad of the rear left foot with $3x10^6$ wild-type or transgenic parasites. Groups of 8 mice were tested. 3 weeks post injection footpad measurements were taken in a blind manner from both rear feet. At week 8 final footpad measurements were taken, the infected foot removed for parasite recovery analysis and popliteal lymph nodes harvested for intracellular cytokine analysis.

2.16 Growth curves of *Leishmania* promastigotes transfected with pSSU, Bm-VAL or Ce-VAL.

Before undertaking another *in vivo* experiment to look at the immunological impact of transgenic *Leishmania* parasites I decided to generate fresh, low passage number, lines of transgenic parasites. The first two *in vivo* experiments had given directly contradicting results, thus to remove any doubt over the virulence of the lines used, wild type parasites (passage 9) were transfected with either:

1) Empty vector: pSSU
2) Bm-VAL in pSSU
3) Ce-VAL in pSSU.

The *C.elegans* VAL gene was used here as a control, given that *C.elegans* is a non-parasitic nematode but has a number of genes encoding VAL proteins.
Parasites were plated into 6-well plates at $1x10^6$ parasites/ml with a total volume of 5ml per well. Parasite numbers were monitored by daily counting where 10µl of parasites were diluted in 190µl of 4% paraformaldehyde and were then counted using a haemocytometer. Parasites were kept in culture for 7 days.

Wild type parasites appeared to reach stationary phase at 5 days, which was slightly earlier than all 3 transgenic lines. However there was no significant difference between parasites transfected with vector alone (pSSU- Fig 2.16 A) and those transfected with the vector containing a gene encoding the VAL gene (Fig 2.16B&C).

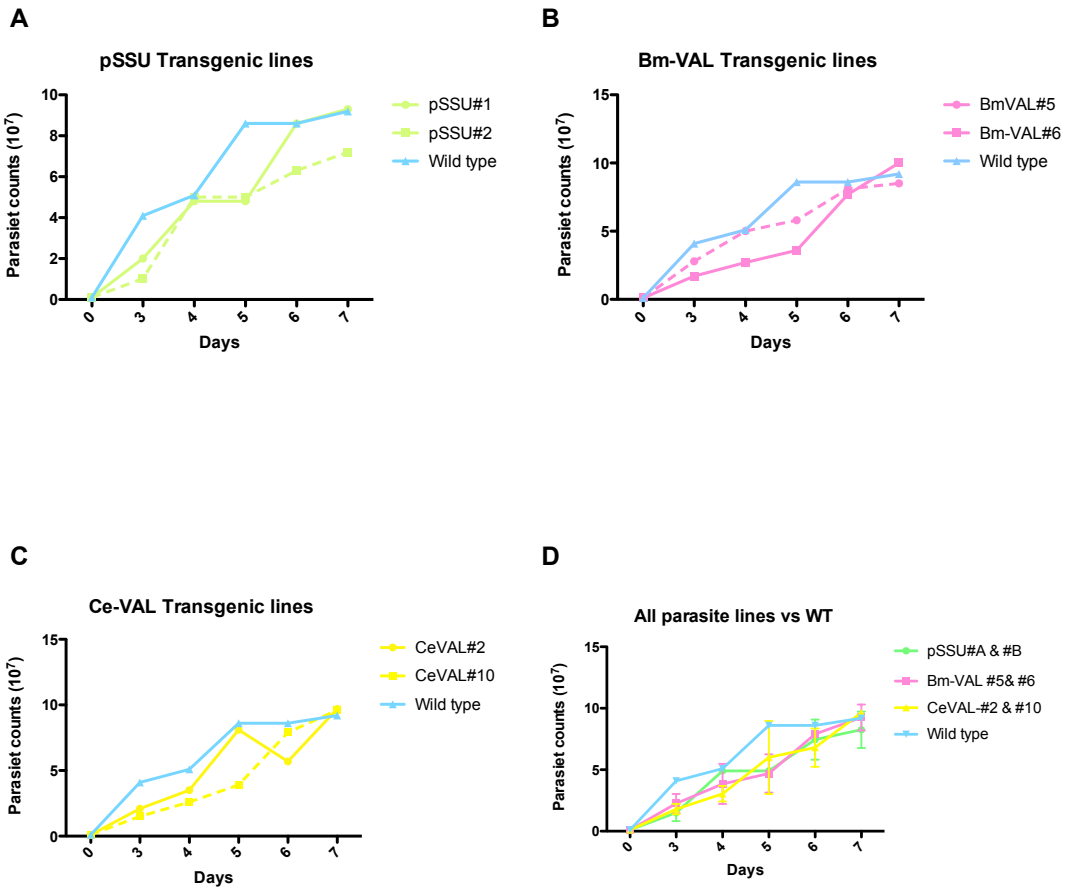

Fig 2.16 Growth curves of *Leishmania* promastigotes transfected with pSSU, Bm-VAL or Ce-VAL.

Two lines of either wild type parasites transfected with empty vector (A) or parasites transfected with Bm-VAL (B) or Ce-VAL (C) were cultured for 7 days. Parasite numbers were determined daily from day 3 onwards. Panel D shows that wild type parasites appear to reach stationary phase around day 5, slightly earlier than the two transgenic lines.

2.17 Time course of Lesion Development.

Lesion development or footpad swelling was again measured over the period of the *in vivo* experiment, which in this case was 8 weeks. As described before the infected footpad was measured and compared to a measurement from the contra-lateral uninfected foot. This was carried out weekly from 3 weeks-post infection and was performed in a blind fashion. Mice were caged in groups of 4 mice per cage with data being pooled for Fig 2.17C.

In this experiment after an initial peak at week 4, mice infected with wild type parasites showed less footpad swelling than mice infected Bm-VAL parasites. Although there seemed to be more variability within the groups in this experiment the data agreed with results seen in the first *in vivo* experiment. However it is notable that overall the footpad swelling in this instance was quite low.

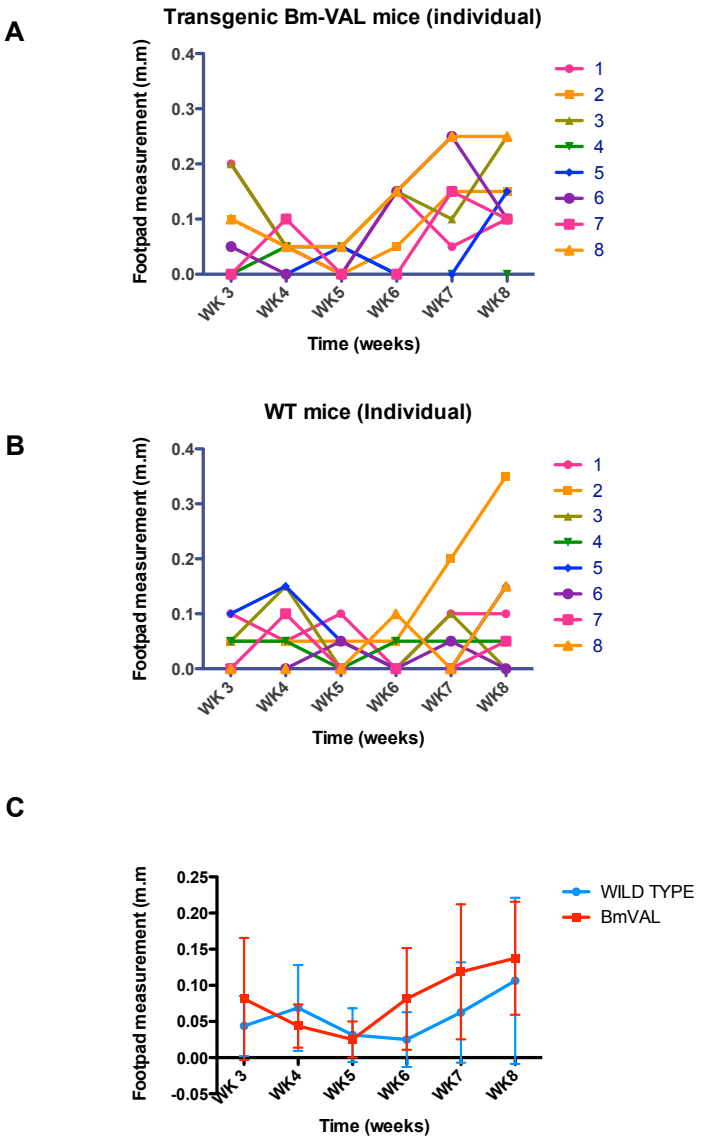

Fig 2.17 Time course of Lesion Development.

A & B Time-course of footpad swelling (lesion development) in individual mice from groups of mice infected with either wild type *L.mexicana* or Bm-VAL transgenic *L.mexicana*. **C** Time-course showing grouped mice measurements. All mice were infected with newly generated transgenic lines.

For **A,B & C** Groups of 8 female C57/B6 mice were mice were injected subcutaneously in the footpad of the rear left foot with $3x10^6$ wild-type or transgenic parasites. 3 weeks post injection footpad measurements were taken using a digital micrometer from both the infected foot and the contralateral uninfected foot. At week 8 final footpad measurements were taken, the infected foot removed for parasite recovery analysis and popliteal lymph nodes harvested for intracellular cytokine analysis.
Panel C shows the mean measurements for the 8 mice. Error bars show standard deviation.

2.18 Parasites recovered from foot and spleen of infected mice.

Removal and culture of footpads and spleens from infected mice is another way by which parasite virulence can be measured. In the first *in vivo* experiment parasites were detected at a higher dilution from mice infected with Bm-VAL parasites than wild type parasites although this did not reach statistical significance. This would indicate that the transgenic parasites, in this instance, were more infectious than the wild type parasites. As with the footpad swelling data, this was not reproduced in the second *in vivo* experiment. Bm-VAL transfected parasites were once more detected at a higher dilution than wild type parasites but again failing to reach statistical significance. In this instance no parasites were recovered from the spleen of either wild type *L.mexicana* or Bm-VAL parasite infected mice.

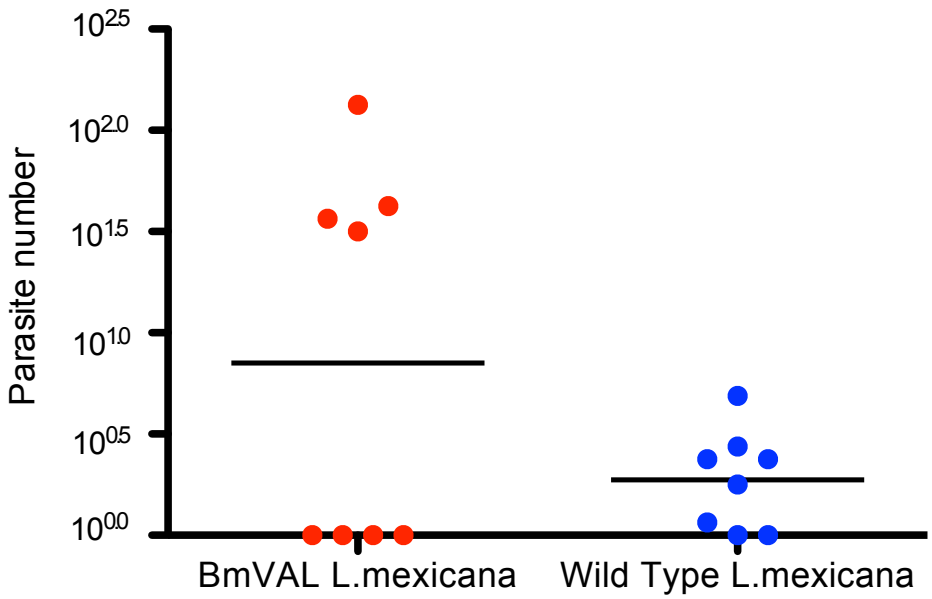

*** No parasites recovered from spleen for either group**

Fig 2.18 Parasites recovered from foot and spleen of infected mice.

The foot was recovered from infected mice and was manually disrupted using a syringe plunger. Extracts were centrifuged and then resuspended in 1ml of SDM media prior to serial dilution across a 96-well plate. In this instance no parasites were recovered from the spleens of either WT or Bm-VAL infected mice.

2.19 Immune responses in popliteal lymph node.

The draining lymph nodes were harvested at the end of the *in vivo* experiment and were analysed for the production of intra cellular cytokines. In the first experiment lymph node cell numbers were decreased in mice infected with wild type parasites, however in this experiment even though the lesion development in mice infected with BmVAL parasites was more pronounced than those infected with wild type parasites, cell numbers from lymph nodes showed no difference between groups. The percentage of CD4+ cells was elevated in mice infected with wild type parasites in the first *in vivo* experiment; however again in this experiment no difference was observed between groups for CD4+ cell numbers. Intracellular IL-4. IL-10 and IFN-γ were all measured with no differences apparent.

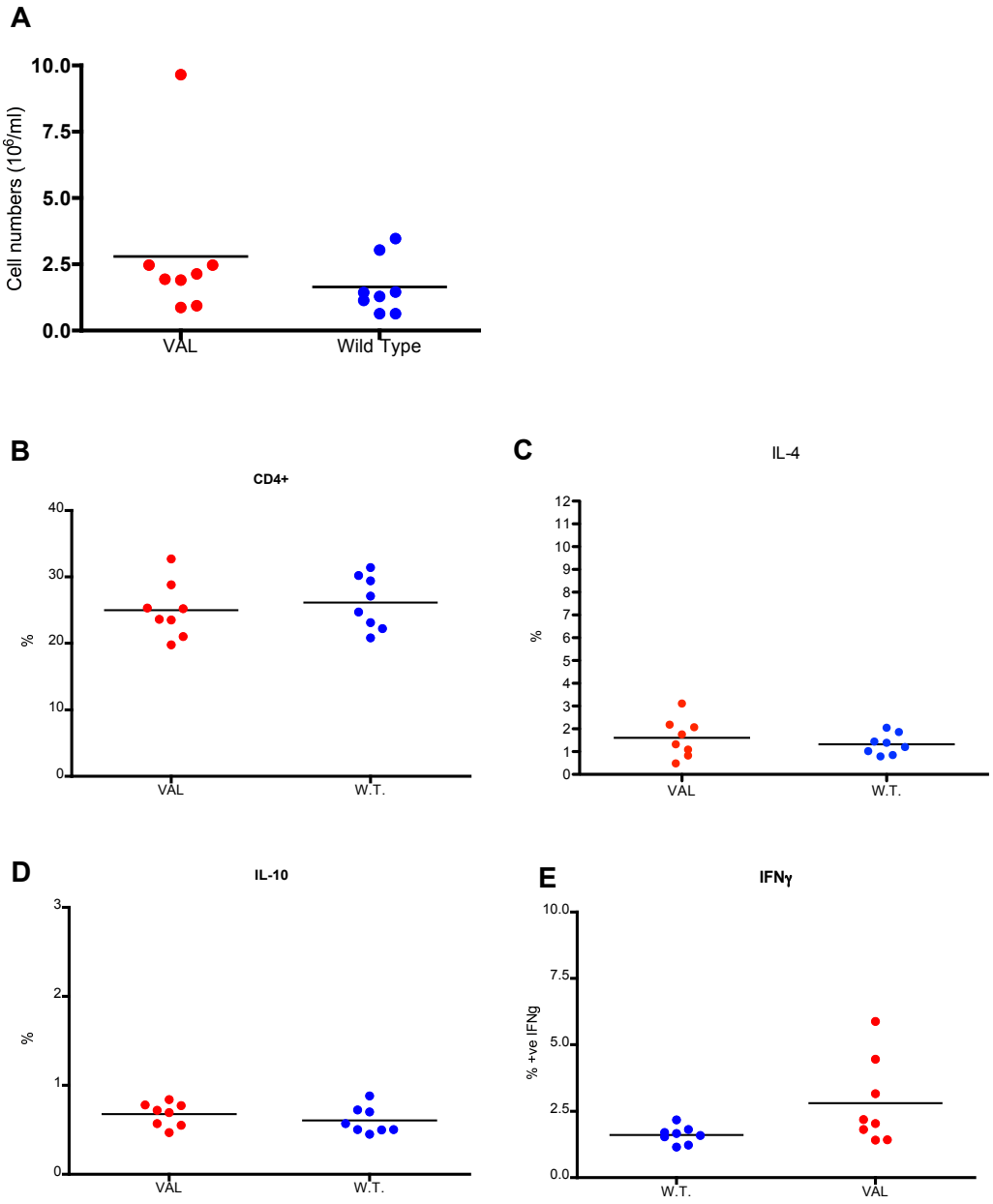

Fig 2.19 Immune responses in popliteal lymph node.

Cells harvested from the draining popliteal lymph node and were stained for the production of intracellular cytokines. Briefly, cells were counted (**A**) and then stimulated with PMA/ Ionomycin and Brefeldin A for 4 hours prior to CD4 cell surface staining (**B**) followed by a permeabilistaion step with BD Bioscieces cytofix/ Cytoperm and subsequent staining for intracellular cytokines, in this case IL10 (**C**) and IFNγ(**D**).

2.20 Experimental protocol for *In vivo* assessment of Bm-VAL-1 gene function.

In an effort to untangle the somewhat confusing results obtained from the *in vivo* experiments thus far one final infection was set up. The 8-week protocol (Fig 2.15) was repeated with mice being injected with either wild type or Bm-VAL *Leishmania* parasites. Lesion development, parasite recovery from footpad and spleen and intracellular cytokine data were all collected as for previous experiments.

2.21 Time course of Lesion Development.

Footpad swelling was monitored as for previous experiments by the measurement of the infected and uninfected foot for each mouse. Differences in the swelling seen in mice infected with wild type parasites compared to those infected with transgenic parasites were again observed. Less variation within the groups was seen in this experiment compared to the previous experiment with animals infected with wild type parasites showing more footpad swelling than those infected with transgenic parasites. This result was in agreement with the lesion development observed in the second *in vivo* experiment which followed the same protocol but was extended for a further 4 weeks.

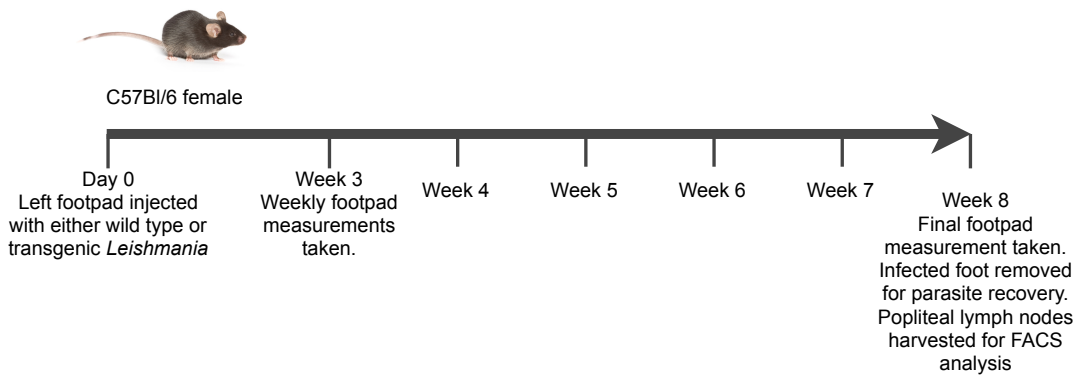

Fig 2.20 Experimental protocol for *In vivo* assessment of Bm-VAL-1 gene function.

Mice were injected subcutaneously in the footpad of the rear left foot with $3x10^6$ wild-type or transgenic parasites. Groups of 8 mice were tested. 3 weeks post injection footpad measurements were taken from both the infected foot and the contralateral uninfected foot.
At week 8 final footpad measurements were taken, the infected foot removed for parasite recovery analysis and popliteal lymph nodes harvested for intracellular cytokine analysis.

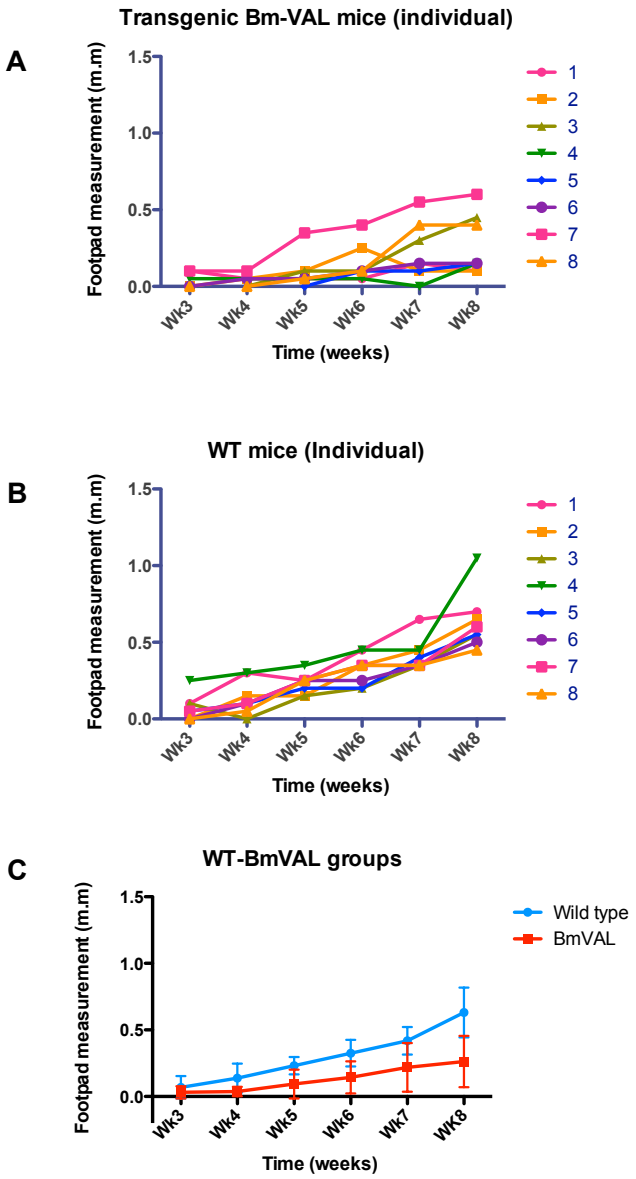

Fig 2.21 Time course of Lesion Development.

A & B Time-course of footpad swelling (lesion development) in individual mice from groups of mice infected with either wild type *L.mexicana* or Bm-VAL transgenic *L.mexicana*. **C** Time-course showing grouped mice measurements. For **A,B & C** Groups of 8 mice were mice were injected subcutaneously in the footpad of the rear left foot with $3x10^6$ wild-type or transgenic parasites. 3 weeks post injection footpad measurements were taken using a digital micrometer from both the infected foot and the contralateral uninfected foot. At week 8 final footpad measurements were taken, the infected foot removed for parasite recovery analysis and popliteal lymph nodes harvested for intracellular cytokine analysis.
Panel C shows the mean measurements for the 8 mice. Error bars show standard deviation.

2.22 Parasites recovered from foot and spleen of infected mice.

In this experiment parasites were recovered from both the footpad and the spleen after these tissues had been recovered at the end of week eight. These were then cultured for 7 days to examine parasite virulence.

In both the footpad and spleen parasites were observed at a higher dilution from mice infected with wild type parasites, implying that the transgenic parasites were less virulent than the wild type parasites and supporting the lesion development data in Fig 2.21.

2.23 Immune responses in popliteal lymph node.

Popliteal lymph nodes were harvested from both groups of mice and were stained for surface CD4+ and then assayed for the production of intracellular IL-4, IL-10 and IFN-γ.

The percentage of CD4+ T cells was significantly lower in mice infected with wild type *Leishmania* than in mice infected with Bm-VAL transgenic parasites. Also IL-10 and Il-4 levels were significantly reduced in the presence of transgenic parasites. These cytokines are able to deactivate macrophages and therefore help intracellular parasite growth and disease progression, which is seen in the lesion development data in Fig. 2.21 and parasite recovery data in Fig. 2.22.

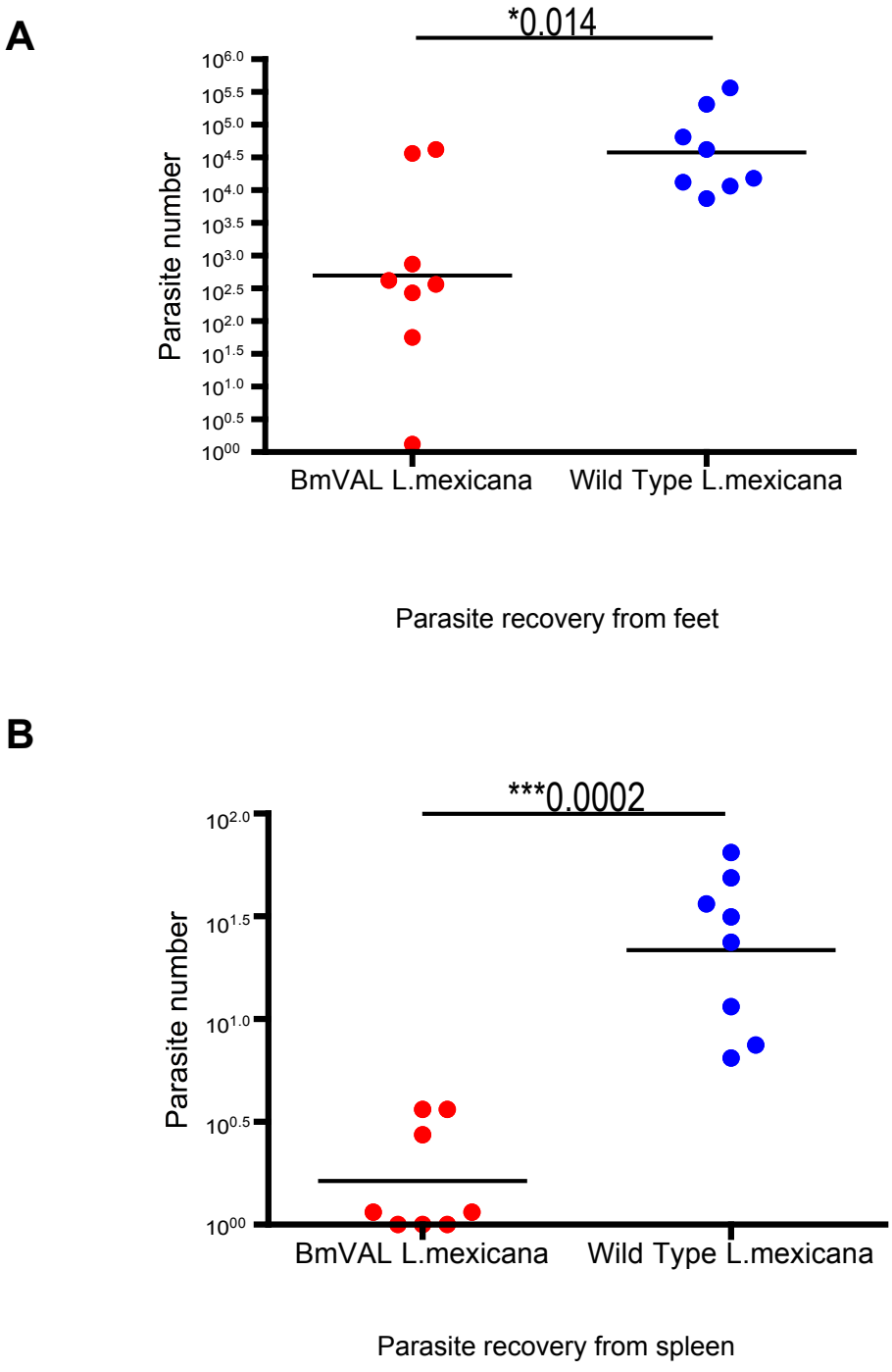

Fig 2.22 Parasites recovered from foot and spleen of infected mice.

The foot (**A**) and spleen (**B**) were recovered from infected mice and were manually disrupted using a syringe plunger. Extracts were centrifuged and then resuspended in 1ml of SDM media prior to serial dilution across a 96-well plate.

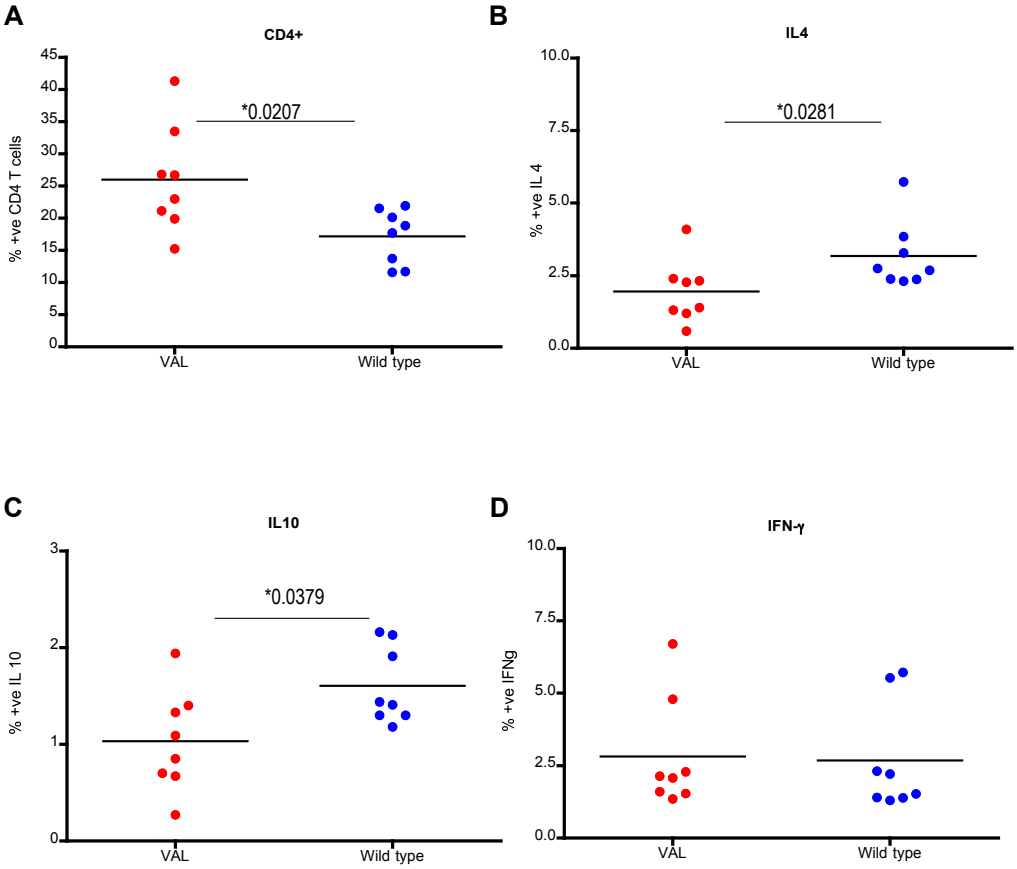

Fig 2.23 Immune responses in popliteal lymph node.

Cells harvested from the draining popliteal lymph node and were stained for the production of intracellular cytokines. Briefly, cells were counted (**A**) and then stimulated with PMA/ Ionomycin and Brefeldin A for 4 hours prior to CD4 cell surface staining (**B**) followed by a permeabilistaion step with BD Bioscieces cytofix/ Cytoperm and subsequent staining for intracellular cytokines, in this case IL10 (**C**) and IFNγ(**D**).

2.24 Collated lesion development time course data from *Leishmania in vivo* experiments.

Lesion development, or footpad swelling, is a standard and well-known parameter which is used to monitor the progress of a *Leishmania* infection in an *in vivo* setting. This data when examined along with supporting data such as parasite recovery and cytokine information can give an insight into host immune responses to a particular parasite.

Lesion development in two of the four *in vivo* experiments (*in vivo* 1&3) indicated that the wild type parasites had mounted a weaker infection, evident by larger lesions in the infected mice measurements, whilst experiments 2&4 indicated to the contrary (Fig 2.24A). When this data was pooled however there is little difference between the wild type and transgenic parasites until week 7 where upon the swelling in the wild type parasites continues until week 11 (Fig 2.24B).

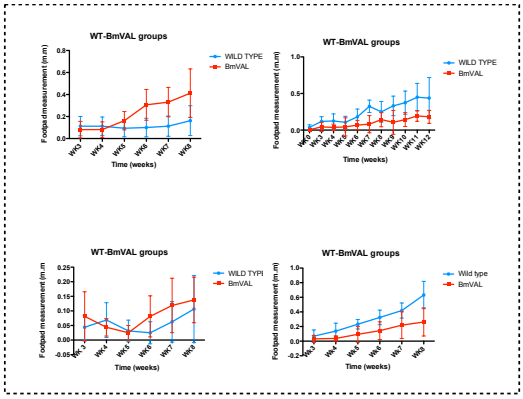

B

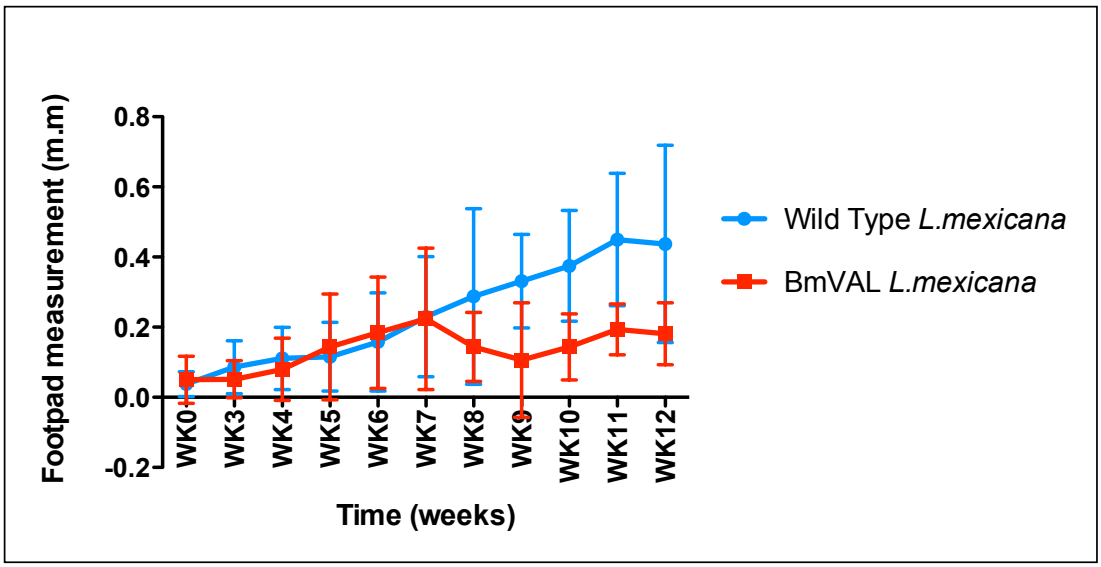

Fig 2.24 Collated lesion development time course data from *Leishmania in vivo* experiments.

Following infection with wild type or transfected *Leishmania* parasites footpad measurements were taken at weekly intervals from the uninfected and the contralateral infected foot. Measurements were carried out using a digital micrometer and were done blind.

A. Data shown is from 4 individual experiments.
B. Data shown is pooled from 4 individual experiments. Error bars show standard deviation.

2.25 Collated parasite recovery data from *Leishmania in vivo* experiments.

Where wild type parasites had mounted a stronger infection than the transgenic parasites (Exp. 2&4) this was accompanied by an increase in parasite virulence as demonstrated in the data shown after serial dilution analysis and was consistent whether parasites had been recovered from the footpad (A) or the spleen (B), always achieving statistical significance (Fig 2.25A). All data was then pooled from the 4 individual *in vivo* experiments. Parasite recovery from animals infected with wild type parasites continued to be higher than for those recovered from transgenic parasite infections however now being unable to reach statistical significance.

Experiments 1&3 showed that the transgenic parasites had mounted a more severe infection by lesion development (Fig 2.24) and this data was supported by the parasite recovery data. In both experiments, parasites were recovered at a higher dilution from the feet from mice infected with transgenic parasites. However, the data achieved statistical significance only in the first experiment. Parasites were not detected at all in the spleen in the 3rd experiment.

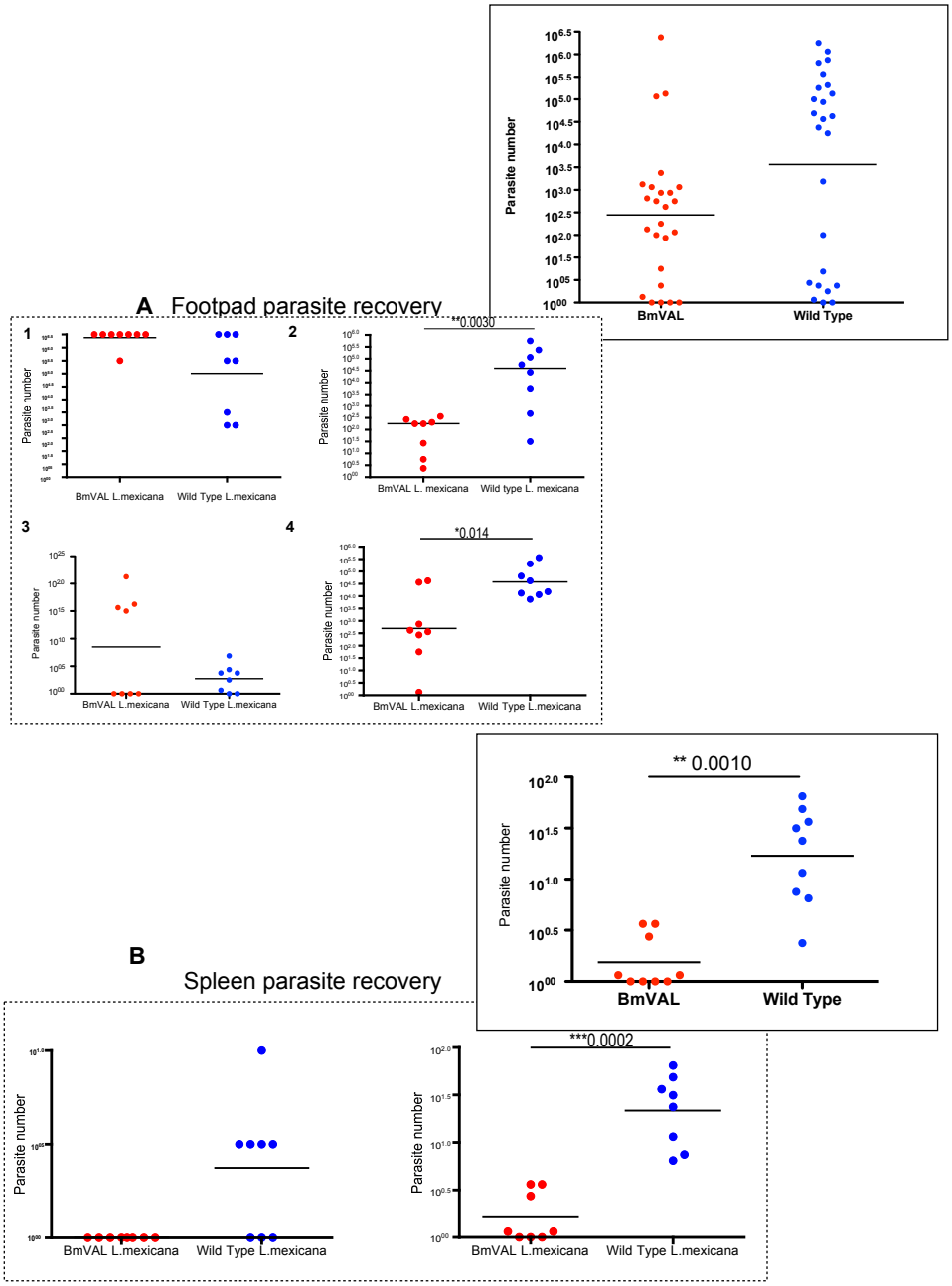

Fig 2.25 Collated parasite recovery data from *Leishmania in vivo* experiments.

The foot or spleen was recovered from infected mice and was manually disrupted using a syringe plunger. Extracts were centrifuged and then resuspended in 1ml of SDM media prior to serial dilution across a 96-well plate. **A** Parasite recovery from the infected foot of the mouse. **B** Data from the spleen.
Data shown is pooled from 4 individual experiments (A) and two individual experiments (B).

2.26 Summary of experimental readouts from 4 *in vivo* infection experiments.

Data from the four *in vivo* experiments although contradictory followed two distinct patterns:

1) Where mice infected with wild type parasites had greater footpad swelling than mice infected with transgenic parasites, these mice also had higher levels of parasite recovery from either the footpad or the spleen and they also had higher levels of IL-4 and IL-10.
2) Where mice infected with transgenic parasites had higher levels of footpad swelling this was always accompanied by higher levels of parasite recovery from the footpad.

Thus regardless of parasite provenance high levels of parasite lesion development are accompanied by high levels of parasite recovery from the footpad or spleen after serial dilution and increased levels of IL4 & Il-10.

A

***In vivo* 1**: 8 week experiment BmVAL and wild type Footpad measurements, parasite recovery from feet only, intra-cellular cytokines
***In vivo* 2**: 12 week experiment BmVAL and wild type Footpad measurements, parasite recovery from feet & spleen, intra-cellular cytokines, cytokines by ELISA
***In vivo* 3**: 8 week experiment BmVAL(newly derived line) and wild type Parasite growth curves, footpad measurements, parasite recovery from feet none found in spleen, intra-cellular cytokines
***In vivo* 4**: 8 week experiment BmVAL and wild type Footpad measurements, parasite recovery from feet & spleen, intra-cellular cytokines

B

BmVAL data in relation to wild type

	In vivo **1**	*In vivo* **2**	*In vivo* **3**	*In vivo* **4**
Footpad Measurements	BmVAL ↑	BmVAL ↓	BmVAL ↑	BmVAL ↓
Footpad Parasite Recoveries	BmVAL ↑	BmVAL ↓	BmVAL ↑	BmVAL ↓
Spleen Parasite Recoveries		BmVAL ↓	↔	BmVAL ↓

Fig 2.26 Summary of experimental readouts from 4 *in vivo* infection experiments.

A. *Leishmania in vivo* experiments. A brief description of each in vivo experiment.

B. Summary of experimental readouts from 4 *in vivo* infection experiments.
Comparison of data from 4 individual infection experiments. Experimental readouts comprised of:
1) Measurement of footpad swelling or lesion development.
2) Recoveries of parasites from the foot or spleen of infected mice.
3) Intracellular cytokine data not shown here.

Discussion

In this chapter I have used what could be described as a rather interesting and alternative method to examine the function of a gene and the effects this gene may have on either the parasite itself or the host within which it resides. This method was previously used and published to study the function of another *Brugia malayi* gene, Bm-ALT (Gomez-Escobar et al., 2005). In that study it was observed that parasites expressing the Bm-ALT gene reached higher levels of infectivity in bone marrow derived macrophages an *in vitro* situation, that they had an accelerated infection profile *in vivo* and that they were indeed more resistant to IFN-γ killing by macrophages. A truncated mutant of the Bm-ALT gene was also tested and this did not possess the same parasitic qualities as the native gene.

A lot of preliminary data had been gathered relating to the *in vitro* properties of the Bm-VAL-1 gene in this transfection system and this was discussed in my MSc thesis (Murray, 2007). This showed expression of the BmVAL-1 gene in *Leishmania mexicana* promastigotes by RT-PCR and also by immunofluorescence using a BmVAL-1 specific antibody. Promastigotes exhibited staining of the flagella indicating that the gene product had been exported to the plasma membrane and transgenic amastigotes within bone marrow derived macrophages were also stained using anti-VAL monoclonal and polyclonal antibodies. Given the *in vitro* information already gathered the next step was to elucidate the impact of the gene *in vivo*.

There has been much published with regards to the roles of arginase, iNOS, IL-13 and IL-10 cytokines and regulatory enzymes during *Leishmania* infection and maintenance within the macrophage environment. (Iniesta et al., 2005), (Shweash et al., 2011), (Gaur et al., 2007), (Kane & Mosser, 2001). Arginase levels detected in infected BMDM were slightly higher where transgenic parasites had been used for infection rather than wild type. This would lead to a more favourable environment for parasite survival within the macrophage. The increase seen in IL-13 may be responsible for the rise in arginase levels (Mosser, 2003). This may have correlated

with the increase found in iNOS expression found with wild type infection perhaps leading to a more classically activated macrophage. Unfortunately none of the data reached statistical significance and was more indicative of an observational trend.

Lesion development and parasite recovery results were inconclusive between experiments however as stand alone tests they followed definite trends. In the two experiments where the lesion development was slower and less marked with transgenic parasites than wild type, fewer parasites were recovered at high serial dilutions from both the footpad and the spleen. Whereas when the infections with transgenic parasite mounted a more vigorous infection resulting in larger lesion development than the wild type, the parasite recovery from the spleen in this case was higher. Thus as a general rule infections with more intense footpad swelling have higher numbers of parasites present at higher dilutions, an indication of increased virulence.

In the case of the Bm-VAL gene, using the heterologous expression system in *Leishmania* may not have yielded as definitive results as were achieved when the Bm-ALT gene was examined. Other genes, Bm-MIF (L.Prieto-Lafuente, unpublished), have been examined in the lab with varying levels of success. As with most experimental systems the function of a particular gene being investigated may in fact prohibit its activity in an artificial setting. Where a gene normally exerts a strong effect in its natural biological setting then the heterologous expression system being utilised here may have been more informative. However, if the gene in question has a more subtle role then the transfection of *Leishmania* parasites may not be sensitive enough to detect this.

Transfection of a gene into *Leishmania major* parasites may help to tackle some of the issues mentioned above by allowing direct questions to be addressed between mouse strains: BALB/c mice show resistance to *L.major* whereas C57BL/6 are susceptible, thus questions addressing the ability of transgenic parasites to switch host responses from resistant to susceptible can be asked.

Chapter 3

VAL, a component of HES, and its effect in the Allergic Airway Inflammation model

Introduction

Immune mediated diseases such as asthma, inflammatory bowel disease and multiple sclerosis are on the increase in Western societies (Braman, 2006), (Loftus, 2004), (Marrie, 2004). The fact that the same societies are now relatively free of parasitic companions in the form of helminth infections has not gone unnoticed. This phenomenon has become known as "The Hygiene Hypothesis": the idea that as we have rid ourselves of helminth parasites, we find ourselves at the mercy of an over-active, unregulated immune system (Elliott & Weinstock, 2012), (Guarner et al., 2006), (Kitagaki et al., 2006).

A related theory is "The old friends hypothesis" (Fig 3.1) which draws on a similar situation that by improving food hygiene, we have removed a population of environmental saprophytes that had evolved with us. This gives weight to the idea that as the loss of constitutive elements such as helminths and pseudo commensals, which would have resulted in a more regulatory immune environment, the incidence of allergy and autoimmune diseased has increased.

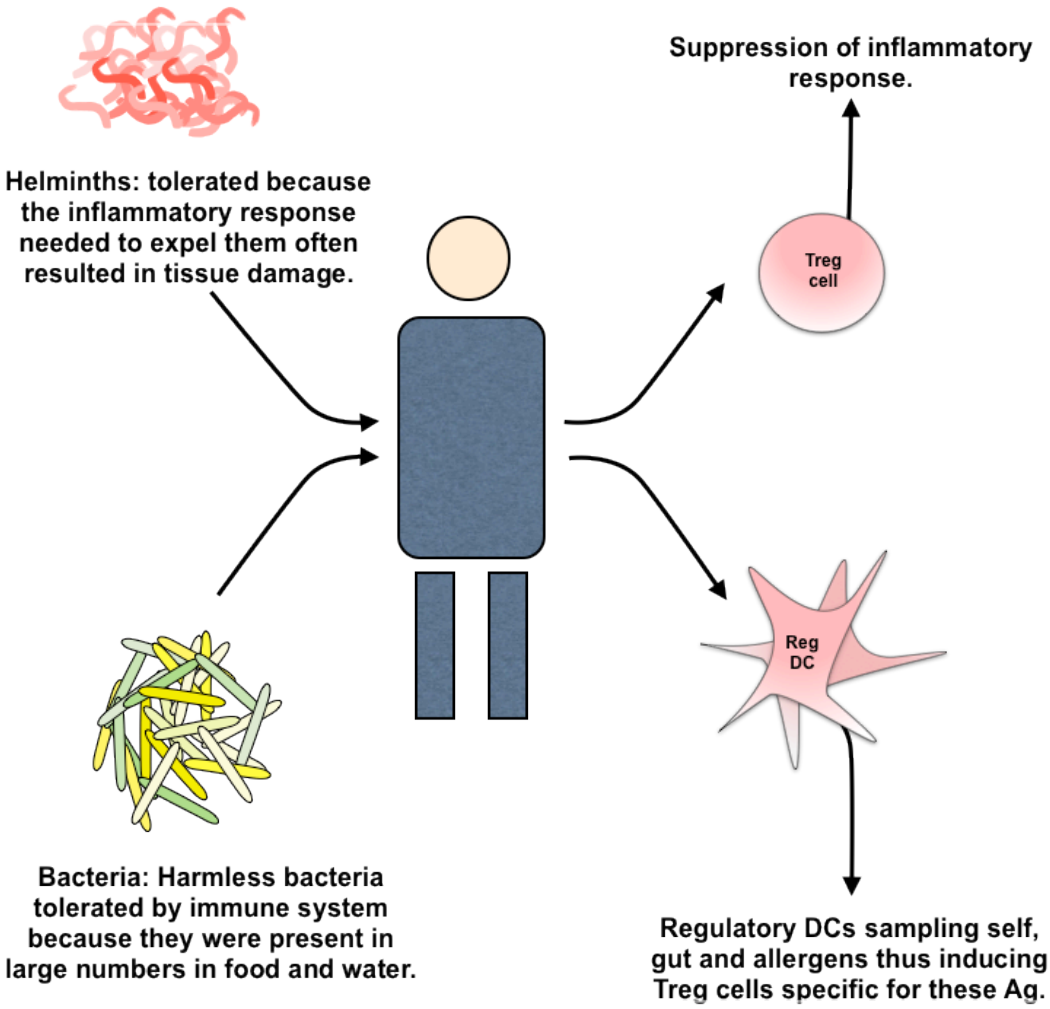

Fig 3.1 Immunoregulatory setting induced by the presence of helminths and bacteria.

The presence of helminth parasites or bacteria, that were not necessarily "good" for us but were often tolerated, allowed dendritic cells to initiate Treg cells rather than Th1 or Th2 effector cells. This created conditions where the immunological backdrop was one in which inflammatory cytokines were suppressed (Rook, 2009). Here atopy, characterized by high IgE, IL-4, IL-5 and IL-13, accompanied by high numbers of eosinophils and mast cells, is reduced.

Many other factors may also be implicated in the likelihood of an individual being predisposed to allergies and asthma. An individual may be at higher risk of these conditions if they are from an urban environment as opposed to a rural one. Also the number of infections they encountered as a child may predetermine their "at risk" status (Yazdanbakhsh, Kremsner, & van Ree, 2002). Thus the association between parasitic infection and allergy is not as simple as the swing of the Th1/Th2 dichotomy but more of regulation and education of the responding immune cells.

The argument however remains that the prevalence of allergies is not as high in developing countries where helminth infections are common. Data to support the idea that helminths have at least some sort of protective effect for their host is increasing, with researchers frequently looking to molecules produced by these parasites to provide the answer. One of the main possibilities lies in products secreted or excreted by the parasites (the ES products), which have direct contact with various important host cell types (Harnett, 2014), (Aranzamendi et al., 2013).

To help study interactions between host cells (Fig 3.2) and parasite produced products animal models have become an invaluable tool for the molecular parasitologist. In this chapter, one such model, the **a**llergic **a**irway **i**nflammation (A.A.I.) model is used to examine the effect of HpVAL proteins in an asthmatic situation.

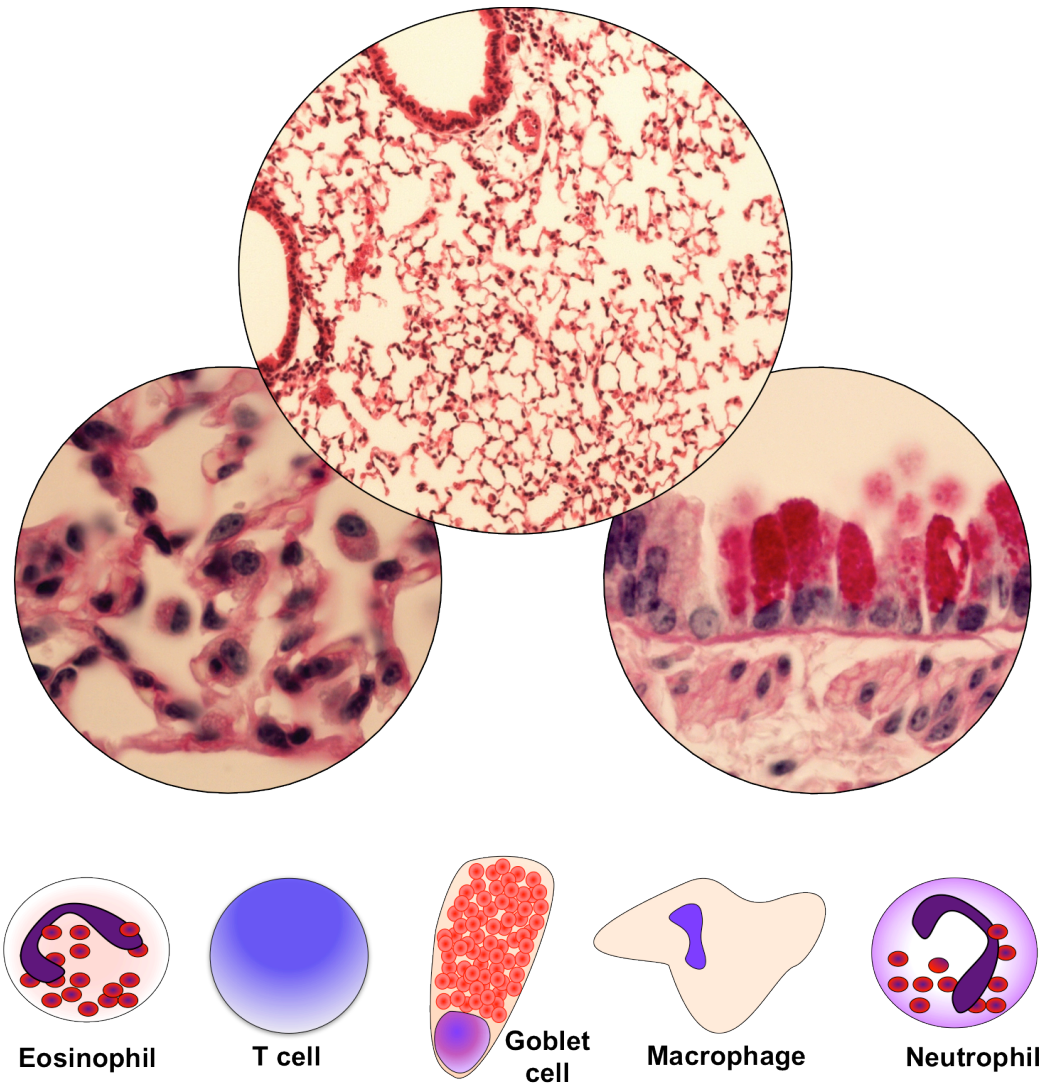

Fig 3.2 Lung tissue and cells that may come into contact with *H.polygyrus* ES in the A.A.I. model.

Previously in our lab (Wilson et al., 2005) showed that the presence of an infection with the murine intestinal helminth *H.polygyrus* helped to down-regulate allergen induced lung pathology in the DerP1 and OVA allergy models. Allergens were administered I.P. to C57BL/6 or BALB/c mice, followed two weeks later by an intra-tracheal allergen airway challenge. This resulted in significantly reduced airway cellular infiltrates accompanied by a reduction in airway eosinophilia and neutrophilia. Common allergy associated Th2 cytokines IL-4, IL-5 and IL-13 were all reduced in mice carrying an infection. Tissue pathology, measured by H&E and PAS staining to examine cellular infiltrate and mucus producing goblet cells

respectively, showed that the presence of the infection ameliorated these physical hallmarks of A.A.I. Much of this suppression was attributed to the presence of a population of $CD4^+CD25^+$ T cells, which transferred protection to allergen-sensitized recipients.

The immunomodulatory effects of infection with *H.polygyrus* were further characterized when it was shown that a population of $CD4^-CD19^+$ MLN B cells from infected mice was able to reduce airway eosinophilia, lower IL-5 secretion and reduce pathology in uninfected, sensitized mice. These same cells were also shown to reduce symptoms of EAE in experimental mice, thus demonstrating modulating properties in both allergic and autoimmune disorders (Wilson et al., 2010).

It was subsequently demonstrated that the protective properties of harbouring an infection could be reproduced by administration of the parasite excretory secretory products alone. Using the OVA-alum model of AAI, HES was added to an OVA-alum suspension and was injected I.P. to uninfected mice. Following an OVA challenge, which was delivered on three consecutive days, a suppression of infiltrating cells in the bronchioalveolar lavage fluid was accompanied by reductions in eosinophil numbers and $CD4^+$ T helper cells. Once more levels of IL-4, IL-5 and IL-13 were all reduced when HES had been administered at the point of sensitization and also at the point of airway challenge, indicating that HES was able to suppress an already established response (McSorley et al., 2012).

In this chapter I examine if a single molecule, VAL, isolated from HES can exert the same immunomodulatory qualities as those seen during parasite infection or administration of the total mixture of parasite secretions.

Results

3.3 Can recombinant HpVALs induce a Th2 response?

An initial assessment of the *in vivo* immunological activity of insect cell derived recombinant HpVAL proteins was carried out. HES, recombinant HpVAL-1, heat-treated recombinant HpVAL-1 or recombinant HpVAL-4 were injected into the peritoneal cavity of Balb/c mice on Day 0. Th2 cytokines, IL-4, IL-10 and Il-13 were measured at Day 7 post injection from the peritoneal cavity and popliteal lymph nodes (Fig. 3.3A).

Helminth parasites are known to induce Th2 responses, as described by (Girgis, Gundra, & Loke, 2013), (McSorley & Maizels, 2012), (Anthony et al., 2007) and yet, in an airway allergy model, the presence of these parasites or release of their excretory secretory products can be seen to alter these Th2 responses with reductions in IL-4, IL-5 and IL-13. For example, a recombinant cystatin from *Nippostrongylus brasiliensis* (nippocystatin) was shown to suppress OVA-specific cytokine production in mice and profoundly suppressed OVA-specific proliferation of splenocytes (Dainichi et al., 2001). Also, treatment of mice with recombinant Av-cystatin from *Acanthocheilonema viteae* during of after sensitisation in the OVA-induced allergic airway model reduced levels of OVA-specific and total IgE, down-regulated IL-4 production, inhibited eosinophil recruitment and suppressed allergic airway hyperreactivity (Schnoeller et al., 2008). Recombinant macrophage migration inhibitory factor (MIF) from *Anisakis simplex* (As) induced a complete inhibition of eosinophilia and goblet cell hyperplasia within the lung in the same model with recruitment of a population of CD4(+) CD25(+)Foxp3(+) T cells (regulatory T) occurring to the spleen and lungs of the rAs-MIF-treated mice (Park et al., 2009).

Cell numbers in the lymph node were significantly reduced, in comparison to HES, where HpVAL-1, -4 or heat-treated HpVAL-1 had been administered (Fig 3.3 Bi). This data was not reflected in peritoneal lavage counts, with all groups having similar cell counts to the HES group (Fig 3.3 Bii).

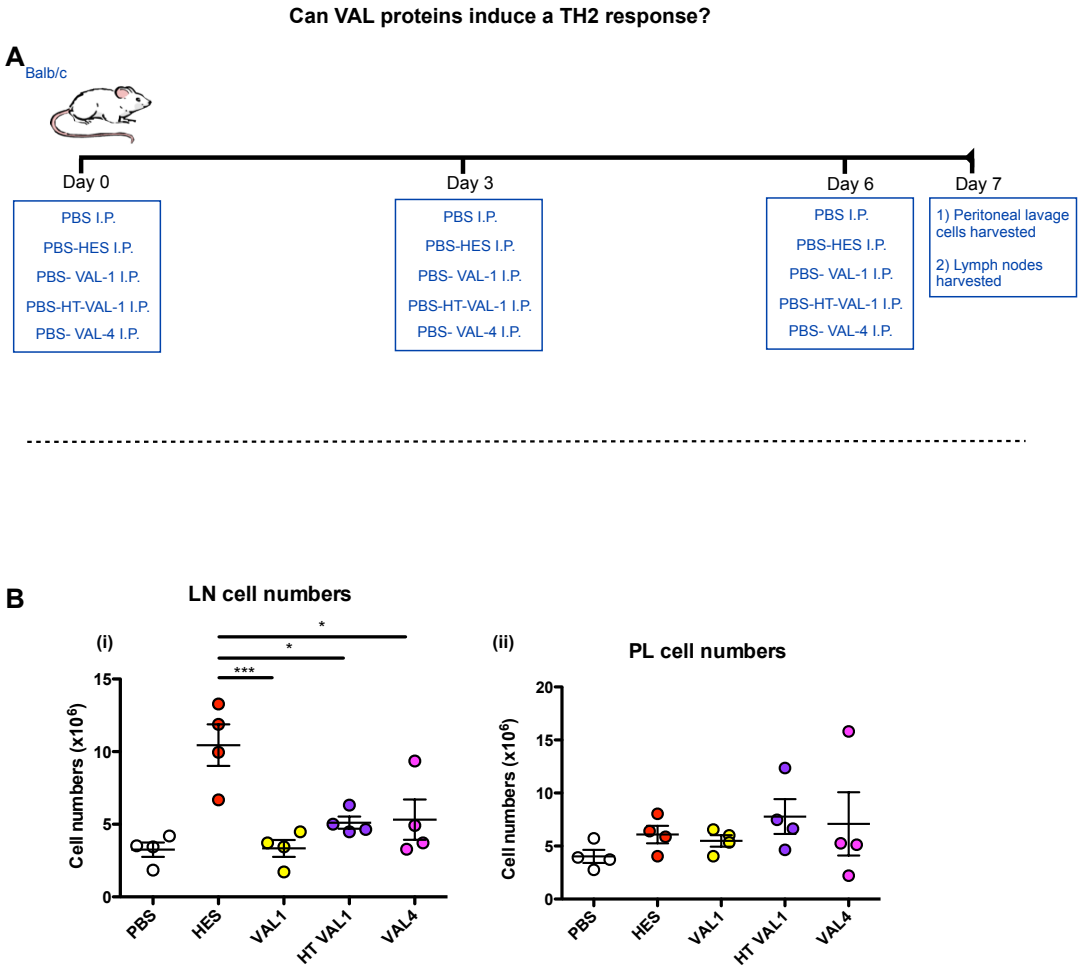

Fig 3.3 Can recombinant HpVALs induce a TH2 response?

A. Experimental protocol. BALB/c mice were injected I.P. at Day 0, day 3 and day 6 with either 200µl PBS or 200µl of PBS containing HES, recombinant Hp-VAL1, heat-treated Hp-VAL1 or Hp-VAL4. Mice were killed at Day 7. Peritoneal lavage cells and lymph nodes were harvested.

B. Total cell numbers from lymph nodes**(i)** and peritoneal lavage fluid(ii) were enumerated by haemocytometer counting.
*=p<0.05, **=p<0.01, ***=p<0.001

3.4 Cytokines produced in response to recombinant VALs are significantly lower than seen in response to HES.

In order to further describe the immune response generated by directly injecting recombinant VAL proteins into the peritoneum of a mouse, cytokines were measured in the lymph nodes (Fig 3.4 A) and peritoneal lavage fluid (Fig 3.4 B). Levels of IFN-γ, IL-4, IL-10 and IL-13 were measured by flow cytometry and shown as a percentage of CD4+ cells. Levels of macrophage activating IFN-γ from T cells were highest in mice treated with HES (Fig 3.4 Ai) where as mice treated with VAL proteins produced significantly less. IL-4 and IL-13 levels were also significantly higher for mice treated with HES (Fig 3.4 A and B ii and iii) compared to VAL treated mice. Production of IL-10 in the lymph nodes and peritoneal lavage, where HES was administered, was also significantly greater than where HpVAL had been given. These results were consistent between lymph nodes and peritoneal lavage.

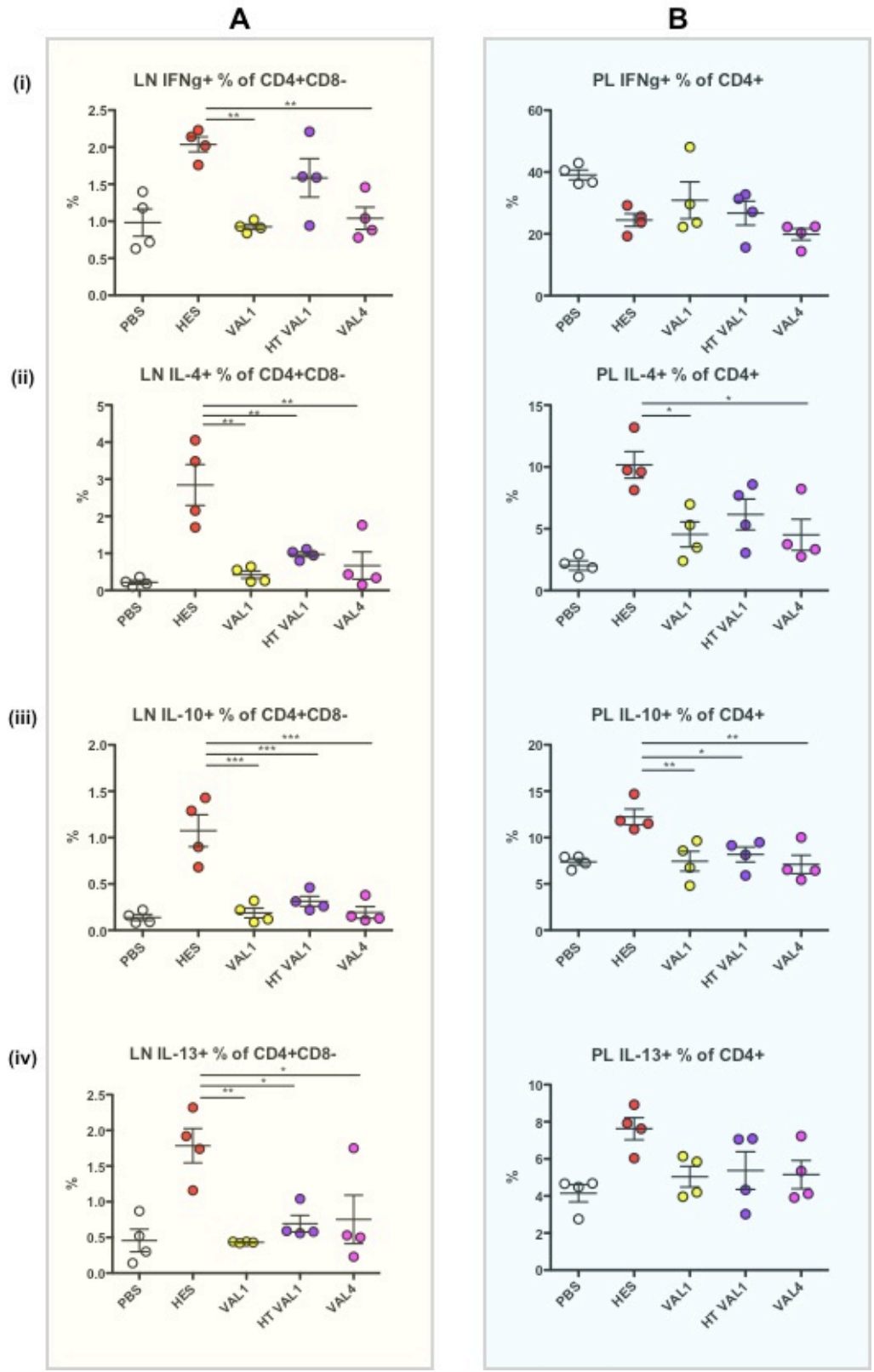

Fig 3.4 Cytokines produced in response to recombinant VALs are significantly lower than seen in response to HES.

Fig 3.4 Cytokines produced in response to recombinant VALs are significantly lower than seen in response to HES.

Female BALB/c mice were injected I.P. on days 0, 3 and 6 with either PBS, HES, Hp-VAL1, heat-treated Hp-VAL1 or Hp-VAL4. On day 7 lymph nodes **(A)** and peritoneal lavage fluid **(B)** were analysed for the presence of **(i)** IFNγ, **(ii)** IL-4, **(iii)** IL-10 and **(iv)** IL-13 cytokines by FACS staining.
*=p<0.05, **=p<0.01, ***=p<0.001

3.5- 3.6 Profile of cells recruited in response to HES and recombinant VALs.

Cell types recruited into the peritoneum after the administration of either HES or VAL proteins were determined by flow cytometry. T cells ($CD4^+$, Fig 3.5A), eosinophils ($SiglecF^+F4/80^-$, Fig 3.5B), macrophages ($F4/80^+SiglecF^-$, Fig 3.5C) and neutrophils ($GR1^+SiglecF^-$, Fig 3.5D) were enumerated as a percentage of cells and as absolute numbers. Macrophages recruited in response to HES or VAL proteins accounted for 20% of the total cells recruited (Fig 3.5 C) with the exception of HpVAL-4, where this was reduced 15%, although nevertheless accounted for the largest proportional cell type.

These data are summarized in Fig 3.6 and shows that macrophages and eosinophils are the primary cell types recruited to the peritoneal cavity.

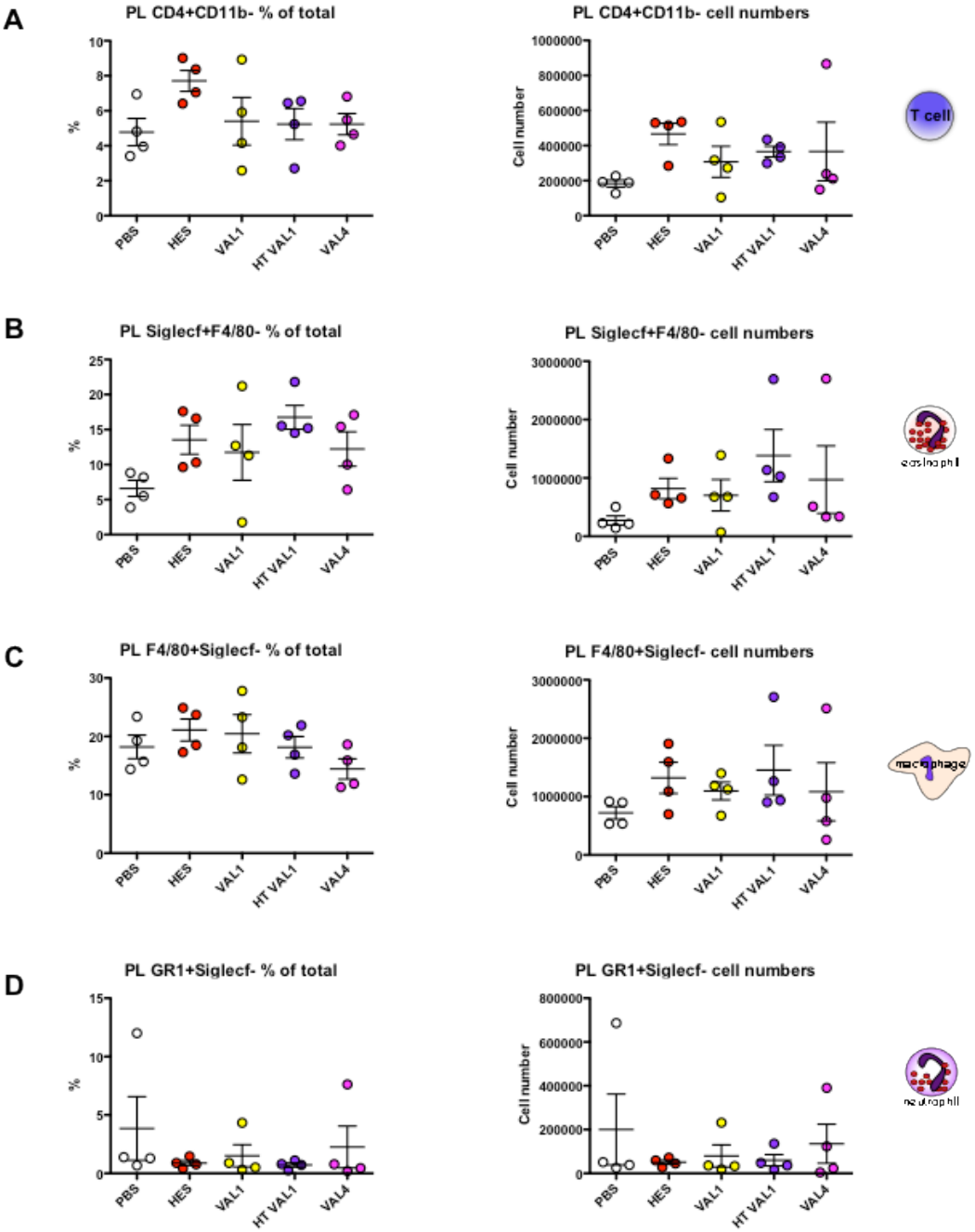

Fig 3.5 Profile of cells recruited in response to HES and recombinant VALs.
Female BALB/c mice were injected I.P. on days 0, 3 and 6 with either PBS, HES, Hp-VAL1, heat-treated Hp-VAL1 or Hp-VAL4. On day 7 peritoneal lavage fluid was analysed for (**A**) T helper cells (CD4+CD11b-), (**B**) eosinophils (SiglecF+ F4/80-), (**C**) alveolar macrophages (F4/80+ SiglecF-) and (**D**) neutrophils (GR1+ SglecF-).
*=p<0.05, **=p<0.01, ***=p<0.001

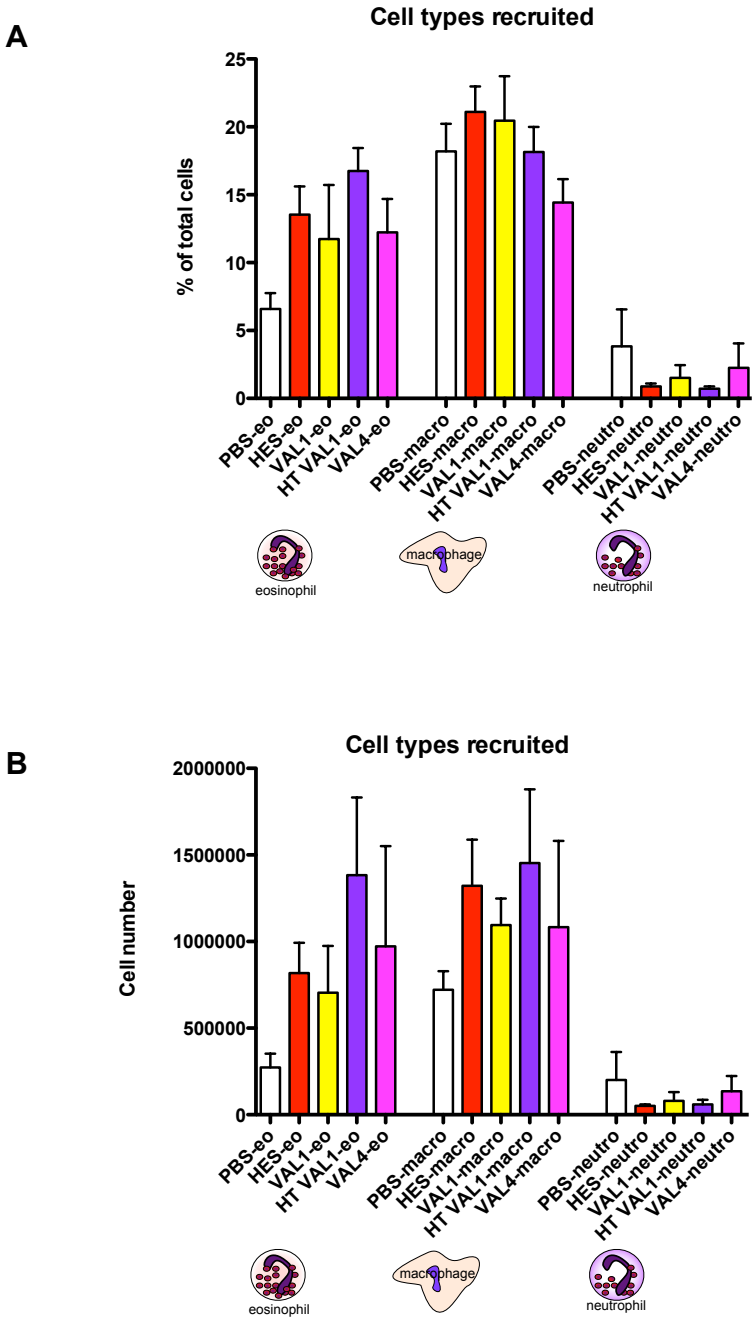

Fig 3.6 Summary of cell types recruited to peritoneal cavity.

Female BALB/c mice were injected I.P. on days 0, 3 and 6 with either PBS, HES, Hp-VAL1, heat-treated Hp-VAL1 or Hp-VAL4. On day 7 peritoneal lavage fluid was analysed for T helper cells (CD4+CD11b-), eosinophils (SiglecF+ F4/80-), alveolar macrophages (F4/80+ SiglecF-) and neutrophils (GR1+ SglecF-).
Percentages **(A)** and numbers **(B)** and percentages of cells are shown above.

3.7- 3.8 Levels of RELM-α and YM-1 in peritoneal lavage fluid

As macrophages were one of the main cell types to be recruited to the peritoneum upon injection with HES, HpVAL-1 or HpVAL-4, classification of these cells, with regards to their expression of RELM-α and YM-1, was measured by FACS. Both RELM-α **(**Fig 3.7A**)** and YM-1 (Fig 3.7B) levels showed a slight increase in groups treated with VAL proteins in comparison to those treated with HES, although none of these increases reached statistical significance. Representative flow plots are shown in Fig 3.7C for all groups.

Fig 3.8 shows a summary of findings from this experiment.

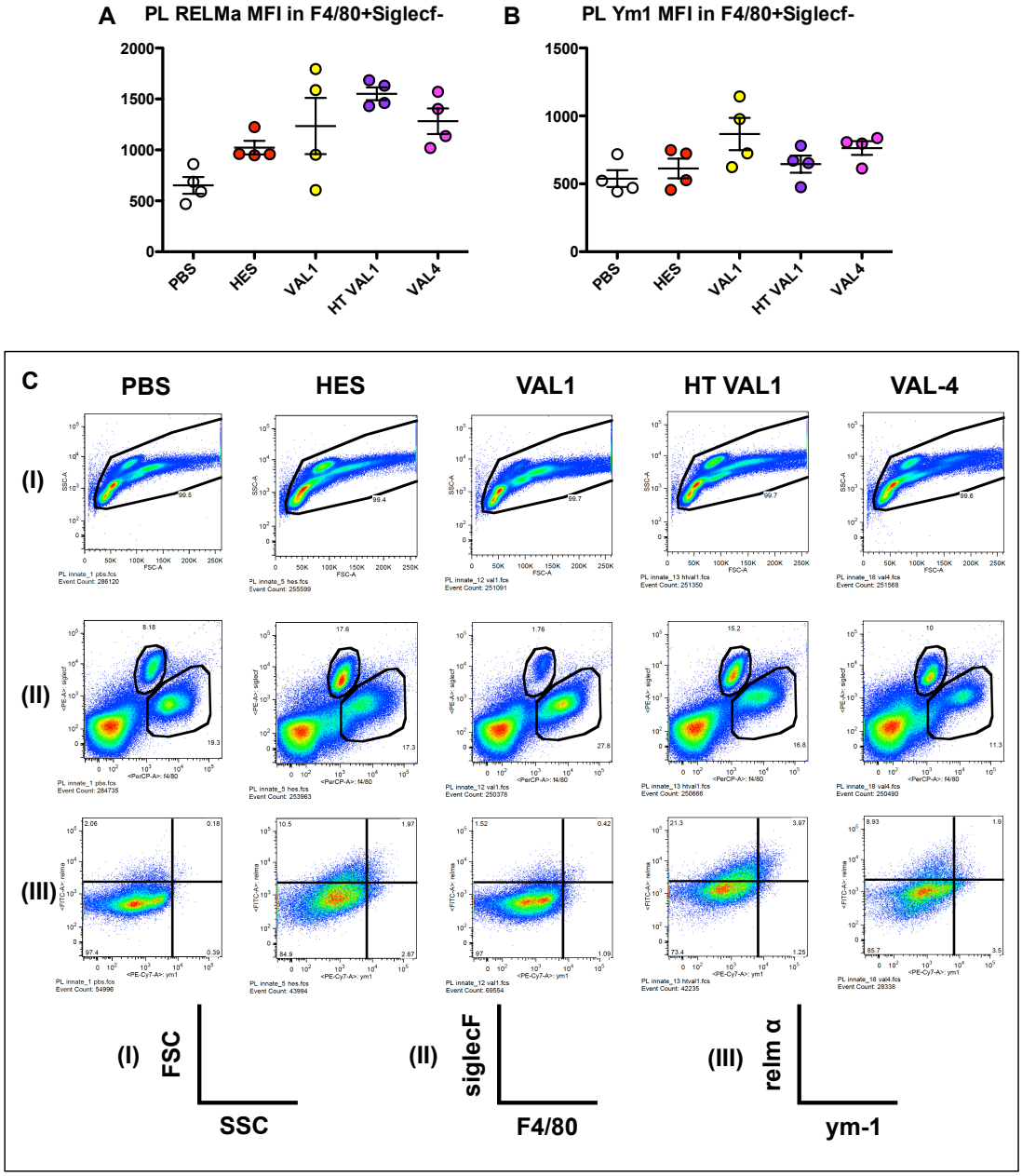

Fig 3.7 Levels of RELM-α and YM-1 in peritoneal lavage fluid

Female BALB/c mice were injected I.P. on days 0, 3 and 6 with either PBS, HES, Hp-VAL1, heat-treated Hp-VAL1 or Hp-VAL4. Type 2 myeloid cell response markers, Relm-α **(A)** and YM-1 **(B)** in the PL fluid were measured by FACS.
(**C**) Representative Flow plots for (I) FSC/SSC, (II) siglecF/F4/80 and (III) relmα/ym-1.

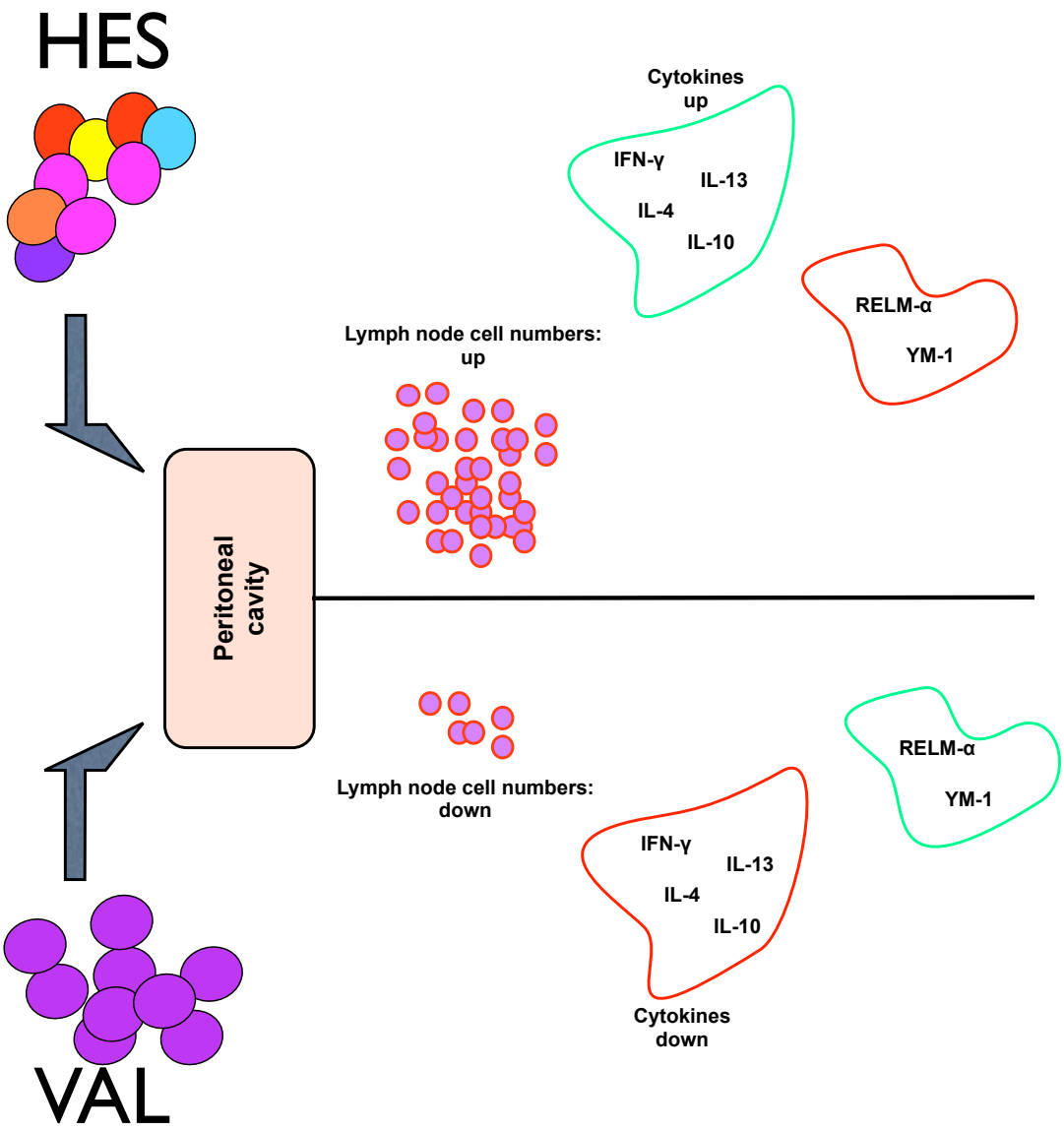

Fig 3.8 Summary of the effects seen upon injection of the peritoneal cavity with HES or VAL proteins.

Lymph node numbers increase upon HES administration compared to a lower number seen in mice given VAL. Higher levels of IFN-γ, IL-4, IL-10 and IL-13 were measured in HES mice. However levels of RELM-α and YM-1 were lower than observed in mice treated with any of the VAL proteins, although this did not reach statistical significance.

The following four experiments were carried out utilising the A.A.I. model to examine immunomodulatory properties of recombinant VAL proteins.

3.9- 3.10 Experiment 1: Hp-VAL, a component of HES, reduces cell numbers and eosinophil numbers in BAL fluid in the A.A.I. model.

The excretory secretory products of *H.polygyrus* have been shown to ameliorate symptoms that occur in the allergic airway inflammation model (Fig 3.9) (McSorley et al., 2012). As discussed previously (Chapter 1), the excretory secretory products of *H.polygyrus* and many other parasites are an extremely complex mixture of proteins, carbohydrates and lipids (Hewitson et al., 2011b). HpVAL-4 is the most abundant single domain VAL molecule from that mixture, and as such was chosen to examine the potential of a single protein from this suppressive HES cocktail. Recombinant HpVAL-4 was administered to female BALB/c mice at days 0 and 14 through the A.A.I. protocol described in Fig 3.9A. After 28 days an ova-aerosol challenge was given to the mice on three consecutive days where after the bronchioalveoar lavage (BAL) fluid and tissues as shown in Fig 3.9B were harvested for analysis.

One of the primary read-outs for this model is analysis of the bronchioalveoar lavage fluid or BAL. BAL cell counts for mice treated with HES were significantly reduced when compared to OVA treatment (Fig 3.10 B (i)). Cell counts for mice treated with Hp-VAL4 were also reduced but this did not reach statistical significance. The reduction in cell numbers observed with HpVAL-4 treatment was reversed upon heat-treatment of the recombinant. In studies described by (McSorley et al., 2012) heat-treatment of HES had no affect on its ability to reduce inflammation or recruit cells, in particular eosinophils to the lung.
BAL fluid was also assayed for the presence of eosinophils, their cellular profile being SiglecF^{+} CD11c^{-}. The proportion of the total BAL infiltrate that were eosinophils is shown in Fig 3.10 B (ii) whereas the total number of eosinophils present is presented in Fig 3.10 B (iii). In both cases the percentage and number of

eosinophils is reduced in mice treated with HES and Hp-VAL4. Representative staining is shown for a sample treated with OVA and HpVAL-4 (Fig 3.10C).

Allergic Airway Inflammation (AAI) Model

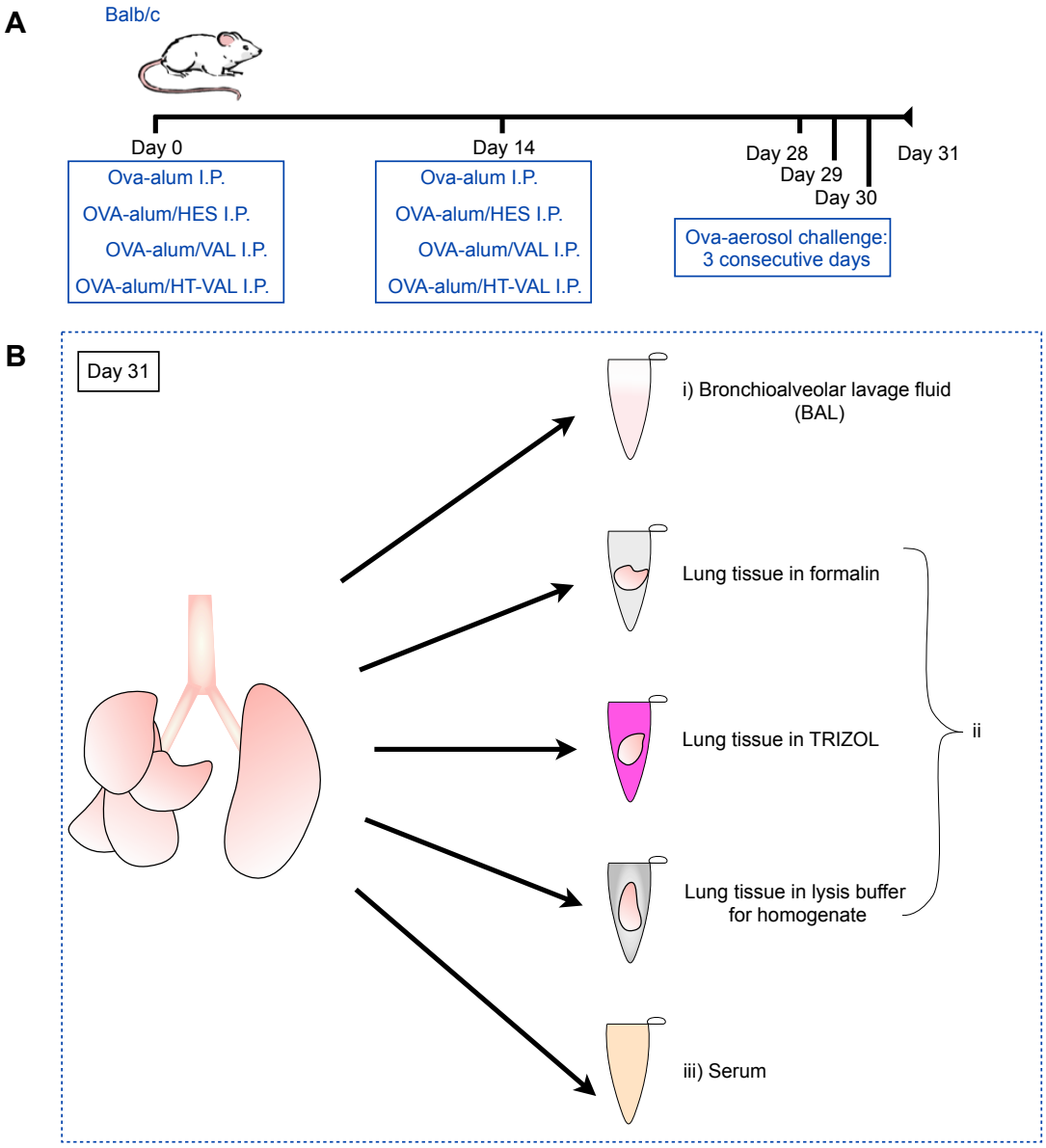

Fig 3.9 Allergic Airway Inflammation model

A. Sensitisation of /c mice was achieved by intra-peritoneal injection at day 0 and day 14 with mixtures of either OVA+ alum, HES+ alum, VAL+ alum or heat-treated VAL+ alum. Challenge with 1% OVA/PBS was performed intra-nasally for 3 consecutive days (Day 28, 29 & 30).

B Samples collected at Day 31 included i) bronchioalveolar lavage fluid (BAL), ii) lung tissue samples in formalin, TRIzol & lysis buffer and iii) serum.

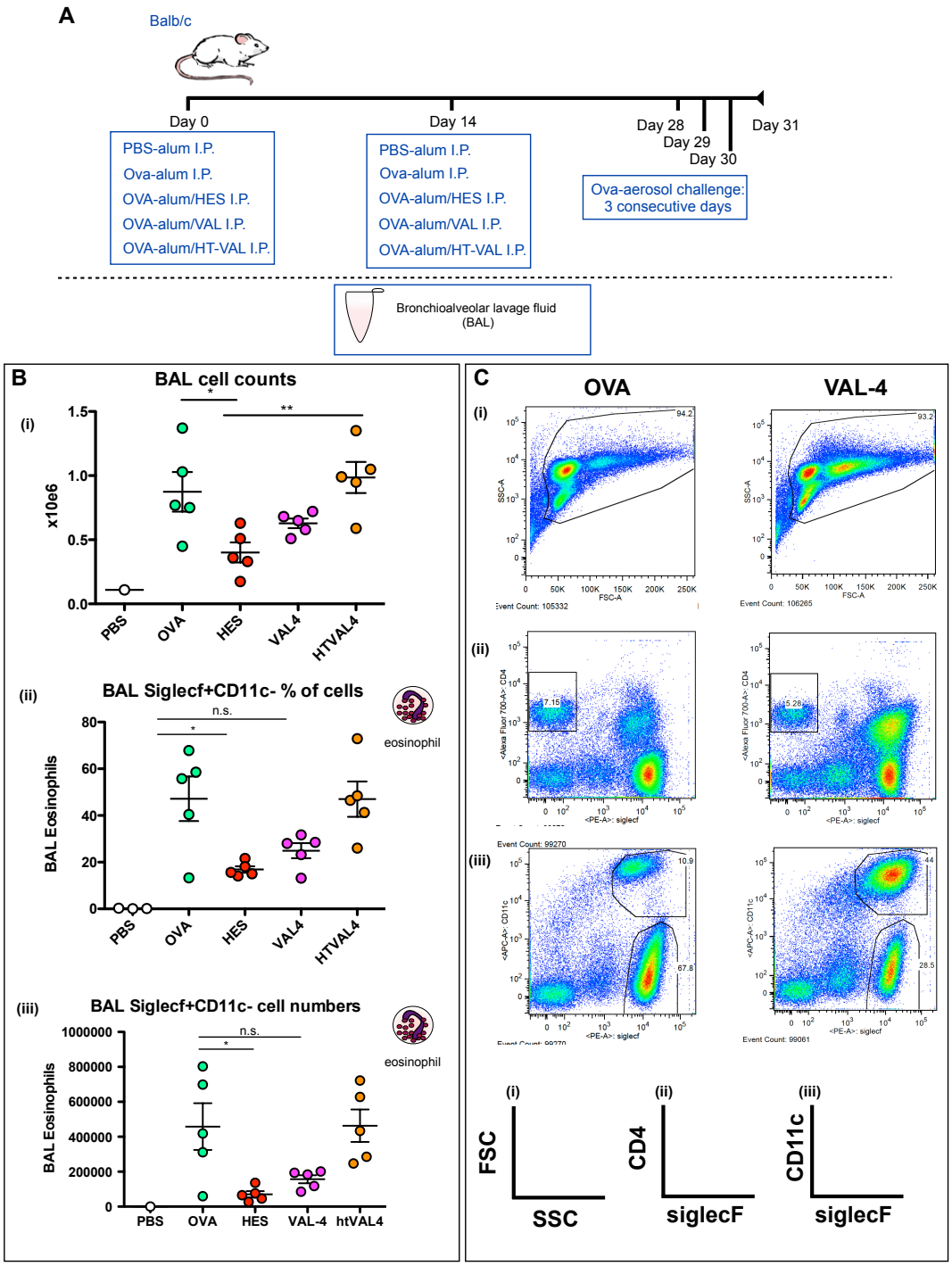

Fig 3.10 Experiment 1: Hp-VAL, a component of HES, reduces cell numbers and eosinophil numbers in BAL fluid in the A.A.I. model.

Fig 3.10 Experiment 1: Hp-VAL, a component of HES, reduces cell numbers and eosinophil numbers in BAL fluid in the A.A.I. model.

A. Experimental protocol for A.A.I. model. BALB/c mice were injected I.P. at Day 0 and Day 14 with either 200µl PBS, 200µl 20µg/ml Ovalbumin(Ova)-alum, 200µl 20µg/ml HES, 200µl 20µg/ml Hp-VAL4 or heat-treated (HT) Hp-VAL4. 1% Ova protein in PBS was used as an aerosol challenge and was administered at Days 28, 29 & 30. The experiment was terminated at Day 31 by terminal anaesthesia.

B. (i) Total cell numbers from BAL fluid were enumerated by haemocytometer counting. Eosinophil (SiglecF^{+}, CD11c^{-}) numbers were enumerated as a percentage of all cells **(ii)** or shown as total number of eosinophils **(iii)**. *=p<0.05, **=p<0.01, ***=p<0.001

C. Representative flow cytometry plots showing (i) FSC/SSC (ii) CD4/siglecF (iii) CD11c/siglecF

3.11 Analysis of BAL fluid shows a reduction in proportions and absolute numbers of T helper cells after administration of HES and Hp-VAL4.

The potential of $CD4^+$ T cells to ameliorate asthmatic symptoms in the A.A.I. model has been illustrated by (Wilson et al., 2005). $CD4^+$ and $CD4^-$ cells were isolated from the mesenteric lymph nodes of *H.polygyrus* infected mice and were transferred into uninfected OV-sensitized recipient mice. Reductions of total BAL cell numbers accompanied a suppression of airway eosinophilia in mice treated with $CD4^+$ cells.

To examine cell numbers and phenotypes, BAL cells were assayed using flow cytometry for the presence of $CD4^+$ T cells, alveolar macrophages ($CD11c^+$ $SiglecF^+$) and neutrophils ($GR1^+$ $SiglecF^-$ $CD11c^-$) (Fig 3.11) as well as eosinophils ($SiglecF^+$ $CD11c^-$) (Fig 3.10B ii and iii). Where mice had been treated with either HES or HpVAL-4 overall percentages and total numbers of $CD4^+$ T cells were significantly reduced relative to the OVA treated group (Fig 3.11A). This effect was lost or diminished in mice treated with heat-treated HpVAL-4 indicating that the effect was possibly conformation dependent. In the same mice the percentage of alveolar macrophages had increased but only reached significance in mice treated with HES treatment (Fig. 3.11B). Airway neutrophilia was raised in mice treated with HES and also in mice treated with HpVAL-4 but to a lesser extent and neither treatment reached statistical significance. Again neutrophilia responses to heat-treated HpVAL-4 were equivalent to OVA treatment alone (Fig 3.11C).

Thus preliminary indications were that HpVAL-4 functioned in a similar manner to HES in the A.A.I. model with regards to the extent and quality of the cellular response.

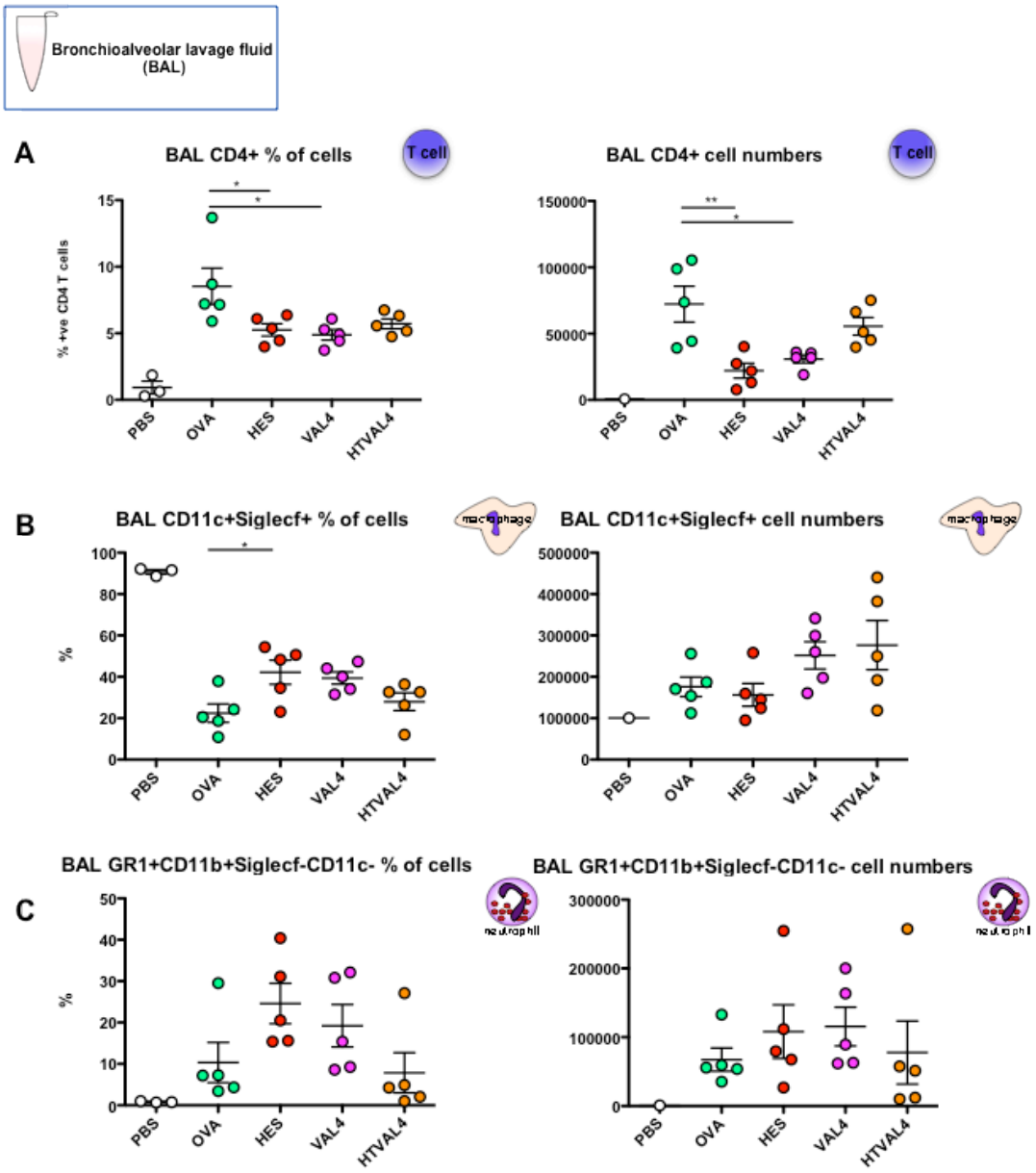

3.11 Analysis of BAL fluid shows a reduction in proportions and absolute numbers of T helper cells after administration of HES and Hp-VAL4.

Following the AAI protocol where by mice were injected IP with either PBS, OVA, HES, Hp-VAL4 or HT-Hp-VAL4 cells from the BAL fluid were stained to identify **(A)** CD4+ T cells, **(B)** alveloar macrophages and **(C)** neutrophils. *=p<0.05, **=p<0.01, ***=p<0.001

3.12- 3.13(i) & (ii) An overall reduction in cytokines produced is observed in mice treated with HES and HpVAL-4.

In the same model the cytokines present in both the BAL and the lung tissue were measured using a bead based immunoassay: BD Cytometric Bead Array. This technique allows the analysis of a large number of cytokines to be measured at the same time in a small sample volume.

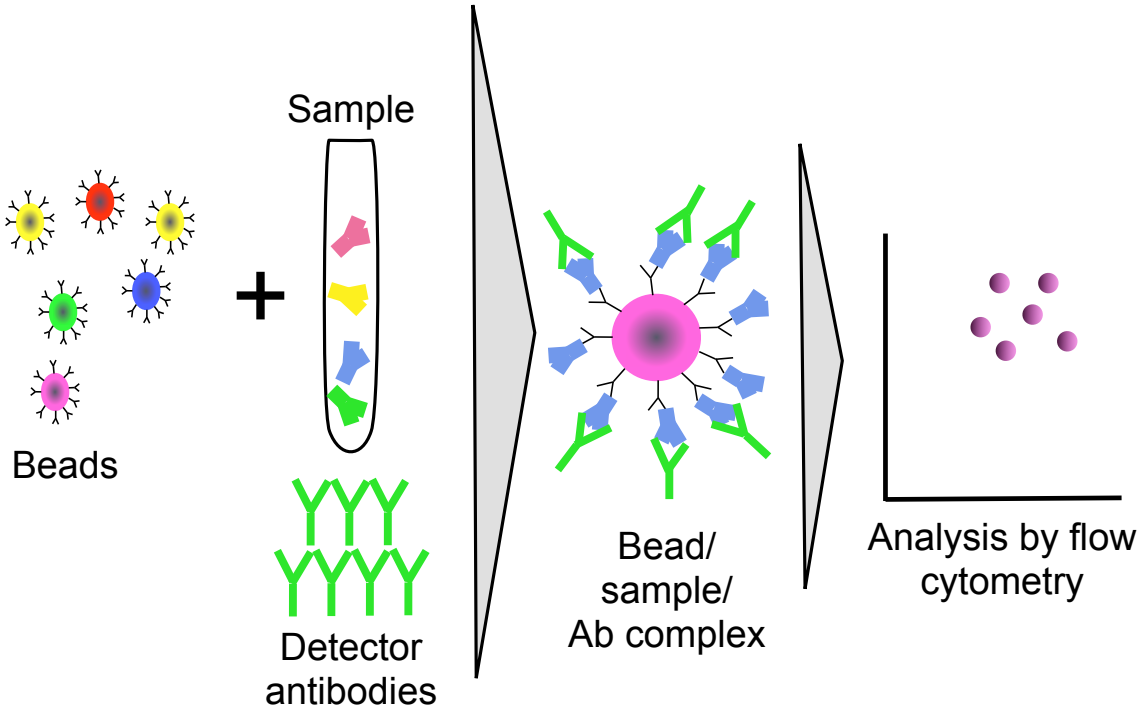

Fig. 3.12 BD Cytometric Bead Array

A combination of antibody specific fluorescent beads is incubated with the sample of interest along with reporter conjugated detector antibodies. After incubation and subsequent wash steps the complex is then acquired on a flow cytometer. Individual bead populations fluoresce at varying intensities depending on the sample being analysed. Concentration of individual analytes can then be generated from a standard curve.

When an active *H.polygyrus* infection is present levels of IFN-γ, IL-5 and IL-13 are reduced (Wilson et al., 2005). This cytokine profile is replicated when animals are treated with Hp-VAL4 with slight reductions in IFN-γ, IL-4, IL-5, IL-6 (Fig 3.13i) and IL-10, IL-13, IL17A and TNF-α (Fig 3.13ii) when compared to cytokine produced when OVA or heat treated HpVAL-4 was administered. Due to high variance in the OVA group none of these reductions (BAL IFN-γ: 100%, BAL IL-5: 50%, BAL IL-13: 30%, Fig 3.13i A and C, Fig 3.13ii B) reached statistical significance, although a significant reduction of IL-4 produced in the lung homogenate where HES treatment was administered was noted.
Heat-treatment of HpVAL-4 resulted in significantly more IL-10 in the BAL fluid and IL-13 in the lung homogenate. However levels of IL-10 were extremely low and perhaps an alternative method to measure this cytokine should be considered.

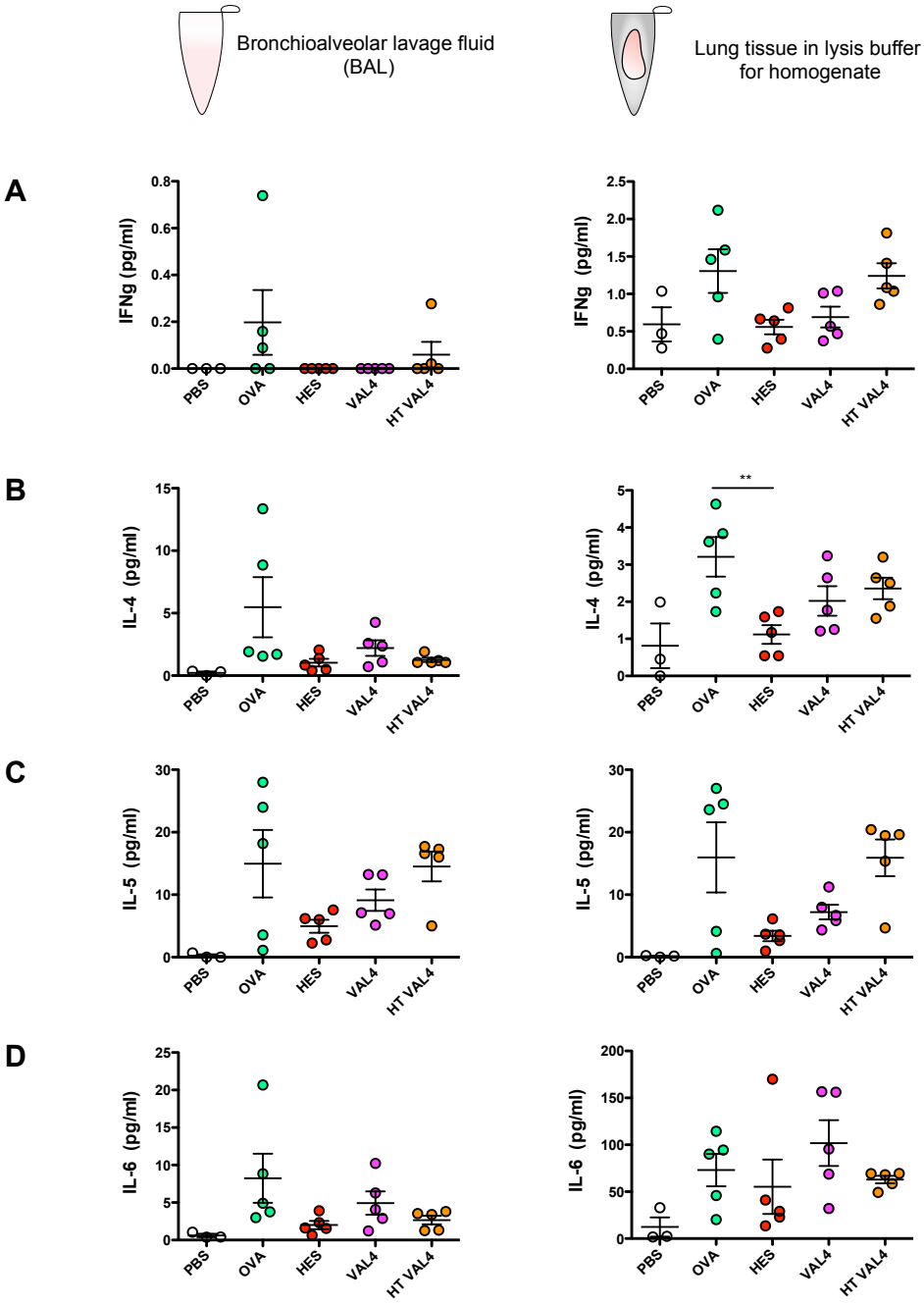

Fig 3.13 (i) An overall reduction in cytokines produced is observed in mice treated with HES and HpVAL-4.

Bronchioalveolar lavage cells and tissue homogenate were harvested and analysed for cytokine production using a cytometric bead array kit (CBA- BD Biosciences). Cytokines shown here are **(A)** IFNγ, **(B**) IL-4, **(C)** IL-5 and **(D)** IL-6. Continued over Fig 3.11 (ii).
*=p<0.05, **=p<0.01, ***=p<0.001

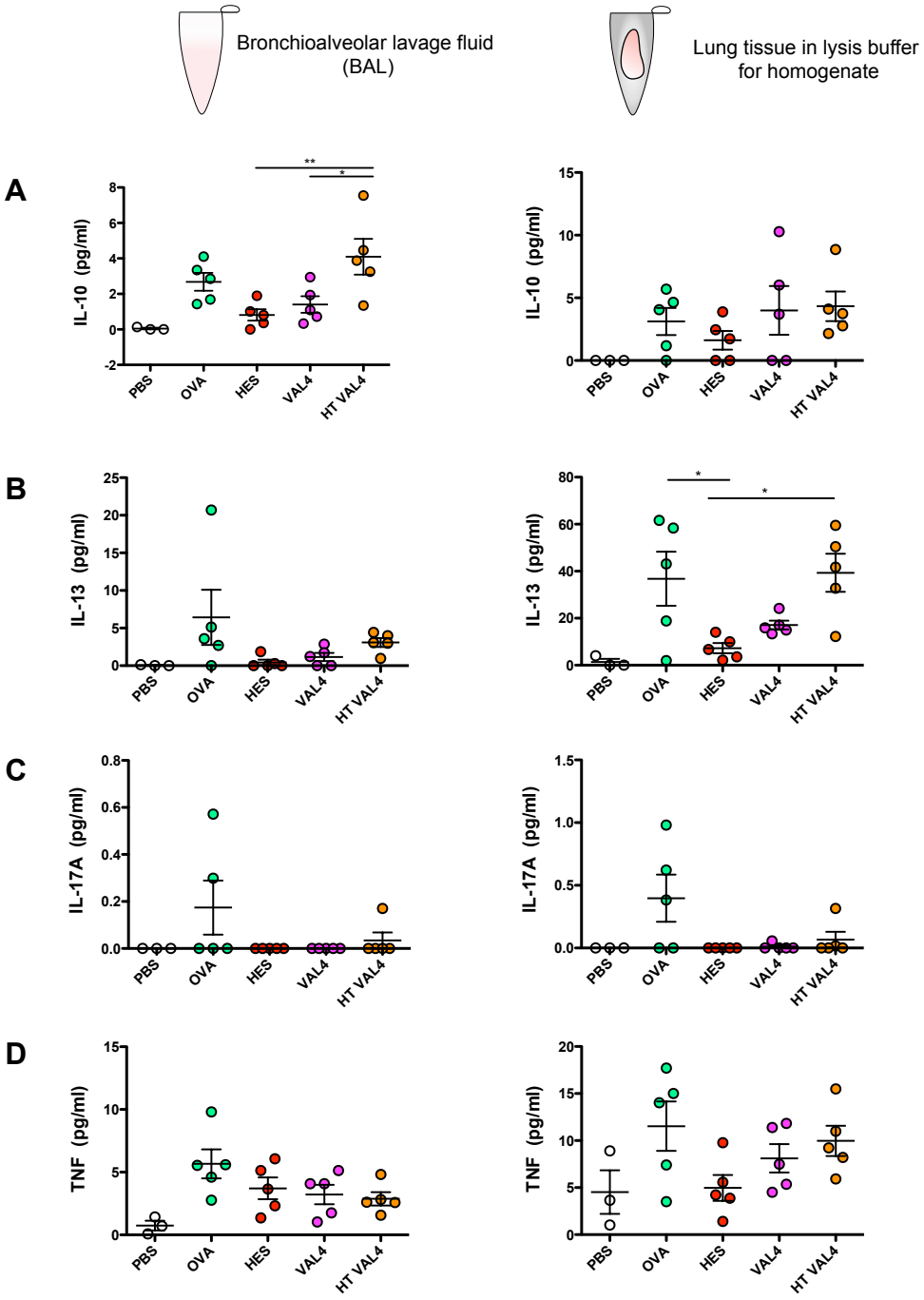

Fig 3.13 (ii) An overall reduction in cytokines produced is observed in mice treated with HES and HpVAL-4 (cont'd).

Bronchioalveolar lavage cells and tissue homogenate were harvested and analysed for cytokine production using a cytometric bead array kit (CBA- BD Biosciences). Cytokines shown here are **(A)** IL-10, **(B**) IL-13, **(C)** IL-17A and **(D)** TNF. *=p<0.05, **=p<0.01, ***=p<0.001

3.14 Levels of OVA specific IgE are reduced with HES treatment but not by HpVAL-4.

Antibody isotype responses have been reported either during *H.polygyrus* infection throughout the A.A.I. model or in the case of HES being administered at the point of sensitisation (Table 3.1).

Antibody	Response	H.polygyrus infection or HES treatment	Author
OVA specific IgE	↑	Worm infection	Kitagaki et al.
	↓	HES treatment	McSorley et al.
Total IgE	↑	Worm infection	Wilson et al.
	↑	Worm infection	Kitagaki et al.
IgG2a	↑	Worm infection	Wilson et al.
	↓	HES treatment	McSorley et al.
	↓	Worm infection	Kitagaki et al.
IgG1	↑↑	Worm infection	Wilson et al.
	↓	HES treatment	McSorley et al.

Table 3.1 Antibody responses throughout A.A.I model in response to either H.polygyrus infection or treatment with HES.

These responses appear to show some disparity between the presence of a live parasite infection and treatment with the parasite secretions.

Analysis of the antibody responses when Hp-VAL4, which is a single component of HES, is administered would further examine the outcome in a more reductionist

manner i.e. the parasite produces a mixture of molecules which can be separated to individual components.

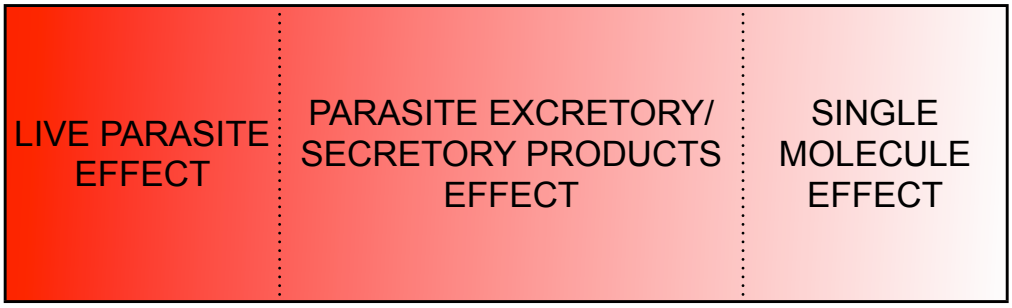

Where OVA specific IgE was measured levels were reduced when HES had been administered as seen by (McSorley et al., 2012). However when HpVAL-4 was used the levels of IgE were very slightly elevated but not reaching statistical significance (Fig 3.14A). IgG2a and IgG1, (Fig 3.14 B and C), showed matching trends with HES administration as noted on Table 3.1. Antibody levels when HpVAL-4 was given were very similar to HES in the case of IgG2a but notably elevated for IgG1. These results, although not statistically significant, contrast with those seen where HES is administered at the point of sensitization with HpVAL-4 behaving in a similar manner to a live parasite infection. Denaturing HpVAL-4 appeared to have little effect on levels of OVA-specific IgE whereas levels of IgG2a were elevated and IgG1were reduced.

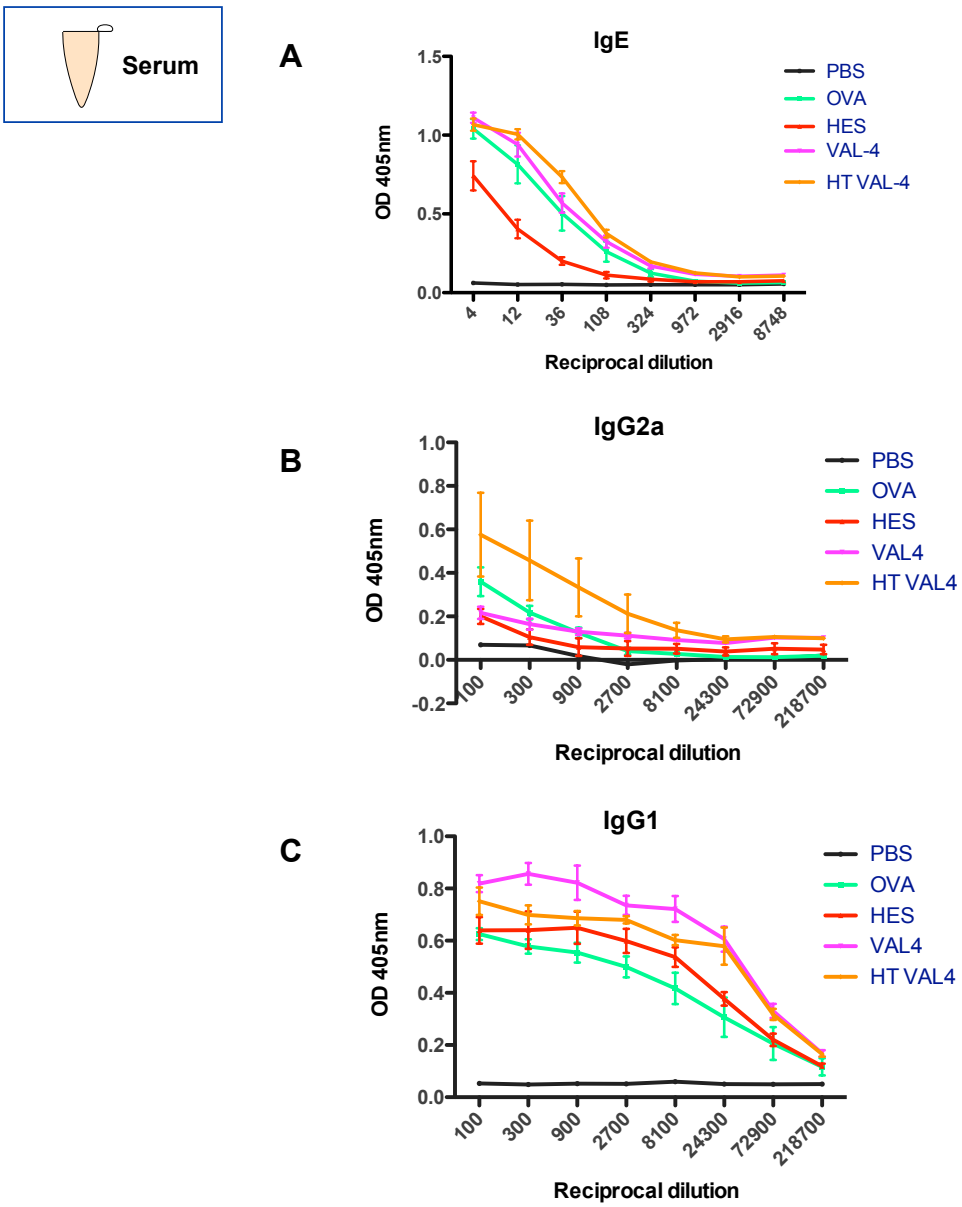

Fig 3.14 Levels of OVA specific IgE are reduced with HES treatment but not Hp-VAL4.
Antigen specific IgE **(A)**, IgG2a **(B)** and IgG1 **(C)** were measured in the serum by ELISA. For IgE assay serum was initially IgG depleted by incubation with Protein G sepharose beads. Ovalbumin was coated onto ELISA plates at a concentration of 25µg/ml overnight at 4°C. Plates were blocked using 2% BSA in carbonate buffer before washing and subsequent addition of sera which was serially diluted across the plate. After overnight incubation detection antibodies were added at the following diltuons: IgE 1:4000, IgG2a 1:4000 and IgG1 1:6000. ABTS substrate was then used to detect positive signals, which were read at an O.D. of 405nm. Error bars show SEM.

3.15 Levels of RELM-α in BAL and lung homogenate are reduced by HES treatment, whereas YM-1 levels appear to increase.

Type 2 innate response markers RELM-α and YM-1 are closely involved in the immune response to an asthmatic situation (Byers & Holtzman, 2010). Levels of these proteins, which are secreted by alternatively activated macrophages (AAMs) and alveolar macrophages (Sutherland, Maizels, & Allen, 2009), have been shown to be significantly reduced in the presence of HES during the A.A.I. model (McSorley et al., 2012). In a second model of airway allergy, where the fungal extract allergen *Alternaria* is administered intra-nasally (Kobayashi et al., 2009), similarly significant reductions in RELM-α and to a lesser extent YM-1 were observed with HES administration (McSorley et al., 2014).

To examine whether or not a single molecule from HES can exert the same down regulation of RELM-α and YM-1, levels of these two markers in BAL fluid and lung homogenate were examined by ELISA. As seen for HES, levels of RELM-α in the BAL fluid and the lung homogenate were reduced (Fig 3.15 A and B), with this reduction reaching statistical significance in the BAL fluid (Fig 3.15A). However levels of YM-1 in the BAL fluid (Fig 3.15C), although slighty reduced with HES treatment were actually higher when HpVAL-4 had been administered. YM-1 levels in the lung homogenate changed little between OVA, HES and HpVAL-4 treatment but were significantly elevated with the administration of heat-treated HpVAL-4 (Fig 3.15D).

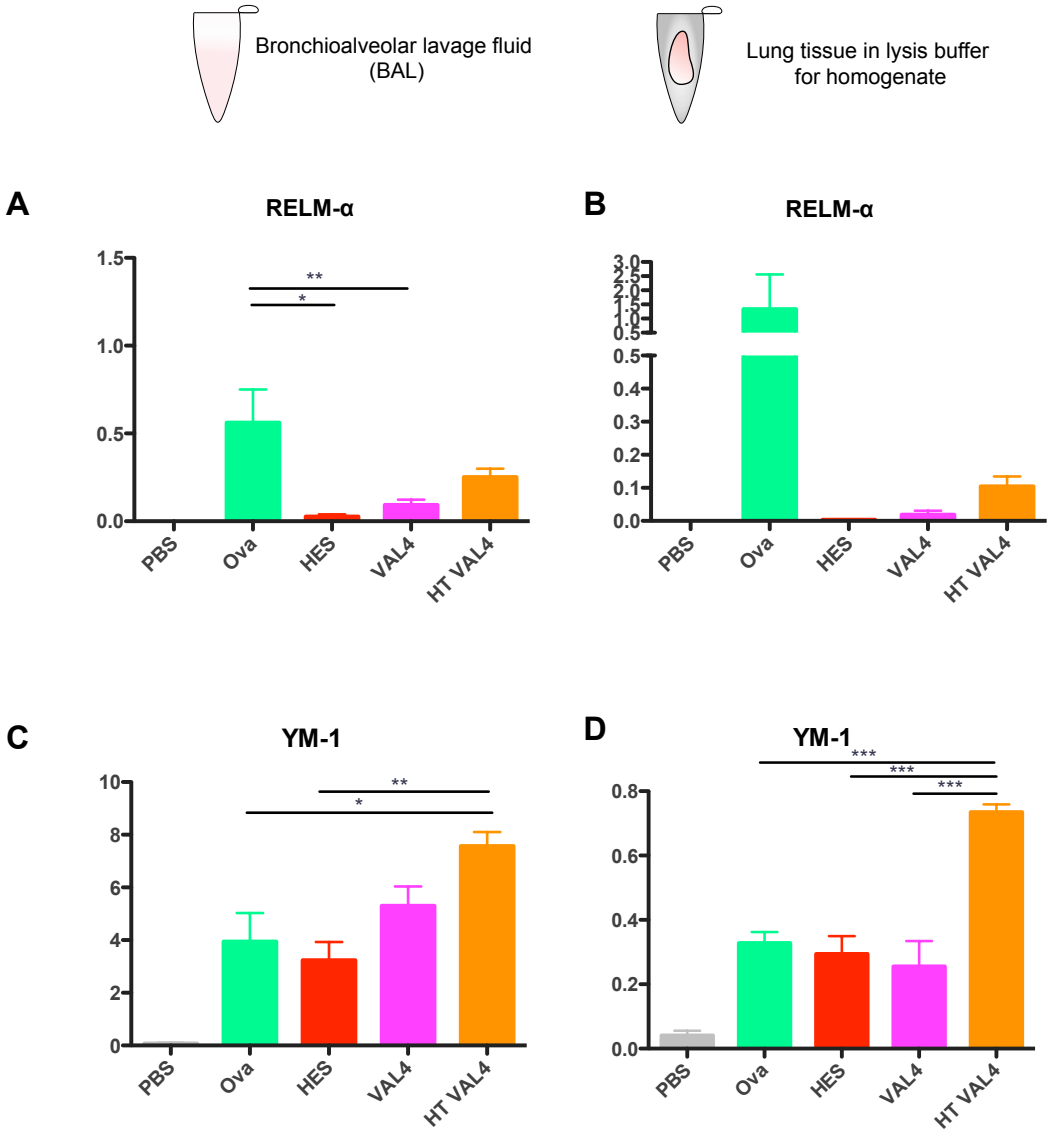

Fig 3.15 Levels of RELM-α in BAL and lung homogenate are reduced by HES treatment, whereas YM-1 levels appear to increase.

Type 2 myeloid cell response markers, RELM-α **(A & B)** and YM-1 **(C & D)**, in the BAL fluid and lung homogenate were measured by ELISA. For lung homogenate measurements, levels of Relm-α and YM-1 were normalised to protein content by Bradford assay.
*=p<0.05, **=p<0.01, ***=p<0.001

3.16 Differences between treatment groups illustrated by immunohistochemistry.

Wax embedded sections of lung tissue were prepared from formalin fixed samples and these were subsequently stained with hematoxylin and eosin (H&E) to identify inflammatory infiltrate and Periodic acid- Schiff (PAS) to localize mucus production.

Sections stained with H&E (Fig 3.16, yellow box), in some instances, showed an increase in inflammatory infiltrate where mice had been treated with OVA. Also an increase in mucus producing goblet cells was evident from PAS stained sections of lungs from mice treated with OVA (Fig 3.16, blue box). HES and HpVAL-4 treated mice had fewer goblet cells although this was not quantified numerically. Wax embedded sections could be stained in future with an α-MUC2 antibody in order to allow easier quantitation of goblet cell hyperplasia.

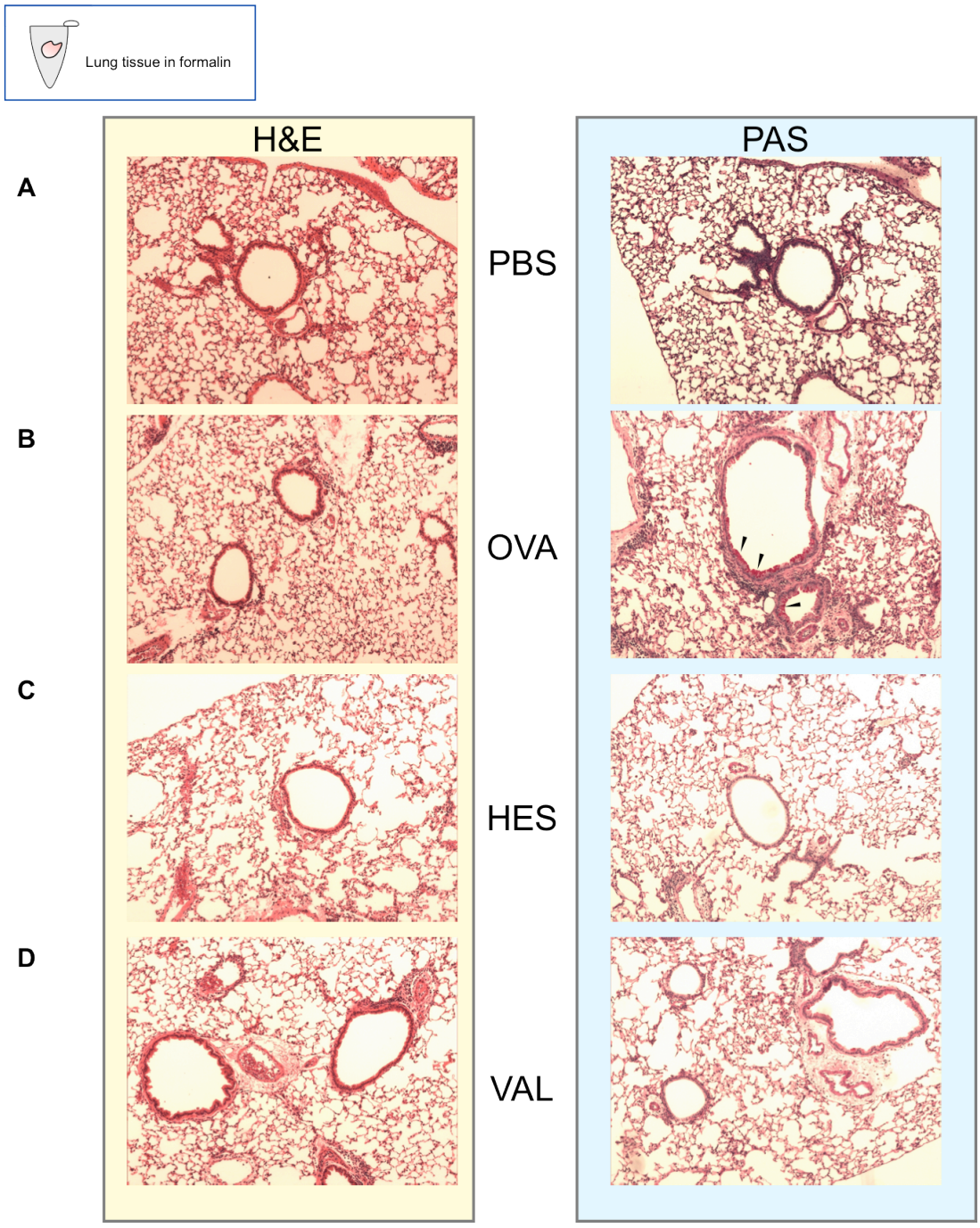

Fig 3.16 Differences between treatment groups illustrated by immunohistochemistry.
Lung tissue was fixed in formalin prior to wax embedding and sectioning. Black arrowheads show presence of goblet cells on PAS stained sections (10X magnification). Representative staining shown for mice treated with PBS **(A)**, OVA **(B)**, HES **(C)** and Hp-VAL4 **(D)**.

3.17 Experiment 2: Do other VAL molecules suppress AAI?

Data from the previous experiment indicated that administration of HpVAL-4, a single domain VAL molecule, altered the immune response in the A.A.I. model in the same way that a live infection of *H.polygyrus* parasites or secretions from that parasite do, albeit not as potently. BAL fluid cell counts, eosinophilia, cell recruitment and cytokine responses all behaved in a similar manner.

As has been discussed in previous chapters HpVAL-4 is one of a large and diverse family of VAL molecules. Thus it would be imprudent to assume all behaved in the same or a similar manner.

The following experiment tested the administration of two further VAL molecules during the sensitization phase of the A.A.I. model. The first, HpVAL-1, is a double-domain VAL molecule, expressed in an insect cell expression system, from *H.polygyrus* excretory-secretory products. The second, CeVAL, another single domain VAL molecule, was isolated from the free-living nematode *Caenorhabditis elegans.* This was also expressed in the same insect cell expression system as the previous proteins.

These proteins were administered I.P. to female BALB/c mice at Day 0 and 14, followed by an OVA-aerosol challenge on days 28,29 and 30 (Fig 3.17 A). On day 31 total BAL cell numbers were enumerated, with mice treated with HpVAL-1 showing the largest and significant reduction in cell numbers (Fig 3.17 Bi). Both HpVAL4 and CeVAL showed reduced BAL cell counts when compared to the OVA treatment group, however these did not achieve statistical significance (Fig 3.17 Bi). Numbers of eosinophils, characterized as SiglecF^{+}CD11c^{-} (Fig 3.17 Bii and iii), were significantly lower again in mice treated with HpVAL-1 and although also lower as a percentage of the total number of cells this failed to reach statistical significance. Thus all three VAL molecules reduce cell infiltrate and achieve a reduction in airway eosinophilia.

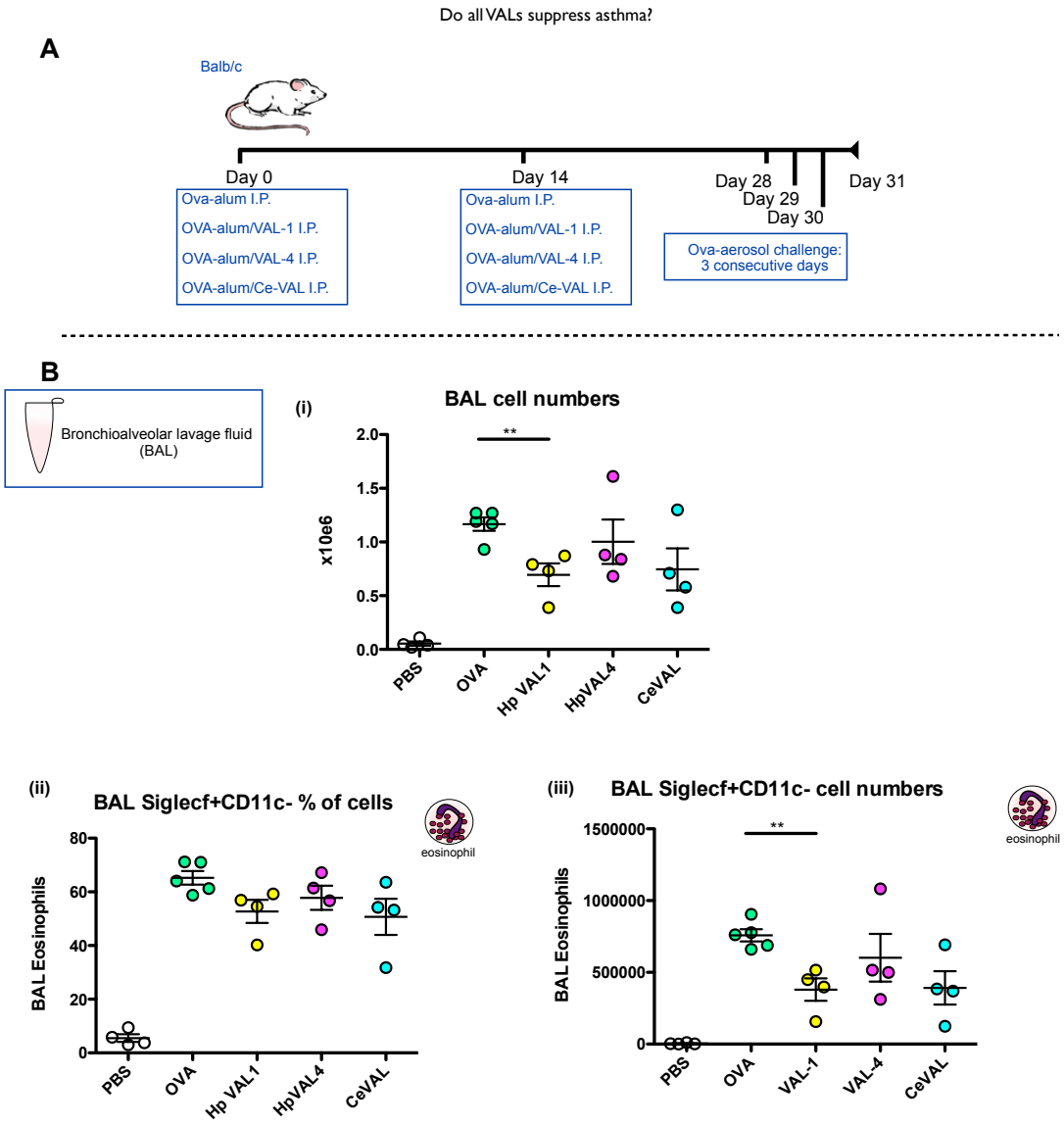

Fig 3.17 Experiment 2: Do other VAL molecules suppress AAI
A. Experimental protocol for A.A.I. model.

BALB/c mice were injected I.P. at Day 0 and Day 14 with either 200µl PBS, 200µl 20µg/ml Ovalbumin(Ova)-alum, 200µl 20µg/ml Hp-VAL1, 200µl 20µg/ml Hp-VAL4 or 20µg/ml Ce-VAL. 1% Ova protein in PBS was used as an aerosol challenge and was administered at Days 28, 29 & 30. The experiment was terminated at Day 31 by terminal anaesthesia.
B. (i) Total cell numbers from BAL fluid were enumerated by haemocytometer counting. Eosinophil ($SiglecF^+$, $CD11c^-$) numbers were enumerated as a percentage of all cells **(ii)** or shown as total number of eosinophils **(iii)**.
*=p<0.05, **=p<0.01, ***=p<0.001

3.18 Enumeration and characterization of BAL cells.

As discussed in the previous experiment, characterization of the cells being recruited into the lungs gives an indication of the type of immune response being mounted by the mouse and whether or not administration of the VAL molecules has altered this as a potential immunomodulatory molecule would.

T cells ($CD4^+$), alveolar macrophages ($CD11c^+SiglecF^+$) and neutrophils ($GR1^+CD11c^-SiglecF^-$) were all enumerated as a percentage of total cells recruited and as total cell numbers (Fig 3.18 A-C). Generally little difference was observed with administration of any of the VAL molecules. The percentage of $CD4^+$ T helper cells with OVA administration
(Fig 3.18A), at fewer than 5%, was lower than the 8-9% seen in the previous experiment (Fig 3.11A). This result was echoed not only in the absolute numbers of $CD4^+$ T helper cells but across the cell types measured. This may have been an indication that the level of asthma achieved in this experiment was lower than in the previous, however total BAL cell numbers are comparable between the two experiments (Fig 3.10 Bi and Fig 3.17 Bi) thus indicating asthma levels were similar.

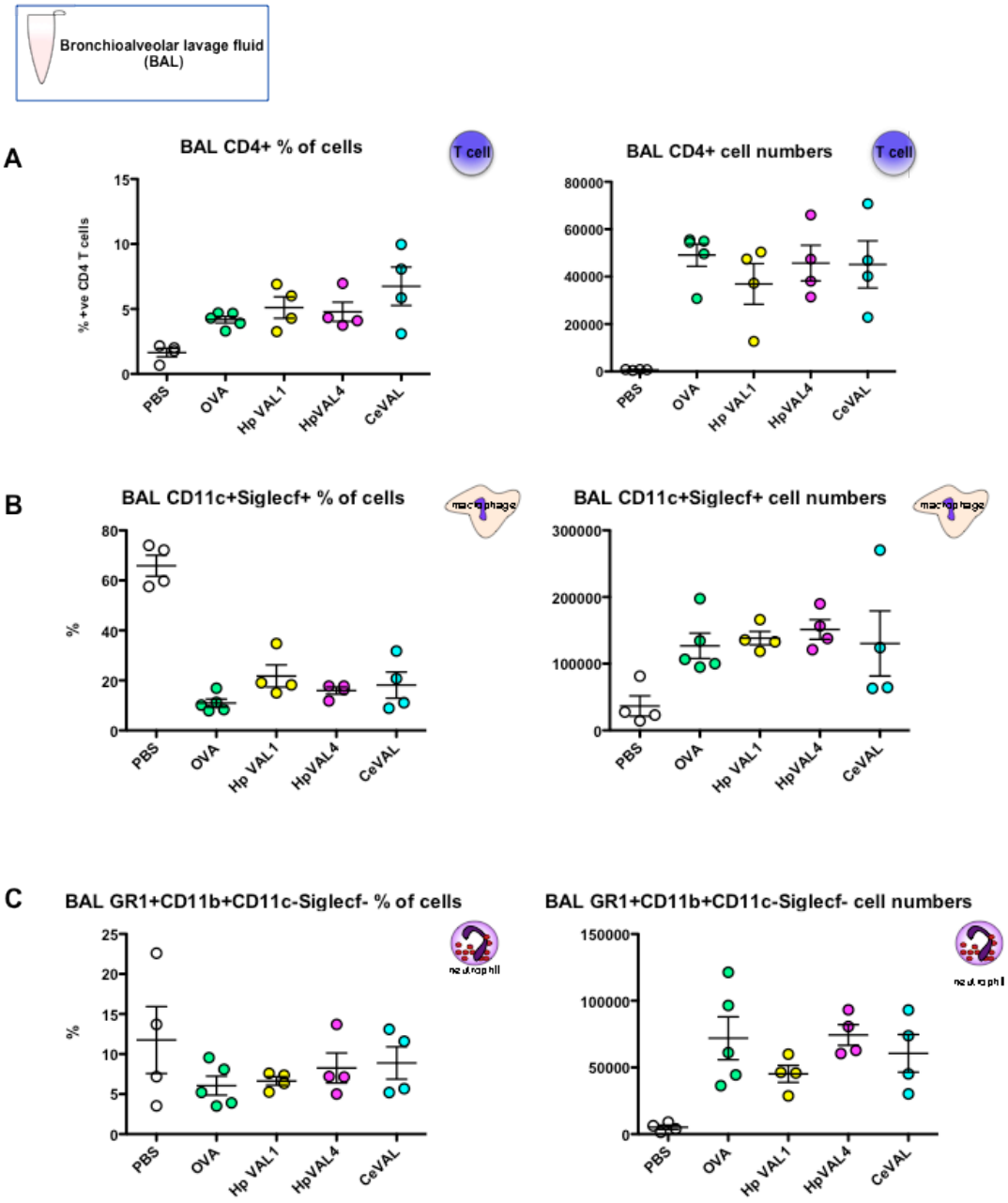

Fig 3.18 Enumeration and characterisation of BAL cells.

Following the AAI protocol where by mice were injected IP with either PBS, OVA, Hp-VAL1, Hp-VAL4 or Ce-VAL cells from the BAL fluid were stained to identify **(A)** CD4+ T cells, **(B)** alveloar macrophages and **(C)** neutrophils. *=p<0.05, **=p<0.01, ***=p<0.001

3.19 Enumeration and characterization of lung homogenate cells.

Total cell numbers from the lung homogenate showed reductions after administration of the 3 individual VAL molecules (Fig 3.19A). The nature of this cell recruitment is described further with enumeration of eosinophils and neutrophils present in the lung homogenate. The proportion and number of eosinophils was reduced in all treatment groups with this reaching a significant reduction in mice treated with HpVAL-1 and CeVAL (Fig 3.19 B). Neutrophil cell numbers tended to decrease upon VAL treatment although this did not reach statistical significance (Fig 3.19C).
Thus, as shown in Fig 3.19D, the main cell type recruited in the BAL fluid is eosinophils and these are reduced in proportion and number upon administration of all 3 VAL molecules.

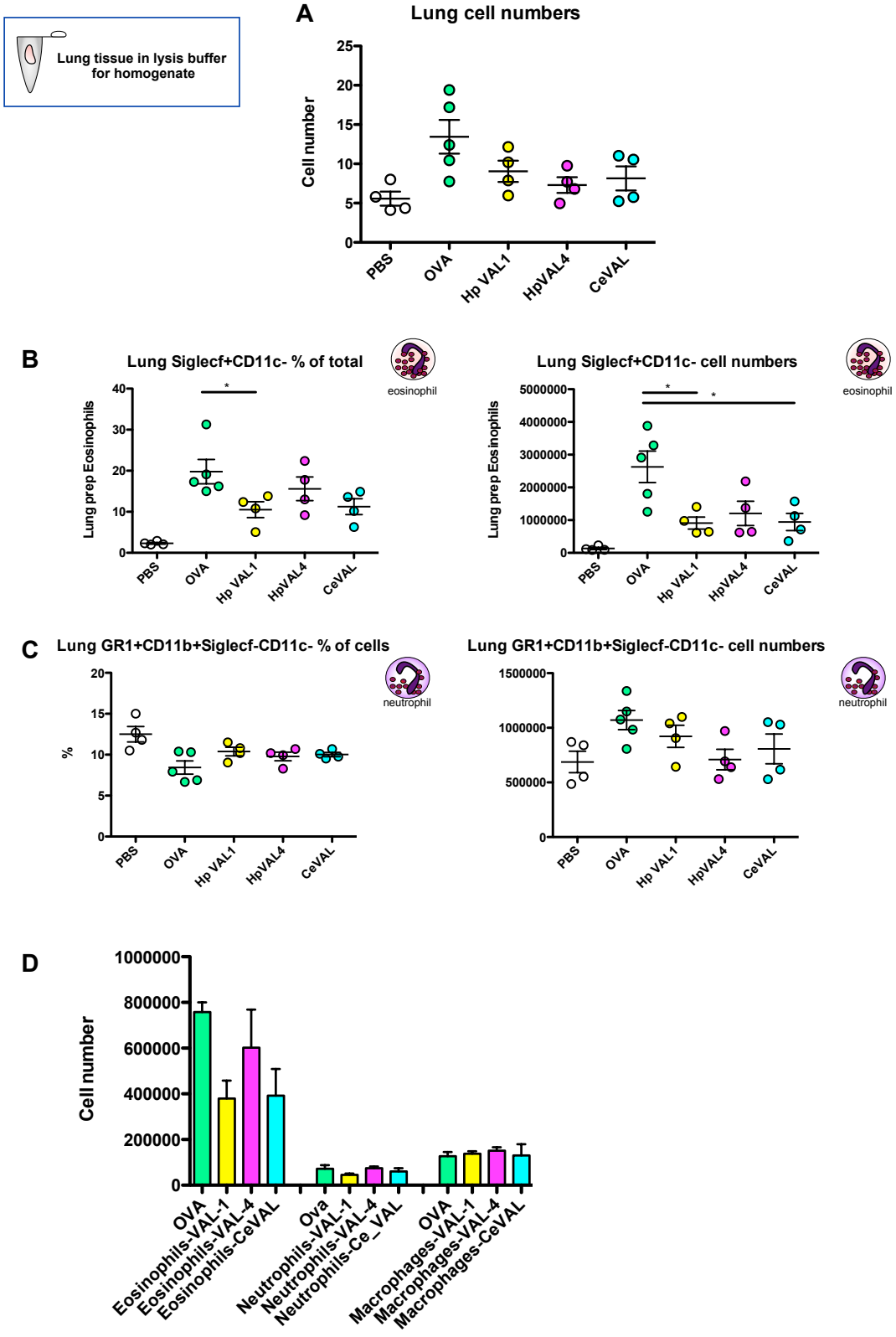

Fig 3.19 Enumeration and characterisation of lung homogenate cells.

Fig 3.19 Enumeration and characterisation of lung homogenate cells.

Following the AAI protocol where by mice were injected IP with either PBS, OVA, Hp-VAL1, Hp-VAL4 or Ce-VAL cells from the lung homogenate were first counted **(A)** then stained to identify eosinophils **(B)** and neutrophils **(C)**. Numbers of eosinophils, neutrophils and alveolar macrophages in the BAL fluid were plotted against OVA **(D)**.
*=p<0.05, **=p<0.01, ***=p<0.001

3.20 (i-iii) Intracellular cytokine profile of BAL and lung homogenate cells by CBA assay.

The BD CBA assay was used as described previously to measure levels of cytokine present in BAL fluid and lung homogenate collected from mice at the end of the A.A.I. model experimental protocol.

Here IFNγ, IL-4, IL-5, IL-6 (Fig 3.20 i), IL-9, IL-10, IL-13, IL17A (Fig 3.20 ii) and TNF (Fig 3.18 iii) were measured. Results relative to mice treated with OVA are summarized below in Table 3.2.

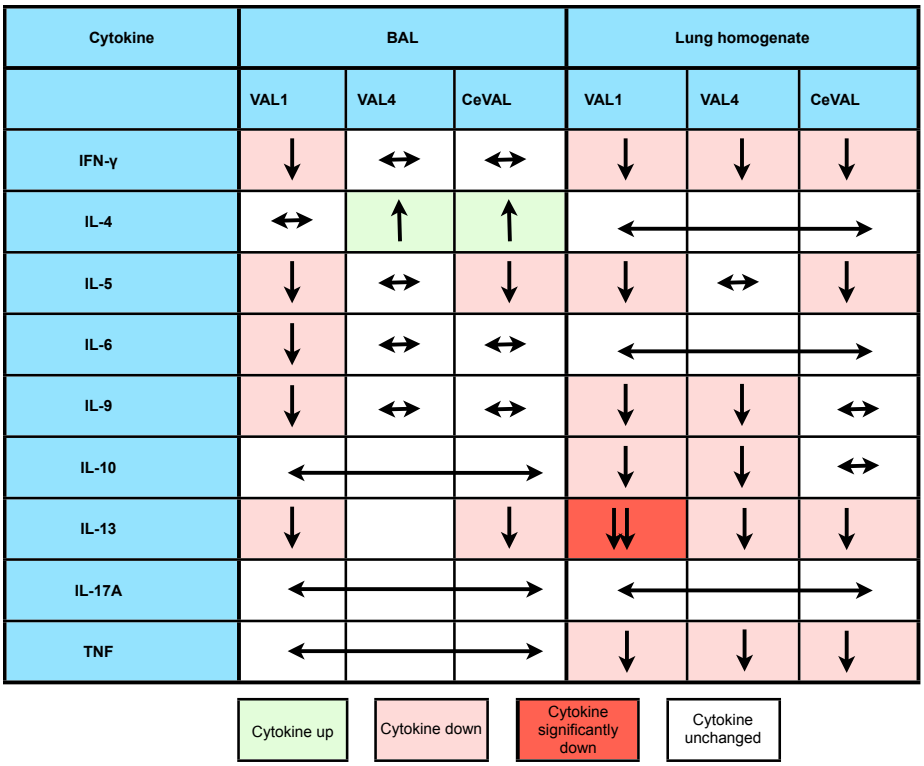

Table 3.2 Summary of CBA cytokine data
Results tabulated above show cytokine responses against OVA in the BAL fluid and in lung homogenate. Pale green boxes indicate levels of cytokine are higher, pink indicates lower and red indicates a significant decrease in cytokine levels.

As seen in the previous experiment, generally cytokine levels were lower or unchanged after VAL administration. In particular, IFN-γ, IL-5 and IL-13 were reduced in both experiments, data that concur with those seen by (Wilson et al., 2005) and (McSorley et al., 2012).

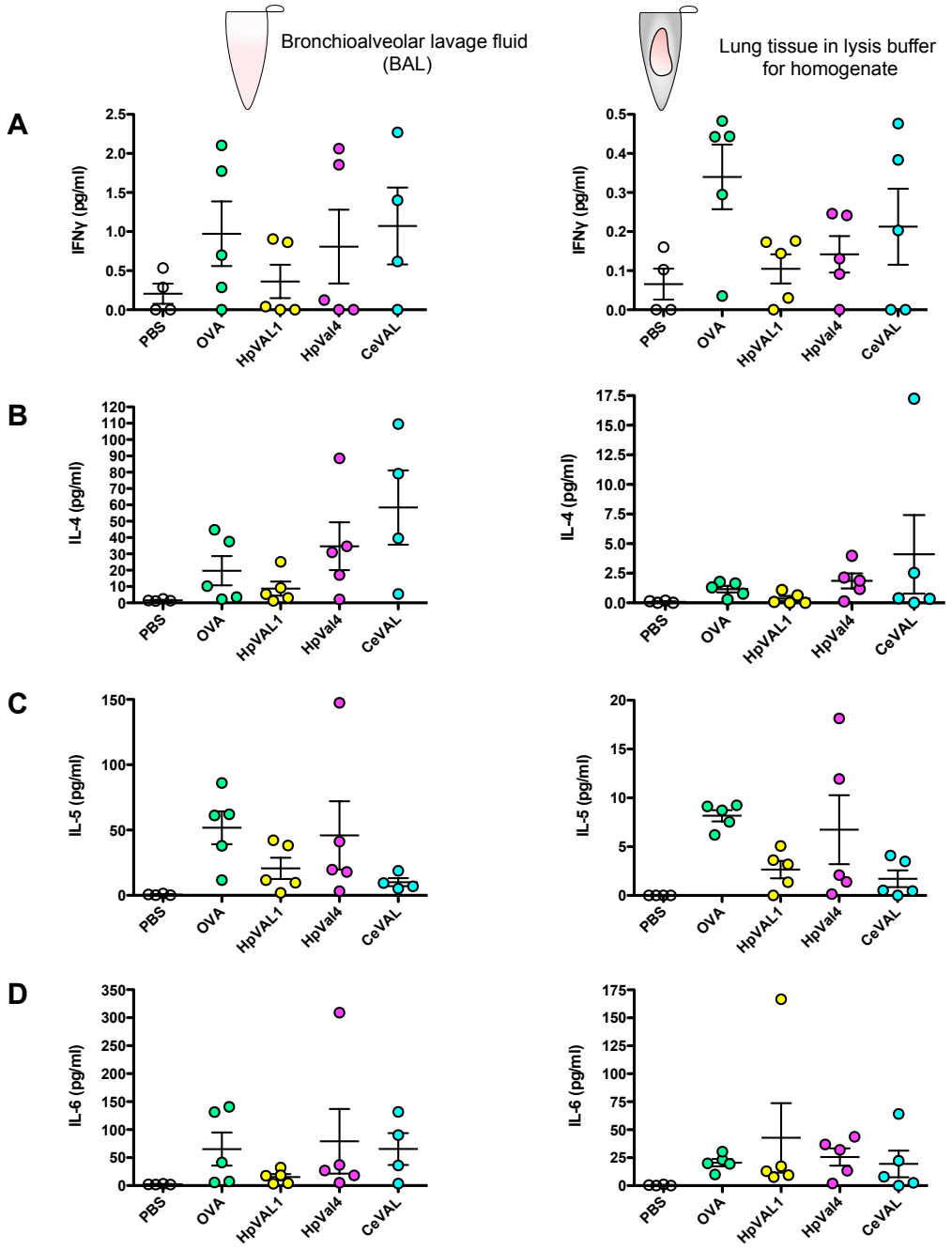

Fig 3.20(i) Intracellular cytokine profile of BAL and lung homogenate cells by CBA assay.

Bronchioalveolar lavage cells and tissue homogenate were harvested and analysed for cytokine production using a cytometric bead array kit (CBA- BD Biosciences). Cytokines shown here are **(A)** IFNγ, **(B**) IL-4, **(C)** IL-5 and **(D)** IL-6. Continued over Fig 3.5 (ii).
*=p<0.05, **=p<0.01, ***=p<0.001

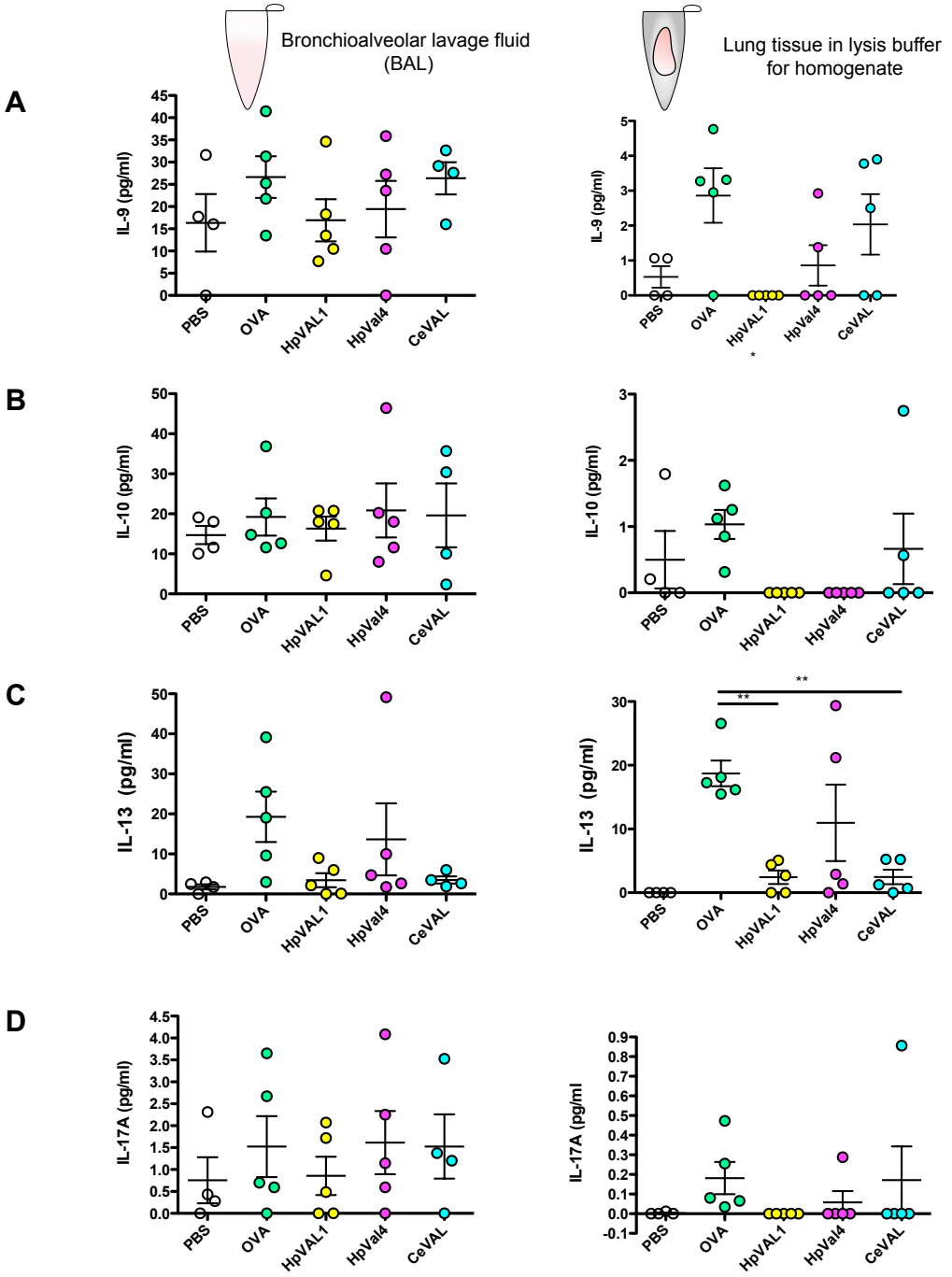

Fig 3.20 (ii) Intracellular cytokine profile of BAL cells by CBA assay (contd.)

Bronchioalveolar lavage cells and tissue homogenate were harvested and analysed for cytokine production using a cytometric bead array kit (CBA- BD Biosciences). Cytokines shown here are **(A)** IL-9, **(B**) IL-10, **(C)** IL-13 and **(D)** IL-17A. *=p<0.05, **=p<0.01, ***=p<0.001

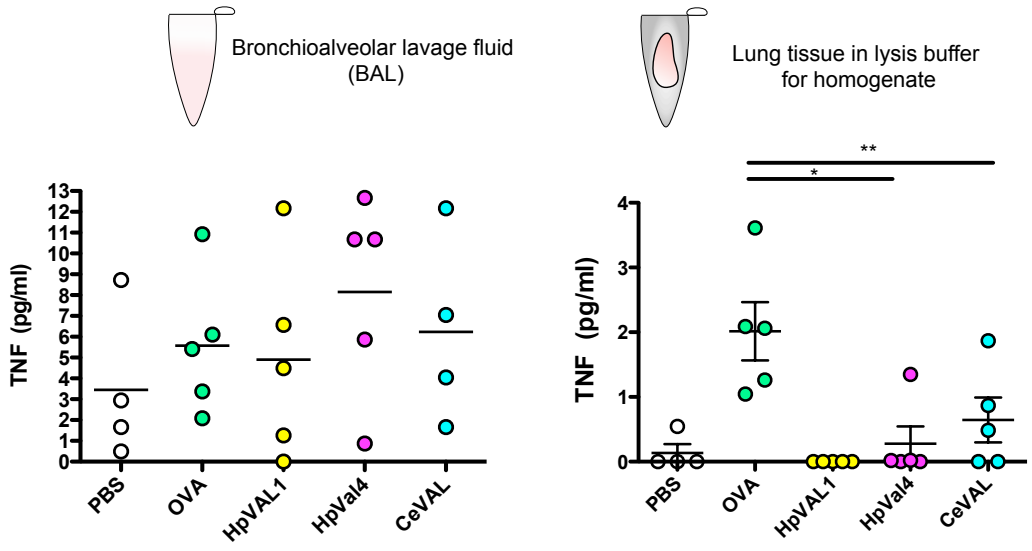

Fig 3.20 (iii) Intracellular cytokine profile of BAL cells by CBA assay (contd.)

Bronchioalveolar lavage cells and tissue homogenate were harvested and analysed for cytokine production using a cytometric bead array kit (CBA- BD Biosciences).
Cytokine shown here are is TNF-α.
*=p<0.05, **=p<0.01, ***=p<0.001

3.21 Levels of RELM-α in BAL and lung homogenate are reduced by VAL treatment. Conversely, YM-1 levels increase upon treatment with CeVAL.

To further characterize the cells that were recruited to the lung during the experiment RELM-α and YM-1 levels were measured by ELISA in both the BAL fluid (Fig 3.21 A and C) and the lung homogenate (Fig 3.21 B and D). In the previous experiment where HES or HpVAL-4 were administered during the sensitization phase of the model, levels of RELM-α were reduced (Fig 3.15 A and B) whereas levels of YM-1, when HpVAL-4 was administered, increased (Fig 3.15 C and D). This result was repeated here, where mice were given one of three different VAL moleclues, each representing variants of the the molecule found througout the VAL family. All measurements are relative to the OVA treated group of mice.

RELM-α was reduced in response to all three VALs in both the BAL fluid (Fig 3.21 A) and the lung homogenate (Fig 3.21 B) as was seen when HES was administered. Interestingly, levels of YM-1 again were increased upon treatment with all 3 VALs (Fig 3.21 C and D), in particular with CeVAL in the lung homogenate (Fig 3.21 D).

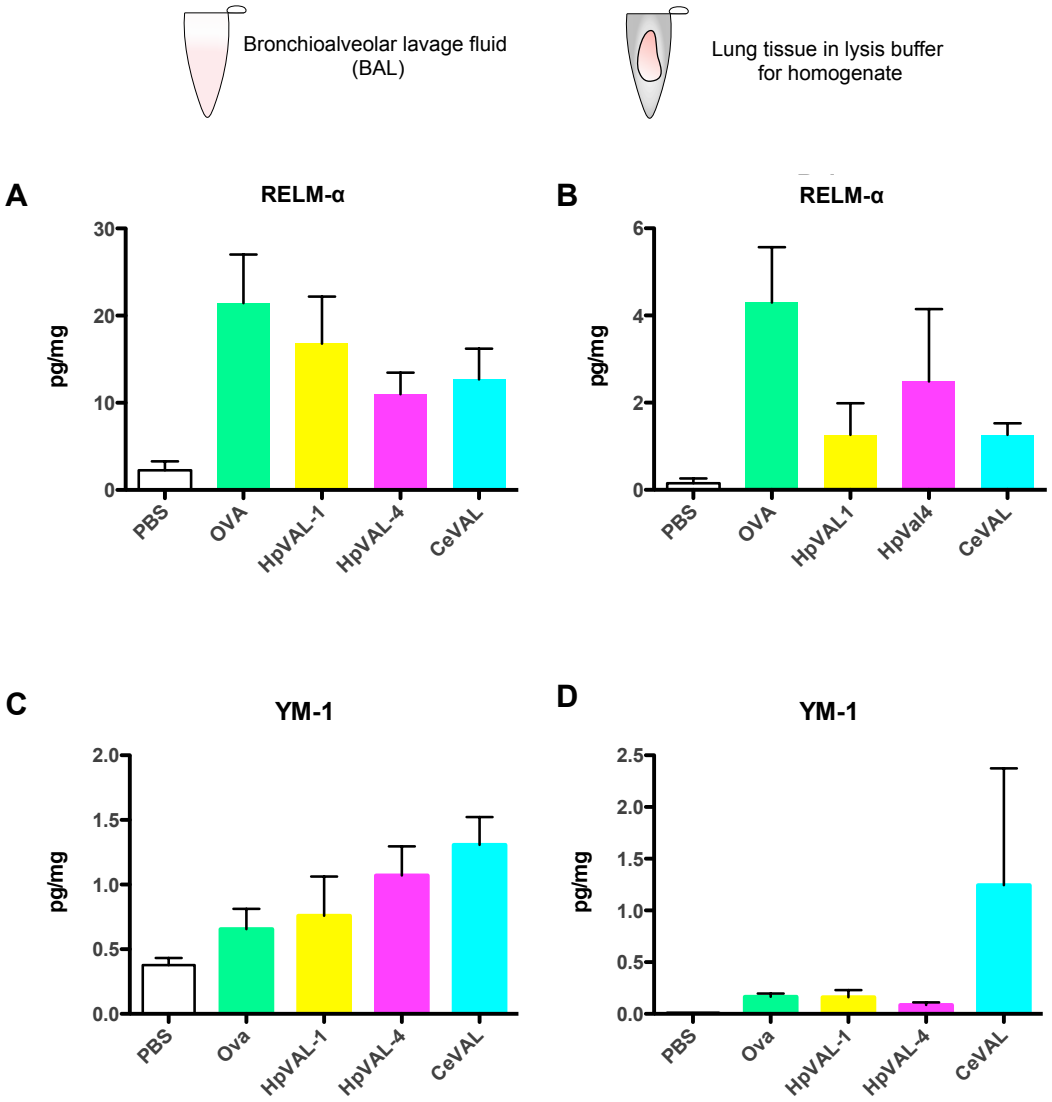

Fig 3.21 Levels of RELM-α in BAL and lung homogenate are reduced by VAL treatment. Conversely, YM-1 levels increase upon treatment with CeVAL.

Type 2 myeloid cell response markers, Relm-α (A & B) and YM-1 (C & D), in the BAL fluid and lung homogenate were measured by ELISA. For lung homogenate measurements, levels of Relm-α and YM-1 were normalised to protein content by Bradford assay.
*=p<0.05, **=p<0.01, ***=p<0.001

3.22 Experiment 3: Is the reduction of airway eosinophilia dependent on VAL structure?

Results from earlier experiments saw levels of eosinophils fall dramatically in mice that had been given HpVAL-4, an effect that was completely lost by boiling the recombinant. These mice also had lower levels of $CD4^+$ cells and higher neutrophil counts. IFN-γ, IL-5 and Il-13 were all reduced although levels of OVA specific IgE were much higher than those observed in HES treated mice.

Subsequent experiments have, for the most part, agreed with these initial data. HpVAL-4 is a single domain VAL molecule and when a double domain VAL protein was tested, in the form of HpVAL-1, this also resulted in a significant reduction in eosinophil numbers. A second single domain VAL was tested, CeVAL. Administration of this molecule also resulted in reductions in eosinophil numbers; in fact a more potent effect was observed than was seen with HpVAL-4.

These experiments however had not examined the possibility that the effect seen on eosinophil recruitment was one determined by the structure of the VAL molecule and that this could be reversed by heat-treatment of the protein.

In Experiment 3, both the single and double domain variants were tested in the original 31-day A.A.I. protocol. Both VAL proteins were administered at Day 0 and day 14 with and without prior heat-treatment. A third protein, *Nippostongylus brasiliensis* C-type lectin (NbCTL), was included in this experiment as a recombinant protein control. This protein had been produced using the same insect cell expression system as all of the VAL proteins used throughout this chapter.

Although cell counts achieved for mice treated with OVA alone were comparable to previous experiments (Fig 3.22 Bi), the same reductions in eosinophil numbers when animals were treated with VAL proteins were not achieved (Fig 3.22 B ii and iii). A slight reduction in eosinophil numbers and percentages where VALs had been administered in comparison to OVA was noted, this being greater than any effect from administration of NbCTL.

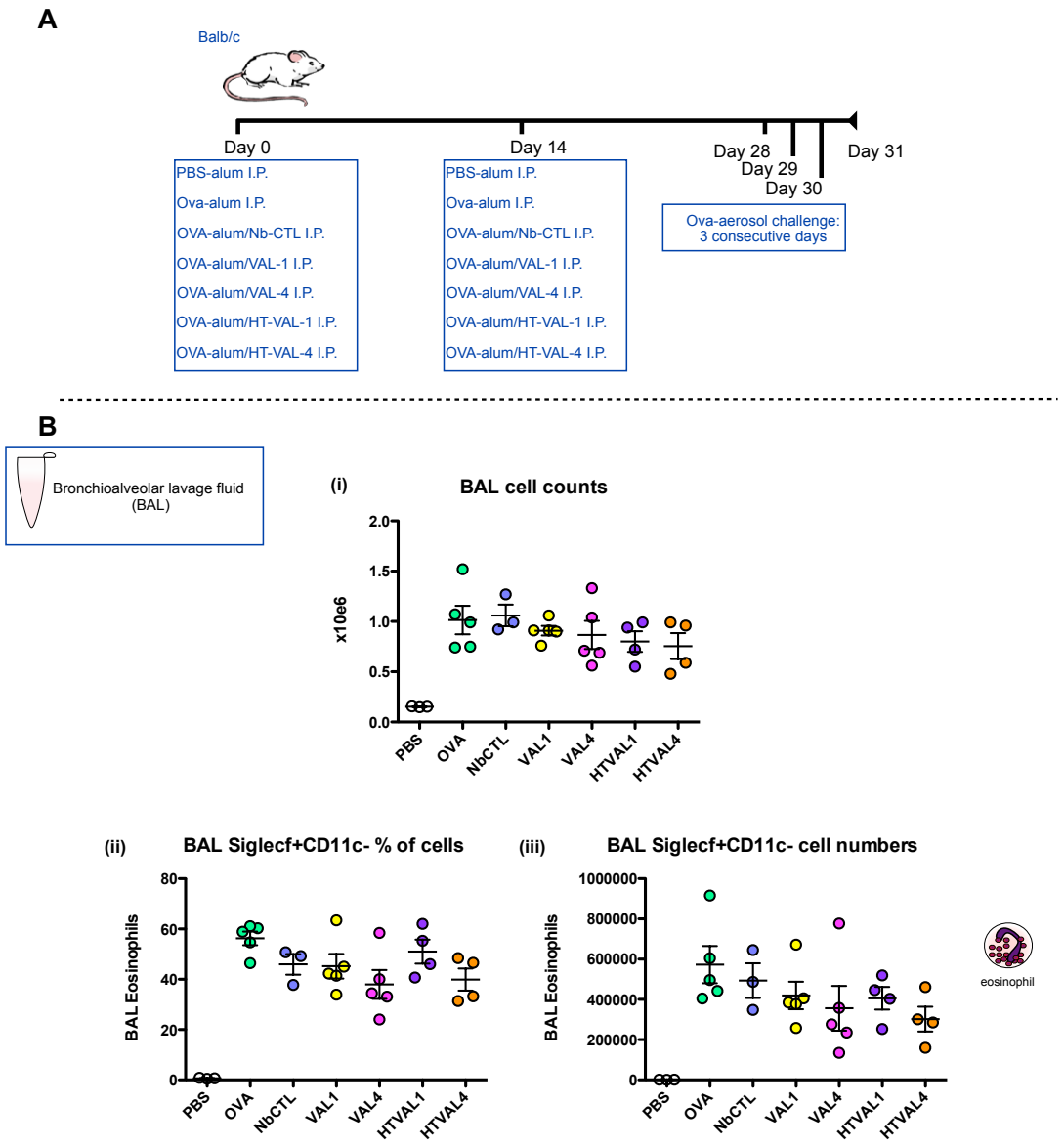

Fig 3.22 Experiment 3: Is the reduction of airway eosinophilia dependent on VAL structure?

A. Experimental protocol for A.A.I. model. BALB/c mice were injected I.P. at Day 0 and Day 14 with either 200µl PBS, 200µl 20µg/ml Ovalbumin(Ova)-alum, 200µl 20µg/ml Nb-CTL, 200µl 20µg/ml Hp-VAL1, 200µl 20µg/ml Hp-VAL4 or 200µl 20µg/ml heat treated Hp-VAL1 or 200µl 20µg/ml heat treated Hp-VAL4. 1% Ova protein in PBS was used as an aerosol challenge and was administered at Days 28, 29 & 30. The experiment was terminated at Day 31 by terminal anaesthesia.

B. (i) Total cell numbers from BAL fluid were enumerated by haemocytometer counting. Eosinophil (SiglecF^{+}, CD11c^{-}) numbers were enumerated as a percentage of all cells **(ii)** or shown as total number of eosinophils **(iii)**.

3.23 Enumeration and characterization of BAL cells.

Cell from the bronchioalveolar lavage fluid were stained with markers to identify various cell types by flow cytometry. Very slight reductions in T cell numbers were seen after administration of VAL recombinants, but this did not reach statistical significance (Fig 3.23 A). Numbers of T cells were somewhat increased with NbCTL treatment (Fig 3.32A). Percentages of macrophages regardless of treatment were between 20% and 30% with heat treatment of the recombinant proteins having little effect on macrophage recruitment (Fig 3.23 B). Where mice had been treated with HpVAL-4, neutrophil recruitment was increased; this however only reached statistical significance when an outlying point was omitted (Fig 3.23C). Generally heat-treatment of these recombinant proteins resulted in a slight reduction of neutrophils but overall little effect was seen.

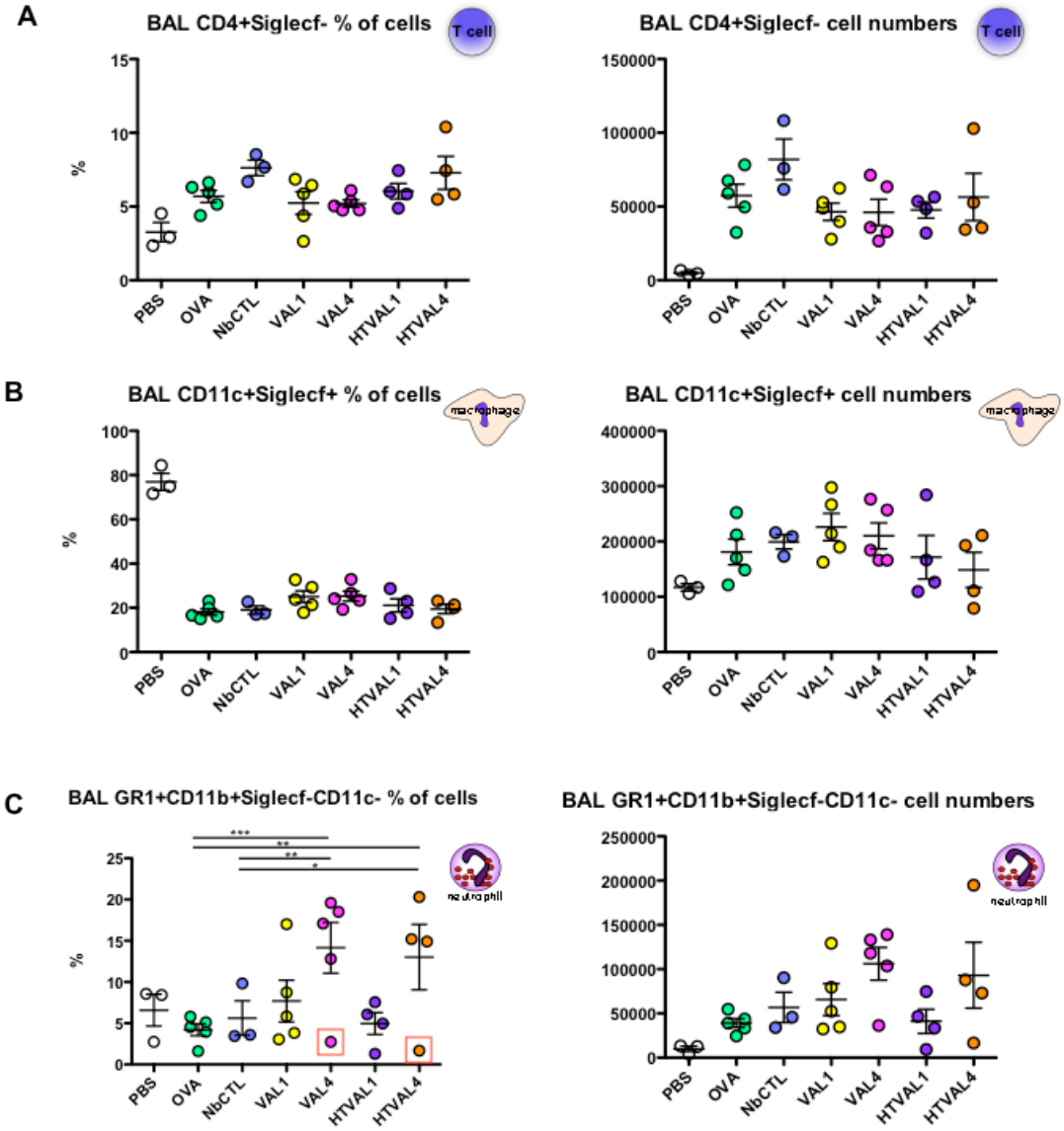

Fig 3.23 Enumeration and characterisation of BAL cells.

Following the A.A.I. protocol where by mice were injected IP with either PBS, OVA, Nb-CTL, Hp-VAL1,Hp-VAL4, HT-Hp-VAL1 or HT-Hp-VAL4, cells from the BAL fluid were stained to identify **(A)** CD4+ T cells, **(B)** alveloar macrophages and **(C)** neutrophils.

N.B. Statistics for Fig. 3.23C: % of cells, was carried out after boxed points were omitted.

*=p<0.05, **=p<0.01, ***=p<0.001

3.24 Experiment 4: Can the initial suppression of AAI by HpVAL be repeated?

The effect of VAL on the A.A.I. model was initially very convincing, with reductions in eosinophilia that were reversed by heat treatment of the protein. This was however in direct contradiction of results seen with HES (McSorley et al., 2012). Here, when HES was heat-treated, reductions in total BAL cell counts and BAL eosinophil numbers remained reduced.

Thus, recombinant HpVAL 4 was administered to female BALB/c mice on Days 0 and 14 of a 31-day A.A.I. protocol (Fig 3.24A). Recombinant protein was again heat-treated to examine the effects on cell recruitment of disrupting the protein structure.

Clear reductions in cell numbers counted in the BAL fluid, after treatment with HES, were enumerated (Fig 3.24 Bi). Reductions were also seen in mice treated with HpVAL4 as seen previously (Fig 3.10), however these effects were not reversed by heat-treatment of the protein (Fig 3.24 Bi). Moreover, cell counts from mice treated with boiled HpVAL4 were actually lower than those treated with HpVAL4 that had not been denatured.

Fig 3.24 Bii shows that eosinophil numbers enumerated from the BAL fluid were also significantly reduced in mice treated with HES (89% reduction) and HpVAL4 (54% reduction), however numbers remained significantly reduced with a 68% reduction occurring when recombinant HpVAL-4 protein had been heat-treated.

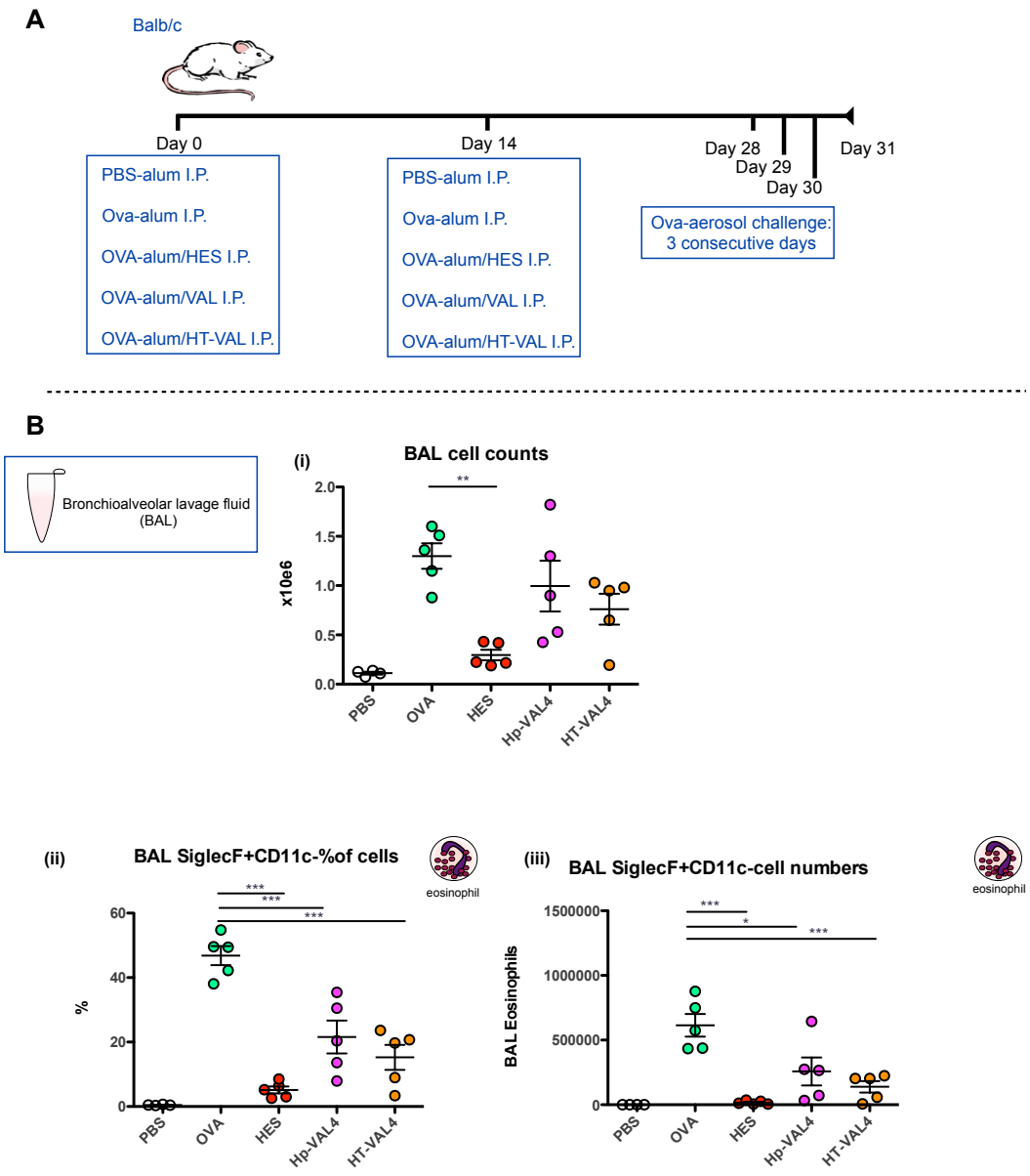

Fig 3.24 Experiment 4: Can the initial suppression of AAI by HpVAL be repeated?

A. Experimental protocol for A.A.I. model. BALB/c mice were injected I.P. at Day 0 and Day 14 with either 200µl PBS, 200µl 20µg/ml Ovalbumin(Ova)-alum, 200µl 20µg/ml HES, 200µl 20µg/ml Hp-VAL4 or heat-treated (HT) Hp-VAL4. 1% Ova protein in PBS was used as an aerosol challenge and was administered at Days 28, 29 & 30. The experiment was terminated at Day 31 by terminal anaesthesia.

B. (i) Total cell numbers from BAL fluid were enumerated by haemocytometer counting. Eosinophil ($SiglecF^+$, $CD11c^-$) numbers were enumerated as a percentage of all cells **(ii)** or shown as total number of eosinophils **(iii)**. *=p<0.05, **=p<0.01, ***=p<0.001

3.25 Enumeration and characterization of BAL cells.

Cells harvested in the BAL fluid were counted and stained for analysis by flow cytometry. T cells, alveolar macrophages and neutrophils were graphed in Fig 3.25 A-C.

In mice treated with HES and HpVAL4, CD4+ T cell numbers were reduced (Fig 3.25A). This reached statistical significance for the HES treated group (40% reduction) but not for the group treated with HpVAL (17%). Again, no difference in T cell or macrophage percentages was noted between groups treated with HpVAL and heat-treated HpVAL (Fig 3.25A and B, red boxes) indicating that these effects were being enabled by a heat stable element. However, the percentage of neutrophils present increased after heat-treatment of HpVAL-4 protein (Fig 3.25C).

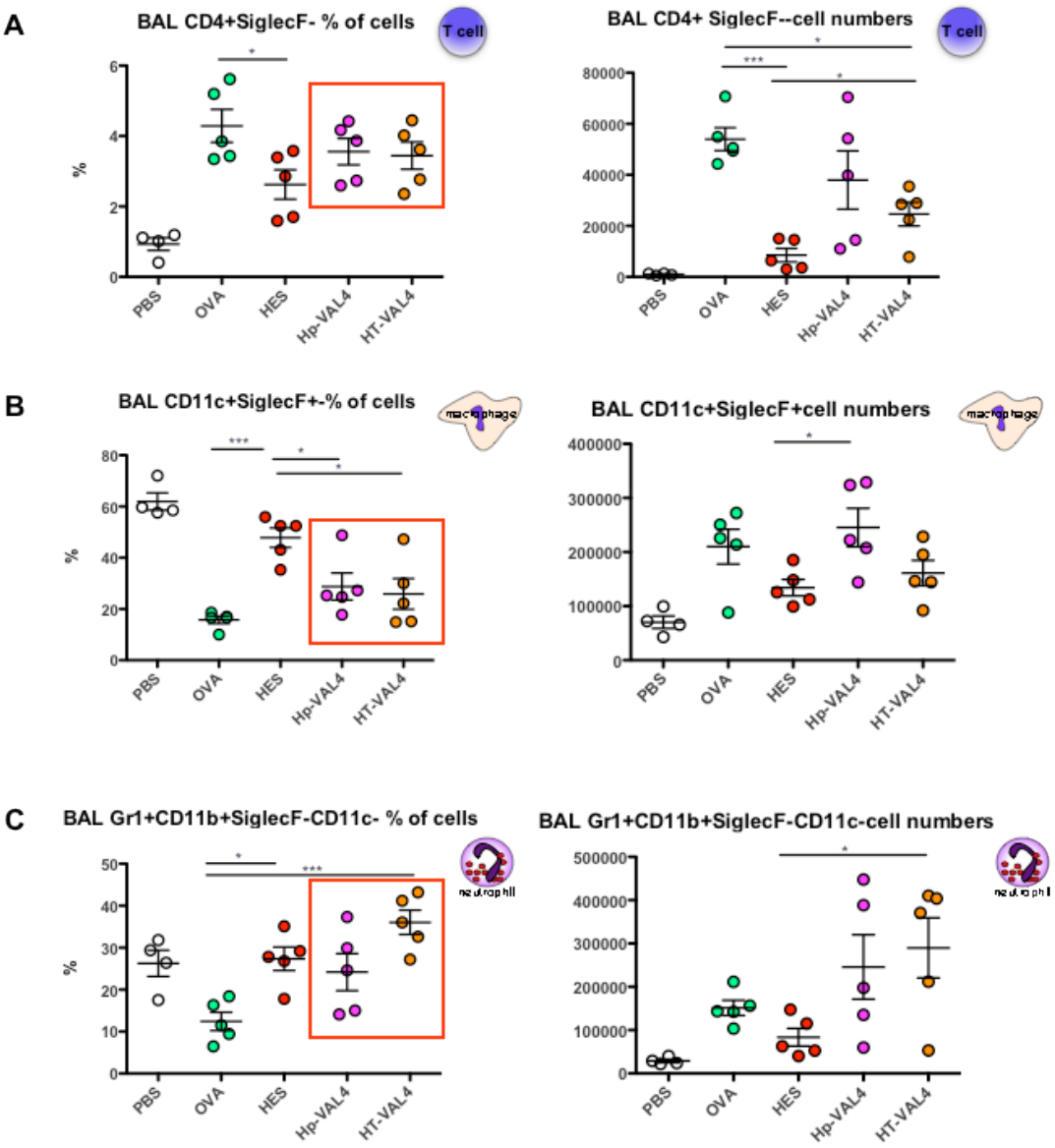

Fig 3.25 Enumeration and characterisation of BAL cells.

Female BALB/c mice were injected IP with either PBS, OVA, HES, Hp-VAL4 or HT-Hp-VAL4. Cells from the BAL fluid were stained to identify **(A)** CD4+ T cells, **(B)** alveloar macrophages and **(C)** neutrophils.

Boxed data highlights HpVAL-4 and heat-treated HpVAL-4.
***=p<0.05, **=p<0.01, ***=p<0.001**

3.26 Pooled data from 4 investigations showing that Hp-VAL4 reduces numbers of eosinophils as seen with HES.

One of the main readouts form the A.A.I. model is the effect the treatment in question has on eosinophil numbers in the lung. Data pooled from the investigations described in this chapter show quite varied results (Fig 3.26A); however only experiment one and four followed exactly the same protocol so this may account for some of the variability.

Focusing in on the responses to one of the main molecules being examined, HpVAL-4, a reduction in eosinophil numbers of 61% was observed (Fig 3.26 B). Overall HES repeatedly reduces airway eosinophilia significantly, a property shared by, albeit to a lesser extent, HpVAL4 (Fig 3.26 B&C). The disparity comes however in whether or not this effect is heat stable. As can clearly be seen in Fig 3.26C data is split but the general trend, after combining the two data sets, would indicate that the effect of eosinophil reduction remains after heat-treatment of the protein.

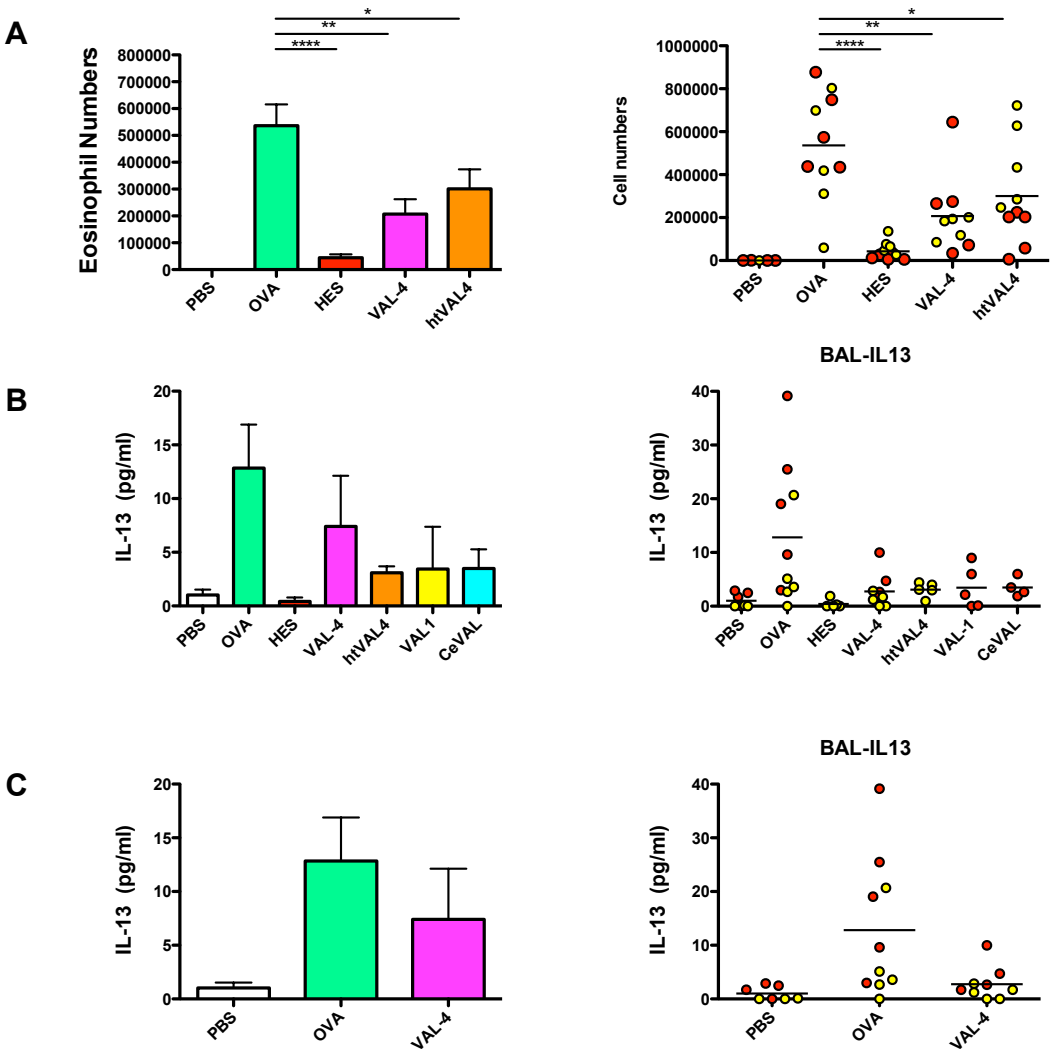

Fig 3.26 Pooled data from 4 investigations showing that Hp-VAL4 reduces numbers of eosinophils as seen with HES.

A. Data from 4 independent AAI experiments was pooled and eosinophil numbers shown. In each experiment female BALB/c mice were injected I.P. at Day 0 and Day 14 with either HES or recombinant protein.

B&C. Comparative data from two A.A.I. experiments in which HpVAL4 was administered I.P. to female BALB/c mice at Days 0 and 14 and boiled Hp-VAL4 was given as a control protein. Graph B shows the overall statistical significance for the two experiments and graph C shows how the effect of heat treatment varied dramatically between the two experiments.
*=p<0.05, **=p<0.01, ***=p<0.001

Discussion

The Hygiene Hypothesis was originally formulated more than 20 years ago by Strachan (Strachan, 1989) who suggested that exposure to infection early in life educated an immature immune system. This conclusion was drawn from an epidemiological study in which he examined family size and the age of a child with relation to his or her siblings, thus the first connection between an appropriate immune response and the "immune history" of that individual was made. The "immune history", in developed countries, of an individual nowadays would be a very different one to that of an individual from 50 years ago, and even more so from 150 years hence. Improvements in vaccinations, health provision, housing, food hygiene and general cleanliness have resulted in a population who have had a different range and severity of childhood ailments and who now harbor few, if any, parasitic companions. This leads to, as we have seen, an undoubted increase in immune mediated diseases such as asthma, autoimmune diseases, atopic dermatitis, colitis and Crohn's which all continue to increase in industrialized nations.

With increases in diseases such as asthma and colitis, so too has the amount of scientific research into the immune responses which have either caused the disease or responded to it. In order to investigate the aforementioned ailments various epidemiological and human reports, alongside new and developing animal model studies are being utilized and developed. When considering research into these immune mediated diseases and the potential for helminths to reduce if not clear symptoms, it is important to first consider the various stages at which the parasite could influence the immune response. Epithelial and dendritic cells would be the first point of contact that the host immune system has with the parasite antigens. At this stage the immune response would normally be pushed towards either a Th1 or Th2 response. If the parasite ES products contain components that interfere at this stage then the host response could be one of tolerance not an inflammatory Th1 situation. Many parasite-originated products have already been shown to exert these qualities; *Nippostrongylus brasiliensis* ES (Holland, Harcus, Riches, & Maizels, 2000), *H.polygyrus* ES (Segura, Su, Piccirillo, & Stevenson, 2007), *Trichinella spiralis* ES

(Aranzamendi et al., 2012), *Trichuris suis* (Kuijk et al., 2012) as well as S*chistosoma mansonii* soluble egg antigen (SEA) (Jankovic, Kullberg, Caspar, & Sher, 2004).

It is also important to consider where the parasite resides throughout its lifecycle and to which cells it and the secretions it produces, come into contact with. The mouse intestinal parasite *H.polygyrus* for example, has an entirely enteric lifecycle, thus only coming into contact with cells related to the intestines. *Strongyloides stercoralis* on the other hand has a fairly complicated lifecycle, comprising of a free-living exogenous phase and a parasitic endogenous phase where the parasite will migrate through the skin, travel to the lungs via the circulatory system where they are then coughed up and swallowed, thus entering the digestive system. Consequently these parasites come into contact with no fewer than 4 different host environments, each possessing their own set of specialized cells.

Research into **A**llergic **A**irway **I**nflammation (**AAI**) and asthma in humans highlights the number of complex interactive process, which can be studied using *in vitro* systems and animal models (Meurs, Gosens, & Zaagsma, 2008). Mechanisms of airway inflammation and airway hyperresponsiveness can now be more easily studied using a number of experimental mouse models, each being able to address various stages or symptoms displayed in an asthmatic individual. For example, the three phases involved in the development of allergic asthma cannot all be studied using the same model. These phases, namely 1) the induction phase, 2) the early-phase asthmatic reaction-EAR and 3) the late-phase asthmatic reaction-LAR, all have characteristic cells and more particularly timings involved (Verstraelen et al., 2008). The ovalbumin model described in this chapter (Fig 3.9) relies on intra-peritoneal administration of the allergen, a route that is obviously far from the natural method of allergen exposure. The model does however, in the presence of an alum adjuvant (Brewer et al., 1999), produce a clearly defined Th2 response. An alternative model, which offers a more natural administration of allergen, is the house dust mite model (Johnson et al., 2004). This involves repeated intra-nasal administration of the allergen in the absence of any adjuvants. However variances in mouse strain used must be taken into consideration when using this model as

BALB/c and C57BL/6 mice showed milder responses when sensitized in this manner (Shinagawa & Kojima, 2003).

In this chapter I have focused on an animal model, widely used in our lab, to look at the potential immunomodulatory properties of a group of proteins found throughout not only the parasite kingdom, but across many different phyla. As discussed in Chapter 1 the VAL family is rather extensively represented in the *H.polygyrus* genome and proteome. To examine every VAL variant would have been unfeasible thus I assessed a representative from the two main subsets of VAL molecules to examine their function in the OVA-alum model of AAI.

Initially HpVAL-4 (single domain VAL) was examined to see if it behaved in a similar way to HES as described by McSorley in the AAI model (McSorley et al., 2012). Immune responses as measured by total BAL cell counts; eosinophilia and cytokine production all replicated observations found for HES; notably in a heat dependent manner i.e. boiling the HpVAL recombinant reversed the result. Levels of IgE however were not reduced as seen when HES was administered with levels remaining at similar levels for OVA treatment alone.

As previously mentioned the VAL family in *H.polygyrus* is extensive. Initial findings demonstrated that HpVAL-4, a single domain VAL molecule, gave similar immunological results to HES. HpVAL-1, a double domain VAL, along with a VAL molecule from *C.elegans*, were therefore tested in the AAI model. BAL cell counts were significantly reduced where HpVAL-1 had been administered, a pattern duplicated by HpVAL-4 and CeVAL although in these instances not reaching statistical significance. Eosinophil numbers were also reduced, again only reaching statistical significance where HpVAL-1 had been used. Other readouts such as cytokine measurements showed a general reduction in cytokine production for all VAL molecules with HpVAL-1 being the most notable.

The ability of recombinant VAL molecules to inhibit an allergic Th2 response was then assessed, along with that of total HES. For both HpVAL-1 and 4 groups,

reductions in lymph node cell numbers were significantly reduced compared to the HES group. Reduced levels of all cytokines measured (IFN-γ, IL-4, IL-10 and IL-13) were observed upon administration of HpVAL-1 and 4. For all groups treated the main cell type recruited was macrophages. High numbers of eosinophils were also detected with very few neutrophils present for all groups. Thus the "HES phenotype" described after peritoneal administration was one of increased cellular infiltrate accompanied by higher levels of IFN-γ, IL-4, IL-10 and IL-13. The "VAL phenotype" saw a reduced cellular infiltrate and low levels of the aforementioned cytokines.

The reductions in BAL and eosinophil numbers were lost when HpVAL-4 was denatured by boiling. This was contrary to observations seen by McSorely where boiled HES retained the ability to reduce total BAL cell counts and eosinophil numbers (McSorley et al., 2012). HpVAL-1, being a double domain VAL molecule, may behave in a different manner to its relative HpVAL-4. Thus heat-treated HpVAL-1 was administered at sensitization and compared to HpVAL-1, HpVAL-4, heat-treated HpVAL-4 and an un-related recombinant protein that had been produced in the same insect cell system as the *H.polygyrus* molecules. In this instance, heat-treatment of the VAL proteins appeared to have no effect on BAL cell counts and eosinophil numbers, implying that the suppressive effect first observed was in this case heat stable. A further experiment was carried out to repeat the observation seen when the recombinant protein was denatured by heat-treatment. Again heat-treatment of HpVAL-4 made no difference to BAL cell numbers or eosinophils counted. When data from these two experiments was pooled there was a trend towards reduced numbers of eosinophils, which was not lost upon denaturation of the protein. This would indicate that conformation of the protein is not critical to facilitate these findings.

The results obtained with both HpVAL-1 and HpVAL-4, two members of the highly represented VAL family in *H.polygyrus,* have not only replicated some of the observations described when an active *H.polygyrus* infection is present throughout the AAI model but also those noted when the excretory/ secretory products of this helminth are used (McSorley et al., 2012). However these results should be considered as very much preliminary data in the light of various studies pertaining to

the allergenic properties of VAL molecules themselves. A recent study examining the allergic responses to two VAL molecules from *Schistosoma mansoni* showed that one of the recombinant proteins exhibited an allergic Th2 response when used in place of OVA in the ova-alum AAI model (Farias et al., 2012). Increases in total BAL cell numbers were accompanied by high numbers of eosinophils and macrophages along with increases in IgG1, IgE and IL-5. What *Schistosoma mansoni* does have in common with *H.polygyrus* is a large and complicated family of VAL molecules, members of which are invariably expressed at different points throughout the parasite lifecycle. In the same study where SmVAL4 was found to be allergenic another VAL protein, SmVAL26 did not demonstrate the same findings. These two molecules are expressed by the parasite at quite different stages throughout the development of the parasite; SmVAL4 being expressed by the cercariae and SmVAL26 being found in the egg and the hatched egg's fluid. It is however not the first report of allergic responses to VAL molecules; a Phase I clinical trial which saw individuals being immunized with the *Necator americanus* ortholog Na-ASP-2, saw some participants developing generalized urticarial reactions after only one immunization thus halting the trial (Diemert et al., 2012).

Thus investigations into the function and mechanisms of VAL molecules from *H.polygyrus* have been shown, using the ova-alum AAI model, to have the potential to act as immunomodulatory elements in the same way as infection with *H.polygyrus* or administration of the excretory secretory molecules from *H.polygyrus*. Use of another model, which utilizes the common fungus *Alternaria alternata,* could be employed to further study the VAL family; in particular to study the potential of VALs to suppress early IL-33 release and production of Th2 cytokines IL-4, IL-5 and IL-13 by innate lymphoid cells (ILCs) as seen when mice are treated with HES (McSorley et al., 2014). A further, more detailed study of the effect of VAL molecules on the epithelial cells with which it comes into contact could also be undertaken.

Finally, one rather poignant question remains; in our efforts to eradicate all things helminthic in developing countries are we inadvertently leaving them to deal with an equally debilitating epidemic of allergies and immune mediated diseases?

Chapter 4

Interactions concerning HES, VAL, *H.polygyrus* and the gut.

Introduction

During the lifecycle of a parasite there are often many junctures at which the host can and may mount an immune response. Take for example the hookworm; during its lifecycle it visits no less than 4 separate locations in its host. The infective larval stage of the hookworm enters its host though the skin: host-parasite interaction number 1 (Fig 4.1 A). From there it travels to the heart via the blood stream and onwards to the lungs (Fig 4.1 B & C): host-parasite interaction numbers 2 and 3. At this point the parasite migrates upwards through the oesophagus to be swallowed thus moving from a lung/ airway setting into the gut: host-parasite interaction number 4(Hotez, Bethony, Bottazzi, Brooker, & Buss, 2005). These moments define how the parasite and the host recognise and subsequently interact with each other and are critical in determining the outcome of infection.

The model used in this chapter is the murine intestinal helminth *Heligmosomoides polygyrus,* which has been introduced and discussed in previous chapters. Here I examine how the parasite and its excretory secretory products, in particular HpVAL proteins, interact and recognise the murine gut and its related tissues and cells.

Cells within the intestine have evolved to perform specific and essential functions. The first hindrance an intestinal parasite will come across is the extensive mucous layer covering the epithelium. Synthesised by goblet cells, this layer is comprised of two layers of mucus. The outer most layer consists of secreted, large glycoproteins, which prevent resident commensal bacteria gaining access to the gut epithelial cells.

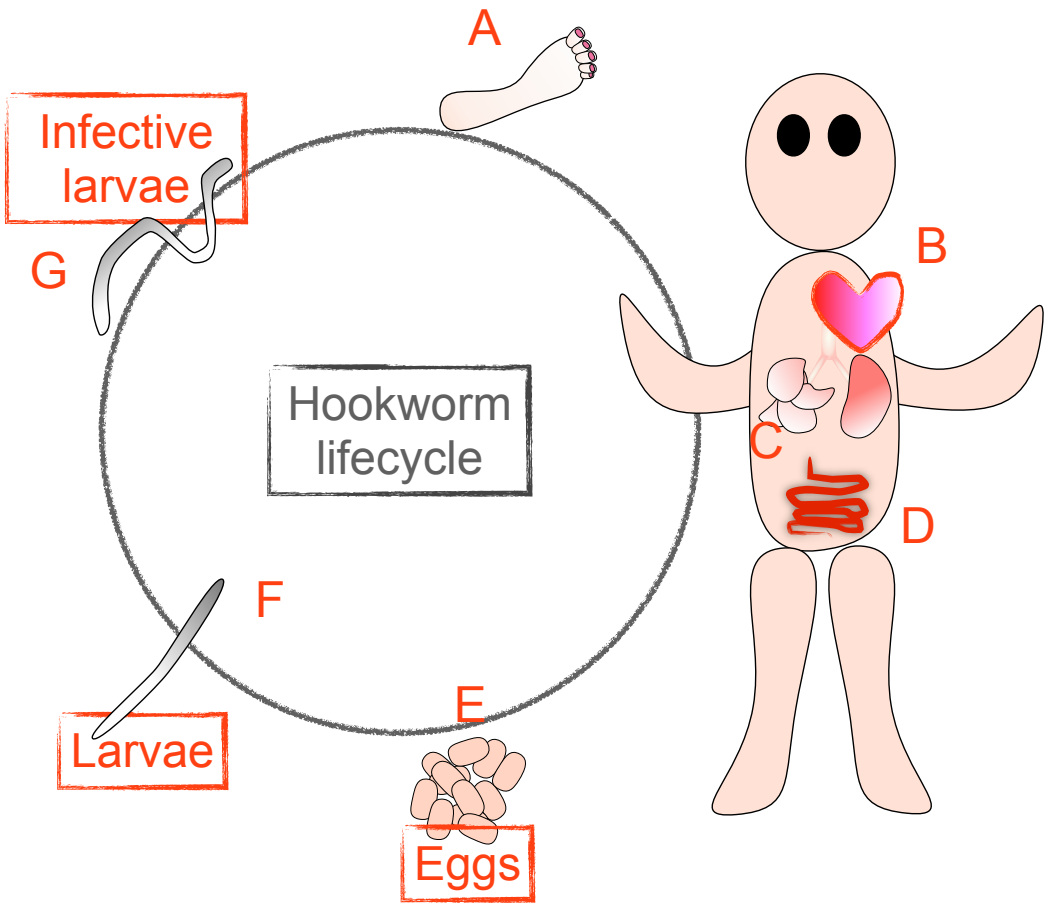

Fig 4.1 The hookworm lifecycle.

A. Infective hookworm larvae penetrate the skin and migrate via the blood system to the heart (B) and hence to the lungs (C). Larvae mature into adult worms in the small intestine where they mate and commence egg production (D). Eggs are passed into the environment in the faeces where they hatch within 1-2 days (E & F). Following a further two moults the larvae become 3rd stage infective larvae capable of infecting the mammalian host (G).

These bacteria, although trapped in the mucous layer also thrive there. Being comprised mainly of the mucin Muc2, the oligosaccharides from this mucin provide microbial attachment opportunities and a suitable energy source (Martens, Roth, Heuser, & Gordon, 2009). Thus the outermost mucus layer helps maintain the host microbiota. Below this loosely attached layer of mucus lies a thinner but adherent layer of mucus. This is devoid of microbes and provides a protective barrier over the cells of the epithelium (Johansson et al., 2008). Forming another protective layer immediately over the epithelial cells lies a sheet of glycocalyx, composed primarily of the membrane bound Muc3 mucin (Frey et al., 1996), (Artis, 2008). Throughout the adherent layer of mucous, antimicrobial products secreted by Paneth and goblet cells and secretory IgA also can be found. These add to a multi-layered defence system set up and maintained by the intestinal epithelial cells (Fig 4.2).

Goblet cells are largely responsible for the secretion of mucins found in the mucous layers covering the epithelium, and are also responsible for the secretion of products such as TFF3 (intestinal trefoil factor 3) which aids wound healing and increases mucous viscosity (Taupin & Podolsky, 2003) and RELMβ, suggested to act as an immune effector molecule by binding to nematode structures that detect the chemokine microenvironment (Artis et al., 2004). Interestingly it has also been shown that RELMβ has a more potent effect on luminal residing parasites, such as *H.polygyrus* and *N.brasiliensis,* by hampering the ability of the parasite to feed and as a result reducing ATP levels (Herbert et al., 2009).

It is well documented that goblet cell hyperplasia accompanies acute gut helminth infections, (Marillier et al., 2008), (Peterson & Artis, 2014) and with this an increase in mucus production ensues. The Th2 environment, which can occur during intestinal helminth infections, has been shown to be a possible cause for an increase in goblet cell numbers; with adoptive transfer experiments showing stem cells, located at the base of intestinal crypts, being differentiated into goblet cells (Ishikawa, Wakelin, & Mahida, 1997).

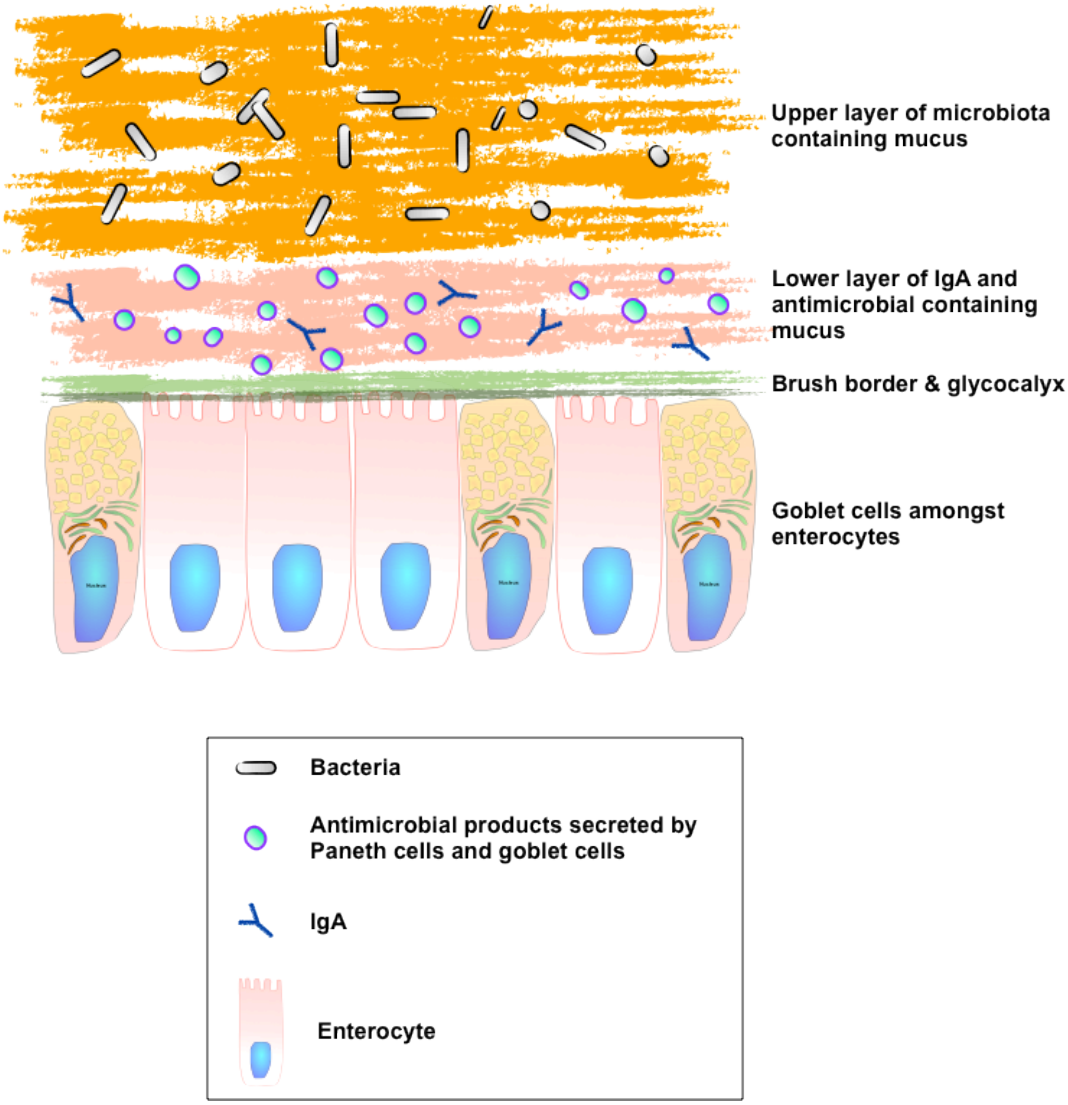

Fig 4.2 The intestinal epithelial layers.

In addition to secretion of mucous, RELMβ and TFF3 it has also been suggested that goblet cells may be responsible for a degree of antigen presentation to intestinal dendritic cells (McDole et al., 2012). All the while it must be remembered that the function and activity of the goblet cell is highly dependent upon its location and the infection/ immune status of the host.

The intestinal environment is further defined by the activity of Paneth cells. Located at the base of the crypts of Lieberkühn, these cells contain secretory granules, which can be stained with haemotoxylin and eosin (see Fig 4.18), are filled with antimicrobial peptides and proteins (Ayabe et al., 2000), (Bevins & Salzman, 2011). Unlike all other cells in the crypt, which migrate from the bottom of the crypt towards the intestinal lumen, the Paneth cells migrate towards the base of the crypt where they reside for up to 30 days.

The content of these secretory granules lends an insight into their role within the intestine. Lysozyme (Nevalainen & Haapanen, 1993), crytpidins (α-defensins present in the crypt) (Bergenfeldt et al., 1996) and phospholipase A2 (Bergenfeldt et al., 1996) have all been identified as Paneth cell granule components with antimicrobial properties, and these can be released when certain conditions are detected. With Paneth cell numbers varying along the length on the intestine, large numbers of Paneth cells are present in the small intestine accompanied by a relatively few microbes. Compare this with the established microbiota present in the large intestine where Paneth cells are absent. Release of Paneth cell contents is under the control of various mechanisms e.g. secretion of granules can occur in the presence of bacterial products such as lipopolysaccharide (LPS) (Ayabe et al., 2000) or when gastrointestinal hormones such as cholecystokinin are detected (Senegas-Balas, Balas, Pradayrol, Laval, & Ribet, 1979).

Alongside the antimicrobial properties exhibited by contents of the Paneth cell they are also responsible for maintaining an environment conducive to the proliferation, differentiation and migration of the population stem cells present in the crypts (Sato et al., 2011), (Barker et al., 2007), (Morrison & Spradling, 2008). These stem cells

replenish a population of enterocytes, goblet cells and other intestinal epithelial cells, which is lost on a daily basis. Control of stem cell differentiation is mediated by the Wnt pathway (Gregorieff & Clevers, 2005), (Reya & Clevers, 2005), (Pinto, Gregorieff, Begthel, & Clevers, 2003) namely the renewal of Paneth, goblet and enteroendocrine cells (Gregorieff & Clevers, 2005).

Thus, the goblet cell and Paneth cell together regulate not only the innate immune environment in the gut by influencing the mucosa and microbiota, but also regeneration of the very cells required that facilitate this. Given the position of these cells, it is hypothesized that they become bathed in products secreted by the parasite, therefore representing one of the main points of contact where parasite and host come into contact with each other. In this chapter, interactions between the parasite, excretory secretory products from that parasite and the cells of the intestine are examined, using a combination of immunohistological techniques for light, fluorescent and confocal microscopy.

Results

Section 1: Probing the adult surface of *H.polygyrus*.

4.3 Monoclonal antibody binds to carbohydrates on the surface of the parasite.

The cuticle of *H.polygyrus* is not alone with regards to the abundance of surface carbohydrates, which have been described amongst others for *Teladorsagia circumcincta* (Hillrichs et al., 2012), *C.elegans* (Page & Johnstone, 2007), *Trichinella* (Denkers, Wassom, Krco, & Hayes, 1990), (Bolas-Fernandez & Corral Bezara, 2006), and *Nippostrongylus brasiliensis* (Harcus et al., 2009). In the case of *T.circumcincta* and *Haemonchus contortus* the display of carbohydrates on the surface of the parasite is actually being exploited in order to distinguish between the two when examining egg, third stage larvae and adult worms in the field (Hillrichs et al., 2012).

Here mAb 13.1, which recognizes O-linked glycans on the surface of the parasite (Hewitson et al., 2011a), was used to stain the surface of whole adult *H.polygyrus* parasites. Staining was carried out in round-bottomed 96 well plates where parasites were incubated for 1 hour with Ab diluted 1:100 in PBS. Parasites were washed prior to the addition of an anti-mouse TRITC secondary antibody (Sigma). Samples were mounted in Vectashield anti-fade mountant before analysis by fluorescence microscopy.

The surface of the adult cuticle clearly shows annuli (E) and furrows (F) similar to those described for *C.elegans* (Page & Johnstone, 2007) where the annuli are coated by a glycoprotein layer. These form ridges (C & H), which run down the length of the parasite and stop just before the end as shown in panel D.

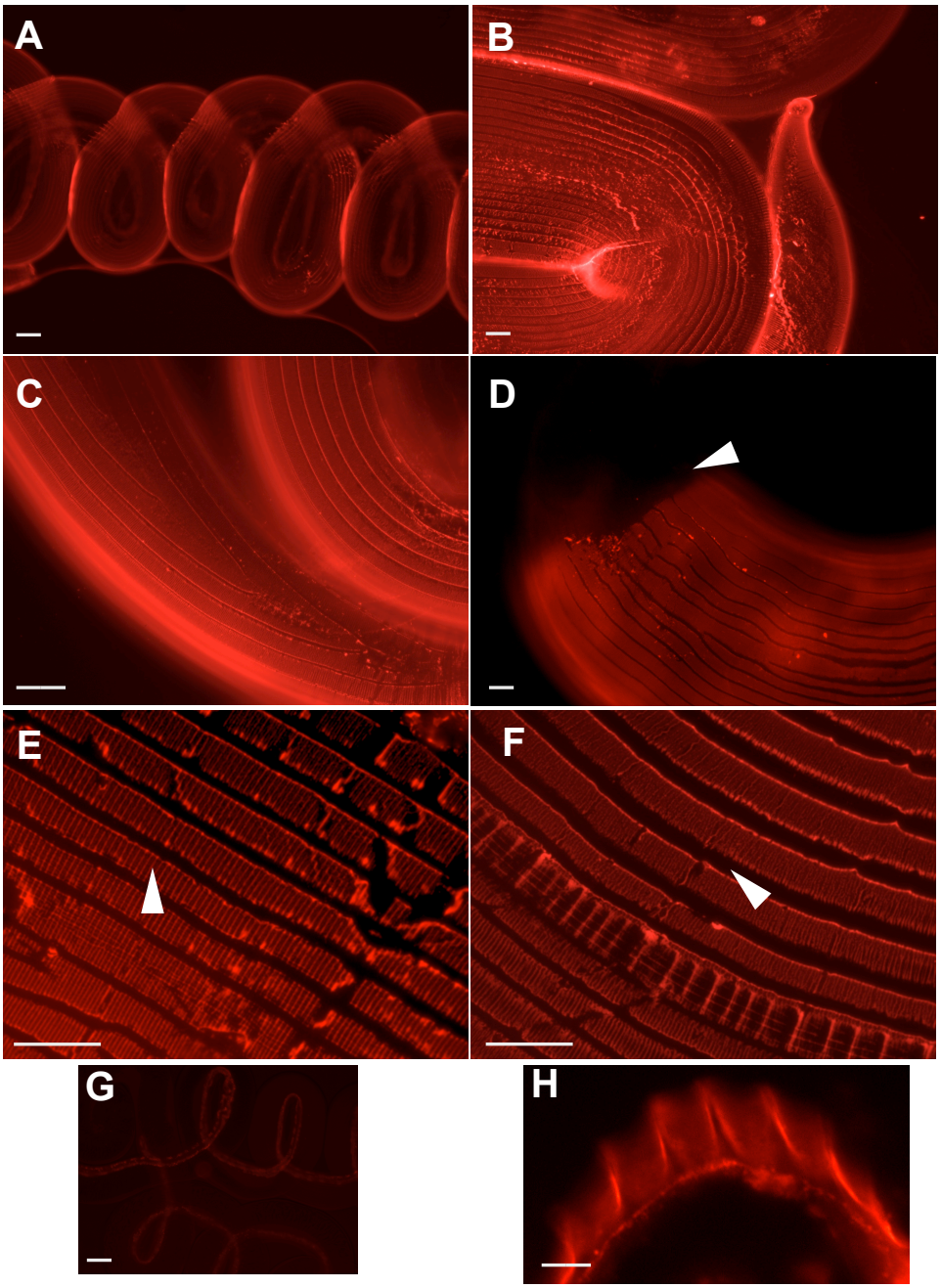

Fig 4.3 Monoclonal antibody binds to carbohydrates on the surface of the parasite.
Live adult *H.polygyrus* worms were collected from culture and were placed into wells of a 96-well plate in 200µl PBS. Parasites were washed twice in PBS by carefully removing most of the PBS from the well and replacing it with fresh buffer (parasites were clearly visible at the bottom of the well). Parasites were then incubated with αVAL-CHO mAB 131, diluted 1:100 in PBS for 1 hour on ice. Parasites were then washed twice with PBS before the addition of an α-mouse TRITC conjugate (Sigma T2402) diluted 1:100 in PBS for 1 hour. Prior to mounting in Vectashield parasites were washed three times in PBS. Scale bar = 100µm.

4.4 Polyclonal α-HES and α- Glycan A antibodies recognise the surface and some internal structures of the parasite.

The surface of the parasite, known as the cuticle, is the first point of contact for parasite and host interactions, allowing the parasite to move throughout its environment whilst simultaneously protecting it. Composed mainly of collagens it also contains cuticulins, glycoproteins and lipids (Page & Johnstone, 2007), (Blaxter, Page, Rudin, & Maizels, 1992). A set of moults throughout the parasitic lifecycle, which result in the loss of one cuticle and replacement with another, allows the parasite to shed surface bound antibodies collected along the way thus aiding its attempts to hide from immune attack (Blaxter et al., 1992).

To help visualize the parasite surface coat, adult *H.polygyrus* parasites were first immunostained with a polyclonal antibody raised against the excretory secretory products (HES). Parasites were removed from culture flasks and were placed into wells on a 96-well, round bottomed tissue culture plate for staining. The parasites were washed twice in PBS before adding a diluted rat α-HES antibody and incubating on ice for an hour. In between primary and secondary antibodies parasites were carefully washed with PBS. α-rat TRITC (Sigma) conjugate was diluted 1:100 in PBS and added to parasites for 1 hour. Parasites were then mounted using an anti-fade mountant (Vectashield) and sealed onto polysine slides for analysis by fluorescent microscopy. Where sections of adult worms were stained the parasites were first mounted in Cryo-m-bed (Bright Instruments) and frozen on dry ice. 5μm sections were cut onto polysine slides using a Leica cryostat and were allowed to dry for 1 hour before fixing in 100% acetone. Primary antibodies were diluted in PBS/1% FCS and were incubated on sections or on whole parasites for one two hours respectively.

The surface coat of the parasite bound the anti-HES Ab both in whole female and male adult worms (Fig.4.4 A & B) and fixed frozen sections (Fig.4.4 C & D). The antibody also bound to structures within the parasite's body cavity as well as a layer of collagens and muscle under the outer cuticle as shown in Fig 4.4 C.

A striking observation occurred with a monoclonal antibody termed α-Glycan A (Fig 4.4 D). This monoclonal recognises HpVAL-1, 2 & 5 and binds to these proteins by means of O-linked glycan side chains (Hewitson et al., 2011a). Here it bound the cuticle of adult parasites potentially binding carbohydrates present on the parasite surface, and, depending on where the parasite had been sectioned, also bound to some internal structures presumably via a similar carbohydrate moiety.

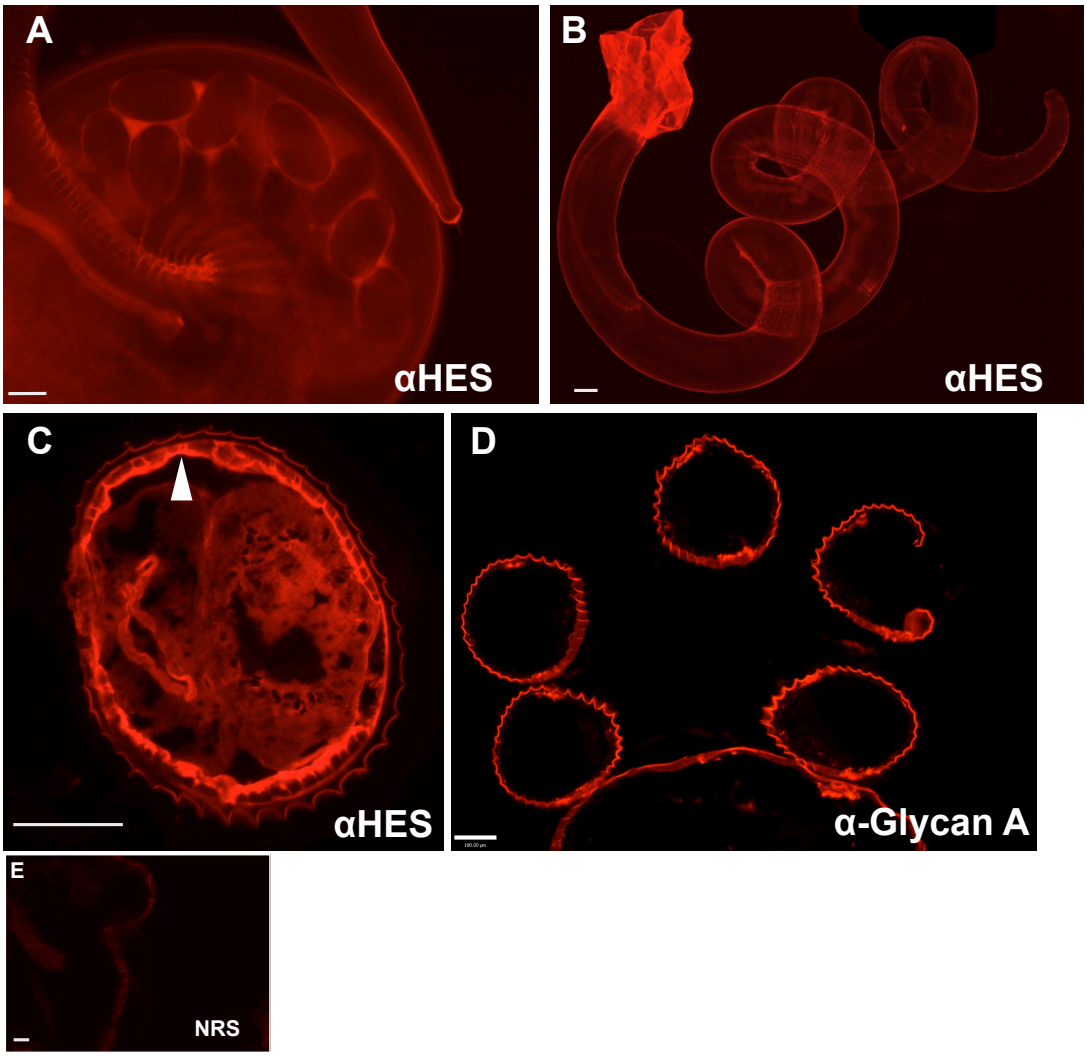

Fig 4.4 Polyclonal α-HES and α- Glycan A antibodies recognise the surface and some internal structures of the parasite.

A, B & E. Live adult female (A & E) and male (B) *H.polygyrus* worms were collected from culture and were placed into wells of a 96-well plate in 200µl PBS. Parasites were washed twice in PBS by carefully removing most of the PBS from the well and replacing it with fresh buffer (parasites were clearly visible at the bottom of the well). Parasites were then incubated with an α-HES antibody or normal rat serum diluted 1:100 in PBS for 1 hour on ice. Parasites were then washed twice with PBS before the addition of an α-rat TRITC conjugate (Sigma T4280) diluted 1:100 in PBS for 1 hour. Prior to mounting in Vectashield parasites were washed three times in PBS.

C & D. 5µm sections were cut onto Polysine^{TM} slides (VWR) using a Leica cryostat from samples of adult male or female *H.polygyrus* frozen in Cryo-m-Bed (Bright Instruments). These were allowed to dry for 1 hour before fixing in 100% acetone for 10 minutes. Sections were then washed in PBS for 10 minutes before incubation with primary antibodies (α- Glycan A mAb 13.1).

Fig 4.4 Polyclonal α-HES and α- Glycan A antibodies recognise the surface and some internal structures of the parasite (cont'd).

mAb was diluted to 50µg/ml in PBS/1% FCS and was incubated on sections for 2 hours at room temperature. Samples were washed in PBS before being incubated with secondary antibodies diluted 1:100 (α-mouse TRITC, Sigma T2402) for 1 hour. After incubation with a secondary antibody slides were washed in PBS for 1 hour (several changes of buffer) and were then mounted using Vectashield , an anti-fade mountant (Vector Labs). Staining was visualised using an Olympus fluorescent microscope and Openlab (Perkin Elmer) software.
Arrow in panel C showing binding of α-Glycan A mAb 13.1 to sub cuticular muscle layer.
Panel D shows a frozen section which has cut through the rings of a single parasite. Binding of α-Glycan A mAb 13.1 to the glycan rich cuticle can be seen.

Scale bar = 100µm.

4.5 Characterisation of antibody binding reveals that monoclonal and polyclonal antibodies, which recognise HpVAL-1 & -4, bind to different structures of the parasite.

As previously mentioned the cuticle of a parasite would be the first point of contact for the immune system of the host. Generation of antibodies against molecules on the cuticle of the parasite is important when determining the longevity of infection (McCoy et al., 2008), (Denkers et al., 1990), (Hewitson et al., 2011a), (Bowles, Brandon, & Meeusen, 1995). In order to examine more closely the antigenic targets produced by *H.polygyrus* a panel of monoclonal antibodies was generated using spleen and draining lymph node cells from a Day-28 infected mouse (Hewitson et al., 2011a). Two of these antibodies (Table 4.1), along-side polyclonal antibodies raised against recombinant HpVAL-1 and HpVAL-4 (Yvonne Harcus), were then used to stain whole adult parasites and frozen sections of adult *H.polygyrus* tissue.

Table 4.1

Ag specificity	Clone name	Spleen or LN	Isotype
Glycan A (HpVAL-1, 2 &5) and recombinant HpVAL-1. Recombinant proteins for HpVALs 2 and 5 have not been made.	13.1	Spleen	IgM
αHpVAL-1 (and recombinant HpVAL-1)	4-M15	MLN	IgG1
αHpVAL-4 (and recombinant HpVAL-4)	2-11	Spleen	IgG1

Adult male and female *H.polygyrus* were separated from culture flasks and were frozen on dry ice in Cryo-m-Bed for sectioning and staining as described previously. Sections of adult, male *H.polygyrus* were prepared as described previously (Fig 4.2) and were stained using mAb 4-M15 and mAb 2-11 (HpVAL-1 & 4 respectively), both diluted to 50µg/ml in PBS/1% FCS. Polyclonal antibodies were diluted 1:100. Staining was carried out as for previous sections (Fig 4.2) and was visualized using an Olympus fluorescent microscope.

Both monoclonal and polyclonal antibodies, which recognize HpVAL-1, bind to the surface of the parasite on whole or sectioned samples, with α-HpVAL-1 monoclonal binding to 4 structures within the body wall (yellow triangles in Panel C). These may be secretory tissues or neuronal fibers running along the length of the parasite. Interestingly neither the monoclonal or polyclonal antibodies, which recognize HpVAL-4, bind to the parasite surface (Fig 4.4 D-F).

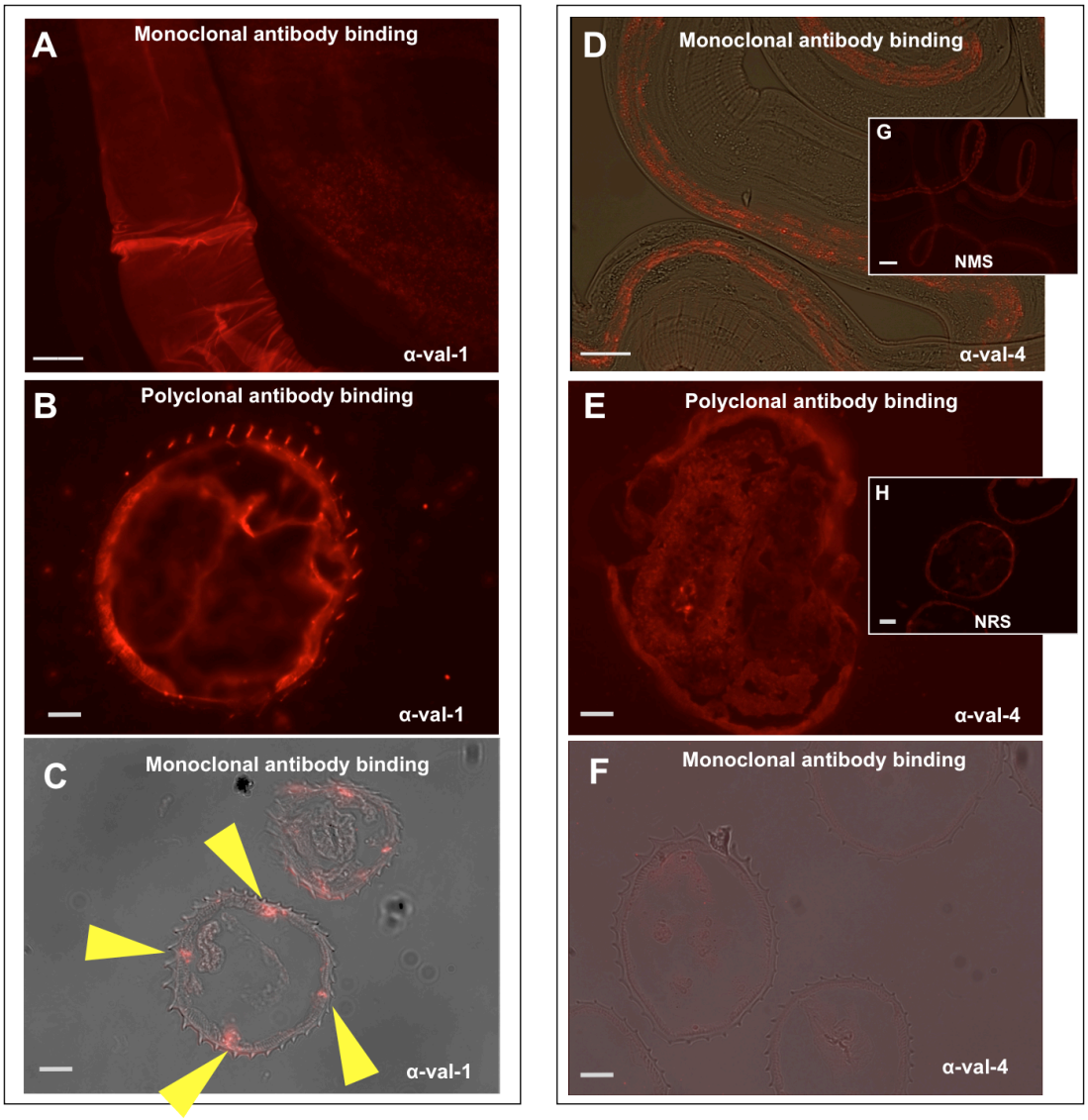

Fig 4.5 Characterisation of antibody binding reveals that monoclonal and polyclonal antibodies, which recognise HpVAL-1 & -4, bind to different structures of the parasite.

Whole parasite staining (**A**&**D**) was performed as previously described (Fig 4.3).
5µm sections (**B,C,E**&**F**) were cut and stained as previously described (Fig 4.4).

A α-HpVAL-1 (4-M15), monoclonal, 50µg/ml.
B α-HpVAL-1, polyclonal, 1:100
C α-HpVAL-1 (4-M15), monoclonal, 50µg/ml. (Bright-field overlay)

Scale bar = 100µm.

D α-HpVAL-4 (2-11), monoclonal, 50µg/ml. (Bright-field overlay)
E α-HpVAL-4, polyclonal, 1:100
F α-HpVAL-4 (2-11), monoclonal, 50µg/ml. (Bright-field overlay)

G&**H** NMS & NRS controls

4.6 Biotinylated lectins do not bind cuticle carbohydrates.

Panels of labeled lectins have been used previously to identify sugars present on the surface of nematodes (Spiegel & Robertson, 1988). Here a panel of biotinylated lectins (Vector BK-1000) was also used to identify the carbohydrates present on the cuticle (Table 4.2).

Table 4.2

Lectin	Abbreviation	Primary sugar specificity
Concanavalin A	Con A	Mannose
Dolichos biflorus agglutinin	DBA	N-acetylgalactosamine
Peanut agglutinin	PNA	Galactose
Ricinus communis agglutinin 1	RCA 1	Galactose, N-acetylgalactosamine
Soybean agglutinin	SBA	N-acetylgalactosamine
Ulex Europaeus agglutinin 1	UEA 1	Fucose
Wheat germ agglutinin	WGA	N-acetylglucosamine

Lectins were reconstituted according to the manufacturer's instructions. All lectins were used at a concentration of 5µg/ml and were incubated on whole, adult *H.polygyrus* parasites for 1.5 hours. Extravidin TRITC was diluted 1:200 and incubated on washed parasites for one hour prior to washing and mounting parasites as described previously (Fig 4.2).

The lectin panel chosen covers a range of sugar binding activities, however none of the lectins tested bound to the surface cuticle of the parasite. ConA, PNA and SBA all bound to spicules in the body cavity of the parasite indicating the presence of manose, galactose and N-acetylglucosamine.
Panel D shows an adult male *H.polygyrus* parasite stained with a α-HES polyclonal antibody. The arrow marks the location of the male spicules, which are found in close proximity to the bursa and assist with copulation (Massoni, Durette-Desset, Quere, & Audebert, 2012).

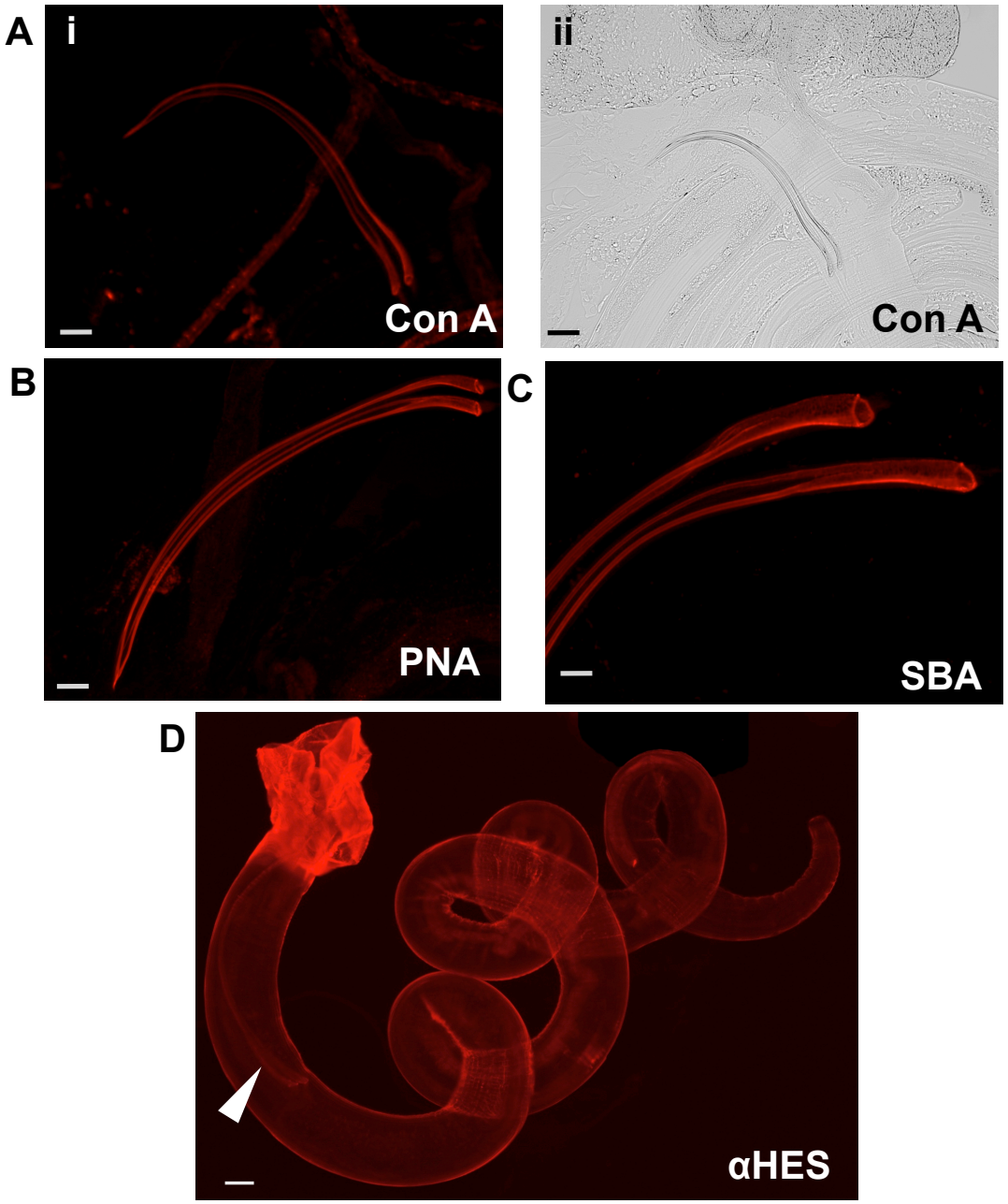

Fig 4.6 Biotinylated lectins do not bind cuticle carbohydrates.

Staining of live adult *H.polygyrus* worms was performd as described previously (Fig 4.3).

Parasites were incubated with biotinylated lectins diluted to 5µg/ml for 1.5 hours. Parasites were then washed twice with PBS before the addition of an α-mouse TRITC conjugate (Sigma T2402) diluted 1:200 in PBS for 1 hour. Prior to mounting in Vectashield parasites were washed three times in PBS.

Scale bar = 100µm.

Panel A i: Concanavalin A
Panel A ii: Concanavalin A (bright-field)
Panel B: Peanut agglutinin
Panel C: Soybean agglutinin
Panel D: Adult male *H.polygyrus* stained with α-HES polyclonal. Arrow shows location of the spicules.

4.7 - 4.10 Are VAL proteins associated with the cuticle and can they be recovered by chemical or detergent treatment?

Information on the composition of the cuticle can provide clues to possible antigenic targets presented by the parasite. Collecting information on the cuticle can be achieved in a variety of ways such as visualization by electron microscopy or analysing the surface with lectin probes (Blaxter et al., 1992). Surface staining on whole parasite cuticles as shown earlier (Fig 4.6), immunostaining sections of fixed parasites (Fig 4.5) or by removal of the labeled parasite cuticle and subsequent molecular analysis (Hewitson et al., 2011b), (Page, Rudin, Fluri, Blaxter, & Maizels, 1992), (Page et al., 1992). Removal of the cuticle or of surface molecules can be achieved in a variety of ways; encouragement of the parasite to exsheath naturally using dilute bleach (Chpt 1) or CO_2 (Boisvenue, Stiff, Tonkinson, & Cox, 1991), detergent removal of the cuticle (Cui et al., 2013a) or a more unusual method of analyzing molecules associated with the cuticle is described by Wharton et al, where as nematodes had become desiccated on glass cover slips, parts of the cuticle had adhered and left what was termed a "cuticle print". This was then stained and visualized by epifluorescence or confocal microscopy (Wharton, Petrone, Duncan, & McQuillan, 2008).

To examine further the cuticle of *H.polygyrus,* parasites were put through a series of washes moving from ethanol to Tween-20. Cetyltrimethylammonium cationic detergent (CTAB) was also used with no pre-incubations in any other detergents. Live adult worms were incubated in ethanol dilutions ranging from 0.1% to 10%. Parasites were then stained or removed and incubated further in diluted Tween-20. To visualise the parasite coat an anti-Glycan A monoclonal antibody (13.1) or anti-HES polyclonal Ab was used. Anti-rat and anti-mouse TRITC secondary antibodies were used to detect primary antibody binding. Stained worms were visualized using an Olympus fluorescent microscope.

Treatment of parasites with 0.1% ethanol (Fig 4.7i) and 1% (Fig 4.7ii) removed some but not all of the surface carbohydrate. 10% ethanol (Fig 4.7iii) removed most of the

carbohydrate on the annuli surface but however the longitudinal ridges present on the surface of the parasite remained unaffected (Fig 4.7 ii & iii). Subsequent incubation in 0.1% and 1% Tween-20 (Fig 4.8i & ii) had little effect on the remaining carbohydrates present however when parasites were incubated in 10% Tween-20 little on no carbohydrate remained demonstrated by staining with αCHO-13.1 and α-HES Ab (Fig 4.8iii).

The removal of cuticle associated carbohydrates was incomplete after an overnight incubation in 0.25% CTAB as can be seen in Fig 4.9ii. Some areas of the parasite displayed no α-carbohydrate staining at all (Fig 4.9i) whereas other regions appeared unaffected. This may have been resolved with an increase in CTAB concentration or a longer incubation period.

H.polygyrus eggs can be visualised within the female parasite (Fig 4.10A), however it is not possible to determine if treatment with detergent Tween-20 has any effect on eggs whilst still inside the parasite. Fig 4.10B shows *H.polygyrus* eggs that had been collected from culture and treated with CTAB. These treatments had little or no effect on the surface of parasite eggs, with only treatment in CTAB having any noticeable effect on the binding ability of the α-HES Ab.

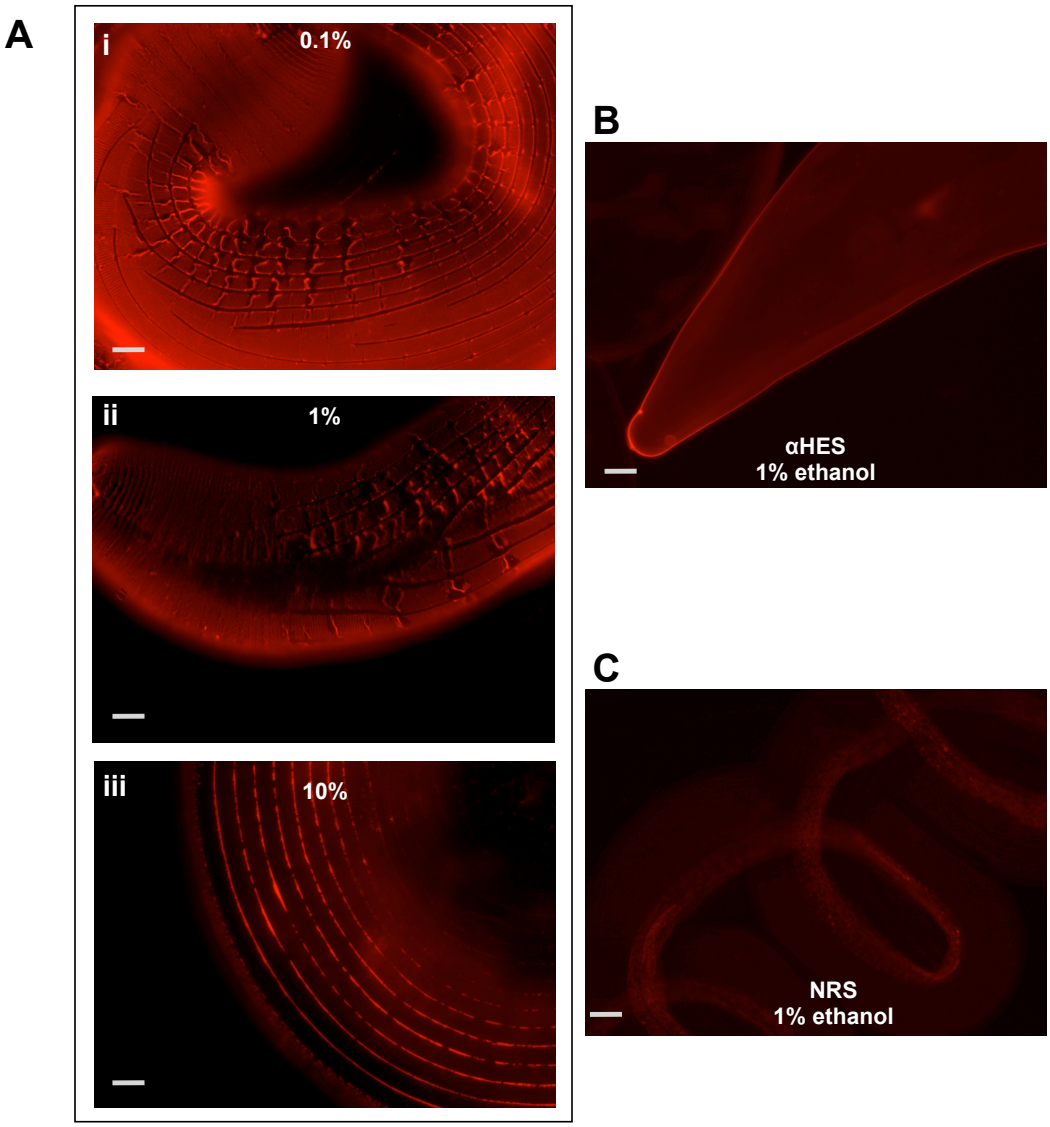

Fig 4.7 Sequential treatments to remove parasite cuticle components: Ethanol.

Live adult *H.polygyrus* worms were collected from culture,washed once in PBS before incubating in ethanol, 0.1% (i), 1.0 % (ii) or 10% (iii) for 15 minutes on ice. Some parasites were removed at this stage for staining whilst the remaining parasites were given a further incubation in Tween20 (1.0 %, Fig 4.7 (i)& (iii) or 10% Fig 4.7(ii)). Parasites were stained with an αHES polyclonal antibody (1:100) or 13.1 monoclonal antibody (1:20) for 2 hours followed by an α-rat TRITC conjugate (Sigma T4280) diluted 1:200 or α-mouse TRITC conjugate (Sigma T2402) diluted 1:200 in PBS in PBS for 1 hour. Prior to mounting in Vectashield parasites were washed three times in PBS.
A. Parasites stained with α-Glycan A 13.1 monoclonal antibody.
B. Parasites stained with α-HES polyclonal antibody.
C. Parasites stained with normal rat serum.
Scale bar = 100μm.

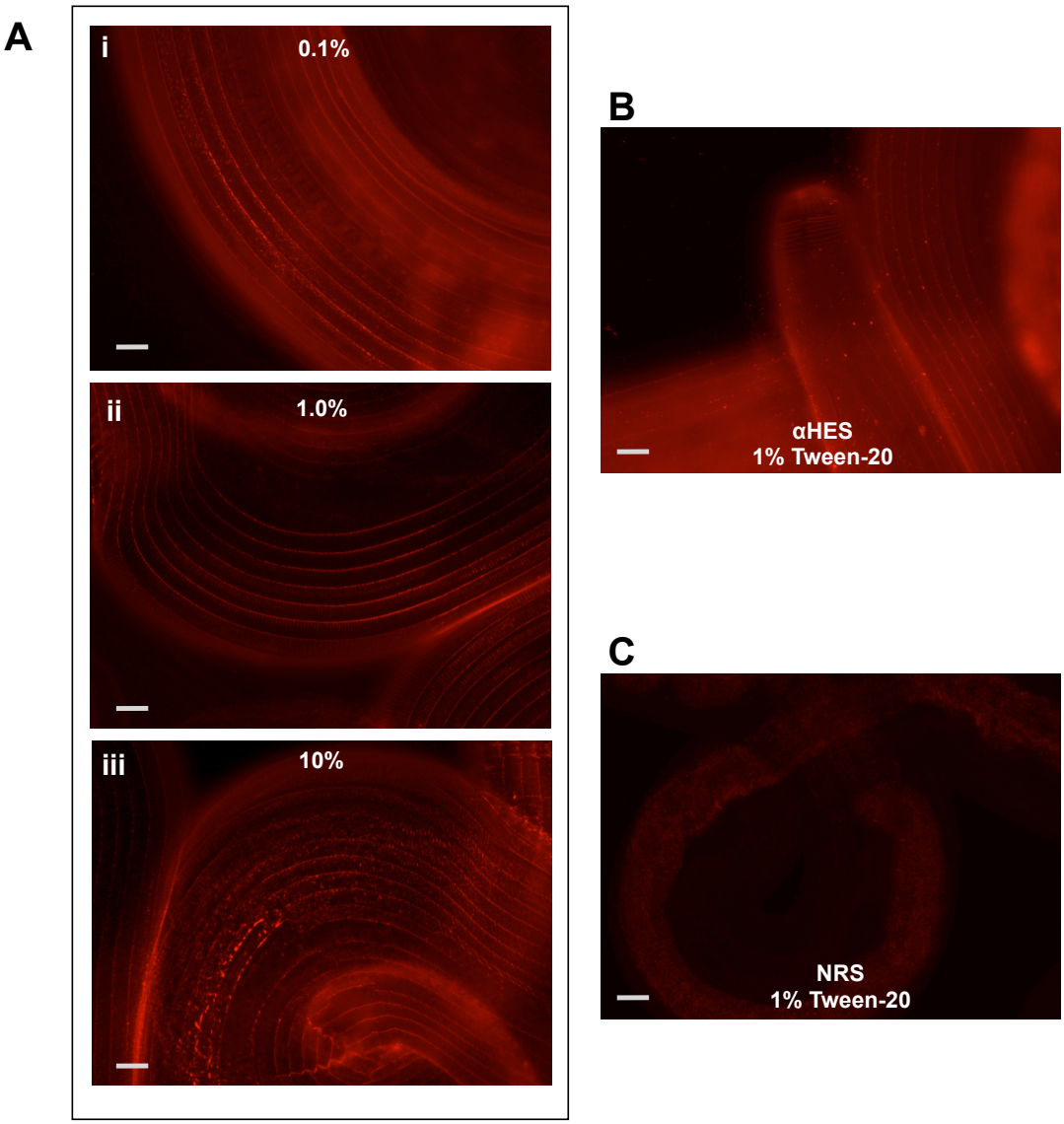

Fig 4.8 Sequential treatments to remove parasite cuticle components: Tween-20

Live adult *H.polygyrus* worms which had been incubated in various dilutions of ethanol were then further incubated in Tween20 (1.0 %, Fig 4.7 (i)& (iii) or 10% Fig 4.7(ii)). Parasites were stained with an αHES polyclonal antibody (1:100) or 13.1 monoclonal antibody (1:20) for 2 hours followed by an α-rat TRITC conjugate (Sigma T4280) diluted 1:200 or α-mouse TRITC conjugate (Sigma T2402) diluted 1:200 in PBS in PBS for 1 hour. Prior to mounting in Vectashield parasites were washed three times in PBS.

A. Parasites stained with α-Glycan A 13.1 monoclonal antibody.
B. Parasites stained with α-HES polyclonal antibody.
C. Parasites stained with normal rat serum.
Scale bar = 100μm.

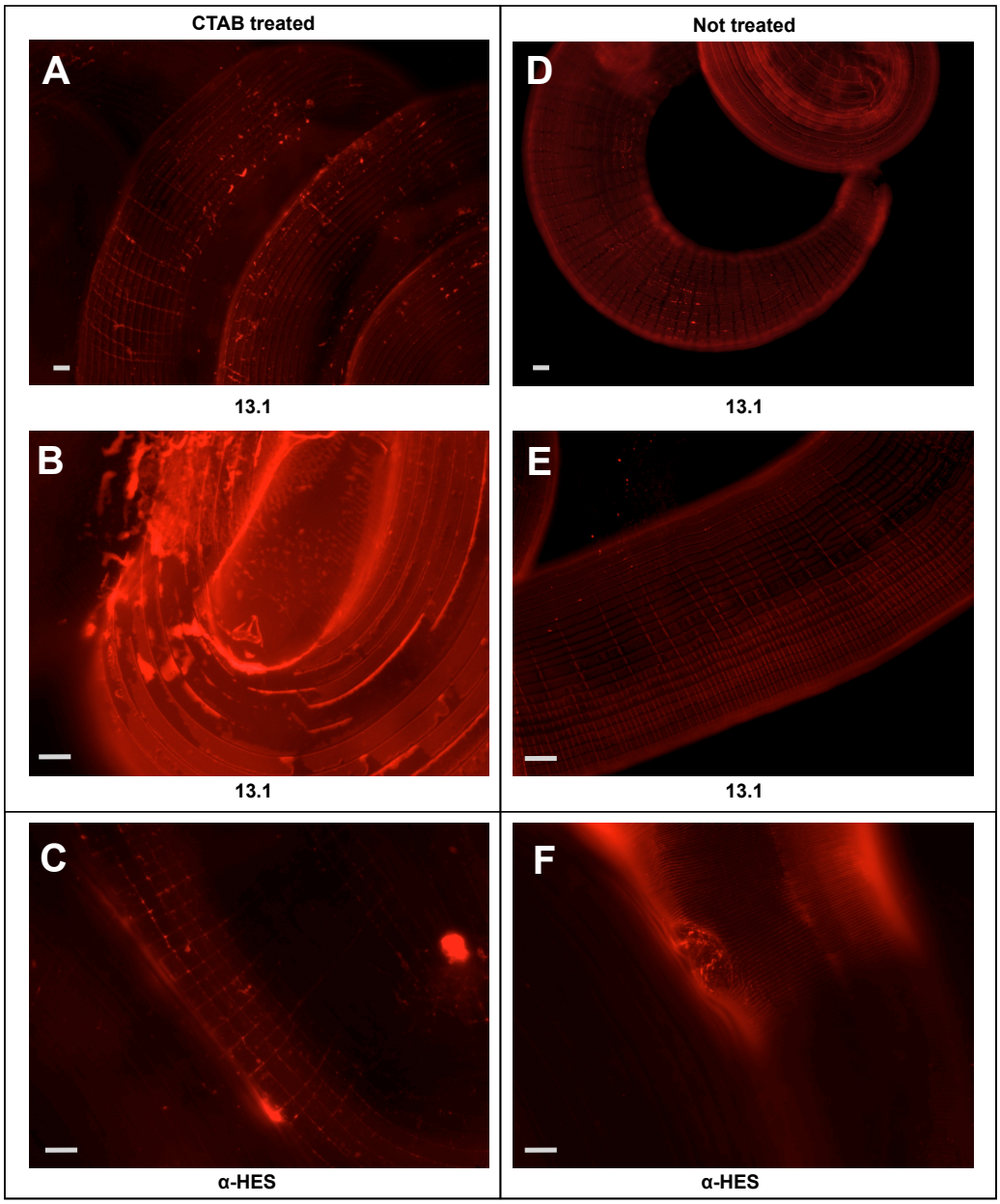

Fig 4.9 Sequential treatments to remove parasite cuticle components: Cetyltrimethylammonium cationic detergent (CTAB)

Adult *H.polygyrus* parasites were cultured overnight at 37°C in *H.polygyrus* culture media containing 0.25% CTAB. Parasites were then incubated with α-Glycan-A mAB 13.1, diluted 1:20 in PBS for 1 hour on ice or α-HES polyclonal Ab, diluted 1:100. Parasites were subsequently washed twice with PBS before the addition of an α-mouse or α-rat TRITC conjugate diluted 1:100 in PBS for 1 hour. Prior to mounting in Vectashield parasites were washed three times in PBS.

A,B &C Parasites treated with CTAB:
A & **B** stained with α-Glycan A mAB 13.1 (X20 & X40 obj).
C stained with α-HES polyclonal Ab.

D,E & F Untreated parasites:
D & **E** stained with α-Glycan A mAB13.1 (X20 & X40 obj).
F stained with α-HES polyclonal Ab.

Scale bar = 100μm.

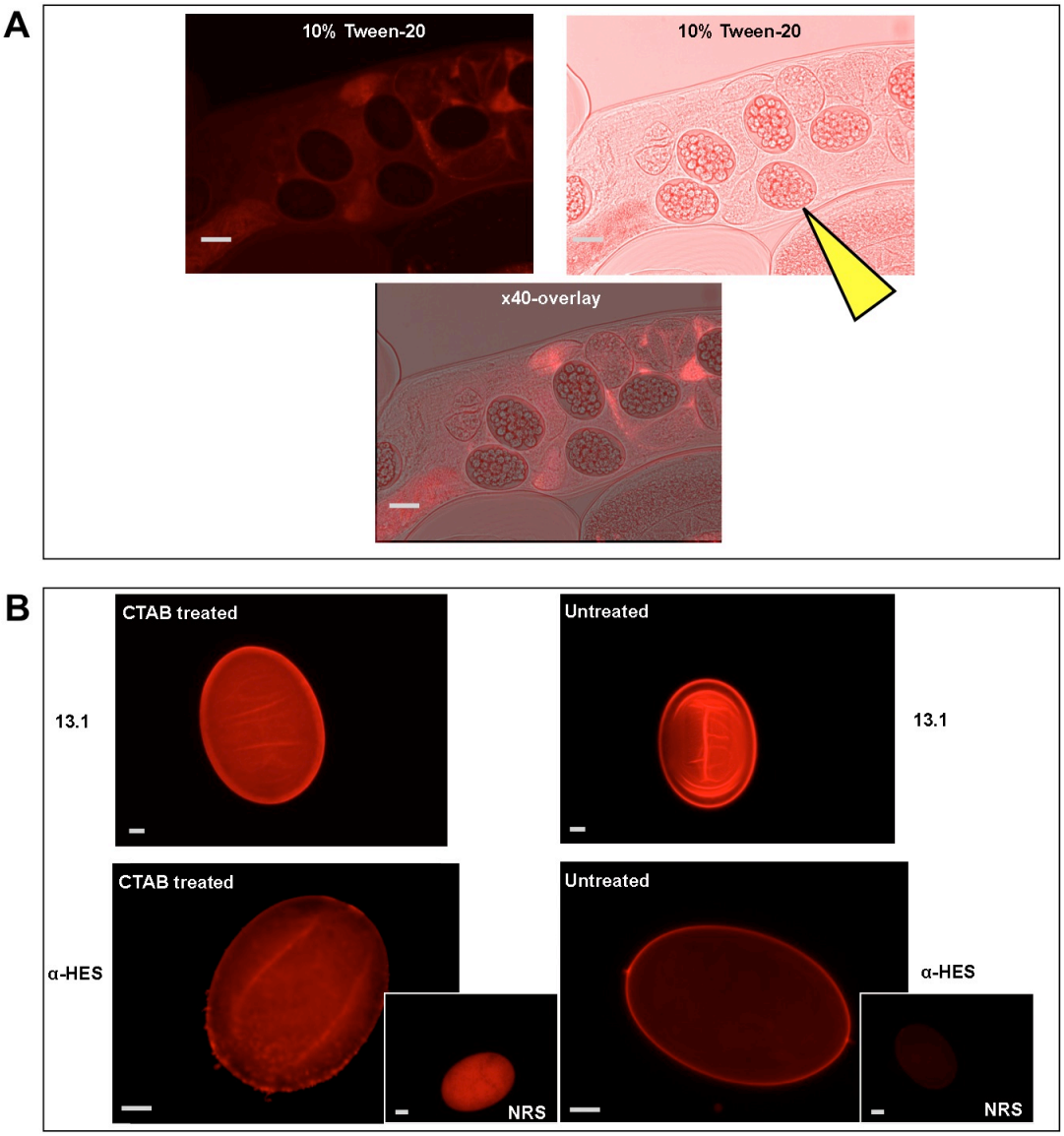

Fig 4.10 Tween & CTAB treatment of eggs

Eggs (and adult parasites) were were cultured overnight at 37°C in *H.polygyrus* culture media containing 0.25% CTAB. Adult parasites were incubated in an αHES polyclonal antibody 1:100 (A) and eggs were incubated with α-Glycan A mAB 13.1, diluted 1:20 (B) both in PBS for 1 hour. Parasites were then washed twice with PBS before the addition of an α-mouse or α-rat TRITC conjugate diluted 1:100 in PBS for 1 hour. Prior to mounting in Vectashield parasites were washed three times in PBS.

A. Whole adult female parasites containing eggs (yellow arrow): Treatment with Tween-20.
B. Treatment with CTAB.
Scale bar = 100μm.

4.11 Acetone precipitated parasite cuticle reveals a 62kDa protein which is recognised by α-HES and α-Glycan A antibodies.

The stripped cuticle contents were examined by western blot in order to see if VAL proteins could be identified. Proteins in the media from both ethanol and CTAB strips were precipitated using acetone and were separated on an SDS-PAGE gel for analysis by western blot. Using a monoclonal antibody that recognizes Glycan A, which is associated with HpVAL-1, the separated proteins were probed and visualized using chemiluminescent substrate.

Anti-HES polyclonal sera bound to bands at 62 kDa present in the acetone precipitated CTAB sample (Fig 4.11A). Following ethanol stripping, no proteins were detected using the anti-carbohydrate antibody (13.1), which recognizes carbohydrates present on, amongst others, HpVAL-1. After CTAB treatment however, 3 main bands were detected using anti-Glycan A (Fig 4.11B). This profile was very similar to that seen after surface radiolabelling labeling of *H.polygyrus* (Hewitson et al., 2011a) (Fig 4.11C) with subsequent nOG removal of labeled proteins, which showed binding to a band at approximately 62kDa.

Further characterization of proteins removed by treatment with CTAB needs to be undertaken. Anti-HpVAL monoclonal antibodies could be used to probe western blots or separated proteins could be identified by mass-spectrometry analysis. Isolated proteins may indeed prove to have protective qualities against future infections as was noted for a set of proteins isolated from the surface of *Trichinella spiralis*. These CTAB isolated proteins provided protection against a challenge infection. The CTAB treatment had no adverse effect on parasites, which were able to go on and mount successful infections (Grencis, Crawford, Pritchard, Behnke, & Wakelin, 1986). As *H.polygyrus* undergoes a number of moults, comparisons of proteins from each cuticle stage could also be achieved and may give information regarding immune evasion strategies throughout the life-cycle.

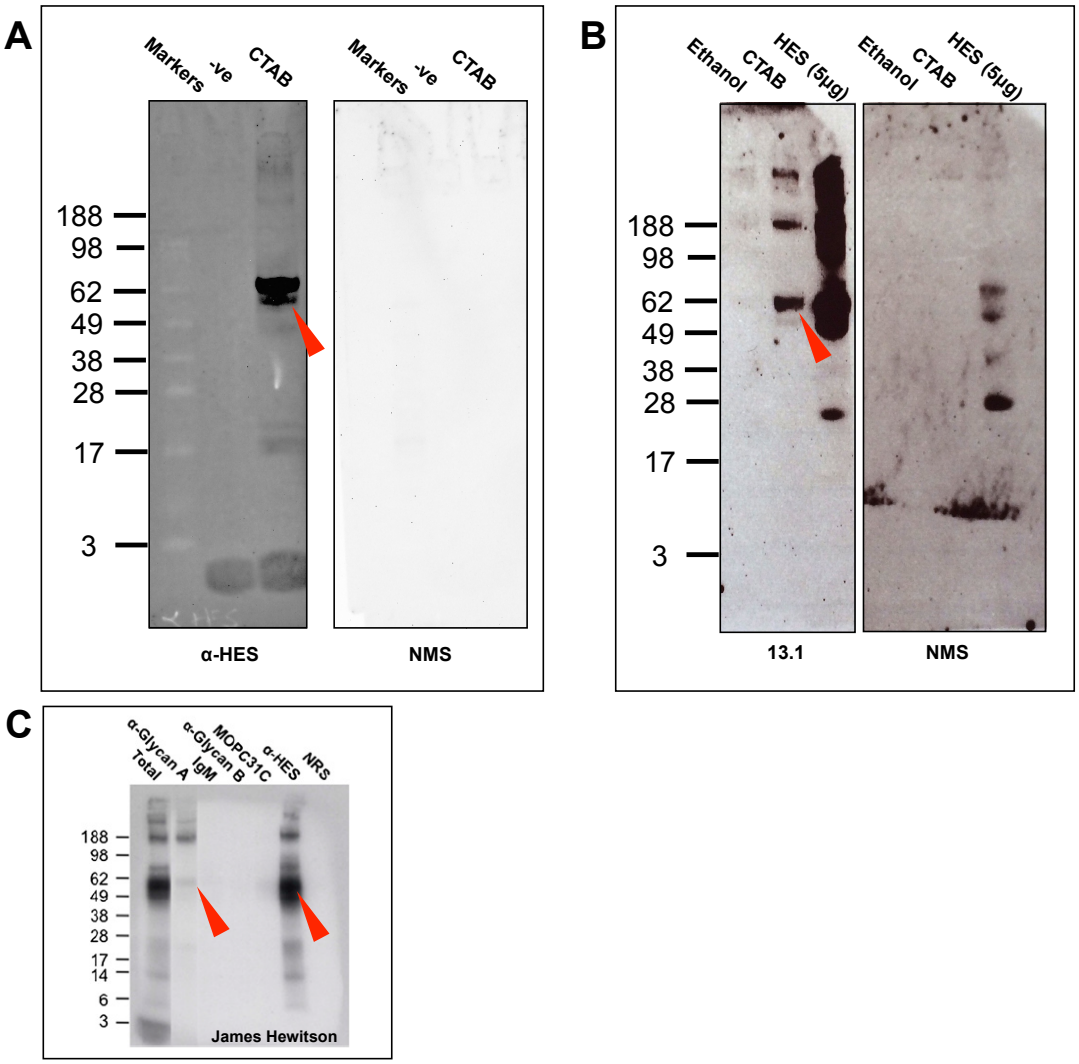

Fig 4.11 Acetone precipitated parasite cuticle reveals a 62kDa protein which is recognised by α-HES and α-Glycan A antibodies.

15ml of media from ethanol and CTAB washes was acetone precipitated by adding 35ml ice cold 100% acetone and freezing at -20°C for 48 hours. Frozen samples were allowed to defrost before centrifugation at 15,000g for 20 minutes. The resulting pellet was air dried then resuspended in 500µl PBS and 50µl of 4XSDS PAGE loading buffer.

A. Western blot of acetone precipitated media from untreated and CTAB treated *H.polygyrus* parasites.
B. Western blot of acetone precipitated media from ethanol and CTAB treated *H.polygyrus* parasites.
C. Western blot (αHES pAb) of 125I surface-labeled adult proteins immunoprecipitated with anti-glycan A mAb 13.1

Arrow indicates 62kDa band.

Section 2: Do *H.polygyrus* products bind to host cells?

4.12 Alexa647 labeled HES binds to cells recruited to granulomas present in *H.polygyrus* infection.

As previously discussed in Chapter 1 (Fig 1.17A), biotinylated HES binds to a population of naïve B cells in a CD24 dependent manner demonstrated by the loss of binding to B cells in CD24-/- mice. This binding indicated that HES can and does interact with host cells. The extent of these interactions is examined more closely here.

To enable further characterization of the binding properties of HES, immunostaining was performed using HES, which had been directly labeled with Alexa647 (Life Technologies). Murine gut tissue from naïve and day 7 infected C57BL/6 mice was embedded in histological wax and 5µm sections were prepared. Staining was done by first dewaxing the sections with Histoclear followed by rehydration through 100%, 95% and 70% ethanol. Sections were immersed in citrate buffer at 95°C to facilitate antigen retrieval. The citrate buffer was then allowed to cool for 20 minutes before sections were washed twice in PBS/Tween 20 for 5 minutes. Sections were blocked using TBS-T/ FCS 10%/ BSA 1% for 1 hour at room temperature followed by two incubations in avidin and biotin to block endogenous biotin activity (Banerjee & Pettit, 1984). Sections were washed once in PBS prior to overnight incubation with the HES647 (4µg/ml and 20µg/ml) and biotinylated αCD24 1:200. Following overnight incubation sections were washed and where a biotinylated primary antibody was used the streptavidin secondary was applied: streptavidin FITC@ 1:100 which was then incubated on sections for 30 minutes prior to final washes in PBS followed by H_2O and mounting of coverslips using an anti-fade mountant containing DAPI.
Alexa647 labelled HES bound to host cells present in the cyst-like structures (granulomas) found in the gut wall (Fig 4.12 B-E). HES647 also bound to the surface of the parasite. Both concentrations (4µg/ml and 20µg/ml) of HES labelled successfully to cells within the granulomas.

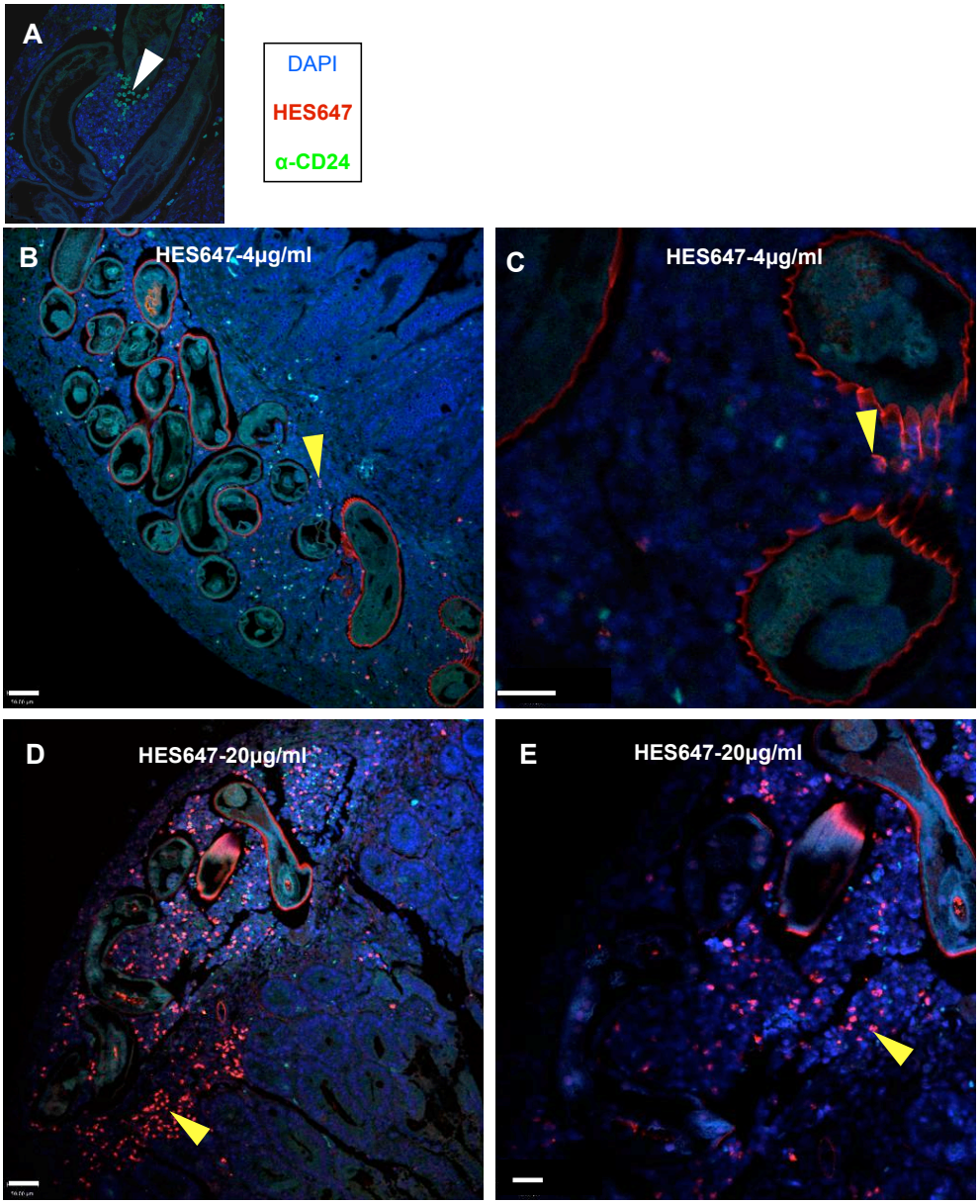

Fig 4.12 Alexa647 labelled HES binds to the surface of the parasite and to cells recruited to the resulting granuloma.

Murine gut tissue from naive and infected C57BL/6 mice was fixed in formalin before embedding in paraffin wax. 5µm sections were cut for staining. Sections were stained with HES647 or αCD24 followed by a FITC secondary.

<u>Day 7 infection</u>.
A. Negative control= Day 7 infected mouse, no stain. (White arrow shows autofluorescent red blood cells. Scale bar: 75µm
B. & **C**. HES 647 4µg/ml (Yellow arrow showing HES647 labelled cells) Scale bar: 50 & 75µm

D. & **E**. HES 647 20µg/ml (Yellow arrow showing HES647 labelled cells) Scale bar: 50µm

4.13 (i) & (ii). Alexa647 labelled HES binds to the surface of the parasite throughout an infection time-course.

As an infection proceeds in a laboratory setting, larvae that have been gavaged into the mouse migrate though the intestinal sub-mucosa where they undergo two molts(Reynolds, Filbey, & Maizels, 2012). During this transit through the gut, parasites become enclosed in cyst-like structures, termed granulomas, in the gut wall as seen in Fig 4.12. The number of these structures varies between mouse strains with BALB/c mice much more prone to cyst development than C57BL/6 mice (Filbey et al., 2014). Parasites then leave the granuloma and return to the lumen of the gut, where as adults they mate resulting in the production of eggs, which are passed in the faeces. To assess the binding of HES to murine cells in the gut, sections of murine intestinal tissue were taken at 4 separate time-points through the *H.polygyrus* infection. Gut tissues and sections were processed as described previously (Fig 4.12). Here, HES647 was used at a concentration of 4µg/ml and αCD24 was used at a dilution of 1:150.

Staining of Day 2 sections onwards shows an infiltrate of host cells around the parasite; to which HES647 and to a lesser extent CD24 both bind (Fig 4.13 IB, yellow arrows). Upon closer observation (Fig 4.13 IC and inset) it became apparent that some of the cells binding to HES647 were located at the bottom of intestinal crypts, which due to their location were very likely to be Paneth cells. These cells however, were lacking the CD24 binding pattern that has been described previously by Limbergen (Van Limbergen et al., 2013) and Sato (Sato et al., 2011). Perhaps fixation of gut tissue prior to sectioning alter CD24 given that it is a highly glycosylated protein. Paneth cell staining was observed throughout the time course, although with fewer cells and less pronounced staining at Day 2. Cell infiltrate in the granuloma at Day7 (Fig 4.13 I C) shows a large number of host cells surrounding the parasite. In the same panel it was noted that there was a lack of Paneth cells directly adjacent to the parasite location. This was also noted at Day 7 and 9 around the

vicinity of the granuloma. It is currently unclear as to why this may occur; possibly secretions from the parasite have caused the Paneth cells to release their contents or perhaps the tissue architecture has been disrupted when then parasite migrated through the wall of the gut.

H.polygyrus parasites can be observed in the wall of the gut tissue from Day 2 post-infection onwards, however binding of HES647 to the cuticle is not visible until Day 5 onwards. As mentioned previously, parasites undergo a number of moults in the sub mucosa of the gut. At Day 2 post infection the parasite has yet to undergo moults and is still at the larval L3 stage. Thus larval and adult parasites most probably have distinctive cuticles therefore explaining the lack of HES647 binding at this stage. Further examination of the cuticle composition is required; furthermore research by Pritchard (Pritchard, Maizels, Behnke, & Appleby, 1984) demonstrated the stage specific expression of cuticular antigens, which may also be significant with regards to the binding ability of parasite products.

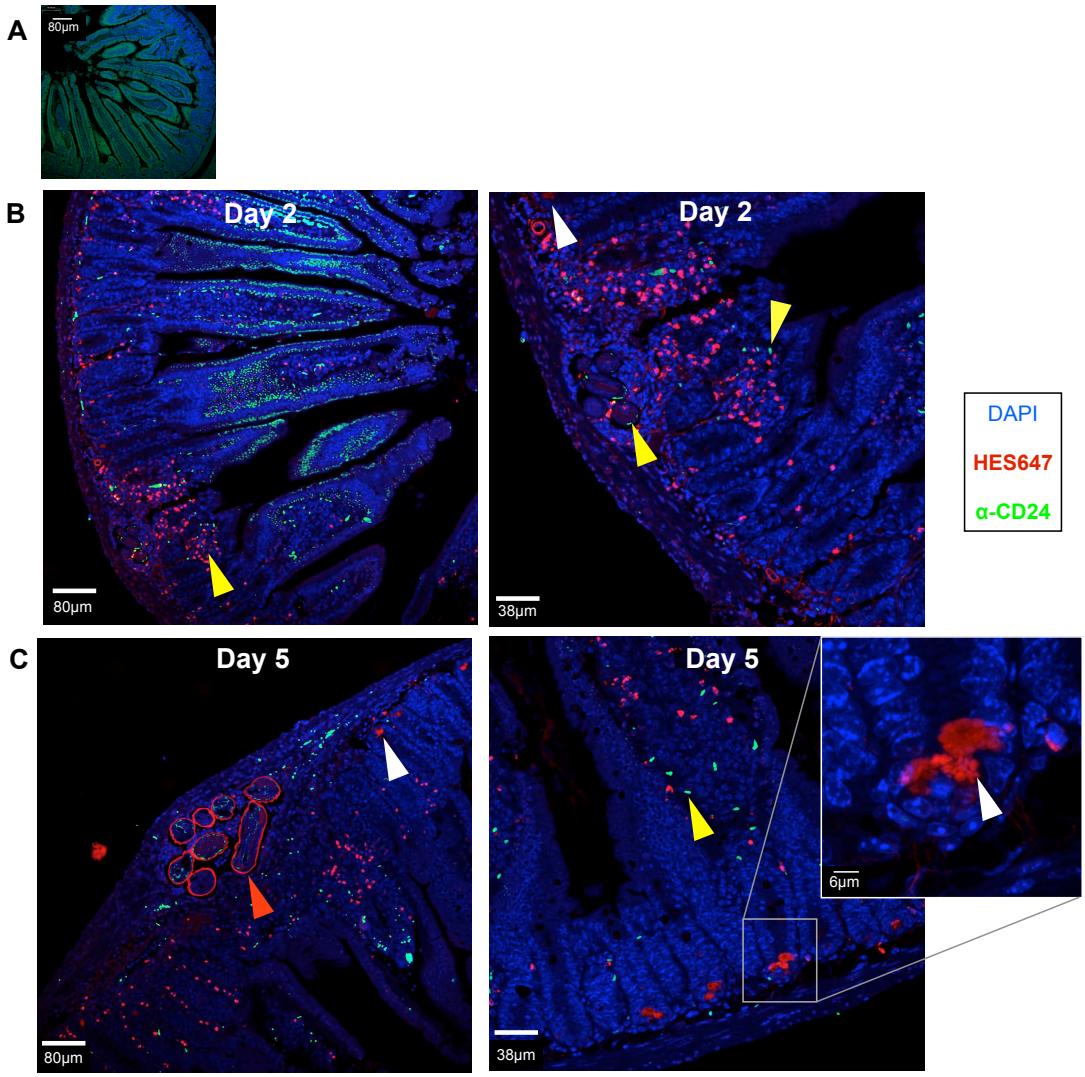

Fig 4.13(i) Alexa647 labeled HES binds to the surface of the parasite throughout an infection time-course.

Murine gut tissue from an infection time course with *H.polygyrus,* comprising Days 2, 5 7 and 9 with Day 0= naive, was processed as described previously (Fig 4.10). **HES647: 4µg/ml αCD24: 1:150.**

A. Naive
B. Day 2 (X20 & X40 magnification)
C. Day 5 (X20 & X40 magnification. Insert= X40 zoom)
White arrows= Paneth cells
Yellow arrows= host cells
Red arrows= *H.polygyrus*

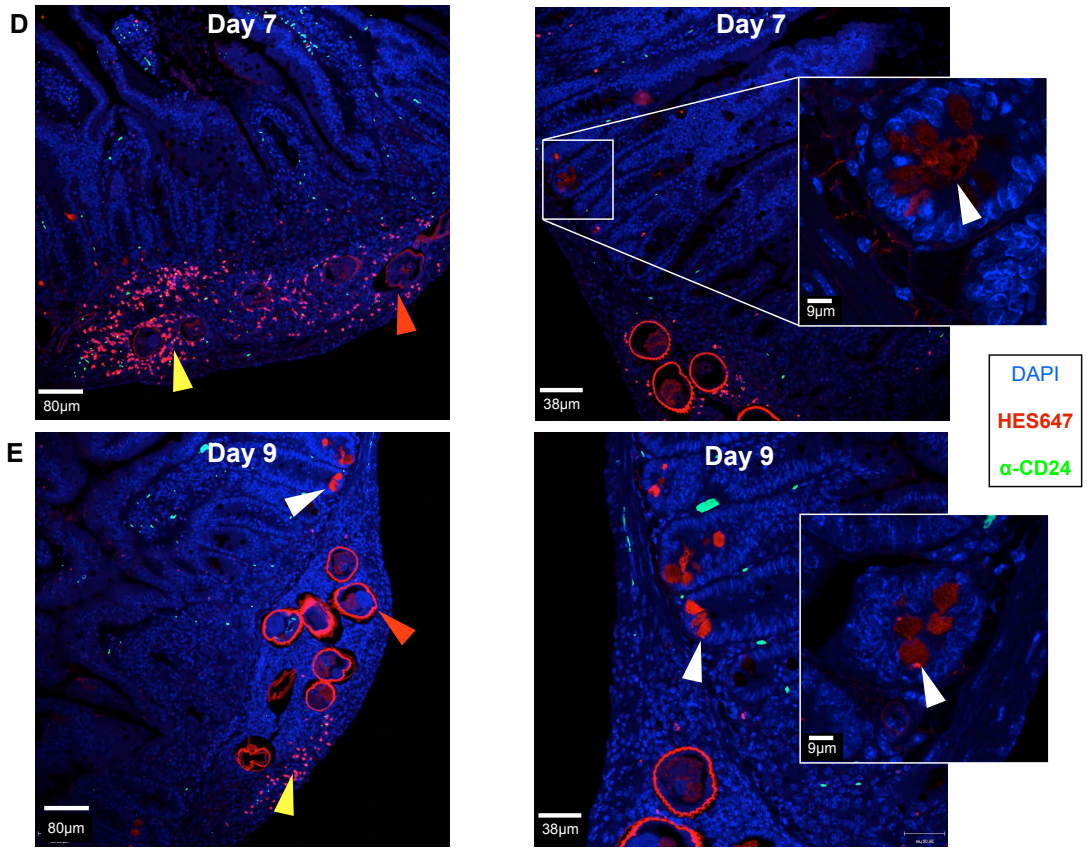

Fig 4.13(ii) Alexa647 labeled HES binds to the surface of the parasite throughout an infection time-course.

Murine gut tissue from an infection time course with *H.polygyrus,* comprising Days 2, 5 7 and 9 with Day 0= naive, was processed as described previously (Fig 4.10). **HES647: 4µg/ml αCD24: 1:150.**

D. Day 7 (X20 & X40 magnification. Insert= X40 zoom)
E. Day 9 (X20 & X40 magnification. Insert= X40 zoom)
White arrows= Paneth cells
Yellow arrows= host cells
Red arrows= *H.polygyrus*

4.14 - 4.16 Is the binding of HES to *H.polygyrus* and Paneth cells CD24 dependent?

To further assess the binding properties of HES to the cuticle of *H.polygyrus* and to Paneth cells in the gut, C57BL/6 and CD24-/- deficient mice were infected with *H.polygyrus* larvae for 7 or 28 days. Gut tissue was harvested and fixed sections were prepared for staining with Hemotoxylin and Eosin (H&E), Periodic acid Schiff (PAS) or stained with HES647 and CD11b-FITC for confocal analysis. CD11b is a marker for B cells, dendritic cells, granulocytes, macrophages, monocytes, NK cells, T cells.

4.15-(i) & (ii) Binding of HES to *H.polygyrus* and Paneth cells is not CD24 dependent (DAY 7).

Binding of HES647 to Paneth cells (white arrows) was evident in both naïve and infected C57Bl/6 mice as shown in Fig 4.15-I A-D. The infection status of CD24-/- mice also has no bearing on the ability of HES647 to bind to Paneth cells (Fig 4.15-II A&D). In the sections examined there were fewer Paneth cells apparent in the CD24-/- than C57BL/6. Alkazami previously described reductions in Paneth cell numbers in hamsters following primary hookworm infections (Alkazmi, Dehlawi, & Behnke, 2008), (Alkazmi & Behnke, 2013).

Panel E (Fig 4.15-i) shows a large influx of host cells around the parasite, which have stained with both HES647 and CD11b (these cells appear orange in colour) or CD11b alone. Macrophage infiltration to tissues surrounding *H.polygyrus* have been shown to contain alternatively activated macrophages (Filbey et al., 2014), however activation status cannot be determined with the staining carried out here. Goblet cells generally appear as black “hole like” structures in the tissue. However the pink and yellow arrow indicates a goblet cell showing faint HES647 staining (Fig 4.15-I D). Goblet cell hyperplasia is well documented in *H.polygyrus* and other gut parasite infections (Cywinska, Czuminska, & Schollenberger, 2004), (Masure et al., 2013), (Khan & Collins, 2004) and is evident in both C57B/6 and CD24-/- mice.

It should also be noted that HES647 binds to the parasite cuticle (red arrows) in both strains of mice as can be seen in the confocal stained panels from both Fig 4.15-(i) & (ii).

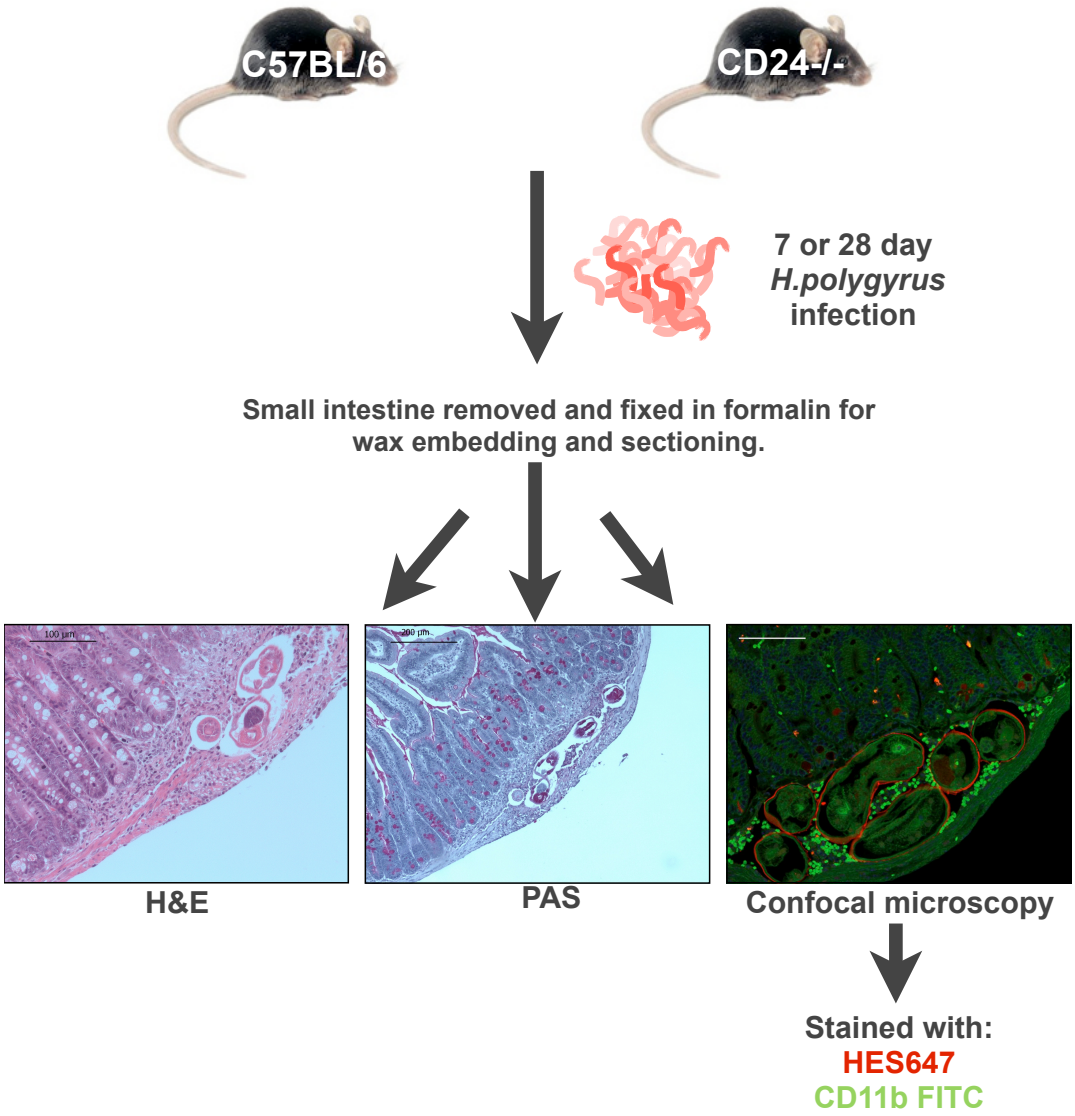

Fig 4.14 Is the binding of HES to *H.polygyrus* and Paneth cells CD24 dependent?

C57BL/6 and CD24-/- mice were infected with *H.polygyrus* for 7 and 28 days. The small intestine was removed and fixed in formalin before embedding in paraffin wax. 5µm sections were then stained with Hemotoxylin and Eosin (H&E), Periodic acid Schiff (PAS) or prepared for confocal analysis. For confocal analysis sections were stained with HES647 and CD11b/FITC.

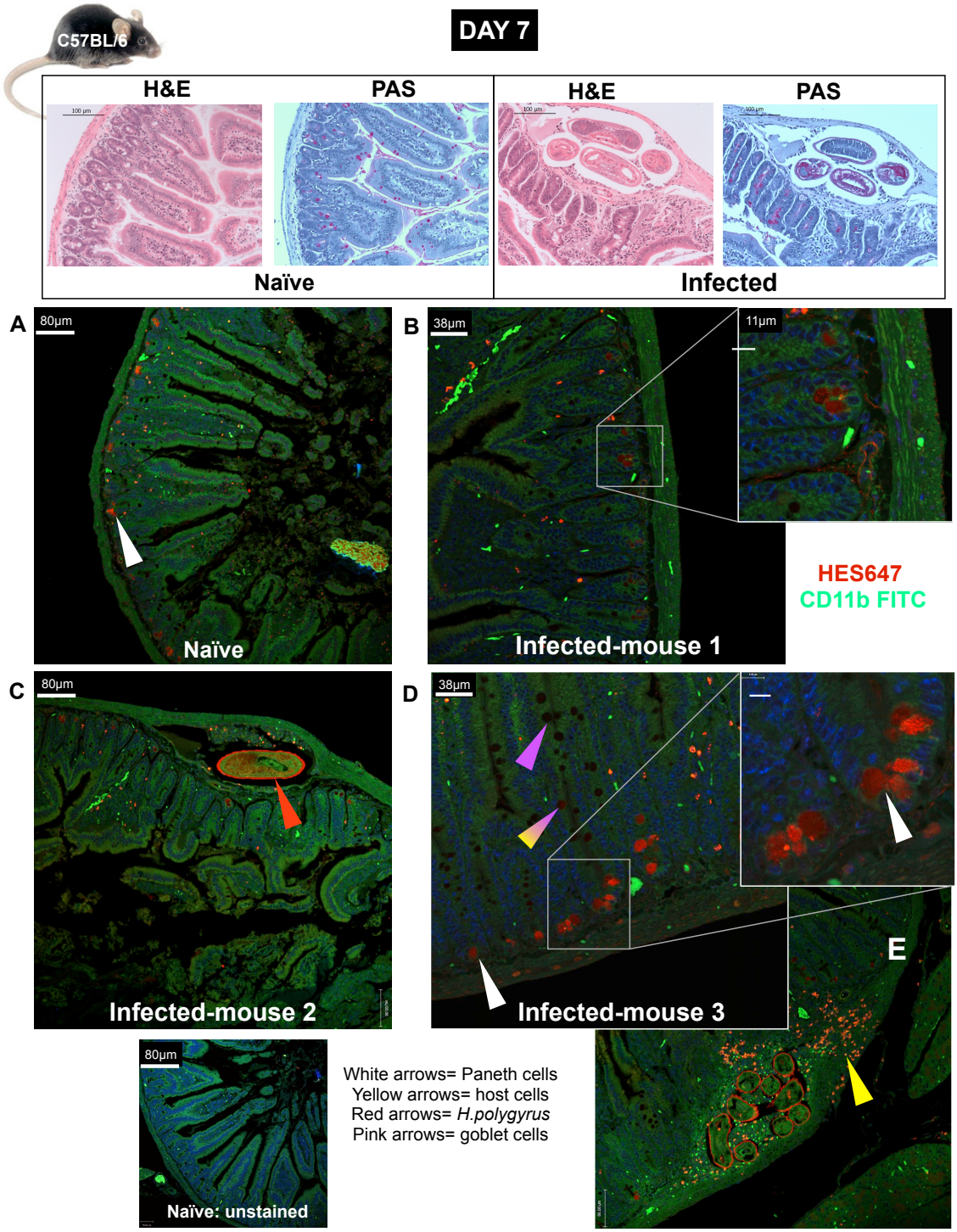
C57BL/6
DAY 7
H&E
PAS
H&E
PAS
Naïve
Infected
A
80µm
Naïve
B
38µm
11µm
Infected-mouse 1
HES647
CD11b FITC
C
80µm
Infected-mouse 2
D
38µm
Infected-mouse 3
E
80µm
Naïve: unstained
White arrows= Paneth cells
Yellow arrows= host cells
Red arrows= H.polygyrus
Pink arrows= goblet cells

Fig 4.15-i

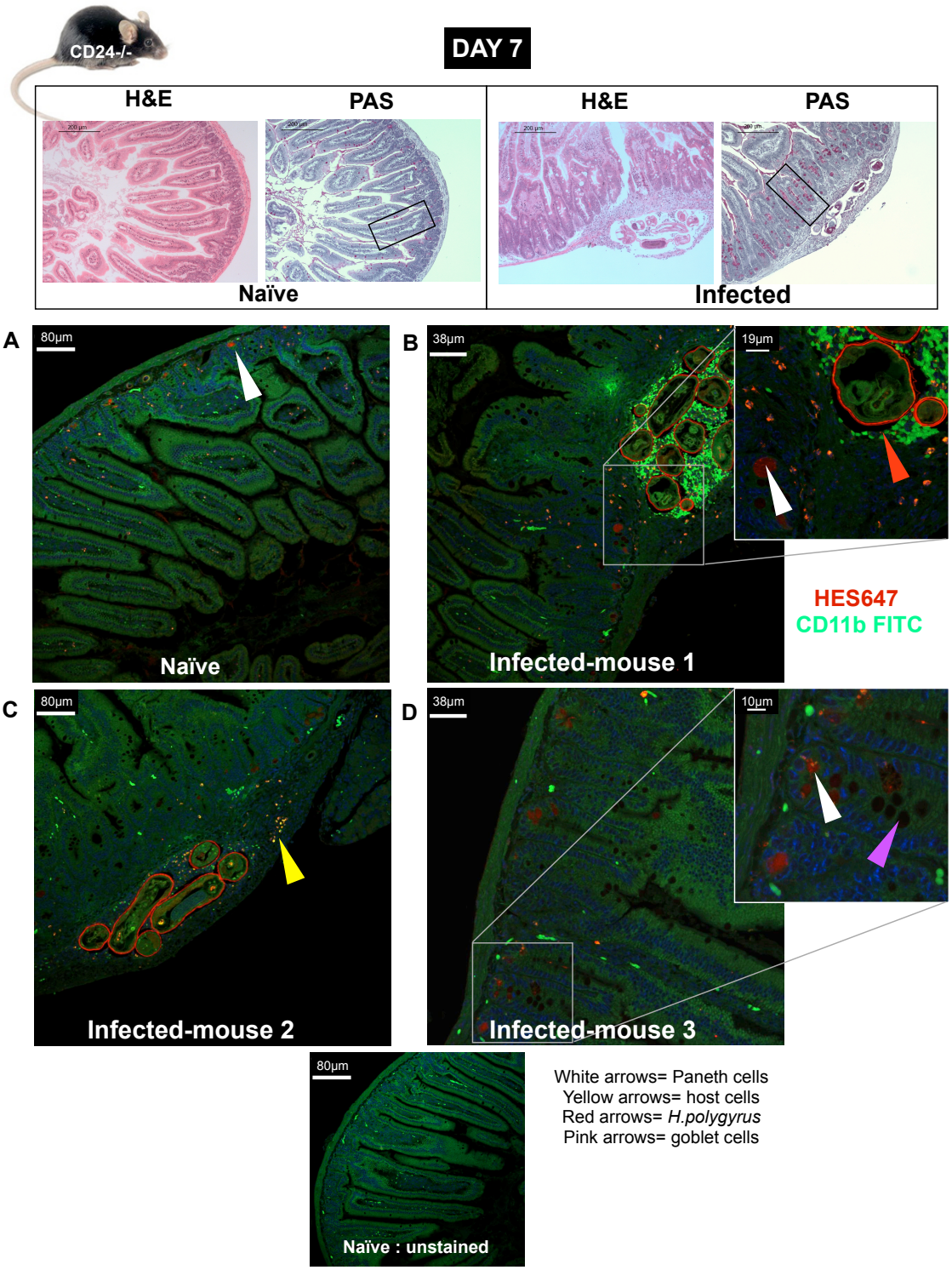
CD24-/-
DAY 7
H&E
PAS
H&E
PAS
Naïve
Infected
A
80µm
Naïve
B
38µm
19µm
Infected-mouse 1
HES647
CD11b FITC
C
80µm
Infected-mouse 2
D
38µm
10µm
Infected-mouse 3
80µm
Naïve : unstained
White arrows= Paneth cells
Yellow arrows= host cells
Red arrows= H.polygyrus
Pink arrows= goblet cells

Fig 4.15-ii

Fig 4.15 (i) & (ii) Binding of HES to *H.polygyrus* and Paneth cells is not CD24 dependent. (DAY 7)

C57BL/6 and CD24-/- mice were infected with *H.polygyrus* for 7 and 28 days. The small intestine was removed and fixed in formalin before embedding in paraffin wax. 5µm sections were then stained with Hemotoxylin and Eosin (H&E), Periodic acid Schiff (PAS) or prepared for confocal analysis. Here sections were stained with HES647 and CD11b/FITC.

I. Sections of gut tissue from **Day 7** infected C57BL/6 mice was stained with H&E, PAS and HES647/CD11b/FITC.

II. Sections of gut tissue from **Day 7** infected CD24-/- mice was stained with H&E, PAS and HES647/CD11b/FITC.

White arrows= Paneth cells
Yellow arrows= host cells
Red arrows= *H.polygyrus*
Pink arrows= goblet cells

Confocal scale bars as shown in µm.

4.16 (i)-(ii) Binding of HES to *H.polygyrus* and Paneth cells is not CD24 dependent (DAY 28).

By day 28 post-infection, parasites have emerged from the wall of the gut and are now adult stage parasites, with the ability to produce eggs, residing in the gut lumen. HES that is collected in a laboratory setting is collected from adult parasites in culture, thus observing adult parasites in the lumen of the gut could indicate how HES molecules would interact with gut cells and tissues *in vivo*.

HES647 and CD11b have stained cells present in the granuloma found in the infected C57BL/6 section (Fig 4.16-I B). These granulomas were characterized by Filbey et al. (Filbey et al., 2014) and were found to contain a large proportion of macrophages. CD11b staining shown here replicates previous staining (Fig 4.16-I F) of a Day 7 granuloma with F4/80:Alexa647 & αGlycanA: FITC. These results confirm the presence of granuloma macrophages at Day 7 and Day 28. Yellow staining seen in the Day 28 granuloma is HES647 and CD11b/FITC co-localization.

Infected tissue also clearly shows the presence of parasites now in the lumen of the gut (red arrows in Fig 4.16-I C&D & Fig 4.16-II B) in both C57B/6 and CD24-/- strains of mice. Fig 4.16-I C & Fig 4.16-II B show sections of an infected mouse where the parasite is nestled in at the base of the villi. Here and in Fig 4.16-I D the surface of the parasite is again clearly labelled with HES647 (yellow arrows). Although there are Paneth cells present in these sections (white arrows) the degree to which they have stained with HES647 appears to be less than at Day 7. As Paneth cells are known to release their contents upon detection of certain stimuli this may result less of the HES binding component being present (Ayabe et al., 2000), (Clevers & Bevins, 2013).

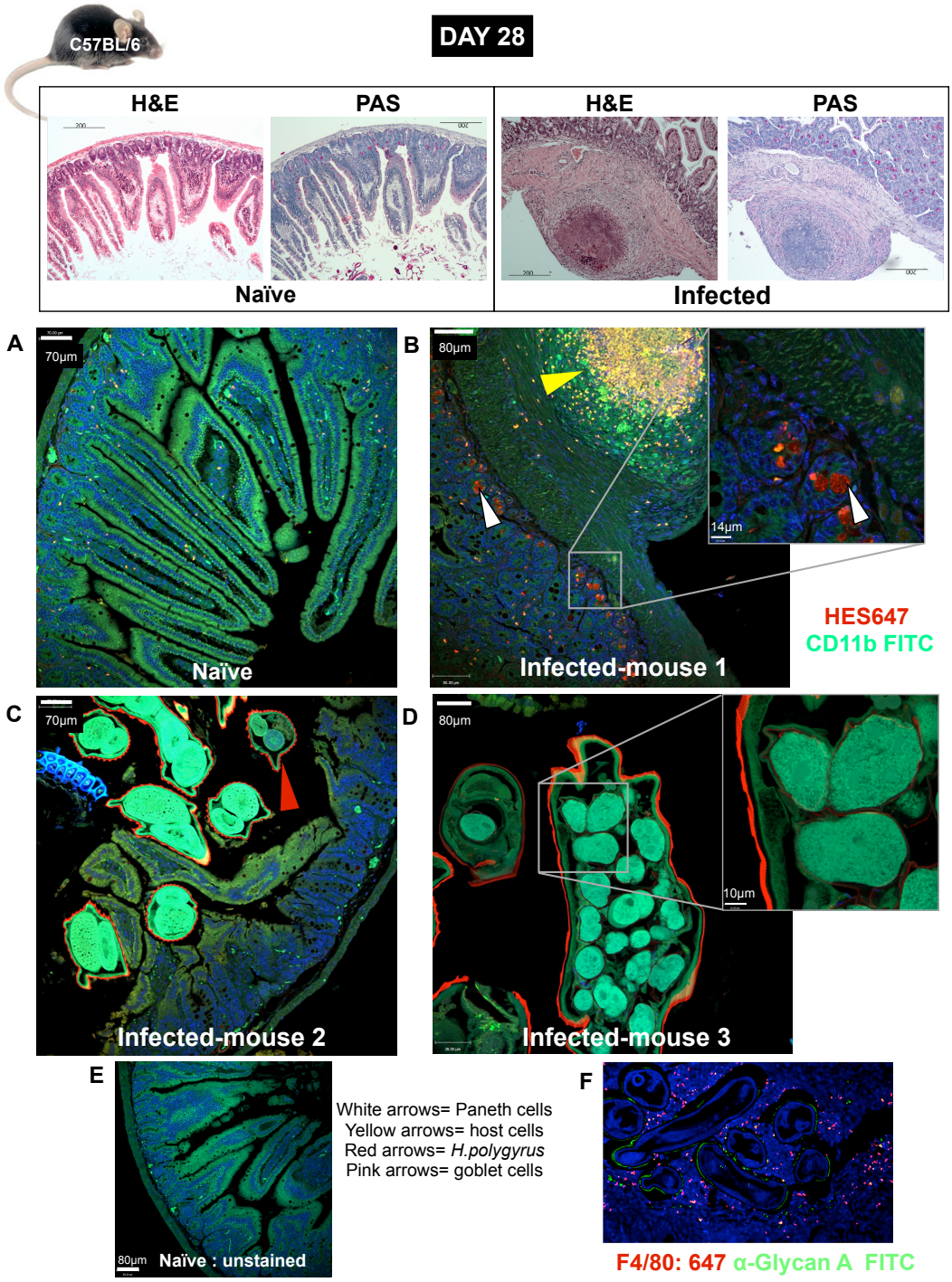
C57BL/6
DAY 28
H&E
PAS
H&E
PAS
Naïve
Infected
A
70µm
Naïve
B
80µm
14µm
Infected-mouse 1
HES647
CD11b FITC
C
70µm
Infected-mouse 2
D
80µm
10µm
Infected-mouse 3
E
80µm
Naïve : unstained
White arrows= Paneth cells
Yellow arrows= host cells
Red arrows= H.polygyrus
Pink arrows= goblet cells
F
F4/80: 647 α-Glycan A FITC

Fig 4.16-(i)

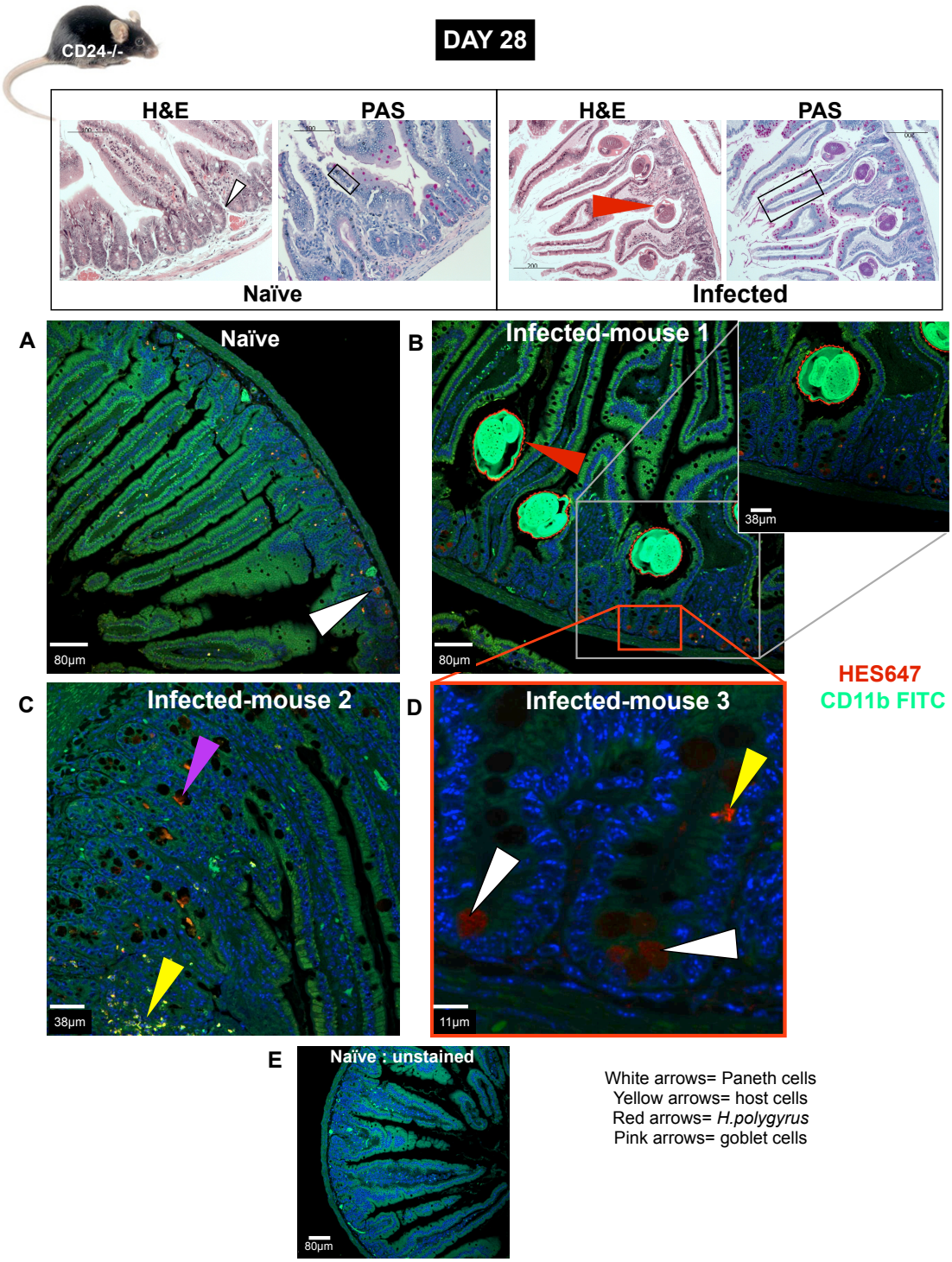
CD24-/-
DAY 28
H&E
PAS
H&E
PAS
Naïve
Infected
A
Naïve
80µm
B
Infected-mouse 1
80µm
38µm
HES647
CD11b FITC
C
Infected-mouse 2
38µm
D
Infected-mouse 3
11µm
E
Naïve : unstained
80µm
White arrows= Paneth cells
Yellow arrows= host cells
Red arrows= H.polygyrus
Pink arrows= goblet cells

Fig 4.16-(ii)

Fig 4.16 (i) & (ii) Binding of HES to *H.polygyrus* and Paneth cells is not CD24 dependent. (DAY 28)

C57B/6 and CD24-/- mice were infected with *H.polygyrus* for 7 and 28 days. The small intestine was removed and fixed in formalin before embedding in paraffin wax. 5µm sections were then stained with Hemotoxylin and Eosin (H&E), Periodic acid Schiff (PAS) or prepared for confocal analysis. Here sections were stained with HES647 and CD11b/FITC.

I. Sections of gut tissue from **Day 28** infected C57B/6 mice was stained with H&E, PAS and HES647/CD11b/FITC.

II. Sections of gut tissue from **Day 28** infected CD24-/- mice was stained with H&E, PAS and HES647/CD11b/FITC.

White arrows= Paneth cells
Yellow arrows= host cells
Red arrows= *H.polygyrus*
Pink arrows= goblet cells

Confocal scale bars as shown in µm.

4.17 HES binding to Paneth cells is heat stabile.

Interactions between proteins and cells are hugely complex, however successful ligation between the two can often be dependent upon structure. To further explore possible mechanisms by which HES binds to both the Paneth cells and the surface of the parasite, Alexa labeled HES647, was denatured by boiling before being used to stain slides from Day 7 infected C56B/6 and CD24-/- mice. Sections were stained with boiled HES647 and CD11b FITC and were subsequently examined by confocal microscopy.

Staining of the parasite cuticle was unaffected, although appeared more diffuse, by denaturing HES as can be seen in Fig 4.17 B (white and yellow arrows respectively). This observation was made in CD24-/- mice, however sections stained from C57BL6/6 mice had no parasites present but presumably parasite cuticle staining here would also have been unaffected. Paneth cell staining was also unaffected by denaturing HES and can be seen in both mouse strains (Fig 4.17 A & B, white arrows).
This data would indicate a heat stable epitope is responsible for binding of HES to both the cuticle of the parasite and to the Paneth cells.

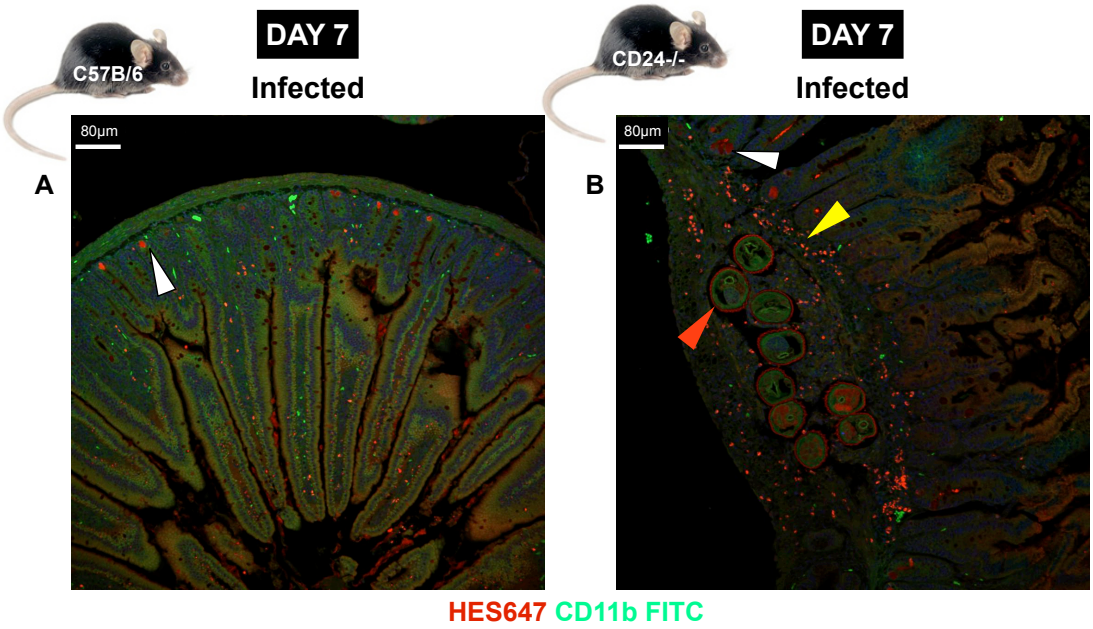

Fig 4.17 Paneth cell binding of HES is heat stabile.

C57BL/6 and CD24-/- mice were infected with *H.polygyrus* for 7 days. The small intestine was removed and fixed in formalin before embedding in paraffin wax. 5µm sections were then prepared for confocal analysis. Here sections of gut tissue from Day 7 infected C57BL/6 and CD24-/-mice were stained with HES647/CD11b/FITC where the HES had been denatured by boiling for 10 minutes.

White arrows= Paneth cells
Yellow arrows= host cells
Red arrows= *H.polygyrus*

Confocal scale bars as shown in µm.

4.18-4.19 Cuticle binding of HES in *H.polygyrus* is not antibody mediated.

One possibility to explain binding of HES to the cuticle of the parasite is that as the mouse responds to the *H.polygyrus* infection by mounting an immune response, antibodies generated bind to the surface of the parasite. These in turn could bind to excretory secretory products produced by the parasite, thus explaining cuticular binding. To test this hypothesis, C57BL/6 mice and μMT mice, which cannot produce an antibody response, were infected with *H.polygyrus* larvae for 7 days. Gut tissue was harvested at Day 7 post-infection and was fixed in formaldehyde prior to wax embedding and sectioning. Sections were stained with H&E and PAS and were prepared for confocal analysis as described previously (Fig 4.12). Sections for confocal analysis were stained with **1**) HES647 & F4/80 FITC or **2**) F4/80 647 & αCHO 13.1FITC.

Parasite cuticle stained with HES647 in μMT mice indicating that the presence of antibody was not required for this binding to take place (Fig 4.19 B, red arrows). Interestingly the αCHO 13.1 antibody binds to the surface of the parasite in the same way as seen for HES. Given that the binding of HES to the cuticle is a heat stable interaction and the αCHO 13.1 antibody binds via a glycan moiety, the binding seen for HES may also be carbohydrate mediated. Macrophages (F4/80FITC +ve) can be seen surrounding the parasite within the granuloma structure in the μMT infected mouse. Most of the cellular infiltrate stains with both HES647 and F4/80 (white box).
Binding of the αCHO 13.1 Ab to the carbohydrate rich serosal layer is apparent in sections from both C57B/6 and μMT mice (blue arrows).

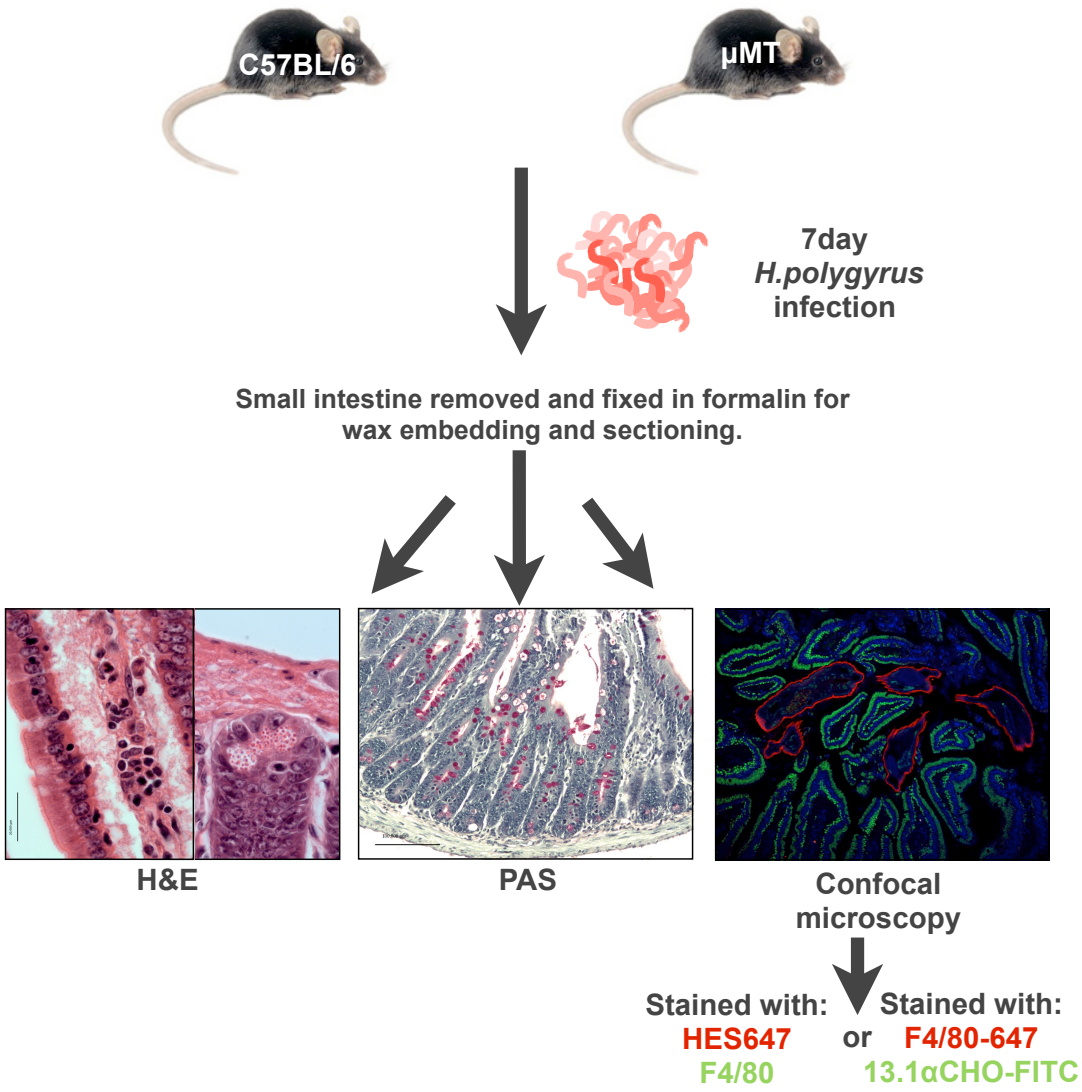

Fig 4.18 Cuticle binding of HES in *H.polygyrus* is not antibody mediated.

C57B/6 and µMTmice were infected with *H.polygyrus* for 7 days. The small intestine was removed and fixed in formalin before embedding in paraffin wax. 5µm sections were then stained with Hemotoxylin and Eosin (H&E), Periodic acid Schiff (PAS) or prepared for confocal analysis. Here sections were stained with HES647 and CD11b/FITC.

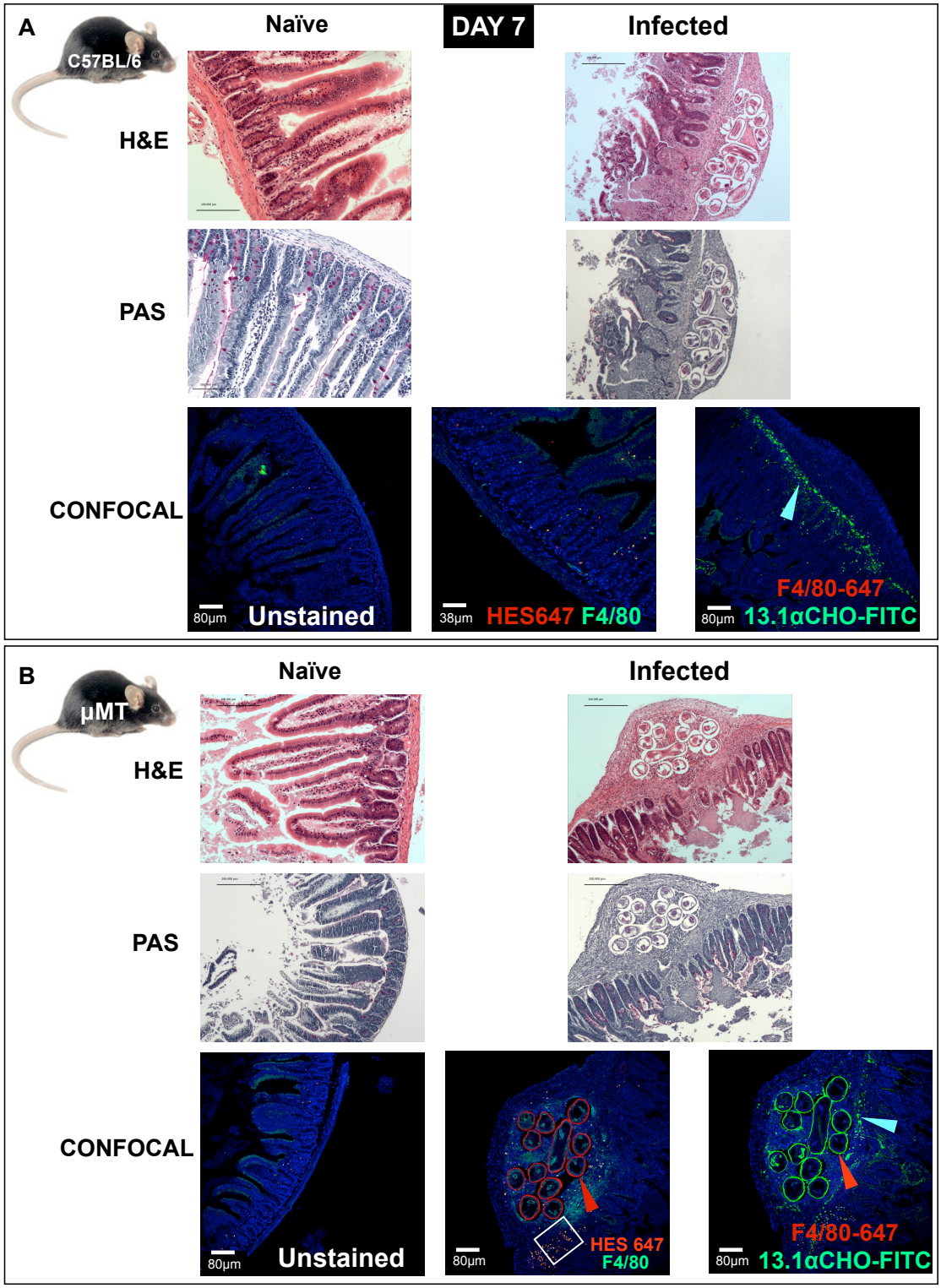

Fig 4.19 Cuticle binding of HES in *H.polygyrus* is not antibody mediated.

Fig 4.19 Cuticle binding of HES in *H.polygyrus* is not antibody mediated.

C57BL/6 and μMTmice mice were infected with *H.polygyrus* for 7. The small intestine was removed and fixed in formalin before embedding in paraffin wax. 5μm sections were then stained with Hemotoxylin and Eosin (H&E), Periodic acid Schiff (PAS) or prepared for confocal analysis. Here sections were stained with HES647 and CD11b/FITC.

A. Sections of gut tissue from **Day 7** infected C57BL/6 mice was stained with H&E, PAS and HES647/F4/80 or F4/80/ 13.1.

B. Sections of gut tissue from **Day 7** infected μMT mice was stained with H&E, PAS and HES647/F4/80 or F4/80/ 13.1.

Blue arrows= serosal binding
Red arrows= *H.polygyrus*

Confocal scale bars as shown in μm.

4.20 Preparation of intestinal epithelium for whole mount staining.

One of the limitations of staining sections of tissue is that when a large area of tissue may be affected by a treatment or an infection, as is the case with an *H.polygyrus* infection in the gut, examining sections if tissue illustrates a very small area, which may not be representative of what is occurring throughout. To allow a more global examination of the locality of Paneth and goblet cells a method, which allows the examination of whole gut villi, was used (Gerbe et al., 2011).

Gut tissue was removed from the mouse and with minimal time passing the tissue was processed. Ice-cold HBSS was used to flush gently through the intestine (a) before turning the gut inside out on a wooden stick. This allowed the interior of the gut to be washed gently in HBSS (b). After washing the gut tissue was removed from the stick by gently slicing along its length with a scalpel blade (c). The open tissue was then transferred to HBSS containing EDTA (30mM) and was incubated on ice for 10 minutes (d). Following a brief wash in HBSS the tissue was carefully laid out, villi side up (f), on a glass plate and two bent needles were used to scrape the surface and remove the villi, which were fixed in 4% PFA overnight (e). Following overnight fixation tissues were then processed for immunostaining and confocal microscopy.

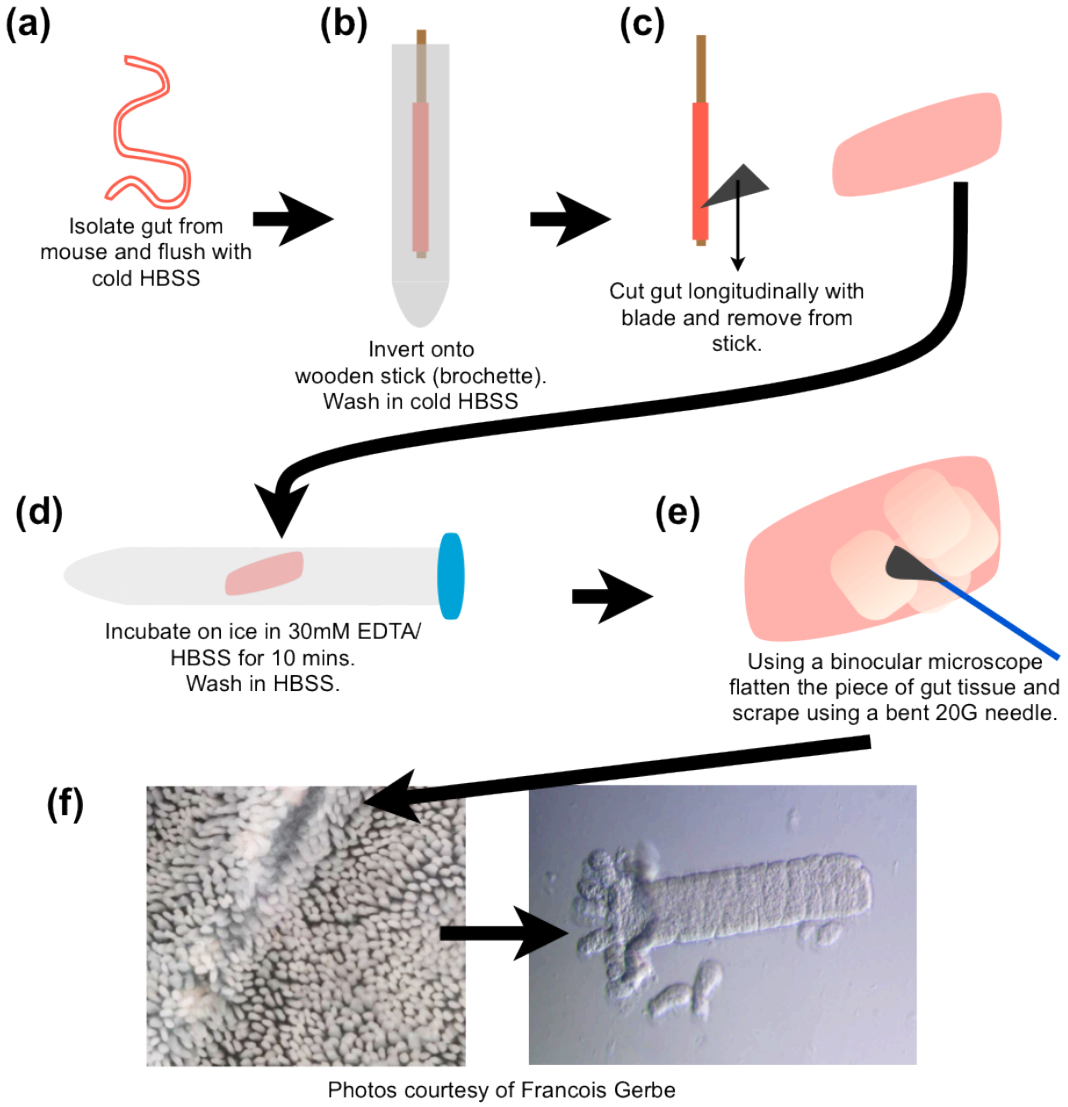

Fig 4.20 Preparation of intestinal epithelium for whole mount staining.

a) The small intestine was removed from the mouse and flushed through with cold HBSS. **b**) The intestine was then carefully inverted on a wooden stick that had been pre-wetted in HBSS buffer. This results in the intestine being turned inside out on the stick. Inverted gut tissue was then placed into cold HBSS in 15ml tubes for 5 minutes on ice. **c**) After washing the tissue was removed by gently slicing along the stick with a scalpel blade. **d**) The tissue was then placed in a solution of 30mM EDTA in HBSS and incubated on ice for 10 minutes and was then washed in HBSS twice for two minutes. **e**) Tissue was then placed on a glass plate and with the aid of a binocular microscope and two 20G needles, the epithelium was gently scraped of and placed into tubes containing 4% PFA. **f**) The epithelium was then gently shaken to break it up into single crypt/villi.

4.21 Immunostaining of intestinal villi and crypts.

Intestinal villi can be stained to visualise different cells type and their locations. The epithelium of the intestine has a range of cell types each with a distinctive role to play (Table 4.3).

Table 4.3 Murine intestinal cell types.

Cell Type	Function	Reference
Enteroendocrine	Endocrine signalling	Ashok et al, 2011
Paneth	Maintenance of stem cells, innate immune response.	Sato et al, 2011
Tuft	Source of prostanoids	Bezencon et al, 2008 Gerbe et al, 2011
Goblet	Mucus secretion	Specian et al, 1991
M-cell	Phagocytosis and transcytosis of macromolecules	Mabbott et al, 2013
Enterocyte	Absorption	Abreau, 2010

Here, preliminary staining was carried out on villi and crypt preps to identify some of the main cell types and structures. PFA fixative was removed from the tissues by washing in PBS/Triton X-100 0.1%. The tissue was then fixed in PBS/Triton X-100 0.05% for 30 minutes on ice before a brief wash prior to blocking for 1 hour in TBS/ 0.1% Triton X100, 5% dry milk powder (Marvel). After blocking the samples were incubated overnight at 4°C in primary antibodies which had been diluted in blocking

buffer. The following day samples were washed in PBS-tween for 5, 10 15 and 20 minutes periods before a 1-hour incubation with secondary antibodies diluted in PBS/tween. Finally samples were washed for 5, 10 and 15 minute periods in PBS/tween followed by a 5-minute final wash in PBS alone. Samples were mounted in
Vectashield ® containing DAPI and were then sealed onto Polysine slides using nail varnish. Samples were visualized using a Leica scanning confocal microscope and images generated using Velocity software in the Pathogen Imaging Facility (PIF), University of Edinburgh.

Lysosyme present in the Paneth cells, located at the bottom of the crypt, was stained with an α-Lysosyme antibody followed by an α-rabbit 647 secondary (Fig 4.21 Panels A-E). β-catenin, which binds to e-cahedrin was used to highlight cell membranes and the nuclear stain DAPI was present in the mounting fluid. Panel E shows individual Paneth cells at the end of a single crypt.
Antibodies used for staining the gut cells are listed in Table 4.4 along with secondary antibodies and their associated fluorophore.

Table 4.4 Antibodies and fluorescent conjugates for confocal microscopy on VCP tissue.

Primary antibodies	Supplier and dilution	Secondary antibodies	Supplier and dilution
Rabbit anti-lysozyme	DAKO (A0099) 1:500	α-rabbit 647 α-mouse 488	Life Technologies 225308 Life Technologies A11001
Mouse anti-βcatenin	BD Biosciences (610154) 1:200	α-mouse 488	Life Technologies A11001
Rabbit anti-MUC2	Santa Cruz (sc-15334) 1:400	α-rabbit 488 α-rabbit 647	Invitrogen A11034 Life Technologies 225308
biotinylated VAL proteins	Insect cell drived, biotinylated	streptavidin 488	Vector SA-5488

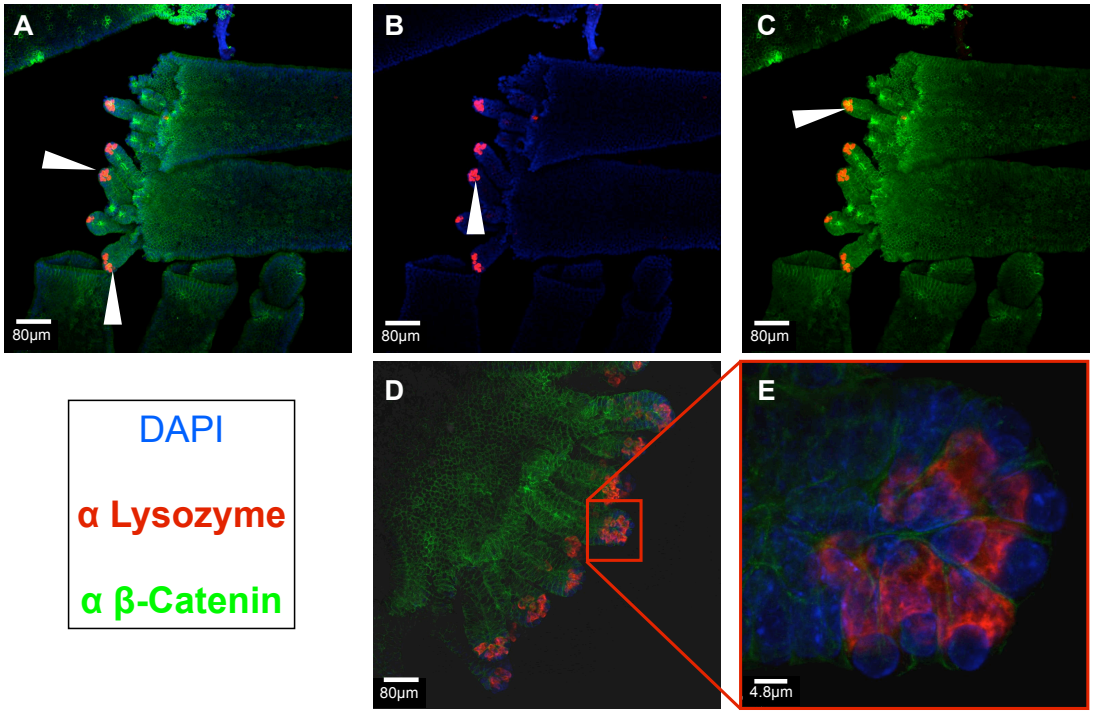

Fig 4.21 Immunostaining of intestinal villi and crypts.

1ml of crypt/villi prep (Fig 4.18) was placed into a 1.5ml tube. At this stage the tissue is in PFA. The fixative was removed and the tissue washed for 5 minutes, 3 times in PBS/ Triton X-100 0.1%. After washing the tissue was fixed for 30 minutes on ice in PBS/ Triton X-100 0.5%. Following fixation the tissue was washed for 5 minutes in PBS / Triton 0.1% and then blocked for 1 hour in TBS/ 5% dry milk (Marvel), 0.1% Triton X-100. Primary antibodies were diluted in blocking buffer. Samples were incubated with 1° Ab overnight at 4°C. Following incubation with the 1°Ab samples were washed 4 times with PBS-T for 5, 10, 15 and 20 minutes. Incubation with 2° Ab (diluted in PBS-T) was preformed at room temperature for 1 hour and generally done in the dark. Samples were then washed 3 times for 5, 10 and 15 minutes in PBS-T followed by a 5 minute wash in PBS. Vectashield containing DAPI was used to mount the samples onto polysine slides. Samples were then sealed with nail varnish before anaylsis using a Leica confocal laser scanning microscope SP5. Confocal microscopy was carried out with advice from Dr Dianne Murray within the PIF facility of the University of Edinburgh.

A-C Arrows show crypts present at the bottom of a villus. Paneth cells have stained with lysozyme (red). Cell walls are labelled with α β-Catenin which binds to the cytpolasmic tail of E-Cahedrin, a trans-membrane adhesion molecule and is conjugated here to an α-mouse 488 seconday Ab.
D-E Paneth cells at the bottom of the crypt stained with an α-lysozyme antibody (red). **E**. Shows individual paneth cells with the nucleus staining with DAPI (blue), cell junctions with β-Catenin (green) and lysozyme (red).

Confocal scale bars as shown in µm.

4.22 HES binds to cells on the surface of the villus.

Previous staining of gut sections showed that Paneth cells stained with HES647 (Fig 4.13). To investigate further the binding potential of the excretory secretory products of *H.polygyrus*, a villi and crypt prep was stained with whole HES labelled with Alexa647 along with an α-lysozyme antibody. Tissue from a naïve C57BL/6 mouse was used and staining was carried out as described for Fig 4.21.

Paneth cells at the base of the crypts stained again with the α-lysozyme antibody, this time detected with an α-rabbit 488 secondary antibody (white arrows on panels A, C & D). Interestingly HES647 also bound to the paneth cells (Panel E) but due to the intensity of the staining it is difficult to visualise at the same time as the lysozyme staining.

In addition to the Paneth cell staining, HES647 also stained many cells present on the surface of the villi (blue arrows on panels A.B &C). It was hypothesized that due to the number and position of these cells that they may be intestinal goblet cells.

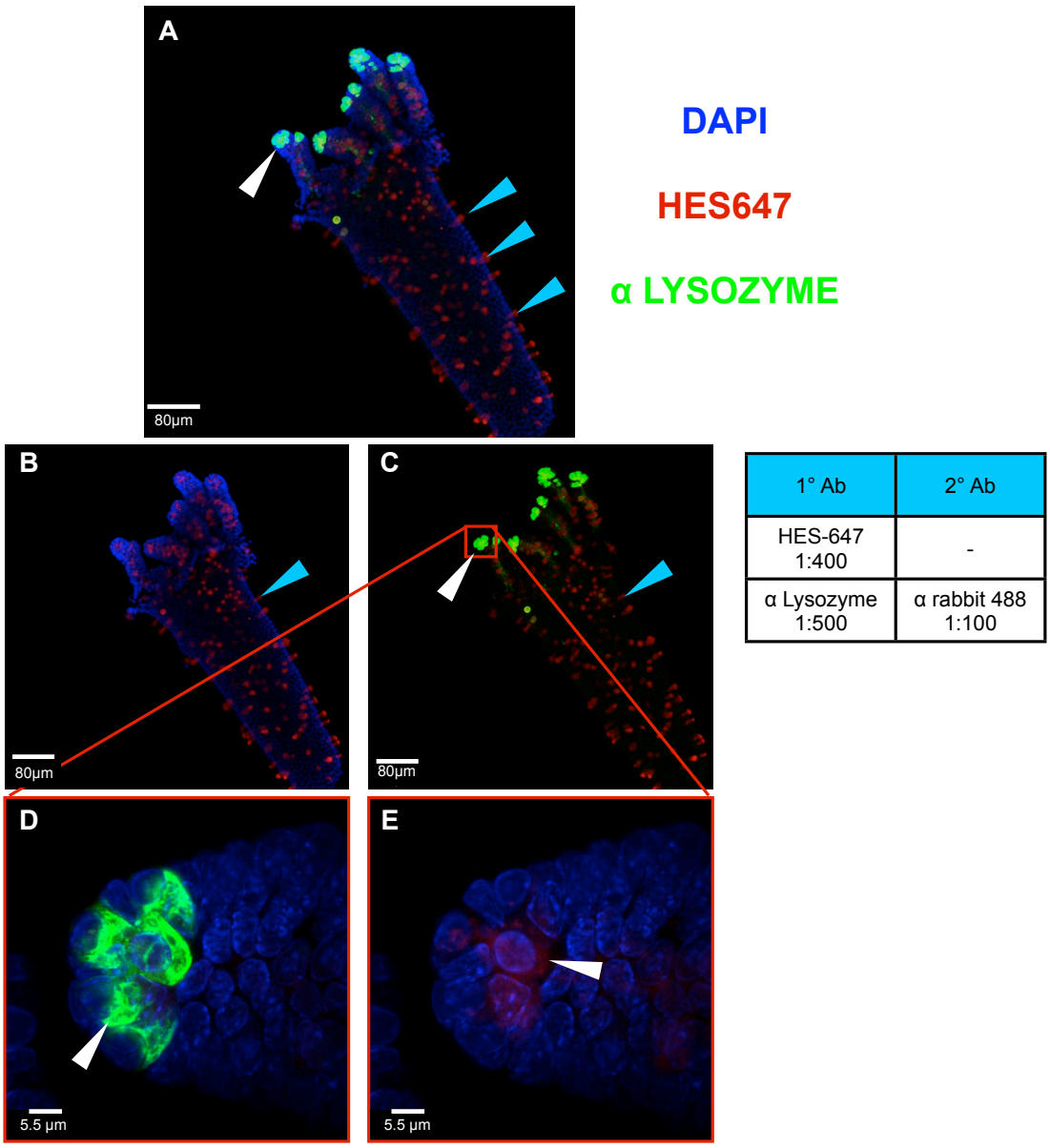

1° Ab	2° Ab
HES-647 1:400	-
α Lysozyme 1:500	α rabbit 488 1:100

Fig 4.22 HES binds to cells on the surface of the villus.

Intestinal epithelium was prepared from naive C56BL/6 mice as described previously (Fig 4.20).
Staining was carried out as described in Fig 4.21.

Paneth cells can be seen binding α-lysozyme (green) in Fig **A**, **C** and **D**. *H.polygyrus* ES (HES) was labelled with AlexaFluor 647 (Life Technologies) as per manufacturers instructions. This was diluted 1:400 and used as described previously (Fig 4.21). Binding of labelled HES to cells on the surface of the villus can be seen in **A-C**.
D & **E** show the paneth cells located at the bottom of the crypt. These cells have labelled with lysozyme (**D**) and HES (**E**).

Confocal scale bars as shown in µm.

4.23 HES and HpVAL-4 bind to villus goblet cells.

The mucosal surface of the gut is covered and protected by a layer of mucus produced by intestinal goblet cells (Escande et al., 2004). The secreted mucin in the intestine is MUC2 thus, in order to confirm the hypothesis that HES647 was indeed binding to goblet cells, tissue from a villi and crypt prep was stained with HES647 and an αMUC2 antibody.

Naïve gut tissue was prepared from C57B/6 mice and was stained with HES647 and αMUC2. As the VAL proteins, discussed previously, represent a large proportion of HES, HpVAL-4, a single domain VAL molecule, was biotinylated and used to stain a villi and crypt prep tissue. HpVAL-4 was used in this instance because the reaction to label it with biotin was more efficient than for its double domain counterpart HpVAL-1.

HES647 and the α-MUC2 antibody bind to the same cells (Fig 4.23A-C) indicating that HES647 binds to murine goblet cells as well as earlier described Paneth cells. Panel A shows an overlay of the two stains (HES647: Panel B & αMUC2 488:Panel C).

Interestingly, biotinylated HpVAL-4 also binds to the goblet cell, shown by the overlapping staining profiles in Fig 4.23 D-E.

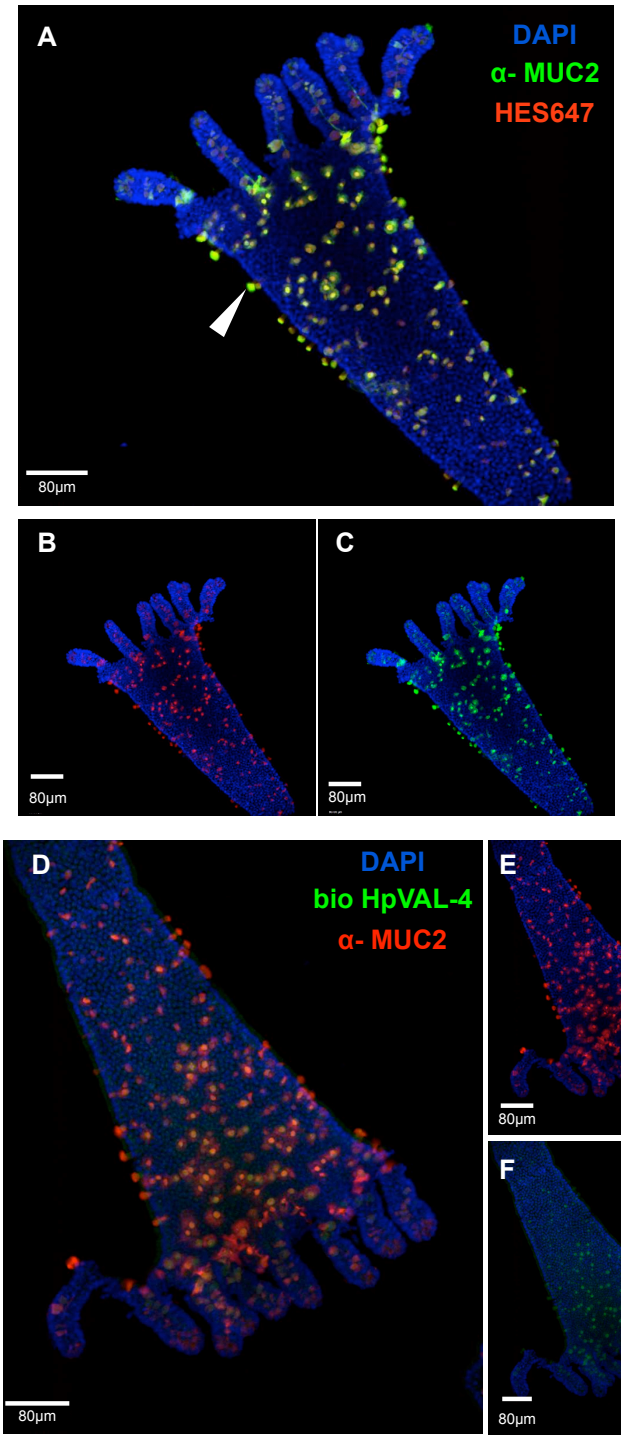

4.23 HES and HpVAL-4 bind to villus goblet cells.

Intestinal epithelium was prepared from naive C56B/6 mice as described previously (Fig 4.20).
Staining was carried out as described in Fig 4.21.

A-C. HES647 and α- MUC2 bind to goblet cells, yellow dual staining in panel **A**.
Panel **B** shows HES647 stain.
Panel **C** shows α- MUC2 stain.

D-F. Biotinylated HpVAL-4 and α- MUC2 bind to goblet cells, yellow dual staining in panel **D**.
Panel **E** shows α- MUC2 stain.
Panel **F** shows bio HpVAL-4 stain.

Confocal scale bars as shown in µm.

1° Ab	2° Ab
HES-647 1:400	-
α MUC-2 1:400	α rabbit 488 1:100
α MUC-2 1:400	α rabbit 647 1:100
bio HpVAL-4 1:400	strep 488 1:100

4.24 HpVAL-4, not HpVAL-1, binds intestinal goblet cells.

As discussed in Chapter 1, the SCP/TAPS family is well represented by the VAL proteins in *H.polygyrus* (Hewitson et al., 2011b). This highly expressed family of proteins is comprised of two distinct sets of molecules, single and double domain proteins. One of the single domain VAL proteins, HpVAL-4, binds to goblet cells present on villi that have been isolated from naïve murine gut tissue (Fig 4.23). To examine if double domain VAL proteins can also bind the goblet cell, biotinylated HpVAL-1, was used to stain a villi and crypt prep. Structurally the single and double domain VAL proteins are quite different therefore if attachment to a goblet cell relies on the assembly of a binding site, single and double domain proteins may exhibit somewhat different characteristics.

Intestinal epithelial tissue was prepared as described previously (Fig 4.20) from both naïve and Day 7 infected C57BL/6 mice. Both HpVAL-1 & HpVAL-4 had been previously biotinylated (Chapter 1, Fig 1.15). These, along with an αMUC2 antibody were incubated on tissue samples as for Fig 4.21.

HES647 bound goblet cells from both naïve and infected mice (A&B). Infected tissue displayed higher levels of MUC2 staining and an increased number of goblet cells as would be expected in a helminth infection setting (Anthony et al., 2007), (Ishikawa, Horii, Oinuma, Suganuma, & Nawa, 1994). HpVAL-1 (C&D), unlike HpVAL-4 (E&F), did not bind to goblet cells on the villus.

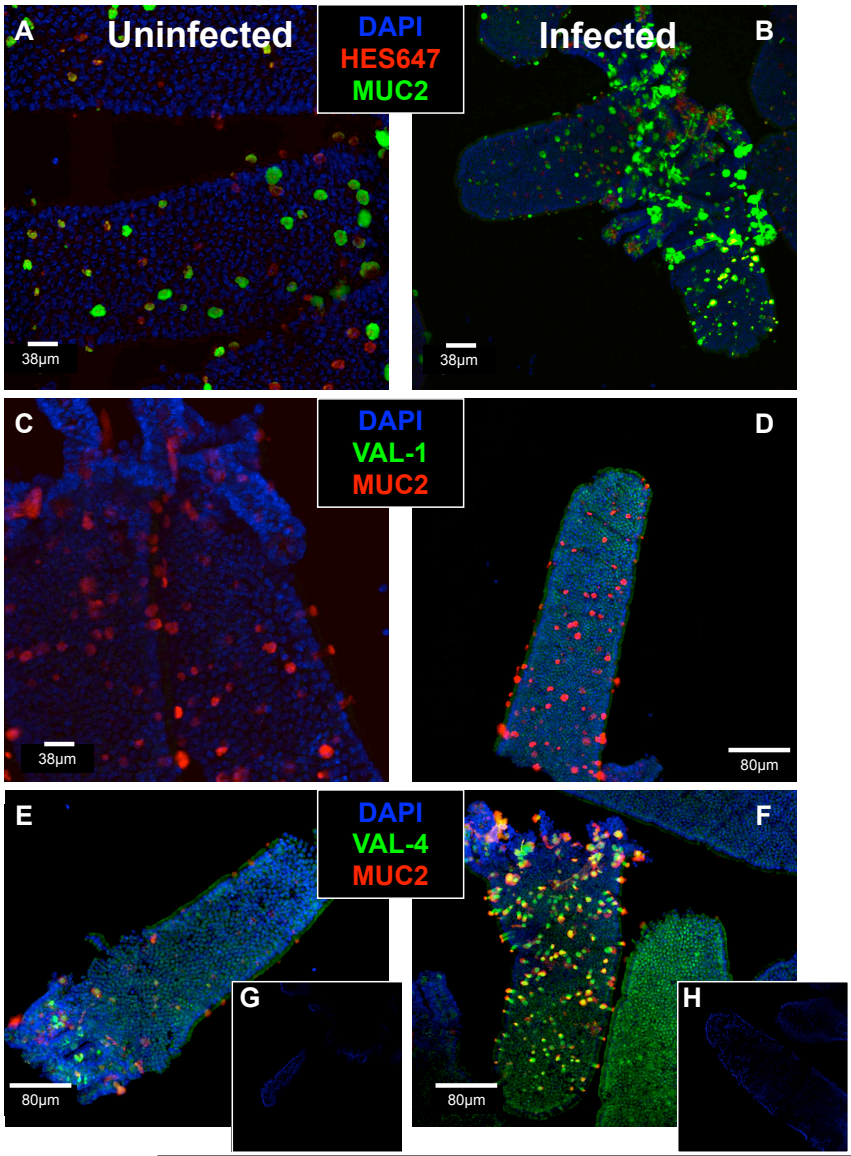

1° Ab	2° Ab
HES-647 1:400	-
α MUC-2 1:400	α rabbit 488 1:100
α MUC-2 1:400	α rabbit 647 1:100
bio HpVAL-1 1:400	strep 488 1:100
bio HpVAL-4 1:400	strep 488 1:100

4.24 HpVAL-4, not HpVAL-1, binds intestinal goblet cells.

Intestinal epithelium was prepared from naive C57BL/6 mice as described previously in Fig 4.20. Staining was carried out as described in Fig 4.21.

Intestinal epithelial tissue from naive (**A**) and infected (**B**) mice was stained with HES647 and α- MUC2.

Intestinal epithelial tissue from naive (**C**) and infected (**D**) mice was stained with Biotinylated HpVAL-1 and α- MUC2.

Intestinal epithelial tissue from naive (**E**) and infected (**F**) mice was stained with Biotinylated HpVAL-4 and α- MUC2.

Panels **G**&**H**: Control staining. Confocal scale bars as shown in µm.

4.25 - 4.26 HpVAL-4 and MUC2 binding within the goblet cell.

The intestinal goblet cell has two main characteristics 1) numerous mucin containing secretory vesicles at the luminal side of the cell and 2) a large nucleus embedded within the epithelium of the villus (Fig. 4.25).

The αMUC2 antibody binds to the mucins present in the vesicles, and also to mucin, which has been expelled from the goblet cell and is now lining the surface of the gut epithelium. To further examine HpVAL binding of goblet cells gut tissue was removed from Day 7 infected C57BL/6 mice and was prepared as described in Fig 4.20. HES647 and biotinylated HpVAL-4 were then used to stain the prepared tissue, which was visualised on a Leica confocal microscope.

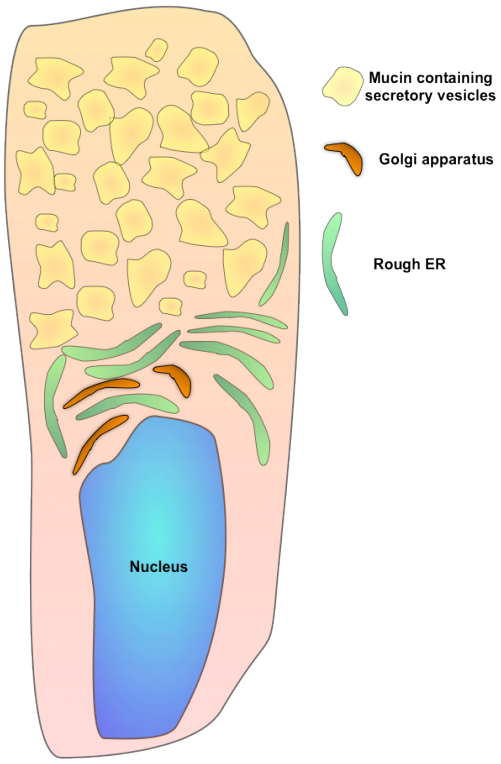

The single domain VAL protein from *H.polygyrus,* HpVAL-4, binds to an area of the cell towards the nucleus as can be seen in Fig 4.26. The green HpVAL-4 staining appears towards the base of the cell and is especially clear in Panels D & E. The αMUC2 antibody stains mucins at the top of the cell (Fig 4.26 D-F) apparently forming a cap at the end of the goblet cell with mucin dispersing into the lumen of the gut.

Fig 4.25 Goblet cell structure

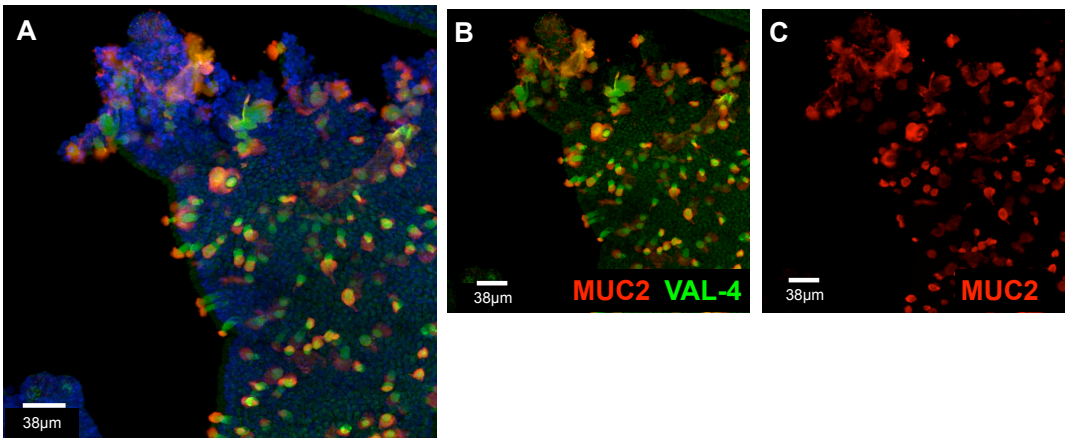

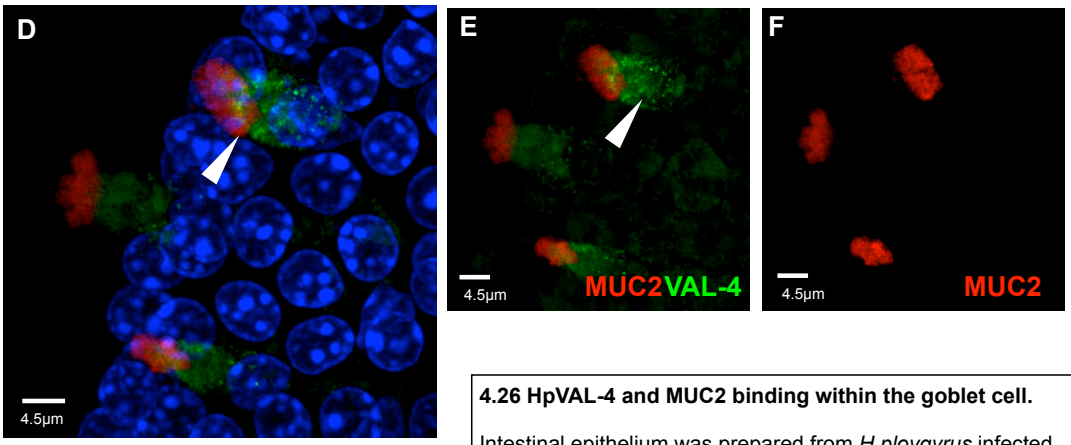

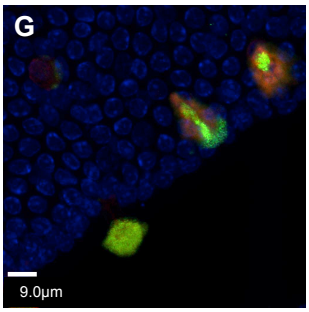

1° Ab	2° Ab
α MUC-2 1:400	α rabbit 647 1:100
bio HpVAL-4 1:400	strep 488 1:100

4.26 HpVAL-4 and MUC2 binding within the goblet cell.

Intestinal epithelium was prepared from *H.ploygyrus* infected C56BL/6 mice as described previously in Fig 4.20. Staining was carried out as described in Fig 4.21.

All panels show biotinylated HpVAL-4 and αMUC2 binding to goblet cells in the murine intestinal epithelium.

(**A**) Biotinylated HpVAL-4 & α- MUC2 staining with DAPI (X40 obj)
(**B**) Biotinylated HpVAL-4 & α- MUC2 staining.
(**C**) α- MUC2 staining alone.

(**D**) Biotinylated HpVAL-4 & α- MUC2 staining with DAPI. (X63 zoom obj)
(**E**) Biotinylated HpVAL-4 & α- MUC2 staining.
(**F**) α- MUC2 staining alone.

(**G**) HES647 & α- MUC2 staining with DAPI. (X63 zoom obj)

Confocal scale bars as shown in µm.

4.27 Intestinal goblet cells from CD24-/- mice bind HES and HpVAL-4 but not HpVAL-1; Paneth cells bind all three.

$CD24^+$ Paneth cells reside at the base of the crypt and are interspersed by Lgr5 stem cells. The relationship between the two cell types provides benefits to each, with the Lgr5 stem cells generating the Paneth cell and the Paneth cell expressing EGF, TGF, Wnt3 and Notch, all essential signals for stem cell maintenance (Sato et al., 2011). As shown earlier binding of HES647 to Paneth cells is not CD24 dependent (Fig 4.15) however the binding of the VAL proteins had not yet been examined.

To confirm previous observations of Paneth cell/HES647 binding and also to examine binding to the goblet cell, HES647 was used to stain a villi and crypt prep from naïve and Day 7 *H.polygyrus* infected CD24-/- mice. Similarly the binding capability of HpVAL-1 and HpVAL-4 to both cell types was examined.

A villi and crypt prep was prepared as described previously in Fig 4.20 and staining was performed with HES647, biotinylated HpVAL-1 and biotinylated HpVAL-4. Both biotinylated proteins were detected using a streptavidin 488 secondary antibody. The goblet cell marker, αMUC2, was included in all staining panels to localise intestinal goblet cells. Tissue was mounted using Vectashield anti-fade mountant containing DAPI on polysine slides, which were sealed with nail varnish prior to confocal microscopy.

Panel **A** (Fig 4.27) shows tissue staining from naïve CD24 -/- mice.
Panel **B** (Fig 4.27) shows staining from Day 7 *H.polygyrus* infected CD24-/- mice.
For both naïve and infected groups:

i & **ii** show HES647/ MUC2 staining.
iii & **iv** show HpVAL-1/MUC2 staining.
v & **vi** show HpVAL-4 staining.

HES647 (Fig 4.27Ai), HpVAL-1 (Fig 4.27Aii) and HpVAL-4 (Fig 4.27Aiii) all bound to Paneth cells in gut tissue from both naïve and infected mice (White arrows, Fig 4.27 A & B) although this binding appeared more diffuse than previously seen. However, only HES647 (Fig 4.27 Ai&ii, Bi&ii) and HpVAL-4 (Fig 4.27 Av&vi, Bv&vi) bound to the goblet cells, regardless of infection status, with HpVAL-1 showing no goblet cell binding.

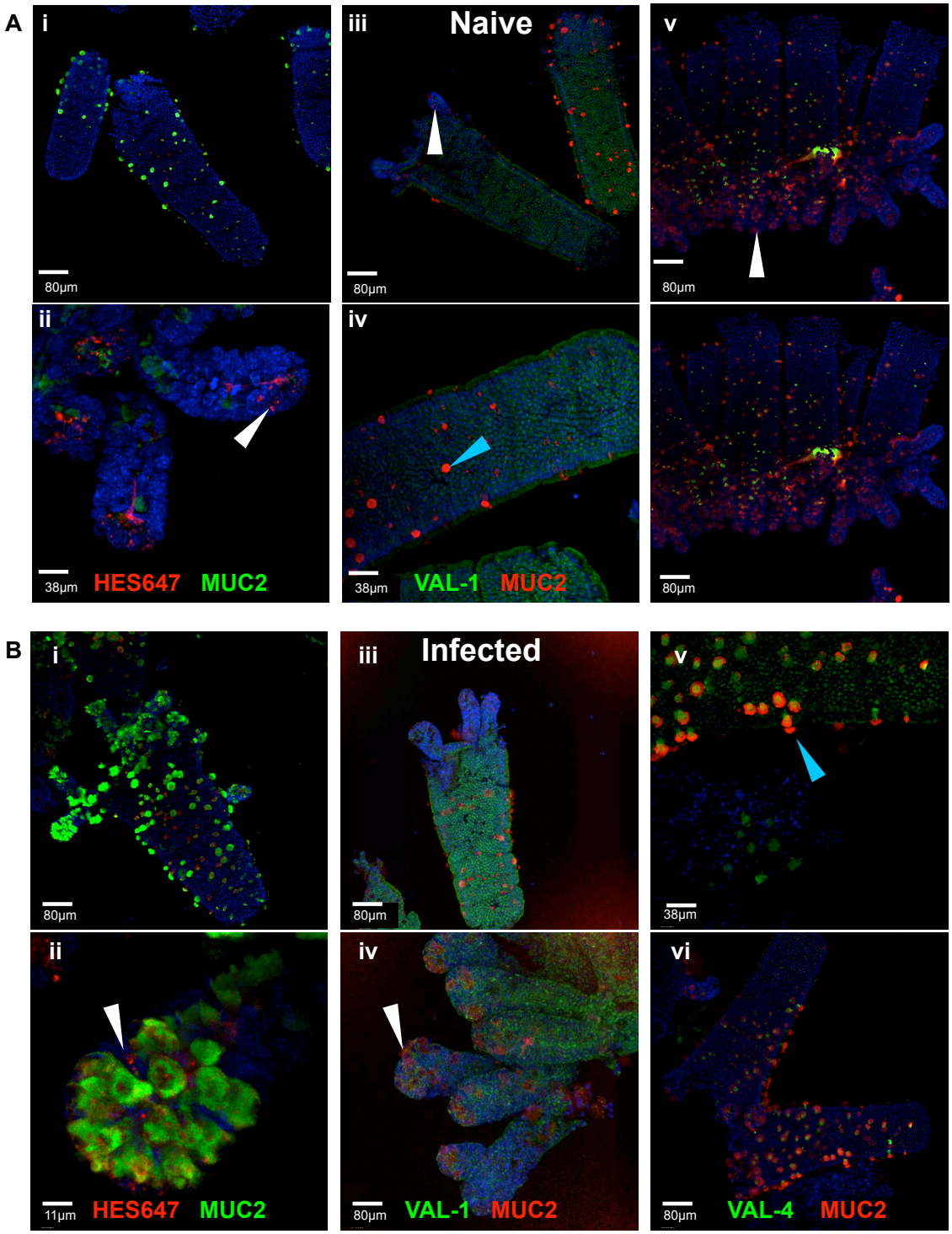

Fig 4.27 Intestinal goblet cells from CD24-/- mice bind HES and HpVAL-4 but not HpVAL-1; Paneth cells bind all three.

4.27 Intestinal goblet and Paneth cells from CD24-/- mice bind HES and HpVAL-4 but not HpVAL-1.

CD24-/- mice were infected with *H.polygyrus* for 7 days. The small intestine was prepared as described previously in Fig 4.20. Staining was carried out as described in Fig 4.21.

A Uninfected epithelial tissue was stained with:
i & ii) HES674 & MUC2
iii & iv) HpVAL-1 & MUC2
v & vi) HpVAL-4 & MUC2

B Infected epithelial tissue was stained with:
i & ii) HES674 & MUC2
iii & iv) HpVAL-1 & MUC2
v & vi) HpVAL-4 & MUC2

Confocal scale bars as shown in μm.

1° Ab	2° Ab
HES-647 1:400	-
α MUC-2 1:400	α rabbit 488 1:100
α MUC-2 1:400	α rabbit 647 1:100
bio HpVAL-1 1:400	strep 488 1:100
bio HpVAL-4 1:400	strep 488 1:100

4.28 Summary of villi and crypt staining.

A summary of staining to date shows the ability of HES647, Hp-VAL-1 and HpVAL-4 proteins and polyclonal antibodies raised against these recombinant proteins to bind to cells on and within the gut epithelium.

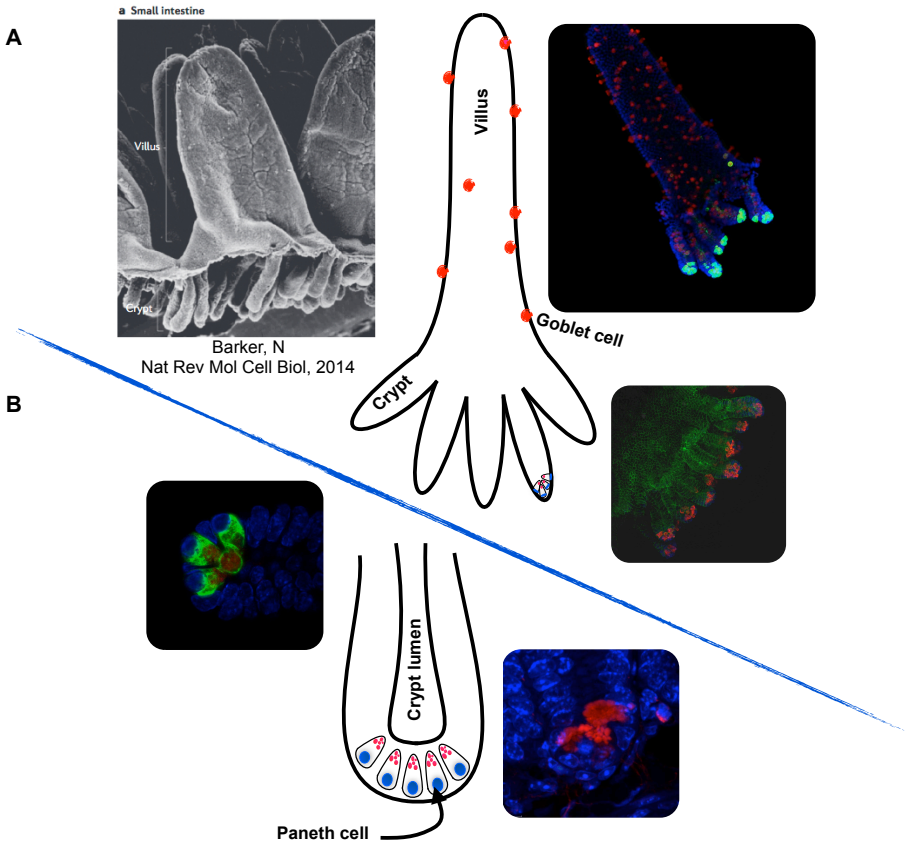

	HES647	HpVAL-1	HpVAL-4	α-HpVAL-1	α-HpVAL-4
Surface of *H.polygyrus*	✓	~	✗	✓	✗
Paneth cell	✓	✓	✓	~	~
Goblet cell	✓	✗	✓	~	~

Fig 4.28 Summary of villi and crypt staining.

A. Staining on intestinal villi
B. Staining on intestinal crypt.

Discussion

Interactions between gut helminths and the products they release, and the cells and tissues of the intestine, are key to survival of the parasite and the level of tissue distress suffered by the host (Garside, Kennedy, Wakelin, & Lawrence, 2000). Whether the parasite resides in the lumen of the gut, as is the case with *Nippostrongylus brasiliensis* (Min, Le Gros, & Paul, 2006), or is an invader of the intestinal epithelium e.g. *Trichinella spiralis* (Khan, 2008), (Patel, Kreider, Urban, & Gause, 2009), or perhaps, as with *Heligmosomoides polygyrus* (Patel et al., 2009), the parasite succeeds in penetrating through the mucosal layer and the underlying tissue, the host immune response to the assault will determine the outcome for the parasite and also the level of pathology experienced by the host. We hypothesise that the excretory secretory products produced by a parasite should have a direct effect on the cells with which they come into contact, in the case of *H.polygyrus*, cells of the intestinal epithelium. These interactions of course would occur in the reverse manner too, with host immune cells coming into contact initially with the parasite cuticle. In this chapter I have tried to examine each of the players in this cohabitation scenario.

Studies examining the whole parasite indicated that antibodies, which had been raised against the parasite secretions, bound to the cuticle, highlighting the surface structure. When used to stain a cross-section of the parasite αHES also bound to structures within the worm including the sub-cuticular muscle layer. A panel of monoclonal antibodies, which were generated from an infection of C57BL/6 mice with *H.polygyrus* ((Hewitson et al., 2011a), was also extremely important in characterization of the cuticle, one of the protective mechanisms of the parasite. In particular, an antibody (α-Glycan A 13.1), which had been characterised previously and revealed binding via O-linked glycans present on HpVAL-1 (Hewitson et al., 2011a), bound the cuticle of both male and female parasites highlighting the cuticular ridges and furrows which run down the length of the parasite. These are very similar to ridges described on *N.brasiliensis* (Lee, 1965). After treatment of the cuticle with ethanol and CTAB washes, the binding of αCHO 13.1 to constituents of the cuticle was confirmed by western blot. The resulting blot produced very similar

results to those observed following surface iodination and detection of labelled proteins with an αHES polyclonal antibody.

Another very informative tool was the direct labeling of the excretory secretory products from the parasite with Alexa Fluor ®647.
Parasites located within granuloma structures, which are formed during an *H.polygyrus* infection, were stained with the labelled HES in both naïve and infected C57BL/6 mice. Although granulomas are a well-described consequence of infection with *H.polygyrus,* their function has not yet been fully explained (Harris & Gause, 2011), (Patel et al., 2009), (Reynolds et al., 2012). Surrounding the parasites within the granuloma the cells infiltrate has been previously characterized with the presence of macrophages being confirmed here by F4/80 and CD11b staining. Interestingly, some of these cells were also stained with HES647. The cuticle staining seen with HES647 remained throughout 9 days of infection, which sees a parasite move from its initial penetration of the duodenal wall as an infective larvae, followed by encystment and molting within the wall of the gut, to its eventual reemergence into the gut lumen as an adult.

Examination of stained sections from infected gut tissue throughout the 9-day infection uncovered staining of another gut cell type not previously observed; the Paneth cell. Located deep within the Crypts of Lieberkühn, the roles of the Paneth cells include creating a suitable environment for the neighbouring epithelial stem cells, along with production of antimicrobial peptides and proteins, which are released during microbial challenge (Clevers & Bevins, 2013), (van Es & Clevers, 2014), (Porter, Bevins, Ghosh, & Ganz, 2002).

As discussed in Chapter 1 (Fig 1.16), HES binds to naïve B cells in a CD24 dependent manner (James Hewitson). Paneth cells are known to express CD24 (Sato et al., 2011), however the binding of HES to Paneth cells is independent of CD24, as Paneth cells in sections from CD24-/- mice stained with HES647 both at an early (Day 7 post infection) and a late (Day 28 post infection) time point. It was also apparent that the binding of HES647 to Paneth cells was a heat stable interaction, as

HES647, which had been boiled prior to staining, still recognized the cells in the sections. The cuticle of parasites infecting μMT mice also labeled with HES647, interestingly, the same staining was observed using the anti-glycan A antibody (α-Glycan A 13.1), suggesting the mechanism for HES binding to the cuticle of the parasite may be carbohydrate mediated. This would explain the heat stable nature of the interaction.

Examining sections of gut tissue, although informative, is very much dependent on the exact location from which the tissue section was taken, and may on occasion not represent the whole picture. To enable a more global picture of the events happening in the gut, whole mount tissue samples were prepared to allow visualization of whole villi and intact crypts. This procedure was used to define the secretory abilities of tuft cells and allows for an overall depiction of gut/ parasite interactions (Gerbe et al., 2011). Staining of the villi confirmed, in a most dynamic manner, the binding of HES to Paneth cells. Intriguingly, it was at this point that the binding of HES to a second cell type was observed; the goblet cell. Confirmation of goblet cell binding was achieved using an αMUC2 antibody, which co-localized strikingly with HES647.

A second method utilized to follow the interactions of a protein involved the use of biotin and subsequent detection of the biotinylated protein with a streptavidin conjugate. Thus, HpVAL-1 & 4 were labelled with biotin and their ability to bind cells or tissue on the villi was examined. HpVAL-1 displayed binding to Paneth cells only, however, its single domain counterpart, HpVAL-4, bound to both Paneth and goblet cells in a similar manner to HES647. Both HES647 and HpVAL-4 bound to part of the goblet cell with the closest proximity to the nucleus, with the αMUC2 antibody binding to form a labeled mucin cap. It was also demonstrated that binding patterns observed for HpVAL-1 and HpVAL-4 were not affected by the infection status of the mouse i.e. naïve vs infected.

Thus, in this chapter I have shown that *H.polygyrus* excretory secretory products bind to the cuticle of the parasite and more interestingly to specific cells of the murine gut. These cells, the Paneth and goblet cell, play key roles within the intestine.

The Paneth cell has more than one significant role in the gut environment. Firstly, via the release of anti-microbial peptides and proteins, the balance between pathogenic bacteria and the host resident microbiota can be maintained. Secondly through the expression of EGF, TGF, Wnt3 and Notch ligand, all of which are necessary for the maintenance of stem cells, a suitable environment is created for the columnar stem cells located between the Paneth cells (Sato et al., 2011), (Clevers & Bevins, 2013), (Ayabe et al., 2000). Indirectly, maintenance of the stem cell population in the crypts has a knock-on effect on the second cell type that was recognized by HES and HpVALs. Microbial protection of the stem cells ensures renewal of intestinal epithelium cells as required, including the goblet cell.

The main function of the goblet cell is mucus production (Specian & Oliver, 1991), (Khan, 2013) although recently it has been suggested they are involved in antigen presentation to intestinal dendritic cells (McDole et al., 2012). In the intestinal environment this layer of mucus effectively separates the resident commensal bacteria from the epithelial cell layer. Compromising this mucus in any way allows entry for the bacteria to the epithelium and subsequent host inflammation.

Binding of HES and of the VAL proteins to these two key intestinal cell types may have detrimental effects on their function and in so doing change the nature of the gut environment, however this possibility has yet to be studied.

Final Discussion and Future Directions

The focus of this thesis has been the examination of the ability of a parasite to remain within a host for extended periods without triggering an immune response. To be successful a parasite must achieve a fine balance between adapting the surrounding environment to meet its lifecycle requirements and yet, at the same time, not causing such upset that a strong immune response results. Such a response could trigger expulsion of the parasite and eliciting a damaging inflammatory event for the host. Manipulation of host immune responses has been a central feature of my research, with particular emphasis on the interactions of parasite products with host cells.

In Chapter 1 a family of proteins was introduced which is highly represented not only in chronic parasites such as *H.polygyrus*, but is also in plants and free-living nematodes, hymenopteran insects and mammals (Gao et al., 2001b), (Suck et al., 2000), (Gibbs et al., 2006), (Hawdon et al., 1999). The VAL proteins are characterised by the presence of a signature sequence motif, the SCP/TAPS domain, and have been described structurally from a number of helminths. The function of these proteins however remains unclear with putative functions including lipid binding, inhibition of neutrophil function and B-cell receptor binding (Rieu, Ueda, Haruta, Sharma, & Arnaout, 1994), (Kelleher et al., 2014), (Chapter 1, Fig 1.17) & (Tribolet et al., 2014). Attribution of a single function for these proteins is unlikely, given the hugely diverse circumstances and locations in which VAL-like proteins are located. Indeed, diversity also occurs within VAL proteins from a single parasite such as *H.polygyrus* or *Haemonchus contortus*, with a number of sequence polymorphisms identified (Hewitson et al., 2011b), (Yatsuda, Krijgsveld, Cornelissen, Heck, & de Vries, 2003).

The study of VAL proteins, and other potential immunomodulatory molecules which are produced by a parasite, presents a number of practical issues. *In vitro* studies undertaken with recombinant proteins give huge insights into potential interactions between the parasite and the host, nonetheless careful consideration must be taken when choosing the method by which recombinant proteins are generated. Many

studies have been carried out using VAL proteins, which have been generated using either bacterial, or yeast based expression systems. Each system comes with a number of caveats to bear in mind. Often proteins generated using *Escherichia coli* are insoluble and hence incorrectly folded. Moreover, the inevitable presence of lipopolysaccharide (LPS) makes cellular assays such as the measurement of cytokine responses especially difficult. When considering recombinant protein production it may be desirable to codon optimise a gene for the chosen expression system. Finally, each recombinant expression system generates proteins decorated with post-translational modifications (Chapter 1, Fig 1.27). These should be considered when examining different recombinant protein expression systems. Moreover, as each newly expressed protein will undoubtedly behave differently in each expression system, the ability to easily move a gene construct from one system to another would be ideal.

In Chapter 2 the focus switches to allow investigation into the effects of the VAL protein *in vivo.* Studies on the effects of parasite proteins *in vivo* remain difficult in parasitic helminths, as transgenesis and targeted gene deletion are not yet possible. Thus, putative gene function was examined using a heterologous expression system in *Leishmania mexicana*. Although initial results suggested that insertion of the Bm-VAL-1 gene increased parasite virulence, as indicated by an increased footpad swelling and parasite recovery, results from subsequent experiments were equally conclusive however, they were alternately contradictory. Perhaps insertion of the Bm-VAL-1 gene produced a very subtle effect, one where slight variations in experimental constituents could affect the outcome. Examining the effect of expression of a protein from a human filarial parasite in a murine system may also have overextended the potential for this experimental set-up. Thus investigation into the effects of HpVAL-4, a murine gene product, may be more informative. RNAi examination of gene function remains a promising avenue for further perusal, however as the gene table in Chapter 1, Table 1.2 shows, it is unclear if *H.polygyrus* expresses all of the machinery required for efficient knockdown to occur.

Chapter 3 investigated the potential immunomodulatory function of VAL proteins using an allergic airway inflammation model. This model has been used to investigate the immunomodulatory properties of excretory/secretory products from *H.polygyrus* (HES) previously (McSorley et al., 2012), thus its use to study single proteins (VALs) isolated from HES not only provided information about these proteins but also supplemented data produced with HES. The AAI model has also been used to study effects of various parasite-derived moieties such as *S.mansoni* antigens (Cardoso et al., 2010), *S.japonicum* (Mo et al., 2008) and *Ansiakis simplex* (Park et al., 2009). Whilst results from the experiments carried out in Chapter 3 show that HpVAL-4 is able to reduce eosinophilia in this model, reductions are not as striking as observed with HES. It should be considered that HpVAL-4 is one of many VAL proteins present in HES, and that these proteins may function together as a group or in conjunction with other HES derived molecules.

There are many models examining airway inflammation, with aspects of each model able to address different characteristics of the disease. An interesting article by Allen et al reviewed a number of animal models used to study airway inflammation. This highlighted the fact that the model used in this study, although providing valuable data regarding immune-mediated events, does not address tissue remodelling that occurs during a chronic asthmatic situation (Allen et al., 2009). When considering VAL proteins in an *H.polygyrus* infection setting, they are represented during most life-cycle stages (Hewitson et al., 2013), thus exposure of the host to these molecules would be over a relatively long period. However, investigators examining homologous proteins in hookworms believe these to be secreted mainly as the parasite enters the host forming a more acute insult (Hawdon et al., 1999). As VAL/ASP family proteins are so diverse perhaps, they have evolved for functions in both acute and chronic settings.

To extend the study of HpVAL proteins further, a second model of asthma could be examined which involves the use of *Alternaria alternata*, a fungal extract that induces a strong Th2 allergic response (Kobayashi et al., 2009). This model sensitises the mouse using intranasal administration of allergen, thus inducing better responses at the lung airway epithelium. As *H.polygyrus* inhabits the murine

intestine, secretions from the parasite will come into direct contact with epithelial cells, consequently VAL proteins may have become adapted to interact with these cells directly.

Chapter 4 examined interactions occurring between the parasite (*H.polygyrus*) and the host (mouse). The nature of parasite-host relationships requires an intimate level of contact between the two, thus in order to coexist these interactions have developed to be mutually beneficial. As *H.polygyrus* resides in the intestine, interactions between intestinal epithelial cells and the excretory/secretory products from the parasite would be expected. A combination of detailed microscopy techniques revealed that products from the parasite do indeed interact with host cells, although any consequences of these interactions now have to be explored. Two key cell types in intestinal epithelium were shown to bind to HES and VAL proteins, the goblet cell and Paneth cells. These cells are hugely important for effective host immunity; goblet cells are responsible for the production of mucus, which has dual roles of 1) aiding parasite expulsion and 2) provision of a suitable eco-environment for the resident microflora. Intimately linked to goblet cells, the Paneth cell nurtures the crypt niche and in so doing, provides optimal conditions for resident stem cell population whilst secreting a cocktail of molecules, which may also affect favourably the gut microbiota (Artis, 2008), (Sato et al., 2011), (Clevers & Bevins, 2013).

Goblet cells have been discussed throughout this thesis (Chapter 3 and 4). Binding of HES and VAL proteins was demonstrated in gut epithelial cells, however it would be interesting to determine if this interaction was a mucin based reaction or specific to gut derived goblet cells. Staining of airway epithelial cells following an *Alternaria alternata* protocol would demonstrate if HES and HpVAL bound to all goblet cells, or alternatively show if this was a gut specific interaction occurring given that *H.polygyrus* is a gut dwelling nematode. Equally, if binding of HES and VAL is a mucus dependent interaction, this could indeed be for a specific mucin and could be addressed by whole mount staining of Muc5 -/- mice.

Paneth cells contain a complex collection of molecules within their secretory granules. Alpha-defensins, cryptidins and anti-microbial molecules all play a role in maintenance of the crypt environment with further influences reaching into the gut lumen (Wilson et al., 1999), (Ayabe et al., 2000). It is not clear from results shown in Chapter 4 if HES or HpVAL proteins bind to one specific molecule within these granules. These may be identified by RT-PCR from known granule components; however dissecting granule information from the surrounding tissue may prove difficult. Paneth cells could be isolated from epithelial tissue using laser capture microdissection, which would refine the cells being examined by RT-PCR (Erickson, Gillespie, & Emmert-Buck, 2008). Equally, the effect of parasite derived protein binding may be affected by the infection status of the host. Paneth cells are understood to release the contents of their granules upon detection of bacterial products, perhaps this also occurs upon detection of parasite-derived products (Bevins & Salzman, 2011). Thus, microdissection of crypts from infected and naïve mice could give indications of changes undergone in the Paneth cell granule contents.

Another protocol recently describe by Sato et al, which has been used to study cell death in intestinal epithelial cells, is that of *in vitro* organoid culture (Sato et al., 2009), (Grabinger et al., 2014). The ability to grow intestinal crypts is a relatively new procedure, which could allow for further investigation into molecular binding properties of the resident cells.

By binding to both Paneth and goblet cells, HES and HpVAL-4 may be influential in adjusting the commensal bacteria found within the gut to favour parasite development. Indeed, Reynolds et al demonstrated that *Lactobacillus* spp were found in particular abundance in *H.polygyrus* infected mice and this positively correlated with parasite infection (Reynolds et al., 2014). The binding of parasite molecules to these two key cell types may also be instrumental in changing the gut mucus that has been suggested to have a key role in parasite establishment. Thus, *H.polygyrus* may exert influences on two key factors that influence the gut environment and physiology, ensuring parasite survival.

It appears then that *H.polygyrus* may be more tightly entwined in the functions of these two key cell types and immunity in the gut than previously thought.

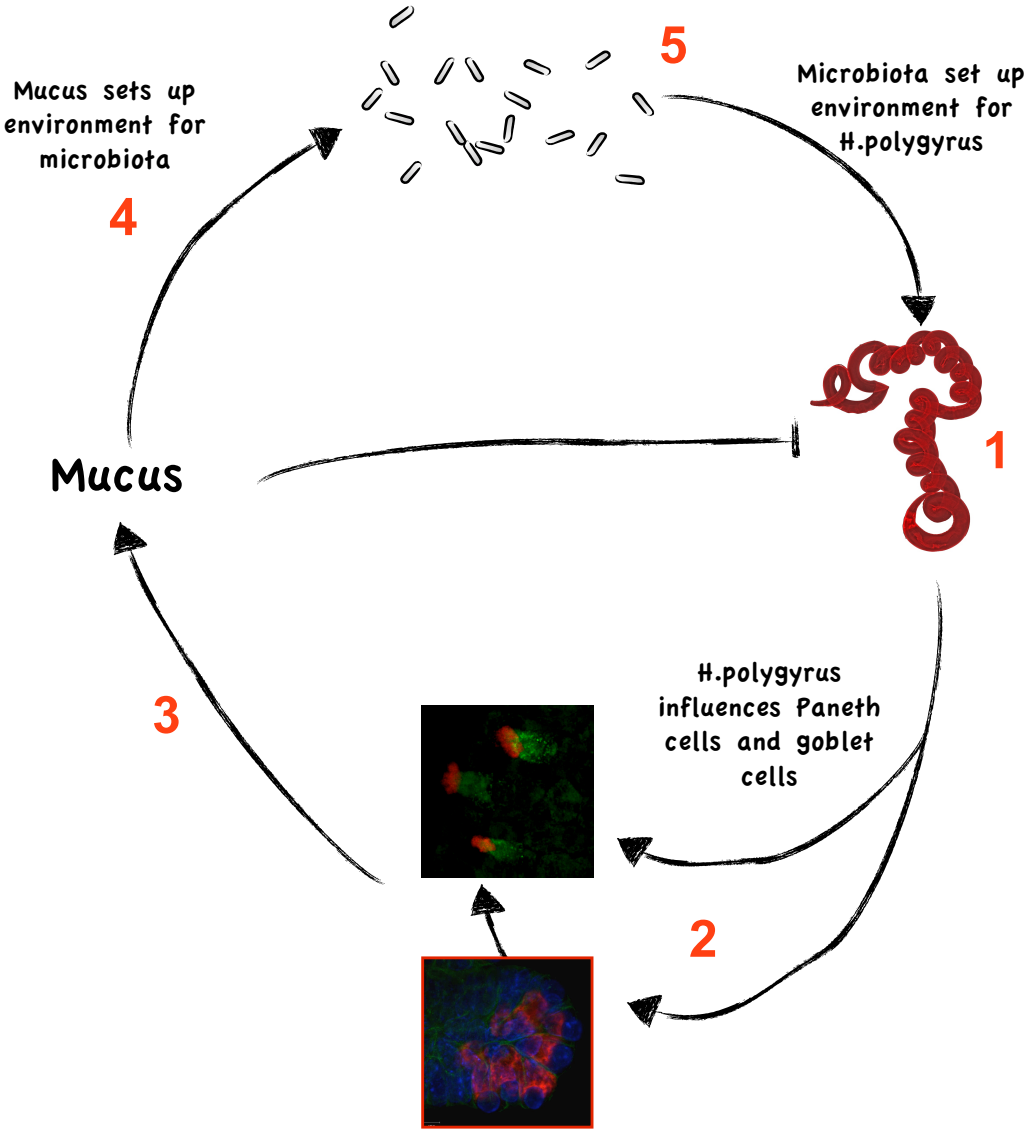

Fig D1. Interactions between *H.polygyrus*, intestinal cells, mucus and the microbiota.

1 *H.polygyrus* interacts directly with Paneth and goblet cells although the consequences of these interactions are as yet not understood.

2 Paneth cell function may be altered and subsequently affect goblet cell numbers and/or function.

3 Mucus produced by goblet cells is important for the microbiota (4) inhabiting in intestine, which, are in turn linked to parasite's ability to establish and proliferate (5).

Finally, the experiments described throughout this thesis were designed to examine the close relationship shared by parasite and host. This is defined by suites of molecules produced by the both parasite and host, and how these molecules interact with the cells and tissue with which they come into contact. Both parasite and host and equally the molecules produced by each, are highly complex, and as such require continued research to unravel the consequences they exert over each other.

References

Abreu, M. T. 2010. Toll-like receptor signalling in the intestinal epithelium: how bacterial recognition shapes intestinal function. ***Nat Rev Immunol***, 10(2): 131-144.

Aebischer, T. 2014. Leishmania spp. Proteome Data Sets: A Comprehensive Resource for Vaccine Development to Target Visceral Leishmaniasis. ***Front Immunol***, 5: 260.

Aguilar Torrentera, F., Lambot, M. A., Laman, J. D., Van Meurs, M., Kiss, R., Noel, J. C., & Carlier, Y. 2002. Parasitic load and histopathology of cutaneous lesions, lymph node, spleen, and liver from BALB/c and C57BL/6 mice infected with Leishmania mexicana. ***Am J Trop Med Hyg***, 66(3): 273-279.

Akira, S., Uematsu, S., & Takeuchi, O. 2006. Pathogen recognition and innate immunity. ***Cell***, 124(4): 783-801.

Alberts B, J. A., Lewis J, et al. 2002. ***Molecular Biology of the Cell. 4th edition.***: Garland Science.

Alkazmi, L. M., & Behnke, J. M. 2013. The mucosal response of hamsters exposed to weekly repeated infections with the hookworm Ancylostoma ceylanicum. ***J Helminthol***, 87(3): 309-317.

Alkazmi, L. M., Dehlawi, M. S., & Behnke, J. M. 2008. The mucosal cellular response to infection with Ancylostoma ceylanicum. ***J Helminthol***, 82(1): 33-44.

Allen, J. E., Bischof, R. J., Sucie Chang, H. Y., Hirota, J. A., Hirst, S. J., Inman, M. D., Mitzner, W., & Sutherland, T. E. 2009. Animal models of airway inflammation and airway smooth muscle remodelling in asthma. ***Pulm Pharmacol Ther***, 22(5): 455-465.

Allen, J. E., Daub, J., Guiliano, D., McDonnell, A., Lizotte-Waniewski, M., Taylor, D. W., & Blaxter, M. 2000. Analysis of genes expressed at the infective larval stage validates utility of Litomosoides sigmodontis as a murine model for filarial vaccine development. ***Infect Immun***, 68(9): 5454-5458.

Allen, J. E., & Maizels, R. M. 2011. Diversity and dialogue in immunity to helminths. ***Nat Rev Immunol***, 11(6): 375-388.

Anthony, R. M., Rutitzky, L. I., Urban, J. F., Jr., Stadecker, M. J., & Gause, W. C. 2007. Protective immune mechanisms in helminth infection. ***Nat Rev Immunol***, 7(12): 975-987.

Anthony, R. M., Urban, J. F., Jr., Alem, F., Hamed, H. A., Rozo, C. T., Boucher, J.-L., Van Rooijen, N., & Gause, W. C. 2006. Memory T(H)2 cells induce alternatively activated macrophages to mediate protection against nematode parasites. ***Nat Med***, 12(8): 955-960.

Aranzamendi, C., de Bruin, A., Kuiper, R., Boog, C. J., van Eden, W., Rutten, V., & Pinelli, E. 2013. Protection against allergic airway inflammation during the chronic and acute phases of Trichinella spiralis infection. ***Clin Exp Allergy***, 43(1): 103-115.

Aranzamendi, C., Fransen, F., Langelaar, M., Franssen, F., van der Ley, P., van Putten, J. P., Rutten, V., & Pinelli, E. 2012. Trichinella spiralis-secreted products modulate DC functionality and expand regulatory T cells in vitro. ***Parasite Immunol***, 34(4): 210-223.

Artis, D. 2008. Epithelial-cell recognition of commensal bacteria and maintenance of immune homeostasis in the gut. ***Nat Rev Immunol***, 8(6): 411-420.

Artis, D., Wang, M. L., Keilbaugh, S. A., He, W., Brenes, M., Swain, G. P., Knight, P. A., Donaldson, D. D., Lazar, M. A., Miller, H. R., Schad, G. A., Scott, P., & Wu, G. D. 2004. RELMbeta/FIZZ2 is a goblet cell-specific immune-effector molecule in the gastrointestinal tract. ***Proc Natl Acad Sci U S A***, 101(37): 13596-13600.

Asojo, O. A., Goud, G., Dhar, K., Loukas, A., Zhan, B., Deumic, V., Liu, S., Borgstahl, G. E., & Hotez, P. J. 2005. X-ray structure of Na-ASP-2, a pathogenesis-related-1 protein from the nematode parasite, Necator americanus, and a vaccine antigen for human hookworm infection. ***J Mol Biol***, 346(3): 801-814.

Aumuller, E., Schramm, G., Gronow, A., Brehm, K., Gibbs, B. F., Doenhoff, M. J., & Haas, H. 2004. Echinococcus multilocularis metacestode extract triggers human basophils to release interleukin-4. ***Parasite Immunol***, 26(10): 387-395.

Ayabe, T., Satchell, D. P., Wilson, C. L., Parks, W. C., Selsted, M. E., & Ouellette, A. J. 2000. Secretion of microbicidal alpha-defensins by intestinal Paneth cells in response to bacteria. ***Nat Immunol***, 1(2): 113-118.

Babu, S., & Nutman, T. B. 2012. Immunopathogenesis of lymphatic filarial disease. ***Semin Immunopathol***, 34(6): 847-861.

Bahlool, Q. Z., Skovgaard, A., Kania, P. W., & Buchmann, K. 2013. Effects of excretory/secretory products from Anisakis simplex (Nematoda) on immune gene expression in rainbow trout (Oncorhynchus mykiss). ***Fish Shellfish Immunol***, 35(3): 734-739.

Balazovich, K. J., Fernandez, R., Hinkovska-Galcheva, V., Suchard, S. J., & Boxer, L. A. 1996. Transforming growth factor-beta1 stimulates degranulation and oxidant release by adherent human neutrophils. ***J Leukoc Biol***, 60(6): 772-777.

Balic, A., Harcus, Y., Holland, M. J., & Maizels, R. M. 2004. Selective maturation of dendritic cells by Nippostrongylus brasiliensis-secreted proteins drives Th2 immune responses. ***Eur J Immunol***, 34(11): 3047-3059.

Banerjee, D., & Pettit, S. 1984. Endogenous avidin-binding activity in human lymphoid tissue. ***J Clin Pathol***, 37(2): 223-225.

Bansemir, A. D., & Sukhdeo, M. V. 1994. The food resource of adult Heligmosomoides polygyrus in the small intestine. ***J Parasitol***, 80(1): 24-28.

Bansemir, A. D., & Sukhdeo, M. V. 2001. Intestinal distribution of worms and host ingesta in Nippostrongylus brasiliensis. ***J Parasitol***, 87(6): 1470-1472.

Barker, N., van Es, J. H., Kuipers, J., Kujala, P., van den Born, M., Cozijnsen, M., Haegebarth, A., Korving, J., Begthel, H., Peters, P. J., & Clevers, H. 2007. Identification of stem cells in small intestine and colon by marker gene Lgr5. ***Nature***, 449(7165): 1003-1007.

Barlow, J. L., Bellosi, A., Hardman, C. S., Drynan, L. F., Wong, S. H., Cruickshank, J. P., & McKenzie, A. N. J. 2012. Innate IL-13-producing nuocytes arise during allergic lung inflammation and contribute to airways hyperreactivity. ***J Allergy Clin Immunol***, 129(1): 191-198.e191-194.

Bartemes, K. R., Iijima, K., Kobayashi, T., Kephart, G. M., McKenzie, A. N., & Kita, H. 2012. IL-33-responsive lineage- CD25+ CD44(hi) lymphoid cells

mediate innate type 2 immunity and allergic inflammation in the lungs. ***Journal of immunology (Baltimore, Md : 1950)***, 188(3): 1503-1513.
Baumgart, M., Tompkins, F., Leng, J., & Hesse, M. 2006. Naturally occurring CD4+Foxp3+ regulatory T cells are an essential, IL-10-independent part of the immunoregulatory network in Schistosoma mansoni egg-induced inflammation. ***Journal of immunology (Baltimore, Md : 1950)***, 176(9): 5374-5387.
Behnke, J., & Harris, P. D. 2010. Heligmosomoides bakeri: a new name for an old worm? ***Trends Parasitol***, 26(11): 524-529.
Behnke, J. M., Keymer, A. E., & Lewis, J. W. 1991. Heligmosomoides polygyrus or Nematospiroides dubius? ***Parasitol Today***, 7(7): 177-179.
Belkaid, Y., & Rouse, B. T. 2005. Natural regulatory T cells in infectious disease. ***Nat Immunol***, 6(4): 353-360.
Bennett, C. L., Misslitz, A., Colledge, L., Aebischer, T., & Blackburn, C. C. 2001. Silent infection of bone marrow-derived dendritic cells by Leishmania mexicana amastigotes. ***Eur J Immunol***, 31(3): 876-883.
Benoit, M., Desnues, B., & Mege, J.-L. 2008. Macrophage polarization in bacterial infections. ***Journal of immunology (Baltimore, Md : 1950)***, 181(6): 3733-3739.
Bergenfeldt, M., Nystrom, M., Bohe, M., Lindstrom, C., Polling, A., & Ohlsson, K. 1996. Localization of immunoreactive secretory leukocyte protease inhibitor (SLPI) in intestinal mucosa. ***J Gastroenterol***, 31(1): 18-23.
Berger, A. 2000. Th1 and Th2 responses: what are they? ***BMJ***, 321(7258): 424.
Bernhagen, J., Calandra, T., & Bucala, R. 1998. Regulation of the immune response by macrophage migration inhibitory factor: biological and structural features. ***J Mol Med (Berl)***, 76(3-4): 151-161.
Bernhagen, J., Calandra, T., Mitchell, R. A., Martin, S. B., Tracey, K. J., Voelter, W., Manogue, K. R., Cerami, A., & Bucala, R. 1993. MIF is a pituitary-derived cytokine that potentiates lethal endotoxaemia. ***Nature***, 365(6448): 756-759.
Bevins, C. L., & Salzman, N. H. 2011. Paneth cells, antimicrobial peptides and maintenance of intestinal homeostasis. ***Nat Rev Microbiol***, 9(5): 356-368.
Bezencon, C., Furholz, A., Raymond, F., Mansourian, R., Metairon, S., Le Coutre, J., & Damak, S. 2008. Murine intestinal cells expressing Trpm5 are mostly brush cells and express markers of neuronal and inflammatory cells. ***J Comp Neurol***, 509(5): 514-525.
Bhopale, G. M. 2003. Pathogenesis of toxoplasmosis. ***Comp Immunol Microbiol Infect Dis***, 26(4): 213-222.
Biasucci, G., Benenati, B., Morelli, L., Bessi, E., & Boehm, G. 2008. Cesarean delivery may affect the early biodiversity of intestinal bacteria. ***The Journal of nutrition***, 138(9): 1796S-1800S.
Bickle, Q. D. 2009. Radiation-attenuated schistosome vaccination--a brief historical perspective. ***Parasitology***, 136(12): 1621-1632.
Blaxter, M. L., Page, A. P., Rudin, W., & Maizels, R. M. 1992. Nematode surface coats: actively evading immunity. ***Parasitol Today***, 8(7): 243-247.
Bloom, B. R. 1979. Games parasites play: how parasites evade immune surveillance. ***Nature***, 279(5708): 21-26.

Bloom, B. R., & Bennett, B. 1966. Mechanism of a reaction in vitro associated with delayed-type hypersensitivity. ***Science***, 153(3731): 80-82.

Bluestone, J. A., & Abbas, A. K. 2003. Natural versus adaptive regulatory T cells. ***Nat Rev Immunol***, 3(3): 253-257.

Boisvenue, R. J., Stiff, M. I., Tonkinson, L. V., & Cox, G. N. 1991. Protective studies in sheep immunized with cuticular collagen proteins and peptides of Haemonchus contortus. ***Parasite Immunol***, 13(3): 227-240.

Bolas-Fernandez, F., & Corral Bezara, L. D. 2006. TSL-1 antigens of Trichinella: an overview of their potential role in parasite invasion, survival and serodiagnosis of trichinellosis. ***Res Vet Sci***, 81(3): 297-303.

Borloo, J., Geldhof, P., Peelaers, I., Van Meulder, F., Ameloot, P., Callewaert, N., Vercruysse, J., Claerebout, E., Strelkov, S. V., & Weeks, S. D. 2013. Structure of Ostertagia ostertagi ASP-1: insights into disulfide-mediated cyclization and dimerization. ***Acta Crystallogr D Biol Crystallogr***, 69(Pt 4): 493-503.

Bottner, M., Krieglstein, K., & Unsicker, K. 2000. The transforming growth factor-betas: structure, signaling, and roles in nervous system development and functions. ***J Neurochem***, 75(6): 2227-2240.

Bowles, V. M., Brandon, M. R., & Meeusen, E. 1995. Characterization of local antibody responses to the gastrointestinal parasite Haemonchus contortus. ***Immunology***, 84(4): 669-674.

Bozza, M., Satoskar, A. R., Lin, G., Lu, B., Humbles, A. A., Gerard, C., & David, J. R. 1999. Targeted disruption of migration inhibitory factor gene reveals its critical role in sepsis. ***J Exp Med***, 189(2): 341-346.

Braman, S. S. 2006. The global burden of asthma. ***Chest***, 130(1 Suppl): 4S-12S.

Brandt, E., Woerly, G., Younes, A. B., Loiseau, S., & Capron, M. 2000. IL-4 production by human polymorphonuclear neutrophils. ***J Leukoc Biol***, 68(1): 125-130.

Brewer, J. M., Conacher, M., Hunter, C. A., Mohrs, M., Brombacher, F., & Alexander, J. 1999. Aluminium hydroxide adjuvant initiates strong antigen-specific Th2 responses in the absence of IL-4- or IL-13-mediated signaling. ***J Immunol***, 163(12): 6448-6454.

Sutas Suttipara**,** Gabriel Rinaldi, and Paul J. Brindley 2012. Genetic manipulation of schistosomes – progress with integration competent vectors. **Parasitology** . 139(5): 641–650

Brown, C. R., & McLeod, R. 1990. Class I MHC genes and CD8+ T cells determine cyst number in Toxoplasma gondii infection. ***J Immunol***, 145(10): 3438-3441.

Brown, M., Kizza, M., Watera, C., Quigley, M. A., Rowland, S., Hughes, P., Whitworth, J. A., & Elliott, A. M. 2004. Helminth infection is not associated with faster progression of HIV disease in coinfected adults in Uganda. ***J Infect Dis***, 190(10): 1869-1879.

Bryant, V. 1973. The life cycle of Nematospiroides dubius, Baylis, 1926 (Nematoda: Heligmosomidae). ***J Helminthol***, 47(3): 263-268.

Buffet, P. A., Sulahian, A., Garin, Y. J., Nassar, N., & Derouin, F. 1995. Culture microtitration: a sensitive method for quantifying Leishmania infantum in tissues of infected mice. ***Antimicrob Agents Chemother***, 39(9): 2167-2168.

Butter, F., Bucerius, F., Michel, M., Cicova, Z., Mann, M., & Janzen, C. J. 2013. Comparative proteomics of two life cycle stages of stable isotope-labeled Trypanosoma brucei reveals novel components of the parasite's host adaptation machinery. ***Mol Cell Proteomics***, 12(1): 172-179.

Buxbaum, L. U. 2013. Leishmania mexicana infection induces IgG to parasite surface glycoinositol phospholipids that can induce IL-10 in mice and humans. ***PLoS Negl Trop Dis***, 7(5): e2224.

Byers, D. E., & Holtzman, M. J. 2010. Alternatively activated macrophages as cause or effect in airway disease. ***Am J Respir Cell Mol Biol***, 43(1): 1-4.

Calandra, T., & Roger, T. 2003. Macrophage migration inhibitory factor: a regulator of innate immunity. ***Nat Rev Immunol***, 3(10): 791-800.

Camberis, M., Le Gros, G., & Urban, J., Jr. 2003. Animal model of Nippostrongylus brasiliensis and Heligmosomoides polygyrus. ***Curr Protoc Immunol***, Chapter 19: Unit 19 12.

Cantacessi, C., Campbell, B. E., Visser, A., Geldhof, P., Nolan, M. J., Nisbet, A. J., Matthews, J. B., Loukas, A., Hofmann, A., Otranto, D., Sternberg, P. W., & Gasser, R. B. 2009. A portrait of the "SCP/TAPS" proteins of eukaryotes--developing a framework for fundamental research and biotechnological outcomes, ***Biotechnology Advances***, Vol. 27: 376-388.

Cantacessi, C., Hofmann, A., Young, N. D., Broder, U., Hall, R. S., Loukas, A., & Gasser, R. B. 2012. Insights into SCP/TAPS proteins of liver flukes based on large-scale bioinformatic analyses of sequence datasets. ***PLoS One***, 7(2): e31164.

Cardoso, L. S., Oliveira, S. C., Goes, A. M., Oliveira, R. R., Pacifico, L. G., Marinho, F. V., Fonseca, C. T., Cardoso, F. C., Carvalho, E. M., & Araujo, M. I. 2010. Schistosoma mansoni antigens modulate the allergic response in a murine model of ovalbumin-induced airway inflammation. ***Clin Exp Immunol***, 160(2): 266-274.

Cash, H. L., Whitham, C. V., Behrendt, C. L., & Hooper, L. V. 2006. Symbiotic bacteria direct expression of an intestinal bactericidal lectin. ***Science***, 313(5790): 1126-1130.

Chalmers, I. W., & Hoffmann, K. F. 2012. Platyhelminth Venom Allergen-Like (VAL) proteins: revealing structural diversity, class-specific features and biological associations across the phylum. ***Parasitology***, 139(10): 1231-1245.

Chalmers, I. W., Mcardle, A. J., Coulson, R. M., Wagner, M. A., Schmid, R., Hirai, H., & Hoffmann, K. F. 2008. Developmentally regulated expression, alternative splicing and distinct sub-groupings in members of the Schistosoma mansoni venom allergen-like (SmVAL) gene family, ***BMC Genomics***, Vol. 9: 89.

Chapman, C. B., Knopf, P. M., Hicks, J. D., & Mitchell, G. F. 1979. IgG1 hypergammaglobulinaemia in chronic parasitic infections in mice: magnitude of the response in mice infected with various parasites. ***Aust J Exp Biol Med Sci***, 57(4): 369-387.

Chen, C.-C., Louie, S., McCormick, B., Walker, W. A., & Shi, H. N. 2005. Concurrent infection with an intestinal helminth parasite impairs host resistance to enteric Citrobacter rodentium and enhances Citrobacter-induced colitis in mice. ***Infect Immun***, 73(9): 5468-5481.

Chen, G., Korfhagen, T. R., Xu, Y., Kitzmiller, J., Wert, S. E., Maeda, Y., Gregorieff, A., Clevers, H., & Whitsett, J. A. 2009. SPDEF is required for mouse pulmonary goblet cell differentiation and regulates a network of genes associated with mucus production. ***J Clin Invest***, 119(10): 2914-2924.

Chu, P. G., & Arber, D. A. 2001. CD79: a review. ***Appl Immunohistochem Mol Morphol***, 9(2): 97-106.

Clevers, H. C., & Bevins, C. L. 2013. Paneth cells: maestros of the small intestinal crypts. ***Annu Rev Physiol***, 75: 289-311.

Cram, E. B. 1927. Bird parasites of the Nematode suborders Strongylata, Ascaridata, and Spirurata. ***Bulletin of the United States National Museum***, 140.

Crivellato, E., Nico, B., Mallardi, F., Beltrami, C. A., & Ribatti, D. 2003. Piecemeal degranulation as a general secretory mechanism? ***The anatomical record Part A, Discoveries in molecular, cellular, and evolutionary biology***, 274(1): 778-784.

Crowle, P. K., & Reed, N. D. 1981. Rejection of the intestinal parasite Nippostrongylus brasiliensis by mast cell-deficient W/Wv anemic mice. ***Infect Immun***, 33(1): 54-58.

Cui, J., Liu, R. D., Wang, L., Zhang, X., Jiang, P., Liu, M. Y., & Wang, Z. Q. 2013a. Proteomic analysis of surface proteins of Trichinella spiralis muscle larvae by two-dimensional gel electrophoresis and mass spectrometry. ***Parasit Vectors***, 6: 355.

Cui, S. J., Xu, L. L., Zhang, T., Xu, M., Yao, J., Fang, C. Y., Feng, Z., Yang, P. Y., Hu, W., & Liu, F. 2013b. Proteomic characterization of larval and adult developmental stages in Echinococcus granulosus reveals novel insight into host-parasite interactions. ***J Proteomics***, 84: 158-175.

Cywinska, A., Czuminska, K., & Schollenberger, A. 2004. Granulomatous inflammation during Heligmosomoides polygyrus primary infections in FVB mice. ***J Helminthol***, 78(1): 17-24.

Dahl, K. E., Shiratsuchi, H., Hamilton, B. D., Ellner, J. J., & Toossi, Z. 1996. Selective induction of transforming growth factor beta in human monocytes by lipoarabinomannan of Mycobacterium tuberculosis. ***Infect Immun***, 64(2): 399-405.

Dainichi, T., Maekawa, Y., Ishii, K., Zhang, T., Nashed, B. F., Sakai, T., Takashima, M., & Himeno, K. 2001. Nippocystatin, a cysteine protease inhibitor from Nippostrongylus brasiliensis, inhibits antigen processing and modulates antigen-specific immune response. ***Infect Immun***, 69(12): 7380-7386.

Dale, D. C., Boxer, L., & Liles, W. C. 2008. The phagocytes: neutrophils and monocytes. ***Blood***, 112(4): 935-945.

Dalzell, J. J., Warnock, N. D., McVeigh, P., Marks, N. J., Mousley, A., Atkinson, L., & Maule, A. G. 2012. Considering RNAi experimental design in parasitic helminths. ***Parasitology***, 139(5): 589-604.

Davies, S. J., Shoemaker, C. B., & Pearce, E. J. 1998. A divergent member of the transforming growth factor beta receptor family from Schistosoma mansoni is expressed on the parasite surface membrane. ***J Biol Chem***, 273(18): 11234-11240.

de Jong, Y. P., Abadia-Molina, A. C., Satoskar, A. R., Clarke, K., Rietdijk, S. T., Faubion, W. A., Mizoguchi, E., Metz, C. N., Alsahli, M., ten Hove, T., Keates, A. C., Lubetsky, J. B., Farrell, R. J., Michetti, P., van Deventer, S. J.,

Lolis, E., David, J. R., Bhan, A. K., & Terhorst, C. 2001. Development of chronic colitis is dependent on the cytokine MIF. ***Nat Immunol***, 2(11): 1061-1066.

Decker, E., Engelmann, G., Findeisen, A., Gerner, P., Laass, M., Ney, D., Posovszky, C., Hoy, L., & Hornef, M. W. 2010. Cesarean delivery is associated with celiac disease but not inflammatory bowel disease in children. ***Pediatrics***, 125(6): e1433-1440.

Dembele, L., Franetich, J. F., Lorthiois, A., Gego, A., Zeeman, A. M., Kocken, C. H., Le Grand, R., Dereuddre-Bosquet, N., van Gemert, G. J., Sauerwein, R., Vaillant, J. C., Hannoun, L., Fuchter, M. J., Diagana, T. T., Malmquist, N. A., Scherf, A., Snounou, G., & Mazier, D. 2014. Persistence and activation of malaria hypnozoites in long-term primary hepatocyte cultures. ***Nat Med***, 20(3): 307-312.

Denkers, E. Y., Wassom, D. L., Krco, C. J., & Hayes, C. E. 1990. The mouse antibody response to Trichinella spiralis defines a single, immunodominant epitope shared by multiple antigens. ***J Immunol***, 144(8): 3152-3159.

Desper, R., & Gascuel, O. 2004. Theoretical foundation of the balanced minimum evolution method of phylogenetic inference and its relationship to weighted least-squares tree fitting. ***Mol Biol Evol***, 21(3): 587-598.

Diemert, D. J., Pinto, A. G., Freire, J., Jariwala, A., Santiago, H., Hamilton, R. G., Periago, M. V., Loukas, A., Tribolet, L., Mulvenna, J., Correa-Oliveira, R., Hotez, P. J., & Bethony, J. M. 2012. Generalized urticaria induced by the Na-ASP-2 hookworm vaccine: implications for the development of vaccines against helminths. ***J Allergy Clin Immunol***, 130(1): 169-176 e166.

Ding, Z. M., Babensee, J. E., Simon, S. I., Lu, H., Perrard, J. L., Bullard, D. C., Dai, X. Y., Bromley, S. K., Dustin, M. L., Entman, M. L., Smith, C. W., & Ballantyne, C. M. 1999. Relative contribution of LFA-1 and Mac-1 to neutrophil adhesion and migration. ***J Immunol***, 163(9): 5029-5038.

Dominguez-Bello, M. G., Costello, E. K., Contreras, M., Magris, M., Hidalgo, G., Fierer, N., & Knight, R. 2010. Delivery mode shapes the acquisition and structure of the initial microbiota across multiple body habitats in newborns. ***Proc Natl Acad Sci U S A***, 107(26): 11971-11975.

Du, C., & Sriram, S. 1998. Mechanism of inhibition of LPS-induced IL-12p40 production by IL-10 and TGF-beta in ANA-1 cells. ***J Leukoc Biol***, 64(1): 92-97.

Dujardin, F. 1845. ***Histoire naturelle des helminthes ou vers intestinaux***.

Dvorak, A. M., & Weller, P. F. 2000. Ultrastructural analysis of human eosinophils. ***Chem Immunol***, 76: 1-28.

El Ridi, R., & Tallima, H. 2009. Schistosoma mansoni ex vivo lung-stage larvae excretory-secretory antigens as vaccine candidates against schistosomiasis. ***Vaccine***, 27(5): 666-673.

El Ridi, R., & Tallima, H. 2013. Vaccine-induced protection against murine schistosomiasis mansoni with larval excretory-secretory antigens and papain or type-2 cytokines. ***J Parasitol***, 99(2): 194-202.

Elliott, D. E., Setiawan, T., Metwali, A., Blum, A., Urban, J. F., Jr., & Weinstock, J. V. 2004. Heligmosomoides polygyrus inhibits established colitis in IL-10-deficient mice. ***Eur J Immunol***, 34(10): 2690-2698.

Elliott, D. E., & Weinstock, J. V. 2012. Where are we on worms? ***Curr Opin Gastroenterol***, 28(6): 551-556.

Erickson, H. S., Gillespie, J. W., & Emmert-Buck, M. R. 2008. Tissue microdissection. ***Methods in molecular biology (Clifton, N J)***, 424: 433-448.

Erwig, L. P., & Henson, P. M. 2007. Immunological consequences of apoptotic cell phagocytosis. ***Am J Pathol***, 171(1): 2-8.

Escande, F., Porchet, N., Bernigaud, A., Petitprez, D., Aubert, J. P., & Buisine, M. P. 2004. The mouse secreted gel-forming mucin gene cluster. ***Biochim Biophys Acta***, 1676(3): 240-250.

Everts, B., Hussaarts, L., Driessen, N. N., Meevissen, M. H., Schramm, G., van der Ham, A. J., van der Hoeven, B., Scholzen, T., Burgdorf, S., Mohrs, M., Pearce, E. J., Hokke, C. H., Haas, H., Smits, H. H., & Yazdanbakhsh, M. 2012. Schistosome-derived omega-1 drives Th2 polarization by suppressing protein synthesis following internalization by the mannose receptor. ***J Exp Med***, 209(10): 1753-1767, S1751.

Falcone, F. H., Dahinden, C. A., Gibbs, B. F., Noll, T., Amon, U., Hebestreit, H., Abrahamsen, O., Klaucke, J., Schlaak, M., & Haas, H. 1996. Human basophils release interleukin-4 after stimulation with Schistosoma mansoni egg antigen. ***Eur J Immunol***, 26(5): 1147-1155.

Fallon, P. G., Ballantyne, S. J., Mangan, N. E., Barlow, J. L., Dasvarma, A., Hewett, D. R., McIlgorm, A., Jolin, H. E., & McKenzie, A. N. J. 2006. Identification of an interleukin (IL)-25-dependent cell population that provides IL-4, IL-5, and IL-13 at the onset of helminth expulsion. ***J Exp Med***, 203(4): 1105-1116.

Fallon, P. G., Jolin, H. E., Smith, P., Emson, C. L., Townsend, M. J., Fallon, R., Smith, P., & McKenzie, A. N. 2002. IL-4 induces characteristic Th2 responses even in the combined absence of IL-5, IL-9, and IL-13. ***Immunity***, 17(1): 7-17.

Farias, L. P., Rodrigues, D., Cunna, V., Rofatto, H. K., Faquim-Mauro, E. L., & Leite, L. C. 2012. Schistosoma mansoni venom allergen like proteins present differential allergic responses in a murine model of airway inflammation. ***PLoS Negl Trop Dis***, 6(2): e1510.

Fernandez, C., Szyperski, T., Bruyere, T., Ramage, P., Mosinger, E., & Wuthrich, K. 1997. NMR solution structure of the pathogenesis-related protein P14a. ***J Mol Biol***, 266(3): 576-593.

Figueiredo, A. S., Hofer, T., Klotz, C., Sers, C., Hartmann, S., Lucius, R., & Hammerstein, P. 2009. Modelling and simulating interleukin-10 production and regulation by macrophages after stimulation with an immunomodulator of parasitic nematodes. ***FEBS J***, 276(13): 3454-3469.

Filbey, K. J., Grainger, J. R., Smith, K. A., Boon, L., van Rooijen, N., Harcus, Y., Jenkins, S., Hewitson, J. P., & Maizels, R. M. 2014. Innate and adaptive type 2 immune cell responses in genetically controlled resistance to intestinal helminth infection. ***Immunol Cell Biol***, 92(5): 436-448.

Filipe-Santos, O., Bustamante, J., Chapgier, A., Vogt, G., de Beaucoudrey, L., Feinberg, J., Jouanguy, E., Boisson-Dupuis, S., Fieschi, C., Picard, C., & Casanova, J.-L. 2006. Inborn errors of IL-12/23- and IFN-gamma-mediated immunity: molecular, cellular, and clinical features. ***Semin Immunol***, 18(6): 347-361.

Finkelman, F. D., Shea-Donohue, T., Morris, S. C., Gildea, L., Strait, R., Madden, K. B., Schopf, L., & Urban, J. F., Jr. 2004. Interleukin-4- and interleukin-13-mediated host protection against intestinal nematode parasites. ***Immunol Rev***, 201: 139-155.

Finney, C. A., Taylor, M. D., Wilson, M. S., & Maizels, R. M. 2007. Expansion and activation of CD4(+)CD25(+) regulatory T cells in Heligmosomoides polygyrus infection. ***Eur J Immunol***, 37(7): 1874-1886.

Fire, A., Xu, S., Montgomery, M. K., Kostas, S. A., Driver, S. E., & Mello, C. C. 1998. Potent and specific genetic interference by double-stranded RNA in Caenorhabditis elegans. ***Nature***, 391(6669): 806-811.

Flaherty, D. M., Monick, M. M., & Hinde, S. L. 2006. Human alveolar macrophages are deficient in PTEN. The role of endogenous oxidants. ***J Biol Chem***, 281(8): 5058-5064.

Forchielli, M. L., & Walker, W. A. 2005. The role of gut-associated lymphoid tissues and mucosal defence. ***Br J Nutr***, 93 Suppl 1: S41-48.

Fort, M. M., Cheung, J., Yen, D., Li, J., Zurawski, S. M., Lo, S., Menon, S., Clifford, T., Hunte, B., Lesley, R., Muchamuel, T., Hurst, S. D., Zurawski, G., Leach, M. W., Gorman, D. M., & Rennick, D. M. 2001. IL-25 induces IL-4, IL-5, and IL-13 and Th2-associated pathologies in vivo. ***Immunity***, 15(6): 985-995.

Frank, G. R., Wisnewski, N., Brandt, K. S., Carter, C. R., Jennings, N. S., & Selkirk, M. E. 1999. Molecular cloning of the 22-24 kDa excretory-secretory 22U protein of Dirofilaria immitis and other filarial nematode parasites. ***Mol Biochem Parasitol***, 98(2): 297-302.

Frey, A., Giannasca, K. T., Weltzin, R., Giannasca, P. J., Reggio, H., Lencer, W. I., & Neutra, M. R. 1996. Role of the glycocalyx in regulating access of microparticles to apical plasma membranes of intestinal epithelial cells: implications for microbial attachment and oral vaccine targeting. ***J Exp Med***, 184(3): 1045-1059.

Frohlich, A., Marsland, B. J., Sonderegger, I., Kurrer, M., Hodge, M. R., Harris, N. L., & Kopf, M. 2007. IL-21 receptor signaling is integral to the development of Th2 effector responses in vivo. ***Blood***, 109(5): 2023-2031.

Gao, B., Allen, R., Maier, T., Davis, E. L., Baum, T. J., & Hussey, R. S. 2001a. Identification of putative parasitism genes expressed in the esophageal gland cells of the soybean cyst nematode Heterodera glycines. ***Mol Plant Microbe Interact***, 14(10): 1247-1254.

Gao, B., Allen, R., Maier, T., Davis, E. L., Baum, T. J., & Hussey, R. S. 2001b. Molecular characterisation and expression of two venom allergen-like protein genes in Heterodera glycines. ***Int J Parasitol***, 31(14): 1617-1625.

Garside, P., Kennedy, M. W., Wakelin, D., & Lawrence, C. E. 2000. Immunopathology of intestinal helminth infection. ***Parasite Immunol***, 22(12): 605-612.

Gaur, U., Roberts, S. C., Dalvi, R. P., Corraliza, I., Ullman, B., & Wilson, M. E. 2007. An effect of parasite-encoded arginase on the outcome of murine cutaneous leishmaniasis. ***J Immunol***, 179(12): 8446-8453.

Geissmann, F., Revy, P., Regnault, A., Lepelletier, Y., Dy, M., Brousse, N., Amigorena, S., Hermine, O., & Durandy, A. 1999. TGF-beta 1 prevents the noncognate maturation of human dendritic Langerhans cells. ***J Immunol***, 162(8): 4567-4575.

Geldhof, P., Meyvis, Y., Vercruysse, J., & Claerebout, E. 2008. Vaccine testing of a recombinant activation-associated secreted protein (ASP1) from Ostertagia ostertagi. ***Parasite Immunol***, 30(1): 57-60.

Geldhof, P., Murray, L., Couthier, A., Gilleard, J. S., McLauchlan, G., Knox, D. P., & Britton, C. 2006. Testing the efficacy of RNA interference in Haemonchus contortus. ***Int J Parasitol***, 36(7): 801-810.

Gerbe, F., van Es, J. H., Makrini, L., Brulin, B., Mellitzer, G., Robine, S., Romagnolo, B., Shroyer, N. F., Bourgaux, J. F., Pignodel, C., Clevers, H., & Jay, P. 2011. Distinct ATOH1 and Neurog3 requirements define tuft cells as a new secretory cell type in the intestinal epithelium. ***J Cell Biol***, 192(5): 767-780.

Gibbs, G. M., Roelants, K., & O'Bryan, M. K. 2008. The CAP superfamily: cysteine-rich secretory proteins, antigen 5, and pathogenesis-related 1 proteins--roles in reproduction, cancer, and immune defense. ***Endocr Rev***, 29(7): 865-897.

Gibbs, G. M., Scanlon, M. J., Swarbrick, J., Curtis, S., Gallant, E., Dulhunty, A. F., & O'Bryan, M. K. 2006. The cysteine-rich secretory protein domain of Tpx-1 is related to ion channel toxins and regulates ryanodine receptor Ca2+ signaling. ***J Biol Chem***, 281(7): 4156-4163.

Girgis, N. M., Gundra, U. M., & Loke, P. 2013. Immune regulation during helminth infections. ***PLoS Pathog***, 9(4): e1003250.

Goldenberg, R. L., Culhane, J. F., Iams, J. D., & Romero, R. 2008. Epidemiology and causes of preterm birth. ***Lancet***, 371(9606): 75-84.

Gomes-Santos, C. S., Braks, J., Prudencio, M., Carret, C., Gomes, A. R., Pain, A., Feltwell, T., Khan, S., Waters, A., Janse, C., Mair, G. R., & Mota, M. M. 2011. Transition of Plasmodium sporozoites into liver stage-like forms is regulated by the RNA binding protein Pumilio. ***PLoS Pathog***, 7(5): e1002046.

Gomez, G., Ramirez, C. D., Rivera, J., Patel, M., Norozian, F., Wright, H. V., Kashyap, M. V., Barnstein, B. O., Fischer-Stenger, K., Schwartz, L. B., Kepley, C. L., & Ryan, J. J. 2005. TGF-beta 1 inhibits mast cell Fc epsilon RI expression. ***Journal of immunology (Baltimore, Md : 1950)***, 174(10): 5987-5993.

Gomez-Escobar, N., Bennett, C., Prieto-Lafuente, L., Aebischer, T., Blackburn, C. C., & Maizels, R. M. 2005. Heterologous expression of the filarial nematode alt gene products reveals their potential to inhibit immune function. ***BMC Biol***, 3: 8.

Gomez-Escobar, N., Lewis, E., & Maizels, R. M. 1998. A novel member of the transforming growth factor-beta (TGF-beta) superfamily from the filarial nematodes Brugia malayi and B. pahangi. ***Exp Parasitol***, 88(3): 200-209.

Gomez-Escobar, N., van den Biggelaar, A., & Maizels, R. 1997. A member of the TGF-beta receptor gene family in the parasitic nematode Brugia pahangi. ***Gene***, 199(1-2): 101-109.

Goodridge, H. S., Wilson, E. H., Harnett, W., Campbell, C. C., Harnett, M. M., & Liew, F. Y. 2001. Modulation of macrophage cytokine production by ES-62, a secreted product of the filarial nematode Acanthocheilonema viteae. ***J Immunol***, 167(2): 940-945.

Gorelik, L., & Flavell, R. A. 2002. Transforming growth factor-beta in T-cell biology. ***Nat Rev Immunol***, 2(1): 46-53.

Goud, G. N., Bottazzi, M. E., Zhan, B., Mendez, S., Deumic, V., Plieskatt, J., Liu, S., Wang, Y., Bueno, L., Fujiwara, R., Samuel, A., Ahn, S. Y., Solanki, M., Asojo, O. A., Wang, J., Bethony, J. M., Loukas, A., Roy, M., & Hotez, P. J. 2005. Expression of the Necator americanus hookworm larval antigen Na-ASP-2 in Pichia pastoris and purification of the recombinant protein for use in human clinical trials. ***Vaccine***, 23(39): 4754-4764.

Goud, G. N., Zhan, B., Ghosh, K., Loukas, A., Hawdon, J., Dobardzic, A., Deumic, V., Liu, S., Dobardzic, R., Zook, B. C., Jin, Q., Liu, Y., Hoffman, L., Chung-Debose, S., Patel, R., Mendez, S., & Hotez, P. J. 2004. Cloning, yeast expression, isolation, and vaccine testing of recombinant Ancylostoma-secreted protein (ASP)-1 and ASP-2 from Ancylostoma ceylanicum, ***J Infect Dis***, Vol. 189: 919-929.

Grabinger, T., Luks, L., Kostadinova, F., Zimberlin, C., Medema, J. P., Leist, M., & Brunner, T. 2014. Ex vivo culture of intestinal crypt organoids as a model system for assessing cell death induction in intestinal epithelial cells and enteropathy. ***Cell Death Dis***, 5: e1228.

Grainger, J. R., Smith, K. A., Hewitson, J. P., McSorley, H. J., Harcus, Y., Filbey, K. J., Finney, C. A., Greenwood, E. J., Knox, D. P., Wilson, M. S., Belkaid, Y., Rudensky, A. Y., & Maizels, R. M. 2010. Helminth secretions induce de novo T cell Foxp3 expression and regulatory function through the TGF-beta pathway. ***J Exp Med***, 207(11): 2331-2341.

Gregorieff, A., & Clevers, H. 2005. Wnt signaling in the intestinal epithelium: from endoderm to cancer. ***Genes Dev***, 19(8): 877-890.

Gregory, W. F., Atmadja, A. K., Allen, J. E., & Maizels, R. M. 2000. The abundant larval transcript-1 and -2 genes of Brugia malayi encode stage-specific candidate vaccine antigens for filariasis. ***Infect Immun***, 68(7): 4174-4179.

Gregory, W. F., Blaxter, M. L., & Maizels, R. M. 1997. Differentially expressed, abundant trans-spliced cDNAs from larval Brugia malayi. ***Mol Biochem Parasitol***, 87(1): 85-95.

Grencis, R. K., Crawford, C., Pritchard, D. I., Behnke, J. M., & Wakelin, D. 1986. Immunization of mice with surface antigens from the muscle larvae of Trichinella spiralis. ***Parasite Immunol***, 8(6): 587-596.

Gronlund, M. M., Lehtonen, O. P., Eerola, E., & Kero, P. 1999. Fecal microflora in healthy infants born by different methods of delivery: permanent changes in intestinal flora after cesarean delivery. ***Journal of pediatric gastroenterology and nutrition***, 28(1): 19-25.

Gruber, B. L., Marchese, M. J., & Kew, R. R. 1994. Transforming growth factor-beta 1 mediates mast cell chemotaxis. ***Journal of immunology (Baltimore, Md : 1950)***, 152(12): 5860-5867.

Guarner, F., Bourdet-Sicard, R., Brandtzaeg, P., Gill, H. S., McGuirk, P., van Eden, W., Versalovic, J., Weinstock, J. V., & Rook, G. A. 2006. Mechanisms of disease: the hygiene hypothesis revisited. ***Nat Clin Pract Gastroenterol Hepatol***, 3(5): 275-284.

Gunawardene, A. R., Corfe, B. M., & Staton, C. A. 2011. Classification and functions of enteroendocrine cells of the lower gastrointestinal tract. ***Int J Exp Pathol***, 92(4): 219-231.

Haile, S., Lefort, J., Joseph, D., Gounon, P., Huerre, M., & Vargaftig, B. B. 1999. Mucous-cell metaplasia and inflammatory-cell recruitment are dissociated in

allergic mice after antibody- and drug-dependent cell depletion in a murine model of asthma. ***Am J Respir Cell Mol Biol***, 20(5): 891-902.
Haisch, K., Schramm, G., Falcone, F. H., Alexander, C., Schlaak, M., & Haas, H. 2001. A glycoprotein from Schistosoma mansoni eggs binds non-antigen-specific immunoglobulin E and releases interleukin-4 from human basophils. ***Parasite Immunol***, 23(8): 427-434.
Hall, M. C. 1878. Neue beobachtungen an helminthen. ***Arch. Naturgeschichte***, 44: 218–245.
Hamann, K. J., Gleich, G. J., Checkel, J. L., Loegering, D. A., McCall, J. W., & Barker, R. L. 1990. In vitro killing of microfilariae of Brugia pahangi and Brugia malayi by eosinophil granule proteins. ***Journal of immunology (Baltimore, Md : 1950)***, 144(8): 3166-3173.
Harcus, Y., Nicoll, G., Murray, J., Filbey, K., Gomez-Escobar, N., & Maizels, R. M. 2009. C-type lectins from the nematode parasites Heligmosomoides polygyrus and Nippostrongylus brasiliensis. ***Parasitol Int***, 58(4): 461-470.
Harnett, W. 2014. Secretory products of helminth parasites as immunomodulators. ***Mol Biochem Parasitol***.
Harnett, W., Goodridge, H. S., Allen, J. M., & Harnett, M. 2012. Receptor usage by the Acanthocheilonema viteae-derived immunomodulator, ES-62. ***Exp Parasitol***, 132(1): 97-102.
Harris, N., & Gause, W. C. 2011. To B or not to B: B cells and the Th2-type immune response to helminths. ***Trends Immunol***, 32(2): 80-88.
Harrod, K. S., Mounday, A. D., Stripp, B. R., & Whitsett, J. A. 1998. Clara cell secretory protein decreases lung inflammation after acute virus infection. ***Am J Physiol***, 275(5 Pt 1): L924-930.
Hartmann, S., Kyewski, B., Sonnenburg, B., & Lucius, R. 1997. A filarial cysteine protease inhibitor down-regulates T cell proliferation and enhances interleukin-10 production. ***Eur J Immunol***, 27(9): 2253-2260.
Harty, J. T., & Bevan, M. J. 1999. Responses of CD8(+) T cells to intracellular bacteria. ***Curr Opin Immunol***, 11(1): 89-93.
Harty, J. T., Tvinnereim, A. R., & White, D. W. 2000. CD8+ T cell effector mechanisms in resistance to infection. ***Annual review of immunology***, 18: 275-308.
Hawdon, J. M., Jones, B. F., Hoffman, D. R., & Hotez, P. J. 1996. Cloning and characterization of Ancylostoma-secreted protein. A novel protein associated with the transition to parasitism by infective hookworm larvae, ***J Biol Chem***, Vol. 271: 6672-6678.
Hawdon, J. M., Narasimhan, S., & Hotez, P. J. 1999. Ancylostoma secreted protein 2: cloning and characterization of a second member of a family of nematode secreted proteins from Ancylostoma caninum, ***Molecular and Biochemical Parasitology***, Vol. 99: 149-165.
Henriksen, A., King, T. P., Mirza, O., Monsalve, R. I., Meno, K., Ipsen, H., Larsen, J. N., Gajhede, M., & Spangfort, M. D. 2001. Major venom allergen of yellow jackets, Ves v 5: structural characterization of a pathogenesis-related protein superfamily. ***Proteins***, 45(4): 438-448.
Herbert, D. R., Yang, J. Q., Hogan, S. P., Groschwitz, K., Khodoun, M., Munitz, A., Orekov, T., Perkins, C., Wang, Q., Brombacher, F., Urban, J. F., Jr., Rothenberg, M. E., & Finkelman, F. D. 2009. Intestinal epithelial cell

secretion of RELM-beta protects against gastrointestinal worm infection. ***J Exp Med***, 206(13): 2947-2957.

Hesse, M., Piccirillo, C. A., Belkaid, Y., Prufer, J., Mentink-Kane, M., Leusink, M., Cheever, A. W., Shevach, E. M., & Wynn, T. A. 2004. The pathogenesis of schistosomiasis is controlled by cooperating IL-10-producing innate effector and regulatory T cells. ***Journal of immunology (Baltimore, Md : 1950)***, 172(5): 3157-3166.

Hewitson, J. P., Filbey, K. J., Grainger, J. R., Dowle, A. A., Pearson, M., Murray, J., Harcus, Y., & Maizels, R. M. 2011a. Heligmosomoides polygyrus elicits a dominant nonprotective antibody response directed against restricted glycan and peptide epitopes. ***J Immunol***, 187(9): 4764-4777.

Hewitson, J. P., Grainger, J. R., & Maizels, R. M. 2009. Helminth immunoregulation: the role of parasite secreted proteins in modulating host immunity. ***Mol Biochem Parasitol***, 167(1): 1-11.

Hewitson, J. P., Harcus, Y., Murray, J., van Agtmaal, M., Filbey, K. J., Grainger, J. R., Bridgett, S., Blaxter, M. L., Ashton, P. D., Ashford, D. A., Curwen, R. S., Wilson, R. A., Dowle, A. A., & Maizels, R. M. 2011b. Proteomic analysis of secretory products from the model gastrointestinal nematode Heligmosomoides polygyrus reveals dominance of venom allergen-like (VAL) proteins. ***J Proteomics***, 74(9): 1573-1594.

Hewitson, J. P., Ivens, A. C., Harcus, Y., Filbey, K. J., McSorley, H. J., Murray, J., Bridgett, S., Ashford, D., Dowle, A. A., & Maizels, R. M. 2013. Secretion of protective antigens by tissue-stage nematode larvae revealed by proteomic analysis and vaccination-induced sterile immunity. ***PLoS Pathog***, 9(8): e1003492.

Hillrichs, K., Schnieder, T., Forbes, A. B., Simcock, D. C., Pedley, K. C., & Simpson, H. V. 2012. Use of fluorescent lectin binding to distinguish Teladorsagia circumcincta and Haemonchus contortus eggs, third-stage larvae and adult worms. ***Parasitol Res***, 110(1): 449-458.

Hogan, S. P., Rosenberg, H. F., Moqbel, R., Phipps, S., Foster, P. S., Lacy, P., Kay, A. B., & Rothenberg, M. E. 2008. Eosinophils: biological properties and role in health and disease. ***Clin Exp Allergy***, 38(5): 709-750.

Holcomb, I. N., Kabakoff, R. C., Chan, B., Baker, T. W., Gurney, A., Henzel, W., Nelson, C., Lowman, H. B., Wright, B. D., Skelton, N. J., Frantz, G. D., Tumas, D. B., Peale, F. V., Jr., Shelton, D. L., & Hebert, C. C. 2000. FIZZ1, a novel cysteine-rich secreted protein associated with pulmonary inflammation, defines a new gene family. ***EMBO J***, 19(15): 4046-4055.

Holland, M. J., Harcus, Y. M., Riches, P. L., & Maizels, R. M. 2000. Proteins secreted by the parasitic nematode Nippostrongylus brasiliensis act as adjuvants for Th2 responses. ***Eur J Immunol***, 30(7): 1977-1987.

Hooper, L. V., Wong, M. H., Thelin, A., Hansson, L., Falk, P. G., & Gordon, J. I. 2001. Molecular analysis of commensal host-microbial relationships in the intestine. ***Science (New York, N Y)***, 291(5505): 881-884.

Horsnell, W. G. C., & Brombacher, F. 2008. Key roles for specific and nonspecific antibody in intestinal nematode expulsion. ***Cell Host Microbe***, 4(4): 303-305.

Hotez, P. J., Bethony, J., Bottazzi, M. E., Brooker, S., & Buss, P. 2005. Hookworm: "the great infection of mankind". ***PLoS Med***, 2(3): e67.

Hovenberg, H. W., Davies, J. R., & Carlstedt, I. 1996. Different mucins are produced by the surface epithelium and the submucosa in human trachea: identification of MUC5AC as a major mucin from the goblet cells. ***Biochem J***, 318 (Pt 1): 319-324.

Hurdayal, R., & Brombacher, F. 2014. The role of IL-4 and IL-13 in cutaneous Leishmaniasis. ***Immunol Lett***.

Hurst, S. D., Muchamuel, T., Gorman, D. M., Gilbert, J. M., Clifford, T., Kwan, S., Menon, S., Seymour, B., Jackson, C., Kung, T. T., Brieland, J. K., Zurawski, S. M., Chapman, R. W., Zurawski, G., & Coffman, R. L. 2002. New IL-17 family members promote Th1 or Th2 responses in the lung: in vivo function of the novel cytokine IL-25. ***Journal of immunology (Baltimore, Md : 1950)***, 169(1): 443-453.

Iniesta, V., Carcelen, J., Molano, I., Peixoto, P. M., Redondo, E., Parra, P., Mangas, M., Monroy, I., Campo, M. L., Nieto, C. G., & Corraliza, I. 2005. Arginase I induction during Leishmania major infection mediates the development of disease. ***Infect Immun***, 73(9): 6085-6090.

Irwin, R. S., Augustyn, N., French, C. T., Rice, J., Tedeschi, V., Welch, S. J., Editorial Leadership, T., Barnes, P. J., Brightling, C. E., Collop, N. A., Davidson, B. L., Gutterman, D. D., Hall, J. B., Heffner, J. E., Hill, N. S., Ip, M. S.-M., Jindal, S. K., Johnson, R. G., Manaker, S., Moss, J., Murin, S., O'Byrne, P. M., Olivieri, D., Rubin, B. K., Schwarz, M. I., Somers, V. K., Anderson, B. J., Lipsey, L., Micek, P. A., Miller, C., Popa, M., & Markowski, P. A. 2013. Spread the word about the journal in 2013: from citation manipulation to invalidation of patient-reported outcomes measures to renaming the Clara cell to new journal features. ***Chest***, 143(1): 1-4.

Ishikawa, N., Horii, Y., Oinuma, T., Suganuma, T., & Nawa, Y. 1994. Goblet cell mucins as the selective barrier for the intestinal helminths: T-cell-independent alteration of goblet cell mucins by immunologically 'damaged' Nippostrongylus brasiliensis worms and its significance on the challenge infection with homologous and heterologous parasites. ***Immunology***, 81(3): 480-486.

Ishikawa, N., Wakelin, D., & Mahida, Y. R. 1997. Role of T helper 2 cells in intestinal goblet cell hyperplasia in mice infected with Trichinella spiralis. ***Gastroenterology***, 113(2): 542-549.

Jackson, A. D. 2001. Airway goblet-cell mucus secretion. ***Trends Pharmacol Sci***, 22(1): 39-45.

Jalkanen, J., Huhtaniemi, I., & Poutanen, M. 2005. Mouse cysteine-rich secretory protein 4 (CRISP4): a member of the Crisp family exclusively expressed in the epididymis in an androgen-dependent manner. ***Biol Reprod***, 72(5): 1268-1274.

Jankovic, D., Kullberg, M. C., Caspar, P., & Sher, A. 2004. Parasite-induced Th2 polarization is associated with down-regulated dendritic cell responsiveness to Th1 stimuli and a transient delay in T lymphocyte cycling. ***J Immunol***, 173(4): 2419-2427.

Jenkins, S. J., & Allen, J. E. 2010. Similarity and diversity in macrophage activation by nematodes, trematodes, and cestodes. ***J Biomed Biotechnol***, 2010: 262609.

Johansson, M. E., Phillipson, M., Petersson, J., Velcich, A., Holm, L., & Hansson, G. C. 2008. The inner of the two Muc2 mucin-dependent mucus layers in colon is devoid of bacteria. ***Proc Natl Acad Sci U S A***, 105(39): 15064-15069.

Johnson, J. R., Wiley, R. E., Fattouh, R., Swirski, F. K., Gajewska, B. U., Coyle, A. J., Gutierrez-Ramos, J. C., Ellis, R., Inman, M. D., & Jordana, M. 2004. Continuous exposure to house dust mite elicits chronic airway inflammation and structural remodeling. ***Am J Respir Crit Care Med***, 169(3): 378-385.

Joseph, G. T., Huima, T., & Lustigman, S. 1998. Characterization of an Onchocerca volvulus L3-specific larval antigen, Ov-ALT-1. ***Mol Biochem Parasitol***, 96(1-2): 177-183.

Jovanovic, D. V., Di Battista, J. A., Martel-Pelletier, J., Jolicoeur, F. C., He, Y., Zhang, M., Mineau, F., & Pelletier, J. P. 1998. IL-17 stimulates the production and expression of proinflammatory cytokines, IL-beta and TNF-alpha, by human macrophages. ***Journal of immunology (Baltimore, Md : 1950)***, 160(7): 3513-3521.

Kamath, R. S., Fraser, A. G., Dong, Y., Poulin, G., Durbin, R., Gotta, M., Kanapin, A., Le Bot, N., Moreno, S., Sohrmann, M., Welchman, D. P., Zipperlen, P., & Ahringer, J. 2003. Systematic functional analysis of the Caenorhabditis elegans genome using RNAi, ***Nature***, Vol. 421: 231-237.

Kane, M. M., & Mosser, D. M. 2001. The role of IL-10 in promoting disease progression in leishmaniasis. ***J Immunol***, 166(2): 1141-1147.

Kapsenberg, M. L. 2003. Dendritic-cell control of pathogen-driven T-cell polarization. ***Nat Rev Immunol***, 3(12): 984-993.

Kelleher, A., Darwiche, R., Rezende, W. C., Farias, L. P., Leite, L. C. C., Schneiter, R., & Asojo, O. A. 2014. Schistosoma mansoni venom allergen-like protein 4 (SmVAL4) is a novel lipid-binding SCP/TAPS protein that lacks the prototypical CAP motifs. ***Acta crystallographica Section D, Biological crystallography***, 70(Pt 8): 2186-2196.

Kero, J., Gissler, M., Gronlund, M. M., Kero, P., Koskinen, P., Hemminki, E., & Isolauri, E. 2002. Mode of delivery and asthma -- is there a connection? ***Pediatr Res***, 52(1): 6-11.

Khan, I. A., Hakak, R., Eberle, K., Sayles, P., Weiss, L. M., & Urban, J. F., Jr. 2008. Coinfection with Heligmosomoides polygyrus fails to establish CD8+ T-cell immunity against Toxoplasma gondii. ***Infect Immun***, 76(3): 1305-1313.

Khan, J. J. K. W. I. 2013. Goblet Cells and Mucins: Role in Innate Defense in Enteric Infections. ***Pathogens***: 55-70.

Khan, W. I. 2008. Physiological changes in the gastrointestinal tract and host protective immunity: learning from the mouse-Trichinella spiralis model. ***Parasitology***, 135(6): 671-682.

Khan, W. I., & Collins, S. M. 2004. Immune-mediated alteration in gut physiology and its role in host defence in nematode infection. ***Parasite Immunol***, 26(8-9): 319-326.

Kiessling, R., Klein, E., Pross, H., & Wigzell, H. 1975. "Natural" killer cells in the mouse. II. Cytotoxic cells with specificity for mouse Moloney leukemia cells. Characteristics of the killer cell. ***Eur J Immunol***, 5(2): 117-121.

Kim, J. Y., Cho, M. K., Choi, S. H., Lee, K. H., Ahn, S. C., Kim, D. H., & Yu, H. S. 2010. Inhibition of dextran sulfate sodium (DSS)-induced intestinal inflammation via enhanced IL-10 and TGF-beta production by galectin-9

homologues isolated from intestinal parasites. ***Mol Biochem Parasitol***, 174(1): 53-61.

Kitagaki, K., Businga, T. R., Racila, D., Elliott, D. E., Weinstock, J. V., & Kline, J. N. 2006. Intestinal helminths protect in a murine model of asthma. ***J Immunol***, 177(3): 1628-1635.

Kleemann, R., Kapurniotu, A., Frank, R. W., Gessner, A., Mischke, R., Flieger, O., Juttner, S., Brunner, H., & Bernhagen, J. 1998. Disulfide analysis reveals a role for macrophage migration inhibitory factor (MIF) as thiol-protein oxidoreductase. ***J Mol Biol***, 280(1): 85-102.

Klein Wolterink, R. G. J., Kleinjan, A., van Nimwegen, M., Bergen, I., de Bruijn, M., Levani, Y., & Hendriks, R. W. 2012. Pulmonary innate lymphoid cells are major producers of IL-5 and IL-13 in murine models of allergic asthma. ***Eur J Immunol***, 42(5): 1106-1116.

Knight, P. A., Wright, S. H., Lawrence, C. E., Paterson, Y. Y., & Miller, H. R. 2000. Delayed expulsion of the nematode Trichinella spiralis in mice lacking the mucosal mast cell-specific granule chymase, mouse mast cell protease-1. ***J Exp Med***, 192(12): 1849-1856.

Knox, D. P., Geldhof, P., Visser, A., & Britton, C. 2007. RNA interference in parasitic nematodes of animals: a reality check? ***Trends Parasitol***, 23(3): 105-107.

Kobayashi, T., Iijima, K., Radhakrishnan, S., Mehta, V., Vassallo, R., Lawrence, C. B., Cyong, J. C., Pease, L. R., Oguchi, K., & Kita, H. 2009. Asthma-related environmental fungus, Alternaria, activates dendritic cells and produces potent Th2 adjuvant activity. ***J Immunol***, 182(4): 2502-2510.

Koblansky, A. A., Jankovic, D., Oh, H., Hieny, S., Sungnak, W., Mathur, R., Hayden, M. S., Akira, S., Sher, A., & Ghosh, S. 2013. Recognition of profilin by Toll-like receptor 12 is critical for host resistance to Toxoplasma gondii. ***Immunity***, 38(1): 119-130.

Korten, S., Buttner, D. W., Schmetz, C., Hoerauf, A., Mand, S., & Brattig, N. 2009. The nematode parasite Onchocerca volvulus generates the transforming growth factor-beta (TGF-beta). ***Parasitol Res***, 105(3): 731-741.

Kovalick, G. E., & Griffin, D. L. 2005. Characterization of the SCP/TAPS gene family in Drosophila melanogaster. ***Insect Biochem Mol Biol***, 35(8): 825-835.

Kreider, T., Anthony, R. M., Urban, J. F., Jr., & Gause, W. C. 2007. Alternatively activated macrophages in helminth infections. ***Curr Opin Immunol***, 19(4): 448-453.

Kropf, P., K. Brunson, R. Etges and I. Müller. 1998. ***The Leishmaniasis Model.***: Academic Press Ltd, London.

Kucera, K., Harrison, L. M., Cappello, M., & Modis, Y. 2011. Ancylostoma ceylanicum Excretory-Secretory Protein 2 Adopts a Netrin-Like Fold and Defines a Novel Family of Nematode Proteins, ***Journal of Molecular Biology***.

Kuijk, L. M., Klaver, E. J., Kooij, G., van der Pol, S. M., Heijnen, P., Bruijns, S. C., Kringel, H., Pinelli, E., Kraal, G., de Vries, H. E., Dijkstra, C. D., Bouma, G., & van Die, I. 2012. Soluble helminth products suppress clinical signs in murine experimental autoimmune encephalomyelitis and differentially modulate human dendritic cell activation. ***Mol Immunol***, 51(2): 210-218.

Kumar, P., Chen, K., & Kolls, J. K. 2013. Th17 cell based vaccines in mucosal immunity. ***Curr Opin Immunol***, 25(3): 373-380.

Kunzmann, S., Collins, J. J., Kuypers, E., & Kramer, B. W. 2013. Thrown off balance: the effect of antenatal inflammation on the developing lung and immune system. ***Am J Obstet Gynecol***, 208(6): 429-437.

Langrish, C. L., Chen, Y., Blumenschein, W. M., Mattson, J., Basham, B., Sedgwick, J. D., McClanahan, T., Kastelein, R. A., & Cua, D. J. 2005. IL-23 drives a pathogenic T cell population that induces autoimmune inflammation. ***J Exp Med***, 201(2): 233-240.

Lantz, C. S., Boesiger, J., Song, C. H., Mach, N., Kobayashi, T., Mulligan, R. C., Nawa, Y., Dranoff, G., & Galli, S. J. 1998. Role for interleukin-3 in mast-cell and basophil development and in immunity to parasites. ***Nature***, 392(6671): 90-93.

Lee, D. L. 1965. The Cuticle of Adult Nippostrongylus Brasiliensis. ***Parasitology***, 55: 173-181.

Lefrancois, L., & Goodman, T. 1989. In vivo modulation of cytolytic activity and Thy-1 expression in TCR-gamma delta+ intraepithelial lymphocytes. ***Science (New York, N Y)***, 243(4899): 1716-1718.

Lendner, M., Doligalska, M., Lucius, R., & Hartmann, S. 2008. Attempts to establish RNA interference in the parasitic nematode Heligmosomoides polygyrus☆, ***Molecular and Biochemical Parasitology***: 11.

Licona-Limon, P., Kim, L. K., Palm, N. W., & Flavell, R. A. 2013. TH2, allergy and group 2 innate lymphoid cells. ***Nat Immunol***, 14(6): 536-542.

Liddell, S., & Knox, D. P. 1998. Extracellular and cytoplasmic Cu/Zn superoxide dismutases from Haemonchus contortus. ***Parasitology***, 116 (Pt 4): 383-394.

Liese, J., Schleicher, U., & Bogdan, C. 2008. The innate immune response against Leishmania parasites. ***Immunobiology***, 213(3-4): 377-387.

Lightowlers, M. W., & Rickard, M. D. 1988. Excretory-secretory products of helminth parasites: effects on host immune responses. ***Parasitology***, 96 Suppl: S123-166.

Liu, D., & Uzonna, J. E. 2012. The early interaction of Leishmania with macrophages and dendritic cells and its influence on the host immune response. ***Front Cell Infect Microbiol***, 2: 83.

Liu, Q., Kreider, T., Bowdridge, S., Liu, Z., Song, Y., Gaydo, A. G., Urban, J. F., Jr., & Gause, W. C. 2010. B cells have distinct roles in host protection against different nematode parasites. ***Journal of immunology (Baltimore, Md : 1950)***, 184(9): 5213-5223.

Liu, S. K., Cypess, R. H., & van Zandt, P. 1974. Gastritis caused by multiple Nematospiroides dubius infections. ***J Parasitol***, 60(5): 790-793.

Loftus, E. V., Jr. 2004. Clinical epidemiology of inflammatory bowel disease: Incidence, prevalence, and environmental influences. ***Gastroenterology***, 126(6): 1504-1517.

Loke, P., Nair, M. G., Parkinson, J., Guiliano, D., Blaxter, M., & Allen, J. E. 2002. IL-4 dependent alternatively-activated macrophages have a distinctive in vivo gene expression phenotype. ***BMC Immunol***, 3: 7.

Lubetsky, J. B., Swope, M., Dealwis, C., Blake, P., & Lolis, E. 1999. Pro-1 of macrophage migration inhibitory factor functions as a catalytic base in the phenylpyruvate tautomerase activity. ***Biochemistry***, 38(22): 7346-7354.

Lue, H., Kleemann, R., Calandra, T., Roger, T., & Bernhagen, J. 2002. Macrophage migration inhibitory factor (MIF): mechanisms of action and role in disease. ***Microbes Infect***, 4(4): 449-460.

Lustigman, S., Brotman, B., Huima, T., Prince, A. M., & McKerrow, J. H. 1992. Molecular cloning and characterization of onchocystatin, a cysteine proteinase inhibitor of Onchocerca volvulus. ***J Biol Chem***, 267(24): 17339-17346.

Lustigman, S., Geldhof, P., Grant, W. N., Osei-Atweneboana, M. Y., Sripa, B., & Basanez, M. G. 2012. A research agenda for helminth diseases of humans: basic research and enabling technologies to support control and elimination of helminthiases. ***PLoS Negl Trop Dis***, 6(4): e1445.

Maaser, C., Eckmann, L., Paesold, G., Kim, H. S., & Kagnoff, M. F. 2002. Ubiquitous production of macrophage migration inhibitory factor by human gastric and intestinal epithelium. ***Gastroenterology***, 122(3): 667-680.

Mabbott, N. A., Donaldson, D. S., Ohno, H., Williams, I. R., & Mahajan, A. 2013. Microfold (M) cells: important immunosurveillance posts in the intestinal epithelium. ***Mucosal Immunol***, 6(4): 666-677.

MacDonald, A. J., Cao, L., He, Y., Zhao, Q., Jiang, S., & Lustigman, S. 2005. rOv-ASP-1, a recombinant secreted protein of the helminth Onchocercavolvulus, is a potent adjuvant for inducing antibodies to ovalbumin, HIV-1 polypeptide and SARS-CoV peptide antigens, ***Vaccine***, Vol. 23: 3446-3452.

MacDonald, A. S., & Maizels, R. M. 2008. Alarming dendritic cells for Th2 induction. ***J Exp Med***, 205(1): 13-17.

MacDonald, A. S., Maizels, R. M., Lawrence, R. A., Dransfield, I., & Allen, J. E. 1998. Requirement for in vivo production of IL-4, but not IL-10, in the induction of proliferative suppression by filarial parasites. ***J Immunol***, 160(3): 1304-1312.

MacDonald AS, M. R., Lawrence RA, Dransfield I, Allen JE. 1998 Requirement for in vivo production of IL-4, but not IL-10, in the induction of proliferative suppression by filarial parasites. ***J Immunol***, 15: 4124-4132.

MacLennan, K., McLean, K., & Knox, D. P. 2005. Serpin expression in the parasitic stages of Trichostrongylus vitrinus, an ovine intestinal nematode. ***Parasitology***, 130(Pt 3): 349-357.

Magalhaes, E. S., Mourao-Sa, D. S., Vieira-de-Abreu, A., Figueiredo, R. T., Pires, A. L., Farias-Filho, F. A., Fonseca, B. P., Viola, J. P., Metz, C., Martins, M. A., Castro-Faria-Neto, H. C., Bozza, P. T., & Bozza, M. T. 2007. Macrophage migration inhibitory factor is essential for allergic asthma but not for Th2 differentiation. ***Eur J Immunol***, 37(4): 1097-1106.

Magalhaes, E. S., Paiva, C. N., Souza, H. S., Pyrrho, A. S., Mourao-Sa, D., Figueiredo, R. T., Vieira-de-Abreu, A., Dutra, H. S., Silveira, M. S., Gaspar-Elsas, M. I., Xavier-Elsas, P., Bozza, P. T., & Bozza, M. T. 2009. Macrophage migration inhibitory factor is critical to interleukin-5-driven eosinophilopoiesis and tissue eosinophilia triggered by Schistosoma mansoni infection. ***FASEB J***, 23(4): 1262-1271.

Maizels, R. M., Gomez-Escobar, N., Gregory, W. F., Murray, J., & Zang, X. 2001. Immune evasion genes from filarial nematodes. ***Int J Parasitol***, 31(9): 889-898.

Maizels, R. M., Hewitson, J. P., & Gause, W. C. 2011. Heligmosomoides polygyrus: one species still. ***Trends Parasitol***, 27(3): 100-101.

Maizels, R. M., Hewitson, J. P., Murray, J., Harcus, Y. M., Dayer, B., Filbey, K. J., Grainger, J. R., McSorley, H. J., Reynolds, L. A., & Smith, K. A. 2012. Immune modulation and modulators in Heligmosomoides polygyrus infection. ***Exp Parasitol***, 132(1): 76-89.

Manoury, B., Gregory, W. F., Maizels, R. M., & Watts, C. 2001. Bm-CPI-2, a cystatin homolog secreted by the filarial parasite Brugia malayi, inhibits class II MHC-restricted antigen processing. ***Curr Biol***, 11(6): 447-451.

Mantovani, A., Cassatella, M. A., Costantini, C., & Jaillon, S. 2011. Neutrophils in the activation and regulation of innate and adaptive immunity. ***Nature reviews Immunology***, 11(8): 519-531.

Marillier, R. G., Michels, C., Smith, E. M., Fick, L. C., Leeto, M., Dewals, B., Horsnell, W. G., & Brombacher, F. 2008. IL-4/IL-13 independent goblet cell hyperplasia in experimental helminth infections. ***BMC Immunol***, 9: 11.

Markus, M. B. 2011. Malaria: origin of the term "hypnozoite". ***J Hist Biol***, 44(4): 781-786.

Marrie, R. A. 2004. Environmental risk factors in multiple sclerosis aetiology. ***Lancet Neurol***, 3(12): 709-718.

Martens, E. C., Roth, R., Heuser, J. E., & Gordon, J. I. 2009. Coordinate regulation of glycan degradation and polysaccharide capsule biosynthesis by a prominent human gut symbiont. ***J Biol Chem***, 284(27): 18445-18457.

Martin, C., Saeftel, M., Vuong, P. N., Babayan, S., Fischer, K., Bain, O., & Hoerauf, A. 2001. B-cell deficiency suppresses vaccine-induced protection against murine filariasis but does not increase the recovery rate for primary infection. ***Infect Immun***, 69(11): 7067-7073.

Mason, L., Tribolet, L., Simon, A., von Gnielinski, N., Nienaber, L., Taylor, P., Willis, C., Jones, M. K., Sternberg, P. W., Gasser, R. B., Loukas, A., & Hofmann, A. 2014. Probing the equatorial groove of the hookworm protein and vaccine candidate antigen, Na-ASP-2. ***Int J Biochem Cell Biol***, 50: 146-155.

Massacand, J. C., Stettler, R. C., Meier, R., Humphreys, N. E., Grencis, R. K., Marsland, B. J., & Harris, N. L. 2009. Helminth products bypass the need for TSLP in Th2 immune responses by directly modulating dendritic cell function. ***Proc Natl Acad Sci U S A***, 106(33): 13968-13973.

Massoni, J., Durette-Desset, M. C., Quere, J. P., & Audebert, F. 2012. Redescription of Heligmosomoides neopolygyrus, Asakawa and Ohbayashi, 1986 (Nematoda: Heligmosomidae) from a Chinese rodent, Apodemus peninsulae (Rodentia: Muridae); with comments on Heligmosomoides polygyrus polygyrus (Dujardin, 1845) and related species in China and Japan. ***Parasite***, 19(4): 367-374.

Masure, D., Vlaminck, J., Wang, T., Chiers, K., Van den Broeck, W., Vercruysse, J., & Geldhof, P. 2013. A role for eosinophils in the intestinal immunity against infective Ascaris suum larvae. ***PLoS Negl Trop Dis***, 7(3): e2138.

McCoy, K. D., Stoel, M., Stettler, R., Merky, P., Fink, K., Senn, B. M., Schaer, C., Massacand, J., Odermatt, B., Oettgen, H. C., Zinkernagel, R. M., Bos, N. A., Hengartner, H., Macpherson, A. J., & Harris, N. L. 2008. Polyclonal and

specific antibodies mediate protective immunity against enteric helminth infection. ***Cell Host Microbe***, 4(4): 362-373.
McCulloch, R., & Barry, J. D. 1999. A role for RAD51 and homologous recombination in Trypanosoma brucei antigenic variation. ***Genes Dev***, 13(21): 2875-2888.
McDole, J. R., Wheeler, L. W., McDonald, K. G., Wang, B., Konjufca, V., Knoop, K. A., Newberry, R. D., & Miller, M. J. 2012. Goblet cells deliver luminal antigen to CD103+ dendritic cells in the small intestine. ***Nature***, 483(7389): 345-349.
McLaren, D. J., Mackenzie, C. D., & Ramalho-Pinto, F. J. 1977. Ultrastructural observations on the in vitro interaction between rat eosinophils and some parasitic helminths (Schistosoma mansoni, Trichinella spiralis and Nippostrongylus brasiliensis). ***Clin Exp Immunol***, 30(1): 105-118.
McNeilly, T. N., & Nisbet, A. J. 2014. Immune modulation by helminth parasites of ruminants: implications for vaccine development and host immune competence. ***Parasite***, 21: 51.
McSorley, H. J., Blair, N. F., Smith, K. A., McKenzie, A. N., & Maizels, R. M. 2014. Blockade of IL-33 release and suppression of type 2 innate lymphoid cell responses by helminth secreted products in airway allergy. ***Mucosal Immunol***.
McSorley, H. J., Hewitson, J. P., & Maizels, R. M. 2013. Immunomodulation by helminth parasites: defining mechanisms and mediators, ***Int J Parasitol***, Vol. 43: 301-310.
McSorley, H. J., & Maizels, R. M. 2012. Helminth infections and host immune regulation. ***Clin Microbiol Rev***, 25(4): 585-608.
McSorley, H. J., O'Gorman, M. T., Blair, N., Sutherland, T. E., Filbey, K. J., & Maizels, R. M. 2012. Suppression of type 2 immunity and allergic airway inflammation by secreted products of the helminth Heligmosomoides polygyrus, ***Eur J Immunol***, Vol. 42: 2667-2682.
Mege, J. L., Mehraj, V., & Capo, C. 2011. Macrophage polarization and bacterial infections. ***Curr Opin Infect Dis***, 24(3): 230-234.
Mehr, I. J., & Seifert, H. S. 1998. Differential roles of homologous recombination pathways in Neisseria gonorrhoeae pilin antigenic variation, DNA transformation and DNA repair. ***Mol Microbiol***, 30(4): 697-710.
Metwali, A., Setiawan, T., Blum, A. M., Urban, J., Elliott, D. E., Hang, L., & Weinstock, J. V. 2006. Induction of CD8+ regulatory T cells in the intestine by Heligmosomoides polygyrus infection. ***Am J Physiol Gastrointest Liver Physiol***, 291(2): G253-259.
Meurs, H., Gosens, R., & Zaagsma, J. 2008. Airway hyperresponsiveness in asthma: lessons from in vitro model systems and animal models, ***European Respiratory Journal***, Vol. 32: 487-502.
Meyvis, Y., Geldhof, P., Gevaert, K., Timmerman, E., Vercruysse, J., & Claerebout, E. 2007. Vaccination against Ostertagia ostertagi with subfractions of the protective ES-thiol fraction. ***Vet Parasitol***, 149(3-4): 239-245.
Mills, K. H. 2008. Induction, function and regulation of IL-17-producing T cells. ***Eur J Immunol***, 38(10): 2636-2649.
Min, B., Le Gros, G., & Paul, W. E. 2006. Basophils: a potential liaison between innate and adaptive immunity. ***Allergol Int***, 55(2): 99-104.

Misslitz, A., Mottram, J. C., Overath, P., & Aebischer, T. 2000. Targeted integration into a rRNA locus results in uniform and high level expression of transgenes in Leishmania amastigotes. ***Mol Biochem Parasitol***, 107(2): 251-261.

Mitre, E., & Nutman, T. B. 2003. Lack of basophilia in human parasitic infections. ***Am J Trop Med Hyg***, 69(1): 87-91.

Mo, H. M., Lei, J. H., Jiang, Z. W., Wang, C. Z., Cheng, Y. L., Li, Y. L., & Liu, W. Q. 2008. Schistosoma japonicum infection modulates the development of allergen-induced airway inflammation in mice. ***Parasitol Res***, 103(5): 1183-1189.

Moreau, M. C., & Corthier, G. 1988. Effect of the gastrointestinal microflora on induction and maintenance of oral tolerance to ovalbumin in C3H/HeJ mice. ***Infect Immun***, 56(10): 2766-2768.

Morelli, A. E., Zahorchak, A. F., Larregina, A. T., Colvin, B. L., Logar, A. J., Takayama, T., Falo, L. D., & Thomson, A. W. 2001. Cytokine production by mouse myeloid dendritic cells in relation to differentiation and terminal maturation induced by lipopolysaccharide or CD40 ligation. ***Blood***, 98(5): 1512-1523.

Morimoto, M., Morimoto, M., Whitmire, J., Xiao, S., Anthony, R. M., Mirakami, H., Star, R. A., Urban, J. F., Jr., & Gause, W. C. 2004. Peripheral CD4 T cells rapidly accumulate at the host: parasite interface during an inflammatory Th2 memory response. ***Journal of immunology (Baltimore, Md : 1950)***, 172(4): 2424-2430.

Morrison, S. J., & Spradling, A. C. 2008. Stem cells and niches: mechanisms that promote stem cell maintenance throughout life. ***Cell***, 132(4): 598-611.

Mosser, D. M. 2003. The many faces of macrophage activation. ***J Leukoc Biol***, 73(2): 209-212.

Mosser, D. M., & Edwards, J. P. 2008. Exploring the full spectrum of macrophage activation. ***Nat Rev Immunol***, 8(12): 958-969.

Mulder, N. J., Apweiler, R., Attwood, T. K., Bairoch, A., Barrell, D., Bateman, A., Binns, D., Biswas, M., Bradley, P., Bork, P., Bucher, P., Copley, R. R., Courcelle, E., Das, U., Durbin, R., Falquet, L., Fleischmann, W., Griffiths-Jones, S., Haft, D., Harte, N., Hulo, N., Kahn, D., Kanapin, A., Krestyaninova, M., Lopez, R., Letunic, I., Lonsdale, D., Silventoinen, V., Orchard, S. E., Pagni, M., Peyruc, D., Ponting, C. P., Selengut, J. D., Servant, F., Sigrist, C. J., Vaughan, R., & Zdobnov, E. M. 2003. The InterPro Database, 2003 brings increased coverage and new features. ***Nucleic Acids Res***, 31(1): 315-318.

Mulu, A., Legesse, M., Erko, B., Belyhun, Y., Nugussie, D., Shimelis, T., Kassu, A., Elias, D., & Moges, B. 2013. Epidemiological and clinical correlates of malaria-helminth co-infections in Southern Ethiopia. ***Malar J***, 12: 227.

Murray, J. 2007. Structure and Function of the VAL family in Brugia malayi.

Murray, J., Gregory, W. F., Gomez-Escobar, N., Atmadja, A. K., & Maizels, R. M. 2001. Expression and immune recognition of Brugia malayi VAL-1, a homologue of vespid venom allergens and Ancylostoma secreted proteins. ***Mol Biochem Parasitol***, 118(1): 89-96.

Murray, J., Manoury, B., Balic, A., Watts, C., & Maizels, R. M. 2005. Bm-CPI-2, a cystatin from Brugia malayi nematode parasites, differs from Caenorhabditis

elegans cystatins in a specific site mediating inhibition of the antigen-processing enzyme AEP. ***Mol Biochem Parasitol***, 139(2): 197-203.
Nandan, D., & Reiner, N. E. 1997. TGF-beta attenuates the class II transactivator and reveals an accessory pathway of IFN-gamma action. ***J Immunol***, 158(3): 1095-1101.
Neu, J., & Rushing, J. 2011. Cesarean versus vaginal delivery: long-term infant outcomes and the hygiene hypothesis. ***Clin Perinatol***, 38(2): 321-331.
Nevalainen, T. J., & Haapanen, T. J. 1993. Distribution of pancreatic (group I) and synovial-type (group II) phospholipases A2 in human tissues. ***Inflammation***, 17(4): 453-464.
Nisbet, A. J., Zarlenga, D. S., Knox, D. P., Meikle, L. I., Wildblood, L. A., & Matthews, J. B. 2011. A calcium-activated apyrase from Teladorsagia circumcincta: an excretory/secretory antigen capable of modulating host immune responses? ***Parasite Immunol***, 33(4): 236-243.
O'Connell, A. E., Hess, J. A., Santiago, G. A., Nolan, T. J., Lok, J. B., Lee, J. J., & Abraham, D. 2011. Major basic protein from eosinophils and myeloperoxidase from neutrophils are required for protective immunity to Strongyloides stercoralis in mice. ***Infect Immun***, 79(7): 2770-2778.
Ogilvie, B. M., & Jones, V. E. 1971. Parasitological review. Nippostrongylus brasiliensis: a review of immunity and host-parasite relationship in the rat. ***Exp Parasitol***, 29(1): 138-177.
Organization, W. H. 2014a. Lymphatic filariasis, ***Fact Sheet***.
Organization, W. H. 2014b. Onchocerciasis, ***Fact Sheet***.
Organization, W. H. 2014c. Schistosomiasis, ***Fact Sheet***.
Organization, W. H. 2014d. Soil-transmitted helminth infections, ***Fact Sheet***.
Osman, A., Wang, C. K., Winter, A., Loukas, A., Tribolet, L., Gasser, R. B., & Hofmann, A. 2012. Hookworm SCP/TAPS protein structure--A key to understanding host-parasite interactions and developing new interventions. ***Biotechnol Adv***, 30(3): 652-657.
Owhashi, M., Arita, H., & Hayai, N. 2000. Identification of a novel eosinophil chemotactic cytokine (ECF-L) as a chitinase family protein. ***J Biol Chem***, 275(2): 1279-1286.
Page, A. P., & Johnstone, I. L. 2007. The cuticle. ***WormBook***: 1-15.
Page, A. P., Rudin, W., Fluri, E., Blaxter, M. L., & Maizels, R. M. 1992. Toxocara canis: a labile antigenic surface coat overlying the epicuticle of infective larvae. ***Exp Parasitol***, 75(1): 72-86.
Park, K. S., Korfhagen, T. R., Bruno, M. D., Kitzmiller, J. A., Wan, H., Wert, S. E., Khurana Hershey, G. K., Chen, G., & Whitsett, J. A. 2007. SPDEF regulates goblet cell hyperplasia in the airway epithelium. ***J Clin Invest***, 117(4): 978-988.
Park, S. K., Cho, M. K., Park, H. K., Lee, K. H., Lee, S. J., Choi, S. H., Ock, M. S., Jeong, H. J., Lee, M. H., & Yu, H. S. 2009. Macrophage migration inhibitory factor homologs of anisakis simplex suppress Th2 response in allergic airway inflammation model via CD4+CD25+Foxp3+ T cell recruitment. ***J Immunol***, 182(11): 6907-6914.
Pastrana, D. V., Raghavan, N., FitzGerald, P., Eisinger, S. W., Metz, C., Bucala, R., Schleimer, R. P., Bickel, C., & Scott, A. L. 1998. Filarial nematode parasites

secrete a homologue of the human cytokine macrophage migration inhibitory factor. ***Infect Immun***, 66(12): 5955-5963.
Patel, N., Kreider, T., Urban, J. F., Jr., & Gause, W. C. 2009. Characterisation of effector mechanisms at the host:parasite interface during the immune response to tissue-dwelling intestinal nematode parasites. ***Int J Parasitol***, 39(1): 13-21.
Pawlowski Z. Schad G and Stott G. 1991. Hookworm infection and anaemia : approaches to prevention and control Geneva : World Health Organization.
Pays, E., Vanhamme, L., & Perez-Morga, D. 2004. Antigenic variation in Trypanosoma brucei: facts, challenges and mysteries. ***Curr Opin Microbiol***, 7(4): 369-374.
Peao, M. N., Aguas, A. P., de Sa, C. M., & Grande, N. R. 1993. Anatomy of Clara cell secretion: surface changes observed by scanning electron microscopy. ***J Anat***, 182 (Pt 3): 377-388.
Pederson, J. L., Chapot, M. S., Simms, S. R., Sohbati, R., Rittenour, T. M., Murray, A. S., & Cox, G. 2014. Age of Barrier Canyon-style rock art constrained by cross-cutting relations and luminescence dating techniques. ***Proc Natl Acad Sci U S A***, 111(36): 12986-12991.
Pennock, J. L., Behnke, J. M., Bickle, Q. D., Devaney, E., Grencis, R. K., Isaac, R. E., Joshua, G. W., Selkirk, M. E., Zhang, Y., & Meyer, D. J. 1998. Rapid purification and characterization of L-dopachrome-methyl ester tautomerase (macrophage-migration-inhibitory factor) from Trichinella spiralis, Trichuris muris and Brugia pahangi. ***Biochem J***, 335 (Pt 3): 495-498.
Penttila, I. A., Ey, P. L., & Jenkin, C. R. 1983. Adherence of murine peripheral blood eosinophils and neutrophils to the different parasitic stages of Nematospiroides dubius. ***Aust J Exp Biol Med Sci***, 61 (Pt 6): 617-627.
Perona-Wright, G., Jenkins, S. J., & MacDonald, A. S. 2006. Dendritic cell activation and function in response to Schistosoma mansoni. ***Int J Parasitol***, 36(6): 711-721.
Pesce, J. T., Ramalingam, T. R., Mentink-Kane, M. M., Wilson, M. S., El Kasmi, K. C., Smith, A. M., Thompson, R. W., Cheever, A. W., Murray, P. J., & Wynn, T. A. 2009a. Arginase-1-expressing macrophages suppress Th2 cytokine-driven inflammation and fibrosis. ***PLoS Pathog***, 5(4): e1000371.
Pesce, J. T., Ramalingam, T. R., Wilson, M. S., Mentink-Kane, M. M., Thompson, R. W., Cheever, A. W., Urban, J. F., Jr., & Wynn, T. A. 2009b. Retnla (relmalpha/fizz1) suppresses helminth-induced Th2-type immunity. ***PLoS Pathog***, 5(4): e1000393.
Peters, N. C., Egen, J. G., Secundino, N., Debrabant, A., Kimblin, N., Kamhawi, S., Lawyer, P., Fay, M. P., Germain, R. N., & Sacks, D. 2008. In vivo imaging reveals an essential role for neutrophils in leishmaniasis transmitted by sand flies. ***Science***, 321(5891): 970-974.
Peterson, L. W., & Artis, D. 2014. Intestinal epithelial cells: regulators of barrier function and immune homeostasis. ***Nat Rev Immunol***, 14(3): 141-153.
Pfaff, A. W., Schulz-Key, H., Soboslay, P. T., Taylor, D. W., MacLennan, K., & Hoffmann, W. H. 2002. Litomosoides sigmodontis cystatin acts as an immunomodulator during experimental filariasis. ***Int J Parasitol***, 32(2): 171-178.

Pinto, D., Gregorieff, A., Begthel, H., & Clevers, H. 2003. Canonical Wnt signals are essential for homeostasis of the intestinal epithelium. ***Genes Dev***, 17(14): 1709-1713.

Pogonka, T., Oberlander, U., Marti, T., & Lucius, R. 1999. Acanthocheilonema viteae: characterization of a molt-associated excretory/secretory 18-kDa protein. ***Exp Parasitol***, 93(2): 73-81.

Porter, E. M., Bevins, C. L., Ghosh, D., & Ganz, T. 2002. The multifaceted Paneth cell. ***Cell Mol Life Sci***, 59(1): 156-170.

Pritchard, D. I., Maizels, R. M., Behnke, J. M., & Appleby, P. 1984. Stage-specific antigens of Nematospiroides dubius. ***Immunology***, 53(2): 325-335.

Prucca, C. G., & Lujan, H. D. 2009. Antigenic variation in Giardia lamblia. ***Cell Microbiol***, 11(12): 1706-1715.

Qiang, S., Bin, Z., Shu-hua, X., Zheng, F., Hotez, P., & Hawdon, J. M. 2000. Variation between ASP-1 molecules from Ancylostoma caninum in China and the United States. ***J Parasitol***, 86(1): 181-185.

Ramirez, G., Valck, C., Aguilar, L., Kemmerling, U., Lopez-Munoz, R., Cabrera, G., Morello, A., Ferreira, J., Maya, J. D., Galanti, N., & Ferreira, A. 2012. Roles of Trypanosoma cruzi calreticulin in parasite-host interactions and in tumor growth. ***Mol Immunol***, 52(3-4): 133-140.

Reece, J. J., Siracusa, M. C., & Scott, A. L. 2006. Innate immune responses to lung-stage helminth infection induce alternatively activated alveolar macrophages. ***Infect Immun***, 74(9): 4970-4981.

Reibman, J., Meixler, S., Lee, T. C., Gold, L. I., Cronstein, B. N., Haines, K. A., Kolasinski, S. L., & Weissmann, G. 1991. Transforming growth factor beta 1, a potent chemoattractant for human neutrophils, bypasses classic signal-transduction pathways. ***Proc Natl Acad Sci U S A***, 88(15): 6805-6809.

Reya, T., & Clevers, H. 2005. Wnt signalling in stem cells and cancer. ***Nature***, 434(7035): 843-850.

Reynolds, L., Smith, K., Filbey, K., Harcus, Y., Hewitson, J., Redpath, S., Valdez, Y., Yebra, M., Finlay, B. B., & Maizels, R. 2014. Commensal-pathogen interactions in the intestinal tract: Lactobacilli promote infection with, and are promoted by, helminth parasites. ***Gut Microbes***, 5(4).

Reynolds, L. A., Filbey, K. J., & Maizels, R. M. 2012. Immunity to the model intestinal helminth parasite Heligmosomoides polygyrus. ***Semin Immunopathol***, 34(6): 829-846.

Reynolds, S. D., & Malkinson, A. M. 2010. Clara cell: progenitor for the bronchiolar epithelium. ***Int J Biochem Cell Biol***, 42(1): 1-4.

Ribeiro-Gomes, F. L., Peters, N. C., Debrabant, A., & Sacks, D. L. 2012. Efficient capture of infected neutrophils by dendritic cells in the skin inhibits the early anti-leishmania response. ***PLoS Pathog***, 8(2): e1002536.

Rieu, P., Ueda, T., Haruta, I., Sharma, C. P., & Arnaout, M. A. 1994. The A-domain of beta 2 integrin CR3 (CD11b/CD18) is a receptor for the hookworm-derived neutrophil adhesion inhibitor NIF. ***J Cell Biol***, 127(6 Pt 2): 2081-2091.

Mann VH[1], Suttiprapa S, Skinner DE, Brindley PJ, Rinaldi G. 2014. Pseudotyped murine leukemia virus for schistosome transgenesis: approaches, methods and perspectives. **Transgenic Res.** 23(3):539-56

Roberts, S. C., Tancer, M. J., Polinsky, M. R., Gibson, K. M., Heby, O., & Ullman, B. 2004. Arginase plays a pivotal role in polyamine precursor metabolism in Leishmania. Characterization of gene deletion mutants. ***J Biol Chem***, 279(22): 23668-23678.

Rogers, D. F. 1994. Airway goblet cells: responsive and adaptable front-line defenders. ***Eur Respir J***, 7(9): 1690-1706.

Rogers, D. F. 2003. The airway goblet cell. ***Int J Biochem Cell Biol***, 35(1): 1-6.

Ronger-Savle, S., Valladeau, J., Claudy, A., Schmitt, D., Peguet-Navarro, J., Dezutter-Dambuyant, C., Thomas, L., & Jullien, D. 2005. TGFbeta inhibits CD1d expression on dendritic cells. ***J Invest Dermatol***, 124(1): 116-118.

Rook, G. A. 2009. Review series on helminths, immune modulation and the hygiene hypothesis: the broader implications of the hygiene hypothesis. ***Immunology***, 126(1): 3-11.

Rook, G. A. W. 2010. 99th Dahlem conference on infection, inflammation and chronic inflammatory disorders: darwinian medicine and the 'hygiene' or 'old friends' hypothesis. ***Clin Exp Immunol***, 160(1): 70-79.

Rosas, L. E., Keiser, T., Barbi, J., Satoskar, A. A., Septer, A., Kaczmarek, J., Lezama-Davila, C. M., & Satoskar, A. R. 2005. Genetic background influences immune responses and disease outcome of cutaneous L. mexicana infection in mice. ***Int Immunol***, 17(10): 1347-1357.

Rosengren, E., Bucala, R., Aman, P., Jacobsson, L., Odh, G., Metz, C. N., & Rorsman, H. 1996. The immunoregulatory mediator macrophage migration inhibitory factor (MIF) catalyzes a tautomerization reaction. ***Mol Med***, 2(1): 143-149.

Ruemmele, F. M., & Garnier-Lengline, H. 2013. Transforming growth factor and intestinal inflammation: the role of nutrition. ***Nestle Nutr Inst Workshop Ser***, 77: 91-98.

Rzepecka, J., Donskow-Schmelter, K., & Doligalska, M. 2007. Heligmosomoides polygyrus infection down-regulates eotaxin concentration and CCR3 expression on lung eosinophils in murine allergic pulmonary inflammation. ***Parasite Immunol***, 29(8): 405-413.

Samarasinghe, B., Knox, D. P., & Britton, C. 2010. Factors affecting susceptibility to RNA interference in Haemonchuscontortus and in vivo silencing of an H11 aminopeptidase gene, ***International Journal for Parasitology***.

Samarasinghe, B., Knox, D. P., & Britton, C. 2011. Factors affecting susceptibility to RNA interference in Haemonchus contortus and in vivo silencing of an H11 aminopeptidase gene. ***Int J Parasitol***, 41(1): 51-59.

Sato, T., van Es, J. H., Snippert, H. J., Stange, D. E., Vries, R. G., van den Born, M., Barker, N., Shroyer, N. F., van de Wetering, M., & Clevers, H. 2011. Paneth cells constitute the niche for Lgr5 stem cells in intestinal crypts. ***Nature***, 469(7330): 415-418.

Sato, T., Vries, R. G., Snippert, H. J., van de Wetering, M., Barker, N., Stange, D. E., van Es, J. H., Abo, A., Kujala, P., Peters, P. J., & Clevers, H. 2009. Single Lgr5 stem cells build crypt-villus structures in vitro without a mesenchymal niche. ***Nature***, 459(7244): 262-265.

Satoh-Takayama, N., Vosshenrich, C. A. J., Lesjean-Pottier, S., Sawa, S., Lochner, M., Rattis, F., Mention, J.-J., Thiam, K., Cerf-Bensussan, N., Mandelboim, O., Eberl, G., & Di Santo, J. P. 2008. Microbial flora drives interleukin 22

production in intestinal NKp46+ cells that provide innate mucosal immune defense. ***Immunity***, 29(6): 958-970.
Satoskar, A. R., Bozza, M., Rodriguez Sosa, M., Lin, G., & David, J. R. 2001. Migration-inhibitory factor gene-deficient mice are susceptible to cutaneous Leishmania major infection. ***Infect Immun***, 69(2): 906-911.
Saverwyns, H., Visser, A., Nisbet, A. J., Peelaers, I., Gevaert, K., Vercruysse, J., Claerebout, E., & Geldhof, P. 2008. Identification and characterization of a novel specific secreted protein family for selected members of the subfamily Ostertagiinae (Nematoda). ***Parasitology***, 135(Pt 1): 63-70.
Scherf, A., Lopez-Rubio, J. J., & Riviere, L. 2008. Antigenic variation in Plasmodium falciparum. ***Annu Rev Microbiol***, 62: 445-470.
Schnoeller, C., Rausch, S., Pillai, S., Avagyan, A., Wittig, B. M., Loddenkemper, C., Hamann, A., Hamelmann, E., Lucius, R., & Hartmann, S. 2008. A helminth immunomodulator reduces allergic and inflammatory responses by induction of IL-10-producing macrophages. ***J Immunol***, 180(6): 4265-4272.
Schonemeyer, A., Lucius, R., Sonnenburg, B., Brattig, N., Sabat, R., Schilling, K., Bradley, J., & Hartmann, S. 2001. Modulation of human T cell responses and macrophage functions by onchocystatin, a secreted protein of the filarial nematode Onchocerca volvulus. ***J Immunol***, 167(6): 3207-3215.
Schramm, G., Mohrs, K., Wodrich, M., Doenhoff, M. J., Pearce, E. J., Haas, H., & Mohrs, M. 2007. Cutting edge: IPSE/alpha-1, a glycoprotein from Schistosoma mansoni eggs, induces IgE-dependent, antigen-independent IL-4 production by murine basophils in vivo. ***Journal of immunology (Baltimore, Md : 1950)***, 178(10): 6023-6027.
Segura, M., Su, Z., Piccirillo, C., & Stevenson, M. M. 2007. Impairment of dendritic cell function by excretory-secretory products: a potential mechanism for nematode-induced immunosuppression. ***Eur J Immunol***, 37(7): 1887-1904.
Senegas-Balas, F., Balas, D., Pradayrol, L., Laval, J., & Ribet, A. 1979. Comparative effects of CCK-PZ on certain intestinal hydrolases in the mucosa and in the luminal content of the hamster jejuno-ileum. ***Acta Hepatogastroenterol (Stuttg)***, 26(6): 486-492.
Shamri, R., Xenakis, J. J., & Spencer, L. A. 2011. Eosinophils in innate immunity: an evolving story. ***Cell and tissue research***, 343(1): 57-83.
Shin, M. H., Lee, Y. A., & Min, D. Y. 2009. Eosinophil-mediated tissue inflammatory responses in helminth infection. ***Korean J Parasitol***, 47 Suppl: S125-131.
Shinagawa, K., & Kojima, M. 2003. Mouse model of airway remodeling: strain differences. ***Am J Respir Crit Care Med***, 168(8): 959-967.
Shweash, M., Adrienne McGachy, H., Schroeder, J., Neamatallah, T., Bryant, C. E., Millington, O., Mottram, J. C., Alexander, J., & Plevin, R. 2011. Leishmania mexicana promastigotes inhibit macrophage IL-12 production via TLR-4 dependent COX-2, iNOS and arginase-1 expression. ***Mol Immunol***, 48(15-16): 1800-1808.
Simpson, K. J., Davis, G. M., & Boag, P. R. 2012. Comparative high-throughput RNAi screening methodologies in C. elegans and mammalian cells. ***N Biotechnol***, 29(4): 459-470.
Siracusa, M. C., Saenz, S. A., Hill, D. A., Kim, B. S., Headley, M. B., Doering, T. A., Wherry, E. J., Jessup, H. K., Siegel, L. A., Kambayashi, T., Dudek, E. C.,

Kubo, M., Cianferoni, A., Spergel, J. M., Ziegler, S. F., Comeau, M. R., & Artis, D. 2011. TSLP promotes interleukin-3-independent basophil haematopoiesis and type 2 inflammation. ***Nature***, 477(7363): 229-233.

Sorci, G., & Faivre, B. 2009. Inflammation and oxidative stress in vertebrate host-parasite systems. ***Philosophical transactions of the Royal Society of London Series B, Biological sciences***, 364(1513): 71-83.

Specian, R. D., & Oliver, M. G. 1991. Functional biology of intestinal goblet cells. ***Am J Physiol***, 260(2 Pt 1): C183-193.

Spiegel, Y., & Robertson, W. M. 1988. Wheat Germ Agglutinin Binding to the Outer Cuticle of the Plant-parasitic Nematode Anguina tritici. ***J Nematol***, 20(3): 499-501.

Spits, H., Artis, D., Colonna, M., Diefenbach, A., Di Santo, J. P., Eberl, G., Koyasu, S., Locksley, R. M., McKenzie, A. N. J., Mebius, R. E., Powrie, F., & Vivier, E. 2013. Innate lymphoid cells--a proposal for uniform nomenclature. ***Nature reviews Immunology***, 13(2): 145-149.

Spurlock, G. M. 1943. Observations on Host-Parasite Relations between Laboratory Mice and Nematospiroides dubius Baylis. ***The Journal of Parasitology***, 29(5): 303-311.

Stavnezer, J. 1995. Regulation of antibody production and class switching by TGF-beta. ***J Immunol***, 155(4): 1647-1651.

Stein, M., Keshav, S., Harris, N., & Gordon, S. 1992. Interleukin 4 potently enhances murine macrophage mannose receptor activity: a marker of alternative immunologic macrophage activation. ***J Exp Med***, 176(1): 287-292.

Stockdale, C., Swiderski, M. R., Barry, J. D., & McCulloch, R. 2008. Antigenic variation in Trypanosoma brucei: joining the DOTs. ***PLoS Biol***, 6(7): e185.

Strachan, D. P. 1989. Hay fever, hygiene, and household size. ***BMJ***, 299(6710): 1259-1260.

Su, Z., Segura, M., & Stevenson, M. M. 2006. Reduced protective efficacy of a blood-stage malaria vaccine by concurrent nematode infection. ***Infect Immun***, 74(4): 2138-2144.

Suck, R., Weber, B., Kahlert, H., Hagen, S., Cromwell, O., & Fiebig, H. 2000. Purification and immunobiochemical characterization of folding variants of the recombinant major wasp allergen Ves v 5 (antigen 5). ***Int Arch Allergy Immunol***, 121(4): 284-291.

Sullivan, B. M., & Locksley, R. M. 2009. Basophils: a nonredundant contributor to host immunity. ***Immunity***, 30(1): 12-20.

Sutherland, T. E., Maizels, R. M., & Allen, J. E. 2009. Chitinases and chitinase-like proteins: potential therapeutic targets for the treatment of T-helper type 2 allergies. ***Clin Exp Allergy***, 39(7): 943-955.

Swope, M., Sun, H. W., Blake, P. R., & Lolis, E. 1998. Direct link between cytokine activity and a catalytic site for macrophage migration inhibitory factor. ***EMBO J***, 17(13): 3534-3541.

Szekanecz, Z., & Koch, A. E. 2007. Macrophages and their products in rheumatoid arthritis. ***Current opinion in rheumatology***, 19(3): 289-295.

Szyperski, T., Fernández, C., Mumenthaler, C., & Wüthrich, K. 1998. Structure comparison of human glioma pathogenesis-related protein GliPR and the plant pathogenesis-related protein P14a indicates a functional link between

the human immune system and a plant defense system, ***Proc Natl Acad Sci USA***, Vol. 95: 2262-2266.
Takatori, H., Kanno, Y., Watford, W. T., Tato, C. M., Weiss, G., Ivanov, I. I., Littman, D. R., & O'Shea, J. J. 2009. Lymphoid tissue inducer-like cells are an innate source of IL-17 and IL-22. ***J Exp Med***, 206(1): 35-41.
Takeuchi, M., Alard, P., & Streilein, J. W. 1998. TGF-beta promotes immune deviation by altering accessory signals of antigen-presenting cells. ***J Immunol***, 160(4): 1589-1597.
Takeuchi, S., Hirayama, K., Ueda, K., Sakai, H., & Yonehara, H. 1958. Blasticidin S, a new antibiotic. ***J Antibiot (Tokyo)***, 11(1): 1-5.
Taupin, D., & Podolsky, D. K. 2003. Trefoil factors: initiators of mucosal healing. ***Nat Rev Mol Cell Biol***, 4(9): 721-732.
Taylor, J. J., Mohrs, M., & Pearce, E. J. 2006. Regulatory T cell responses develop in parallel to Th responses and control the magnitude and phenotype of the Th effector population. ***Journal of immunology (Baltimore, Md : 1950)***, 176(10): 5839-5847.
Telford, G., Wheeler, D. J., Appleby, P., Bowen, J. G., & Pritchard, D. I. 1998. Heligmosomoides polygyrus immunomodulatory factor (IMF), targets T-lymphocytes. ***Parasite Immunol***, 20(12): 601-611.
Terrazas, C. A., Juarez, I., Terrazas, L. I., Saavedra, R., Calleja, E. A., & Rodriguez-Sosa, M. 2010. Toxoplasma gondii: impaired maturation and pro-inflammatory response of dendritic cells in MIF-deficient mice favors susceptibility to infection. ***Exp Parasitol***, 126(3): 348-358.
Tessier, D. C., Thomas, D. Y., Khouri, H. E., Laliberte, F., & Vernet, T. 1991. Enhanced secretion from insect cells of a foreign protein fused to the honeybee melittin signal peptide. ***Gene***, 98(2): 177-183.
Tetteh, K. K., Loukas, A., Tripp, C., & Maizels, R. M. 1999. Identification of abundantly expressed novel and conserved genes from the infective larval stage of Toxocara canis by an expressed sequence tag strategy. ***Infect Immun***, 67(9): 4771-4779.
Thompson, R. C. A., & Monis, P. 2012. Giardia--from genome to proteome. ***Adv Parasitol***, 78: 57-95.
Thornton, D. J., Carlstedt, I., Howard, M., Devine, P. L., Price, M. R., & Sheehan, J. K. 1996. Respiratory mucins: identification of core proteins and glycoforms. ***Biochem J***, 316 (Pt 3): 967-975.
Timmons, L., Court, D. L., & Fire, A. 2001. Ingestion of bacterially expressed dsRNAs can produce specific and potent genetic interference in Caenorhabditis elegans. ***Gene***, 263(1-2): 103-112.
Timmons, L., & Fire, A. 1998. Specific interference by ingested dsRNA. ***Nature***, 395(6705): 854.
Tkalcevic, J., Novelli, M., Phylactides, M., Iredale, J. P., Segal, A. W., & Roes, J. 2000. Impaired immunity and enhanced resistance to endotoxin in the absence of neutrophil elastase and cathepsin G. ***Immunity***, 12(2): 201-210.
Tomita, M., Kobayashi, T., Itoh, H., Onitsuka, T., & Nawa, Y. 2000. Goblet cell hyperplasia in the airway of Nippostrongylus brasiliensis-infected rats. ***Respiration***, 67(5): 565-569.
Tribolet, L., Cantacessi, C., Pickering, D. A., Navarro, S., Doolan, D. L., Trieu, A., Fei, H., Chao, Y., Hofmann, A., Gasser, R. B., Giacomin, P. R., & Loukas,

A. 2014. Probing of a Human Proteome Microarray With a Recombinant Pathogen Protein Reveals a Novel Mechanism by Which Hookworms Suppress B-Cell Receptor Signaling. ***J Infect Dis***.

Tridandapani, S., Wardrop, R., Baran, C. P., Wang, Y., Opalek, J. M., Caligiuri, M. A., & Marsh, C. B. 2003. TGF-beta 1 suppresses [correction of supresses] myeloid Fc gamma receptor function by regulating the expression and function of the common gamma-subunit. ***J Immunol***, 170(9): 4572-4577.

Triglia, T., Duraisingh, M. T., Good, R. T., & Cowman, A. F. 2005. Reticulocyte-binding protein homologue 1 is required for sialic acid-dependent invasion into human erythrocytes by Plasmodium falciparum. ***Mol Microbiol***, 55(1): 162-174.

Trujillo-Vargas, C. M., Werner-Klein, M., Wohlleben, G., Polte, T., Hansen, G., Ehlers, S., & Erb, K. J. 2007. Helminth-derived products inhibit the development of allergic responses in mice. ***Am J Respir Crit Care Med***, 175(4): 336-344.

Tsubokawa, D., Goso, Y., Nakamura, T., Maruyama, H., Yatabe, F., Kurihara, M., Ichikawa, T., & Ishihara, K. 2012. Rapid and specific alterations of goblet cell mucin in rat airway and small intestine associated with resistance against Nippostrongylus brasiliensis reinfection. ***Exp Parasitol***, 130(3): 209-217.

Vamadevan, A. S., Fukata, M., Arnold, E. T., Thomas, L. S., Hsu, D., & Abreu, M. T. 2010. Regulation of Toll-like receptor 4-associated MD-2 in intestinal epithelial cells: a comprehensive analysis. ***Innate Immun***, 16(2): 93-103.

van Es, J. H., & Clevers, H. 2014. Paneth cells. ***Curr Biol***, 24(12): R547-548.

Van Limbergen, J., Geddes, K., Henderson, P., Russell, R. K., Drummond, H. E., Satsangi, J., Griffiths, A. M., Philpott, D. J., & Wilson, D. C. 2013. Paneth cell marker CD24 in NOD2 knockout organoids and in inflammatory bowel disease (IBD). ***Gut***.

Veldhoen, M., Hocking, R. J., Atkins, C. J., Locksley, R. M., & Stockinger, B. 2006. TGFbeta in the context of an inflammatory cytokine milieu supports de novo differentiation of IL-17-producing T cells. ***Immunity***, 24(2): 179-189.

Verstraelen, S., Bloemen, K., Nelissen, I., Witters, H., Schoeters, G., & Van Den Heuvel, R. 2008. Cell types involved in allergic asthma and their use in in vitro models to assess respiratory sensitization, ***Toxicol In Vitro***, Vol. 22: 1419-1431.

Viney, M. E., & Thompson, F. J. 2008. Two hypotheses to explain why RNA interference does not work in animal parasitic nematodes. ***Int J Parasitol***, 38(1): 43-47.

Visser, A., Geldhof, P., de Maere, V., Knox, D. P., Vercruysse, J., & Claerebout, E. 2006. Efficacy and specificity of RNA interference in larval life-stages of Ostertagia ostertagi. ***Parasitology***, 133(Pt 6): 777-783.

Vivier, E., Raulet, D. H., Moretta, A., Caligiuri, M. A., Zitvogel, L., Lanier, L. L., Yokoyama, W. M., & Ugolini, S. 2011. Innate or adaptive immunity? The example of natural killer cells. ***Science***, 331(6013): 44-49.

Wahl, S. M., Allen, J. B., Weeks, B. S., Wong, H. L., & Klotman, P. E. 1993. Transforming growth factor beta enhances integrin expression and type IV collagenase secretion in human monocytes. ***Proc Natl Acad Sci U S A***, 90(10): 4577-4581.

Wahl, S. M., Hunt, D. A., Wakefield, L. M., McCartney-Francis, N., Wahl, L. M., Roberts, A. B., & Sporn, M. B. 1987. Transforming growth factor type beta induces monocyte chemotaxis and growth factor production. ***Proc Natl Acad Sci U S A***, 84(16): 5788-5792.

Walker, J. A., Barlow, J. L., & McKenzie, A. N. J. 2013. Innate lymphoid cells--how did we miss them? ***Nature reviews Immunology***, 13(2): 75-87.

Walsh, K. P., & Mills, K. H. 2013. Dendritic cells and other innate determinants of T helper cell polarisation. ***Trends Immunol***, 34(11): 521-530.

Wang, S. Z., Rosenberger, C. L., Bao, Y. X., Stark, J. M., & Harrod, K. S. 2003. Clara cell secretory protein modulates lung inflammatory and immune responses to respiratory syncytial virus infection. ***J Immunol***, 171(2): 1051-1060.

Watts, C. 2001. Antigen processing in the endocytic compartment. ***Curr Opin Immunol***, 13(1): 26-31.

Werner, A., Ramlau-Hansen, C. H., Jeppesen, S. K., Thulstrup, A. M., & Olsen, J. 2007. Caesarean delivery and risk of developing asthma in the offspring. ***Acta paediatrica (Oslo, Norway : 1992)***, 96(4): 595-596.

Werner, F., Jain, M. K., Feinberg, M. W., Sibinga, N. E., Pellacani, A., Wiesel, P., Chin, M. T., Topper, J. N., Perrella, M. A., & Lee, M. E. 2000. Transforming growth factor-beta 1 inhibition of macrophage activation is mediated via Smad3. ***J Biol Chem***, 275(47): 36653-36658.

Wharton, D. A., Petrone, L., Duncan, A., & McQuillan, A. J. 2008. A surface lipid may control the permeability slump associated with entry into anhydrobiosis in the plant parasitic nematode Ditylenchus dipsaci. ***J Exp Biol***, 211(Pt 18): 2901-2908.

Whelan, M., Harnett, M. M., Houston, K. M., Patel, V., Harnett, W., & Rigley, K. P. 2000. A filarial nematode-secreted product signals dendritic cells to acquire a phenotype that drives development of Th2 cells. ***Journal of immunology (Baltimore, Md : 1950)***, 164(12): 6453-6460.

Whelan, R. A., Rausch, S., Ebner, F., Gunzel, D., Richter, J. F., Hering, N. A., Schulzke, J. D., Kuhl, A. A., Keles, A., Janczyk, P., Nockler, K., Wieler, L. H., & Hartmann, S. 2014. A transgenic probiotic secreting a parasite immunomodulator for site-directed treatment of gut inflammation. ***Mol Ther***, 22(10): 1730-1740.

White, R. R., & Artavanis-Tsakonas, K. 2012. How helminths use excretory secretory fractions to modulate dendritic cells. ***Virulence***, 3(7): 668-677.

Williams, D. J., & Behnke, J. M. 1983. Host protective antibodies and serum immunoglobulin isotypes in mice chronically infected or repeatedly immunized with the nematode parasite Nematospiroides dubius. ***Immunology***, 48(1): 37-47.

Williams, S. A., Lizotte-Waniewski, M. R., Foster, J., Guiliano, D., Daub, J., Scott, A. L., Slatko, B., & Blaxter, M. L. 2000. The filarial genome project: analysis of the nuclear, mitochondrial and endosymbiont genomes of Brugia malayi. ***Int J Parasitol***, 30(4): 411-419.

Wilson, C. L., Ouellette, A. J., Satchell, D. P., Ayabe, T., Lopez-Boado, Y. S., Stratman, J. L., Hultgren, S. J., Matrisian, L. M., & Parks, W. C. 1999. Regulation of intestinal alpha-defensin activation by the metalloproteinase matrilysin in innate host defense. ***Science***, 286(5437): 113-117.

Wilson, M. S., Taylor, M. D., Balic, A., Finney, C. A., Lamb, J. R., & Maizels, R. M. 2005. Suppression of allergic airway inflammation by helminth-induced regulatory T cells. ***J Exp Med***, 202(9): 1199-1212.

Wilson, M. S., Taylor, M. D., O'Gorman, M. T., Balic, A., Barr, T. A., Filbey, K., Anderton, S. M., & Maizels, R. M. 2010. Helminth-induced CD19+CD23hi B cells modulate experimental allergic and autoimmune inflammation. ***Eur J Immunol***, 40(6): 1682-1696.

Winston, W. M., Sutherlin, M., Wright, A. J., Feinberg, E. H., & Hunter, C. P. 2007. Caenorhabditis elegans SID-2 is required for environmental RNA interference. ***Proc Natl Acad Sci U S A***, 104(25): 10565-10570.

Winter, A. D., McCormack, G., Myllyharju, J., & Page, A. P. 2013. Prolyl 4-hydroxlase activity is essential for development and cuticle formation in the human infective parasitic nematode Brugia malayi. ***J Biol Chem***, 288(3): 1750-1761.

Wohlleben, G., Trujillo, C., Muller, J., Ritze, Y., Grunewald, S., Tatsch, U., & Erb, K. J. 2004. Helminth infection modulates the development of allergen-induced airway inflammation. ***Int Immunol***, 16(4): 585-596.

Wojciechowski, W., Harris, D. P., Sprague, F., Mousseau, B., Makris, M., Kusser, K., Honjo, T., Mohrs, K., Mohrs, M., Randall, T., & Lund, F. E. 2009. Cytokine-producing effector B cells regulate type 2 immunity to H. polygyrus. ***Immunity***, 30(3): 421-433.

Yamaguchi, H., Yamamoto, C., & Tanaka, N. 1965. Inhibition of protein synthesis by blasticidin S. I. Studies with cell-free systems from bacterial and mammalian cells. ***J Biochem***, 57(5): 667-677.

Yamaguchi, Y. 1998. Regulation of GM-CSF-induced dendritic cell development by TGF-beta1 and co-developing macrophages. ***Microbiol Immunol***, 42(9): 627-637.

Yamazaki, Y., & Morita, T. 2004. Structure and function of snake venom cysteine-rich secretory proteins. ***Toxicon***, 44(3): 227-231.

Yatsuda, A. P., Eysker, M., Vieira-Bressan, M. C., & De Vries, E. 2002. A family of activation associated secreted protein (ASP) homologues of Cooperia punctata. ***Res Vet Sci***, 73(3): 297-306.

Yatsuda, A. P., Krijgsveld, J., Cornelissen, A. W. C. A., Heck, A. J. R., & de Vries, E. 2003. Comprehensive analysis of the secreted proteins of the parasite Haemonchus contortus reveals extensive sequence variation and differential immune recognition. ***J Biol Chem***, 278(19): 16941-16951.

Yazdanbakhsh, M., Kremsner, P. G., & van Ree, R. 2002. Allergy, parasites, and the hygiene hypothesis. ***Science***, 296(5567): 490-494.

Yoshimura, A., & Muto, G. 2011. TGF-beta function in immune suppression. ***Curr Top Microbiol Immunol***, 350: 127-147.

Yoshino, T. P., Brown, M., Wu, X. J., Jackson, C. J., Ocadiz-Ruiz, R., Chalmers, I. W., Kolb, M., Hokke, C. H., & Hoffmann, K. F. 2014. Excreted/secreted Schistosoma mansoni venom allergen-like 9 (SmVAL9) modulates host extracellular matrix remodelling gene expression. ***Int J Parasitol***, 44(8): 551-563.

Zang, X., Taylor, P., Wang, J. M., Meyer, D. J., Scott, A. L., Walkinshaw, M. D., & Maizels, R. M. 2002. Homologues of human macrophage migration

inhibitory factor from a parasitic nematode. Gene cloning, protein activity, and crystal structure. ***J Biol Chem***, 277(46): 44261-44267.

Zang, X., Yazdanbakhsh, M., Jiang, H., Kanost, M. R., & Maizels, R. M. 1999. A novel serpin expressed by blood-borne microfilariae of the parasitic nematode Brugia malayi inhibits human neutrophil serine proteinases. ***Blood***, 94(4): 1418-1428.

Zhang, X., & Mosser, D. M. 2008. Macrophage activation by endogenous danger signals. ***J Pathol***, 214(2): 161-178.

Zhao, A., Urban, J. F., Jr., Anthony, R. M., Sun, R., Stiltz, J., van Rooijen, N., Wynn, T. A., Gause, W. C., & Shea-Donohue, T. 2008. Th2 cytokine-induced alterations in intestinal smooth muscle function depend on alternatively activated macrophages. ***Gastroenterology***, 135(1): 217-225.e211.

Published Papers

JOURNAL OF PROTEOMICS 74 (2011) 1573–1594

available at www.sciencedirect.com

www.elsevier.com/locate/jprot

Proteomic analysis of secretory products from the model gastrointestinal nematode *Heligmosomoides polygyrus* reveals dominance of Venom Allergen-Like (VAL) proteins

James P. Hewitson[a], *Yvonne Harcus*[a], *Janice Murray*[a], *Maaike van Agtmaal*[a], *Kara J. Filbey*[a], *John R. Grainger*[a,1], *Stephen Bridgett*[b], *Mark L. Blaxter*[b], *Peter D. Ashton*[d], *David A. Ashford*[d], *Rachel S. Curwen*[c], *R. Alan Wilson*[c], *Adam A. Dowle*[d], *Rick M. Maizels*[a,*]

[a]*Institute of Immunology and Infection Research, University of Edinburgh, Edinburgh EH9 3JT, UK*
[b]*Gene Pool, Ashworth Laboratories, University of Edinburgh, Edinburgh EH9 3JT, UK*
[c]*Department of Biology, University of York, York YO10 5DD, UK*
[d]*Technology Facility, Proteomics Laboratory, Department of Biology, University of York, York YO10 5DD, UK*

ARTICLE INFO

Available online 29 June 2011

Keywords:
Parasite
Immunomodulation
Protease
Secretion
Signal peptide

ABSTRACT

The intestinal helminth parasite, *Heligmosomoides polygyrus bakeri* offers a tractable experimental model for human hookworm infections such as *Ancylostoma duodenale* and veterinary parasites such as *Haemonchus contortus*. Parasite excretory–secretory (ES) products represent the major focus for immunological and biochemical analyses, and contain immunomodulatory molecules responsible for nematode immune evasion. In a proteomic analysis of adult *H. polygyrus* secretions (termed HES) matched to an extensive transcriptomic dataset, we identified 374 HES proteins by LC–MS/MS, which were distinct from those in somatic extract HEx, comprising 446 identified proteins, confirming selective export of ES proteins. The predominant secreted protein families were proteases (astacins and other metalloproteases, aspartic, cysteine and serine-type proteases), lysozymes, apyrases and acetylcholinesterases. The most abundant products were members of the highly divergent venom allergen-like (VAL) family, related to *Ancylostoma* secreted protein (ASP); 25 homologues were identified, with VAL-1 and -2 also shown to be associated with the parasite surface. The dominance of VAL proteins is similar to profiles reported for *Ancylostoma* and *Haemonchus* ES products. Overall, this study shows that the secretions of *H. polygyrus* closely parallel those of clinically important GI nematodes, confirming the value of this parasite as a model of helminth infection.

1. Introduction

Infection with intestinal nematode parasites such as hookworm, whipworm and *Ascaris* remains an enormous global health problem, with over 25% of the world's population infected [1]. Moreover, similar pathogens account for major morbidity and economic loss among livestock in temperate climates [2]. The high prevalence and longevity of these parasites in immunocompetent hosts reflects a sophisticated array of mechanisms to modulate, disrupt and divert the host

* *Corresponding author at:* Institute of Immunology and Infection Research, University of Edinburgh, West Mains Road, Edinburgh EH9 3JT, UK. Tel.: +44 131 650 5511; fax: +44 131 650 5450.
E-mail address: rick.maizels@ed.ac.uk (R.M. Maizels).
[1] Current address: Mucosal Immunology Unit, Laboratory of Parasitic Diseases, NIAID, National Institutes for Health, Bethesda, MD 20892, USA.

1874-3919/$ – see front matter © 2011 Elsevier B.V. All rights reserved.
doi:10.1016/j.jprot.2011.06.002

immune response [3,4]. However, the identification of molecular mediators of parasite immunomodulation is still at an early stage [5–7]. For these reasons, the recent expansion in genomic [8–11], transcriptomic [12–21] and proteomic [22–30] analyses of parasitic nematodes provides an exciting platform for new discoveries.

A major theme in helminth research is the analysis of products released by live parasites which are likely to fulfil the many biological imperatives faced by a pathogen, including invasion of the host, creation of a suitable niche, and evasion of host immunity. These molecules, termed excretory–secretory (ES) products, have been the particular target of proteomic studies aimed at characterising the "secretome" of the major human [25–27] and veterinary [22,23,28–30] parasites. In addition, many prominent individual ES proteins have been identified, most notably members of a large multi-gene Venom Allergen-Like (VAL) family [28,31,32], first characterised in ES of the canine nematode *Ancylostoma caninum* and named *Ancylostoma* Secreted Protein (ASP) [33]. Members of this gene family include effective vaccine molecules in experimental models [34], indicating also the potential for ES proteins as new immunoprophylactics against helminth infections in man and animals.

Because the major human intestinal helminth species do not normally infect laboratory animals, model systems with natural rodent nematode parasites are invaluable in gaining insights into the factors regulating infection and immunity. The murine intestinal nematode parasite, *Heligmosomoides polygyrus*, provides a widely studied system [35], and much is now known of the immunology of infection and the immune components which combine to protect the host [36–40]. Parasite-infected mice feature multiple levels of immunosuppression, including amelioration of allergy [41,42], autoimmune diabetes [43,44] and colitis [45–48]. At least part of the immunosuppression can be accounted for by expanded regulatory T cell activity [42,49–51] and suppressive B cell populations [52] in infected mice, which are also able to transfer immunosuppression to uninfected recipients [42,52].

Significantly, the immunomodulatory effects of live *H. polygyrus* infection can be reproduced with the soluble products (HES) collected from adult parasites cultivated *in vitro*. HES converts naive murine T cells into suppressive regulatory T cells [53], interferes with the ability of dendritic cells to stimulate effector T cells and suppresses antibody responses to unrelated antigens [54], and can prevent the development of airway allergy in mice (O'Gorman, McSorley et al., manuscript in preparation). Hence the nature of the HES products is of intense interest for potential novel immunomodulators that might be exploited in therapy of allergy and autoimmunity. More broadly, intestinal nematodes co-habit a complex ecosystem with commensal microbes, and bacterial–parasite interactions are also likely to be important in the establishment of a long term nematode infection [55].

Despite the sophistication of the cellular immune analyses of *H. polygyrus* infection, few molecular products from this parasite have yet been described [24,56–60]. Indeed, genomic and transcriptomic datasets are only now being developed for this organism (Harcus et al., manuscripts in preparation). Taking a proteomic approach, we have identified the majority of proteins secreted by adult *H. polygyrus*, and show that there is a predominance of VAL/ASP-like products, which demonstrates that the overall composition and functional profile of HES closely parallels those of *Ancylostoma* and *Haemonchus* parasites. These results pave the way to use the mouse model for more precise determination of the role of many individual proteins in the biological processes of infection, intestinal establishment, and manipulation of the host immune response.

2. Materials and methods

2.1. Parasites and HES

The original stock of *H. polygyrus bakeri* used in these studies was kindly supplied to us by Professor JM Behnke, University of Nottingham, UK. The life cycle of *H. polygyrus* was maintained in CBAxC57BL/6F1 mice infected with 500 infective larvae by gavage, and adult worms were recovered 14 days later. Adult worms were washed extensively before incubation in serum-free RPMI1640 medium supplemented with 1% glucose, 100 U/ml penicillin, 100 μg/ml streptomycin, 2 mM L-glutamine, and 100 μg/ml gentamicin (Gibco). Culture supernatants were recovered at 3–4 day intervals and replaced each time with fresh medium over a 3 week period. Worms remained viable throughout this time frame. Pooled supernatants were diafiltrated into PBS over a 3000 MWCO Amicon membrane, and the resultant HES (*H. polygyrus* excretory/secretory products) material stored at −80 °C [59]. The profile of proteins released each week did not differ significantly (Supplementary Fig. A1). Soluble somatic extracts of adult worms (*H. polygyrus* extract; HEx) were prepared by homogenisation in a ground-glass hand-held homogeniser (VWR-Jencons, UK) in ice-cold PBS, followed by centrifugation at 13,000 *g* for 30 min, from which the supernatant was collected and stored at −80 °C until use.

2.2. 2-D gel electrophoresis and spot identification

HES and HEx (25 μg per gel) were separated and silver stained as previously described [25], then scanned with a Linoscan 1450 (Heidelberg). Protein spots of interest were prepared for mass spectrometry analysis as before [25], and positive-ion MALDI mass spectra were obtained using a Bruker ultraflex III in reflectron mode, equipped with a Nd:YAG smart beam laser. MS spectra were acquired over a mass range of m/z 800–4000, and monoisotopic masses were obtained using a SNAP averaging algorithm. The ten strongest peaks of interest, with a S/N greater than 30, were selected for MS/MS fragmentation in LIFT mode. Bruker flexAnalysis software (version 3.3) was used to perform the spectral processing and peak list generation for both the MS and MS/MS spectra.

2.3. LC–MS/MS

Tryptic HES peptides were prepared essentially as before [25] and then loaded onto a nanoAcquity UPLC system equipped with a nanoAcquity Symmetry C_{18}, 5 μm trap (180 μm × 20 mm) and a nanoAcquity BEH130 1.7 μm C_{18} capillary column (75 μm × 250 mm; all Waters). The trap was washed for 5 min with 0.1% (v/v) formic acid at 10 μL/min. Subsequently, flow

was switched to the capillary column, and peptides were separated by gradient elution (Solvent A = 0.1% (v/v) formic acid; Solvent B = acetonitrile with 0.1% (v/v) formic acid; Initial gradient conditions 5% solvent B (2 min), then a linear gradient to 35% solvent B over 120 min, followed by a linear gradient to 50% solvent B over 5 min, and finally wash with 95% solvent B for 10 min. Flow rate was 300 nL/min and column temperature was 60 °C). The nanoLC system was interfaced with a maXis UHR-TOF mass spectrometer (Bruker Daltonics) with a nano-electrospray source fitted with a steel emitter needle (180 μm O.D. × 30 μm I.D.; Proxeon). Instrument control, data acquisition and processing were performed using Compass 1.3 SR3 software (microTOF control, Hystar and DataAnalysis; Bruker Daltonics). Positive ESI–MS & MS/MS spectra were acquired using AutoMSMS mode. Instrument settings were: ion spray voltage: 1500 V, dry gas: 6 L/min, dry gas temperature 160 °C, ion acquisition range: *m/z* 50–2200. AutoMSMS settings were: MS: 0.5 s (acquisition of survey spectrum), MS/MS (CID with N_2 as collision gas): ion acquisition range: *m/z* 300–1500, 5 precursor ions, absolute threshold 1000 counts, acquisition time: 0.1 s for precursor intensities ≥100,000 counts increasing linearly to 1 s for precursor intensitities of 1000 counts, collision energy and isolation width settings were calculated automatically using the AutoMSMS fragmentation table, preferred charge states: 2–4, singly charged ions excluded, one fragmentation spectrum was acquired for each precursor and former target ions were excluded for 30 s.

2.4. *Database searching and bioinformatics*

Tandem mass spectral data were submitted to database searching using a locally-running copy of the Mascot program (Matrix Science Ltd., version 2.1), through the Bruker ProteinScape interface (version 2.1). Search parameters required trypsin specificity, the carbamidomethylation of cysteine, allowed a maximum of one missed cleavage, and the possible oxidation of methionine. Spectra were searched against an in-house database composed of >460,000 cDNA sequences from both normalised and non-normalised libraries made from adult worm mRNA (Harcus et al., manuscript in preparation; http://www.nematodes.org/nembase4/overview.shtml). The database was supplemented with existing NCBI depositions for *H. polygyrus*. Sequencing was performed on a Roche 454 instrument yielding reads of ~200 nt, and assembled into isotigs each representing a distinct transcript using Newbler 2.5. For gel spot identifications a peptide tolerance of 250 ppm and MS/MS tolerance of 0.5 Da were employed. For LC–MS/MS Mascot searches, MudPit scoring was used with a peptide tolerance of 10 ppm and MS/MS tolerance of 0.1 Da. The significance threshold was set at $p < 0.05$, and hits were manually inspected for the presence of open reading frames. All LC–MS/MS data were filtered to only accept peptides with expect values <0.05, and single peptide hits were further filtered requiring expect values <0.01. All protein matches were required to contain at least one unique peptide sequence not matched in any higher ranked proteins. The LC–MS/MS data were also searched against a Mascot generated decoy database, containing a random set of sequences with the same average amino acid composition and sequence length as the target database. Comparison of the number of sequences identified in the target and decoy databases estimated a false discovery rate of 2.01% HES and 2.94% for HEx for peptide matches above identity threshold. Spectra were also searched against Swiss-Prot to identify potential murine or bacterial proteins present in HES and HEx. Here the false discovery rate was higher (33.1% for HES and 6.92% for HEx), likely reflecting the paucity of *H. polygyrus* sequences in the database, and their low level of sequence identity with other species. The exponentially Modified Protein Abundance Index (emPAI) for each identification was calculated according to the ratio of observed and observable peptides for each protein.

Identified protein sequences were subject to analysis by SignalP3.0 to ascertain presence of predicted signal peptide [61]. In some instances, protein sequences were judged to be truncated, by the absence of a start methionine and/or by homology to known protein sequences from other organisms. Proteins and conserved domains were identified by BLAST, and gene ontology (GO) categories determined with Interproscan version 31.0 (http://www.ebi.ac.uk/Tools/pfa/ iprscan/). Protein sequences lacking conserved domains, but with significant similarity (BLAST score >40) to nematode proteins were labelled conserved nematode proteins (CSN = Conserved Secreted, No signal peptide; CSP = Conserved Secreted with signal-Peptide; CXN = Conserved eXtract, No signal peptide; CXP = Conserved eXtract with signal-Peptide). Novel sequences (BLAST score <40) were labelled NSN, NSP, NXN and NSP as described above. ClustalW sequence alignments were performed using MacVector version 11.1.1. To identify potential *N*- and *O*-glycosylation sites, NetNGlyc 1.0 (http://www.cbs.dtu.dk/services/NetNGlyc/) and NetOGlyc 3.1 (http://www.cbs.dtu.dk/services/NetOGlyc/) were used respectively. Accession numbers given for nucleotide and protein sequences are those deposited with ENA or NCBI.

2.5. *Antibody generation and Western blotting*

HES (1 μg) was separated by 2-D gel electrophoresis as described above, blotted as before [25], and then blocked in 5% skimmed milk powder (Marvel)-TBS with 0.05% Tween 20 (TBST) for 2 h at room temperature. Polyclonal antibodies to *Hp*-VAL-1, -2 and -4 were generated to 6-His-tagged recombinant proteins expressed in pET21 (Novagen)-transformed *E. coli*, solubilised in 8 M urea and purified by metal chelating chromatography under the same chaotropic conditions; rats were immunised with 100 μg of recombinant protein co-precipitated with alum, boosted on days 28 and 35 with 100 μg protein in alum, and serum collected on day 42. To assess binding to HES, membranes were probed with 1/1000 sera dilutions in block solution overnight at 4 °C, washed extensively in TBST, and then with 1/2000 rabbit anti-rat Ig (1 h room temperature; DakoCytomation). Following further washing in TBST, blots were developed using ChemiGlow West, according to the manufacturer's instructions (Alpha Innotech) and imaged using a FluorChem SP (Alpha Innotech).

2.6. *Surface radio-iodination, immunoprecipitation and surface staining*

Adult *H. polygyrus* were surface radio-labelled as described in earlier publications [62] but using Pierce Iodination Reagent (Iodogen) as the catalyst for generating nascent iodine [63]. Eppendorf tubes (1.5 ml) were coated with 200 μl of a 1 mg/ml solution of Iodination reagent (Pierce) in chloroform, dried, washed with PBS, before transfer of approximately 500 adult

worms and 500 μCi ^{125}Iodine (Perkin Elmer) on ice. The sample was incubated with frequent agitation for 10 min, quenched by the addition of a saturated solution of L-tyrosine (Sigma), and surface radio-labelled parasite material produced as for HEx as described above, except that parasites were homogenised in PBS containing 1.5% nOG detergent and 1% protease inhibitor cocktail (Sigma P8340). Surface labelled parasite proteins were then separated by 2-D gel electrophoresis as above, and then dried and autoradiographed as before [62]. Immunoprecipitates were performed following pre-clearing of radiolabelled parasite extract with Protein G agarose beads (Millipore, 16–266) in the presence of MOPC 31 C IgG1 isotype control (for mouse anti-VAL monoclonal antibodies) or naïve rat serum (for rat anti-VAL polyclonal serum) for 30 min at room temperature. Unbound parasite material was then incubated with 2 μg of mAb to VAL-1 (clone 3–36), VAL-2 (clone 4-S4), VAL-4 (clone 2–11) or MOPC 31 control IgG1 in non-denaturing IP buffer (20 mM Tris pH 8, 150 mM NaCl, 1 mM EDTA, 10% glycerol, 1% Triton-X100) for 2 h, then with Protein G agarose beads overnight, at 4 °C with rotation.

The production and specificity of anti-VAL mAb from the spleens of infected mice is to be described elsewhere [64]. Alternatively, 5 μl polyclonal anti-VAL-1, 2, 4 rat sera or naïve rat sera was used. Beads were washed 5×5 min in IP buffer, and bound proteins eluted by boiling in NuPAGE LDS sample buffer (Invitrogen)/0.5 M 2- mercaptoethanol, before separation on 1-D SDS-PAGE and autoradio graph as before [64]. For sections, adult *H. polygyrus* worms were snap-frozen on dry ice in Cryo-M-Bed mountant (Bright Instruments), cryostat sections (5 μm; Leica) cut onto Polysine™ slides (VWR), dried and then fixed in 100% acetone for 10 min. Sections were washed twice with PBS for 10 min, and then incubated with the mouse mAb described above (50 μg/mL in 1% FCS/PBS) for 2 h at room temperature, washed twice in PBS as before, and then incubated with secondary anti-mouse Ig TRITC (1/100 in PBS) for 1 h at room temperature. Sections were washed extensively and then mounted in anti-fade Vectashield mountant (Vector Labs), before imaging with an Olympus fluorescent microscope.

3. Results

3.1. Mass spectrometric identification of HES proteins from 2D PAGE gels

H. polygyrus adult excretory–secretory (HES) products were collected from parasites cultured in serum-free medium and concentrated over a 3000 MW cut-off membrane. To determine the identity of HES proteins, we used both 2-dimensional gel electrophoresis (2DGE) and 'shotgun' proteomics approaches. HES contained over 100 discernable polypeptides when analysed by silver staining of 2DGE (Fig. 1A), in a pattern clearly distinct from that of *H. polygyrus* somatic soluble protein extract (HEx, Fig. 1B). Analysis of 53 of the spots visible by 2DGE of HES (Fig. 1C) provided identities when matched against an in-house transcriptomic database of adult *H. polygyrus* mRNA (composed of 466,844 Roche 454 sequence reads, Harcus et al., manuscript in preparation). Additional spots were examined but did not provide sufficient material for MS identification (data not shown).

The most abundant products, as judged by intensity of silver staining, were found to be members of the VAL/ASP gene family (*e.g.* spots 4–9, 20–25, 35, 38–40), as well as apyrases, lysozymes, myoglobins and proteases. Table 1 summarises the full list of parasite proteins identified in this manner, which also includes a galectin, vitellogenin, chitinase, enolase and two novel gene sequences. We also observed that some proteins were present in multiple spots (*e.g.* variants of VAL-1 and VAL-2 were present in spots 20–24 and 5–9, respectively, and apyrase-2 in spots 31–33). Consistent with this, a polyclonal rat serum generated against recombinant VAL-1.1 recognised a chain of at least 8 spots by Western blot (Fig. 1D). Although several secreted HES proteins show micro-variation at the amino acid level (see below), this does not fully account for the observed differences in pI, as the same variant may be present in several different spots (*e.g.* VAL-1.2 is present in spots 21–24), and conversely more than one sequence variant was often seen in the same spot (see Table 1 and Supplementary Fig. A2), as the amino acid polymorphisms identified do not lead to large changes in predicted pI (data not shown).

3.2. Mass spectrometric identification by LC–MS/MS

For a more exhaustive analysis of HES components, we employed LC–MS/MS on a total of 40 μg of HES, resulting in the identification of a total of 374 secreted HES proteins; 100 of the most abundant (as ranked by Mascot score) are presented in Table 2, with the full listing given in Supplementary Table A1. Among the HES proteins identified were a selection of proteases, particularly metalloproteases (zinc metalloproteases and a large number of astacins), cysteine proteases (cathepsin B, legumain and necpain), aspartyl proteases (necepsin), and various serine proteases (cathepsin A, dipeptidyl peptidase four, serine carboxypeptidases and trypsin family proteins). Several other classes of enzymes were abundantly secreted, including relatively high levels of acetylcholinesterases, apyrases, chitinases and lysozymes. Protease inhibitors (cystatins, Kunitz inhibitors and serpins), transthyretin-related (TTR) proteins, chondroitin proteoglycans, and lectins (both C-type lectins and galectins) were also detected, as were a large number of proteins of unknown function with homologues in other nematodes (conserved nematode proteins) and novel proteins as yet unidentified in other helminths. In addition, as discussed further below, no fewer than 25 distinct VAL proteins were identified. Most of the abundant proteins had been localised by 2DGE to specific spots, as indicated where appropriate in Table 2. Searching of LC–MS/MS data against Swiss-Prot revealed that HES contained two different Ig kappa light chains (accession numbers P01654 and P01837) and a single IgG1 heavy chain (P01869). No significant matches were found to any bacterial protein sequences. We confirmed the presence of trace amounts of host immunoglobulin by ELISA, which showed that 1 μg of HES contains 0.135±0.010 ng murine IgG1 (data not shown). It is likely that this antibody is bound to the adult worm *in vivo*, and subsequently dissociates from the parasite during the *in vitro* culture period. No murine proteins were detected in HEx.

In parallel, the soluble somatic protein extract (HEx) of the worm was analysed, yielding 446 identities thereby greatly extending analysis beyond previously available information

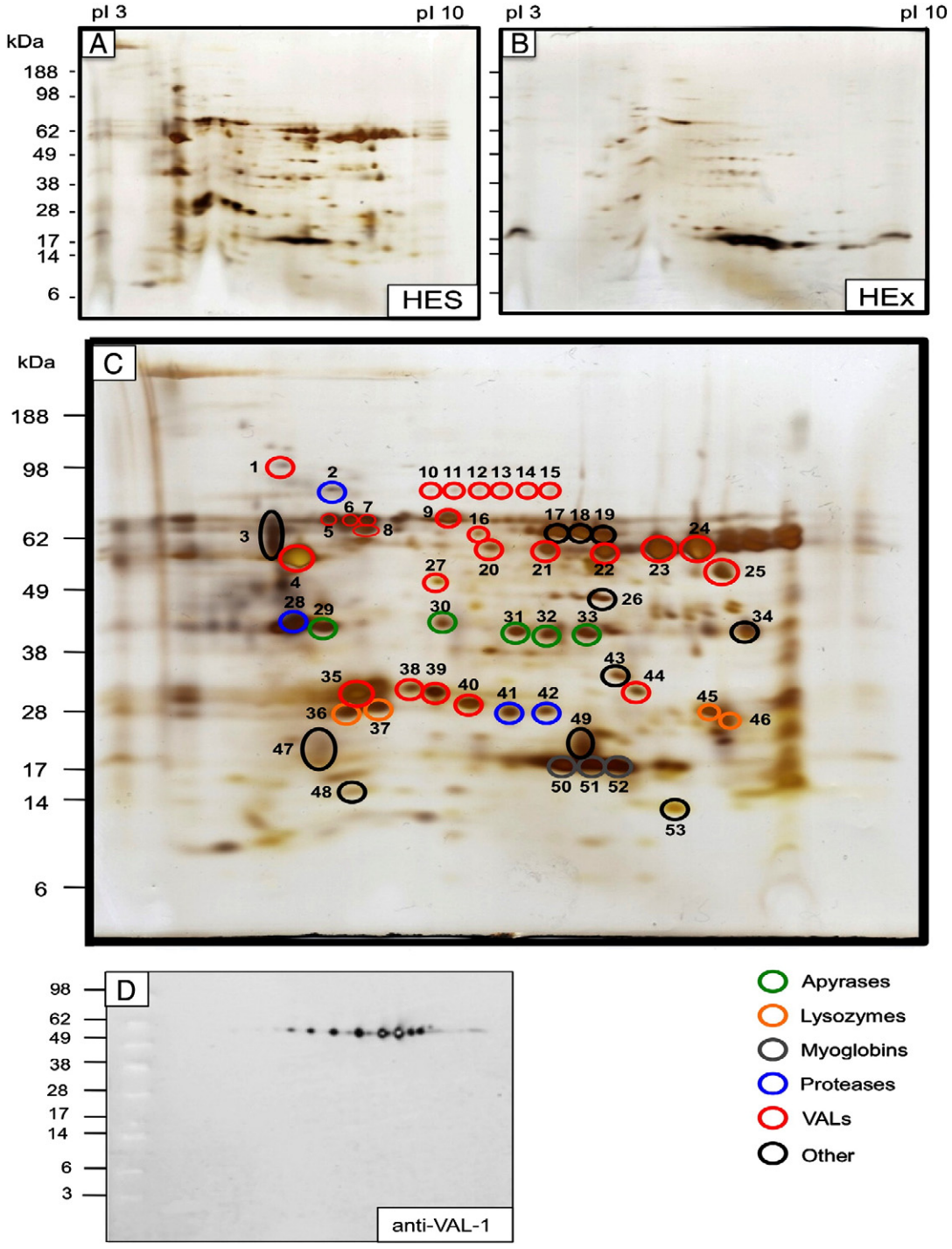

Fig. 1 – 2-Dimensional analysis of *H. polygyrus* secreted proteins (HES) and soluble somatic extract (HEx). A. HES silver stain. B. HEx silver stain. Note that the major spots of 15–18 kDa have previously been identified as myoglobins [24]. C. HES annotated with spots analysed by MS/MS as presented in Table 1. D. Anti-VAL-1 rat polyclonal antibody on Western blot.

[24]. Table 3 presents 100 of the most abundant (ranked by Mascot score) and a full listing is given in Supplementary Table A2. Complete mass spectrometric data for HES and HEx are presented in Supplementary Tables A3 and A4 respectively. In contrast to HES, many of the HEx products were ribosomal proteins and protein synthesis factors, as well as cytoskeletal components (actin, tropomyosin and tubulin) and also cytosolic enzymes involved in glycolysis, lipid binding and redox reactions. GO annotation of HES and HEx (Fig. 2 and Supplementary Table A5) indicated that translation (GO:0006412) was the most common "biological process" term for HEx, and structural component of ribosome (GO:0003735) was the most common "molecular function", indicative of the large number of ribosomal proteins present. In contrast, proteolysis

Table 1 – Proteins identified in HES from spots.

Spot	Identity	Domain	Hpb adult database	Score	Peptides	Accession No
1	VAL-3.1	Double SCP	isotig05790	64	2	JF914909
2	MEP-1 Zinc metalloprotease	Peptidase M13	isotig02967	144	5	(*truncated*)
3	CHI-1 Chitinase	Chitinase GH19	isotig04840	268	3	HE573246
4	VAL-3.1	Double SCP	isotig05790	462	6	JF914909
5	VAL-2.1/2.2/2.3 (*a*)	Double SCP	isotig03106	43	1	JF914906
6	VAL-2.1/2.2/2.3 (*a*)	Double SCP	isotig03106	266	7	JF914906
7	VAL-2.1/2.2/2.3 (*a*)	Double SCP	isotig03106	206	6	JF914906
8	VAL-2.1/2.2/2.3 (*a*)	Double SCP	isotig03106	32	1	JF914906
9	VAL-2.1/2.2/2.3 (*a*)	Double SCP	isotig03106	429	7	JF914906
10	VAL-5	Double SCP	isotig04839	186	8	JF914911
11	VAL-5	Double SCP	isotig04839	146	10	JF914911
12	VAL-5	Double SCP	isotig04839	132	8	JF914911
13	VAL-5	Double SCP	isotig04839	145	5	JF914911
14	VAL-5	Double SCP	isotig04839	169	7	JF914911
15	VAL-5	Double SCP	isotig04839	121	4	JF914911
16	VAL-9	Double SCP	isotig05765	495	10	JF914917
17	ACE-1 Acetylcholinesterase	Esterase lipase	isotig05694	21	1	JF439067
18	ACE-1 Acetylcholinesterase	Esterase lipase	isotig05694	32	2	JF439067
19	ACE-1 Acetylcholinesterase	Esterase lipase	isotig05694	53	2	JF439067
20	VAL-1.1	Double SCP	isotig06320	16	1	JF914902
21A	VAL-1.2	Double SCP	isotig03069	43	1	JF914903
21B	VAL-1.4	Double SCP	isotig01653	38	1	JF914905
22A	VAL-1.2	Double SCP	isotig03069	129	4	JF914903
22B	VAL-1.1	Double SCP	isotig06320	103	4	JF914902
22 C	VAL-1.4	Double SCP	isotig01653	70	2	JF914905
23A	VAL-1.2	Double SCP	isotig03069	419	5	JF914903
23B	VAL-1.1	Double SCP	isotig06320	402	5	JF914902
24A	VAL-1.1	Double SCP	isotig06320	613	6	JF914902
24B	VAL-1.2	Double SCP	isotig03069	385	5	JF914903
25	VAL-6	Double SCP	isotig03505	401	4	JF914912
26	Enolase (*b*)	Enolase	isotig06965	103	3	(*truncated*)
27	VAL-8.1	Double SCP	isotig02308	257	6	JF914916
28	MEP-3 Zinc metalloprotease	Peptidase M13	isotig05155	177	3	(*truncated*)
29	APY-1.1 Apyrase	Apyrase	isotig02250	68	3	JF721961
30	APY-3 Apyrase	Apyrase	isotig03589	188	5	JF721966
31	APY-2 Apyrase	Apyrase	isotig07051	213	6	JF721965
32	APY-2 Apyrase	Apyrase	isotig07051	323	3	JF721965
33	APY-2 Apyrase	Apyrase	isotig07051	185	5	JF721965
34	PHP-1, PHA-domain protein	PHA02954	isotig03547	180	4	HE573241
35	VAL-4	Single SCP	isotig10387	127	3	JF914910
36A	LYS-1 Lysozyme	Muramidase GH25	isotig08802	411	6	HE573247
36B	LYS-3 Lysozyme	Muramidase GH25	isotig08606	126	3	HE573249
37A	LYS-1 Lysozyme	Muramidase GH25	isotig08802	483	6	HE573247
37B	LYS-3 Lysozyme	Muramidase GH25	isotig08606	170	3	HE573249
38A	VAL-7.3	Single SCP	isotig02284	94	3	JF914915
38B	VAL-7.2	Single SCP	isotig01525	61	2	JF914914
39	VAL-7.2	Single SCP	isotig01525	48	1	JF914914
40	VAL-7.1	Single SCP	isotig01524	296	6	JF914913
41	NAS-1.1/1.2 Nematode Astacin (*c*)	ZnMc astacin-like	isotig04178	280	4	(*truncated*)
42	NAS-3.3 Nematode Astacin (*d*)	ZnMc astacin-like	isotig01791	141	2	(*truncated*)
43	Galectin	Double GLECT	isotig09082	219	4	(*truncated*)
44	VAL-10	Single SCP	isotig04979	27	1	JF914918
45	LYS-2 Lysozyme	Muramidase GH25	isotig05074	220	4	HE573248
46	LYS-2 Lysozyme	Muramidase GH25	isotig05074	179	3	HE573248
47	Vitellogenin	VWD	contig00471	64	2	(*truncated*)
48	NSP-4 Novel Secreted Protein	None	isotig11873	60	1	HE573242
49	NSP-16 Novel Secreted Protein	None	isotig05257	39	2	HE573243
50	Myoglobin	Globin	isotig04274	64	1	HE573244
51	Myoglobin	Globin	isotig04274	125	3	HE573244
52	Myoglobin	Globin	isotig04274	94	3	HE573244
53	TTR-1 Transthyretin-related	DUF290	isotig04612	452	6	HE573245

(GO:0006508) and metalloendopeptidase activity (GO:0004222) were the most common biological process and molecular function terms for HES. It is important to note that a greater number of proteins in HES compared to HEx failed to match GO terms (molecular function 54.8% HES *Vs* 23.5% HEx; biological process 68.7% HES *Vs* 41.3% HEx), consistent with the specialised nature of the parasite secretions unique to its intestinal niche, and in contrast to the somatic extract which is generally composed of proteins common to most eukaryotic organisms.

3.3. Comparison of proteins in HES and HEx reveals preferentially secreted proteins

Only 104 of 374 (27.8%) HES proteins were detectable in HEx (Table 4). The most abundant of these "somatic" proteins present in HES were the myoglobins and vitellogenins, both of which are extremely highly expressed by adult worms, the former representing the dominant species on 2D profiles (Fig. 1B). Hence, while the secreted components in HES in general represent a selective subset of the whole worm proteome, abundant somatic constituents such as myoglobin are also found in the *in vitro* parasite culture medium. In this regard it is noteworthy that both myoglobin and vitellogenin contain N-terminal signal sequences. It is also possible that as core egg proteins, vitellogenins diffuse from the eggs released by adult females during *in vitro* culture, or are present in intrauterine contents that accompany egg release. Comparison of exponentially modified Protein Abundance Index (emPAI) values for the 104 proteins common to HES and HEx indicated that there were large differences in the level of certain proteins between the two parasite preparations (*e.g.* VAL-1 and VAL-2 variants were highly abundant in HES and detected at only trace amounts in HEx; Table 4). This is not unexpected given that parasite secretions originate from the worm itself.

3.4. HES and HEx components differ significantly in proportion of predicted signal peptide sequences and in extent of novel gene products

Of the 374 HES proteins identified, 291 (77.8%) contained a predicted N-terminal signal peptide (Fig. 3). In addition, 100 (26.7%) did not correspond to any annotated gene in the NCBI database, and of these 70 (18.7%) were novel proteins with no database match. The remaining 30 sequences matched predicted or hypothetical proteins of unknown function from *C. elegans* or other nematodes, and were classified as conserved nematode proteins. When these 100 secreted proteins of unknown function were examined for the presence of a potential signal peptide, approximately 85% of each (60/70 novel, 25/30 conserved) were signal peptide-positive, indicating that an important set of novel secreted proteins are present in HES. The novel proteins in particular were mostly <150 amino acids, with an average predicted molecular weight of 16.5 kDa (range 5.4–55.5 kDa). In contrast to HES, only 25.1% (112/446) of proteins identified in HEx encoded signal peptides, and HEx also contained noticeably fewer proteins of unknown function, with only 15 conserved nematode proteins (of which 4 were also detected in HES) and 9 novel proteins (4 detected in HES).

3.5. VAL proteins are associated with the parasite surface

In parallel with HES analysis, we also investigated the adult parasite surface proteins accessible to radio-iodination of live worms. When surface iodination was employed, solubilised proteins were analysed by 2D gel electrophoresis and autoradiography, and showed mobilities similar to VAL-1 and -2 (compare Fig. 4A with Fig. 1C) which could be specifically immunoprecipitated with monoclonal and polyclonal antibodies specific for VAL-1 and VAL-2 (Fig. 4B), indicating that both VAL-1 and VAL-2, highly enriched in HES, are present on the surface of the adult worm. In contrast, we did not detect surface expression of the similarly abundantly secreted VAL-4.

The distribution of VAL-1 and -2 was then investigated using monoclonal antibodies specific for each protein [64] to stain frozen sections of adult worms (Fig. 4C–F). Both antibodies gave a highly restricted punctate pattern of labelling the body wall, in a series of structures at contralateral sites that may represent longitudinal neuronal fibres or secretory tissues. Interestingly, in *A. caninum*, different VAL (ASP) products showed distinct localization patterns, with anti-Ac-ASP-4 staining the cuticle of adult worms, while antibodies to ASP-3 and -6 bind to glandular structures, and anti-ASP-5 to the gut, yet all four proteins are also found in adult worm ES [65].

3.6. Sequence analysis of the H. polygyrus VAL gene family

The most striking characteristic of HES is the predominance of members of the VAL gene family, both in terms of the abundance of certain members, particularly VAL-1, 2, 3, 4 and 7, as well as the large number (25) of different VAL proteins detected. VAL proteins show a conserved overall structure built around the SCP modular domain of ~200 amino acids (sperm-coating protein; pfam accession PF00188), typically containing 5 disulphide bonds. Members of this gene family generally contain either a single SCP domain, or two tandem domains, which are not necessarily closely related to each other in sequence. Fig. 5 shows a schematic of the 25 secreted VAL proteins of adult *H. polygyrus*, including 21 full length proteins, 8 of which (VAL-4, 7, 10, 15, 19, 21, 22 and 25) are single domain and 13 double domain (VAL-1, 2, 3, 5, 6, 8, 9, 12, 13, 14, 16, 17 and 20). Phylogenetically, the single- and double-

Notes to Table 1
Accession numbers from NCBI GenBank or European Nucleotide Archive (ENA) are given where full-length sequences are available.
(a) Peptides are common to all three variants of VAL-2; isotig and Accession number given are for VAL-2.1. Isotig and accession numbers for VAL-2.2 and -2.3 are isotig07425/JF914907 and isotig03105/JF914908.
(b) 1 additional peptide matches isotig18996 coding for N-terminal segment of Enolase separated from isotig 06965 by gap of ~27 nt.
(c) Peptides are common to NAS-1.1 and -1.2; latter is isotig04179.
(d) Two additional peptide matches to each of variants NAS 3.1 (isotig01799) and NAS-3.4 (isotig 01793).

Table 2 – Top 100 proteins identified in HES by LC–MS/MS.

Rank	Identity	Conserved domains	Code	Score	SP
1	VAL-1.1	SCP (Double)	isotig06320	6546	SP
2	VAL-1.2	SCP (Double)	isotig03069	5788	SP*
3	VAL-2.2	SCP (Double)	isotig07425	5149	SP*
4	VAL-2.3	SCP (Double)	isotig03105	5039	SP
5	VAL-3.1	SCP (Double)	isotig05790	4754	SP
6	VAL-2.1	SCP (Double)	isotig03106	4003	SP
7	Vitellogenin	Vitellogenin, DUF1943	contig00471	3997	SP
8	LYS-1 Lysozyme	Muramidase GH25	isotig08802	3615	SP
9	VAL-7.2	Single SCP	isotig01525	3369	SP
10	VAL-7.5	Single SCP	isotig01526	3367	SP
11	VAL-7.3	Single SCP	isotig02284	3051	SP
12	LYS-2 Lysozyme	Muramidase GH25	isotig05074	2947	SP
13	VAL-1.3	Double SCP	isotig06456	2668	SP
14	VAL-7.4	Single SCP	isotig02282	2604	SP
15	VAL-7.1	Single SCP	isotig01524	2593	SP
16	TTR-1 Transthyretin-related	DUF290	isotig04612	2130	SP
17	VAL-1.4	Double SCP	isotig01653.	1841	SP
18	APY-1.1 Apyrase	Apyrase	isotig02250	1833	SP
19	APY-1.2 Apyrase	Apyrase	isotig07986	1818	SP
20	VAL-13	Double SCP	isotig06642	1809	SP
21	VAL-4	Single SCP	isotig10387	1770	SP
22	MEP-1 Zinc metalloprotease	Peptidase M13	isotig02967	1624	SP*
23	VAL-1.5	Double SCP	isotig01652	1596	SP*
24	NSP-1 Novel Secreted Protein with SP	None	isotig11973	1584	SP
25	APY-1.3 Apyrase	Apyrase	isotig05261	1583	SP
26	Myoglobin	Globin	isotig04274	1579	SP
27	Peritrophin-A-like protein	Chitin-binding type 2	Isotig05677	1561	SP*
28	Vitellogenin	DUF1943	contig00207	1552	SP*
29	ACE-1 Acetylcholinesterase	Esterase lipase	isotig05694	1527	SP
30	NPA-1 Nematode polyprotein allergen	None	isotig02438	1498	SP
31	APY-2 Apyrase	Apyrase	isotig07051	1474	SP
32	Myoglobin	Globin	isotig11742	1446	SP
33	VAL-9	Double SCP	isotig05765	1431	SP
34	Myoglobin	Globin	isotig04273	1390	SP
35	VAL-11	Single SCP	isotig05330	1303	SP*
36	MSP-1 Major Sperm Protein	Motile Sperm	isotig01565	1278	NO
37	MEP-2 Zinc metalloprotease	Pep0, Peptidase M13 N	isotig05366	1232	SP
38	Vitellogenin	Vitellogenin N, LPN N	contig00203	1205	SP*
39	Vitellogenin	VWD	contig00477	1204	SP*
40	VAL-8.1	Double SCP	isotig02308	1200	SP
41	TTR-2 Transthyretin-related	DUF290	isotig13558	1156	SP
42	NAS-1.1 Nematode Astacin protease	ZnMc astacin-like	isotig04178	1148	SP*
43	ACE-2 Acetylcholinesterase	Esterase lipase	isotig00868	1122	SP
44	PHP-1 PHA domain protein	PHA02954	isotig03547	1120	SP
45	NAS-1.2 Nematode Astacin protease	ZnMc astacin-like	isotig04179	1095	SP*
46	Myoglobin	Globin	isotig05169	1094	SP
47	VAL-8.2	Double SCP	isotig02308	1040	SP*
48	MEP-3 Zinc metalloprotease	Peptidases M13, M13N	isotig05155	1007	SP*
49	ACE-3 Acetylcholinesterase	Esterase lipase	isotig00869	1006	SP
50	Deoxyribonuclease II	Dnase_II	isotig08122	1006	SP*
51	VAL-6	Double SCP	isotig03505	996	SP
52	CHI-1 Chitinase	Chitinase GH19	isotig04840	988	SP
53	Astacin protease (fragment)	None	isotig01219	956	SP*
54	Trypsin family protein	Trypsin SPc	isotig03474	919	NO
55	Vitellogenin	VWD	contig00212	918	SP*
56	Aspartyl protease (necepsin)	Pepsin/retropepsin-like	isotig06497	884	SP
57	Trypsin family protein	Trypsin SPc	isotig03473	883	NO
58	VAL-1.6	Double SCP	isotig01655	867	SP
59	NAS-2.1 Nematode Astacin protease	ZnMc astacin-like	isotig01336	858	SP*
60	MFH-1 Ascaris MFP2b homologue	MFP2b	isotig07283	845	NO
61	NAS-2.2 Nematode Astacin protease	ZnMc astacin-like	isotig01334	836	SP*
62	NAS-3.1 Nematode Astacin protease	ZnMc astacin-like	isotig01799	832	SP*
63	NAS-4 Nematode Astacin protease	ZnMc astacin-like	isotig00214	830	SP*
64	Enolase	Enolase	isotig06965	826	NO
65	VAL-17	Double SCP	isotig05765	825	SP*

Table 2 (*continued*)

Rank	Identity	Conserved domains	Code	Score	SP
66	TTR-3 Transthyretin-related	DUF290	isotig14171	821	SP
67	MEP-4 Zinc metalloprotease	Peptidases M13, M13 N	isotig05402	806	SP
68	VAL-12	Double SCP	isotig06637	803	SP
69	NSP-2 Novel Secreted Protein with SP	None	isotig12022	802	SP
70	NSP-3 Novel Secreted Protein with SP	None	isotig12137	802	SP
71	NAS-5.1 Nematode Astacin protease	ZnMc astacin-like, CUB	isotig01596	779	SP*
72	NSN-1 Novel Secreted Non-signal-peptide protein	None	isotig18405	777	NFL
73	VAL-5	None	isotig04839	746	SP
74	Chondroitin-like protein	None	isotig01493	710	SP
75	Vitellogenin	Vitellogenin N	contig00199	696	SP
76	NAS-5.2 Nematode Astacin protease	ZnMc astacin-like, CUB	isotig01598	691	SP*
77	VAL-14	Double SCP	isotig04896	689	SP
78	LYS-3 Lysozyme	Muramidase GH25	isotig08606	683	SP*
79	NAS-6 Nematode Astacin protease	ZnMc astacin-like, CUB	isotig07866	681	SP*
80	Myoglobin	Globin	isotig11666	683	SP
81	NSP-4 Novel Secreted Protein	None	isotig05257	681	SP
82	MFH-2 Ascaris MFP2b homologue	MFP2b	isotig07373	647	NO
83	APY-3 Apyrase-3	Apyrase	isotig03589	644	SP
84	Complement regulatory protein	CCP	isotig13827	632	SP
85	Aldolase	FBP Aldolase 1a	isotig04915	627	NO
86	Complement regulatory protein	CCP	isotig12552	611	SP*
87	NSP-5 Novel Secreted Protein	None	isotig12800	599	SP
88	NSP-6 Novel Secreted Protein	None	isotig12832	596	SP
89	NSP-7 Novel Secreted Protein	None	isotig12576	592	SP
90	NSN-2 Novel Secreted Non-signal-peptide protein	None	isotig14195	589	NFL
91	FAR-1 Fatty acid/retinol binding protein	Gp-FAR-1	isotig11475	577	SP*
92	HEX-1 Hexokinase	Hexokinases 1, 2	isotig05973	563	NO
93	NSP-8 Novel Secreted Protein	None	isotig16252	557	SP
94	NSP-9 Novel Secreted Protein	None	isotig09200	529	SP
95	SCP-1 Serine carboxypeptidase	Esterase lipase	isotig05975	529	SP
96	CSP-1 Conserved nematode Secreted protein	None	isotig13235	528	SP*
97	SPN-1 Serpin	Serpin	isotig08233	512	NFL
98	NAS-3.2 Nematode Astacin protease	ZnMc astacin-like	isotig01792	509	SP*
99	CSP-2 Conserved nematode Secreted Protein	None	isotig09016	502	SP
100	NAS-3.3 Nematode Astacin protease	ZnMc astacin-like	isotig01791	498	SP*

SCP denotes the PFAM Sperm Coat Protein domain found in either single or double formation in VAL proteins. SS denotes presence of predicted signal sequence; SS* indicates that the sequence is truncated but homologous to known proteins containing signal sequences; NFL denotes transcripts which are not full length and for which no database homologues were found with signal sequences (in the case of novel proteins, no homologues were found at all). Note that VAL-8.1 corresponds to a sequence similar but not identical to isotig02308, while VAL-8.2 matches exactly.

domain proteins appear to have diversified independently, although the single-domain VAL-19 is most likely to have evolved from a double-domain ancestor (Fig. 5). Double-domain VAL proteins include an inter-domain linker "hinge" region, which in the case of VAL-1, 2 and 5 comprise multiple Ser/Thr residues bearing a common antigenic *O*-glycan [64]. Immunodominant serum antibodies target this glycan early in infection, although anti-peptide antibodies such as those tested in Fig. 4 are also represented [64]. Similar stretches of predicted *O*-glycosylation are present in other secreted VAL proteins, particularly VAL-11, 17 and 20 (Fig. 5).

Analysis of individual *H. polygyrus* VAL amino acid sequences reveals extensive variation between genes: for example, within the C-terminal domains of the 13 double-domain proteins, only 15/189 amino acid residues are completely conserved (8%), and a further 10 altered in only 1 gene sequence, while in the N-terminal SCP-1 domain there are only 7 identical positions (of which 6 are cysteines). Similarly, for the single domain VAL proteins there are only 8 fully conserved amino acids, and 7 differing at only 1 position. Additionally, transcriptomic studies have identified significant micro-sequence variation within individual VAL proteins (Harcus et al. manuscript in preparation), and this was evident with respect to proteomic data. For example, five alternative VAL-1 sequences verified by proteomic data are presented in Fig. 6. Note the extensive sequence diversity, particularly in the first SCP domain, suggesting that domain 1 is either under diversifying selection, or that intra-genic recombination is taking place. Similar sequence variation, with multiple variants matching the peptide data, was observed for VAL-2 and VAL-7. As the full genome of this parasite has yet to be assembled, we cannot yet determine whether the micro-variation is due to either allelic polymorphism or recent duplication of the relevant gene loci. Sequence variation has previously been reported for VALs of *A. caninum* [66], *Cooperia punctata* [67] and *H.contortus* [22].

3.7. *Non-VAL gene families represented in HES*

In addition to the 25 VAL proteins, a number of conserved gene family proteins are well represented in HES with particular prominence of the following functional groups.

Table 3 – Top 100 Proteins identified in HEx by LC–MS/MS.

Rank	Identity	Code	Score	SS
1	Vitellogenin	contig00471	3369	
2	Myoglobin	isotig11742	3366	
3	Myoglobin	isotig13336	3098	
4	Actin	isotig01642	2585	
5	Actin	isotig01640	2251	
6	Myoglobin	isotig04274	2208	
7	Myoglobin	isotig11356	2113	
8	Myoglobin	isotig05169	1977	
9	Myoglobin	isotig04273	1833	
10	HSP90	isotig04714	1831	
11	Major sperm protein	isotig01565	1820	
12	Phosphoenolpyruvate carboxykinase	isotig05532	1713	
13	Aldolase	isotig04915	1611	
14	Myoglobin	isotig11666	1607	
15	Nematode polyprotein allergen NPA-1	isotig02438	1562	
16	Enolase	isotig06965	1476	
17	Protein disulphide isomerase	isotig05787	1465	✓
18	Vitellogenin	contig00207	1301	
19	Vitellogenin	contig00212	1295	
20	Eukaryotic translation elongation factor 1A	isotig06220	1223	
21	14-3-3 family member	isotig07975	1218	
22	Actin	isotig08179	1212	
23	Eukaryotic translation elongation factor 1A	isotig02523	1187	
24	Beta-tubulin	isotig06421	1179	
25	HSP70	isotig07134	1167	
26	Vitellogenin	contig00203	1040	
27	Vitellogenin	EST Hp_ADY001C04	1025	
28	Eukaryotic translation elongation factor 2	isotig05363	1015	
29	Ribosomal protein 60S P0	isotig01358	965	
30	HSP60	isotig06093	958	
31	Protein disulphide isomerase	isotig01916	902	✓
32	Vitellogenin	contig00199	884	
33	AAA family ATPase	isotig05378	857	
34	HSP90	isotig05404	851	
35	Serpin	isotig02225	788	
36	Ribosomal protein 40S S8	isotig10482	785	
37	Thioredoxin peroxidase	isotig05188	771	
38	Alpha-tubulin	isotig06550	736	
39	Arginine kinase	isotig06694	736	
40	Fumarase	isotig02533	717	
41	Myoglobin	isotig12632	698	
42	Actin	isotig08340	695	
43	Cystathionine beta-synthase	isotig05473	681	
44	Glyceraldehyde 3-phosphate dehydrogenase	isotig03503	646	
45	Calreticulin	Hpb-CRT	636	
46	Glutamate dehydrogenase	isotig06500	634	
48	HSP70	isotig05458	585	
49	Tropomyosin	Hpb-TRP	585	
50	Nucleosome assembly protein	isotig04959	573	
51	Chondroitin family member	isotig01493	571	
52	Malate dehydrogenase	isotig05076	561	
53	Phosphoglycerate_kinase	isotig06484	533	
54	Myoglobin	isotig13442	531	
55	Ribosomal protein 60S L6	isotig11208	524	
56	Vitellogenin	EST Hp_ADY_001G11	523	
57	Myoglobin (fragment)	isotig19571	521	
58	Fatty acid and retinol binding protein	isotig11475	515	
59	Alpha-tubulin	isotig06165	512	
60	C-type lectin	isotig02337	499	✓
61	Phosphatidylethanolamine-binding protein	isotig05126	469	✓
62	Ribosomal protein 60S L18	isotig10630	465	
63	Ribosomal protein 40S S4	isotig05116	463	
64	CSN-2 Conserved secreted protein, No signal sequence	isotig04423	449	
65	Chondroitin family member	isotig06559	433	
66	Eukaryotic translation initiation factor 4A	isotig06491	432	
67	Retinol binding protein	Hpb-RBP	419	
68	Enolase (fragment)	isotig18996	404	
69	Nucleoside diphosphate kinase	isotig05236	401	
70	Ribosomal protein 60S L7a	isotig09109	397	
71	CSN-5 Conserved secreted protein, No signal sequence	isotig03664	393	
72	Glutathione S-transferase	isotig10292	389	
73	Macrophage migration inhibitory factor	isotig14093	383	
74	Vitellogenin	contig00211	372	
75	Cyclophilin	isotig11124	364	
76	Dehydrogenase	isotig03780	363	
77	Cytochrome C	isotig11144	361	
78	Ribosomal protein 60S L14	isotig14543	359	
79	RACK family member	isotig07754	358	
80	Aspartyl protease inhibitor	isotig05063	355	
81	Glutathione S-transferase	isotig07073	351	
82	VAL-3.1	isotig05790	349	✓
83	Ribosomal protein 60S L10	isotig12696	346	
84	Transketolase	isotig02953	346	
85	HSP70	isotig13132	345	
86	Ribosomal protein 40S S3	isotig09688	345	
87	Aldehyde dehydrogenase family member	isotig04738	339	
88	Oxidoreductase	isotig08193	323	
89	Glutathione S-transferase	isotig11588	322	
90	Adenosylhomocysteinase	isotig08907	308	
91	TTR-13 Transthyretin-related	isotig13284	304	
92	Glutathione S-transferase	isotig04128	302	
93	Ureidopropionase	isotig08079	300	
94	HSP70	isotig08182	296	
95	CSN-6 Conserved secreted protein, No signal sequence	isotig04424	288	
96	Fructose-1,6-bisphosphatase	isotig07764	284	
97	NAC domain-containing protein	isotig10507	283	
98	Alpha-tubulin	isotig06090	282	
99	Isocitrate lyase-malate synthase	isotig05351	282	
100	Ribosomal protein 60S L12	isotig11621	278	

3.7.1. *Acetylcholinesterases*

Three acetylcholinesterases are among the 100 most abundant HES proteins (Table 2), with Hpb-ACE-1 represented by 3 distinct spots (Table 1). Two additional proteins, ACE-2 and -3, differ by only 18 amino acids (3.1%) from each other but show ~32% divergence from ACE-1. The secretion of AChE by adult

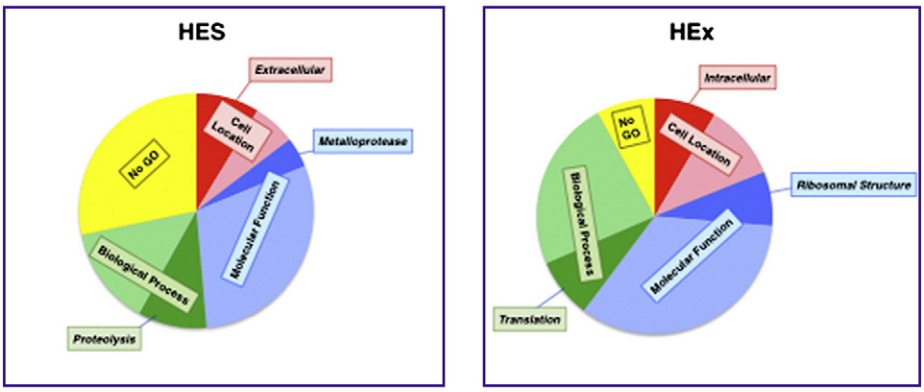

Fig. 2 – GO distribution of the proteins in HES and HEx. All identified proteins in HES and HEx were analysed by Gene Ontology and categorised firstly into 4 broad categories: cell localation (Red), molecular function (Blue), biological process (Green), and no recognised GO similarity (Yellow). Within each category, the most frequent term is shown (darker colours). Some proteins are included in more than one category. A more detailed listing of GO identifications is given in Supplementary Table A3.

H. polygyrus has been previously reported [68] and is a general feature of most nematode ES products [69]. In *N. brasiliensis*, the expression of three AChE isoforms has been shown to be differentially regulated according to the immune status of the host [70–73], and the 3 *H. polygyrus* proteins show highest similarity to isoform A of *N. brasiliensis*.

3.7.2. *Apyrases*

Four distinct apyrases were identified, one of which (Hpb-APY-1) was found as three minor sequence variants, all but one in the most abundant 100 HES proteins. Apyrases are adenosine diphosphatases, similar to mammalian CD73-like proteins, which catalyse the hydrolysis of ATP/ADP to AMP, and can often act also on other NDPs. Two recent reports have identified arthropod (*Cimex*)-like apyrases from related trichostrongylid nematodes *T. circumcincta* [74] and *Ostertagia ostertagi* [75] sharing 92% amino acid identity; in the latter case the enzyme was localised to the oesophageal glands. While all 4 *H. polygyrus* apyrases are homologous to these enzymes, levels of amino acid identity are less than 60%, indicating considerable diversification since divergence of the murine and ruminant parasites.

3.7.3. *Lipid-binding proteins*

Several structurally unrelated lipid-binding protein families are represented in HES. HES contains two distinct homologues of the Fatty acid/Retinol-binding (FAR) protein that has been recorded in ES of many other parasitic nematodes [76,77] and which in the case of *A. caninum* FAR-1 has been shown to functionally bind fatty acids and retinol [78]. A nematode polyprotein allergen (NPA) is also secreted by *H. polygyrus*, homologues of which bind the same ligands in *Ascaris* [79] and *Dictyocaulus viviparus* [80]. In addition, a total of 12 transthyretins are represented in HES, members of a widespread and diverse family of small proteins believed to recognise small hydrophobic ligands such as thyroid hormone, retinol or phosphatidylserine [81–83].

3.7.4. *Lysozymes*

Lysozymes or muramidases are present in multiple forms in HES, with 8 distinct gene products identified. All are related to *C. elegans* and the 7 full-length sequences contain a potential signal peptide. In other organisms, lysozymes degrade the glycosidic bond linking *N*-acetylglucosamine and *N*-acetylmuramic acid in the murein proteoglycan of bacterial cell walls. Since adult *H. polygurus* cohabit with microbial flora, and Gram-positive bacteria are more susceptible to lysozyme-mediated lysis, it is possible that these lysozymes modify the bacterial population sharing the intestinal niche of the worm.

3.7.5. *Proteases*

Five aspartyl proteases (PF00026) in HES correspond to a major enzymatic class from parasitic nematodes. Aspartyl proteases play a key role in the ability of *A. caninum* hookworms to degrade haemoglobin [84], and are the target of protective antibodies against the human parasite *Necator americanus* [85]. We identified no fewer than 20 astacins, Zn-metalloproteases distributed across the animal kingdom with particular frequency in nematodes [86,87].

Cysteine proteases have a major role in nematode parasites, particularly within the hookworm family. However, while 7 ES cathepsin B products have been defined in *H. contortus* [88], part of a larger gene family which show a particularly high level of transcription in intestinal tissue [89], only 4 are found in HES, a cathepsin B-like cysteine protease, a homologue of *N. americanus* necpain and two legumains (asparaginyl endopeptidases). Serine proteases are also less prominent in HES than aspartyl or metallo-enzymes, but include Cathepsin A, aminopeptidase, serine carboxypeptidases, trypsin family proteases and dipeptidyl peptidase four (DPF) proteins.

3.7.6. *Protease inhibitors*

Three broad classes of protease inhibitor are found in HES. Cystatins are a broadly conserved family of cysteine protease inhibitors found across plant and animal phyla, with an especial role in immune modulation by parasitic nematodes [90,91]. Inhibition of the protease active site involves a QVVAG sequence which is perfectly conserved in the *H. polygyrus* homologue, as also in Nippocystatin from *N. brasiliensis* ES [92] and in *B. malayi* Bm-CPI-2 [93]. However, while *Bm*-CPI-2 has a second inhibitory motif (SND) that blocks the legumain

Table 4 – Proteins common to both HES and HEx.

Rank	Name	CODE	HES score	HES emPAI	HEx score	HEx emPAI	HES/HEx emPAI
1	VAL-2.1	isotig03106	5149	8.35	103	0.12	69.6
2	TTR-1 Transthyretin-related	isotig04612	2130	29.24	144	0.86	34.0
3	VAL-1.3	isotig06456	2668	1.97	47	0.06	32.8
4	VAL-7.5	isotig01526	3367	11.23	100	0.35	32.1
5	VAL-1.1	isotig06320	6546	4.05	77	0.18	22.5
6	NAS-3.1 Astacin protease	isotig01799	832	2.02	47	0.12	16.8
7	VAL-3.1	isotig05790	4754	3.66	349	0.25	14.6
8	VAL-7.1	isotig01524	2593	8.84	129	0.64	13.8
9	NSN-1 Novel secreted protein, No SP	isotig18405	777	4.03	40	0.31	13.0
10	Astacin protease family member	isotig01791	419	1.41	67	0.12	11.8
11	CSP-4 Conserved secreted protein with SP	isotig13290	482	1.82	37	0.16	11.4
12	VAL-4	isotig10387	1770	4.08	53	0.42	9.7
13	Aspartyl protease (necepsin)	isotig06497	884	1.17	136	0.18	6.5
14	Kunitz inhibitor	isotig01217	273	0.76	88	0.12	6.3
15	VAL-12	isotig06637	803	1.02	130	0.19	5.4
16	Astacin protease family member (fragment)	isotig01219	956	3.05	89	0.59	5.2
17	Superoxide dismutase	isotig09104	235	0.47	48	0.10	4.7
18	C-type lectin mannose receptor-like	isotig00496	366	0.97	61	0.23	4.2
19	MFH-1 Ascaris MFP2b homologue	isotig07283	845	1.17	137	0.29	4.0
20	Cystatin	isotig02700	261	0.41	71	0.12	3.4
21	CSP-2 Conserved secreted protein with SP	isotig09016	502	0.57	434	0.20	2.9
22	Motile sperm domain containing protein	isotig16097	175	0.50	144	0.22	2.3
23	Galectin	isotig09082	120	0.20	44	0.09	2.2
24	TIL domain-containing protein	isotig00779	98	0.27	42	0.13	2.1
25	Arginine kinase	isotig05009	212	0.65	193	0.33	2.0
26	Motile sperm domain containing protein	isotig16375	220	0.89	160	0.53	1.7
27	ERM family member	isotig02815	79	0.08	100	0.05	1.6
28	Cyclophilin	isotig09088	111	0.31	71	0.20	1.6
29	Actin depolymerising factor	isotig07522	145	0.23	144	0.15	1.5
30	Macrophage migration inhibitory factor	isotig14093	256	0.96	383	0.65	1.5
31	TTR-5 Transthyretin-like	isotig13207	397	0.89	88	0.61	1.5
32	MFH-3 Ascaris MFP2b homologue	isotig07980	463	0.84	148	0.58	1.4
33	TTR-10 Transthyretin-like	isotig11792	108	0.67	84	0.47	1.4
34	NSP-30 Novel secreted protein with SP	isotig12701	194	0.99	166	0.73	1.4
35	Chondroitin family member	isotig01493	710	0.48	571	0.38	1.3
36	Ferritin	isotig15727	117	0.74	140	0.73	1.0
37	NSP-39 Novel secreted protein with SP	isotig16333	108	0.78	187	0.77	1.0
38	Vitellogenin	contig00207	1552	5.73	1301	5.70	1.0
39	Myoglobin (fragment)	isotig19571	415	3.10	521	3.09	1.0
40	Calmodulin	isotig07710	53	0.07	57	0.07	1.0
41	Cathepsin-B like cysteine protease	isotig07017	147	0.06	136	0.06	1.0
42	Galectin	isotig09713	81	0.10	69	0.10	1.0
43	Kunitz inhibitor	isotig02721	82	0.13	82	0.13	1.0
44	Kunitz inhibitor	isotig02378	35	0.20	36	0.20	1.0
45	ML-domain containing protein	isotig10098	110	0.23	88	0.23	1.0
46	Motile sperm domain containing protein	isotig16212	138	0.22	92	0.22	1.0
47	NSP-59 Novel secreted protein with SP	isotig13319	38	0.16	35	0.16	1.0
48	Triose phosphate isomerase	isotig05016	276	0.44	198	0.44	1.0
49	VAL-15	isotig02149	133	0.20	200	0.20	1.0
50	Chondroitin family member	isotig08745	82	0.21	92	0.22	1.0
51	NPA-1 Nematode polyprotein allergen	isotig02438	1498	0.67	1562	0.75	0.9
52	Vitellogenin	contig00471	3997	3.05	3369	3.74	0.8
53	Nucleoside diphosphate kinase	isotig05236	462	1.18	401	1.55	0.8
54	TTR-6 Transthyretin related	isotig05212	304	0.62	210	0.83	0.7
55	Rab GDP dissociation inhibitor	isotig06129	54	0.16	168	0.22	0.7
56	Chondroitin family member	isotig06559	284	0.48	433	0.66	0.7
57	Vitellogenin	contig00199	696	2.38	884	3.29	0.7
58	Myoglobin	isotig11742	1446	3.31	3366	4.60	0.7
59	Enolase	isotig06965	826	2.13	1476	3.02	0.7
60	Transaldolase	isotig07176	59	0.14	62	0.21	0.7
61	Vitellogenin	contig00203	1205	4.87	1040	7.34	0.7
62	Aldolase	isotig04899	67	0.13	114	0.20	0.7
63	Vitellogenin (fragment)	sing00711	131	1.60	179	2.57	0.6
64	Myoglobin	isotig05169	1094	1.64	1977	2.64	0.6

Table 4 (*continued*)

Rank	Name	CODE	HES score	HES emPAI	HEx score	HEx emPAI	HES/HEx emPAI
65	Myoglobin	isotig04274	1579	3.13	2208	5.07	0.6
66	TTR-11 Transthyretin related	isotig04258	83	0.29	95	0.47	0.6
67	Ribosomal protein 60S L40/Ubiquitin	isotig13199	108	0.34	116	0.56	0.6
68	Serpin	isotig02225	281	0.33	788	0.59	0.6
69	Vitellogenin	contig00212	918	2.24	1295	4.24	0.5
70	Vitellogenin	contig00211	263	1.29	374	2.46	0.5
71	Chondroitin family member	isotig04525	51	0.13	75	0.27	0.5
72	Fatty acid/retinol binding protein	isotig11475	577	1.47	515	3.12	0.5
73	Fatty acid/retinol binding protein (fragment)	sing12372	71	0.27	78	0.61	0.4
74	Phosphatidylethanolamine-binding protein	isotig05126	339	0.64	469	1.67	0.4
75	Independent phosphoglycerate mutase	isotig01699	48	0.05	136	0.14	0.4
76	Vitellogenin	Hp_ADY_001G11	144	2.05	523	5.75	0.4
77	Cyclophilin	isotig11124	256	0.87	364	2.48	0.4
78	Thioredoxin peroxidase	isotig05188	498	1.79	771	5.19	0.3
79	Enolase (fragment)	isotig18996	326	1.08	404	3.30	0.3
80	Glutathione S-transferase	isotig11588	219	0.47	322	1.45	0.3
81	HSP70 (fragment)	isotig13132	148	0.35	345	1.11	0.3
82	Myoglobin	isotig11356	398	0.63	2113	2.00	0.3
83	Calreticulin	Hpb-CRT	74	0.21	636	0.67	0.3
84	Lipocalin domain-containing protein	isotig05316	104	0.34	229	1.09	0.3
85	Myoglobin	isotig11666	683	4.48	1607	14.53	0.3
86	CSN-5 Conserved secreted protein, No SP	isotig03664	43	0.08	393	0.27	0.3
87	Aldolase	isotig04915	627	0.77	1611	3.00	0.3
88	Major sperm protein	isotig01565	1278	2.10	1820	8.59	0.2
89	HSP60	isotig06093	195	0.43	958	1.76	0.2
90	Piwi domain-containing protein	isotig04875	77	0.06	167	0.25	0.2
91	14-3-3 family member	isotig07975	324	0.94	1218	3.98	0.2
92	CSN-2 Conserved secreted protein, No SP	isotig04423	127	1.08	449	4.75	0.2
93	Actin	isotig08340	102	0.27	695	1.38	0.2
94	Cytochrome C	isotig11144	50	0.13	361	0.86	0.2
95	Actin	isotig01640	340	0.47	2251	3.21	0.1
96	Eukaryotic translation elongation factor 2	isotig05363	86	0.09	1015	0.87	0.1
97	Protein disulfide isomerase	isotig01916	81	0.16	902	1.62	0.1
98	Eukaryotic translation elongation factor 1A	isotig02523	44	0.12	1187	1.64	0.1
99	Protein disulfide isomerase	isotig05787	133	0.24	1465	3.42	0.1
100	HSP70	isotig07134	100	0.22	1167	3.18	0.1
101	Glutathione S-transferase	isotig10292	47	0.24	389	3.88	0.1
102	Malate dehydrogenase	isotig05076	44	0.07	561	1.31	0.1
103	Ribosomal protein 60S P0	isotig01358	38	0.04	965	0.77	0.1
104	Retinol binding protein	Hpb-RBP	29	0.16	419	5.15	0.0

is altered in *H. polygyrus* (SNA) and may therefore not function in an identical fashion. Seven Kunitz type serine protease inhibitors are represented in HES, and again this gene is found in multiple forms in many helminth products [94]. Notably, a related secreted product from adult *A. ceylanicum* (AceK1) acts against a broad range of serine proteases, including trypsin, chymotrypsin and pancreatic elastase [95,96]. In *C. elegans*, a Kunitz-type inhibitor is important in collagen processing for cuticle formation, with mutations causing the blister-5 (*bli*-5) phenotype [97]. A structurally unrelated family of serine inhibitors are the serpins, large globular proteins that include most dominant ES antigen of *B. malayi* MF [98,99]. Three HES serpins were identified but are only distantly related to Bm-SPN-2, all being most similar to a serpin from *Trichostrongylus vitrinus*.

3.8. *Similarity to other Strongylid nematodes*

The overall profile of gene sets represented in HES shows many similarities to those reported in Trichostrongylid nematode *T. circumcincta*[30] as well as the more distantly related hookworm *Ancylostoma caninum*[28], as shown in Table 5, and a number of specific homologies are noted above. In each species, VAL family members predominate, and similar findings have been reported for other members of the Trichostronglyid taxon such as *Ostertagia ostertagi* [100].

4. Discussion

The secretome of extracellular pathogens provides fascinating insights into the biological strategy of infectious organisms, in particular those such as long-lived helminth species that must attain an optimal physiological and immunological balance with their hosts [7]. The spectrum of parasite secreted proteins represents the elaborate adaptions demanded by the parasitic mode of life, over and above nematode-specific functions evident in free-living relatives such as *C. elegans*, many of which are likely to have evolved to interact with a precise host pathway, often with a specific ligand or receptor, and each of

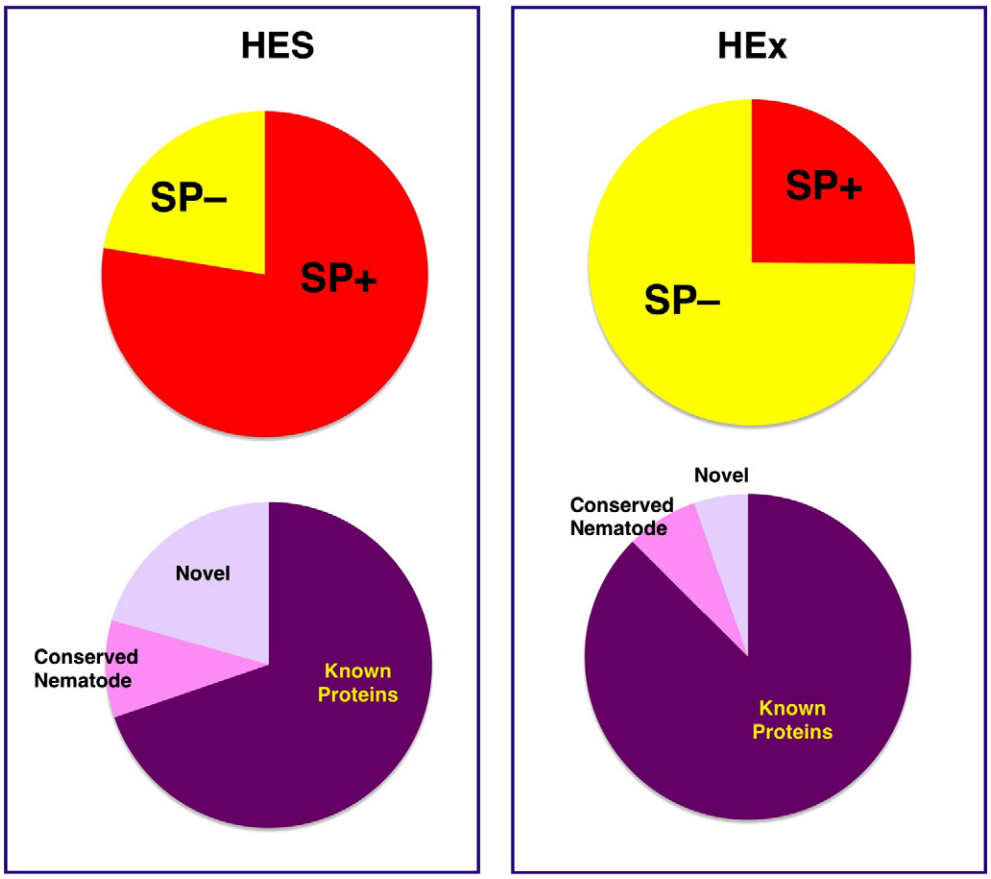

Fig. 3 – Novel genes and signal peptides of the proteins in HES and HEx. Upper diagrams: Distribution of signal peptide-containing protein sequences. Lower diagrams: Proportions of novel and nematode-conserved genes containing signal peptides.

which may offer a novel and effective route to intervention and therapy.

The analytical power of modern proteomics enabled us to identify 374 ES products of adult *H. polygyrus*, holding open the prospect of a complete "worm pharmacopoeia" of potential host-modulating proteins [101]. Comparisons with the whole worm somatic protein extracts indicate a high level of selectivity, with many proteins only detectable in the secretions of the parasite, and conversely most somatic products being absent from HES. The likelihood that HES collected *in vitro* faithfully reflects release *in vivo*, is supported by recent work detecting circulating HES antigen in the serum of infected mice (Hewitson, unpublished), and demonstrating that host antibody responses are predominantly directed against HES, rather than HEx, antigens [64]. Validation of the methodological focus on ES products is further offered by the contrast in signal peptide-positive sequences within HES compared to HEx. Moreover, the concept that ES proteins may have evolved more rapidly to interact with host systems is supported by the higher number of novel (and novel signal peptide-positive) gene sequences among HES proteins than in the general body components, as previously noted in *N. brasiliensis* [13].

We also established that two of the major HES proteins, VAL-1 and -2, are represented on the surface of adult parasites. This finding reiterates work with other nematode species that found concordance between surface and secreted proteins of adult *B. malayi* [63,102] and larval *T. canis* [103,104]. These studies raise interesting questions regarding the route of secretion by live parasitic nematodes: while they possess specialised secretory apparatus such as oesophageal glands [103,105], there is also evidence of direct trans-cuticular secretion deriving from the syncytial hypodermal tissue underlying the extracellular cuticle [106]. Now that the adult ES proteins are well defined, and with a number of monoclonal antibodies to these proteins [64], these issues can be directly addressed at the microscopic level.

The most striking feature of the HES analysis is the dominance of multiple VAL proteins. The VAL family is an extraordinary one in being so widely distributed in nature, with alternative names from diverse systems including Cysteine-RIch Secretory Protein (CRISP), Sperm Coat Protein (SCP) in mammals and plant Pathogenesis-Related protein (PR), without any clear indication as to their functional role(s) [107,108]. Within the nematodes, the archetypal VAL protein is the *Ancylostoma* secreted protein (ASP), a homologue of which (ASP-2) has been taken forward for human hookworm vaccine trials [109]. Interestingly, in *Ancylostoma* species from dogs and humans, multiple and divergent ASPs are known. For example, some 25 distinct VAL family transcripts were identified by Mitreva and colleagues from *A. caninum* [16]. For potential vaccines, it is important to target products of the initial

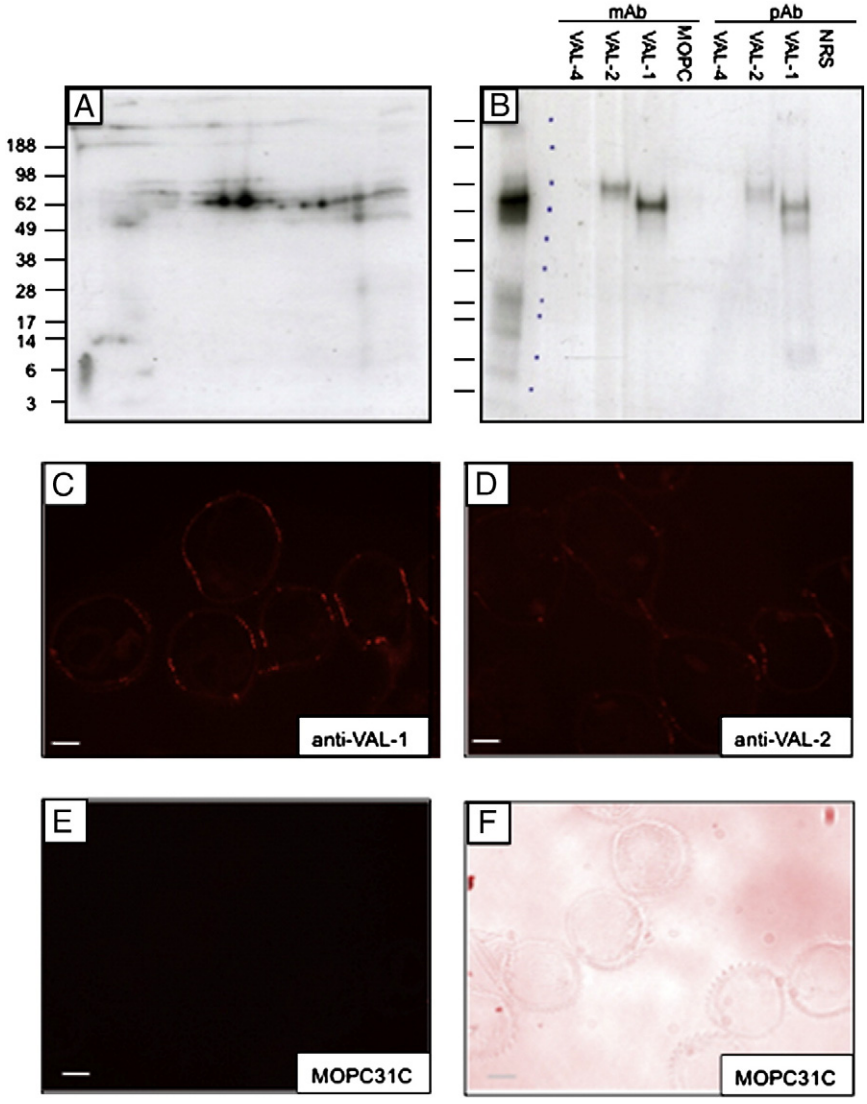

Fig. 4 – Surface labelling of adult *H. polygyrus* reveals VAL-1 and VAL-2 are surface associated. A. Surface iodination, 2D gel. B. Immunoprecipitation of surface labelled VAL-1 and -2 with specific antibodies. C. Anti-VAL-1 monoclonal antibody on adult worm section. D. Anti-VAL-2 monoclonal antibody on adult worm section. E and F. MOPC control antibody on adult worm section with corresponding bright field image.

infective stages as well as of established adults; thus future work with *H. polygyrus* will investigate VAL gene expression in immature as well as adult stages of the parasite. Additionally, we are currently assessing the protective potential of both the total adult secretions and individual VAL proteins.

VAL genes are also expressed in non-parasitic organisms, but with an intriguing association with the interface between different species, as for example in snake and insect venoms and haematophagous insect saliva, as well as in the response of plants to microbial infection. Moreover, numerous homologues exist in the free-living nematode *C. elegans* [108], arguing that these genes must have many functions outside the frame of host–parasite interactions. Indeed, *lon-1* is such a gene that controls body length downstream of TGF-β signalling [110]. It is plausible, therefore, that the SCP domain is simply an adaptable protein framework that facilitates the evolution of diverse specialised functions, and that such diversity is accentuated by inter-species interactions; certainly the extensive radiation within the *H. polygyrus* lineage is consistent with this notion. Intriguingly, VAL proteins found in HES differ from those of *C. elegans* in terms of both the enrichment of double domain proteins and in the presence of a serine/threonine rich linker region between SCP domains, the site of highly antigenic *O*-glycans in the HES proteins [64].

The comparison with related nematode species (Table 5) is instructive, not only in confirming that dominant VAL secretion is shared among different members of the taxon, but also identifying many common, and some particular, gene sets associated with intestinal parasitism. Most conspicuous across all these species is the level of protease production, predominantly astacins and other metalloproteases, but also including the aspartyl, cysteine and serine protease classes. Together with the

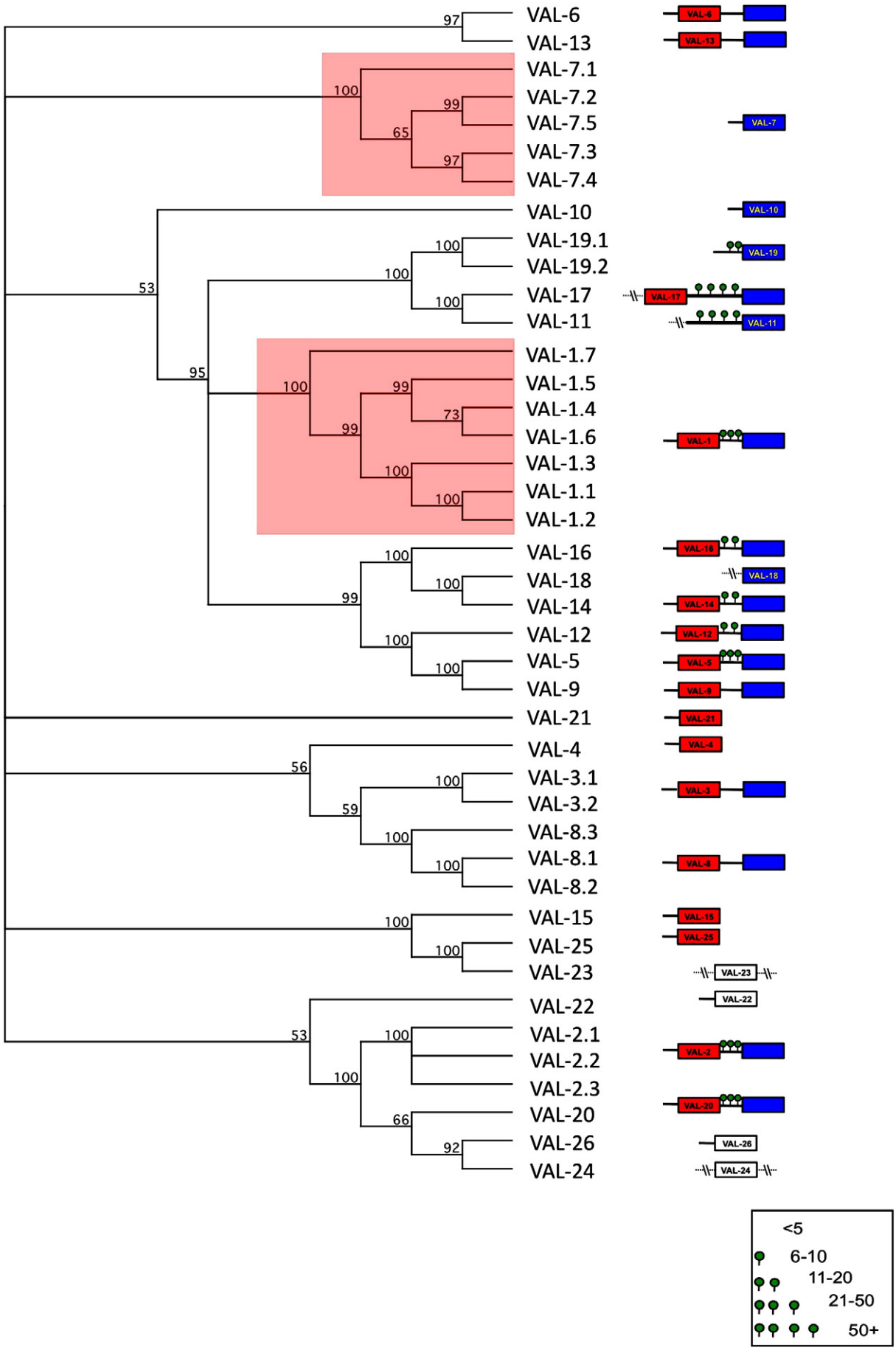
VAL-6
VAL-13
VAL-7.1
VAL-7.2
VAL-7.5
VAL-7.3
VAL-7.4
VAL-10
VAL-19.1
VAL-19.2
VAL-17
VAL-11
VAL-1.7
VAL-1.5
VAL-1.4
VAL-1.6
VAL-1.3
VAL-1.1
VAL-1.2
VAL-16
VAL-18
VAL-14
VAL-12
VAL-5
VAL-9
VAL-21
VAL-4
VAL-3.1
VAL-3.2
VAL-8.3
VAL-8.1
VAL-8.2
VAL-15
VAL-25
VAL-23
VAL-22
VAL-2.1
VAL-2.2
VAL-2.3
VAL-20
VAL-26
VAL-24
<5
6-10
11-20
21-50
50+

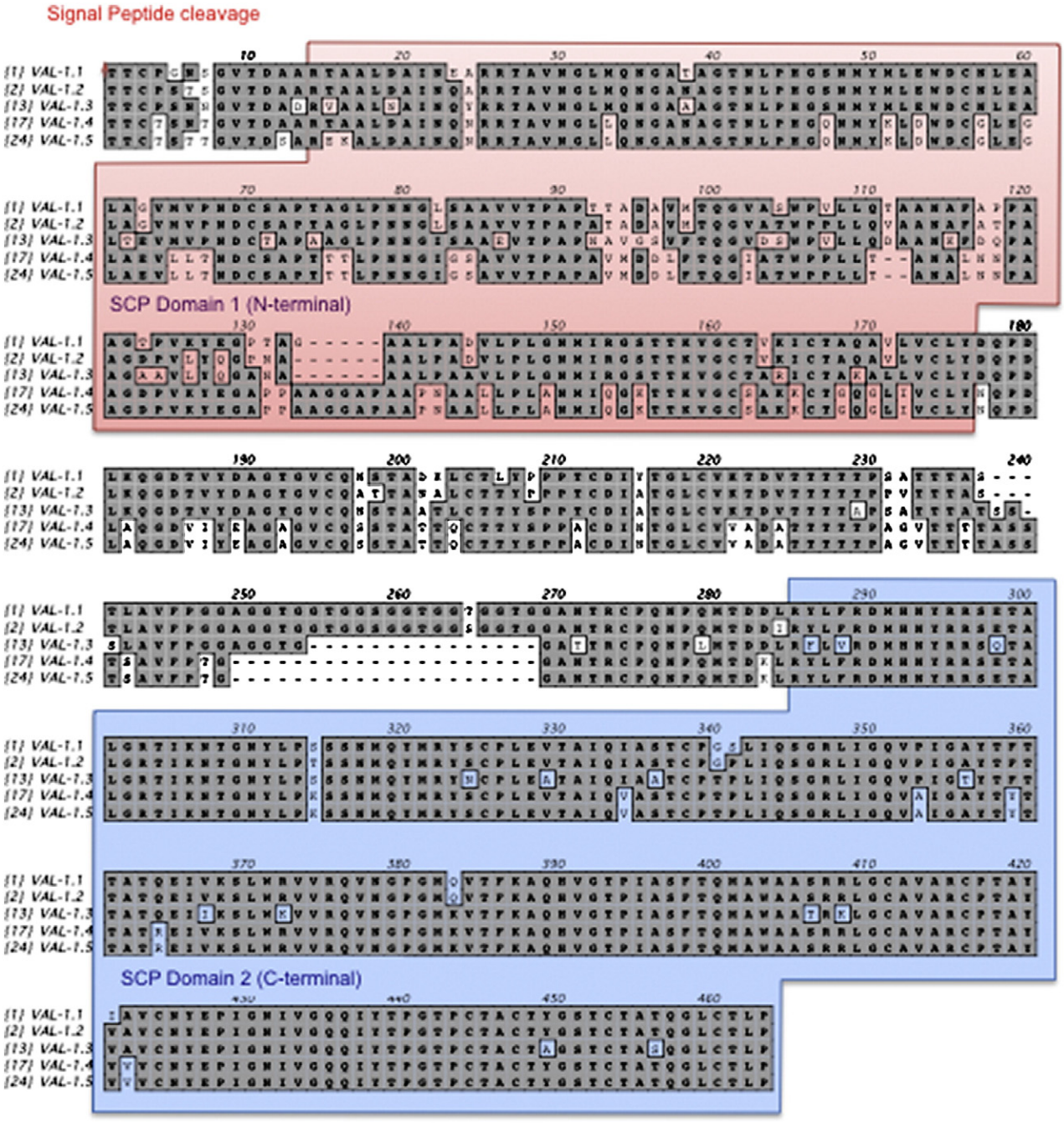

Fig. 6 – Sequence variation within *H polygyrus* VAL-1 proteins. Mature proteins with signal cleavage site and N and C-terminal SCP domains indicated.

release of a series of protease inhibitors (cystatins, serpins, Kunitz inhibitors *etc.*) this suggests that nematodes can reset the hydrolytic and proteolytic environment of the gastrointestinal tract, possibly to avoid enzymatic attack but also quite probably to degrade host mediators and obstacles such as mucins, immunoglobulins and innate defence molecules.

A further set of parallels are seen with the production of apyrases, with four different proteins identified. Whilst

Fig. 5 – Schematic of relatedness of *H. polygyrus* HES VAL-1-25, and VAL-26 identified in HEx. The domain structure of Hpb-VAL-1 to -26 are depicted including signal sequences, linker regions (predicted O-glycosylation is indicated with green circles) and SCP homology domains (N-terminal red, C-terminal blue). Single SCP domain proteins are coloured according to whether they are related to N (red) or C-terminal (blue) SCP domains. Divergent sequences equally distinct from both are white. Sequence truncation is indicated by (–\\–).

Table 5 – Table of common ES proteins between *H. polygyrus*, *Ancylostoma caninum*, *Haemonchus contortus* and *Teladorsagia circumcincta*.

	A. caninum	*H. contortus*	*H. polygyrus*	*T. circumcincta* (L4 not adult)
	[28]	[22]	Hewitson, this paper	[30]
n	105	107	374	32
VAL/ASP	24	13	25	8
Metalloproteases/Astacins/Aminopeptidases	4	14	25	2
Transthyretins	5	2	12	0
Lysozymes	2	0	8	0
Serine proteases	0	8	8	0
Galectins	2	0	5	0
Aspartyl proteases	1	1	5	0
Cysteine proteases/necpains	3	0	4	13
CTLs	3	0	3	0
15-kDa ES	8	21	2	0
Cyclophilins	0	2	2	0
Protein disulphide isomerases	1	0	2	2
Nucleoside diphosphate kinases	0	1	1	0
GA1	0	21	0	0

apyrases have been associated with the inhibition of blood clotting by blood feeding insects [111], they do not appear to be secreted by blood feeding hookworms [28]. An alternative role may be immunomodulatory through conversion of pro-inflammatory ATP/ADP to anti-inflammatory AMP [112]. ATP, released by intestinal bacteria, can activate dendritic cells (DC) to secrete the pro-inflammatory cytokines IL-6 and IL-23, resulting in the induction of inflammatory Th17 cells [113]. Similarly, ATP-dependent DC activation is essential for Th2-dependent lung pathology in asthma models, and this can be inhibited through the administration of an apyrase [114]. In this context, adenosine generation may both induce Foxp3+ regulatory T cells and be used by this cell type as a mechanism of suppression [115]. Finally, in *C. elegans*, an endo-apyrase, APY-1, fulfils a more homeostatic role in the stress response of the organism [116], a role that cannot be excluded for *H. polygyrus* homologues.

Whilst we have catalogued the identity of several hundred of the most abundant proteins in the search for helminth immunomodulators, we did not detect expression of the TGFβ family member encoded by *H. polygyrus*, and expressed by all mammalian stages [60]. Such activity appears linked to the ability of HES to induce de novo Foxp3-positive regulatory T cells [53]. This may be because TGFβ is active at sub-nM levels, beyond the level of detection of our MS analysis. Alternatively, it is not known whether the TGFβ activity in HES is due to a true-TGFβ homolog. We are currently fractionating HES to determine this. Another potential immunomodulator previously considered is calreticulin, which has been reported to drive the Th2 response that is strongly provoked in *H. polygyrus* infection [58]; as calreticulin is present at only low levels in HES, but is readily detectable in worm extract, it remains to be determined if this product emanates from active secretion or leakage from compromised parasites.

In conclusion, we have embarked on a fine-detail molecular dissection of an important nematode parasite, which serves as an excellent model for both human and veterinary helminth diseases. Whilst RNAi has not yet been successfully demonstrated with *H. polygyrus* [117], more recent studies have established that secretory proteins may be optimally positioned for silencing in this way [118], which should allow functional testing of the various potentially immunomodulatory proteins described here. It is important to note that so far we have analysed only adult HES, but that infection is initiated by L3 which embed in the intestinal submucosa and clearly elaborate a set of equally fascinating mediators; hence in due course we hope to analyse the ES of immature stages and complete the proteomic characterization of this organism.

Supplementary materials related to this article can be found online at doi:10.1016/j.jprot.2011.06.002

Acknowledgements

We thank the Wellcome Trust for Programme Grant support. KJF is supported by an MRC CASE studentship with UCB Celltech. JRG was supported by a Wellcome Trust PhD studentship.

REFERENCES

[1] Hotez PJ, Brindley PJ, Bethony JM, King CH, Pearce EJ, Jacobson J. Helminth infections: the great neglected tropical diseases. J Clin Invest 2008;118:1311–21.
[2] Miller JE, Horohov DW. Immunological aspects of nematode parasite control in sheep. J Anim Sci 2006;84: E124–32 suppl.
[3] Maizels RM, Yazdanbakhsh M. Regulation of the immune response by helminth parasites: cellular and molecular mechanisms. Nat Rev Immunol 2003;3:733–43.
[4] Elliott DE, Summers RW, Weinstock JV. Helminths as governors of immune-mediated inflammation. Int J Parasitol 2007;37:457–64.
[5] Harnett W, Harnett MM. Therapeutic immunomodulators from nematode parasites. Expert Rev Mol Med 2008;10:e18.
[6] Adisakwattana P, Saunders SP, Nel HJ, Fallon PG. Helminth-derived immunomodulatory molecules. Adv Exp Med Biol 2009;666:95–107.
[7] Hewitson JP, Grainger JR, Maizels RM. Helminth immunoregulation: the role of parasite secreted proteins in

modulating host immunity. Mol Biochem Parasitol 2009;167: 1–11.
[8] Ghedin E, Wang S, Spiro D, Caler E, Zhao Q, Crabtree J, et al. Draft genome of the filarial nematode parasite *Brugia malayi*. Science 2007;317:1756–60.
[9] Abad P, Gouzy J, Aury JM, Castagnone-Sereno P, Danchin EG, Deleury E, et al. Genome sequence of the metazoan plant-parasitic nematode *Meloidogyne incognita*. Nat Biotechnol 2008;26:909–15.
[10] Opperman CH, Bird DM, Williamson VM, Rokhsar DS, Burke M, Cohn J, et al. Sequence and genetic map of *Meloidogyne hapla:* a compact nematode genome for plant parasitism. Proc Natl Acad Sci USA 2008;105:14802–7.
[11] Mitreva M, Jasmer DP, Zarlenga DS, Wang Z, Abubucker S, Martin J, et al. The draft genome of the parasitic nematode *Trichinella spiralis*. Nat Genet 2011;43:228–35.
[12] Tetteh KKA, Loukas A, Tripp C, Maizels RM. Identification of abundantly-expressed novel and conserved genes from infective stage larvae of *Toxocara canis* by an expressed sequence tag strategy. Infect Immun 1999;67:4771–9.
[13] Harcus YM, Parkinson J, Fernández C, Daub J, Selkirk ME, Blaxter ML, et al. Signal sequence analysis of expressed sequence tags from the nematode *Nippostrongylus brasiliensis* and the evolution of secreted proteins in parasites. Genome Biol 2004;5:R39.
[14] Mitreva M, Jasmer DP, Appleton J, Martin J, Dante M, Wylie T, et al. Gene discovery in the adenophorean nematode *Trichinella spiralis*: an analysis of transcription from three life cycle stages. Mol Biochem Parasitol 2004;137: 277–91.
[15] Parkinson J, Mitreva M, Whitton C, Thomson M, Daub J, Martin J, et al. A transcriptomic analysis of the phylum Nematoda. Nat Genet 2004;36:1259–67.
[16] Mitreva M, McCarter JP, Arasu P, Hawdon J, Martin J, Dante M, et al. Investigating hookworm genomes by comparative analysis of two *Ancylostoma* species. BMC Genomics 2005;6:58.
[17] Nisbet AJ, Redmond DL, Matthews JB, Watkins C, Yaga R, Jones JT, et al. Stage-specific gene expression in *Teladorsagia circumcincta* (Nematoda: Strongylida) infective larvae and early parasitic stages. Int J Parasitol 2008;38:829–38.
[18] Yin Y, Martin J, Abubucker S, Scott AL, McCarter JP, Wilson RK, et al. Intestinal transcriptomes of nematodes: comparison of the parasites *Ascaris suum* and *Haemonchus contortus* with the free-living *Caenorhabditis elegans*. PLoS Negl Trop Dis 2008;2: e269.
[19] Abubucker S, Zarlenga DS, Martin J, Yin Y, Wang Z, McCarter JP, et al. The transcriptomes of the cattle parasitic nematode *Ostertagia ostartagi*. Vet Parasitol 2009;162:89–99.
[20] Cantacessi C, Mitreva M, Jex AR, Young ND, Campbell BE, Hall RS, et al. Massively parallel sequencing and analysis of the *Necator americanus* transcriptome. PLoS Negl Trop Dis 2010;4:e684.
[21] Cantacessi C, Mitreva M, Campbell BE, Hall RS, Young ND, Jex AR, et al. First transcriptomic analysis of the economically important parasitic nematode, *Trichostrongylus colubriformis*, using a next-generation sequencing approach. Infect Genet Evol 2010;10:1199–207.
[22] Yatsuda AP, Krijgsveld J, Cornelissen AWCA, Heck AJ, De Vries E. Comprehensive analysis of the secreted proteins of the parasite *Haemonchus contortus* reveals extensive sequence variation and differential immune recognition. J Biol Chem 2003;278:16941–51.
[23] Craig H, Wastling JM, Knox DP. A preliminary proteomic survey of the in vitro excretory/secretory products of fourth-stage larval and adult *Teladorsagia circumcincta*. Parasitology 2006;132:535–43.
[24] Morgan C, LaCourse EJ, Rushbrook BJ, Greetham D, Hamilton JV, Barrett J, et al. Plasticity demonstrated in the proteome of a parasitic nematode within the intestine of different host strains. Proteomics 2006;6:4633–45.
[25] Hewitson JP, Harcus YM, Curwen RS, Dowle AA, Atmadja AK, Ashton PD, et al. The secretome of the filarial parasite, *Brugia malayi*: proteomic profile of adult excretory–secretory products. Mol Biochem Parasitol 2008;160:8–21.
[26] Moreno Y, Geary TG. Stage- and gender-specific proteomic analysis of *Brugia malayi* excretory–secretory products. PLoS Negl Trop Dis 2008;2:e326.
[27] Bennuru S, Semnani R, Meng Z, Ribeiro JM, Veenstra TD, Nutman TB. *Brugia malayi* excreted/secreted proteins at the host/parasite interface: stage- and gender-specific proteomic profiling. PLoS Negl Trop Dis 2009;3:e410.
[28] Mulvenna J, Hamilton B, Nagaraj SH, Smyth D, Loukas A, Gorman JJ. Proteomics analysis of the excretory/secretory component of the blood-feeding stage of the hookworm, *Ancylostoma caninum*. Mol Cell Proteomics 2009;8:109–21.
[29] Smith SK, Nisbet AJ, Meikle LI, Inglis NF, Sales J, Beynon RJ, et al. Proteomic analysis of excretory/secretory products released by *Teladorsagia circumcincta* larvae early post-infection. Parasite Immunol 2009;31:10–9.
[30] Nisbet AJ, Smith SK, Armstrong S, Meikle LI, Wildblood LA, Beynon RJ, et al. *Teladorsagia circumcincta:* activation-associated secreted proteins in excretory/secretory products of fourth stage larvae are targets of early IgA responses in infected sheep. Exp Parasitol 2010;125:329–37.
[31] Murray J, Gregory WF, Gomez-Escobar N, Atmadja AK, Maizels RM. Expression and immune recognition of *Brugia malayi* VAL-1, a homologue of vespid venom allergens and *Ancylostoma* secreted proteins. Mol Biochem Parasitol 2001;118:89–96.
[32] Asojo OA, Goud GN, Dhar K, Loukas A, Zhan B, Deumic V, et al. X-ray structure of Na-ASP-2, a pathogenesis related-1 protein from the nematode parasite, *Necator americanus*, and a vaccine antigen for human hookworm infection. J Mol Biol 2005;346:801–14.
[33] Hawdon JM, Jones BF, Hoffman DR, Hotez PJ. Cloning and characterization of *Ancylostoma*-secreted protein. A novel protein associated with the transition to parasitism by infective hookworm larvae. J Biol Chem 1996;271:6672–8.
[34] Hotez PJ, Zhan B, Bethony JM, Loukas A, Williamson A, Goud GN, et al. Progress in the development of a recombinant vaccine for human hookworm disease: the Human Hookworm Vaccine Initiative. Int J Parasitol 2003;33:1245–58.
[35] Monroy FG, Enriquez FJ. *Heligmosomoides polygyrus*: a model for chronic gastrointestinal helminthiasis. Parasitol Today 1992;8:49–54.
[36] Finkelman FD, Shea-Donohue T, Morris SC, Gildea L, Strait R, Madden KB, et al. Interleukin-4- and interleukin-13-mediated host protection against intestinal nematode parasites. Immunol Rev 2004;201:139–55.
[37] Anthony RM, Rutitzky LI, Urban Jr JF, Stadecker MJ, Gause WC. Protective immune mechanisms in helminth infection. Nat Rev Immunol 2007;7:975–87.
[38] McCoy KD, Stoel M, Stettler R, Merky P, Fink K, Senn BM, et al. Polyclonal and specific antibodies mediate protective immunity against enteric helminth infection. Cell Host Microbe 2008;4: 362–73.
[39] Herbert DR, Yang J-Q, Hogan SP, Groschwitz K, Khodoun MV, Munitz A, et al. Intestinal epithelial cell secretion of RELM-b protects against gastrointestinal worm infection. J Exp Med 2009;206:2947–57.
[40] Wojciechowski W, Harris DP, Sprague F, Mousseau B, Makris M, Kusser K, et al. Cytokine-producing effector B cells regulate type 2 immunity to *H. polygyrus*. Immunity 2009;30: 421–33.
[41] Bashir ME, Andersen P, Fuss IJ, Shi HN, Nagler-Anderson C. An enteric helminth infection protects against an allergic response to dietary antigen. J Immunol 2002;169:3284–92.

[42] Wilson MS, Taylor M, Balic A, Finney CAM, Lamb JR, Maizels RM. Suppression of allergic airway inflammation by helminth-induced regulatory T cells. J Exp Med 2005;202: 1199–212.
[43] Saunders KA, Raine T, Cooke A, Lawrence CE. Inhibition of autoimmune type 1 diabetes by gastrointestinal helminth infection. Infect Immun 2006;75:397–407.
[44] Liu Q, Sundar K, Mishra PK, Mousavi G, Liu Z, Gaydo A, et al. Helminth infection can reduce insulitis and type 1 diabetes through CD25- and IL-10-independent mechanisms. Infect Immun 2009;77:5347–58.
[45] Khan WI, Blennerhasset PA, Varghese AK, Chowdhury SK, Omsted P, Deng Y, et al. Intestinal nematode infection ameliorates experimental colitis in mice. Infect Immun 2002;70:5931–7.
[46] Elliott DE, Setiawan T, Metwali A, Blum A, Urban Jr JF, Weinstock JV. *Heligmosomoides polygyrus* inhibits established colitis in IL-10-deficient mice. Eur J Immunol 2004;34:2690–8.
[47] Sutton TL, Zhao A, Madden KB, Elfrey JE, Tuft BA, Sullivan CA, et al. Anti-inflammatory mechanisms of enteric *Heligmosomoides polygyrus* infection against trinitrobenzene sulfonic acid-induced colitis in a murine model. Infect Immun 2008;76:4772–82.
[48] Hang L, Setiawan T, Blum AM, Urban J, Stoyanoff K, Arihiro S, et al. *Heligmosomoides polygyrus* infection can inhibit colitis through direct interaction with innate immunity. J Immunol 2010;185:3184–9.
[49] Metwali A, Setiawan T, Blum AM, Urban J, Elliott DE, Hang L, et al. Induction of $CD8^+$ regulatory T cells in the intestine by *Heligmosomoides polygyrus* infection. Am J Physiol Gastrointest Liver Physiol 2006;291:G253–9.
[50] Finney CAM, Taylor MD, Wilson MS, Maizels RM. Expansion and activation of $CD4^+CD25+$ regulatory T cells in *Heligmosomoides polygyrus* infection. Eur J Immunol 2007;37:1874–86.
[51] Rausch S, Huehn J, Kirchhoff D, Rzepecka J, Schnoeller C, Pillai S, et al. Functional analysis of effector and regulatory T cells in a parasitic nematode infection. Infect Immun 2008;76:1908–19.
[52] Wilson MS, Taylor MD, O'Gorman MT, Balic A, Barr TA, Filbey K, et al. Helminth-induced CD19+CD23hi B cells modulate experimental allergic and autoimmune inflammation. Eur J Immunol 2010;40:1682–96.
[53] Grainger JR, Smith KA, Hewitson JP, McSorley HJ, Harcus Y, Filbey KJ, et al. Helminth secretions induce de novo T cell Foxp3 expression and regulatory function through the TGF-β pathway. J Exp Med 2010;207:2331–41.
[54] Segura M, Su Z, Piccirillo C, Stevenson MM. Impairment of dendritic cell function by excretory–secretory products: a potential mechanism for nematode-induced immunosuppression. Eur J Immunol 2007;37:1887–904.
[55] Belkaid Y, Liefenfeld O, Maizels RM. Induction and control of regulatory T cells in the GI tract: consequences for local and peripheral immune responses. Clin Exp Immunol 2009;160: 35–41.
[56] Hoselton S, Piche L, Gustad T, Robinson M. Production of a recombinant version of a *Heligmosomoides polygyrus* antigen that is preferentially recognized by resistant mouse strains. Parasite Immunol 2002;24:429–35.
[57] Rzepecka J, Lucius R, Doligalska M, Beck S, Rausch S, Hartmann S. Screening for immunomodulatory proteins of the intestinal parasitic nematode *Heligmosomoides polygyrus*. Parasite Immunol 2006;28:463–72.
[58] Rzepecka J, Rausch S, Klotz C, Schnöller C, Kornprobst T, Hagen J, et al. Calreticulin from the intestinal nematode *Heligmosomoides polygyrus* is a Th2-skewing protein and interacts with murine scavenger receptor-A. Mol Immunol 2008;46:1109–19.
[59] Harcus Y, Nicoll G, Murray J, Filbey K, Gomez-Escobar N, Maizels RM. C-type lectins from the nematode parasites *Heligmosomoides polygyrus* and *Nippostrongylus brasiliensis*. Parasitol Int 2009;58:461–70.
[60] McSorley HJ, Grainger JR, Harcus YM, Murray J, Nisbet A, Knox DP, et al. *daf-7*-related TGF-β homologues from trichostrongyloid nematodes show contrasting life cycle expression patterns. Parasitology 2010;137:159–71.
[61] Bendtsen JD, Nielsen H, von Heijne G, Brunak S. Improved prediction of signal peptides: SignalP 3.0. J Mol Biol 2004;340: 783–95.
[62] Pritchard DI, Maizels RM, Behnke JM, Appleby P. Stage-specific antigens of *Nematospiroides dubius*. Immunology 1984;53: 325–35.
[63] Maizels RM, Gregory WF, Kwan-Lim G-E, Selkirk ME. Filarial surface antigens: the major 29,000 mol.wt. glycoprotein and a novel 17,000–200,000 mol.wt. complex from adult *Brugia malayi* parasites. Mol Biochem Parasitol 1989;32:213–27.
[64] Hewitson JP, Filbey KJ, Grainger JR, Dowle AA, Pearson M, Murray J, Harcus Y, Maizels RM. *Heligmosomoides polygyrus* elicits a dominant nonprotective antibody response directed at restricted glycan and peptide epitopes. Manuscript submitted for publication 2011.
[65] Zhan B, Liu Y, Badamchian M, Williamson A, Feng J, Loukas A, et al. Molecular characterisation of the *Ancylostoma*-secreted protein family from the adult stage of *Ancylostoma caninum*. Int J Parasitol 2003;33:897–907.
[66] Qiang S, Bin Z, Shu-hua X, Zheng F, Hotez P, Hawdon JM. Variation between ASP-1 molecules from *Ancylostoma caninum* in China and the United States. J Parasitol 2000;86:181–5.
[67] Yatsuda AP, Eysker M, Vieria-Bressan MCR, De Vries E. A family of activation associated secreted protein (ASP) homologues of *Cooperia punctata*. Res Vet Sci 2002;73:297–306.
[68] Lawrence CE, Pritchard DI. Differential secretion of acetylcholinesterase and proteases during the development of *Heligmosomoides polygyrus*. Int J Parasitol 1993;23:309–14.
[69] Selkirk ME, Lazari O, Hussein AS, Matthews JB. Nematode acetylcholinesterases are encoded by multiple genes and perform non-overlapping functions. Chem Biol Interact 2005;157–158:263–8.
[70] Blackburn CC, Selkirk ME. Characterisation of the secretory acetylcholinesterases from adult *Nippostrongylus brasiliensis*. Mol Biochem Parasitol 1992;53:79–88.
[71] Grigg ME, Tang L, Hussein AS, Selkirk ME. Purification and properties of monomeric (G_1) forms of acetylcholinesterase secreted by *Nippostrongylus brasiliensis*. Mol Biochem Parasitol 1997;90:513–24.
[72] Hussein AS, Chacón MR, Smith AM, Tosado-Acevedo R, Selkirk ME. Cloning, expression, and properties of a nonneuronal secreted acetylcholinesterase from the parasitic nematode *Nippostrongylus brasiliensis*. J Biol Chem 1999;274:9312–9.
[73] Hussein A, Harel M, Selkirk M. A distinct family of acetylcholinesterases is secreted by *Nippostrongylus brasiliensis*. Mol Biochem Parasitol 2002;123:125–34.
[74] Nisbet AJ, Zarlenga DS, Knox DP, Meikle LI, Wildblood LA, Matthews JB. A calcium-activated apyrase from *Teladorsagia circumcincta*: an excretory/secretory antigen capable of modulating host immune responses? Parasite Immunol 2011.
[75] Zarlenga DS, Nisbet AJ, Gasbarre LC, Garrett WM. A calcium-activated nucleotidase secreted from *Ostertagia ostertagi* 4th-stage larvae is a member of the novel salivary apyrases present in blood-feeding arthropods. Parasitology 2011;138:333–43.
[76] Kennedy MW, Garside LH, Goodrick LE, McDermott L, Brass A, Price NC, et al. The Ov20 protein of the parasitic nematode *Onchocerca volvulus*. A structurally novel class of small helix-rich retinol-binding proteins. J Biol Chem 1997;272: 29442–8.

[77] Garofolo A, Kläger SL, Rowlinson M-C, Nirmalan N, Klion A, Allen JE, et al. The FAR proteins of filarial nematodes: secretion, glycosylation and lipid binding characteristics. Mol Biochem Parasitol 2002;122:161–70.
[78] Basavaraju S, Zhan B, Kennedy MW, Liu Y, Hawdon J, Hotez PJ. Ac-FAR-1, a 20 kDa fatty acid- and retinol-binding protein secreted by adult *Ancylostoma caninum* hookworms: gene transcription pattern, ligand binding properties and structural characterisation. Mol Biochem Parasitol 2003;126: 63–71.
[79] Kennedy MW, Brass A, McCruden AB, Price NC, Kelly SM, Cooper A. The ABA-1 allergen of the parasitic nematode *Ascaris suum:* fatty acid and retinoid binding function and structural characterization. Biochemistry 1995;34:6700–10.
[80] Kennedy MW, Britton C, Price NC, Kelly SM, Cooper A. The DvA-1 polyprotein of the parasitic nematode Dictyocaulus viviparus. A small helix-rich lipid-binding protein. Journal of Biological Chemistry 1995;270:19277–81.
[81] Eneqvist T, Lundberg E, Nilsson L, Abagyan R, Sauer-Eriksson AE. The transthyretin-related protein family. Eur J Biochem 2003;270:518–32.
[82] Hennebry SC. Evolutionary changes to transthyretin: structure and function of a transthyretin-like ancestral protein. FEBS J 2009;276:5367–79.
[83] Wang X, Li W, Zhao D, Liu B, Shi Y, Chen B, et al. *Caenorhabditis elegans* transthyretin-like protein TTR-52 mediates recognition of apoptotic cells by the CED-1 phagocyte receptor. Nat Cell Biol 2010;12:655–64.
[84] Brinkworth RI, Prociv P, Loukas A, Brindley PJ. Hemoglobin-degrading, aspartic proteases of blood-feeding parasites: substrate specificity revealed by homology models. J Biol Chem 2001;276:38844–51.
[85] Pearson MS, Bethony JM, Pickering DA, de Oliveira LM, Jariwala A, Santiago H, et al. An enzymatically inactivated hemoglobinase from *Necator americanus* induces neutralizing antibodies against multiple hookworm species and protects dogs against heterologous hookworm infection. FASEB J 2009;23:3007–19.
[86] Hawdon JM, Jones BF, Perregaux MA, Hotez PJ. *Ancylostoma caninum*: metalloprotease release coincides with activation of infective larvae *in vitro*. Exp Parasitol 1995;80:205–11.
[87] Williamson AL, Lustigman S, Oksov Y, Deumic V, Plieskatt J, Mendez S, et al. *Ancylostoma caninum* MTP-1, an astacin-like metalloprotease secreted by infective hookworm larvae, is involved in tissue migration. Infect Immun 2006;74:961–7.
[88] Yatsuda AP, Bakker N, Krijgsveld J, Knox DP, Heck AJ, de Vries E. Identification of secreted cysteine proteases from the parasitic nematode *Haemonchus contortus* detected by biotinylated inhibitors. Infect Immun 2006;74:1989–93.
[89] Jasmer DP, Mitreva MD, McCarter JP. mRNA sequences for *Haemonchus contortus* intestinal cathepsin B-like cysteine proteases display an extreme in abundance and diversity compared with other adult mammalian parasitic nematodes. Mol Biochem Parasitol 2004;137:297–305.
[90] Hartmann S, Lucius R. Modulation of host immune responses by nematode cystatins. Int J Parasitol 2003;33:1291–302.
[91] Klotz C, Ziegler T, Figueiredo AS, Rausch S, Hepworth MR, Obsivac N, et al. A helminth immunomodulator exploits host signaling events to regulate cytokine production in macrophages. PLoS Pathog 2011;7:e1001248.
[92] Dainichi T, Maekawa Y, Ishii K, Zhang T, Nashed BF, Sakai T, et al. Nippocystatin, a cysteine protease inhibitor from *Nippostrongylus brasiliensis*, inhibits antigen processing and modulates antigen-specific immune response. Infect Immun 2001;69:7380–6.
[93] Murray J, Manoury B, Balic A, Watts C, Maizels RM. *Bm*-CPI-2, a cystatin from *Brugia malayi* nematode parasites, differs from *C. elegans* cystatins in a specific site mediating inhibition of the antigen-processing enzyme AEP. Mol Biochem Parasitol 2005;139:197–203.
[94] Gonzalez S, Flo M, Margenat M, Duran R, Gonzalez-Sapienza G, Grana M, et al. A family of diverse Kunitz inhibitors from *Echinococcus granulosus* potentially involved in host–parasite cross-talk. PLoS One 2009;4:e7009.
[95] Milstone AM, Harrison LM, Bungiro RD, Kuzmic P, Cappello M. A broad spectrum Kunitz type serine protease inhibitor secreted by the hookworm *Ancylostoma ceylanicum*. J Biol Chem 2000;275:29391–9.
[96] Chu D, Bungiro RD, Ibanez M, Harrison LM, Campodonico E, Jones BF, et al. Molecular characterization of *Ancylostoma ceylanicum* Kunitz-type serine protease inhibitor: evidence for a role in hookworm-associated growth delay. Infect Immun 2004;72:2214–21.
[97] Page AP, McCormack G, Birnie AJ. Biosynthesis and enzymology of the *Caenorhabditis elegans* cuticle: identification and characterization of a novel serine protease inhibitor. Int J Parasitol 2006;36:681–9.
[98] Zang XX, Yazdanbakhsh M, Kiang H, Kanost MR, Maizels RM. A novel serpin expressed by the blood-borne microfilariae of the parasitic nematode *Brugia malayi* inhibits human neutrophil serine proteinases. Blood 1999;94:1418–28.
[99] Zang XX, Atmadja AK, Gray P, Allen JE, Gray CA, Lawrence RA, et al. The serpin secreted by *Brugia malayi* microfilariae, Bm-SPN-2, elicits strong, but short-lived, immune responses in mice and humans. J Immunol 2000;165:5161–9.
[100] Saverwyns H, Visser A, Nisbet AJ, Peelaers I, Gevaert K, Vercruysse J, et al. Identification and characterization of a novel specific secreted protein family for selected members of the subfamily Ostertagiinae (Nematoda). Parasitology 2008;135:63–70.
[101] Johnston MJG, Macdonald JA, McKay DM. Parasitic helminths: a pharmacopeia of anti-inflammatory molecules. Parasitology 2009;136:125–47.
[102] Kwan-Lim G-E, Gregory WF, Selkirk ME, Partono F, Maizels RM. Secreted antigens of filarial nematodes: survey and characterisation of in vitro excretory/secretory (E/S) products of adult *Brugia malayi* filarial parasites. Parasite Immunol 1989;11: 629–54.
[103] Page AP, Hamilton AJ, Maizels RM. *Toxocara canis:* monoclonal antibodies to carbohydrate epitopes of secreted (TES) antigens localize to different secretion-related structures in infective larvae. Exp Parasitol 1992;75: 56–71.
[104] Page AP, Rudin W, Fluri E, Blaxter ML, Maizels RM. *Toxocara canis*: a labile antigenic coat overlying the epicuticle of infective larvae. Exp Parasitol 1992;75:72–86.
[105] Wu Y, Egerton G, Pappins DJC, Harrison RA, Wilkinson M, Underwood A, et al. The secreted larval acidic proteins (SLAPs) of *Onchocerca* spp. are encoded by orthologues of the *alt* gene family of *Brugia malayi* and have host protective potential. Mol Biochem Parasitol 2004;134:213–24.
[106] Selkirk ME, Gregory WF, Yazdanbakhsh M, Jenkins RE, Maizels RM. Cuticular localisation and turnover of the major surface glycoprotein (gp29) of adult *Brugia malayi*. Mol Biochem Parasitol 1990;42:31–44.
[107] Gibbs GM, Roelants K, O'Bryan MK. The CAP superfamily: cysteine-rich secretory proteins, antigen 5, and pathogenesis-related 1 proteins—roles in reproduction, cancer, and immune defense. Endocr Rev 2008;29:865–97.
[108] Cantacessi C, Campbell BE, Visser A, Geldhof P, Nolan MJ, Nisbet AJ, et al. A portrait of the "SCP/TAPS" proteins of eukaryotes — developing a framework for fundamental research and biotechnological outcomes. Biotechnol Adv 2009;27:376–88.
[109] Bethony J, Loukas A, Smout M, Brooker S, Mendez S, Plieskatt J, et al. Antibodies against a secreted protein from hookworm larvae reduce the intensity of hookworm infection in

humans and vaccinated laboratory animals. FASEB J 2005;19: 1743–5.
[110] Morita K, Flemming AJ, Sugihara Y, Mochii M, Suzuki Y, Yoshida S, et al. A *Caenorhabditis elegans* TGF-beta, DBL-1, controls the expression of LON-1, a PR-related protein, that regulates polyploidization and body length. EMBO J 2002;21: 1063–73.
[111] Valenzuela JG, Belkaid Y, Rowton E, Ribeiro JM. The salivary apyrase of the blood-sucking sand fly *Phlebotomus papatasi* belongs to the novel Cimex family of apyrases. J Exp Biol 2001;204:229–37.
[112] Gounaris K, Selkirk ME. Parasite nucleotide-metabolizing enzymes and host purinergic signalling. Trends Parasitol 2005;21:17–21.
[113] Atarashi K, Nishimura J, Shima T, Umesaki Y, Yamamoto M, Onoue M, et al. ATP drives lamina propria T(H)17 cell differentiation. Nature 2008;455:808–12.
[114] Idzko M, Hammad H, van Nimwegen M, Kool M, Willart MA, Muskens F, et al. Extracellular ATP triggers and maintains asthmatic airway inflammation by activating dendritic cells. Nat Med 2007;13:913–9.
[115] Fletcher JM, Lonergan R, Costelloe L, Kinsella K, Moran B, O'Farrelly C, et al. CD39+Foxp3+ regulatory T Cells suppress pathogenic Th17 cells and are impaired in multiple sclerosis. J Immunol 2009;183:7602–10.
[116] Uccelletti D, Pascoli A, Farina F, Alberti A, Mancini P, Hirschberg CB, et al. APY-1, a novel *Caenorhabditis elegans* apyrase involved in unfolded protein response signalling and stress responses. Mol Biol Cell 2008;19: 1337–45.
[117] Lendner M, Doligalska M, Lucius R, Hartmann S. Attempts to establish RNA interference in the parasitic nematode *Heligmosomoides polygyrus*. Mol Biochem Parasitol 2008;161: 21–31.
[118] Samarasinghe B, Knox DP, Britton C. Factors affecting susceptibility to RNA interference in *Haemonchus contortus* and in vivo silencing of an H11 aminopeptidase gene. Int J Parasitol 2011;41:51–9.

Heligmosomoides polygyrus Elicits a Dominant Nonprotective Antibody Response Directed against Restricted Glycan and Peptide Epitopes

James P. Hewitson, Kara J. Filbey, John R. Grainger, Adam A. Dowle, Mark Pearson, Janice Murray, Yvonne Harcus and Rick M. Maizels

J Immunol 2011; 187:4764-4777; Prepublished online 30 September 2011;
doi: 10.4049/jimmunol.1004140
http://www.jimmunol.org/content/187/9/4764

The Journal of Immunology is published twice each month by
The American Association of Immunologists, Inc.,
9650 Rockville Pike, Bethesda, MD 20814-3994.

Print ISSN: 0022-1767 Online ISSN: 1550-6606.

Heligmosomoides polygyrus Elicits a Dominant Nonprotective Antibody Response Directed against Restricted Glycan and Peptide Epitopes

James P. Hewitson,*[,1] Kara J. Filbey,*[,1] John R. Grainger,*[,2] Adam A. Dowle,[†] Mark Pearson,* Janice Murray,* Yvonne Harcus,* and Rick M. Maizels*

Heligmosomoides polygyrus **is a widely used gastrointestinal helminth model of long-term chronic infection in mice, which has not been well-characterized at the antigenic level. We now identify the major targets of the murine primary Ab response as a subset of the secreted products in *H. polygyrus* excretory–secretory (HES) Ag. An immunodominant epitope is an O-linked glycan (named glycan A) carried on three highly expressed HES glycoproteins (venom allergen *Ancylostoma*-secreted protein-like [VAL]-1, -2, and -5), which stimulates only IgM Abs, is exposed on the adult worm surface, and is poorly represented in somatic parasite extracts. A second carbohydrate epitope (glycan B), present on both a non-protein high molecular mass component and a 65-kDa molecule, is widely distributed in adult somatic tissues. Whereas the high molecular mass component and 65-kDa molecules bear phosphorylcholine, the glycan B epitope itself is not phosphorylcholine. Class-switched IgG1 Abs are found to glycan B, but the dominant primary IgG1 response is to the polypeptides of VAL proteins, including also VAL-3 and VAL-4. Secondary Ab responses include the same specificities while also recognizing VAL-7. Although vaccination with HES conferred complete protection against challenge *H. polygyrus* infection, mAbs raised against each of the glycan epitopes and against VAL-1, VAL-2, and VAL-4 proteins were unable to do so, even though these specificities (with the exception of VAL-2) are also secreted by tissue-phase L4 larvae. The primary immune response in susceptible mice is, therefore, dominated by nonprotective Abs against a small subset of antigenic epitopes, raising the possibility that these act as decoy specificities that generate ineffective humoral immunity.** ***The Journal of Immunology*****, 2011, 187: 4764–4777.**

Heligmosomoides polygyrus is a widely used experimental mouse model for the highly prevalent human and animal gastrointestinal helminth infections (1, 2). This system has provided major new findings in parasite immunology (3, 4), immune regulation (5, 6), nutrition (7), and ecology (8), and yet little information is available on the specific parasite Ags to which the host immune system is exposed. In this study, we set out to identify the molecular targets of murine humoral Abs, to define individual *H. polygyrus* Ags, and to investigate the role of major Ab specificities in the host–parasite relationship.

Among the interesting facets of *H. polygyrus* is its ability to establish a chronic infection in most strains of laboratory mice, with the genetic background influencing the rate of expulsion rather than susceptibility per se (9–11). Genetically resistant mice mount a more rapid serum Ab response measured against adult worm somatic extract (12) or excretory–secretory (ES) Ags from cultured adult parasites (13, 14), and immunity to reinfection is compromised in B cell-deficient mice (4, 15–17). Early investigations had reported that passive transfer of serum from infected mice can confer a degree of immunity to *H. polygyrus* both in terms of worm number and in fecundity (18); this effect was associated with IgG1 isotype Abs (19, 20). More recently, IgG1 serum Abs have been demonstrated to reduce the fecundity and viability of adult worms and shown to require affinity maturation to confer any resistant effect (15).

As has been recently pointed out (21), in current nematode model systems, few serologically important Ags have yet been identified. Previous studies have relied on either crude whole-worm homogenates or collected secreted products as a more restricted but nevertheless complex antigenic set. Therefore, we decided to analyze the humoral Ab response to *H. polygyrus* in terms of specific Igs, to define the molecular targets of parasite-specific Abs, and to test whether these played any protective role against the infection in vivo. We tested Ab reactivities both to crude parasite antigenic extracts and also to preparations collected from in vitro culture of adult worms, termed "excretory–secretory" (ES) Ags, which are strongly implicated in immunomodulation of the host (6, 22). We report in this article that several major constituents are homologs of venom allergen *Ancylostoma*-

*Institute of Immunology and Infection Research, University of Edinburgh, Edinburgh EH9 3JT, United Kingdom; and [†]Technology Facility, Department of Biology, University of York, York YO10 5YW, United Kingdom

[1]J.P.H. and K.J.F. are joint first authors.

[2]Current address: Mucosal Immunology Unit, Laboratory of Parasitic Diseases, National Institute of Allergy and Infectious Diseases, National Institutes for Health, Bethesda, MD.

Received for publication December 21, 2010. Accepted for publication August 24, 2011.

This work was supported by a Wellcome Trust Programme grant and a Wellcome Trust Ph.D. studentship (to J.R.G.). K.J.F. is supported by a Medical Research Council Collaborative Awards in Science and Engineering studentship through UCB Celltech.

Address correspondence and reprint requests to Dr. Rick M. Maizels, Institute of Immunology and Infection Research, University of Edinburgh, West Mains Road, Edinburgh EH9 3JT, United Kingdom. E-mail address: rick.maizels@ed.ac.uk

The online version of this article contains supplemental material.

Abbreviations used in this article: ASP, *Ancylostoma*-secreted protein; ES, excretory–secretory; ESI, electrospray ionization; HES, *Heligmosomoides polygyrus* adult excretory–secretory products; HEx, *Heligmosomoides polygyrus* adult somatic extract; HM-65, high molecular mass 65 kDa antigenic complex; IP, immunoprecipitation; LC, liquid chromatography; MLN, mesenteric lymph node; MS/MS, tandem mass spectrometry; PC, phosphorylcholine; PNGase, peptide:N-glycanase; TFH, T follicular helper cell; TFMS, trifluoromethanesulfonic acid; VAL, venom allergen *Ancylostoma*-secreted protein-like.

secreted protein (ASP)-like (VAL) Ags related to the vaccine candidates of human and canine hookworms (23, 24). However, the response to infection is dominated by anti-glycan specificities, and the murine Ab profile is highly restricted with respect to the range of Ags recognized.

Materials and Methods

Parasites, Ags, and mice

The original stock of *H. polygyrus bakeri* used in these studies was kindly supplied to us by Prof. J.M. Behnke (University of Nottingham, Nottingham, U.K.). Parasites, *H. polygyrus* ES (HES) Ag and adult worm somatic extract (HEx) were produced as described previously (6, 25, 26). Day 5 fourth-stage larvae were collected from the intestinal wall of infected mice and ES collected over a 3-d culture period in the same manner as adult HES. Female C57BL/6 and BALB/c mice (6–10 wk old) were bred in-house, and animal studies were performed under U.K. Home Office License. Mice were infected with 200 *H. polygyrus* L3 by oral gavage, and fecal egg counts and adult worm burdens were determined by standard procedures (2). For secondary infection, mice were treated orally with pyrantel embonate (27) in the form of 2.5 mg Strongid P paste in 0.2 ml water on days 28 and 29 postprimary infection. Drug-treated mice were rechallenged with 200 L3 by gavage 2 wk later. Where indicated, HES was heat denatured by incubating at 95˚C for 20 min (6).

One-dimensional and two-dimensional gel electrophoresis and Western blotting

HES and HEx (1–10 μg) were separated, silver stained, or blotted as described previously (28). Blots were blocked in 2% BSA–TBS with 0.05% Tween 20 (TBST) for 2 h at room temperature, before being probed with sera (1/500 dilution) or mAbs (2 μg/ml) at 4˚C overnight. Following extensive washing in TBST, blots were incubated with HRP-conjugated secondary Abs (anti-mouse Ig 1/2000, Dako P0460, DakoCytomation; anti-mouse IgM 1/1000, Southern Biotech 1020-05, and anti-mouse IgG1, 1/2000 Southern Biotech 1070-05; Southern Biotechnology Associates) for 1 h at 37˚C, washed in TBST, and then developed as described previously (28). Alternatively, IgA blots were incubated with biotinylated anti-mouse IgA (1/500, M31115; Invitrogen), followed by HRP–streptavidin (1/2000; Sigma-Aldrich), and developed as above. Mouse IgM mAb Bp-1 (29) was used for anti-phosphorylcholine (PC) blots at 1/1000 dilution and detected with anti-mouse Ig as above.

ELISA

HES and HEx (1 μg/ml) were coated on Immunoplates (Nunc) in 0.06 M carbonate buffer overnight (4˚C), blocked with block solution (2% BSA–TBST) for 2 h (37˚C), and then incubated with doubling dilutions of sera (in block solution) for 2 h (37˚C). For comparison of HES and L4 ES, each were used to coat plates at a range of dilutions. Worm-specific Ab titers were detected using the secondary reagents described above and developed with ABTS (Insight Biotech). Titer was determined as the reciprocal dilution at which the sample dropped below background levels. For anti-PC ELISA, plates were coated with 1 μg/ml PC-conjugated BSA (30), serum was used at a 1/500 dilution and mAb at 5 μg/ml. Anti-*H. polygyrus* mAbs were used at 5 μg/ml for all ELISAs, unless stated. Goat anti-rat Ig (1/2000, Dako P0450; DakoCytomation) was used as a secondary for experiments with rat sera.

mAb and polyclonal Ab production

For mAbs, spleens and mesenteric lymph nodes (MLN) were recovered from C57BL/6 mice at day 28 postinfection and fused with SP2 cells. Fused cells were cultured for 12–14 d in HAT selection media (RPMI 1640

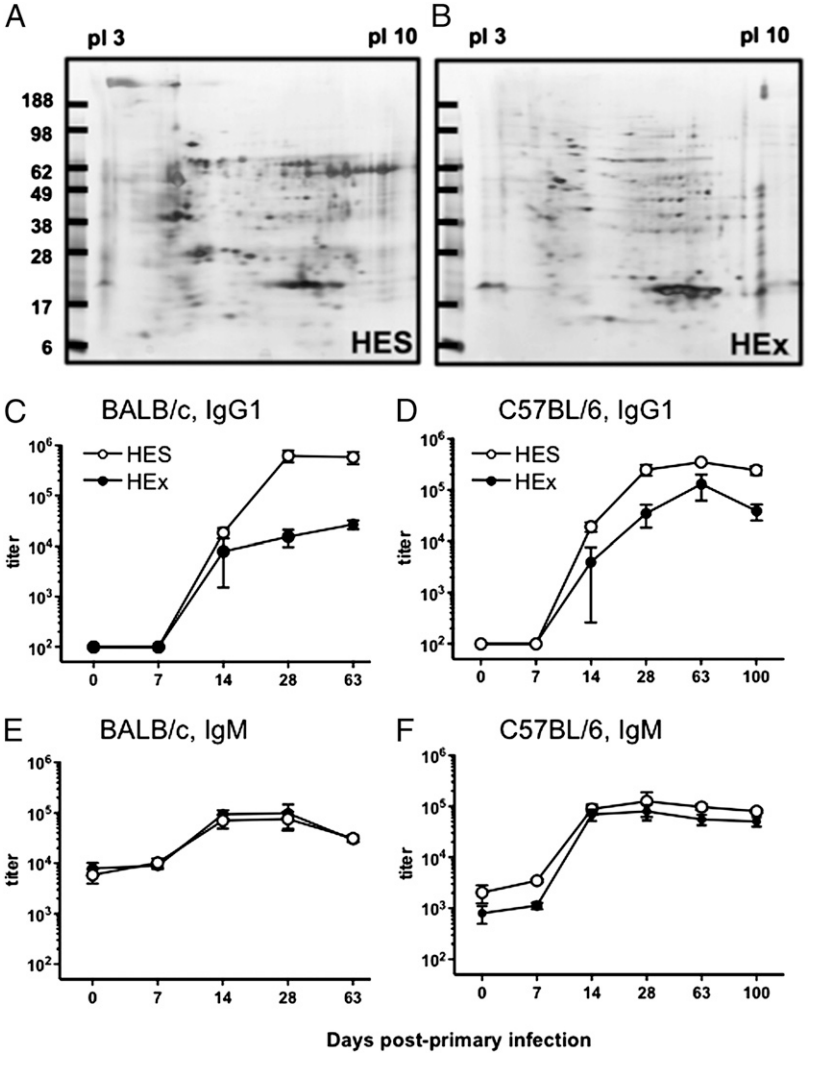

FIGURE 1. The predominant serological Ags of *H. polygyrus* are in HES rather than somatic extract. *A* and *B*, Two-dimensional silver-stained gels of 10 μg HES (*A*) and Hex (*B*). Molecular mass markers (in kDa) are indicated on the left. *C* and *D*, Anti-HES (open symbols) and HEx (solid symbols) IgG1 serum Ab titres from BALB/c (*C*) and C57BL/6 (*D*) mice at various time points following primary infection. *E* and *F*, Anti-HES and HEx IgM serum Ab titres in the same BALB/c (*E*) and C57BL/6 (*F*) mice. Each point represents the mean and SEM of data from five individual mice separately assayed. Data are representative of two independent experiments.

medium supplemented with 20% FCS [Hyclone], 100 U/ml penicillin, 100 μg/ml streptomycin, 2 mM L-glutamine [all Life Technologies], HAT [100 μM hypoxanthine, 0.4 μM aminopterin, and 16 μM thymidine] and OPI [1 mM oxaloacetate, 0.45 mM pyruvate, and 0.2 U/ml insulin; all Sigma-Aldrich]). Plates were ELISA screened for the production of anti-HES Abs as above, and positive wells were cloned by two to three rounds of limiting dilution. Cells were then adapted into standard complete RPMI 1640 medium (RPMI 1640 medium supplemented with 10% FCS and the above concentrations of penicillin, streptomycin, and L-glutamine) and grown in bulk cultures in Vectra Cell Bioreactors (Bio-Vectra) to produce mAb. Ab isotypes were determined either with a mouse Ab isotype kit (Isostrip; Roche) or the anti-mouse Ig secondary Ab described above. Abs were purified using an AKTA prime fast protein liquid chromatography (LC) with a HiTrap protein G HP (IgG1 mAb) or HiTrap IgM purification (IgM and IgA) column, according to the manufacturer's instructions, and then dialyzed extensively into PBS. For the rat polyclonal Abs, rats were immunized with 25 μg HES or recombinant *H. polygyrus* calreticulin (AM296015 (31), produced in *Escherichia coli*) in alum adjuvant i.p., then boosted with 10 μg Ag on days 28 and 35, before serum collection on day 42. The mouse IgG1 myeloma MOPC 31C from American Type Culture Collection was used as an isotype control. A hybridoma-producing mouse anti-DNP IgM control was produced as above from mice immunized with 50 μg DNP-conjugated keyhole limpet hemocyanin in alum adjuvant i.p. and then boosted on days 12 and 13 with 1 μg DNP–keyhole limpet hemocyanin in PBS i.v. before spleen harvest on day 14. Screening was performed using DNP–OVA and anti-mouse IgM secondary Ab as above. Hybridomas were also produced from mice immunized with 25 μg HES in IFA (Sigma-Aldrich) i.p. then boosted on days 48 and 49 with 1 μg HES in PBS i.v. before spleen harvest and fusion on day 50.

Immunoprecipitation

HES was labeled with biotin (~40 μg biotin reagent/100 μg HES) using EZ-link Sulfo-NHS Biotinylation kit (Pierce) for 2 h on ice and then dialyzed overnight into PBS. Biotinylated HES was then precleared with protein G-agarose beads (16-266; Millipore) in the presence of MOPC 31C IgG1 isotype control for 30 min at room temperature. Unbound HES (2 μg) was then incubated with 2 μg various anti-HES IgG1 mAb, MOPC IgG1 control, or 5 μl C57BL/6 day 28 primary or day 14 secondary infection sera, in nondenaturing immunoprecipitation (IP) buffer (20 mM Tris [pH 8], 150 mM NaCl, 1 mM EDTA, 10% glycerol, and 1% Triton X-100) for 2 h, and then with protein G-agarose beads overnight at 4˚C with rotation. Beads were then washed 5 × 5 min in IP buffer, and bound proteins were eluted with 0.1 M glycine (pH 2.7). Eluted proteins were buffer exchanged into PBS (with MicroBio-Spin 6 chromatography columns; Bio-Rad), run on one-dimensional and two-dimensional gels and Western blotted as described above, and then probed with 1/2000 streptavidin-horseradish peroxidase (Sigma-Aldrich) before developing to allow visualization of biotinylated proteins.

Deglycosylation

For peptide:N-glycanase (PNGase) F treatment, HES or RNase B (Sigma-Aldrich) was denatured by heating to 95˚C for 5 min in the presence of 0.1% SDS and 100 mM 2-ME, before the addition of 10 U PNGase F (Sigma-Aldrich) and 1% Triton X-100. Samples were incubated at 37˚C for 3 h. For PNGase A treatment, HES was diluted in 100 mM ammonium bicarbonate (pH 8.5), heat denatured, and digested overnight with 1 μg proteomics grade trypsin at 37˚C (Sigma-Aldrich), after which trypsin was inactivated by boiling. Complete digestion of HES was confirmed by SDS-PAGE analysis (data not shown). Tryptic peptides were then lyophilized and resuspended in 100 mM sodium acetate (pH 5) and treated with 0.2 mU PNGase A (Roche) for 24 h at 37˚C. For subsequent ELISA analysis, peptides were bound to plates in carbonate buffer at 1 μg/ml and then tested for Ab binding as above. For PNGase F and A digestions, control proteins were treated in an identical manner but in the absence of enzyme. For chemical deglycosylation of HES with trifluoromethanesulfonic acid (TFMS), HES, or RNase B were dialyzed into 0.1 M ammonium acetate then lyophilized until completely dry. The pellet was resuspended in 10% anisole in TFMS (both Sigma-Aldrich) at 4˚C, and the reaction was allowed to proceed for 2 h before neutralization with a 60% pyridine solution in a methanol–dry ice bath. The soluble fraction of HES was dialyzed into PBS, and the residual precipitate was solubilized in 1% SDS.

Affinity purification of VAL proteins

Twenty milligrams each of anti–VAL-1 (4-M15), 2 (4-S4), and 4 (2-11) mAbs were dialyzed into coupling buffer (0.1 M sodium bicarbonate and 0.5 M NaCl [pH 8.4]) and then reacted with swollen cyanogen bromide-activated Sepharose beads (Sigma-Aldrich) overnight at 4˚C with rotation. Unreacted groups were blocked with 0.2 M glycine (pH 8) for 2 h at room temperature, after which the beads were washed in five cycles of coupling

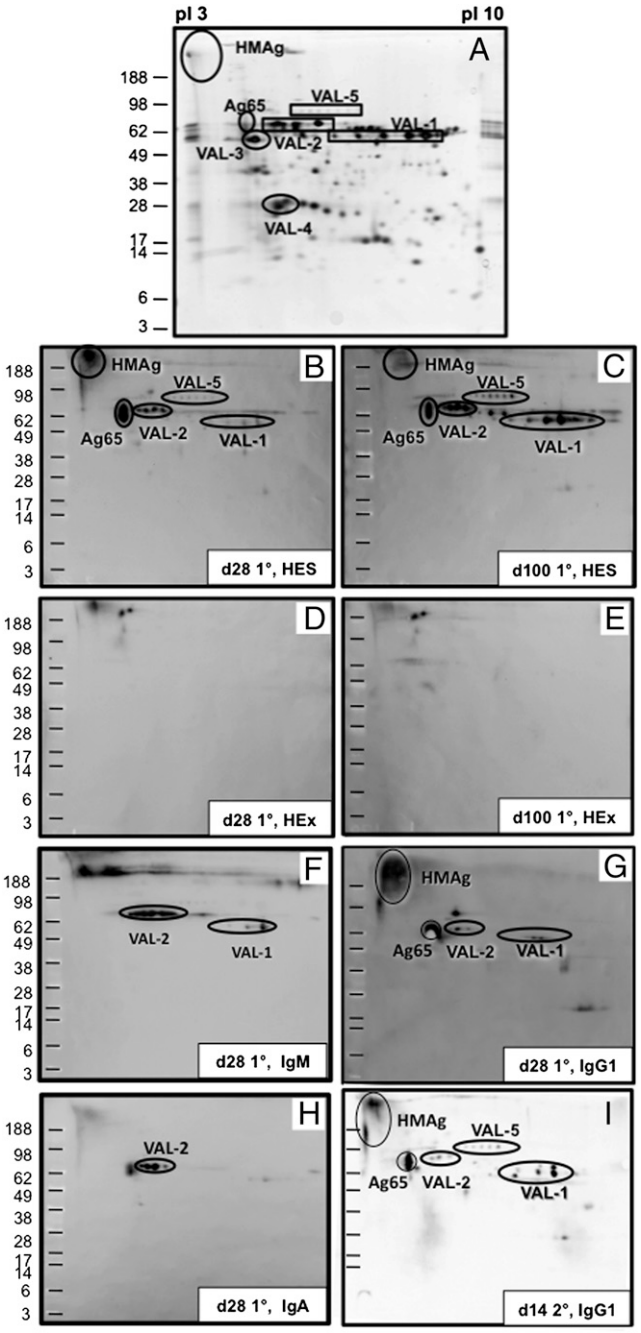

FIGURE 2. Polyclonal Abs recognize a restricted set of *H. polygyrus* Ags by Western blot. *A*, Silver-stained two-dimensional gel of HES indicating major components identified by mass spectrometry (34). HMAg and Ag65 indicate the position of Ags (subsequently termed HM-65; see Fig. 3*D*) that do not stain with silver. *B* and *C*, Two-dimensional Western blot of HES with sera from C57BL/6 mice taken at day 28 (*B*) and day 100 (*C*) following primary infection with *H. polygyrus*, developed with a polyvalent anti-Ig conjugate. *D* and *E*, As above, but with HEx. *F*, Two-dimensional Western blot of anti-HES IgM in sera from 28-d infected C57BL/6 mice. *G*, As above, for anti-HES IgG1. *H*, As above, for anti-HES IgA. *I*, Two-dimensional Western blot of anti-HES IgG1 in sera C57BL/6 mice collected 14 d following a secondary challenge infection. For each assay, sera were pooled from five mice. Molecular mass markers are indicated in kilodaltons, and results are representative of two or more experiments. Naive mouse sera showed no positive binding under the same conditions (data not shown).

buffer, followed by 0.1 M sodium acetate and 0.5 M NaCl (pH 4). For affinity purification, 10 μg HES was treated as before for IP, eluted proteins were run on one-dimensional SDS-PAGE, and bands of interest were excised for mass spectrometry analysis.

Sequence database and mass spectrometry

In studies to be published elsewhere, a database compiled of ~466,000 Roche 454 sequence reads from normalized and non-normalized adult *H polygyrus* cDNA was assembled into ~20,000 predicted gene products (Y. Harcus, J.P. Hewitson, K.J. Filbey, J.R. Grainger, M. van Agtmaal, M. Thompson, N. Wrobel, S. Bridgett, M.L. Blaxter, and R.M. Maizels, manuscript in preparation). This database was used to match peptides identified by mass spectrometry of SDS-PAGE and two-dimensional gel-purified proteins. The individual protein genes described in this article (VAL-1, VAL-2, VAL-3, VAL-4, VAL-5, and VAL-7) were each amplified by PCR from *H. polygyrus* mRNA using gene-specific primers, and multiple independent clones were sequenced to verify the sequences predicted by the assembly algorithm. The full sequences for VAL-1 to VAL-5 and VAL-7 have been deposited with the National Center for Biotechnology Information (http://www.ncbi.nlm.nih.gov/) under accession numbers JF914902, JF914906, JF914909, JF91410, JF914911, and JF914913, respectively. Immunoprecipitated HES proteins were prepared for mass spectrometry analysis as described previously (28). Positive-ion MALDI mass spectra were obtained using a Bruker ultraflex III in reflectron mode, equipped with an Nd:YAG smart beam laser. MS spectra were acquired over a mass range of *m/z* 800–4000, and monoisotopic masses were obtained using a SNAP (sophisticated numerical annotation procedure) averaging algorithm. The 10 strongest peaks of interest, with an signal/noise ratio >30, were selected for tandem mass spectrometry (MS/MS) fragmentation in LIFT mode. Bruker flexAnalysis software (version 3.3) was used to perform the spectral processing and peak list generation for both the MS and MS/MS. Identification of mAb 2-11 target VAL-4 required LC-electrospray ionization (ESI)-MS/MS using an Ultimate nanoLC system (Dionex) equipped with a PepMap C_{18} trap (300 μm × 0.5 cm, Dionex) and an Onyx C_{18} monolithic silica capillary column (100 μm × 15 cm; Phenomenex). Peptides were eluted over with a acetonitrile gradient (solvent A = 2% [v/v] acetonitrile, 0.1% [v/v] formic acid in H_2O; solvent B = acetonitrile, 0.1% [v/v] formic acid; gradient conditions consisted of 3 min solvent A), and then, a linear 0–50% gradient of solvent B over 20 min was applied, followed by a 50-min wash at 95% solvent B. The flow rate was 1.2 μl/min, and the column temperature was 60°C. The nanoLC was interfaced with a high capacity trap ultra ETD II ion-trap LC-MS/MS system (Bruker Daltonics) with an online nanoESI source. Positive ESI-MS and MS/MS were acquired using AutoMSn mode, over the 300- to 1800-*m/z* range. Instrument control, data acquisition, and processing were performed using Compass 1.3 SP1 software (Esquire control, Hystar, and DataAnalysis; Bruker Daltonics). MS/MS data were submitted to database searching against an in-house database containing the predicted gene products using the Mascot program (Matrix Science, version 2.1), through the Bruker ProteinScape interface (version 2.1). Database searching was run with a peptide tolerance of 250 ppm and MS/MS tolerance of 0.5 Da. Peptide matches with expect values <0.05 at a Mowse significance threshold of $p < 0.05$ were considered significant.

Immunofluorescence

For sections, adult *H. polygyrus* worms were snap-frozen on dry ice in Cryo-M-Bed mountant (Bright Instruments). Cryostat sections (5 μm; Leica) were cut onto Polysine slides (VWR), dried, and then fixed in 100% acetone for 10 min. Sections were washed twice with PBS for 10 min and then incubated with the various mAb (50 μg/ml in PBS containing 1% FCS) for 2 h at room temperature, washed twice in PBS as before, and then incubated with secondary anti-mouse Ig tetramethylrhodamine isothiocyanate (1/100 in PBS) for 1 h at room temperature. Following extensive washing, sections were mounted in anti-fade Vectashield mountant (Vector Laboratories). Staining was visualized with an Olympus fluorescent microscope. Non-fixed intact worms were stained on ice in round-bottom 96-well plates and then treated as above.

Radiolabeling of adult worm surface

Adult *H. polygyrus* were surface radiolabeled essentially as described in earlier publications (32, 33). Eppendorf tubes (1.5ml) were coated with 200 μl of a 1 mg/ml solution of Iodination reagent (Pierce) in chloroform. Once dried, the tubes were washed several times with PBS, before transfer of ~500 adult worms and 500 μCi [^{125}I] (PerkinElmer) on ice. The sample was incubated with frequent agitation for 10 min and then quenched by the addition of a saturated solution of *L*-tyrosine (Sigma-Aldrich). Radiolabeled parasite surface material was then produced as described above as with HEx, except parasites were homogenized in 1.5% n-octyl glucoside detergent and 1% protease inhibitor mixture (P8340; Sigma-Aldrich). Immunoprecipitates were performed as above (anti–HM-65 mAb 9.1.3 or rat anti-HES polyclonal Ab) or with anti-mouse IgM-agarose (A4540; Sigma-Aldrich). Autoradiographs were carried out on dried gels as described previously (32, 33).

Vaccination and passive immunization

C57BL/6 females were immunized with 25 μg HES in alum adjuvant i.p., then boosted on days 28 and 35 with 5 μg HES–alum i.p. Mice were challenged with 200 *H. polygyrus* L3 larvae, fecal egg counts were determined at days 14 and 28 postinfection, and adult worms counted at day 28. For passive immunization, C57BL/6 females were treated on day −1 and then every 2–3 d postinfection (with 200 *H. polygyrus* L3 larvae) with either 0.2 or 1 mg mAb i.p. (for IgG1 mAbs) or i.v. (for IgM mAbs) as detailed in the figure legend. Eggs and worm numbers were determined as above.

Results

Ab responses are predominantly directed at secreted, rather than somatic, parasite Ags

As a first step in defining immunogenic products of adult *H. polygyrus*, we compared a conventional antigenic preparation comprising a soluble whole parasite extract (HEx), with products released by live parasites maintained in serum-free tissue culture medium (HES). The overall protein compositions of HES and HEx are very different, as shown in Fig. 1*A* and 1*B*, respectively, and confirmed by recent proteomic analysis (34).

As IgG1 Abs predominate and have a protective role in both primary and secondary *H. polygyrus* infection (15, 19, 20), we then compared IgG1 responses to HES and HEx following a primary infection. Ag-specific IgG1 responses to HES were detected by ELISA in both BALB/c and C57BL/6 mice by day 14 postinfection and by day 28 reached a high titer, which was main-

Table I. mAbs to HES Ags

Ag, Specificity	Clone	Source	Isotype
Glycan A (VAL-1-2-5)	13.1, 2-2, 2-12, 2-13, 2-62, 3-8, 3-11, 3-28, 3-29, 3-40, 3-42, 3-55	d28 SPL	IgM
Glycan B (HM-65)	14.3	d28 SPL	IgA
	3-31	d28 SPL	IgM
	4-M9	d28 MLN	IgM
	4-M7, 4-M17	d28 MLN	IgG1
	9.1.3	HES/IFA	IgG1
VAL-1	2-6, 3-6, 3-10, 3-38, 3-39	d28 SPL	IgG1
	4-M4, 4-M15, 4-M20, 4-M23, 4-M25	d28 MLN	IgG1
VAL-2	4-S4	d28 SPL	IgG1
VAL-4	2-11	d28 SPL	IgG1

d28 SPL, day 28 spleen.

tained for at least 63 (BALB/c; Fig. 1*C*) and 100 d (C57BL/6; Fig. 1*D*). Moreover, IgG1 titers to HES were up to 20-fold higher than those to HEx and showed less variation between individual animals. We therefore focused in the majority of subsequent Ab investigations on HES.

The anti-parasite IgM response differed from the IgG1 response in several regards (Fig. 1*E*, 1*F*). Significant background levels of both anti-HES and anti-HEx IgM Abs were noted in naive mice, and following infection, specific IgM titers reached a relatively early plateau (day 14). Furthermore, reactivity to HES and HEx was equivalent at all time points. We were unable to detect the target of (presumably natural) IgM Abs present in naive mice using both Western blot and mAb techniques, perhaps because of their relatively weak affinity (data not shown).

Ag specificity of polyclonal Ab responses

To identify individual antigenic targets of the Ab responses, we adopted both polyclonal and monoclonal strategies. First, we used two-dimensional SDS-PAGE separation of HES Ags, by which ~100 distinct protein spots are observed (Figs. 1*A*, 2*A*); the identity of most major proteins has been determined by mass spectrometry (34). Despite the abundance of potential Ags, however, the two-dimensional Western blot profile of polyclonal sera from C57BL/6 mice with 28-d primary infection is much more

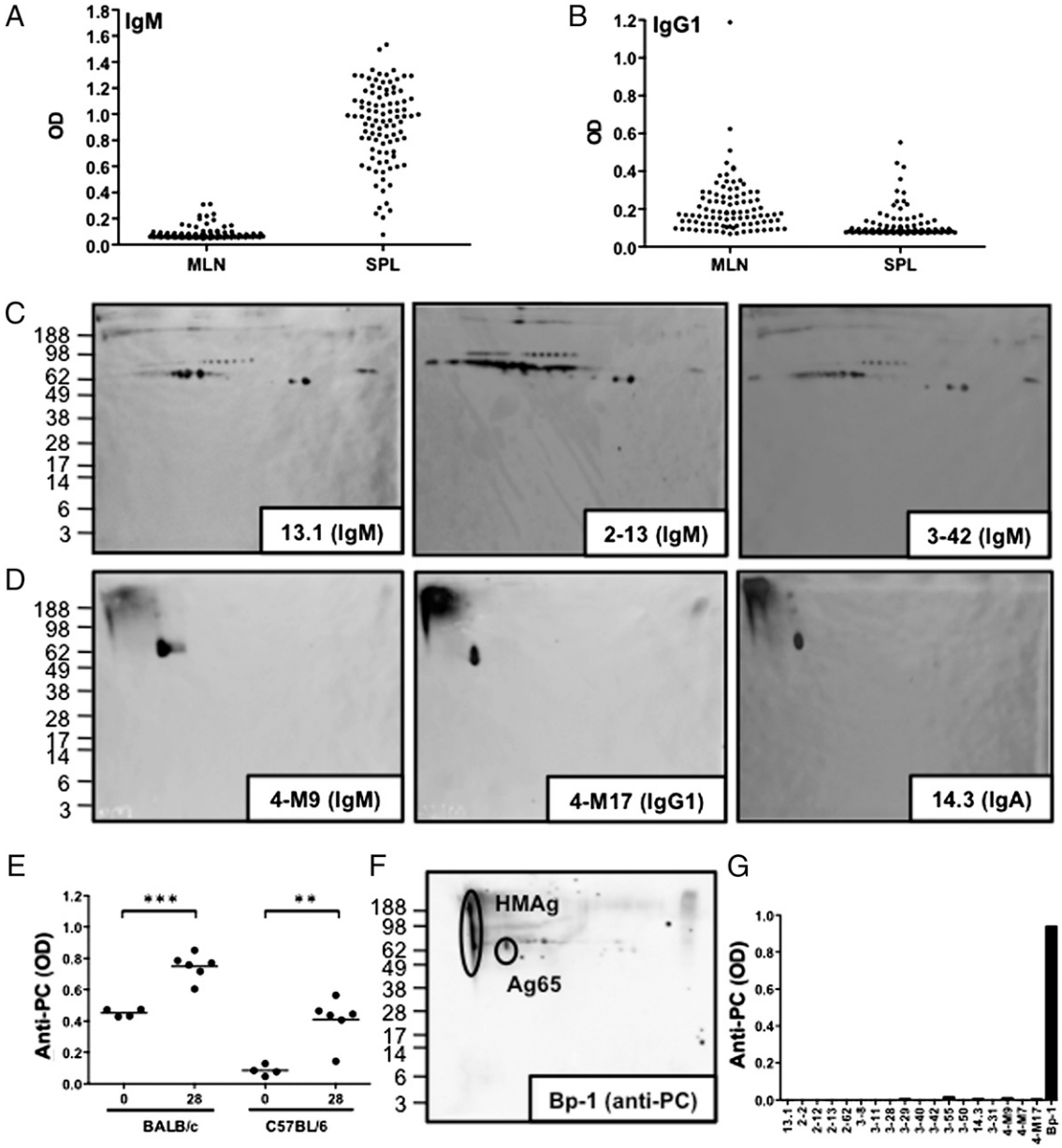

FIGURE 3. HES-specific mAbs from mice infected with *H. polygyrus*. *A* and *B*, Frequency of HES-specific hybridoma cells producing IgM (*A*) or IgG1 (*B*) from the MLNs and spleens of infected C57BL/6 mice at day 28 postinfection, as determined by ELISA. Each dot represents a single well of a 96-well plate. *C*, Representative two-dimensional Western blots of three different IgM anti-HES mAbs derived from infected mice, which bind to glycan A. *D*, Representative two-dimensional Western blots of anti-HES IgM, IgG1, and IgA mAbs recognizing glycan B on the HM-65 Ags. *E*, Anti-PC Abs measured by ELISA against PC-BSA in naive and 28-d infected sera from BALB/c and C57BL/6 mice. *F*, Two-dimensional Western blot of HES probed with anti-PC mAb Bp-1. The positions of the HM-65 Ags are circled. *G*, Reactivity to PC measured by ELISA on BSA–PC-coated plates; data from a panel of anti-HES mAbs are shown, together with Bp-1–positive control. Molecular mass markers are indicated in kilodaltons. $^{**}p < 0.01$, $^{***}p < 0.001$.

restricted (Fig. 2*B*). These were identified by proteomics as members of the venom allergen/VAL family of proteins (35, 36), specifically VAL-1, VAL-2, and VAL-5 (Fig. 2*A*) (34). Additional reactivity was noted to both a high molecular mass component and a smaller 65-kDa Ag, which do not appreciably silver stain and did not give measureable peptides for proteomic analysis; we term this Ag combination HM-65 (see below).

As reactivity increases over a long time frame, and as the C57BL/6 mouse is considered to be a slow responder to infection (37, 38), we also examined the serological response at 100 d postinfection (Fig. 2*C*); at this time point, responses to all the Ags previously noted were substantially stronger, but there remained a restricted repertoire of target Ags.

Consistent with ELISA results indicating that anti-HEx somatic extract responses were relatively weak, the same sera showed only slight reactivity by Western blot (Fig. 2*D*, 2*E*). The primary anti–VAL Ab response to HES was predominantly of the IgM isotype, although a smaller amount of anti–VAL-2 IgA was also noted (Fig. 2*F*, 2*H*). In contrast, anti-HES IgG1 response was detected against HM-65 (Fig. 2*G*). Polyclonal IgE did not provide a measurable signal by Western blot (data not shown).

We also examined the secondary response mounted by genetically susceptible mice cleared of infection by chemotherapy; in these mice, protective immunity is stimulated against challenge infection (9, 39). Importantly, immunity to challenge infection is ablated in B cell- or Ab-deficient mice (4, 15, 16, 40). By Western blot analysis, secondary IgG1 Abs showed a similar profile to samples from primary infection, albeit with a 10- to 30-fold higher titer (data not shown) and correspondingly stronger binding patterns (Fig. 2*I*). In contrast, secondary IgM responses were similar to primary Abs with respect both the titer and specificity profile (data not shown).

mAb specificities

We next generated a panel of monoclonal Abs to dissect the antigenic response in fine detail, using spleens and draining MLN from infected mice at day 28 (Table I). Despite taking cells at this relatively late time point in the primary response, a substantial proportion of monoclonals represented Abs that had not undergone class switch from the IgM isotype, particularly when splenocytes rather than MLN cells were used (Fig. 3*A*). The great majority (12 of 14) of these IgM mAbs displayed a similar Western blot profile against HES (Fig. 3*C*) and bound to proteins previously identified as VAL-1, VAL-2, and VAL-5 by proteomic analysis. In fact, this indicates that the observed specificity of polyclonal serum (Fig. 2*B*, 2*C*) can be largely replicated by a single (monoclonal) Ab specificity and that an immunodominant epitope is shared by at least three members of the VAL family.

A different pattern was shared by a smaller number of Abs, including IgM, IgG1, and IgA isotypes, which bound to HM-65 (Fig. 3*D*). Notably, these components do not stain with silver and do not give measurable peptides for proteomic analysis, mimicking the pattern seen with polyclonal IgG1 from primary infections (Fig. 2*G*).

Because of the prominence of PC in many helminth products, including high molecular mass species with nonproteinaceous composition (30, 41), we tested for PC reactivity in infection sera and for PC epitopes in HES. Serum Abs from *H. polygyrus*-infected mice showed a modest degree of anti-PC binding (Fig. 3*E*), as has been reported previously (42). When two-dimensional Western blots were probed with monoclonal anti-PC Ab, the major positive reaction was with HM-65 (Fig. 3*F*). Despite this, none of the anti-HES monoclonals bound directly to PC (Fig. 3*G*), indicating that they target a non-PC specificity.

IgG Abs recognize heat-labile epitopes of secreted VAL Ags

The majority of IgG1 mAbs raised from infected mice (12 of 14) failed to react with HES by Western blot, despite their strong reactivity to native HES by ELISA (Fig. 4*A* and data not shown). We interpreted this to mean that the IgG1 response is predominantly directed against conformational protein epitopes, which

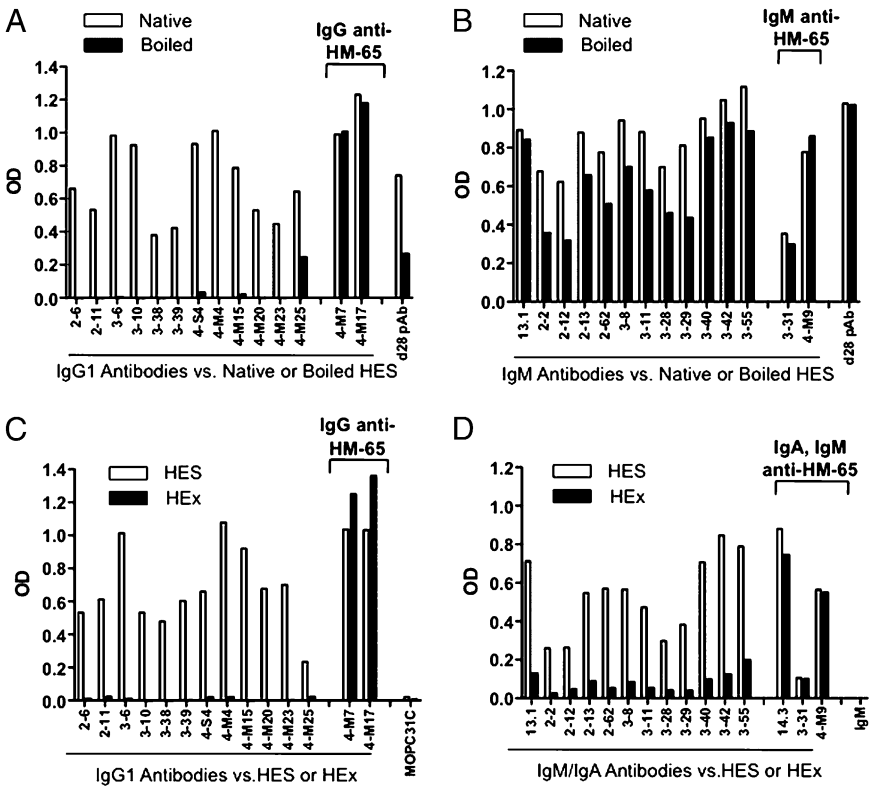

FIGURE 4. Most HES-specific IgG1 Abs recognize heat-labile epitopes absent from parasite extract. *A*, ELISA reactivity of anti-HES IgG1 mAbs to native (□) and boiled (■) HES. Polyclonal sera from 28-d infected C57BL/6 mice were included as a positive control. *B*, As above, for IgM mAbs. *C*, ELISA reactivity of anti-HES IgG1 mAbs to HES (□) and HEx (■). MOPC 31C myeloma IgG1 was included as a negative control. *D*, ELISA reactivity of anti-HES IgM and IgA mAbs to HES (□) and HEx (■). Anti-DNP IgM mAb was included as a negative control.

are destroyed following detergent denaturation during SDS-PAGE. In support of this, although IgM monoclonals are equally reactive to native or heat-denatured HES (Fig. 4*B*), heat denaturation of HES ablated all IgG1 mAb ELISA reactivity, with the exception of the two anti–HM-65 IgG1 Abs (Fig. 4*A*). Furthermore, although most IgG1 mAbs (Fig. 4*C*) and IgM mAbs (Fig. 4*D*) show little reactivity to somatic extract (HEx), all Abs specific for HM-65 show equally strong binding to HES and HEx.

To identify the heat-labile determinant(s) recognized by the IgG1 mAbs, an immunoprecipitation strategy was used using biotin-labeled nondenatured HES and protein G beads. The majority of these IgG1 monoclonals (10 of 14) were specific for a band that migrates in the position of VAL-1, as represented by 4-M15 (Fig. 5*A*). Two additional mAbs immunoprecipitated Ags comigrating with VAL-2 (4-S4) and VAL-4 (2-11).

Two-dimensional analysis of Ags immunoprecipated by day 28 polyclonal infection serum confirmed that the dominant target of primary IgG Ab in C57BL/6 mice was VAL-1 (Fig. 5*D*), as well as a spot that comigrates with another VAL protein abundant in HES, VAL-3 (Fig. 2*A*). Moroever, secondary IgG immunoprecipitated two further homologs, VAL-4 and VAL-7 (Fig. 5*E*). Comparison of profiles from Western blot (Fig. 2*G*, 2*I*) and immunoprecipitation (Fig. 5*D*, 5*E*) indicates that Western blotting gives an incomplete picture of IgG1 Ab specificity, as a result of the predominantly conformationally dependent VAL epitopes, whereas immunoprecipitation of biotinylated Ags omits the HM-65 group of Ags with low protein content.

To formally identify the immunoprecipitated proteins, samples bound by each Ab were eluted from one-dimensional gel bands (Fig. 5*F*) and subjected to mass spectrometry, matching the respective protein sequences (Fig. 5*G*). These assays also indicate that VAL-1, VAL-2, and VAL-4 do not interact with other proteins present in HES, given the absence of any coimmunoprecipitated components.

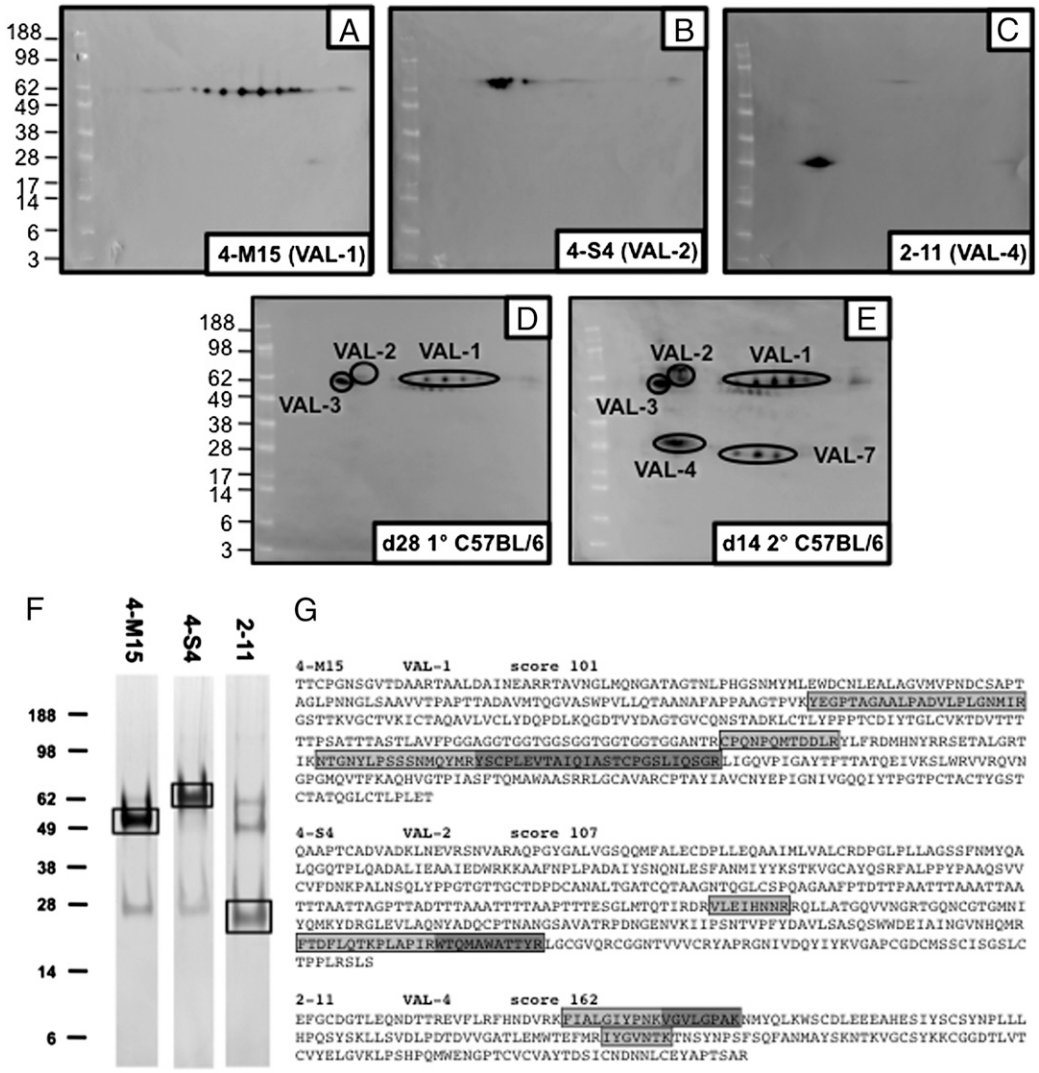

FIGURE 5. Conformation-dependent IgG1 Abs primarily target VAL Ags. *A–E*, Immunoprecipitation of biotin-labeled HES by the indicated mAb or polyclonal infection sera, separated by two-dimensional SDS-PAGE, and visualized by Western blotting with streptavidin–HRP. *A*, Anti–VAL-1 mAb 4-M15. *B*, Anti–VAL-2 mAb 4-S4. *C*, Anti–VAL-4 mAb 2-11. *D*, Primary day 28 C57BL/6 polyclonal infection serum. VAL-1, VAL-2, and VAL-3 are indicated. *E*, Secondary day 14 C57BL/6 polyclonal infection serum. Postions of VAL-4 and VAL-7 are indicated, as well as VAL-1, VAL-2, and VAL-3 as above. *F*, One-dimensional SDS-PAGE of immunoprecipitated (unlabeled) HES proteins using bead-conjugated mAb as indicated; boxes indicate segments eluted for mass spectrometric analysis. Additional bands likely reflect H and L chains of mAb leaching from beads. Molecular mass markers are indicated in kilodaltons. *G*, Peptides of VAL-1, VAL-2, and VAL-4 matched by mass spectrometry indicated by boxes. Mascot scores are also shown.

IgM Abs recognize a common O-linked glycan epitope on VAL glycoproteins

Despite being bound by several IgM monoclonals (Fig. 3*C*), the target Ags VAL-1, VAL-2, and VAL-5 show only limited amino acid homology (14.9% identity, 23.5% similarity; Supplemental Fig. 1), and reactivity is heat stable (Fig. 4*B*). We therefore evaluated the possibility of a carbohydrate nature of the target epitope(s). We also noted that the Ags' predicted molecular masses, based on primary amino acid sequences, were 10–39 kDa lower than their observed gel migration, yet each contained only a single potential N-linked glycosylation site (Fig. 6*A*). However, they encoded abundant serine and threonine residues in a central domain, which were predicted to be O-glycosylated by the NetOGlyc 3.1 program (Fig. 6*A*, Supplemental Fig. 2) (43). This contrasts with another secreted VAL protein of similar abundance, VAL-3 (Fig. 2*A*), which does not appear to be recognized by IgM Abs, lacks predicted O-glycosylation sites (Supplemental Fig. 2), and migrates on two-dimensional gels in a manner consistent with its predicted molecular mass (Figs. 3*A*, 6*A*).

To first confirm that glycan A is carried on VAL-1 and VAL-2, we showed that the anti-glycan A mAb 13.1 bound to VAL-1 and VAL-2 on Western blots following their affinity purification using IgG1 mAbs to the conformational epitopes of the VAL Ags (Fig. 6*B* and data not shown). Comparison with the profile of immunoprecipitated VAL-1 Ag (Fig. 5*A*) indicates that only three of the six VAL-1 spots react with the anti-glycan A mAb, as is also evident from Fig. 3*B*.

To then investigate the potential role of antigenic carbohydrates, we used both enzymatic and chemical deglycosylation strategies. When HES was pretreated with PNGase F to remove N-linked carbohydrates, small mobility shifts were evident in silver-stained gels (Fig. 6*C*) and Western blots (Fig. 6*D*), indicating the removal of *N*-glycans, yet polyclonal sera and IgM mAb reactivity remained intact (Fig. 6*D*, 6*E*). Similarly, the dominant Ag is unlikely to be an PNGase F-resistant *N*-glycan with a core α1,3-fucose, because PNGase A treatment of tryptic HES peptides failed to ablate either polyclonal or mAb binding (Supplemental Fig. 3). Furthermore, mass spectrometric analysis identified a number of peptides containing unconjugated N-glycosylation sites (NxS/T), calling into question whether these are used in the VAL proteins of this species (data not shown).

To assess the role of *O*-glycans, HES was treated with TFMS, which removes both *N*- and *O*-glycans. Such chemical deglycosylation resulted in mobility shifts of silver-stained HES bands, indicative of glycan removal, comparable to that seen with a control glycoprotein, RNase B (Fig. 7*A*). Importantly, TFMS treatment ablated both anti-VAL IgM mAb and polyclonal infection sera recognition of HES (Fig. 7*B*, 7*C*), whereas TFMS-treated HES retained reactivity with an anti-protein Ab, raised against recombinant *H. polygyrus* calreticulin, as well as polyclonal serum from rats immunized with HES (Fig. 7*D*). These data therefore indicate that the dominant and persistent IgM Ab response is to an O-linked glycan shared by several polypeptide secreted Ags of *H. polygyrus*. The status of the HM-65 Ag is less clear; although PNGase F treatment ablates binding of anti-glycan B 14.3 mAb to the 65-kDa component but not the high molecular mass complex, the reverse is true for TFMS (Figs. 6*D*, 7*B*). Because the 65-kDa Ag is less abundant, the overall reactivity of 14.3 to TFMS-treated HES is reduced ~10-fold but not abolished (Fig. 7*E*). Thus, a similar or identical epitope is conjugated through different linkages to different carrier macromolecules. It was also noted that TFMS does not remove the PC moiety from HM-65 (data not shown), indicating that a different linkage is used in *H. polygrus* from that described through N-linked glycans for *Acanthocheilonema viteae* (44).

A

	Predicted Mol.wt (–SP)	Observed Mw (kDa)	Discrepancy (kDa)	*N*-Glyco	*O*-Glyco
VAL-1	46.8	56.5	9.7	1	18
VAL-2	47.8	68.0	10.2	1	26
VAL-3	49.4	53.5	4.1	1	2
VAL-5	50.3	89.5	39.2	1	30

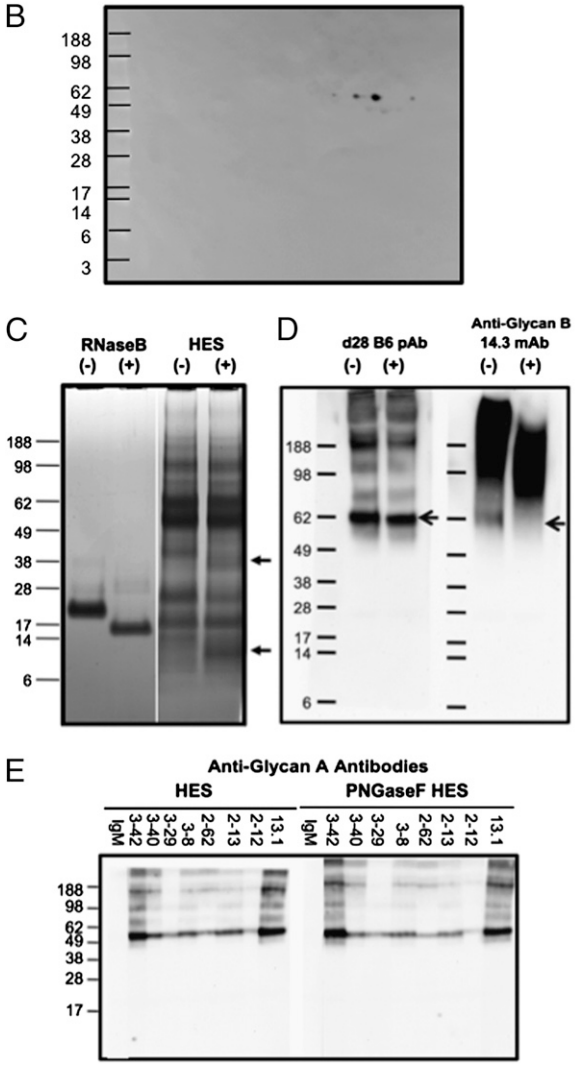

FIGURE 6. The immunodominant IgM target is not an N-linked glycan. *A*, Molecular mass discrepancies between the predicted molecular mass of indicated VAL proteins, based on amino acid sequence and observed migration on two-dimensional gels. Mature molecular mass is that predicted without the signal peptide (SP) sequence, predicted N-glycosylation sites are defined as N(X)S/T, and O-glycosylation sites were predicted using NetOGlyc version 3.1 (43). The proportion of predicted sites used is not known. *B*, Western blot of anti–VAL-1 mAb (4-M15)-precipitated Ag separated on two-dimensional SDS-PAGE and probed with anti-glycan A mAb (13.1). *C*, Silver-stained one-dimensional SDS-PAGE of PNGase F-treated (+) or mock-treated (−) RNase B control glycoprotein and HES. *D*, One-dimensional Western blot of HES with or without PNGase F treatment using day 28 C57BL/6 polyclonal sera and anti-glycan B (HM-65) mAb 14.3. Band shifts associated with enzymatic removal of *N*-glycans are arrowed. *E*, One-dimensional Western blots of HES with or without PNGase F treatment using anti-glycan A mAbs. IgM denotes an anti-DNP IgM mAb negative control. Molecular mass markers are indicated in kilodaltons

Glycans A and B as well as VAL-1 and VAL-4, but not VAL-2, are expressed by tissue-phase larvae

Upon infection of mice, *H. polygyrus* larvae first invade the submucosal tissue of the intestinal tract, molt twice (from L3 to L4

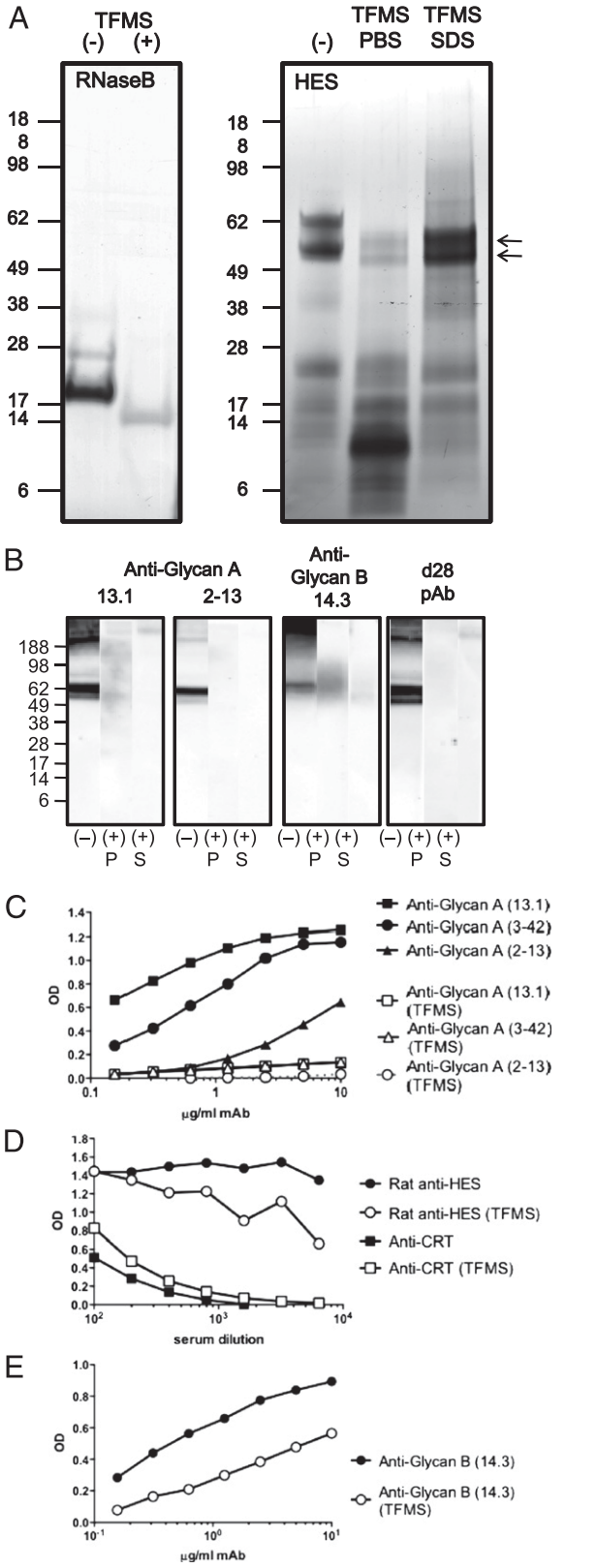

FIGURE 7. Chemical deglycosylation ablates anti-glycan A IgM Ab binding and reduces anti-glycan B binding to HM-65. *A*, Silver-stained one-dimensional SDS-PAGE of TFMS-treated (+) or mock-treated (−) HES and RNase B control glycoprotein. TFMS-treated HES was separated into PBS and SDS-soluble fractions. *B*, One-dimensional Western blots of mock-treated and TFMS-treated HES probed with anti-HES mAbs against glycans A and B and day 28 C57BL/6 polyclonal antiserum. *C*, ELISA of TFMS-treated (open symbols) and mock-treated (solid symbols) HES, used to measure binding of anti-glycan A mAb 13.1 (squares), 2-13 (triangles), and 3-42 (circles). *D*, ELISA of TFMS-treated (open symbols) and mock-treated (solid symbols) HES probed with polyclonal rat anti-HES serum (circles) or rat Ab to recombinant *H. polygyrus* calreticulin (Hp-CRT; squares). *E*, ELISA of TFMS-treated (open symbols) and mock-treated (solid symbols) HES probed with the anti-glycan B (HM-65) mAb 14.3. The PBS-soluble fraction of TFMS was used for ELISA in *C–E*. Molecular mass markers are indicated in kilodaltons.

and then adult), emerging 8 d later into the lumen of the small intestine (1). As immunity to challenge infection is directed, in part at least, at the tissue-phase larvae (3), we investigated whether the Ags defined from adult parasites are also expressed by fourth-stage larvae (L4) recovered from the submucosa at day 5 post-infection. Larvae were cultivated to yield ES Ags, which were probed with each of the specific Ab reagents. Polyclonal anti-HES antiserum reacted strongly with L4 ES (Fig. 8*A*); positive reactions to L4 ES were also seen with mAbs to glycan A (Fig. 8*B*) and glycan B (Fig. 8*C*), although in both cases levels were lower than with HES. Interestingly, among the VAL Ags, it was found that although VAL-1 (Fig. 8*D*) and VAL-4 (Fig. 8*F*) were present at similar levels in HES and L4 ES, VAL-2 was absent from the larval stage (Fig. 8*E*).

Glycan A is strongly represented on the adult cuticle, whereas glycan B is a somatic Ag

To localize glycan A and B epitopes within the adult parasite, we probed intact worms and sections by immunofluorescent microscopy. In sections, anti-glycan A mAb bound the worm surface, highlighting the longitudinal ridges of the cuticle (Fig. 9*A*). Anti-glycan A Ab also bound to the surface of intact adults in a pattern that similarly emphasized the ridges (Fig. 9*B*). At higher magnification, anti-glycan A Ab was seen to stain an ordered array of epitopes organized longitudinally along the cuticular furrows (Fig. 9*C*). In contrast, anti-glycan B Abs failed to bind to intact worms (Fig. 9*D*) while reacting strongly to somatic constituents in cross-sections (Fig. 9*E*); in particular, no cuticular binding was observed with anti-glycan B Ab.

To determine the macromolecules to which cuticular glycan A is conjugated, we surface radiolabeled adult worms and used mAbs to immunoprecipitate glycan A-bearing Ags. As shown in Fig. 9*F*, this procedure indicates that glycan A is expressed on at least four different molecular mass species, with a 180-kDa band predominating (Fig. 9*F*); only a small proportion of ~55-kDa VAL proteins are similarly immunoprecipitated. The conclusion that most surface glycan A is not borne on VAL proteins is supported by studies reported elsewhere that anti–VAL-1 and –VAL-2 mAbs bind only to localized areas of the cuticle (34). In contrast to glycan A, the glycan B-specific Abs were unable to immunoprecipitate radiolabeled surface components (Fig. 9*F*). A remarkable degree of cross-reactivity between ES and surface proteins was indicated as a polyclonal sera raised against HES was able to precipitate essentially all radiolabeled surface components (Fig. 9*F*).

Vaccination with HES confers protection against challenge whereas passive immunization with anti-HES mAb does not

Given the protective ability of VAL family members such as ASP in related helminth infections (45), we determined whether passive immunization with the anti-VAL protein and glycan mAbs were able to confer protection against challenge infection. We first wished to verify that adult worm-derived HES, in which VAL proteins are among the major Ags, could effectively vaccinate against challenge with larval parasites, as negative results have been reported in the literature (46). We found, however, that HES

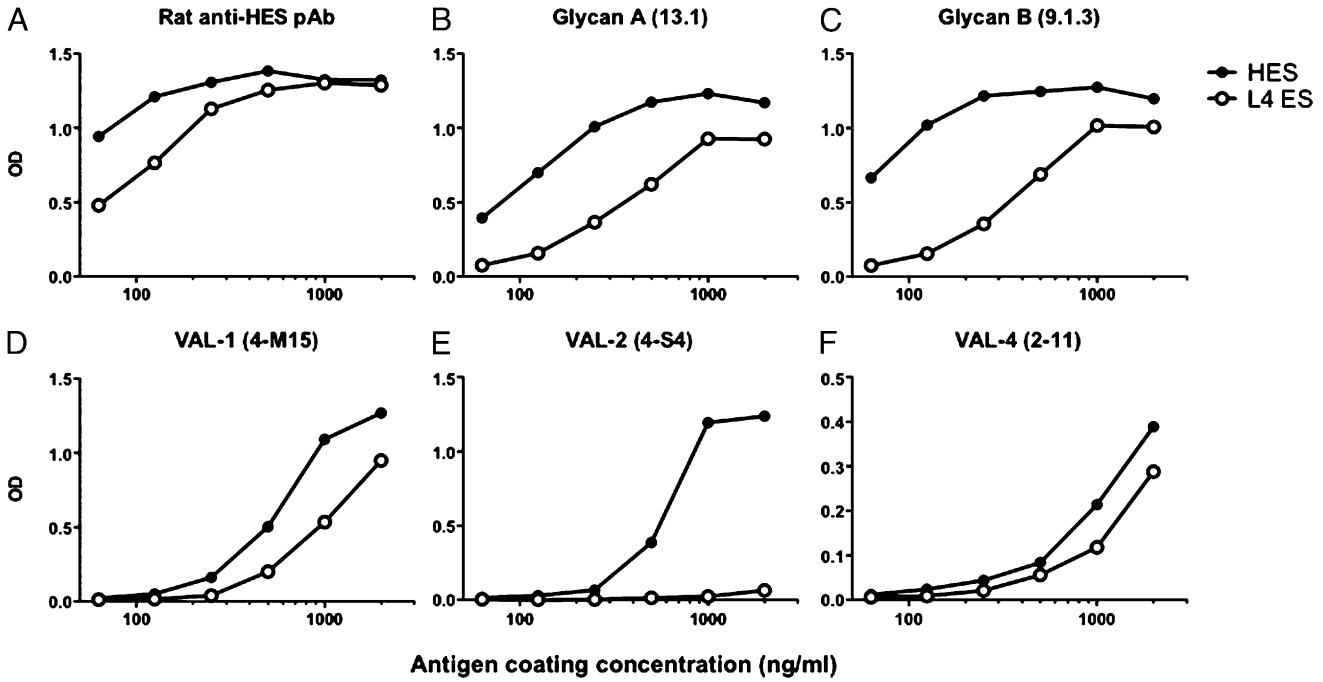

FIGURE 8. Monoclonal binding to ES from the tissue-phase L4 larvae show expression of glycans A and B, VAL-1 and VAL-4, but not VAL-2. *A*, ELISA reactivity of polyclonal rat anti-HES binding to plates coated with range of concentrations of adult HES (solid symbols) or L4 ES (open symbols) *B*, As above, with anti-glycan A mAb 13.1. *C*, As above, with anti-glycan B mAb 9.1.3. *D*, As above, with anti–VAL-1 mAb 4-M15. *E*, As above, with anti–VAL-2 mAb 4-S4. *F*, As above, with anti–VAL-4 mAb 2-11.

vaccination with alum adjuvant induced a potent humoral response, with titers of anti-HES IgG1 comparable to those seen following secondary infection (data not shown). Moreover, vaccinated animals had greatly reduced egg counts at day 14 than animals immunized with PBS-adjuvant alone (Fig. 10*A*), whereas by day 28, HES-immunized animals showed no fecal eggs and had expelled all adult worms (Fig. 10*A*, 10*B*). Thus, immune responses against adult secretions conferred highly effective and significant protection against larval challenge.

We next performed passive immunization experiments with each of the defined specificity mAbs given throughout the infection period. Using either 0.2 or 1 mg doses of mAb every 2–3 d, mice given anti–VAL-1, –VAL-2, or –VAL-4 IgG1 Abs showed no diminution in egg counts at day 14 (Fig. 10*C*) or day 28 (Fig. 10*D*) of infection, and indeed, anti–VAL-4 recipients showed elevated egg numbers in two independent experiments ($p < 0.05$ compared with recipients of MOPC31C). Furthermore, none of the anti-VAL mAbs induced worm expulsion as measured at day 28 (Fig. 10*E*).

In the same experiments, we also tested IgG1 anti-glycan B mAb for ability to passively protect recipient mice; however, as shown in Fig. 10*C–E*, this Ab also failed to reduce egg numbers or elicit expulsion of adult worms. Finally, IgM Ab against glycan A was tested, because no class-switched Abs of this specificity were observed. As with the other mAbs, anti-glycan A did not protect against egg production (data not shown) or worm persistence (Fig. 10*F*).

Discussion

The model system of *H. polygyrus* captures many essential characteristics of the gastrointestinal nematode infections that are highly prevalent in human and animal populations (47, 48). The parasite establishes a chronic infection, driving regulatory T and B cell subsets within a Th2-dominated environment (5, 25, 49–51) and altering innate populations such as dendritic cells (52, 53) and macrophages (54, 55). Immunity to *H. polygyrus* is slow to develop, particularly in the genetically most susceptible hosts (14), but both B cells and the Abs they produce are important constituents of the protective immune response (4, 15, 16). In this study, we aimed primarily to define the Ags of adult parasites recognized by host serum Abs and secondarily to address whether those Ab specificities serve a protective function in the host–parasite relationship.

Previous antigenic analyses of *H. polygyrus* have involved a mixture of approaches and relatively simple characterization such as one-dimensional SDS-PAGE or column fractionation (32, 33, 56) or have investigated individual gene products that are postulated to play a role in immune recognition (26, 31, 57, 58). We have adopted in this study a more global approach to identify the major Ags recognized during primary infection, which we show are well represented in HES, although not in somatic extracts, presumably reflecting the fact that the immune system is exposed in a more continuous fashion to the secreted products of a luminal-dwelling live parasite. Indeed, we have detected glycan A in the serum of 7-d infected mice, demonstrating that products of a gastrointestinal parasite can disseminate to distant sites (J.P. Hewitson, unpublished observations). Ongoing work has also revealed that T cell Ags, driving the secretion of Th2 cytokines, are enriched in HES compared with somatic extract in a similar manner to serological Ags (J.P. Hewitson and K.J. Filbey, unpublished observations).

Murine Ab responses are known to be predominantly IgG1 with primary reactivity to secreted Ags in the 50- to 70-kDa range (14, 59). These Ags correspond to those we have now defined as VAL-1, VAL-2, and VAL-5 and appear likely to represent the products isolated from HES by Monroy et al. (57) to achieve a 40% reduction in egg production following vaccination. Interestingly, these glycoproteins bear a conserved antigenic carbohydrate we have termed glycan A, the structural analysis of which is now under way. Glycan A is also strongly associated with the cuticular surface of the adult worm and is partly responsible for the extensive degree of antigenic sharing between the secretions and

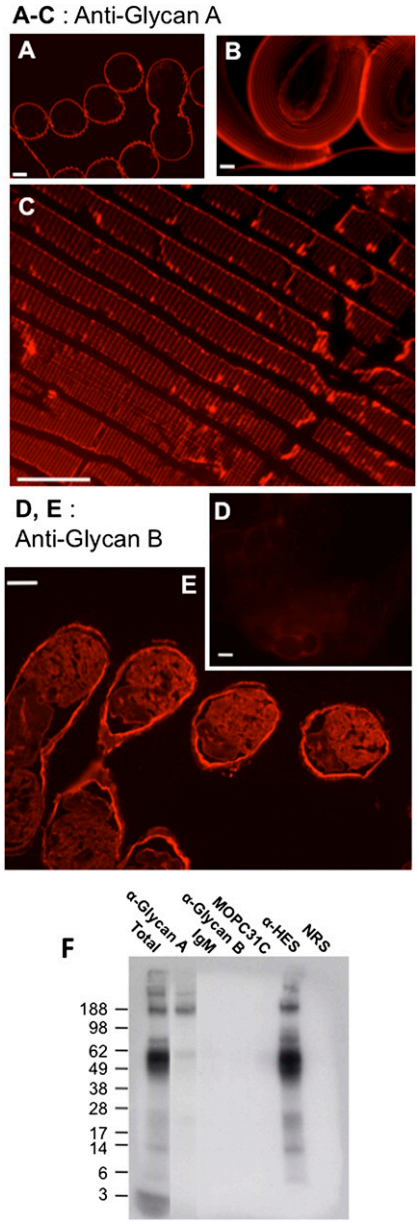

FIGURE 9. The immunodominant glycan A is present on the surface of adult worms. *A*, Binding of anti-glycan A mAb 13.1 to transverse sections of adult *H. polygyrus.* The corrugated cuticular ridges are visible. *B*, Binding of anti-glycan A mAb 13.1 to the surface of intact adult *H. polygyrus. C*, Binding of anti-glycan A mAb 13.1 to ordered structures within cuticular furrows on the surface of *H. polygyrus*. *D*, Failure of anti-glycan B mAb 14.3 to bind to intact worms. *E*, Binding of anti-glycan B mAb 14.3 to muscle layer and other structures in transverse sections of adult worms. *F*, SDS-PAGE of ^{125}I surface-labeled adult proteins immunoprecipitated with anti-glycan A mAb 13.1, revealed by autoradiography; similar analysis with anti-glycan B mAb 9.1.3 is also shown. Control IgM and IgG1 (MOPC31C) proteins are shown, as well as polyclonal rat anti-HES and normal rat serum (NRS). Scale bars (*A–E*), 100 μm. Molecular mass markers are indicated in kilodaltons.

surface of adult *H. polygyrus*, as reported by earlier investigators (33). This may indicate that HES, and the VAL components in particular, are shed from the surface of the worm or alternatively that molecules secreted in HES remain associated in some form with the parasite cuticle.

The VAL glycoproteins represent the immunodominant target of both IgM (against glycan A) and the class-switched IgG1 response (against a conformational epitope, presumably the protein backbone). Most VAL proteins from other species have been reported to be glycosylated based on discrepancies between predicted and observed molecular mass [e.g., *Ancylostoma caninum* VALs (60)], although only *N*-glycans have so far been identified [on a VAL protein from the cattle nematode *Ostertagia ostertagi* (61)]. In this article, we show that a subset of *H. polygyrus* secreted VAL proteins are decorated with highly antigenic *O*-glycans, which are most likely concentrated in a serine/threonine-rich tract linking two conserved sperm coating protein (cd05380) domains. Similar stretches of predicted O-glycosylation can be observed in other nematode VAL proteins, including *Haemonchus contortus* Hc40 (accession number AAC03562; http://www.ncbi.nlm.nih.gov/), *Cooperia punctata* ASPs (AAK35199 and AAK35187), and *A. caninum* ASP-4 and ASP-6 (AAO63576 and AAO63578). It is also important to note that the VAL proteins themselves, rather than only their associated glycans, are likely to play a key role in host–parasite interactions, as *H. polygyrus* secretes a number of abundant nonglycosylated VAL proteins such as VAL-3 (34).

The nematode cuticle is an extracellular matrix assembled from specialized collagens and cuticlins (62), with sugar components that may vary greatly between species. For example, *Trichinella spiralis* conjugates a unique immunodominant glycan with a terminal tyvelose sugar onto multiple peptide backbones (63), providing a target for protective Abs (64, 65), whereas larvae of *Toxocara canis* (which invade the intestinal tract and migrate in tissues) release two unusually methylated and highly antigenic O-linked trisaccharides (66–68). Larvae of *Trichostrongylus colubriformis*, which, like *H. polygyrus*, is a member of the Trichostrongylid family, express a protease-resistant carbohydrate Ag that may act as the target of protective immunity (69). Another antigenic moiety closely related with helminth parasites is phosphorylcholine, which may be associated with high molecular mass proteoglycan-like molecules (30) or individual proteins that resolve on SDS-PAGE (41). Interestingly, both appear to be the case for HES in which PC is present on a high molecular mass product that does not stain for protein, as well as a 65-kDa component. Most intriguingly, mAbs to this combination (termed HM-65) do not react to PC itself, indicating that a distinct but as yet uncharacterized structure (provisionally named glycan B) is expressed. It remains possible that "glycan B" is not a true carbohydrate but a small haptenic group similar to diethylaminoethanol that is found in ES Ags of the filarial nematode *Litomosoides sigmodontis* (70). Hence, although we do not yet know the structural nature of glycans A and B, it is clear that *H. polygyrus* is not unusual in presenting extensive and immunodominant nonprotein specificities to the mammalian host.

Abs may exert a protective effect by several pathways (17); in particular, they may impede growth and migration during the histotrophic larval phase (20, 71), possibly by neutralizing key ES products (6), and may target the exposed epitopes on the surface of adult worms during the luminal phase. A major objective in studying Ab–Ag interactions in *H. polygyrus* is therefore to address whether particular specificities can confer immunological protection against infection. It is known that Abs play an important role in protective immunity to this parasite, as B cell-deficient animals suffer impaired immunity against secondary infection (4, 15, 16) as a result of absence of Ab as well as B cell participation in the cellular response. In tests of polyclonal serum Abs, the passive transfer of secondary infection sera can protect against challenge infection (15, 72), and this was associated with the IgG1 fraction (19). Although attempts to transfer immunity with primary infection sera have been less successful (15), purified IgG1 can reduce worm burdens and lead to stunting of adult parasites

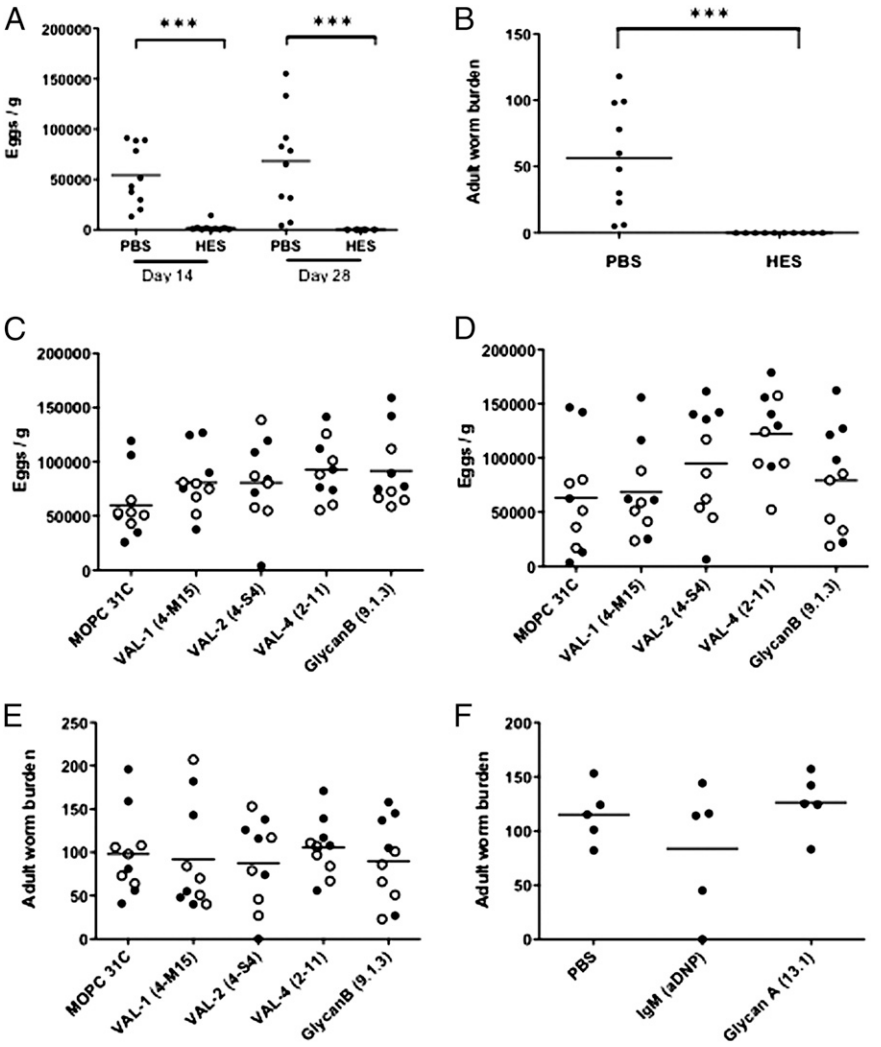

FIGURE 10. Vaccination with adult HES confers sterile immunity to challenge, but passive immunization with mAbs from infected mice does not lead to worm expulsion. *A*, Fecal egg counts at 14 and 28 d postinfection in HES-alum vaccinated mice compared with PBS-alum alone. Each symbol represents a single mouse, and data shown are combined from two independent experiments. ***$p < 0.0001$. *B*, Adult worm burdens at 28 d postinfection in HES-alum vaccinated mice compared with PBS-alum alone. Each symbol represents a single mouse, horizontal bars denote mean values, and data shown are combined from two independent experiments. ***$p < 0.0001$. *C* and *D*, Fecal egg counts at 14 d (*C*) and 28 d (*D*) postinfection in mice receiving passive immunizations of anti-HES IgG1 mAbs or of MOPC31C control IgG1 Ab. Each symbol represents a single mouse, horizontal bars denote mean values, and data shown are combined from two independent experiments using 0.2 mg (open symbols) or 1 mg (closed symbol) mAb for each dose. *E*, Adult worm burdens at day 28 postinfection in the experiments shown in *C* and *D*. *F*, Adult worm burdens at day 28 postinfection in mice passively immunized with PBS alone, control anti-DNP IgM, or IgM anti-glycan A mAb 13.1. i.v. Each symbol represents a single mouse, and horizontal bars denote mean values; similar results were obtained in an independent experiment following i.p. delivery of mAb. Mice receiving i.p. injections of IgG1 Abs were assayed 24 h following the first transfer and were found to have specific anti-HES serum Abs equivalent to between 217 and 633 μg/ml mAb (data not shown).

(20). This may imply that the efficacy of secondary serum Abs over primary sera reflects elevated titers of anti-worm Abs, rather than any difference in specificity induced by repeat exposure.

We therefore tested each of the mAb types generated in this study for their ability to confer protection by passive transfer. However, none exerted any effect on immunity. As we transferred considerable quantities of each, and these mAbs represent the major specificities present in primary infection sera, our data instead argue that the failure of primary sera to protect does not reflect a quantitative insufficiency in terms of concentration but either an inadequate affinity as a result of limited affinity maturation or, most interestingly, the absence of key new specificities that may arise only after multiple infections. The failure of mAb-mediated passive immunization contrasts with the sterile immunity generated following vaccination with HES that generates circulating anti-HES titers comparable to those seen following secondary infection. We also therefore examined the Ab profile following secondary infection, which is broadly similar to the primary but contains some additional specificities (such as the single-domain VAL-7 Ag). Future work will examine whether these are more effective targets of protective immunity. A further possibility to be tested is that combinations of Abs, for example, against each of the related VAL proteins, are required to neutralize a common function and that the full range of anti-VAL Abs are only generated through secondary infection.

An intriguing finding of this study is that the dominant anti-glycan A response, which is rapidly and extensively stimulated by *H. polygyrus*, shows little protective capacity. This epitope may thus represent an example of a decoy Ag that is elaborated by the parasite to distract immune responses without risk of it inducing a lethal attack on the worm. It is also notable that despite strongly binding the adult worm surface, anti-glycan A Abs are not protective in vivo; this could reflect their restriction to IgM, suggesting that in the absence of class-switching Abs may not gain access to the intestinal sites of infection. The lack of other isotypes even after 28 d of infection suggests a deficiency in T cell help, potentially at the level of the TFH. As it is known that there are abundant IL-4–producing TFH in the draining MLN of *H. polygyrus* mice early in primary infection (73), it is surprising that no IgG response to glycan A is mounted, suggesting that this specificity is recognized and/or processed in an unusual manner.

The longevity of parasites can be attributed to their ability to evade or divert host immunity (74), and hence, the molecular basis of immune attack is of paramount interest. Our understanding of immune interactions with gastrointestinal helminths is primarily at the level of effector cell populations (39, 75) rather than identification of target molecules. At this time, the definition of parasite molecules in this important model of chronic gastrointestinal infection will provide an essential platform both to analyze the recognition of Ags and to identify the parasite products (proteins and sugars) that can modulate host immunity and facilitate protection (22). In this article, we have accordingly moved our definition forward from using crude parasite extracts to the more

antigenic and less complex HES, and finally to individual antigenic species, so that future work can study defined glycans and recombinant proteins. We have also established that most of the prominent Ags are secreted not only by the luminal-dwelling mature adult worms but also by the histotrophic larval stage, which is considered to be a major target of protective immunity. We can now begin to investigate how and where Abs act (21), the relative importance of functional neutralization and the recruitment of host effector cells, and the lethal mechanisms that achieve sterilizing immunity against intestinal helminths.

Disclosures

The authors have no financial conflicts of interest.

References

1. Monroy, F. G., and F. J. Enriquez. 1992. *Heligmosomoides polygyrus:* a model for chronic gastrointestinal helminthiasis. *Parasitol. Today (Regul. Ed.)* 8: 49–54.
2. Camberis, M., G. Le Gros, and J. Urban, Jr. 2003. Animal model of *Nippostrongylus brasiliensis* and *Heligmosomoides polygyrus*. In *Current Protocols in Immunology.* R. Coico, ed. John Wiley and Sons, Inc., New York, p. 19.12.11–19.12.27.
3. Anthony, R. M., J. F. Urban, Jr., F. Alem, H. A. Hamed, C. T. Rozo, J. L. Boucher, N. Van Rooijen, and W. C. Gause. 2006. Memory T_H2 cells induce alternatively activated macrophages to mediate protection against nematode parasites. *Nat. Med.* 12: 955–960.
4. Wojciechowski, W., D. P. Harris, F. Sprague, B. Mousseau, M. Makris, K. Kusser, T. Honjo, K. Mohrs, M. Mohrs, T. Randall, et al. 2009. Cytokine-producing effector B cells regulate type 2 immunity to *H. polygyrus. Immunity* 30: 421–433.
5. Wilson, M. S., M. D. Taylor, A. Balic, C. A. M. Finney, J. R. Lamb, and R. M. Maizels. 2005. Suppression of allergic airway inflammation by helminth-induced regulatory T cells. *J. Exp. Med.* 202: 1199–1212.
6. Grainger, J. R., K. A. Smith, J. P. Hewitson, H. J. McSorley, Y. Harcus, K. J. Filbey, C. A. M. Finney, E. J. D. Greenwood, D. P. Knox, M. S. Wilson, et al. 2010. Helminth secretions induce de novo T cell Foxp3 expression and regulatory function through the TGF-β pathway. *J. Exp. Med.* 207: 2331–2341.
7. Ing, R., Z. Su, M. E. Scott, and K. G. Koski. 2000. Suppressed T helper 2 immunity and prolonged survival of a nematode parasite in protein-malnourished mice. *Proc. Natl. Acad. Sci. USA* 97: 7078–7083.
8. Scott, M. E. 1987. Regulation of mouse colony abundance by *Heligmosomoides polygyrus. Parasitology* 95(Pt. 1): 111–124.
9. Behnke, J. M., and D. Wakelin. 1977. *Nematospiroides dubius:* stimulation of acquired immunity in inbred strains of mice. *J. Helminthol.* 51: 167–176.
10. Prowse, S. J., G. F. Mitchell, P. L. Ey, and C. R. Jenkin. 1979. The development of resistance in different inbred strains of mice to infection with *Nematospiroides dubius. Parasite Immunol.* 1: 277–288.
11. Wahid, F. N., and J. M. Behnke. 1993. Immunological relationships during primary infection with *Heligmosomoides polygyrus*: regulation of fast response phenotype by H-2 and non-H-2 genes. *Parasitology* 107: 343–350.
12. Wahid, F. N., and J. M. Behnke. 1993. Immunological relationships during primary infection with *Heligmosomoides polygyrus* (*Nematospiroides dubius*): parasite specific IgG1 antibody responses and primary response phenotype. *Parasite Immunol.* 15: 401–413.
13. Lawrence, C. E., and D. I. Pritchard. 1994. Immune response profiles in responsive and non-responsive mouse strains infected with *Heligmosomoides polygyrus. Int. J. Parasitol.* 24: 487–494.
14. Ben-Smith, A., F. N. Wahid, D. A. Lammas, and J. M. Behnke. 1999. The relationship between circulating and intestinal *Heligmosomoides polygyrus*-specific IgG1 and IgA and resistance to primary infection. *Parasite Immunol.* 21: 383–395.
15. McCoy, K. D., M. Stoel, R. Stettler, P. Merky, K. Fink, B. M. Senn, C. Schaer, J. Massacand, B. Odermatt, H. C. Oettgen, et al. 2008. Polyclonal and specific antibodies mediate protective immunity against enteric helminth infection. *Cell Host Microbe* 4: 362–373.
16. Liu, Q., T. Kreider, S. Bowdridge, Z. Liu, Y. Song, A. G. Gaydo, J. F. Urban, Jr., and W. C. Gause. 2010. B cells have distinct roles in host protection against different nematode parasites. *J. Immunol.* 184: 5213–5223.
17. Harris, N., and W. C. Gause. 2011. To B or not to B: B cells and the Th2-type immune response to helminths. *Trends Immunol.* 32: 80–88.
18. Dobson, C. 1982. Passive transfer of immunity with serum in mice infected with *Nematospiroides dubius*: influence of quality and quantity of immune serum. *Int. J. Parasitol.* 12: 207–213.
19. Pritchard, D. I., D. J. L. Williams, J. M. Behnke, and T. D. G. Lee. 1983. The role of IgG1 hypergammaglobulinaemia in immunity to the gastrointestinal nematode *Nematospiroides dubius*: the immunochemical purification, antigen-specificity and in vivo anti-parasite effect of IgG1 from immune serum. *Immunology* 49: 353–365.
20. Pritchard, D. I., J. M. Behnke, and D. J. Williams. 1984. Primary infection sera and IgG1 do not block host-protective immunity to *Nematospiroides dubius. Immunology* 51: 73–81.
21. Pleass, R. J., and J. M. Behnke. 2009. B-cells get the T-cells but antibodies get the worms. *Trends Parasitol.* 25: 443–446.
22. Hewitson, J. P., J. R. Grainger, and R. M. Maizels. 2009. Helminth immunoregulation: the role of parasite secreted proteins in modulating host immunity. *Mol. Biochem. Parasitol.* 167: 1–11.
23. Bethony, J., A. Loukas, M. Smout, S. Brooker, S. Mendez, J. Plieskatt, G. Goud, M. E. Bottazzi, B. Zhan, Y. Wang, et al. 2005. Antibodies against a secreted protein from hookworm larvae reduce the intensity of hookworm infection in humans and vaccinated laboratory animals. *FASEB J.* 19: 1743–1745.
24. Diemert, D. J., J. M. Bethony, and P. J. Hotez. 2008. Hookworm vaccines. *Clin. Infect. Dis.* 46: 282–288.
25. Finney, C. A. M., M. D. Taylor, M. S. Wilson, and R. M. Maizels. 2007. Expansion and activation of $CD4^+CD25^+$ regulatory T cells in *Heligmosomoides polygyrus* infection. *Eur. J. Immunol.* 37: 1874–1886.
26. Harcus, Y., G. Nicoll, J. Murray, K. Filbey, N. Gomez-Escobar, and R. M. Maizels. 2009. C-type lectins from the nematode parasites *Heligmosomoides polygyrus* and *Nippostrongylus brasiliensis. Parasitol. Int.* 58: 461–470.
27. Pritchard, D. I., and J. M. Behnke. 1985. The suppression of homologous immunity by soluble adult antigens of *Nematospiroides dubius. J. Helminthol.* 59: 251–256.
28. Hewitson, J. P., Y. M. Harcus, R. S. Curwen, A. A. Dowle, A. K. Atmadja, P. D. Ashton, A. Wilson, and R. M. Maizels. 2008. The secretome of the filarial parasite, *Brugia malayi*: proteomic profile of adult excretory-secretory products. *Mol. Biochem. Parasitol.* 160: 8–21.
29. Sutanto, I., R. M. Maizels, and D. A. Denham. 1985. Surface antigens of a filarial nematode: analysis of adult *Brugia pahangi* surface components and their use in monoclonal antibody production. *Mol. Biochem. Parasitol.* 15: 203–214.
30. Maizels, R. M., J. Burke, and D. A. Denham. 1987. Phosphorylcholine-bearing antigens in filarial nematode parasites: analysis of somatic extracts, in-vitro secretions and infection sera from *Brugia malayi* and *B. pahangi*. *Parasite Immunol.* 9: 49–66.
31. Rzepecka, J., S. Rausch, C. Klotz, C. Schnöller, T. Kornprobst, J. Hagen, R. Ignatius, R. Lucius, and S. Hartmann. 2009. Calreticulin from the intestinal nematode *Heligmosomoides polygyrus* is a Th2-skewing protein and interacts with murine scavenger receptor-A. *Mol. Immunol.* 46: 1109–1119.
32. Pritchard, D. I., R. M. Maizels, J. M. Behnke, and P. Appleby. 1984. Stage-specific antigens of *Nematospiroides dubius. Immunology* 53: 325–335.
33. Adams, J. H., F. G. Monroy, I. J. East, and C. Dobson. 1987. Surface and excretory/secretory antigens of *Nematospiroides dubius. Immunol. Cell Biol.* 65: 393–397.
34. Hewitson, J. P., Y. Harcus, J. Murray, M. van Agtmaal, K. J. Filbey, J. R. Grainger, S. Bridgett, M. L. Blaxter, P. D. Ashton, D. A. Ashford, et al. 2011. Proteomic analysis of secretory products from the model gastrointestinal nematode *Heligmosomoides polygyrus* reveals dominance of Venom Allergen-Like (VAL) proteins. *J. Proteomics* 74: 1573–1594.
35. Zhan, B., Y. Liu, M. Badamchian, A. Williamson, J. Feng, A. Loukas, J. M. Hawdon, and P. J. Hotez. 2003. Molecular characterisation of the *Ancylostoma*-secreted protein family from the adult stage of *Ancylostoma caninum. Int. J. Parasitol.* 33: 897–907.
36. Cantacessi, C., B. E. Campbell, A. Visser, P. Geldhof, M. J. Nolan, A. J. Nisbet, J. B. Matthews, A. Loukas, A. Hofmann, D. Otranto, et al. 2009. A portrait of the "SCP/TAPS" proteins of eukaryotes—developing a framework for fundamental research and biotechnological outcomes. *Biotechnol. Adv.* 27: 376–388.
37. Prowse, S. J., and G. F. Mitchell. 1980. On the choice of mice for dissection of strain variations in the development of resistance to infection with *Nematospiroides dubius. Aust. J. Exp. Biol. Med. Sci.* 58: 603–605.
38. Behnke, J. M., J. M. Mugambi, S. Clifford, F. A. Iraqi, R. L. Baker, J. P. Gibson, and D. Wakelin. 2006. Genetic variation in resistance to repeated infections with *Heligmosomoides polygyrus bakeri*, in inbred mouse strains selected for the mouse genome project. *Parasite Immunol.* 28: 85–94.
39. Anthony, R. M., L. I. Rutitzky, J. F. Urban, Jr., M. J. Stadecker, and W. C. Gause. 2007. Protective immune mechanisms in helminth infection. *Nat. Rev. Immunol.* 7: 975–987.
40. Perona-Wright, G., K. Mohrs, J. Taylor, C. Zaph, D. Artis, E. J. Pearce, and M. Mohrs. 2008. Cutting edge: helminth infection induces IgE in the absence of μ- or δ-chain expression. *J. Immunol.* 181: 6697–6701.
41. Harnett, W., and M. M. Harnett. 1999. Phosphorylcholine: friend or foe of the immune system? *Immunol. Today* 20: 125–129.
42. Brown, A. R., and C. A. Crandall. 1976. A phosphorylcholine idiotype related to TEPC 15 in mice infected with *Ascaris suum. J. Immunol.* 116: 1105–1109.
43. Julenius, K., A. Mølgaard, R. Gupta, and S. Brunak. 2005. Prediction, conservation analysis, and structural characterization of mammalian mucin-type O-glycosylation sites. *Glycobiology* 15: 153–164.
44. Harnett, W., K. M. Houston, R. Amess, and M. J. Worms. 1993. *Acanthocheilonema viteae*: phosphorylcholine is attached to the major excretory-secretory product via an N-linked glycan. *Exp. Parasitol.* 77: 498–502.
45. Ghosh, K., J. Hawdon, and P. Hotez. 1996. Vaccination with alum-precipitated recombinant *Ancylostoma*-secreted protein 1 protects mice against challenge infections with infective hookworm (*Ancylostoma caninum*) larvae. *J. Infect. Dis.* 174: 1380–1383.
46. Day, K. P., R. J. Howard, S. J. Prowse, C. B. Chapman, and G. F. Mitchell. 1979. Studies on chronic versus transient intestinal nematode infections in mice. I. A comparison of responses to excretory/secretory (ES) products of *Nippostrongylus brasiliensis* and *Nematospiroides dubius* worms. *Parasite Immunol.* 1: 217–239.

47. Maizels, R. M., A. Balic, N. Gomez-Escobar, M. Nair, M. D. Taylor, and J. E. Allen. 2004. Helminth parasites—masters of regulation. *Immunol. Rev.* 201: 89–116.
48. Patel, N., T. Kreider, J. F. Urban, Jr., and W. C. Gause. 2009. Characterisation of effector mechanisms at the host:parasite interface during the immune response to tissue-dwelling intestinal nematode parasites. *Int. J. Parasitol.* 39: 13–21.
49. Metwali, A., T. Setiawan, A. M. Blum, J. Urban, D. E. Elliott, L. Hang, and J. V. Weinstock. 2006. Induction of $CD8^+$ regulatory T cells in the intestine by *Heligmosomoides polygyrus* infection. *Am. J. Physiol. Gastrointest. Liver Physiol.* 291: G253–G259.
50. Rausch, S., J. Huehn, D. Kirchhoff, J. Rzepecka, C. Schnoeller, S. Pillai, C. Loddenkemper, A. Scheffold, A. Hamann, R. Lucius, and S. Hartmann. 2008. Functional analysis of effector and regulatory T cells in a parasitic nematode infection. *Infect. Immun.* 76: 1908–1919.
51. Wilson, M. S., M. D. Taylor, M. T. O'Gorman, A. Balic, T. A. Barr, K. Filbey, S. M. Anderton, and R. M. Maizels. 2010. Helminth-induced $CD19^+CD23^{hi}$ B cells modulate experimental allergic and autoimmune inflammation. *Eur. J. Immunol.* 40: 1682–1696.
52. Balic, A., K. A. Smith, Y. Harcus, and R. M. Maizels. 2009. Dynamics of $CD11c^+$ dendritic cell subsets in lymph nodes draining the site of intestinal nematode infection. *Immunol. Lett.* 127: 68–75.
53. Smith, K. A., K. Hochweller, G. J. Hämmerling, L. Boon, A. S. Macdonald, and R. M. Maizels. 2011. Chronic helminth infection promotes immune regulation in vivo through dominance of $CD11c^{lo}CD103^-$ dendritic cells. *J. Immunol.* 186: 7098–7109.
54. Bazzone, L. E., P. M. Smith, L. I. Rutitzky, M. G. Shainheit, J. F. Urban, T. Setiawan, A. M. Blum, J. V. Weinstock, and M. J. Stadecker. 2008. Coinfection with the intestinal nematode *Heligmosomoides polygyrus* markedly reduces hepatic egg-induced immunopathology and proinflammatory cytokines in mouse models of severe schistosomiasis. *Infect. Immun.* 76: 5164–5172.
55. Weng, M., D. Huntley, I. F. Huang, O. Foye-Jackson, L. Wang, A. Sarkissian, Q. Zhou, W. A. Walker, B. J. Cherayil, and H. N. Shi. 2007. Alternatively activated macrophages in intestinal helminth infection: effects on concurrent bacterial colitis. *J. Immunol.* 179: 4721–4731.
56. Rzepecka, J., R. Lucius, M. Doligalska, S. Beck, S. Rausch, and S. Hartmann. 2006. Screening for immunomodulatory proteins of the intestinal parasitic nematode *Heligmosomoides polygyrus. Parasite Immunol.* 28: 463–472.
57. Monroy, F. G., I. J. East, C. Dobson, and J. H. Adams. 1989. Immunity in mice vaccinated with a molecular weight 60,000 glycoprotein secreted by adult *Nematospiroides dubius. Int. J. Parasitol.* 19: 71–76.
58. Hoselton, S., L. Piche, T. Gustad, and M. Robinson. 2002. Production of a recombinant version of a *Heligmosomoides polygyrus* antigen that is preferentially recognized by resistant mouse strains. *Parasite Immunol.* 24: 429–435.
59. Pleass, R. J., and A. E. Bianco. 1996. Irradiated larval vaccination and antibody responses evaluated in relation to the expression of immunity to *Heligmosomoides polygyrus. Parasitol. Res.* 82: 445–453.
60. Mulvenna, J., B. Hamilton, S. H. Nagaraj, D. Smyth, A. Loukas, and J. J. Gorman. 2009. Proteomics analysis of the excretory/secretory component of the blood-feeding stage of the hookworm, *Ancylostoma caninum. Mol. Cell. Proteomics* 8: 109–121.
61. Meyvis, Y., N. Callewaert, K. Gevaert, E. Timmerman, J. Van Durme, J. Schymkowitz, F. Rousseau, J. Vercruysse, E. Claerebout, and P. Geldhof. 2008. Hybrid *N*-glycans on the host protective activation-associated secreted proteins of *Ostertagia ostertagi* and their importance in immunogenicity. *Mol. Biochem. Parasitol.* 161: 67–71.
62. Page, A. P., and I. L. Johnstone. 2007. The cuticle. *WormBook*: 1–15.
63. Denkers, E. Y., D. L. Wassom, C. J. Krco, and C. E. Hayes. 1990. The mouse antibody response to *Trichinella spiralis* defines a single, immunodominant epitope shared by multiple antigens. *J. Immunol.* 144: 3152–3159.
64. Ellis, L. A., A. J. Reason, H. R. Morris, A. Dell, R. Iglesias, F. M. Ubeira, and J. A. Appleton. 1994. Glycans as targets for monoclonal antibodies that protect rats against *Trichinella spiralis. Glycobiology* 4: 585–592.
65. McVay, C. S., P. Bracken, L. F. Gagliardo, and J. Appleton. 2000. Antibodies to tyvelose exhibit multiple modes of interference with the epithelial niche of *Trichinella spiralis. Infect. Immun.* 68: 1912–1918.
66. Khoo, K.-H., R. M. Maizels, A. P. Page, G. W. Taylor, N. B. Rendell, and A. Dell. 1991. Characterization of nematode glycoproteins: the major *O*-glycans of *Toxocara* excretory-secretory antigens are O-methylated trisaccharides. *Glycobiology* 1: 163–171.
67. Page, A. P., and R. M. Maizels. 1992. Biosynthesis and glycosylation of serine/threonine-rich secreted proteins from *Toxocara canis* larvae. *Parasitology* 105: 297–308.
68. Schabussova, I., H. Amer, I. van Die, P. Kosma, and R. M. Maizels. 2007. O-Methylated glycans from *Toxocara* are specific targets for antibody binding in human and animal infections. *Int. J. Parasitol.* 37: 97–109.
69. Maass, D. R., G. B. Harrison, W. N. Grant, W. R. Hein, and C. B. Shoemaker. 2009. Intraspecific epitopic variation in a carbohydrate antigen exposed on the surface of *Trichostrongylus colubriformis* infective L3 larvae. *PLoS Pathog.* 5: e1000597.
70. Hintz, M., G. Schares, A. Taubert, R. Geyer, H. Zahner, S. Stirm, and F. J. Conraths. 1998. Juvenile female *Litomosoides sigmodontis* produce an excretory/secretory antigen (Juv-p120) highly modified with dimethylaminoethanol. *Parasitology* 117: 265–271.
71. Ey, P. L. 1988. *Heligmosomoides polygyrus:* retarded development and stunting of larvae by antibodies specific for excretory/secretory antigens. *Exp. Parasitol.* 65: 232–243.
72. Behnke, J. M., and H. A. Parish. 1979. Expulsion of *Nematospiroides dubius* from the intestine of mice treated with immune serum. *Parasite Immunol.* 1: 13–26.
73. King, I. L., and M. Mohrs. 2009. IL-4–producing $CD4^+$ T cells in reactive lymph nodes during helminth infection are T follicular helper cells. *J. Exp. Med.* 206: 1001–1007.
74. Maizels, R. M., and M. Yazdanbakhsh. 2003. Immune regulation by helminth parasites: cellular and molecular mechanisms. *Nat. Rev. Immunol.* 3: 733–743.
75. Allen, J. E., and R. M. Maizels. 2011. Diversity and dialogue in immunity to helminths. *Nat. Rev. Immunol.* 11: 375–388.